Ca^{2+} SIGNALING AND HEART RHYTHM

EDITED BY: Ming Lei, Christopher L.-H. Huang, R. John Solaro and Yunbo Ke

PUBLISHED IN: Frontiers in Physiology

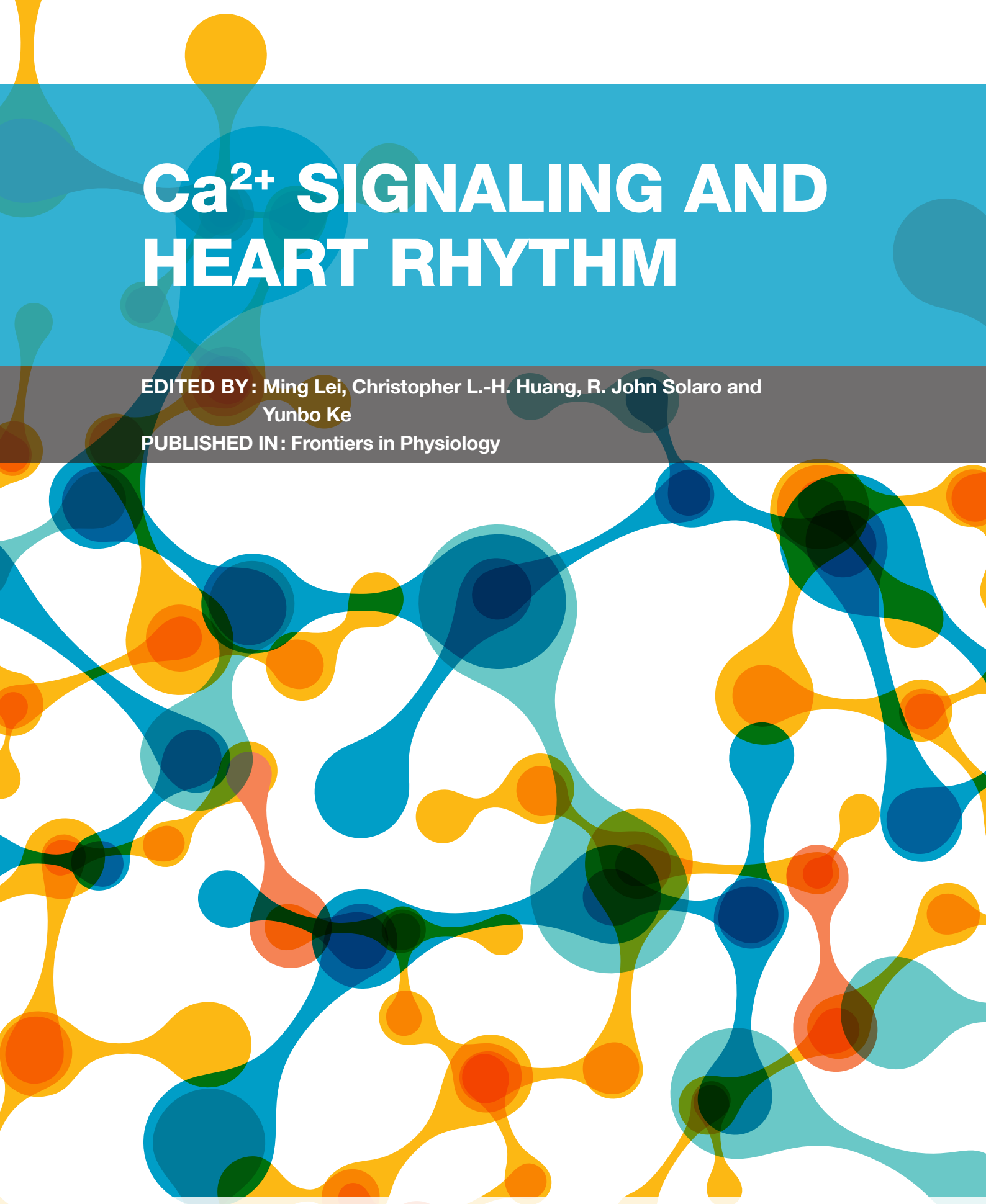

frontiers Research Topics

frontiers

ISSN 1664-8714
ISBN 978-2-88919-874-0
DOI 10.3389/978-2-88919-874-0

About Frontiers

Frontiers is more than just an open-access publisher of scholarly articles: it is a pioneering approach to the world of academia, radically improving the way scholarly research is managed. The grand vision of Frontiers is a world where all people have an equal opportunity to seek, share and generate knowledge. Frontiers provides immediate and permanent online open access to all its publications, but this alone is not enough to realize our grand goals.

Frontiers Journal Series

The Frontiers Journal Series is a multi-tier and interdisciplinary set of open-access, online journals, promising a paradigm shift from the current review, selection and dissemination processes in academic publishing. All Frontiers journals are driven by researchers for researchers; therefore, they constitute a service to the scholarly community. At the same time, the Frontiers Journal Series operates on a revolutionary invention, the tiered publishing system, initially addressing specific communities of scholars, and gradually climbing up to broader public understanding, thus serving the interests of the lay society, too.

Dedication to Quality

Each Frontiers article is a landmark of the highest quality, thanks to genuinely collaborative interactions between authors and review editors, who include some of the world's best academicians. Research must be certified by peers before entering a stream of knowledge that may eventually reach the public - and shape society; therefore, Frontiers only applies the most rigorous and unbiased reviews.
Frontiers revolutionizes research publishing by freely delivering the most outstanding research, evaluated with no bias from both the academic and social point of view.
By applying the most advanced information technologies, Frontiers is catapulting scholarly publishing into a new generation.

What are Frontiers Research Topics?

Frontiers Research Topics are very popular trademarks of the Frontiers Journals Series: they are collections of at least ten articles, all centered on a particular subject. With their unique mix of varied contributions from Original Research to Review Articles, Frontiers Research Topics unify the most influential researchers, the latest key findings and historical advances in a hot research area! Find out more on how to host your own Frontiers Research Topic or contribute to one as an author by contacting the Frontiers Editorial Office: **researchtopics@frontiersin.org**

Ca^{2+} SIGNALING AND HEART RHYTHM

Topic Editors:
Ming Lei, University of Oxford, UK
Christopher L.-H. Huang, University of Cambridge, UK
R. John Solaro, University of Illinois at Chicago, USA
Yunbo Ke, University of Illinois at Chicago, USA

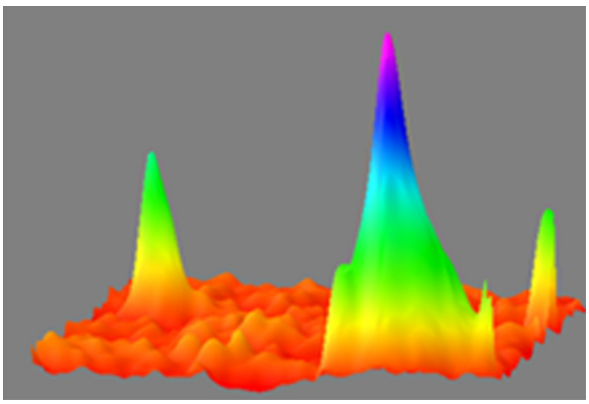

Three dimensional representation of a confocal image of Ca^{2+} sparks and Ca^{2+} wave recorded from a hypertrophied murine ventricular myocyte. Adapted from Rui et al. PLOS One 2014; 9:e101974

Ca^{2+} is a key second messenger in the intricate workings of the heart. In cardiac myocytes, Ca^{2+} signaling controls or modulates electrophysiological function, excitation-contraction coupling, contractile function, energy balance, cell death, and gene transcription. Thus, diverse Ca^{2+}-dependent regulatory processes occur simultaneously within a cell. Yet, distinct signals can be resolved by local Ca^{2+} sensitive protein complexes and differential Ca^{2+} signal integration.

In addition to its importance to normal cardiac function, such regulation is also crucial in disease conditions. Ca^{2+} is likely involved in ectopic cardiac rhythms in both atrial and ventricular tissues through generating triggered activity often appearing as delayed afterdepolarisations, particularly following cellular Ca overloading. Recent studies also implicate Ca^{2+} in Na^{+} channel expression and properties with consequences for conduction velocity and therefore arrhythmic substrate. At the cellular level, such regulation involves control of the activity of membrane ion channels and Ca^{2+} handling proteins. These in turn involve multiple extra- and intracellular signaling pathways.

This e-book assembles review and original articles from experts in this field. It summarises major recent progress bearing on roles of Ca^{2+} in cardiac electrophysiological function encompassing both normal and abnormal cardiac function. These extend from physiological roles of Ca^{2+} signaling in pacemaker function, in particular generation of sino-atrial pacemaker potentials, to pathological roles of abnormal Ca^{2+} signaling in both atrial and ventricular arrhythmogenesis. It also seeks to bridge the gap between advances in basic science and development of new therapies.

Citation: Lei, M., Huang, C. L.-H., Solaro, R. J., Ke, Y., eds. (2016). Ca^{2+} Signaling and Heart Rhythm. Lausanne: Frontiers Media. doi: 10.3389/978-2-88919-874-0

Table of Contents

frontiers in Physiology

EDITORIAL
published: 11 January 2016
doi: 10.3389/fphys.2015.00423

Editorial: Ca^{2+} Signaling and Heart Rhythm

Christopher L.-H. Huang[1], R. John Solaro[2], Yunbo Ke[2] and Ming Lei[3]*

[1] Physiological Laboratory, Department of Biochemistry, University of Cambridge, Cambridge, UK, [2] Department of Physiology and Biophysics, University of Illinois at Chicago, Chicago, USA, [3] Department of Pharmacology, University of Oxford, Oxford, UK

Keywords: calcium, sino-atrial node, atrial arrhythmia, Ca^{2+} clock, Ca^{2+} channels

The Editorial on the Research Topic

Ca^{2+} Signaling and Heart Rhythm

Ca^{2+} is a strategic intracellular second messenger regulating multifarious cardiac cellular processes. This Frontiers issue on Ca^{2+} signaling and cardiac rhythm first focuses on the spontaneous membrane depolarization triggering action potential (AP) pacing by sino-atrial node (SAN) cells. These drive normal rhythmic atrial followed by ventricular depolarization initiating effective systolic contraction (Mangoni and Nargeot, 2008). Classic pharmacological and immunological localization studies had implicated sarcoplasmic reticular (SR)-mediated Ca^{2+} storage and release (Rigg and Terrar, 1996) involving ryanodine receptor (RyR2)-Ca^{2+} release channels (Rigg et al., 2000) as necessary components in an adrenergically-responsive, complex, Ca^{2+}-dependent, sino-atrial pacing process. Subsequent confocal imaging demonstrated spontaneous, precisely timed, rhythmic, local, submembrane, SR Ca^{2+} release events (Bogdanov et al., 2001; Vinogradova et al., 2004; Lakatta et al., 2010). Were these to activate Na^{+}-Ca^{2+} exchange current, I_{NCX}, the resulting depolarization could trigger surface inward L-type Ca^{2+} currents, I_{Ca}, thereby initiating AP firing (Vinogradova et al., 2002). SAN cells possessed high basal cAMP and phosphokinase A-dependent phosphorylation levels (Vinogradova et al., 2006) that could ensure RyR2-mediated Ca^{2+} release activity (Yang et al., 2002) at the requisite frequencies (Vinogradova et al., 2002, 2006). The resulting $[Ca^{2+}]$ (to >100 nM) increases produced the expected I_{NCX} changes (Bogdanov et al., 2001) besides additionally activating strategic enzymes, particularly calcium/calmodulin-dependent protein kinase II (CaMKII). Hyperpolarization-activated cyclic nucleotide-gated (HCN) channels carrying I_f likely also importantly contribute to this process: *Hcn4*-/- and *Hcn4*-R669Q/R669Q mouse embryos were bradycardic with 75–90% reduced I_f before eventual lethality (Stieber et al., 2003; Chandra et al., 2006; Harzheim et al., 2008); tamoxiphen-inducible adult hearts showed ~70% reduced I_f and progressive $\leq$50% reductions in, nevertheless persistent, SAN pacing, compromising its responses to isoproterenol challenge (Sohal et al., 2001; Baruscotti et al., 2011).

The present articles first complete necessary conditions for such a Ca^{2+}-mediated pacing system (Vinogradova et al., 2000; Bogdanov et al., 2001; Sanders et al., 2006; Maltsev and Lakatta, 2007) to exist. They explore recent evidence implicating I_{NCX}, combined with delayed rectifier K^{+} current deactivation, in the pacemaker depolarization triggering I_{Ca} (Capel and Terrar). Furthermore, intracellular $[Ca^{2+}]$ proved instrumental in determining pacing rates: 1,2-bis(o-aminophenoxy)ethane-N,N,N′,N′-tetraacetic acid (BAPTA) dose-dependently slowed, ultimately abolishing, AP firing in isolated guinea-pig SAN myocytes (Capel and Terrar). Involvement of I_{Ca} in both SAN pacing and atrioventricular conduction was indicated in mice homozygously lacking L-type, Cav1.3, or T-type, Cav3.1, channels normally expressed in mouse, rabbit and human

OPEN ACCESS

Edited and reviewed by:
Ruben Coronel, Academic Medical Center, Netherlands

****Correspondence:***
Christopher L.-H. Huang
clh11@cam.ac.uk

Specialty section:
This article was submitted to Cardiac Electrophysiology, a section of the journal Frontiers in Physiology

Received: *10 December 2015*
Accepted: *22 December 2015*
Published: *11 January 2016*

Citation:
Huang CL-H, Solaro RJ, Ke Y and Lei M (2016) Editorial: Ca^{2+} Signaling and Heart Rhythm. Front. Physiol. 6:423. doi: 10.3389/fphys.2015.00423

pacemaker tissue (Mesirca et al.). Volume and pressure overload-induced heart failure in rabbit SAN cells markedly influenced both Ca^{2+} transients and pacemaker activity (Verkerk et al.). Finally, the hypothesis generated schemes amenable to quantitative modeling and reconstruction (Yaniv et al.).

The articles then explore further ion channel mechanisms possibly contributing to this regulation. TRPC3 channels mediating Ca^{2+} entry are up-regulated in clinical and experimental atrial fibrillation (AF), and are implicated in SAN dysfunction and atrioventricular block (Yanni et al., 2011; Harada et al., 2012; Sabourin et al., 2012). Ju et al. report that the *Trpc3-/-* variant rescued pacing-induced AF in angiotensin II-treated mice (Ju et al.). Similarly, intracellular Ca^{2+} store depletion increased Ca^{2+} entry in isolated firing mouse SAN pacemaker cells, findings reduced by store-operated Ca^{2+} entry (SOCE) blockers. SAN pacemaker cells further expressed the endoplasmic reticular, Ca^{2+}-sensing, stromal interacting molecules (STIM) and surface membrane Orai1 channels likely involved in SOCE. Ca^{2+} store depletion redistributed STIM1 to the cell periphery increasing STIM1-Ora1 co-localization (Liu et al.).

SAN and surrounding atrial tissue form a SAN-atrial pacemaker complex. SAN disorders accordingly can produce re-entrant substrate causing AF in addition to bradycardic, sinus node, dysfunction (Nattel et al., 2007). Altered intracellular Ca^{2+} transients and diastolic SR Ca^{2+} release appear to be important AF triggers in murine hearts (Zhang et al., 2009, 2010). Ai explores possible interactions between key Ca^{2+} handling proteins in such arrhythmia. These include RyR2, phospholamban, L-type Ca^{2+} channels (Cav1.2) (Schulman et al., 1992), and possible actions upon these of the intrinsic stress-related family of mitogen-activated protein kinase (MAPK) cascades including c-Jun N-terminal kinase, extracellular signal-regulated kinases, and p38 MAPKs whose activity alters in aging and failing hearts (Ai).

Further articles bear upon modulatory influences upon the complex of Ca^{2+} signaling pathways. Thus, SR Ca^{2+} uptake mechanisms proved affected by p21-activated kinase (Pak1) deficiency, previously identified with hypertrophic ventricular remodeling in heart failure, through altered post-transcriptional activity of key Ca^{2+}-handling proteins, particularly SR Ca^{2+}-ATPase (Wang et al.). Similarly, altered protein phosphatase 2A expression and activity, likely acting downstream of Pak1, may compromise responses to β-adrenergic stimulation with implications for arrhythmia and cardiac failure (Lei et al.). Finally, membrane protein regulation, trafficking and recycling are fundamental to all cellular physiological processes including those involving Ca^{2+} homeostasis. This prompted review of a particular, endosome-based, trafficking process, involving endocytic C-terminal Eps15 homology domain-containing regulatory proteins (Curran et al.).

Ultimately, quantitative analysis of Ca^{2+}-mediated modulatory effects on cardiac function as a whole must extend such molecular and cellular analysis from Ca^{2+} homeostatic to contractile function in entire cardiac chambers (cf. Adeniran et al., 2013; Davies et al., 2014). This reconstruction will require further, more quantitative, data on the processes involved. Nevertheless, one such article succeeds in integrating abnormal Ca^{2+} homeostasis, ion channel and structural remodeling with ventricular electro-mechanical dynamics in the clinical problem of heart failure with preserved ejection fraction. It emerges with testable predictions of reduced systolic Ca^{2+} and therefore systolic force, but increased diastolic Ca^{2+} and therefore residual diastolic force, despite conserved ejection fraction, particularly at increased heart rates (Adeniran et al.). Simulations of this kind offer openings into more detailed and quantitative studies of sino-atrial and atrial intricacies.

Explorations of the kind described in this series of articles thus contribute to development of a systems basis for sinus node disorder (SND), atrial arrhythmia, and their translational consequences (Nattel, 2002). SND is the commonest clinical indication requiring pacemaker implantation. AF, for which available treatment is limited (Kannel and Benjamin, 2009), is a major contributor to cardiovascular morbidity and mortality, particularly in aging human populations (Juhaszova et al., 2005).

AUTHOR CONTRIBUTIONS

CH, Drafting and planning of the editorial, response to editors report; RS, Re-reading and rewriting of the editorial; YK, Re-reading and checking of the editorial; and ML, Final corrections and rewordings, response to editors report.

REFERENCES

Adeniran, I., Hancox, J. C., and Zhang, H. (2013). In silico investigation of the short QT syndrome, using human ventricle models incorporating electromechanical coupling. *Card. Electrophysiol.* 4:166. doi: 10.3389/fphys.2013.00166

Baruscotti, M., Bucchi, A., Viscomi, C., Mandelli, G., Consalez, G., Gnecchi-Rusconi, T., et al. (2011). Deep bradycardia and heart block caused by inducible cardiac-specific knockout of the pacemaker channel gene Hcn4. *Proc. Natl. Acad. Sci. U.S.A.* 108, 1705–1710. doi: 10.1073/pnas.1010122108

Bogdanov, K. Y., Vinogradova, T. M., and Lakatta, E. G. (2001). Sinoatrial nodal cell ryanodine receptor and $Na^{(+)}$-$Ca^{(2+)}$ exchanger: molecular partners in pacemaker regulation. *Circ. Res.* 88, 1254–1258. doi: 10.1161/hh1201.092095

Chandra, R., Portbury, A. L., Ray, A., Ream, M., Groelle, M., and Chikaraishi, D. M. (2006). Beta1-adrenergic receptors maintain fetal heart rate and survival. *Biol. Neonate* 89, 147–158. doi: 10.1159/000088842

Davies, L., Jin, J., Shen, W., Tsui, H., Shi, Y., Wang, Y., et al. (2014). Mkk4 is a negative regulator of the transforming growth factor beta 1 signaling associated with atrial remodeling and arrhythmogenesis with age. *J. Am. Heart Assoc.* 3, 1–19. doi: 10.1161/JAHA.113.000340

Harada, M., Luo, X., Qi, X. Y., Tadevosyan, A., Maguy, A., Ordog, B., et al. (2012). Transient receptor potential canonical-3 channel-dependent fibroblast regulation in atrial fibrillation. *Circulation* 126, 2051–2064. doi: 10.1161/CIRCULATIONAHA.112.121830

Harzheim, D., Pfeiffer, K. H., Fabritz, L., Kremmer, E., Buch, T., Waisman, A., et al. (2008). Cardiac pacemaker function of HCN4 channels in mice is confined to embryonic development and requires cyclic AMP. *EMBO J.* 27, 692–703. doi: 10.1038/emboj.2008.3

Juhaszova, M., Rabuel, C., Zorov, D. B., Lakatta, E. G., and Sollott, S. J. (2005). Protection in the aged heart: preventing the heart-break of old age? *Cardiovasc. Res.* 66, 233–244. doi: 10.1016/j.cardiores.2004.12.020

Kannel, W. B., and Benjamin, E. J. (2009). Current perceptions of the epidemiology of atrial fibrillation. *Cardiol. Clin.* 27, 13–24, vii. doi: 10.1016/j.ccl.2008.09.015

Lakatta, E. G., Maltsev, V. A., and Vinogradova, T. M. (2010). A coupled system of intracellular Ca^{2+} clocks and surface membrane voltage clocks controls the timekeeping mechanism of the heart's pacemaker. *Circ. Res.* 106, 659–673. doi: 10.1161/CIRCRESAHA.109.206078

Maltsev, V. A., and Lakatta, E. G. (2007). Normal heart rhythm is initiated and regulated by an intracellular calcium clock within pacemaker cells. *Heart Lung Circ.* 16, 335–348. doi: 10.1016/j.hlc.2007.07.005

Mangoni, M. E., and Nargeot, J. (2008). Genesis and regulation of the heart automaticity. *Physiol. Rev.* 88, 919–982. doi: 10.1152/physrev.00018.2007

Nattel, S. (2002). New ideas about atrial fibrillation 50 years on. *Nature* 415, 219–226. doi: 10.1038/415219a

Nattel, S., Maguy, A., Le Bouter, S., and Yeh, Y.-H. (2007). Arrhythmogenic ion-channel remodeling in the heart: heart failure, myocardial infarction, and atrial fibrillation. *Physiol. Rev.* 87, 425–456. doi: 10.1152/physrev.00014.2006

Rigg, L., Heath, B. M., Cui, Y., and Terrar, D. A. (2000). Localisation and functional significance of ryanodine receptors during beta-adrenoceptor stimulation in the guinea-pig sino-atrial node. *Cardiovasc. Res.* 48, 254–264. doi: 10.1016/S0008-6363(00)00153-X

Rigg, L., and Terrar, D. A. (1996). Possible role of calcium release from the sarcoplasmic reticulum in pacemaking in guinea-pig sino-atrial node. *Exp. Physiol.* 81, 877–880. doi: 10.1113/expphysiol.1996.sp003983

Sabourin, J., Antigny, F., Robin, E., Frieden, M., and Raddatz, E. (2012). Activation of transient receptor potential canonical 3 (TRPC3)-mediated Ca^{2+} entry by A1 adenosine receptor in cardiomyocytes disturbs atrioventricular conduction. *J. Biol. Chem.* 287, 26688–26701. doi: 10.1074/jbc.M112.378588

Sanders, L., Rakovic, S., Lowe, M., Mattick, P. A. D., and Terrar, D. A. (2006). Fundamental importance of Na^{+}-Ca^{2+} exchange for the pacemaking mechanism in guinea-pig sino-atrial node. *J. Physiol.* 571, 639–649. doi: 10.1113/jphysiol.2005.100305

Schulman, H., Hanson, P. I., and Meyer, T. (1992). Decoding calcium signals by multifunctional CaM kinase. *Cell Calcium* 13, 401–411. doi: 10.1016/0143-4160(92)90053-U

Sohal, D. S., Nghiem, M., Crackower, M. A., Witt, S. A., Kimball, T. R., Tymitz, K. M., et al. (2001). Temporally regulated and tissue-specific gene manipulations in the adult and embryonic heart using a tamoxifen-inducible Cre protein. *Circ. Res.* 89, 20–25. doi: 10.1161/hh1301.092687

Stieber, J., Herrmann, S., Feil, S., Löster, J., Feil, R., Biel, M., et al. (2003). The hyperpolarization-activated channel HCN4 is required for the generation of pacemaker action potentials in the embryonic heart. *Proc. Natl. Acad. Sci. U.S.A.* 100, 15235–15240. doi: 10.1073/pnas.2434235100

Vinogradova, T. M., Bogdanov, K. Y., and Lakatta, E. G. (2002). beta-Adrenergic stimulation modulates ryanodine receptor $Ca^{(2+)}$ release during diastolic depolarization to accelerate pacemaker activity in rabbit sinoatrial nodal cells. *Circ. Res.* 90, 73–79. doi: 10.1161/hh0102.102271

Vinogradova, T. M., Lyashkov, A. E., Zhu, W., Ruknudin, A. M., Sirenko, S., Yang, D., et al. (2006). High basal protein kinase A-dependent phosphorylation drives rhythmic internal Ca^{2+} store oscillations and spontaneous beating of cardiac pacemaker cells. *Circ. Res.* 98, 505–514. doi: 10.1161/01.RES.0000204575.94040.d1

Vinogradova, T. M., Zhou, Y. Y., Bogdanov, K. Y., Yang, D., Kuschel, M., Cheng, H., et al. (2000). Sinoatrial node pacemaker activity requires $Ca^{(2+)}$/calmodulin-dependent protein kinase II activation. *Circ. Res.* 87, 760–767. doi: 10.1161/01.RES.87.9.760

Vinogradova, T. M., Zhou, Y.-Y., Maltsev, V., Lyashkov, A., Stern, M., and Lakatta, E. G. (2004). Rhythmic ryanodine receptor Ca^{2+} releases during diastolic depolarization of sinoatrial pacemaker cells do not require membrane depolarization. *Circ. Res.* 94, 802–809. doi: 10.1161/01.RES.0000122045.55331.0F

Yang, H.-T., Tweedie, D., Wang, S., Guia, A., Vinogradova, T., Bogdanov, K., et al. (2002). The ryanodine receptor modulates the spontaneous beating rate of cardiomyocytes during development. *Proc. Natl. Acad. Sci. U.S.A.* 99, 9225–9230. doi: 10.1073/pnas.142651999

Yanni, J., Tellez, J. O., Maczewski, M., Mackiewicz, U., Beresewicz, A., Billeter, R., et al. (2011). Changes in ion channel gene expression underlying heart failure-induced sinoatrial node dysfunction. *Circ. Heart Fail.* 4, 496–508. doi: 10.1161/CIRCHEARTFAILURE.110.957647

Zhang, Y., Fraser, J. A., Schwiening, C., Zhang, Y., Killeen, M. J., Grace, A. A., et al. (2010). Acute atrial arrhythmogenesis in murine hearts following enhanced extracellular $Ca^{(2+)}$ entry depends on intracellular $Ca^{(2+)}$ stores. *Acta Physiol.* 198, 143–158. doi: 10.1111/j.1748-1716.2009.02055.x

Zhang, Y., Schwiening, C., Killeen, M. J., Zhang, Y., Ma, A., Lei, M., et al. (2009). Pharmacological changes in cellular Ca^{2+} homeostasis parallel initiation of atrial arrhythmogenesis in murine Langendorff-perfused hearts. *Clin. Exp. Pharmacol. Physiol.* 36, 969–980. doi: 10.1111/j.1440-1681.2009.05170.x

Conflict of Interest Statement: The authors declare that the research was conducted in the absence of any commercial or financial relationships that could be construed as a potential conflict of interest.

frontiers in Physiology

REVIEW
published: 25 March 2015
doi: 10.3389/fphys.2015.00080

The importance of Ca^{2+}-dependent mechanisms for the initiation of the heartbeat

*Rebecca A. Capel and Derek A. Terrar**

British Heart Foundation Centre of Research Excellence, Department of Pharmacology, University of Oxford, Oxford, UK

Mechanisms underlying pacemaker activity in the sinus node remain controversial, with some ascribing a dominant role to timing events in the surface membrane ("membrane clock") and others to uptake and release of calcium from the sarcoplasmic reticulum (SR) ("calcium clock"). Here we discuss recent evidence on mechanisms underlying pacemaker activity with a particular emphasis on the many roles of calcium. There are particular areas of controversy concerning the contribution of calcium spark-like events and the importance of I(f) to spontaneous diastolic depolarisation, though it will be suggested that neither of these is essential for pacemaking. Sodium-calcium exchange (NCX) is most often considered in the context of mediating membrane depolarisation after spark-like events. We present evidence for a broader role of this electrogenic exchanger which need not always depend upon these spark-like events. Short (milliseconds or seconds) and long (minutes) term influences of calcium are discussed including direct regulation of ion channels and NCX, and control of the activity of calcium-dependent enzymes (including CaMKII, AC1, and AC8). The balance between the many contributory factors to pacemaker activity may well alter with experimental and clinical conditions, and potentially redundant mechanisms are desirable to ensure the regular spontaneous heart rate that is essential for life. This review presents evidence that calcium is central to the normal control of pacemaking across a range of temporal scales and seeks to broaden the accepted description of the "calcium clock" to cover these important influences.

Keywords: sino-atrial node, cardiac, pacemaking, cytosolic calcium, calcium clock, membrane clock

OPEN ACCESS

Edited by:
Carol Ann Remme, University of Amsterdam, Netherlands

Reviewed by:
Steve Poelzing, Virginia Tech, USA
Thomas Hund, Ohio State University, USA

****Correspondence:***
Derek A. Terrar, Department of Pharmacology, University of Oxford, Mansfield Road, Oxford, Oxon OX1 3QT, UK
derek.terrar@pharm.ox.ac.uk

Specialty section:
This article was submitted to Cardiac Electrophysiology, a section of the journal Frontiers in Physiology

Received: *09 January 2015*
Accepted: *02 March 2015*
Published: *25 March 2015*

Citation:
Capel RA and Terrar DA (2015) The importance of Ca^{2+}-dependent mechanisms for the initiation of the heartbeat. Front. Physiol. 6:80. doi: 10.3389/fphys.2015.00080

A Rudimentary Pacemaker

The aim of this review is to discuss the many different roles of Ca^{2+} in regulating pacemaker function in the sino-atrial node (SAN). The major determinants of pacemaker activity remain controversial, as illustrated by reviews from the Lakatta and DiFrancesco groups (Lakatta and DiFrancesco, 2009; DiFrancesco and Noble, 2012a,b; Lakatta and Maltsev, 2012; Maltsev and Lakatta, 2012). Other important reviews have been published in the last 10 years (Dobrzynski et al., 2007; Imtiaz et al., 2007; Wu and Anderson, 2014). A comprehensive review from Mangoni and Nargeot also presents a valuable overview of pacemaker mechanisms, particularly with respect to conclusions drawn from genetic abnormalities and genetic manipulations (Mangoni and Nargeot, 2008). The starting point for the discussion here will be the broadly excellent review by Irisawa et al. (1993) (see also Irisawa (1978) and Noma (1996)) which is a very comprehensive in its discussion of surface membrane currents.

Irisawa et al. make little or no inclusion of the possible influence of cytosolic Ca^{2+}, particularly that released from the sarcoplasmic reticulum (SR), since little was known on this aspect of pacemaker mechanisms at the time the review was written. In recent years much of the debate concerning the origin of pacemaker activity in the heart has been presented as a choice between two alternative mechanisms, a "membrane clock" in which I(f) activated by hyperpolarization plays the dominant role or a "Ca^{2+} clock" in which the timing of uptake and release of Ca^{2+} by the SR is the major determinant of the cardiac rhythm (DiFrancesco and Noble, 2012a,b; Lakatta and Maltsev, 2012; Maltsev and Lakatta, 2012).

This review seeks to discuss broader aspects of the influence of Ca^{2+} on pacemaker activity than are frequently considered in debates on the relative importance of Ca^{2+} and membrane clocks. The evidence discussed below supports the view that a variety of ionic currents in addition to I(f) can contribute to the timing of the membrane clock, that these events are potentially modulated by intracellular Ca^{2+} in a number of ways and that the relative importance of these pathways might vary under different physiological and clinical conditions. We consider data relating to the role of the Ca^{2+} clock under a range of conditions, and discuss whether such a clock needs to depend solely on spontaneous Ca^{2+} sparks or local calcium releases (LCRs) or whether other rhythmic Ca^{2+}-dependent mechanisms should also be taken into account to form a complete picture. It appears that the Ca^{2+} clock could play a fundamentally important role for the timing mechanism of the cardiac pacemaker under particular conditions, but in many circumstances might play a cooperative interacting role with the membrane clock.

Timing mechanisms for different sorts of pacemaker activity have been discussed in many different tissues including oscillations in smooth muscle, interstitial cells, brain and heart (e.g., Berridge and Galione, 1988). Mechanisms include what have been called membrane oscillators and cytosolic Ca^{2+} oscillators in smooth muscle and brain, and ideas concerning a Ca^{2+} clock are not unique to the heart (Imtiaz et al., 2006; McHale et al., 2006; Berridge, 2008; Imtiaz, 2012).

In the heart, a key feature that distinguishes pacemaker tissue from surrounding atrial muscle is the absence of the stabilizing influence of I_{K1}. Other important characteristics are the presence of the connexin protein Cx45 (Coppen et al., 1999) and I(f) (Biel et al., 2002) and lack of Cx43 (ten Velde et al., 1995), but the lack of I_{K1} is particularly functionally important for the following reasons. The presence of I_{K1} channels in atrial and ventricular myocytes is responsible for the $\sim$−90 mV resting membrane potential in these cells, dominated by the equilibrium potential for potassium ions in physiological solutions. In the absence of I_{K1} the SAN membrane potential is not forced to "rest" at this potential. In addition, lack of the I_{K1} conducting pathway leads to a greatly increased membrane resistance (reduced conductance) in SAN cells in comparison to atrial and ventricular myocytes and this allows very small ionic currents to exert a profound influence on membrane potential. In this regard, it is also relevant to consider that SAN myocytes exhibit small cell capacitance (of the order of 30–40 pF) in turn requiring only small currents to charge or discharge the membrane capacitance. The significance of the lack of I_{K1} in mammalian SAN pacemaker tissue was first demonstrated in an important paper from Irisawa (Noma et al., 1984) (see also Shibata and Giles, 1985 for similar observations in amphibian pacemaker tissue). The susceptibility to oscillations causing spontaneous activity when I_{K1} is suppressed in ventricular tissue was also shown by Miake et al. (2002).

Although there is no "resting" potential in a pacemaker cell showing continuous electrical activity, an important observation is that when pacemaker activity is arrested (for example by the L-type Ca^{2+} channel blocker nifedipine (Kodama et al., 1997), or by blockers of voltage-gated potassium channels (Lei et al., 2001) the membrane adopts a potential at least for a period of seconds at approximately −30 to −40 mV. A similar potential is adopted when spontaneous activity is stopped by chelation of cytosolic Ca^{2+} with intracellular BAPTA (Capel and Terrar, this issue, and see later). A "resting potential" of −38 mV was also described in rabbit SA node by Noma and Irisawa (1975). Again, a similar potential is recorded in amphibian sinus venosus when spontaneous activity is "arrested" by nifedipine (Bramich et al., 1993). Verheijck et al. (1995) also described a "background current with a reversal potential of −32 mV in rabbit SA node in the presence of nifedipine and E-4031."

With this "background" conductance as a starting point, a very simple pacemaker can be constructed in which an action potential upstroke carried by calcium ions leads to a depolarisation that then activates a voltage-gated potassium conductance and this in turn brings about repolarisation. Potassium channel de-activation will then lead to a removal of hyperpolarizing influence and allow the membrane to move back toward its "resting" level as a consequence of the influence of the background conductance pathway (**Figure 1A**). Early modeling work suggested that this mechanism is capable of sustaining spontaneous action potential generation (Hauswirth et al., 1968) and see (Noble et al., 1992).

A more comprehensive model that will be used as a framework for later discussion is shown for comparison in **Figure 1B**.

Even in a review with an emphasis on the many roles for Ca^{2+}, the existence of a background current with a reversal potential in the region of −30 to −40 mV is so fundamentally important for pacemaker mechanisms that it deserves further discussion. It is also conceivable that this poorly understood pathway is itself Ca^{2+}-dependent. The first question that arises from the simple model is how the "pseudo resting" level of −30 to −40 mV is determined and what, in turn, is the selectivity of the membrane to different ions at such a "pseudo resting" potential when voltage-gated channels are not active.

What is Background Current?

Another way of phrasing the question in the previous paragraph is what is the "background current," or perhaps better what is the background conductance because little or no net current will flow at the "pseudo resting" potential. Although the evidence presented above in favor of the existence of a background conductance is compelling, there is surprisingly little evidence or agreement on the ion conducting pathways that give rise to this conductance. One approach is to block everything we think

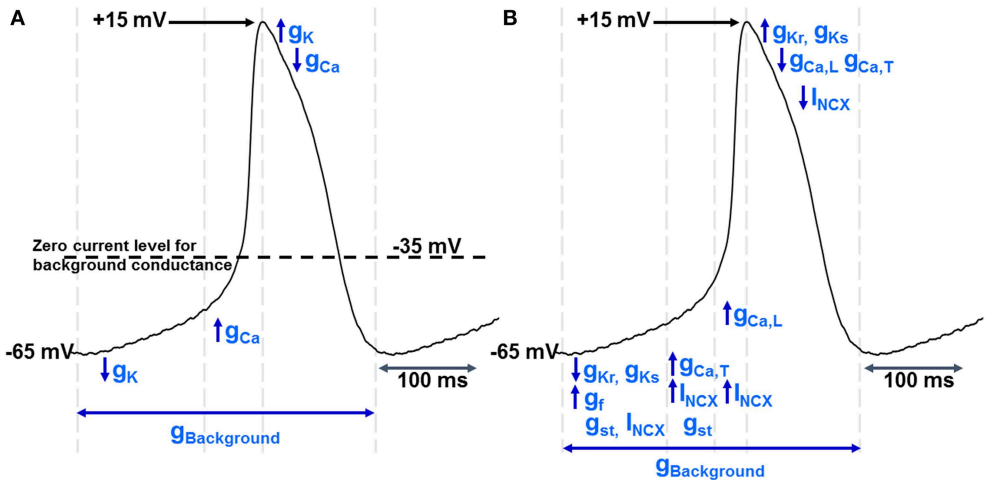

FIGURE 1 | (A) shows a simple model of pacemaker function in which there is a "background" current/conductance with a zero current level between −30 and −40 mV. There is extensive evidence for such a pathway, although as discussed in the text the nature of the conductance(s) contributing to this pathway remain poorly understood. However, given the existence of this pathway, pacemaker activity can be maintained by sequential activation of voltage-gated K^+ and Ca^{2+} ion channels, noting that de-activation of K^+ conductance (g_K) after repolarization will be associated with the "diastolic" or pacemaker depolarization as the potential moves toward the zero current level for the "background" conductance. When the membrane potential reaches the threshold for voltage-gated Ca^{2+} channels, activation of these channels (increasing g_{Ca}) will lead to the upstroke of the action potential and the depolarization will activate voltage-gated potassium channels to complete the cycle of repetitive activity. The vertical dotted lines show an approximate division of the time period of the pacemaker cycle to represent these phases of channel activation and de-activation. The experimental record that is shown to illustrate these phases was recorded from a guinea-pig SAN myocyte in our laboratory and is similar to records in **Figures 2**, **5** (and also to records in Capel and Terrar in this issue). A formal mathematical representation of these changes in conductance was not constructed, but the analysis is broadly similar to the principles used for the basic mathematical model presented by Hauswirth, Noble, and Tsien in 1968 to account for spontaneous activity in Purkinje fibers (Hauswirth et al., 1968).**(B)** shows a more comprehensive description of the ionic conductances and currents underlying pacemaker activity, including g_{CaL} and g_{CaT} (conductance provided by the two varieties of voltage-gated Ca^{2+} channel in cardiac muscle), g_{Ks} and g_{Kr} (the slowly and rapidly activating voltage-gated K^+ channels), g_f (the conductance associated with channels activated by hyperpolarization and carrying the "funny" current), g_{st} (the sustained inward current channels), and I_{NCX} (the NCX current thought to flow throughout the cardiac cycle as outlined in more detail in **Figure 2**). Again, the vertical dotted lines show an approximate division of the time period of the pacemaker cycle to represent different phases of channel activation and de-activation.

we understand and to label what is left as background current e.g., Hagiwara et al. (1992), and this approach leads to the suggestion that background conductance is determined by a balance between potassium conductance (which if dominant would lead to a membrane potential close to the potassium equilibrium potential of perhaps −90 mV) and sodium and/or Ca^{2+} conductances (that if dominant would take the potential to more positive values determined by their equilibrium potentials of ∼+60 mV in the case of Na^+ and more positive than +100 mV in the case of Ca^{2+}). This balance could lead to a "pseudo resting" potential of −30 to −40 mV. Chloride ions cannot be excluded and might also contribute [while a contribution of Cl^- to "background current" was not detected by Hagiwara et al. (1992), other observations from Seyama (1979) and from Huang (Huang et al., 2009) support a role for Cl^-].

At rest, single channels with a zero current potential close to the "pseudo resting" level have not been described. Ito et al. (1994) observed activity of I_{KACh} channels in the absence of ACh. These were the only K^+ channels recorded "at rest" in 105 experiments on SA node cells. These authors concluded that an additional pathway carrying inward current at −50 mV must also exist. These channels could be difficult to find and record from (if they were too scarce, low conductance or too fast and short lived to allow easy detection). One possibility is that a major contributor to background conductance is not an ion channel but NCX in a leak mode as first suggested by Kang and Hilgemann (2004), see later.

Another relevant pathway is the sustained inward current described by Noma and colleagues (Mitsuiye et al., 2000). This pathway cannot contribute to the "pseudo resting" level when nifedipine is used to cause cessation of pacemaker activity, since this drug blocks I(st) in addition to blocking L-type Ca^{2+} channels. However, I(st) is carried by channels that allow passage of monovalent cations and the kinetics of this time and voltage-dependent pathway are sufficiently slow that it could play a role similar to that proposed for the "leak" or background conductance pathway. Under physiological conditions this pathway allows passage of both sodium and potassium ions, with a reversal potential for the current of approximately −20 mV. The single channel conductance of the I(st) pathway has been reported to be 13 pS, and to have an open probability that is regulated by protein kinase A (PKA). In rabbit SAN this pathway gives rise to an approximately 50 pA current at −50 mV in an isolated SAN myocyte (Mitsuiye et al., 1999).

The I(f) current activated by hyperpolarization will be discussed in more detail later, but it is worth mentioning that its kinetics are also slow at potentials close to −60 mV and it could feasibly contribute to conductance over many seconds as well

as playing a role in "pacemaker depolarization" during a single cardiac cycle. In this context, Verkerk and Wilders have argued that de-activation of I(f) near the overshoot of the action potential, though fast, is not instantaneous, and significant I(f) can be present in their models at the start of diastolic depolarization, persisting from activation of this pathway during preceding action potentials (Verkerk and Wilders, 2013). In addition, Proenza et al. (2002) suggested that an "instantaneous" current (that could contribute to steady current) might flow via HCN2 channels.

Store Operated Ca^{2+} Channels (STOCCs) could influence heart rate through the generation of a background current that is modulated through beat to beat SR Ca^{2+} content changes (Ju and Allen, 2007) and (Liu et al., 2015). Roles have also been suggested for TRPM4 (Hof et al., 2013) and TRPM7 (Sah et al., 2013).

Other channels that might contribute include BK channels (Lai et al., 2014), SK channels (Chen et al., 2013) and Ca^{2+} activated Cl channels (Verkerk et al., 2002).

The Roles of NCX

NCX During the Later Stages of the Pacemaker Depolarization, Perhaps Associated with Ca^{2+} Sparks/LCRs

There are at least three possible ways in which electrogenic NCX could contribute to pacemaker activity (**Figure 2**). The most discussed mechanism, often given so much prominence that other possibilities could be overlooked, is the suggestion that there are there are spontaneous events resulting from Ca^{2+} release from the SR [sometimes referred to as Ca^{2+} "sparks" (Huser et al., 2000) or local Ca^{2+} release events (LCRs) (Bogdanov et al., 2001; Vinogradova et al., 2005)] and that the accompanying rises in subsarcolemmal Ca^{2+} cause local depolarizations arising from Ca^{2+} extrusion by electrogenic NCX. These sparks/LCRs can occur in the later stages of the pacemaker depolarization preceding the upstroke of the action potential (Huser et al., 2000; Bogdanov et al., 2001; Vinogradova et al., 2002a, 2005). Although it seems very likely that this is an important component of electrogenic NCX, evidence supports other possibilities listed below that might be equally or under some conditions more important.

NCX Associated with the Upstroke of the Action Potential

In addition to the spontaneous Ca^{2+} release events toward the end of the pacemaker depolarization, there will be the rise in cytosolic Ca^{2+} that is the result of Ca^{2+} entry through Ca^{2+}channels during the upstroke of the action potential, and the consequent Ca^{2+}-induced Ca^{2+} release (CICR) from the SR. CICR occurs as a global release event (meaning a release that occurs synchronously across all of the SR) arising from ryanodine receptor Ca^{2+} release channels. The global, substantial rise in subsarcolemmal Ca^{2+} accompanying CICR during the upstroke of the action potential will nevertheless be accompanied by a major component of Ca^{2+} extrusion through electrogenic NCX (**Figure 2**). Even when SR function is suppressed, the substantial influx of Ca^{2+} through L-type channels during the upstroke of the action potential will be accompanied by extrusion of Ca^{2+} and at least some electrogenic extrusion could be fast enough to re-inforce this action potential upstroke. Note that ryanodine has been reported to reduce the maximum rate of rise of the pacemaker action potential, consistent with a contribution of NCX associated with CICR in addition to the charge carried by L-type Ca^{2+} channels (Rigg and Terrar, 1996; Rigg et al., 2000), although other Ca^{2+} dependent mechanisms such as effects of CaMKII on L-type channels could also contribute to this.

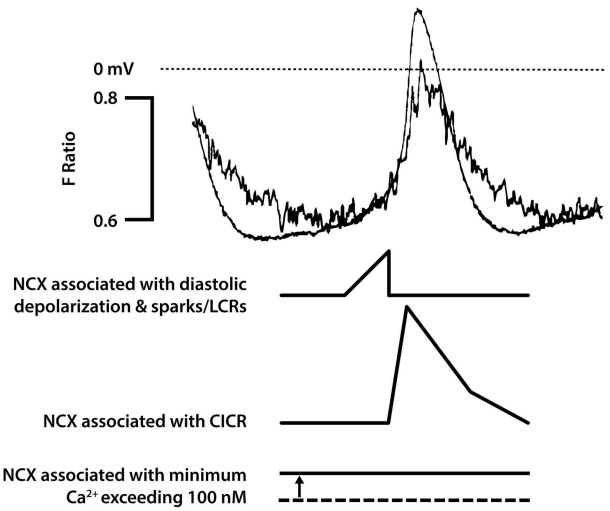

FIGURE 2 | This figure seeks to show in cartoon form the various contributions of NCX to pacemaker activity [that are not confined just to rises in subsarcolemmal Ca^{2+} associated with spontaneous Ca^{2+} release from the SR described as Ca^{2+} sparks or local calcium release events (LCRs)]. The magnitude of the NCX currents will broadly follow the magnitude of the Ca^{2+} transient (though if there are sufficient changes in subsarcolemmal Ca^{2+} and Na^{+}, these changes will influence the equilibrium potentials for these ions and therefore the driving force for NCX). The time course of the Ca^{2+} transient as reported by the Ca^{2+} probe indo-1 (fluorescence ratio with emission at 405 and 485 nm) is shown overlaid with an action potential in a pacemaker cell in the upper pair of traces. It is recognized that the indo-1 fluorescence ratio (noisy trace) will show a lag as a consequence of the kinetics of Ca^{2+} binding to the probe, and there may be a delay in the decline in Ca^{2+} as a consequence of slow dissociation of Ca^{2+} from the probe (although this delay seems not to be severely limiting since isoprenaline was able to speed the Ca^{2+} signals recorded with this probe, see **Figure 5**). There is a rise in Ca^{2+} that precedes the rapid upstroke of the action potential, and under conditions in which spontaneous Ca^{2+} sparks/LCRs occur these events will contribute to the early phase of NCX. This is followed by CICR triggered by Ca^{2+} entry largely through I_{CaL}, and the accompanying large rise in subsarcolemmal Ca^{2+} will be associated with a substantial additional component of NCX. It is thought that the cytosolic and subsarcolemmal Ca^{2+} concentrations remain greater than 100 nM even at the most negative membrane potential between action potentials and this is associated with the third component of NCX represented in the bottom trace, with a dotted line to represent zero NCX current that would be expected to occur at approximately 100 nM Ca^{2+}. Although the components of NCX are shown as separate in this diagrammatic representation to emphasize the many roles of NCX, it is recognized that in reality these components run together as a continuum and cannot easily be dissected experimentally. In addition to these three components of electrogenic NCX with a 3 Ca^{2+}:1 Na^{+} stoichiometry, there may be an additional "leakage" component (see text). The experimental traces are from Rigg et al. (2000).

NCX during Diastole, Including at the Most Negative Potential

The third aspect of possible contribution of NCX to pacemaker activity is a consequence of slower changes in Ca^{2+} concentration. It is clear that the level of Ca^{2+} activity in SAN cells between beats does not typically fall to the ∼100 nM that is measured in quiescent ventricular or atrial myocytes (e.g., Cannell et al., 1987; Schaub et al., 2006), and has been reported as 225 nM (Sanders et al., 2006). If the level of Ca^{2+} concentration between beats were approximately 200 nM, there would be continuous extrusion of Ca^{2+} even during the intervals between beats. Ca^{2+} balance must be maintained in the steady state, but this does not necessitate discrete entry and extrusion phases. Net Ca^{2+} entry is clearly exhibited during the later stages of pacemaker depolarisation and upstroke of the action potential but Sanders et al suggest that the balancing role of Ca^{2+} extrusion (mainly through NCX) occurs throughout the cycle including the most negative potential between beats. Thus, there could be a maintained depolarizing influence of NCX (**Figure 2**).

The three aspects of electrogenic 3:1 NCX have been discussed as separate entities above, in order to emphasize their contributions in different parts of the pacemaker cycle, but it is recognized that in reality they represent a continuum of activity that overlap and cannot be easily distinguished. The clear point is that electrogenic 3:1 NCX can play a role throughout the cardiac cycle and will be dependent on the subsarcolemmal Ca^{2+} concentration under the control of both local and global events.

The average current through the combined contribution of these three components of NCX is substantial since NCX is thought to be the major method of Ca^{2+} extrusion. Every Ca^{2+} ion that enters the cell via a Ca^{2+} channel (L-type or T-type) adds two charges to the cell interior, while extrusion of each Ca^{2+} by NCX adds one charge (with three sodium ions entering in exchange for each divalent Ca^{2+}), and it therefore follows that if the major component of Ca^{2+} extrusion is via NCX then the average depolarizing current through NCX in the steady state throughout the cardiac cycle must be approximately half that through the total Ca^{2+} entry mechanisms.

NCX Acting as a Possible Sodium Leak Pathway

A fourth mechanism by which NCX could contribute to pacemaker activity is the leak pathway proposed by Kang and Hilgemann (2004) that was briefly mentioned above in the context of "background current." The Kang and Hilgemann model was based on extensive experimental evidence using conventional voltage-clamp methods to measure current and voltage across "macro" patches combined with the use of ion sensitive electrodes to give information concerning the sodium and Ca^{2+} gradients close to these membranes. The comprehensive experimental data collected in this way led to the conclusion that the stoichiometry of NCX was 3.2 sodium ions to 1 Ca^{2+}, rather than exactly 3:1. The explanation of a 3.2:1 stoichiometry was that there were additional "modes" of NCX. In particular, a mode with slower kinetics that allowed a single external Ca^{2+} together with a single external sodium ion to be exchanged for a single internal Ca^{2+}, resulting in electrogenic sodium ion leak without net flux of Ca^{2+}, was suggested as a possible contributor to "background current" in pacemaker cells.

The sodium "leak" mode of NCX proposed by Kang and Hilgemann requires the presence of Ca^{2+} on both sides of the membrane, but since there is no net movement of Ca^{2+} this mode is not dependent on the driving force for Ca^{2+} entry into the cell. It seems likely, however, that such a pathway could not operate if the cytosolic Ca^{2+} were too low to occupy the internal site on the NCX protein.

Other Aspects of the Contribution of NCX for Pacemaking

The discussion above focuses on the importance of NCX as a direct contributor to membrane currents. However, in addition to its direct effects as a charge carrier, NCX may have additional functionally important roles in the context of pacemaker mechanisms. In particular these roles include influencing the overall Ca^{2+} balance of the cell (including Ca^{2+} content of the SR), and controlling Ca^{2+} concentrations in cytosolic microdomains within the cell that might influence the behavior/sensitivity of intracellular release channels such as ryanodine receptors (or perhaps IP_3 receptors see Ju et al., 2011) or Ca^{2+}-dependent proteins (see below). Relevant to the present discussion is the thoughtful review by Ottolia et al. (2013) on the importance of NCX in ventricular myocytes. One aspect concerns the balance between NCX and SERCA in determining the amount of Ca^{2+} loaded into the SR which in turn will have an influence on oscillatory Ca^{2+} mechanisms and therefore on Ca^{2+}-dependent currents (whether global or local). Although the interplay between NCX and degree of Ca^{2+} loading of the SR has not yet been studied in detail in pacemaker cells, it seems very likely that the mechanisms that operate in ventricular myocytes will have a close parallel in cardiac pacemaker tissue.

A final point that is relevant here is that NCX might be regulated by protein kinases and these could include Ca^{2+}-sensitive enzymes (Zhang and Hancox, 2009) as discussed below.

Is NCX Essential for Pacemaking?

It is difficult to determine the various contributions of NCX to pacemaker activity by experimental study. There are two problems concerning the use of drugs. The first is selectivity, but even if a drug were available with perfect selectivity for NCX over other cellular targets, the importance of NCX as the major mechanism for Ca^{2+} extrusion under normal conditions means that blockade of NCX would lead to rises in intracellular Ca^{2+} concentrations that would have extensive secondary effects. As discussed below, cytosolic Ca^{2+} influences so many ion channels and other aspects of cell function it is difficult to separate primary and secondary effects of NCX suppression. An "ideal" experiment would require instantaneous blockade of NCX so that effects can be observed before substantial secondary effects have time to occur.

Rapid block of NCX can be achieved by reduction of the extracellular solution by replacing some or all of the Na^+ with Li^+ (which can pass through most of the ion channels that are permeated by sodium ions but which do not substitute for sodium in NCX). Switch to low sodium does suppress the initiation of spontaneous action potentials, but this suppression can take

many beats to establish in toad sinus venosus (Ju and Allen, 1998) and rabbit SA node cells (Bogdanov et al., 2001) when the speed of solution change is modest. When Bogdanov et al caused a rapid but transient solution exchange lasting less than 1 s using a "picospritzer," they showed that replacement of Na^+ with Li^+ could suppress a single action potential (while leaving a slightly depressed Ca^{2+} transient with approximately the same timing as the missing action potential). Sanders et al. (2006) used a rapid switch system that could exchange the solution flowing over individual pacemaker cells in less than 1 s and maintain the flow of this solution. Using this system in guinea-pig SA node cells, rapid switch to low sodium caused immediate cessation of spontaneous activity (both of action potentials and spontaneous Ca^{2+} transients), and this cessation was maintained for the full several seconds of exposure. During this time cytosolic Ca^{2+} as measured by the fluorescent probe fluo-5F fell rather than rose (presumably as a consequence of Ca^{2+} uptake by the SR; see Figure 2 in Sanders et al., 2006).

A possible criticism of sodium replacement experiments is that if the reduction in sodium is very large (e.g., to 14.5 mM or approximately 10%) there may be outward currents through NCX that could complicate interpretation. However, immediate cessation of activity was also seen with smaller reductions of extracellular sodium to 50 mM and even 75 mM (Sanders et al., 2006).

Cessation of SAN myocyte AP firing by low-sodium switch is demonstrably not solely due to suppression of LCR-mediated depolarisation events. Inhibition of Ca^{2+} uptake into the SR using cyclopiazonic acid (CPA), which would be expected after prolonged exposure to abolish SR Ca^{2+} loading, slowed but did not abolish pacemaker activity, and switch to low sodium under these conditions again caused immediate cessation (Sanders et al., 2006). This observation demonstrates the fundamental importance of NCX under these conditions even though the SR is not functional.

Another experimental point arising from the rapid switch experiments is that immediately after the switch back from low sodium to normal sodium the spontaneous rate was restored, but was transiently greater than that observed under control conditions (see Figure 1 in Sanders et al., 2006). This would be consistent with an influence of increased intracellular Ca^{2+} (perhaps an increase in the SR Ca^{2+} load) during the period of exposure to low sodium. In the absence of CPA, when the SR was functional, Sanders et al consistently observed a reduction in cytosolic Ca^{2+} when beating was stopped by the switch to low sodium even though the major mechanism for Ca^{2+} extrusion was inhibited, and this was thought to be accompanied by SR Ca^{2+} uptake (see later).

The observed effects of several drugs that block NCX in causing cessation of pacemaker activity are also consistent with the view that this pathway exerts a profound influence and is probably essential for pacemaking under most conditions (e.g., rapid switch to 5 μM KB-R7943 caused cessation of beating in approximately 20 s, perhaps as a consequence of the time taken to block NCX Sanders et al., 2006), but these observations must be treated with caution because of off target effects of the compounds.

The importance of NCX for pacemaking has also been investigated using genetic approaches to suppress expression of NCX proteins. A knockout of NCX does not survive because it is lethal at the embryonic stage (Cho et al., 2000; Koushik et al., 2001; Reuter et al., 2002). Conditional knockouts in which NCX is selectively suppressed in atrial or SA node tissue have been made. As is the case of drugs, the difficulty of separating direct and indirect effects of NCX suppression applies, and there are compensatory changes that may occur. One recent paper concludes that genetic inhibition (not complete abolition) of NCX1 disables the ability of the SA node to show its normal increase in rate as a "fight or flight" response, but that resting heart rate continues unchanged (Gao et al., 2013). Herrmann et al. (2013) used an inducible SA-node specific Cre transgene to create mice lacking NCX1 in the pacemaker region and showed that ablation of NCX1 was accompanied by a progressive slowing of heart rate and severe arrhythmias. Another recent paper concludes that complete atrial-specific knockout of NCX1 eliminates SA node pacemaker activity (Groenke et al., 2013). In this case the mice were able to survive with the AV node taking over the normal pacemaker function, while the atria appeared to be quiescent. Further, SAN myoyctes isolated when NCX was eliminated also failed to show pacemaker activity.

Taken together the observations above using low sodium, drugs and genetic approaches are consistent with the view that NCX is very important and probably essential for pacemaker mechanisms in the SA node.

The Funny Current I(f)

Is the I(f) Current Essential for Pacemaking?

The "funny" current, I(f) was first described by DiFrancesco and reviewed in DiFrancesco (2010). Similar currents [normally designated I(h)] have been described in neurons showing bursting activity (He et al., 2014). The ion channels carrying the current (HCN channels) are activated by hyperpolarization and the magnitude of the currents in the physiological range is increased when the cyclic nucleotide, cAMP, is bound to the channels [since the activation kinetics are quickened (Wainger et al., 2001) and the activation curve is shifted to less negative potentials, (DiFrancesco and Mangoni, 1994)]. Of the four HCN subtypes, HCN4 is the predominant form in the pacemaker region of the heart, though HCN1 and HCN2 also contribute, and there are species differences between the balance of contributions from different subtypes (Baruscotti and Difrancesco, 2004; Biel et al., 2009; DiFrancesco, 2010).

To answer the question whether or not I(f) is essential for pacemaking, it would be helpful either to block the current pharmacologically, or use the techniques of molecular biology to knock down expression of the channel.

In the case of pharmacological approaches there are a variety of drugs including ZD7288, zetabradine and ivabradine (Baruscotti et al., 2005). Cesium ions have also been used to block the currents (Denyer and Brown, 1990). In all cases the drugs slow but do not completely stop pacemaking. In an early study on SAN myocytes isolated from rabbit SA node 2 mM Cs^+ was observed to cause close to complete blockade of I(f) without

effects on voltage-gated Ca^{2+} and potassium currents. This concentration reduced pacemaker rate by about 30% but did not stop the initiation of action potentials (Denyer and Brown, 1990). The authors concluded that I(f) is not essential, and that there must be an additional "background" current during the pacemaker depolarization (see above discussion). The more recent drugs ZD7288 and ivabradine also slow but do not stop pacemaker activity (BoSmith et al., 1993; Baruscotti et al., 2005). It is, however, difficult to exclude the argument that blockade of I(f) by the drugs is incomplete under the conditions of these experiments, and that only a very small residual current would be necessary for pacemaking. The use of greater concentrations would not be persuasive because of possible non-specific effects such as blockade of L-type Ca^{2+} channels or voltage-gated potassium channels, either or both of which can cause cessation of pacemaker activity.

There has been discussion in the past about whether the I(f) current is sufficiently large to make an important contribution to pacemaking, particularly in the context of conventional experiments in which the cell is held at a constant negative potential (commonly −40 mV) and hyperpolarizing voltage steps are applied. Although large currents are recorded when the cell is hyperpolarized to potentials that are not often experienced in normal physiology (such as −80 or −100 mV), the currents recorded at potentials less negative than −70 mV are small. Convincing evidence for a role of I(f) under conditions that approximate those of normal pacemaker activity is provided by "action potential clamp" experiments (Zaza et al., 1997). The essence of this approach is to record and store the action potential waveform from a single myocyte, and then re-apply this waveform under voltage-clamp conditions. In a single cell the net current under control conditions is zero (since ionic currents charge and discharge the membrane capacitance), but interesting information is provided when blockers are applied to reveal a "difference current" that reflects the particular current pathways that are suppressed by the blocker. Zaza et al. used 2 mM Cs^{+} to block I(f), and concluded that I(f) currents played an important role during the pacemaker depolarization, and that these currents were larger than would have been predicted by conventional voltage-clamp experiments applying only hyperpolarizing pulses, but that other inward currents besides I(f) contribute during this phase.

In the case of genetic experiments, several studies show that suppression of expression of HCN4 proteins also causes a slowing without cessation of activity in the SAN. The most recent uses a conditional knockout system in which HCN4 expression is suppressed only in cardiac tissue of the mouse (Mesirca et al., 2014a). The reduction in spontaneous rate of beating in the SAN reached plateau of about 50% as the I(f) was progressively reduced to very low levels. Interestingly, while the rate reduction in the SAN was reduced by ∼50%, there was a cessation of activity in the AV node leading to heart block and death. The apparently greater sensitivity of AV conduction to I(f) suppression seems surprising, but is consistent with the effect of the I(f) blocker ZD7288, which also stops murine AV function at a concentration of 3 μM while reducing spontaneous activity in the SAN by ∼50% (Yuill and Hancox, 2002).

In summary, both genetic studies to reduce expression of HCN channels and the effects of selective blockers of I(f) in the mouse show similar effects in that as the severity of action increases to a maximal level the effect on spontaneous rate in the SAN appears to plateau at about a 50% reduction in rate.

There may be other functions of I(f) current in the SAN than determining rate. HCN1 and HCN2 proteins are also present in SAN, and show different kinetics of activation and de-activation compared to HCN4 (Wahl-Schott et al., 2014). Recently knockdown of HCN1 proteins has been shown to influence the stability of pacemaking (and the pacemaker region, Fenske et al., 2013) but not to be essential for pacemaker activity.

Are I(f) Currents Influenced by Cytosolic Ca^{2+}?

Observations from Hagiwara and Irisawa (1989) provide very convincing evidence that that the magnitude of I(f) is influenced by cytosolic Ca^{2+}. These authors found that buffering Ca^{2+} at 10^{-10} M caused a substantial (approximately 75%) decrease in current amplitudes, while under the conditions of their experiments 10^{-7} M caused an increase. In experiments in which the cytosol was perfused with different concentrations of Ca^{2+}, it appeared that a log(concentration)-response curve could be established showing increases in the amplitude of I(f) over the range of Ca^{2+} concentrations 10^{-10}–10^{-6} M with the steepest part of the curve covering the range 10^{-8}–10^{-7} M. Although the authors concluded that there was a direct effect of Ca^{2+} on I(f) since the effects of Ca^{2+} were not abolished by the calmodulin inhibitor calmidazolium, it seems likely that the concentration of this compound (10^{-6} M) was not sufficient to cause effective inhibition. This view is supported by the observations of Zaza et al. (1991) who demonstrated that there were no direct effects of Ca^{2+} on I(f) in experiments on inside out patches. Rigg et al. (2003) provided evidence that I(f) is regulated by a Ca^{2+}-calmodulin pathway that could at least in part result from a Ca^{2+}-calmodulin regulation of adenylyl cyclase, and this possibility is discussed in more detail below.

Are T-Type Ca^{2+} Channels Essential for Pacemaking?

The importance of T-type Ca^{2+} channels for cardiac pacemaker activity has recently been reviewed by Mesirca et al. (2014b). The first evidence for a role for T-type Ca^{2+} channels during pacemaking activity in the SA node was provided by drugs with moderate selectivity, and it was concluded that blockade of these channels caused a slowing but not cessation of rate (Hagiwara et al., 1998). Huser et al. (2000) emphasized a role for T-type channels in triggering Ca^{2+} sparks, though others report that Ca^{2+} sparks can occur without involvement of these channels (Vinogradova et al., 2002a). Genetic studies, particularly concerning $Ca_V3.1$ which is the dominant form of T-type Ca^{2+} channel in the adult SA node, show that suppression of this protein causes only modest reduction in heart rate (Mangoni et al., 2006b). It appears from these observations that T-type Ca^{2+} channels can contribute to pacemaker depolarization but make only a modest contribution to pacemaker rate under most conditions.

Ca^{2+} Release from Intracellular Stores

Are Ca^{2+} sparks/LCRs Necessary for Pacemaking?

Huser et al. (2000) first suggested a pacemaker role for Ca^{2+} sparks and associated NCX currents during the later stage of the pacemaker depolarization that precedes the upstroke of the action potential in both subsidiary pacemaker and normal pacemaker myocytes from the cat. Extensive work from the Lakatta laboratory on rabbit SA node cells also shows LCRs as key players in pacemaking (Vinogradova et al., 2002a,b, 2004, 2005, 2006, 2008, 2010; Vinogradova and Lakatta, 2009). Although we have consistently argued for a role of SR Ca^{2+} release in pacemaking (Rigg and Terrar, 1996; Rigg et al., 2000), and this could include an important role for Ca^{2+} sparks/LCRs, it is interesting to note that in our experiments on Ca^{2+} signals in guinea-pig SAN myocytes using both linescan and Nipkow disk techniques (Rakovic et al., 2001; Jackson et al., 2002) we frequently observe cells with apparently normal spontaneous activity that appear to lack detectable Ca^{2+} sparks/LCRs (although the fraction of cells showing this behavior must be regarded as unpublished observations). In addition, it is observed that under most conditions ryanodine slows but does not stop pacemaker activity and as expected this also suppresses LCRs (Vinogradova et al., 2002a). CPA also abolishes LCRs but does not normally cause cessation of pacemaker activity. It therefore appears that Ca^{2+} sparks/LCRs are not essential for pacemaker activity, though when they occur the associated electrogenic Ca^{2+} extrusion via NCX can contribute to the later stages of diastolic depolarization.

Are synchronized Spontaneous Ca^{2+} Releases Associated with a Ca^{2+} clock Essential for Pacemaking?

A Ca^{2+} clock mechanism allows for the possibility that there can be generalized Ca^{2+} releases from the SR alternating with periods of Ca^{2+} uptake. Although such a mechanism is normally discussed in the context of LCRs, it is not a requirement for a Ca^{2+} clock mechanisms to have separate local Ca^{2+} events since the release of Ca^{2+} from the SR could be synchronized over all or a large part of the cell when the Ca^{2+} within the SR reaches a critical concentration (leading to a "global" Ca^{2+} release event similar to the CICR described above but arising from events/conditions within the SR). Note that when membrane potential is clamped at a fixed level close to the most negative potential following a period of normal spontaneous beating it is observed that Ca^{2+} transients can occur with a timing and frequency which is close to the frequency and timing that would have been adopted by spontaneous action potentials if firing had not been interrupted (Vinogradova et al., 2004). The spatial dimensions of these spontaneous releases are frequently much greater than those of LCRs, and it seems possible that these large events arise spontaneously as a consequence of properties of the Ca^{2+} release mechanism in the SR. The timing will depend on the kinetics of Ca^{2+} uptake by SERCA and the time it takes for the Ca^{2+} concentration within the SR to reach a critical level for synchronous Ca^{2+} release. The suggestion of the requirement to reach a critical level of Ca^{2+} within the SR is one way in which such a Ca^{2+} clock could operate, though other timing mechanisms are possible for example arising from the time constants of activation/de-activation of critical proteins in the uptake-release sequence controlling Ca^{2+} handling by the SR. The "global" Ca^{2+} clock (whether arising from the time for Ca^{2+} to reach a critical level or from other kinetic properties of the uptake/release process) could provide a driving mechanism for pacemaker activity, but may not be essential for pacemaker activity. The observation that spontaneous pacemaker activity in the form of action potentials is slowed but not stopped (Rigg and Terrar, 1996; Rigg et al., 2000; Bogdanov et al., 2006) when SR function is suppressed with ryanodine and/or CPA shows that synchronized spontaneous Ca^{2+} release from the Ca^{2+} clock is not always essential for pacemaker activity.

Although under most conditions, ryanodine does not stop spontaneous activity, we have sometimes observed cessation when we have used Ca^{2+} probes with high Ca^{2+} affinity, such as indo-1 (perhaps associated with the additional Ca^{2+} buffering properties of such probes, Rigg et al., 2000). Figure 6 from Rigg et al. is reproduced here showing the progressive development of the effect of ryanodine with a high concentration of isoprenaline present (**Figure 3**). After 4 min exposure to ryanodine, there is oscillating electrical activity that is so small that it must be subthreshold for the normal action potential mechanism but which nevertheless shows a repeating activity with the same period as the underlying Ca^{2+} signal (and is slightly slowed compared with spontaneous action potentials recorded in the same cell). The observed oscillations recorded during the development of the effect are best explained by a Ca^{2+} clock that is driving electrical activity presumably through NCX.

There is a very impressive body of evidence showing that the timing of the Ca^{2+} clock (as judged from the frequency of spontaneous Ca^{2+} events when the membrane potential is held at a constant membrane potential) is correlated with the timing of the action potentials on the surface membrane recorded when spontaneous electrical activity is allowed to occur (Vinogradova et al., 2002a,b, 2004, 2005, 2006, 2008, 2010; Bogdanov et al., 2006; Vinogradova and Lakatta, 2009). This has been examined over a broad range of frequencies when the rate is either increased by adrenoceptor agonists or decreased with muscarinic agonists, and the correlation between membrane and Ca^{2+} oscillations remains very strong throughout the range of frequencies studied. There is a parallel correlation between timing of the Ca^{2+} clock and the degree of phosphorylation and dephosphorylation of functionally important proteins such as L-type Ca^{2+} channels and phospholamban (Vinogradova et al., 2006). Although the correlation between the timing of the Ca^{2+} clock and the frequency of spontaneous action potentials is impressive, this does not establish that the relationship is always causal.

It could be argued that the timing of release and uptake of Ca^{2+} by the SR needs to keep pace with events in the surface membrane in order for a pacemaker mechanism driven primarily by the surface membrane to be maintained in an efficient way, without any disturbance that might otherwise arise from competition with these SR-dependent mechanisms. In other words, the primary mechanism driving the timing of the SA node pacemaker

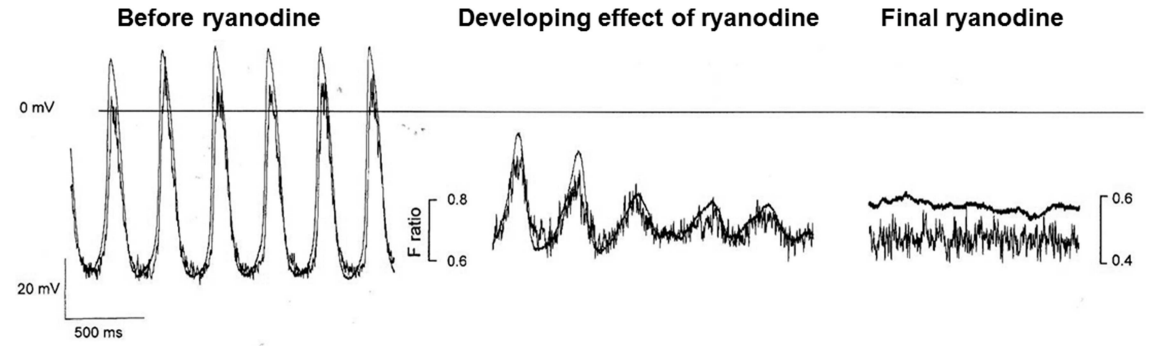

FIGURE 3 | This figure shows the effect of ryanodine in a pacemaker cell in the presence of the calcium probe indo-1 and isoprenaline. Although in our experience, ryanodine slows but does not normally stop spontaneous activity, we have observed cessation of activity after ryanodine when calcium probes are present, particularly those with a high Ca^{2+} affinity, and we have attributed this to the additional Ca^{2+} buffering effects of the probe (see text). Despite these limitations, the trace is instructive in that before cessation of activity (which occurs at a potential close to that shown in **Figure 1A** and described in the text as the zero current level for "background" conductance, see pair of traces on right) subthreshold oscillations occur (middle pair of traces) with a period that is not substantially different from full action potentials at an earlier stage of ryanodine effect. These membrane potential fluctuations are mirrored by corresponding fluctuations in the Ca^{2+} fluorescence signal. The experimental traces are from Rigg et al. (2000).

could still depend on the kinetics of activation and deactivation of membrane proteins making up the membrane clock. However, a coupled clock mechanism (Imtiaz et al., 2006, 2007, 2010; Yaniv et al., 2011, 2013; Imtiaz, 2012; Maltsev et al., 2013, 2014) in which both membrane and Ca^{2+} clocks exert mutually interdependent influences also seems plausible, and perhaps more likely under many circumstances because the system will function most efficiently when the surface membrane and "Ca^{2+} clock" mechanisms are not competing against one another. The two clocks would normally be synchronized, and this may be the optimal configuration. When the Ca^{2+} clock does play a role, there are a variety of ways that cytosolic Ca^{2+} will influence the periodicity of the clock, including influencing the rate of uptake of Ca^{2+} by SERCA and in turn the time taken to reach a critical level within the SR. Other longer term mechanisms for Ca^{2+} to influence the clock by actions on Ca^{2+}-dependent enzymes are considered below. However, it is clear from the discussion above, and particularly from the observation that pacemaker activity can occur without a functional SR, that the Ca^{2+} clock is not essential for spontaneous pacemaker activity supported by a membrane clock.

Do Abnormalities in Ca^{2+} Handling by the SR Influence Pacemaker Rate?

If the Ca^{2+} handling properties of the SR can provide an important timing mechanism that under some conditions drives the generation of action potentials in the SA node, it might be speculated that defects in the function of the SR could lead to rhythm abnormalities.

An abnormality concerning ryanodine receptor Ca^{2+} release channels in the SR membrane supports such a possibility (Neco et al., 2012). This was studied in mice carrying the catecholaminergic polymorphic ventricular tachycardia–linked mutation of ryanodine receptor ($RyR2^{R4496C}$). The SAN region was studied using confocal microscopy and the Ca^{2+} probe fluo-4 at room temperature. The SAN from $RyR2^{R4496C}$ mice showed slowed pacemaker activity and reduced response to catecholamines as compared to myocytes from WT. There were also frequent pauses in the generation of spontaneous action potentials, while the overall frequency of Ca^{2+} sparks/LCRs was increased. Experiments were also carried in SAN preparations loaded with rhod-2 to measure Ca^{2+} and di-4-ANEPPS to measure membrane potential. Pauses interspersed with trains of spontaneous events were observed for both the Ca^{2+} and voltage signals. The pauses were associated with unusually high cytosolic Ca^{2+} concentrations, and it was suggested that the pauses may have resulted from inactivation of the L-type Ca^{2+} channels.

A recent paper from the Federov laboratory (Glukhov et al., 2015) also shows that pacemaker activity is altered when Ca^{2+} handling is modified in mice lacking the SR protein calsequestrin ($Casq2^{-/-}$). These mice showed bradycardia and beat to beat heart rate variability. SAN myocytes isolated from $Casq2^{-/-}$ mice showed an unstable rate with frequent pauses between "trains" of action potentials and the abnormal behavior was associated with abnormal Ca^{2+} release from the SR. In particular the pauses were accompanied by elevated levels of diastolic Ca^{2+} concentration (Glukhov et al., 2015). The effects of calsequestrin lack are complex reflecting the central role of calsequestrin not just as a Ca^{2+} buffer, but as a protein that together with junction and triadin, appears to regulate Ca^{2+} release via ryanodine receptor releases channels in the SR membrane. The responses to isoprenaline were also abnormal for both the chronotropic effect in whole animals and for the change in rate in isolated SAN myocytes. The authors proposed that "the observed pauses in between rhythmic Ca^{2+} transients in $Casq2^{-/-}$ SAN cells are caused by excessive diastolic SR Ca^{2+} release in turn resulting in (i) inhibition of the SAN upstroke I_{CaL} current from partially inactivated L-type Ca^{2+} channels, and/or (ii) decrease in the SR Ca^{2+} content below a threshold level required for the generation of spontaneous SR Ca^{2+} releases."

Another important point in this context is a possible parallel between a Ca^{2+} clock in pacemaker tissue and ventricular arrhythmias in which Ca^{2+} release from the SR is proposed

to occur when the Ca^{2+} concentration within the SR reaches a specific level detected by a "calcium sensing gate" of the ryanodine receptor (RyR2). This "store overload-induced Ca^{2+} release" (SOICR) is modified in ventricular myocytes when a point mutation is introduced in the proposed calcium sensing gate (Chen et al., 2014) [and see (Sitsapesan and Williams, 1994, 1997) for evidence concerning the regulation of RyR2 gating by SR luminal Ca^{2+}]. Carvedilol and a structural analog which lacks ability to block β-adrenoceptors both block SOICR (Zhou et al., 2011; Maruyama et al., 2013). The possible similarity between a pacemaker Ca^{2+} clock and SOICR has received support from another paper involving the same authors in experiments showing that the carvedilol analog and ryanodine both reduced spontaneous rate and also reduced the positive chronotropic effect of isoprenaline (Shinohara et al., 2014).

Taken together, the observations above show very clearly that pacemaker activity is disrupted when Ca^{2+} handling by the SR is abnormal and demonstrate that at least under some conditions the SR can play a central role.

Ca^{2+}-dependent Enzymes

Most of the pacemaker mechanisms described above play a role over times of seconds or less. However, there are important effects of Ca^{2+} that may take much longer to take effect, including activation of a variety of Ca^{2+} dependent enzymes.

CaMKII

An important Ca^{2+}-dependent enzyme for which there is very convincing evidence concerning a role during pacemaking is CaMKII. Evidence using selective drugs supports an important role for CaMKII in maintaining and regulating pacemaker activity in the rabbit SA node (Vinogradova et al., 2000). It was emphasized that CaMKII has properties to function as a "frequency detector" and is therefore well suited to the regulation of pacemaker activity. The CaMKII inhibitor KN93 (but not the inactive analog KN92) substantially slowed or even stopped pacemaker activity. Similar observations were made using the peptide inhibitor AIP. The protein targets for CaMKII activated by Ca^{2+} were shown to include L-type Ca^{2+} channels. Phospholamban regulating the uptake of Ca^{2+} into the SR is another important target. Observations concerning the effects of KN93, KN92, and autocamtide inhibitor peptide (AIP) on spontaneous action potentials in guinea pig SAN myocytes (Xie et al., 2015) were broadly similar to those in the rabbit.

Genetic approaches also provide evidence for the influence of CaMKII on pacemaking at least under stress conditions. One interesting approach is to overexpress an inhibitor peptide for CaMKII (Vinogradova et al., 2000; Chen et al., 2009; Wu et al., 2009; Gao et al., 2011). A "control" is also provided by overexpression of a modified inhibitor protein that lacks ability to suppress CaMKII. In these experiments overexpression of the peptide inhibitor for CaMKII in mouse had little or no effect on resting heart rate (for experiments *in vivo*, in isolated Langendorff perfused hearts and in isolated SA node myocytes), but suppression of CaMKII activity by the peptide did cause a substantial reduction of the positive chronotropic response to isoprenaline. The responses that were reduced by inhibition of CaMKII included the amount of Ca^{2+} loaded in to the SR, the frequency of Ca^{2+} sparks/LCRs and the slope of the diastolic potential. However, interestingly the enhancement of L-type Ca^{2+} current amplitude by isoprenaline was maintained when CaMKII activity was suppressed by the inhibitor peptide. Another mouse model also showed little or no effect of CaMKII knockout on resting rate (Wu et al., 2009) but the positive chronotropic response to isoprenaline was again reduced (and indeed even a slowing of heart rate was seen in the CaMKII KO mice exposed to isoprenaline). These observations support a role for CaMKII in making a major contribution to the "fight or flight" mechanisms in which pacemaker activity is speeded up by adrenoceptor mediated cell signaling. It is clear that CaMKII is a Ca^{2+} stimulated enzyme that can influence pacemaker activity, even if the role of this enzyme under resting conditions remains to be fully established. The importance of CaMKII for pacemaker activity in the SA node has been recently reviewed (Wu and Anderson, 2014).

Adenylyl Cyclases including AC1 and AC8

There are important differences between ventricular myocytes and those in the atria and SA node in terms of the subtypes of adenylyl cyclases, and of the basal activity of these enzymes. In particular it has been shown that actions of ACh at rest in the atria are consistent with inhibition of ongoing basal activity of ACs, while in the ventricle inhibitory actions of ACh are readily detected when adenylyl cyclases are stimulated by aderenoceptor activation but not in the absence of this stimulation (Fischmeister and Hartzell, 1986; Hescheler et al., 1986; Fischmeister and Shrier, 1989; Petit-Jacques et al., 1993). One possibility in the context of the importance of Ca^{2+} for pacemaking mechanisms is the possibility that Ca^{2+}-sensitive adenylyl cyclases are preferentially expressed in the atria and SA node as compared with the ventricle. Evidence that I(f) is regulated by a Ca^{2+}-calmodulin dependent mechanism that is not CaMKII was presented by Rigg et al. (2003) who also speculated that Ca^{2+} regulated adenylyl cyclase could provide such a mechanism. Application of the Ca^{2+} chelator BAPTA reduced I(f) as did calmodulin inhibitors including W7. Although W7 is known to have non-specific effects (Chatelier et al., 2005), these seem unlikely to be solely responsible for the observations since effects of BAPTA on I(f) were no longer seen in the presence of W7. More direct evidence for the presence of Ca^{2+}-stimulated adenylyl cyclases was presented by Mattick et al. (2007). The Ca^{2+}-stimulated adenylyl cyclase AC1 was shown to be expressed in the SAN by RT-PCR methods to detect mRNA as well as by immunoblotting with a specific antibody. Confocal microscopy also showed staining with the specific antibody in SAN myocytes. In addition to AC1, another Ca^{2+}-stimulated adenylyl cyclase AC8, was detected by immunocytochemistry in the SAN myocytes. Functional evidence using BAPTA and selective inhibitors was also presented to show the importance of this pathway for regulating I(f) although it was also pointed out that such a pathway might well have additional effects via PKA and phosphorylation of additional protein targets. Younes et al. (2008) provided further evidence using RT-PCR for the presence of Ca^{2+}-stimulated AC1 and AC8, in addition to

AC types 2, 5, and 6 in SAN myocytes. These experiments also demonstrated the functional importance of the high basal activity of adenylyl cyclase in SA node myocytes for the regulation of a variety of proteins phosphorylated by PKA.

In addition, Kryukova et al. (2012) carried out experiments in which AC1 or AC6 were co-expressed with HCN2 in neonatal rat ventricular myocytes that lack normally AC1, and concluded from their observations that AC1 could play an important Ca^{2+}-dependent role in regulating HCN2.

The importance of the Ca^{2+} stimulated adenylyl cyclases (AC1 and/or AC8) for the regulation of L-type Ca^{2+} currents has recently been demonstrated in atrial myocytes, and the observations may have relevance to SAN function (Collins and Terrar, 2012). In these experiments on atrial myocytes it was observed that buffering of cytosolic Ca^{2+} with BAPTA reduced Ca^{2+} current amplitude, as did inhibition of Ca^{2+} release from the SR using ryanodine and thapsigargin. Interestingly, the effects of BAPTA were prevented by inclusion of cAMP in the patch pipette. The observations are therefore consistent with a role for Ca^{2+} (including those released from the SR) in stimulating adenylyl cyclases and regulating the magnitude of L-type Ca^{2+} currents. It is speculated that similar mechanisms may operate in the SA node.

A variety of other Ca^{2+} dependent enzymes have the potential to influence pacemaker activity but have not yet been studied in detail. These include phophodiesterases, phosphatases and P21-activated kinase (PAK) enzymes that regulate phosphatases (Ke et al., 2007; Chen et al., 2014; Wang et al., 2014). There may also be effects of Ca^{2+} on NO synthase(s) in SAN myocytes since evidence supports actions of NO donors on pacemaker function (e.g., Han et al., 1995; Yoo et al., 1998; Musialek et al., 2000).

Ca^{2+} Regulation of K^+ Channels

The importance of voltage-gated potassium channels, not only for repolarization of the action potential but also as a contributor to pacemaker depolarization as a consequence of time-dependent de-activation, was emphasized at the start of this review (and see Clark et al., 2004). Evidence that the contribution of potassium channels is subject to regulation by cytosolic Ca^{2+} was provided by Zaza et al. (1997) using the "action potential" clamp methods in rabbit SA node mentioned above in relation to I(f). Zaza et al. (1997) concluded that Ca^{2+} influx during the pacemaker cycle also increases a potassium conductance. This potassium conductance could arise from a single channel component or multiple components.

Xie et al. (2015) have recently presented evidence that the slow component of the delayed rectifier current (I_{Ks}) is regulated by a Ca^{2+}-dependent process thought to be CaMKII in guinea-pig SA node. This current was found to be decreased when the cytosolic Ca^{2+} concentration was reduced from 10^{-7} to 10^{-10} M (buffered by EGTA in a ruptured patch conditions). When the cytosolic Ca^{2+} concentration was maintained at 10^{-7} M, addition of calmodulin via the patch pipette increased the current. Inhibitors of CaMKII (autocamtide-2 inhibitor peptide and the less selective KN-93) substantially reduced the current, while in the presence of KN-93 there was no effect of calmodulin addition. Taken together these observations provide convincing evidence that I_{Ks} is modulated by cytosolic Ca^{2+} and that CaMKII plays an important role in this modulation.

Might other channel components be involved? The action potential clamp experiments of Zaza et al. mentioned above were carried out in rabbit SA node, and in this species the rapidly activating I_{Kr} is thought to provide the major voltage-gated potassium current pathway (Verheijck et al., 1995; Lei and Brown, 1996). Although under the conditions of the action potential clamp experiments, a Ca^{2+} dependence of I_{Kr} was not detected, applications of nifedipine to block Ca^{2+} entry may have been too brief (less than 10s in Figure 2 of Zaza et al., 1997 while the full effect of Ca^{2+} on an enzyme pathway might take a period of minutes to develop). More evidence against Ca^{2+} regulation of I_{Kr} is provided by Wu and Anderson (2014). However, it has been shown that I_{Kr} in guinea pig ventricular cells can be influenced by cytosolic Ca^{2+} (Heath and Terrar, 2000) in a complex pathway perhaps involving PKC that depends on Ca^{2+} entry via L-type Ca^{2+} channels leading changes in the amplitude and rectification/inactivation of the channel. It therefore seems premature to exclude an effect of Ca^{2+} on I_{Kr} in SA node at this stage.

An interesting additional point in the debate on Ca^{2+} regulation of potassium conductance in the SA node concerns the possible contribution of the Ca^{2+} activated potassium channel BK (Imlach et al., 2010; Lai et al., 2014) and SK (Chen et al., 2013).

Are there Effects of the SR that are Independent of the Ca^{2+} Clock Mechanism?

As was mentioned above, membrane and Ca^{2+} clocks might normally be synchronized, and consequently CICR could occur at (or very close to) a time when "global" spontaneous Ca^{2+} release would also have occurred. However, it is also possible that CICR can, and perhaps often does, occur without the accompaniment of spontaneous Ca^{2+} release. In this case Ca^{2+} released by CICR from the SR would be expected to drive a significant component of NCX that is independent of the Ca^{2+} clock.

Ca^{2+} released from the SR by CICR that is independent of the Ca^{2+} clock could also drive Ca^{2+}-dependent enzymes. These include CaMKII, AC1 and AC8 as described above. A role for SR-released Ca^{2+} (sensitive to ryanodine and thapsigargin) leading to increased L-type Ca^{2+} currents by a mechanism involving Ca^{2+}-stimulated adenylyl cyclases was recently demonstrated in atrial myocytes (Collins and Terrar, 2012), and it seems very likely that a similar mechanism operates to control pacemaker activity in SAN myocytes. Such a Ca^{2+}-induced stimulation of adenylyl cyclases that is at least partly dependent on Ca^{2+} released from the SR by CICR could also contribute to stimulation of I(f) (by elevation of cAMP) and other ion channels such as I(st) and voltage-gated potassium channels (regulated by PKA).

What are the Functions of L-type Ca^{2+} Channels Associated with SAN Action Potentials?

Voltage-gated L-type Ca^{2+} channels are a major component of the membrane oscillator providing explosive positive feedback

for the upstroke of the action potential which in turn initiates repolarization as a consequence of activation of voltage-gated K^+ channels. The positive feedback for activation of L-type Ca^{2+} channels underlies the fast upstroke and rapid spread of the action potential that synchronizes Ca^{2+} entry and CICR across the cell. The Ca^{2+} entry via L-type Ca^{2+} channels is a major determinant of the degree of Ca^{2+} loading of the SR. The action potential signal is essential for conduction of the pacemaker activity to neighboring myocytes. In addition, it appears that current through $Ca_V1.3$ channels can contribute to the late stage of diastolic depolarization (Zhang et al., 2002; Mangoni et al., 2003, 2006a; Christel et al., 2012). It is also important to note that Ca^{2+} ions entering the cell via L-type Ca^{2+} channels, at any stage during the cardiac cycle but particularly during the rapid upstroke, will drive NCX and cause the extensive secondary effects discussed elsewhere in this review, including enhancement of the activities of PKA and CaMKII (see later).

Application of Ca^{2+} Chelators to Reduce Cytosolic Ca^{2+} to 10 nM or Less

At the present time, it is probably only possible to investigate the effects of Ca^{2+} chelators in single cells, since in multicellular preparations it is difficult to be sure that uptake of Ca^{2+} chelator is complete. It is recognized that isolated myocytes might behave differently from those in the intact myocardium for a variety of reasons including different mechanical influences, lack of paracrine influences from neighboring cells and lack of electrical connections to adjacent myocytes.

In the case of isolated myocytes, Zaza et al. (1997) reported that "under buffering of intracellular Ca^{2+} (ruptured patch, 10 mM intracellular EGTA), spontaneous activity became unstable and ceased in the majority of cells several minutes after achieving the whole-cell configuration." Another approach to apply the Ca^{2+} chelator is to expose the cells to the acetoxymethyl (AM) ester of the Ca^{2+} chelator applied in the extracellular solution. The membrane permeant ester enters the cell and the active chelator is liberated following the action of esterases in the cytosol. Application of EGTA-AM or BAPTA-AM in this way causes cessation of beating (e.g., Sanders et al., 2006), although it is possible that unspecific effects such as blockade of I_{Kr}could contribute to these actions (Tang et al., 2007). Loading of SAN myocytes with AM esters of Ca^{2+} probes such as indo-1 can also lead to cessation of activity, and it was suggested that this could arise from Ca^{2+} chelation by the probe (Rigg et al., 2000). One important exception concerning effects of BAPTA on pacemaker activity is the paper by Himeno et al. (2011) showing that pacemaker activity in the form of action potentials can continue while contraction of the cells is suppressed by application of cytosolic BAPTA. However, these authors also noted that "action potential generation became irregular or stopped completely ∼5 min after the application of BAPTA in our experiments." What is the significance of the observations very soon after breakthrough? In support of their contention that buffering is effective even 20 s after breakthrough the authors show a prolongation of action potentials (thought to arise from slowing of inactivation of Ca^{2+} currents) that would be consistent with the chelating effects of BAPTA. Maltsev et al. (Maltsev et al., 2011; Yaniv et al., 2011) have challenged the significance of these observations with the suggestion that breakthrough from perforated patch to "whole" cell patch weakens the "seal" around the electrode noting that such a weakened seal could allow a "leakage" current that could substitute for a physiological current that is blocked by BAPTA. In other words they maintain that spontaneous activity can continue with little change after chelation of BAPTA since leakage current via a weakened "seal" around the patch pipette can replace the depolarizing influence that would normally be supplied by NCX (or any other Ca^{2+}-sensitive "background" current that occurs when Ca^{2+} is maintained at a physiological level). In support of this suggestion they note that in Figure 5 of Himeno et al. there is an upward deflection on the contraction trace following breakthrough that would be consistent with a small developing contraction associated with entry of Ca^{2+} from the extracellular solution via the leaky seal into the cytosol. Contribution of leakage current around a seal in sustaining pacemaker activity has been considered by other authors, and can make an important contribution under some conditions (Denyer and Brown, 1990), though these authors concluded from observations comparing the effects of Cs^+ under perforated patch conditions and in unpatched cells that the effects of the leakage current can be negligibly small if the seal is sufficiently robust.

This point is addressed in another paper in this issue of Frontiers in Physiology (Capel and Terrar, 2015). It is reported that under the conditions of these experiments, rupture of the membrane beneath a patch pipette to apply BAPTA to the cytosol can cause rapid cessation of activity. When conventional whole-cell patch recording was used with 10 mM BAPTA in the patch pipette solution, this cessation of spontaneous activity was almost immediate (less than 10 s). When the same rupture of the membrane beneath the pipette was made without BAPTA present the spontaneous activity appeared not to be reduced throughout the period of recording (approximately 3 min). When action potentials were first recorded with permeabilised patch (with amphotericin in the pipette to approximate the conditions of Himeno et al.) followed by rupture of the patch membrane, the disruption of spontaneous activity after cytosolic application of 10 mM BAPTA was still clearly observed but slower to develop (perhaps because of effects of amphotericin or its solvent). The speed of disruption depended on the concentration of BAPTA, progressively decreasing over the range 10, 1, and 0.1 mM BAPTA.

The many effects of Ca^{2+} on the mechanisms underlying pacemaker activity and the time windows within which they are thought to act are summarized in **Figure 4**.

Catecholamines and Sympathetic Nerve Stimulation

Evidence concerning the mechanisms underlying the positive chronotropic actions of isoprenaline have been recently discussed with particular reference to computer models of pacemaker activity (Zhang et al., 2012). In the context of the review

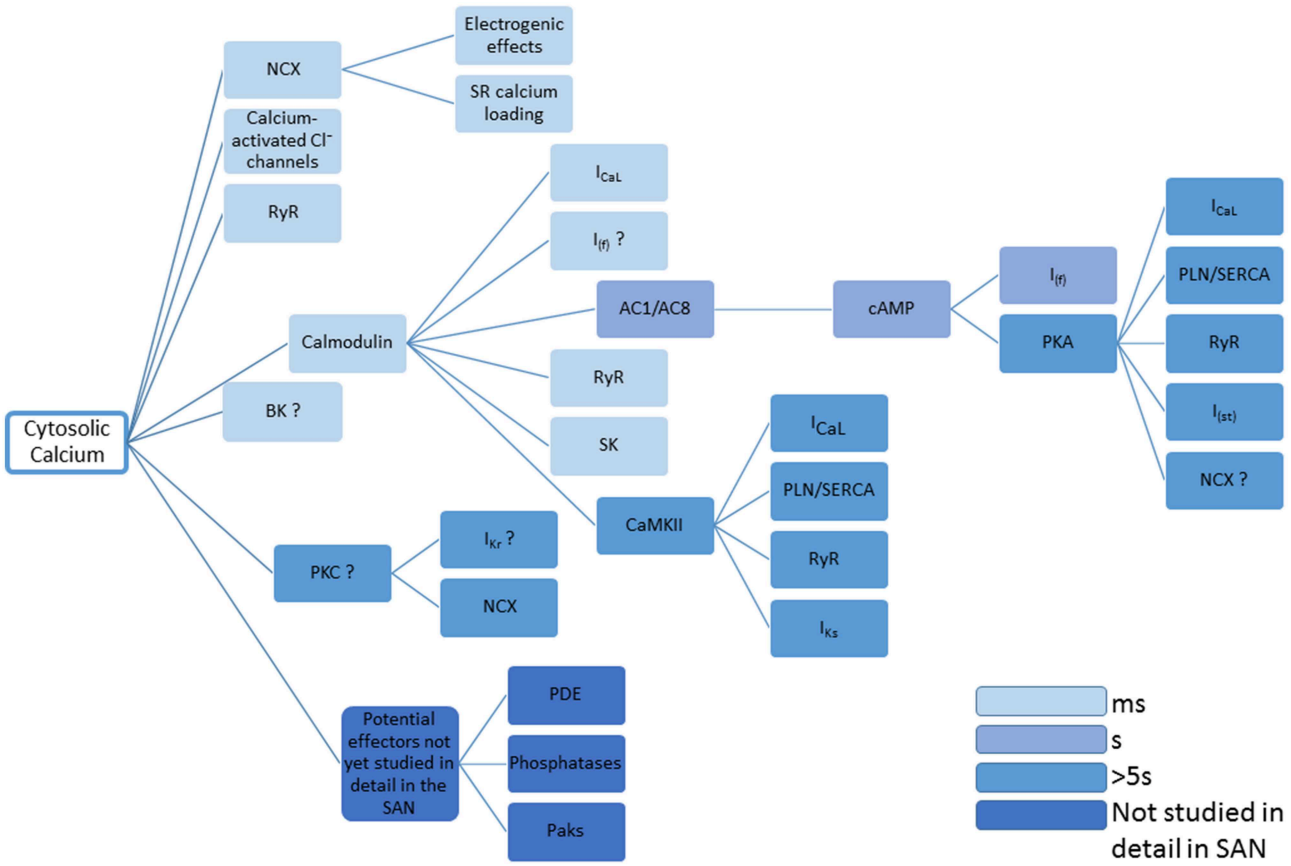

FIGURE 4 | This figure summarizes the many disparate roles for Ca^{2+} in controlling the activity of proteins that determine pacemaker activity. Question marks represent cases in which there is currently limited evidence, and references to support the actions shown can be found in the main text. The entries are color coded to give an approximate indication concerning time taken for changes in cytosolic Ca^{2+} to take effect. The figure concentrates on the effects of cytosolic Ca^{2+}, though it will be the case that Ca^{2+} within the SR will have additional effects, for example through calsequestrin or RyR2 (either via a possible Ca^{2+} sensor within the RyR structure, or through inactivation of RyRs that might be influenced by SR Ca^{2+}). Also omitted are the possible roles of NO produced via Ca^{2+}-stimulated nNOS and eNOS. Small molecules controlling Ca^{2+} signaling (e.g., IP_3, see Ju et al., 2011) are also not included.

presented here, the focus will be on the importance of the many Ca^{2+}-dependent mechanisms that are enhanced during β-adrenoceptor function. The importance of the SR in contributing to the positive chronotropic actions of isoprenaline was first demonstrated by Rigg et al. (2000) in experiments on both intact SA node and isolated SAN myocytes. After exposure to ryanodine, the log(concentration)-response curve for the effects of isoprenaline on intact node was depressed with a reduced slope and maximum effect.

Often effects of isoprenaline (isoproterenol) acting on β-adrenoceptors and of sympathetic nerve stimulation are treated as equivalent, although some have argued that this is oversimplistic (Bramich et al., 1993; Choate et al., 1993; Bramich and Cousins, 1999). There seems justification in this point of view, though a detailed discussion is beyond the scope of this review except to point out that the effects of nerve released noradrenaline on α and β adrenoceptors, as well as the effects of co-transmitters such as ATP and peptides (e.g., Herring, 2014) might have additional effects on Ca^{2+}-dependent pathways.

A major effect of β-adrenoceptor stimulation by isoprenaline is to increase Ca^{2+} currents. Many authors agree that this effect is a major factor in the positive chronotropic effect (Brown et al., 1975; Zhang et al., 2012), and an interesting possibility is that there may be important effects of β-adrenoceptor stimulation to increase current through $Ca_V1.3$ channels that appear to contribute to the later stages of diastolic depolarization (Zhang et al., 2002; Mangoni et al., 2003, 2006a). However, as mentioned above, the effects of β-adrenoceptor stimulation cannot result from the direct effects on the upstroke of the action potential alone as a consequence of increased L-type Ca^{2+} currents. This is because the upstroke makes up only about 10% or less of the cardiac cycle, and so even if the upstroke became infinitely fast (in other words effectively vertical), the pacemaker period would only be reduced to 90% of the value before the increase in Ca^{2+} current (or a rate increase of 1/0.9 giving close to a 10% increase in rate). The increase in upstroke velocity would still be functionally useful in increasing the rate of conduction of the pacemaker message in the form of the action potential to surrounding tissue. However,

in terms of the rate change it seems very likely that an important aspect of the β-adrenoceptor mediated increase in Ca^{2+} current is to increase entry of Ca^{2+} which in turn influences many of the Ca^{2+}-stimulated processes that have been described above.

The most obvious of these is NCX. Broadly if Ca^{2+} entry were to double, the cell would need, in the steady state, to remove twice as much Ca^{2+} and if the major mechanism for achieving this were NCX in its normal 3:1 mode then NCX would also double (and the total charge moved by NCX would remain approximately half that of the total Ca^{2+} entry through channels). Although this seems very likely to be the case, one additional point concerns another effect of β-adrenoceptor stimulation via cAMP and PKA. This is phosphorylation of phospholamban which will lead to increased Ca^{2+} uptake by SERCA into the SR. This might lead to a greater fraction of the Ca^{2+} to be taken up by the SR (or at least a greater rate of uptake into the SR depending on how quickly the Ca^{2+} is released), but in the steady state increased Ca^{2+} entry through the surface membrane must be accompanied by increased extrusion. In terms of the Ca^{2+} clock, the kinetics of Ca^{2+} uptake are expected to have a profound effect, and this might be one factor underlying the reduced effect of isoprenaline after ryanodine (Rigg et al., 2000), though other factors might also contribute as discussed below.

Consistent with the above suggestions of increased Ca^{2+} transients in single SAN myocytes, Rigg et al. (2000) recorded substantial increases in the amplitude as well as decay of Ca^{2+} transients recorded with the Ca^{2+} probe indo-1 in the presence of isoprenaline (see **Figure 5**). The effects of autonomic transmitters on Ca^{2+} transients and action potentials in single SAN myocytes have also been reported by Vinogradova et al. (2002a) and van Borren et al. (2010).

The additional Ca^{2+} both entering through L-type channels, and released from the SR (in individual releases and even more as a time average over many beats) could drive many Ca^{2+}-dependent processes, such as Ca^{2+}-stimulated enzymes and these are expected to contribute to the positive chronotropic effect. The Ca^{2+}-stimulated enzymes include CaMKII as discussed by Wu and Anderson (2014), as well as the Ca^{2+}-stimulated adenylyl cyclases, AC1 and AC8. As discussed above, Ca^{2+}-activation of these enzymes is expected to increase I(f), I(st), I_{Ks}, I_{Kr} and possibly NCX, as well as I_{CaL}.

ACh and Parasympathetic Nerve Stimulation

Effects of acetylcholine include both inhibition of adenylyl cyclase and opening of I_{KACh} channels. The effects on I_{KACh} channels are blocked by tertiapin Q. During parasympathetic nerve stimulation there is a rapid phase of slowing that is sensitive to tertiapin Q and therefore I_{KACh} (Bolter and Turner, 2009). The additional effects of ACh to inhibit adenylyl cyclase are in many respects the opposite of β-adrenoceptor stimulation discussed above. Consequently the inhibition of L-type Ca^{2+} current will again be very important, not so much for direct effect on the rate of rise of the action potential, but for the consequences of reduced Ca^{2+} entry on the many Ca^{2+}-dependent processes discussed above. In the context of Ca^{2+}-dependent mechanisms and in particular the Ca^{2+} clock Lyashkov et al. (2009) show that ACh reduced the number and size of LCRs, and these effects were correlated with the reduction in beating rate. ACh also reduced cAMP levels and the log(concentration)-response curves for reduction in rate and inhibition of phosphorylation of phospholamban were very similar. The authors conclude that there is a tight coupling between suppression of PKA-dependent Ca^{2+} signaling, I_{KACh} activation and reduction of spontaneous rate. van Borren et al. (2010) also investigate the effects of ACh on Ca^{2+} transient, cAMP production and pacemaker frequency. They found that when I(f) was inhibited by 2 mM Cs^{+}, and I_{KACh} was inhibited by tertiapin Q, 1 μM ACh was still able to reduce pacemaker frequency by 72%. Under these conditions, there was a good correlation between the reduction in beating rate and the amplitude of the Ca^{2+} transient. In addition ryanodine and exposure to BAPTA-AM both facilitated ACh mediated slowing. They also showed that inhibition of the Ca^{2+} transient by ryanodine (3 μM) or BAPTA-AM (25 μM) exaggerated the ACh-mediated inhibition of cAMP content, consistent with the proposal that Ca^{2+} affects cAMP production in SAN cells. There may be additional effects of ACh

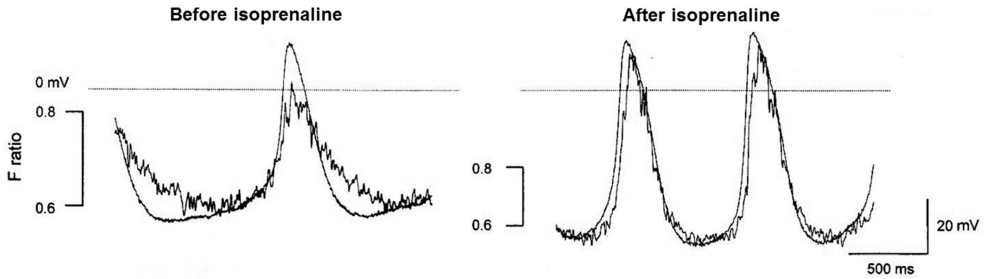

FIGURE 5 | This figure shows the Ca^{2+} transient reported by indo-1 (fluorescence ratio with emission at 405 and 485 nm) accompanying spontaneous action potentials in the same cell in the presence and absence of isoprenaline. It can be seen that the increase in rate of occurrence of spontaneous action potentials caused by isoprenaline was accompanied by an increased amplitude of the Ca^{2+} transient, an increased rate of rise of the Ca^{2+} transient and an increased rate of decay of the transient. The same limitations outlined in **Figure 2** apply here concerning a possible lag in the response of the Ca^{2+} probe to a rise in Ca^{2+} and possible slowing of the time course (though clearly any such delays do not prevent the detection of the speedier decay of the Ca^{2+} transient in the presence of isoprenaline). The experimental traces are from Rigg et al. (2000).

on phosphodiesterases (e.g., Han et al., 1995, for a review of PDE subtypes in SAN see Hua et al., 2012) and phosphatases (Ke et al., 2007).

Summary

The above discussion leads to the view that pacemaker activity in the heart normally requires L-type Ca^{2+} channels and at least one type of voltage-gated potassium channel, while the evidence seems to support the hypothesis that NCX is also essential whether or not it plays a role in determining the poorly understood "background" conductance pathway. The influence of this background conductance pathway allows de-activation of K^+ channels to cause depolarization toward the threshold for voltage-gated Ca^{2+} channels, and future identification of this pathway will be important for our understanding of pacemaker mechanisms. Pacemaker depolarization is enhanced by activation of I(f). The idea that the I(f) pathway is essential for pacemaker depolarization cannot be completely excluded because of the uncertainties concerning whether the pathway is totally suppressed in experiments using drug blockade or techniques of genetic modification, but it seems likely that I(f) is more an important modulator than an essential component of the timing mechanism. Ca^{2+} sparks/LCRs can sometimes contribute to the later stages of pacemaker depolarization preceding the action potential but are not essential for pacemaking. However, "global" properties of Ca^{2+} uptake and release by the SR across the whole myocyte (or at least a substantial fraction of the SR) can give rise to a "Ca^{2+} clock" (as a consequence of the SR filling with Ca^{2+} to a critical level or from other kinetic properties of the proteins involved in uptake and release of Ca^{2+}). The "Ca^{2+} clock" arising in this way frequently plays a modulatory rather than essential role, though there may be conditions in which it is absolutely necessary to re-initiate spontaneous activity if this were to stop. This would mean that Ca^{2+} released from the SR and driving electrogenic NCX may be essential to re-start spontaneous activity under particular conditions. Although a Ca^{2+} clock is not essential for pacemaker activity, it seems probable that under normal conditions there will be a cooperative interaction between membrane and Ca^{2+} clocks that has been referred to as a coupled clock mechanism. Under pathological conditions when the Ca^{2+} clock is not synchronized with the membrane clock the Ca^{2+} clock can lead to disturbed pacemaker rhythms. In normal physiology, Ca^{2+} is thought to drive a depolarizing influence of NCX throughout the cardiac cycle, including during the most negative potential of the pacemaker myocytes, at least under most conditions when the cytosolic Ca^{2+} concentration remains substantially higher than 100 nM. Ca^{2+} also plays important roles in maintaining and regulating pacemaker activity by activating a variety of Ca^{2+}-dependent enzymes including CaMKII, AC1, and AC8. Ca^{2+} seems to exert a direct or indirect influence on most if not all of the proteins providing ionic pathways in the surface membrane.

Acknowledgments

Pacemaking work in the DAT laboratory has been supported for many years by the British Heart Foundation and Wellcome Trust. RAC was supported by a British Heart Foundation Graduate Studentship and, thereafter, a British Heart Foundation research grant.

References

Baruscotti, M., Bucchi, A., and Difrancesco, D. (2005). Physiology and pharmacology of the cardiac pacemaker ("funny") current. *Pharmacol. Ther.* 107, 59–79. doi: 10.1016/j.pharmthera.2005.01.005

Baruscotti, M., and Difrancesco, D. (2004). Pacemaker channels. *Ann. N.Y. Acad. Sci.* 1015, 111–121. doi: 10.1196/annals.1302.009

Berridge, M. J. (2008). Smooth muscle cell calcium activation mechanisms. *J. Physiol.* 586, 5047–5061. doi: 10.1113/jphysiol.2008.160440

Berridge, M. J., and Galione, A. (1988). Cytosolic calcium oscillators. *FASEB J.* 2, 3074–3082.

Biel, M., Schneider, A., and Wahl, C. (2002). Cardiac HCN channels: structure, function, and modulation. *Trends Cardiovasc. Med.* 12, 206–212. doi: 10.1016/S1050-1738(02)00162-7

Biel, M., Wahl-schott, C., Michalakis, S., and Zong, X. (2009). Hyperpolarization-activated cation channels: from genes to function. *Physiol. Rev.* 89, 847–885. doi: 10.1152/physrev.00029.2008

Bogdanov, K. Y., Maltsev, V. A., Vinogradova, T. M., Lyashkov, A. E., Spurgeon, H. A., Stern, M. D., et al. (2006). Membrane potential fluctuations resulting from submembrane Ca2+ releases in rabbit sinoatrial nodal cells impart an exponential phase to the late diastolic depolarization that controls their chronotropic state. *Circ. Res.* 99, 979–987. doi: 10.1161/01.RES.0000247933.66532.0b

Bogdanov, K. Y., Vinogradova, T. M., and Lakatta, E. G. (2001). Sinoatrial nodal cell ryanodine receptor and Na(+)-Ca(2+) exchanger: molecular partners in pacemaker regulation. *Circ. Res.* 88, 1254–1258. doi: 10.1161/hh1201.092095

Bolter, C. P., and Turner, M. J. (2009). Tertiapin-Q removes a large and rapidly acting component of vagal slowing of the guinea-pig cardiac pacemaker. *Auton. Neurosci.* 150, 76–81. doi: 10.1016/j.autneu.2009.05.244

BoSmith, R. E., Briggs, I., and Sturgess, N. C. (1993). Inhibitory actions of ZENECA ZD7288 on whole-cell hyperpolarization activated inward current (If) in guinea-pig dissociated sinoatrial node cells. *Br. J. Pharmacol.* 110, 343–349. doi: 10.1111/j.1476-5381.1993.tb13815.x

Bramich, N. J., Brock, J. A., Edwards, F. R., and Hirst, G. D. (1993). Responses to sympathetic nerve stimulation of the sinus venosus of the toad. *J. Physiol.* 461, 403–430. doi: 10.1113/jphysiol.1993.sp019520

Bramich, N. J., and Cousins, H. M. (1999). Effects of sympathetic nerve stimulation on membrane potential, [Ca2+]i, and force in the toad sinus venosus. *Am. J. Physiol.* 276, H115–H128.

Brown, H. F., McNaughton, P. A., Noble, D., and Noble, S. J. (1975). Adrenergic control of cardian pacemaker currents. *Philos. Trans. R. Soc. Lond. B Biol. Sci.* 270, 527–537. doi: 10.1098/rstb.1975.0029

Cannell, M. B., Berlin, J. R., and Lederer, W. J. (1987). Intracellular calcium in cardiac myocytes: calcium transients measured using fluorescence imaging. *Soc. Gen. Physiol. Ser.* 42, 201–214.

Capel, R. A., and Terrar, D. A. (2015). Cytosolic calcium ions exert a major influence on the firing rate and maintenance of pacemaker activity in guinea-pig sinus node. *Front. Physiol.* 6:23. doi: 10.3389/fphys.2015.00023

Chatelier, A., Renaudon, B., Bescond, J., El Chemaly, A., Demion, M., and Bois, P. (2005). Calmodulin antagonist W7 directly inhibits f-type current in rabbit sino-atrial cells. *Eur. J. Pharmacol.* 521, 29–33. doi: 10.1016/j.ejphar.2005.08.024

Chen, B., Wu, Y., Mohler, P. J., Anderson, M. E., and Song, L. S. (2009). Local control of Ca2+-induced Ca2+ release in mouse sinoatrial node cells. *J. Mol. Cell. Cardiol.* 47, 706–715. doi: 10.1016/j.yjmcc.2009.07.007

Chen, W., Wang, R., Chen, B., Zhong, X., Kong, H., Bai, Y., et al. (2014). The ryanodine receptor store-sensing gate controls Ca2+ waves and Ca2+-triggered arrhythmias. *Nat. Med.* 20, 184–192. doi: 10.1038/nm.3440

Chen, W. T., Chen, Y. C., Lu, Y. Y., Kao, Y. H., Huang, J. H., Lin, Y. K., et al. (2013). Apamin modulates electrophysiological characteristics of the pulmonary vein and the Sinoatrial Node. *Eur. J. Clin. Invest.* 43, 957–963. doi: 10.1111/eci.12125

Cho, C. H., Kim, S. S., Jeong, M. J., Lee, C. O., and Shin, H. S. (2000). The Na^+-Ca^{2+} exchanger is essential for embryonic heart development in mice. *Mol. Cells* 10, 712–722. doi: 10.1007/s100590000034

Choate, J. K., Edwards, F. R., Hirst, G. D., and O'Shea, J. E. (1993). Effects of sympathetic nerve stimulation on the sino-atrial node of the guinea-pig. *J. Physiol.* 471, 707–727. doi: 10.1113/jphysiol.1993.sp019924

Christel, C. J., Cardona, N., Mesirca, P., Herrmann, S., Hofmann, F., Striessnig, J., et al. (2012). Distinct localization and modulation of Cav1.2 and Cav1.3 L-type Ca2+ channels in mouse sinoatrial node. *J. Physiol.* 590, 6327–6342. doi: 10.1113/jphysiol.2012.239954

Clark, R. B., Mangoni, M. E., Lueger, A., Couette, B., Nargeot, J., and Giles, W. R. (2004). A rapidly activating delayed rectifier K+ current regulates pacemaker activity in adult mouse sinoatrial node cells. *Am. J. Physiol. Heart Circ. Physiol.* 286, H1757–H1766. doi: 10.1152/ajpheart.00753.2003

Collins, T. P., and Terrar, D. A. (2012). Ca(2+)-stimulated adenylyl cyclases regulate the L-type Ca(2+) current in guinea-pig atrial myocytes. *J. Physiol.* 590, 1881–1893. doi: 10.1113/jphysiol.2011.227066

Coppen, S. R., Kodama, I., Boyett, M. R., Dobrzynski, H., Takagishi, Y., Honjo, H., et al. (1999). Connexin45, a major connexin of the rabbit sinoatrial node, is co-expressed with connexin43 in a restricted zone at the nodal-crista terminalis border. *J. Histochem. Cytochem.* 47, 907–918. doi: 10.1177/002215549904700708

Denyer, J. C., and Brown, H. F. (1990). Pacemaking in rabbit isolated sino-atrial node cells during Cs+ block of the hyperpolarization-activated current if. *J. Physiol.* 429, 401–409. doi: 10.1113/jphysiol.1990.sp018264

DiFrancesco, D. (2010). The role of the funny current in pacemaker activity. *Circ. Res.* 106, 434–446. doi: 10.1161/CIRCRESAHA.109.208041

DiFrancesco, D., and Mangoni, M. (1994). Modulation of single hyperpolarization-activated channels (i(f)) by cAMP in the rabbit sino-atrial node. *J. Physiol.* 474, 473–482. doi: 10.1113/jphysiol.1994.sp020038

DiFrancesco, D., and Noble, D. (2012a). The funny current has a major pacemaking role in the sinus node. *Heart Rhythm* 9, 299–301. doi: 10.1016/j.hrthm.2011.09.021

DiFrancesco, D., and Noble, D. (2012b). Rebuttal: "The funny current in the context of the coupled clock pacemaker cell system." *Heart Rhythm* 9, 457–458. doi: 10.1016/j.hrthm.2011.09.023

Dobrzynski, H., Boyett, M. R., and Anderson, R. H. (2007). New insights into pacemaker activity: promoting understanding of sick sinus syndrome. *Circulation* 115, 1921–1932. doi: 10.1161/CIRCULATIONAHA.106.616011

Fenske, S., Krause, S. C., Hassan, S. I., Becirovic, E., Auer, F., Bernard, R., et al. (2013). Sick sinus syndrome in HCN1-deficient mice. *Circulation* 128, 2585–2594. doi: 10.1161/CIRCULATIONAHA.113.003712

Fischmeister, R., and Hartzell, H. C. (1986). Mechanism of action of acetylcholine on calcium current in single cells from frog ventricle. *J. Physiol.* 376, 183–202. doi: 10.1113/jphysiol.1986.sp016148

Fischmeister, R., and Shrier, A. (1989). Interactive effects of isoprenaline, forskolin and acetylcholine on Ca2+ current in frog ventricular myocytes. *J. Physiol.* 417, 213–239. doi: 10.1113/jphysiol.1989.sp017798

Gao, Z., Rasmussen, T. P., Li, Y., Kutschke, W., Koval, O. M., Wu, Y., et al. (2013). Genetic inhibition of Na+-Ca2+ exchanger current disables fight or flight sinoatrial node activity without affecting resting heart rate. *Circ. Res.* 112, 309–317. doi: 10.1161/CIRCRESAHA.111.300193

Gao, Z., Singh, M. V., Hall, D. D., Koval, O. M., Luczak, E. D., Joiner, M. L., et al. (2011). Catecholamine-independent heart rate increases require Ca2+/calmodulin-dependent protein kinase II. *Circ. Arrhythm. Electrophysiol.* 4, 379–387. doi: 10.1161/CIRCEP.110.961771

Glukhov, A. V., Kalyanasundaram, A., Lou, Q., Hage, L. T., Hansen, B. J., Belevych, A. E., et al. (2015). Calsequestrin 2 deletion causes sinoatrial node dysfunction and atrial arrhythmias associated with altered sarcoplasmic reticulum calcium cycling and degenerative fibrosis within the mouse atrial pacemaker complex. *Eur. Heart J.* 36, 686–697. doi: 10.1093/eurheartj/eht452

Groenke, S., Larson, E. D., Alber, S., Zhang, R., Lamp, S. T., Ren, X., et al. (2013). Complete atrial-specific knockout of sodium-calcium exchange eliminates sinoatrial node pacemaker activity. *PLoS ONE* 8:e81633. doi: 10.1371/journal.pone.0081633

Hagiwara, N., and Irisawa, H. (1989). Modulation by intracellular Ca2+ of the hyperpolarization-activated inward current in rabbit single sino-atrial node cells. *J. Physiol.* 409, 121–141. doi: 10.1113/jphysiol.1989.sp017488

Hagiwara, N., Irisawa, H., and Kameyama, M. (1998). Contribution of two types of calcium currents to the pacemaker potentials of rabbit sino-atrial node cells. *J. Physiol.* 395, 233–253.

Hagiwara, N., Irisawa, H., Kasanuki, H., and Hosoda, S. (1992). Background current in sino-atrial node cells of the rabbit heart. *J. Physiol.* 448, 53–72. doi: 10.1113/jphysiol.1992.sp019029

Han, X., Shimoni, Y., and Giles, W. R. (1995). A cellular mechanism for nitric oxide-mediated cholinergic control of mammalian heart rate. *J. Gen. Physiol.* 106, 45–65. doi: 10.1085/jgp.106.1.45

Hauswirth, O., Noble, D., and Tsien, R. W. (1968). Adrenaline: mechanism of action on the pacemaker potential in cardiac Purkinje fibers. *Science* 162, 916–917. doi: 10.1126/science.162.3856.916

He, C., Chen, F., Li, B., and Hu, Z. (2014). Neurophysiology of HCN channels: from cellular functions to multiple regulations. *Prog. Neurobiol.* 112, 1–23. doi: 10.1016/j.pneurobio.2013.10.001

Heath, B. M., and Terrar, D. A. (2000). Protein kinase C enhances the rapidly activating delayed rectifier potassium current, IKr, through a reduction in C-type inactivation in guinea-pig ventricular myocytes. *J. Physiol.* 522(Pt 3), 391–402. doi: 10.1111/j.1469-7793.2000.t01-2-00391.x

Herring, N. (2014). Autonomic control of the heart: going beyond the classical neurotransmitters. *Exp. Physiol.* doi: 10.1113/expphysiol.2014.080184. [Epub ahead of print].

Herrmann, S., Lipp, P., Wiesen, K., Stieber, J., Nguyen, H., Kaiser, E., et al. (2013). The cardiac sodium-calcium exchanger NCX1 is a key player in the initiation and maintenance of a stable heart rhythm. *Cardiovasc. Res.* 99, 780–788. doi: 10.1093/cvr/cvt154

Hescheler, J., Kameyama, M., and Trautwein, W. (1986). On the mechanism of muscarinic inhibition of the cardiac Ca current. *Pflugers Arch.* 407, 182–189. doi: 10.1007/BF00580674

Himeno, Y., Toyoda, F., Satoh, H., Amano, A., Cha, C. Y., Matsuura, H., et al. (2011). Minor contribution of cytosolic Ca2+ transients to the pacemaker rhythm in guinea pig sinoatrial node cells. *Am. J. Physiol. Heart Circ. Physiol.* 300, H251–H261. doi: 10.1152/ajpheart.00764.2010

Hof, T., Simard, C., Rouet, R., Salle, L., and Guinamard, R. (2013). Implication of the TRPM4 nonselective cation channel in mammalian sinus rhythm. *Heart Rhythm* 10, 1683–1689. doi: 10.1016/j.hrthm.2013.08.014

Hua, R., Adamczyk, A., Robbins, C., Ray, G., and Rose, R. A. (2012). Distinct patterns of constitutive phosphodiesterase activity in mouse sinoatrial node and atrial myocardium. *PLoS ONE* 7:e47652. doi: 10.1371/journal.pone.0047652

Huang, Z. M., Prasad, C., Britton, F. C., Ye, L. L., Hatton, W. J., and Duan, D. (2009). Functional role of CLC-2 chloride inward rectifier channels in cardiac sinoatrial nodal pacemaker cells. *J. Mol. Cell. Cardiol.* 47, 121–132. doi: 10.1016/j.yjmcc.2009.04.008

Huser, J., Blatter, L. A., and Lipsius, S. L. (2000). Intracellular Ca2+ release contributes to automaticity in cat atrial pacemaker cells. *J. Physiol.* 524(Pt 2), 415–422. doi: 10.1111/j.1469-7793.2000.00415.x

Imlach, W. L., Finch, S. C., Miller, J. H., Meredith, A. L., and Dalziel, J. E. (2010). A role for BK channels in heart rate regulation in rodents. *PLoS ONE* 5:e8698. doi: 10.1371/journal.pone.0008698

Imtiaz, M. S. (2012). Calcium oscillations and pacemaking. *Adv. Exp. Med. Biol.* 740, 511–520. doi: 10.1007/978-94-007-2888-2_22

Imtiaz, M. S., Katnik, C. P., Smith, D. W., and van Helden, D. F. (2006). Role of voltage-dependent modulation of store Ca2+ release in synchronization of Ca2+ oscillations. *Biophys. J.* 90, 1–23. doi: 10.1529/biophysj.104.058743

Imtiaz, M. S., von der Weid, P. Y., Laver, D. R., and van Helden, D. F. (2010). SR Ca2+ store refill–a key factor in cardiac pacemaking. *J. Mol. Cell. Cardiol.* 49, 412–426. doi: 10.1016/j.yjmcc.2010.03.015

Imtiaz, M. S., Zhao, J., Hosaka, K., von der Weid, P. Y., Crowe, M., and van Helden, D. F. (2007). Pacemaking through Ca2+ stores interacting as coupled oscillators via membrane depolarization. *Biophys. J.* 92, 3843–3861. doi: 10.1529/biophysj.106.095687

Irisawa, H. (1978). Comparative physiology of the cardiac pacemaker mechanism. *Physiol. Rev.* 58, 461–498.

Irisawa, H., Brown, H. F., and Giles, W. (1993). Cardiac pacemaking in the sinoatrial node. *Physiol. Rev.* 73, 197–227.

Ito, H., Ono, K., and Noma, A. (1994). Background conductance attributable to spontaneous opening of muscarinic K+ channels in rabbit sino-atrial node cells. *J. Physiol.* 476, 55–68.

Jackson, V. M., Rakovic, S., and Terrar, D. A. (2002). Effects of isoproterenol on calcium transients and calcium sparks in guinea-pig sino-atrial node cells imaged by confocal microscopy. *Biophys. J.* 82, 648A.

Ju, Y. K., and Allen, D. G. (1998). Intracellular calcium and Na^+-Ca^{2+} exchange current in isolated toad pacemaker cells. *J. Physiol.* 508(Pt 1), 153–166. doi: 10.1111/j.1469-7793.1998.153br.x

Ju, Y. K., and Allen, D. G. (2007). Store-operated Ca2+ entry and TRPC expression; possible roles in cardiac pacemaker tissue. *Heart Lung Circ.* 16, 349–355. doi: 10.1016/j.hlc.2007.07.004

Ju, Y. K., Liu, J., Lee, B. H., Lai, D., Woodcock, E. A., Lei, M., et al. (2011). Distribution and functional role of inositol 1,4,5-trisphosphate receptors in mouse sinoatrial node. *Circ. Res.* 109, 848–857. doi: 10.1161/CIRCRESAHA.111.243824

Kang, T. M., and Hilgemann, D. W. (2004). Multiple transport modes of the cardiac Na+/Ca2+ exchanger. *Nature* 427, 544–548. doi: 10.1038/nature02271

Ke, Y., Lei, M., Collins, T. P., Rakovic, S., Mattick, P. A., Yamasaki, M., et al. (2007). Regulation of L-type calcium channel and delayed rectifier potassium channel activity by p21-activated kinase-1 in guinea pig sinoatrial node pacemaker cells. *Circ. Res.* 100, 1317–1327. doi: 10.1161/01.RES.0000266742.51389.a4

Kodama, I., Nikmaram, M. R., Boyett, M. R., Suzuki, R., Honjo, H., and Owen, J. M. (1997). Regional differences in the role of the Ca2+ and Na+ currents in pacemaker activity in the sinoatrial node. *Am. J. Physiol.* 272, H2793–H2806.

Koushik, S. V., Wang, J., Rogers, R., Moskophidis, D., Lambert, N. A., Creazzo, T. L., et al. (2001). Targeted inactivation of the sodium-calcium exchanger (Ncx1) results in the lack of a heartbeat and abnormal myofibrillar organization. *FASEB J.* 15, 1209–1211. doi: 10.1096/fj.00-0696fje

Kryukova, Y. N., Protas, L., and Robinson, R. B. (2012). Ca2+-activated adenylyl cyclase 1 introduces Ca2+-dependence to beta-adrenergic stimulation of HCN2 current. *J. Mol. Cell. Cardiol.* 52, 1233–1239. doi: 10.1016/j.yjmcc.2012.03.010

Lai, M. H., Wu, Y., Gao, Z., Anderson, M. E., Dalziel, J. E., and Meredith, A. L. (2014). BK channels regulate sinoatrial node firing rate and cardiac pacing *in vivo*. *Am. J. Physiol. Heart Circ. Physiol.* 307, H1327–H1338. doi: 10.1152/ajpheart.00354.2014

Lakatta, E. G., and DiFrancesco, D. (2009). What keeps us ticking: a funny current, a calcium clock, or both? *J. Mol. Cell. Cardiol.* 47, 157–170. doi: 10.1016/j.yjmcc.2009.03.022

Lakatta, E. G., and Maltsev, V. A. (2012). Rebuttal: what I(f) the shoe doesn't fit? "The funny current has a major pacemaking role in the sinus node." *Heart Rhythm* 9, 459–460. doi: 10.1016/j.hrthm.2011.09.024

Lei, M., and Brown, H. F. (1996). Two components of the delayed rectifier potassium current, IK, in rabbit sino-atrial node cells. *Exp. Physiol.* 81, 725–741. doi: 10.1113/expphysiol.1996.sp003972

Lei, M., Honjo, H., Kodama, I., and Boyett, M. R. (2001). Heterogeneous expression of the delayed-rectifier K+ currents i(K,r) and i(K,s) in rabbit sinoatrial node cells. *J. Physiol.* 535, 703–714. doi: 10.1111/j.1469-7793.2001.t01-1-00703.x

Liu, J., Xin, L., Benson, V. L., Allen, D. G., and Ju, Y. K. (2015). Store-operated calcium entry and the localization of STIM1 and Orai1 proteins in isolated mouse sinoatrial node cells. *Front. Physiol.* 6:69. doi: 10.3389/fphys.2015.00069

Lyashkov, A. E., Vinogradova, T. M., Zahanich, I., Li, Y., Younes, A., Nuss, H. B., et al. (2009). Cholinergic receptor signaling modulates spontaneous firing of sinoatrial nodal cells via integrated effects on PKA-dependent Ca(2+) cycling and I(KACh). *Am. J. Physiol. Heart Circ. Physiol.* 297, H949–H959. doi: 10.1152/ajpheart.01340.2008

Maltsev, A. V., Yaniv, Y., Stern, M. D., Lakatta, E. G., and Maltsev, V. A. (2013). RyR-NCX-SERCA local cross-talk ensures pacemaker cell function at rest and during the fight-or-flight reflex. *Circ. Res.* 113, e94–e100. doi: 10.1161/CIRCRESAHA.113.302465

Maltsev, V. A., and Lakatta, E. G. (2012). The funny current in the context of the coupled-clock pacemaker cell system. *Heart Rhythm* 9, 302–307. doi: 10.1016/j.hrthm.2011.09.022

Maltsev, V. A., Vinogradova, T. M., Stern, M. D., and Lakatta, E. G. (2011). Letter to the editor: "Validating the requirement for beat-to-beat coupling of the Ca2+ clock and M clock in pacemaker cell normal automaticity." *Am. J. Physiol. Heart Circ. Physiol.* 300, H2323–H2324; author reply H2325–H2326. doi: 10.1152/ajpheart.00110.2011

Maltsev, V. A., Yaniv, Y., Maltsev, A. V., Stern, M. D., and Lakatta, E. G. (2014). Modern perspectives on numerical modeling of cardiac pacemaker cell. *J. Pharmacol. Sci.* 125, 6–38. doi: 10.1254/jphs.13R04CR

Mangoni, M. E., Couette, B., Bourinet, E., Platzer, J., Reimer, D., Striessnig, J., et al. (2003). Functional role of L-type Cav1.3 Ca2+ channels in cardiac pacemaker activity. *Proc. Natl. Acad. Sci. U.S.A.* 100, 5543–5548. doi: 10.1073/pnas.0935295100

Mangoni, M. E., Couette, B., Marger, L., Bourinet, E., Striessnig, J., and Nargeot, J. (2006a). Voltage-dependent calcium channels and cardiac pacemaker activity: from ionic currents to genes. *Prog. Biophys. Mol. Biol.* 90, 38–63. doi: 10.1016/j.pbiomolbio.2005.05.003

Mangoni, M. E., and Nargeot, J. (2008). Genesis and regulation of the heart automaticity. *Physiol. Rev.* 88, 919–982. doi: 10.1152/physrev.00018.2007

Mangoni, M. E., Traboulsie, A., Leoni, A. L., Couette, B., Marger, L., Le Quang, K., et al. (2006b). Bradycardia and slowing of the atrioventricular conduction in mice lacking CaV3.1/alpha1G T-type calcium channels. *Circ. Res.* 98, 1422–1430. doi: 10.1161/01.RES.0000225862.14314.49

Maruyama, M., Xiao, J., Zhou, Q., Vembaiyan, K., Chua, S. K., Rubart-Von Der Lohe, M., et al. (2013). Carvedilol analogue inhibits triggered activities evoked by both early and delayed afterdepolarizations. *Heart Rhythm* 10, 101–107. doi: 10.1016/j.hrthm.2012.09.006

Mattick, P., Parrington, J., Odia, E., Simpson, A., Collins, T., and Terrar, D. (2007). Ca2+-stimulated adenylyl cyclase isoform AC1 is preferentially expressed in guinea-pig sino-atrial node cells and modulates the I(f) pacemaker current. *J. Physiol.* 582, 1195–1203. doi: 10.1113/jphysiol.2007.133439

McHale, N., Hollywood, M., Sergeant, G., and Thornbury, K. (2006). Origin of spontaneous rhythmicity in smooth muscle. *J. Physiol.* 570, 23–28. doi: 10.1113/jphysiol.2005.098376

Mesirca, P., Alig, J., Torrente, A. G., Muller, J. C., Marger, L., Rollin, A., et al. (2014a). Cardiac arrhythmia induced by genetic silencing of 'funny' (f) channels is rescued by GIRK4 inactivation. *Nat. Commun.* 5, 4664. doi: 10.1038/ncomms5664

Mesirca, P., Torrente, A. G., and Mangoni, M. E. (2014b). T-type channels in the sino-atrial and atrioventricular pacemaker mechanism. *Pflugers Arch.* 466, 791–799. doi: 10.1007/s00424-014-1482-6

Miake, J., Marban, E., and Nuss, H. B. (2002). Biological pacemaker created by gene transfer. *Nature* 419, 132–133. doi: 10.1038/419132b

Mitsuiye, T., Guo, J., and Noma, A. (1999). Nicardipine-sensitive Na+-mediated single channel currents in guinea-pig sinoatrial node pacemaker cells. *J. Physiol.* 521(Pt 1), 69–79. doi: 10.1111/j.1469-7793.1999.00069.x

Mitsuiye, T., Shinagawa, Y., and Noma, A. (2000). Sustained inward current during pacemaker depolarization in mammalian sinoatrial node cells. *Circ. Res.* 87, 88–91. doi: 10.1161/01.RES.87.2.88

Musialek, P., Rigg, L., Terrar, D. A., Paterson, D. J., and Casadei, B. (2000). Role of cGMP-inhibited phosphodiesterase and sarcoplasmic calcium in mediating the increase in basal heart rate with nitric oxide donors. *J. Mol. Cell. Cardiol.* 32, 1831–1840. doi: 10.1006/jmcc.2000.1216

Neco, P., Torrente, A. G., Mesirca, P., Zorio, E., Liu, N., Priori, S. G., et al. (2012). Paradoxical effect of increased diastolic Ca(2+) release and decreased sinoatrial node activity in a mouse model of catecholaminergic polymorphic ventricular tachycardia. *Circulation* 126, 392–401. doi: 10.1161/CIRCULATIONAHA.111.075382

Noble, D., Denyer, J. C., Brown, H. F., and Difrancesco, D. (1992). Reciprocal role of the inward currents ib, Na and i(f) in controlling and stabilizing pacemaker frequency of rabbit sino-atrial node cells. *Proc. Biol. Sci.* 250, 199–207. doi: 10.1098/rspb.1992.0150

Noma, A. (1996). Ionic mechanisms of the cardiac pacemaker potential. *Jpn. Heart J.* 37, 673–682. doi: 10.1536/ihj.37.673

Noma, A., and Irisawa, H. (1975). Effects of Na+ and K+ on the resting membrane potential of the rabbit sinoatrial node cell. *Jpn. J. Physiol.* 25, 207–302. doi: 10.2170/jjphysiol.25.287

Noma, A., Nakayama, T., Kurachi, Y., and Irisawa, H. (1984). Resting K conductances in pacemaker and non-pacemaker heart cells of the rabbit. *Jpn. J. Physiol.* 34, 245–254. doi: 10.2170/jjphysiol.34.245

Ottolia, M., Torres, N., Bridge, J. H., Philipson, K. D., and Goldhaber, J. I. (2013). Na/Ca exchange and contraction of the heart. *J. Mol. Cell. Cardiol.* 61, 28–33. doi: 10.1016/j.yjmcc.2013.06.001

Petit-Jacques, J., Bois, P., Bescond, J., and Lenfant, J. (1993). Mechanism of muscarinic control of the high-threshold calcium current in rabbit sino-atrial node myocytes. *Pflugers Arch.* 423, 21–27. doi: 10.1007/BF00374956

Proenza, C., Angoli, D., Agranovich, E., Macri, V., and Accili, E. A. (2002). Pacemaker channels produce an instantaneous current. *J. Biol. Chem.* 277, 5101–5109. doi: 10.1074/jbc.M106974200

Rakovic, S., Rigg, L., Ishida, H., and Terrar, D. A. (2001). Calcium transients in guinea-pig sino-atrial node cells imaged by confocal microscopy. *Biophys. J.* 80, 350A.

Reuter, H., Henderson, S. A., Han, T., Ross, R. S., Goldhaber, J. I., and Philipson, K. D. (2002). The Na+-Ca2+ exchanger is essential for the action of cardiac glycosides. *Circ. Res.* 90, 305–308. doi: 10.1161/hh0302.104562

Rigg, L., Heath, B. M., Cui, Y., and Terrar, D. A. (2000). Localisation and functional significance of ryanodine receptors during beta-adrenoceptor stimulation in the guinea-pig sino-atrial node. *Cardiovasc. Res.* 48, 254–264. doi: 10.1016/S0008-6363(00)00153-X

Rigg, L., Mattick, P. A., Heath, B. M., and Terrar, D. A. (2003). Modulation of the hyperpolarization-activated current (I(f)) by calcium and calmodulin in the guinea-pig sino-atrial node. *Cardiovasc. Res.* 57, 497–504. doi: 10.1016/S0008-6363(02)00668-5

Rigg, L., and Terrar, D. A. (1996). Possible role of calcium release from the sarcoplasmic reticulum in pacemaking in guinea-pig sino-atrial node. *Exp. Physiol.* 81, 877–880. doi: 10.1113/expphysiol.1996.sp003983

Sah, R., Mesirca, P., Van den Boogert, M., Rosen, J., Mably, J., Mangoni, M. E., et al. (2013). Ion channel-kinase TRPM7 is required for maintaining cardiac automaticity. *Proc. Natl. Acad. Sci. U.S.A.* 110, E3037–E3046. doi: 10.1073/pnas.1311865110

Sanders, L., Rakovic, S., Lowe, M., Mattick, P. A., and Terrar, D. A. (2006). Fundamental importance of Na+-Ca2+ exchange for the pacemaking mechanism in guinea-pig sino-atrial node. *J. Physiol.* 571, 639–649. doi: 10.1113/jphysiol.2005.100305

Schaub, M. C., Hefti, M. A., and Zaugg, M. (2006). Integration of calcium with the signaling network in cardiac myocytes. *J. Mol. Cell. Cardiol.* 41, 183–214. doi: 10.1016/j.yjmcc.2006.04.005

Seyama, I. (1979). Characteristics of the anion channel in the sino-atrial node cell of the rabbit. *J. Physiol.* 294, 447–460. doi: 10.1113/jphysiol.1979.sp012940

Shibata, E. F., and Giles, W. R. (1985). Ionic currents that generate the spontaneous diastolic depolarization in individual cardiac pacemaker cells. *Proc. Natl. Acad. Sci. U.S.A.* 82, 7796–7800. doi: 10.1073/pnas.82.22.7796

Shinohara, T., Kim, D., Joung, B., Maruyama, M., Vembaiyan, K., Back, T. G., et al. (2014). Carvedilol analog modulates both basal and stimulated sinoatrial node automaticity. *Heart Vessels* 29, 396–403. doi: 10.1007/s00380-013-0378-2

Sitsapesan, R., and Williams, A. J. (1994). Regulation of the gating of the sheep cardiac sarcoplasmic reticulum Ca(2+)-release channel by luminal Ca2+. *J. Membr. Biol.* 137, 215–226. doi: 10.1007/BF00232590

Sitsapesan, R., and Williams, A. J. (1997). Regulation of current flow through ryanodine receptors by luminal Ca2+. *J. Membr. Biol.* 159, 179–185. doi: 10.1007/s002329900281

Tang, Q., Jin, M. W., Xiang, J. Z., Dong, M. Q., Sun, H. Y., Lau, C. P., et al. (2007). The membrane permeable calcium chelator BAPTA-AM directly blocks human ether a-go-go-related gene potassium channels stably expressed in HEK 293 cells. *Biochem. Pharmacol.* 74, 1596–1607. doi: 10.1016/j.bcp.2007.07.042

ten Velde, I., de Jonge, B., Verheijck, E. E., van Kempen, M. J., Analbers, L., Gros, D., et al. (1995). Spatial distribution of connexin43, the major cardiac gap junction protein, visualizes the cellular network for impulse propagation from sinoatrial node to atrium. *Circ. Res.* 76, 802–811. doi: 10.1161/01.RES.76.5.802

van Borren, M. M., Verkerk, A. O., Wilders, R., Hajji, N., Zegers, J. G., Bourier, J., et al. (2010). Effects of muscarinic receptor stimulation on Ca2+ transient, cAMP production and pacemaker frequency of rabbit sinoatrial node cells. *Basic Res. Cardiol.* 105, 73–87. doi: 10.1007/s00395-009-0048-9

Verheijck, E. E., van Ginneken, A. C., Bourier, J., and Bouman, L. N. (1995). Effects of delayed rectifier current blockade by E-4031 on impulse generation in single sinoatrial nodal myocytes of the rabbit. *Circ. Res.* 76, 607–615. doi: 10.1161/01.RES.76.4.607

Verkerk, A. O., and Wilders, R. (2013). Hyperpolarization-activated current, If, in mathematical models of rabbit sinoatrial node pacemaker cells. *Biomed Res. Int.* 2013, 872454. doi: 10.1155/2013/872454

Verkerk, A. O., Wilders, R., Zegers, J. G., van Borren, M. M., Ravesloot, J. H., and Verheijck, E. E. (2002). Ca(2+)-activated Cl(-) current in rabbit sinoatrial node cells. *J. Physiol.* 540, 105–117. doi: 10.1113/jphysiol.2001.013184

Vinogradova, T. M., Bogdanov, K. Y., and Lakatta, E. G. (2002a). beta-Adrenergic stimulation modulates ryanodine receptor Ca(2+) release during diastolic depolarization to accelerate pacemaker activity in rabbit sinoatrial nodal cells. *Circ. Res.* 90, 73–79. doi: 10.1161/hh0102.102271

Vinogradova, T. M., Bogdanov, K. Y., and Lakatta, E. G. (2002b). Novel perspectives on the beating rate of the heart. *Circ. Res.* 91, e3. doi: 10.1161/01.RES.0000031164.28289.55

Vinogradova, T. M., Brochet, D. X., Sirenko, S., Li, Y., Spurgeon, H., and Lakatta, E. G. (2010). Sarcoplasmic reticulum Ca2+ pumping kinetics regulates timing of local Ca2+ releases and spontaneous beating rate of rabbit sinoatrial node pacemaker cells. *Circ. Res.* 107, 767–775. doi: 10.1161/CIRCRESAHA.110.220517

Vinogradova, T. M., and Lakatta, E. G. (2009). Regulation of basal and reserve cardiac pacemaker function by interactions of cAMP-mediated PKA-dependent Ca2+ cycling with surface membrane channels. *J. Mol. Cell. Cardiol.* 47, 456–474. doi: 10.1016/j.yjmcc.2009.06.014

Vinogradova, T. M., Lyashkov, A. E., Zhu, W., Ruknudin, A. M., Sirenko, S., Yang, D., et al. (2006). High basal protein kinase A-dependent phosphorylation drives rhythmic internal Ca2+ store oscillations and spontaneous beating of cardiac pacemaker cells. *Circ. Res.* 98, 505–514. doi: 10.1161/01.RES.0000204575.94040.d1

Vinogradova, T. M., Maltsev, V. A., Bogdanov, K. Y., Lyashkov, A. E., and Lakatta, E. G. (2005). Rhythmic Ca2+ oscillations drive sinoatrial nodal cell pacemaker function to make the heart tick. *Ann. N.Y. Acad. Sci.* 1047, 138–156. doi: 10.1196/annals.1341.013

Vinogradova, T. M., Sirenko, S., Lyashkov, A. E., Younes, A., Li, Y., Zhu, W., et al. (2008). Constitutive phosphodiesterase activity restricts spontaneous beating rate of cardiac pacemaker cells by suppressing local Ca2+ releases. *Circ. Res.* 102, 761–769. doi: 10.1161/CIRCRESAHA.107.161679

Vinogradova, T. M., Zhou, Y. Y., Bogdanov, K. Y., Yang, D., Kuschel, M., Cheng, H., et al. (2000). Sinoatrial node pacemaker activity requires Ca(2+)/calmodulin-dependent protein kinase II activation. *Circ. Res.* 87, 760–767. doi: 10.1161/01.RES.87.9.760

Vinogradova, T. M., Zhou, Y. Y., Maltsev, V., Lyashkov, A., Stern, M., and Lakatta, E. G. (2004). Rhythmic ryanodine receptor Ca2+ releases during diastolic depolarization of sinoatrial pacemaker cells do not require membrane depolarization. *Circ. Res.* 94, 802–809. doi: 10.1161/01.RES.0000122045.55331.0F

Wahl-Schott, C., Fenske, S., and Biel, M. (2014). HCN channels: new roles in sinoatrial node function. *Curr. Opin. Pharmacol.* 15, 83–90. doi: 10.1016/j.coph.2013.12.005

Wainger, B. J., Degennaro, M., Santoro, B., Siegelbaum, S. A., and Tibbs, G. R. (2001). Molecular mechanism of cAMP modulation of HCN pacemaker channels. *Nature* 411, 805–810. doi: 10.1038/35081088

Wang, Y., Tsui, H., Ke, Y., Shi, Y., Li, Y., Davies, L., et al. (2014). Pak1 is required to maintain ventricular Ca(2)(+) homeostasis and electrophysiological stability through SERCA2a regulation in mice. *Circ. Arrhythm. Electrophysiol.* 7, 938–948. doi: 10.1161/CIRCEP.113.001198

Wu, Y., and Anderson, M. E. (2014). CaMKII in sinoatrial node physiology and dysfunction. *Front. Pharmacol.* 5:48. doi: 10.3389/fphar.2014.00048

Wu, Y., Gao, Z., Chen, B., Koval, O. M., Singh, M. V., Guan, X., et al. (2009). Calmodulin kinase II is required for fight or flight sinoatrial node physiology. *Proc. Natl. Acad. Sci. U.S.A.* 106, 5972–5977. doi: 10.1073/pnas.0806422106

Xie, Y., Ding, W. G., and Matsuura, H. (2015). Ca^{2+}/calmodulin potentiates I Ks in sinoatrial node cells by activating Ca^{2+}/calmodulin-dependent protein kinase II. *Pflugers Arch.* 467, 241–251. doi: 10.1007/s00424-014-1507-1

Yaniv, Y., Maltsev, V. A., Escobar, A. L., Spurgeon, H. A., Ziman, B. D., Stern, M. D., et al. (2011). Beat-to-beat Ca(2+)-dependent regulation of sinoatrial

nodal pacemaker cell rate and rhythm. *J. Mol. Cell. Cardiol.* 51, 902–905. doi: 10.1016/j.yjmcc.2011.08.029

Yaniv, Y., Stern, M. D., Lakatta, E. G., and Maltsev, V. A. (2013). Mechanisms of beat-to-beat regulation of cardiac pacemaker cell function by Ca(2)(+) cycling dynamics. *Biophys. J.* 105, 1551–1561. doi: 10.1016/j.bpj.2013.08.024

Yoo, S., Lee, S. H., Choi, B. H., Yeom, J. B., Ho, W. K., and Earm, Y. E. (1998). Dual effect of nitric oxide on the hyperpolarization-activated inward current (I(f)) in sino-atrial node cells of the rabbit. *J. Mol. Cell. Cardiol.* 30, 2729–2738. doi: 10.1006/jmcc.1998.0845

Younes, A., Lyashkov, A. E., Graham, D., Sheydina, A., Volkova, M. V., Mitsak, M., et al. (2008). Ca(2+) -stimulated basal adenylyl cyclase activity localization in membrane lipid microdomains of cardiac sinoatrial nodal pacemaker cells. *J. Biol. Chem.* 283, 14461–14468. doi: 10.1074/jbc.M707540200

Yuill, K. H., and Hancox, J. C. (2002). Characteristics of single cells isolated from the atrioventricular node of the adult guinea-pig heart. *Pflugers Arch.* 445, 311–320. doi: 10.1007/s00424-002-0932-8

Zaza, A., Maccaferri, G., Mangoni, M., and Difrancesco, D. (1991). Intracellular calcium does not directly modulate cardiac pacemaker (if) channels. *Pflugers Arch.* 419, 662–664. doi: 10.1007/BF00370312

Zaza, A., Micheletti, M., Brioschi, A., and Rocchetti, M. (1997). Ionic currents during sustained pacemaker activity in rabbit sino-atrial myocytes. *J. Physiol.* 505(Pt 3), 677–688. doi: 10.1111/j.1469-7793.1997.677ba.x

Zhang, H., Butters, T., Adeniran, I., Higham, J., Holden, A. V., Boyett, M. R., et al. (2012). Modeling the chronotropic effect of isoprenaline on rabbit sinoatrial node. *Front. Physiol.* 3:241. doi: 10.3389/fphys.2012.00241

Zhang, Y. H., and Hancox, J. C. (2009). Regulation of cardiac Na+-Ca2+ exchanger activity by protein kinase phosphorylation–still a paradox? *Cell Calcium* 45, 1–10. doi: 10.1016/j.ceca.2008.05.005

Zhang, Z., Xu, Y., Song, H., Rodriguez, J., Tuteja, D., Namkung, Y., et al. (2002). Functional Roles of Ca(v)1.3 (alpha(1D)) calcium channel in sinoatrial nodes: insight gained using gene-targeted null mutant mice. *Circ. Res.* 90, 981–987. doi: 10.1161/01.RES.0000018003.14304.E2

Zhou, Q., Xiao, J., Jiang, D., Wang, R., Vembaiyan, K., Wang, A., et al. (2011). Carvedilol and its new analogs suppress arrhythmogenic store overload-induced Ca2+ release. *Nat. Med.* 17, 1003–1009. doi: 10.1038/nm.2406

Conflict of Interest Statement: The authors declare that the research was conducted in the absence of any commercial or financial relationships that could be construed as a potential conflict of interest.

frontiers in Physiology

ORIGINAL RESEARCH
published: 25 March 2015
doi: 10.3389/fphys.2015.00086

The involvement of TRPC3 channels in sinoatrial arrhythmias

Yue-Kun Ju[1], Bon Hyang Lee[1], Sofie Trajanovska[1], Gouliang Hao[2], David G. Allen[1]*, Ming Lei[2] and Mark B. Cannell[3]**

[1] Department of Physiology, School of Medical Sciences, Bosch Institute, University of Sydney, Sydney, NSW, Australia, [2] Department of Pharmacology, University of Oxford, Oxford, UK, [3] Department of Physiology and Pharmacology, University of Bristol, Bristol, UK

Atrial fibrillation (AF) is a significant contributor to cardiovascular morbidity and mortality. The currently available treatments are limited and AF continues to be a major clinical challenge. Clinical studies have shown that AF is frequently associated with dysfunction in the sino-atrial node (SAN). The association between AF and SAN dysfunction is probably related to the communication between the SAN and the surrounding atrial cells that form the SAN-atrial pacemaker complex and/or pathological processes that affect both the SAN and atrial simultaneously. Recent evidence suggests that Ca^{2+} entry through TRPC3 (Transient Receptor Potential Canonical-3) channels may underlie several pathophysiological conditions -including cardiac arrhythmias. However, it is still not known if atrial and sinoatrial node cells are also involved. In this article we will first briefly review TRPC3 and IP_3R signaling that relate to store/receptor-operated Ca^{2+} entry (SOCE/ROCE) mechanisms and cardiac arrhythmias. We will then present some of our recent research progress in this field. Our experiments results suggest that pacing-induced AF in angiotensin II (Ang II) treated mice are significantly reduced in mice lacking the TRPC3 gene ($TRPC3^{-/-}$ mice) compared to wild type controls. We also show that pacemaker cells express TRPC3 and several other molecular components related to SOCE/ROCE signaling, including STIM1 and IP_3R. Activation of G-protein coupled receptors (GPCRs) signaling that is able to modulate SOCE/ROCE and Ang II induced Ca^{2+} homeostasis changes in sinoatrial complex being linked to TRPC3. The results provide new evidence that TRPC3 may play a role in sinoatrial and atrial arrhythmias that are caused by GPCRs activation.

Keywords: TRPC3, receptor-operated Ca^{2+} entry, store-operated Ca^{2+} entry, arrhythmias, sinoatrial node

OPEN ACCESS

Edited by:
Christopher Huang, University of Cambridge, UK

Reviewed by:
Steve Poelzing, Virginia Tech, USA
Thomas Hund, Ohio State University, USA

****Correspondence:***
Yue-kun Ju and David G. Allen, Department of Physiology, School of Medical Sciences (F13), University of Sydney, Anderson Stuart Building, Eastern Ave., Sydney, NSW 2006, Australia
yue-kun.ju@sydney.edu.au; david.allen@sydney.edu.au;
Mark B. Cannell, Department of Physiology and Pharmacology, University of Bristol, Medical Sciences Building, University Walk, Bristol BS8 1TD, UK
mark.cannell@bristol.ac.uk

Specialty section:
This article was submitted to Cardiac Electrophysiology, a section of the journal Frontiers in Physiology

Received: *28 November 2014*
Accepted: *04 March 2015*
Published: *25 March 2015*

Citation:
Ju Y-K, Lee BH, Trajanovska S, Hao G, Allen DG, Lei M and Cannell MB (2015) The involvement of TRPC3 channels in sinoatrial arrhythmias. Front. Physiol. 6:86. doi: 10.3389/fphys.2015.00086

Introduction

The Role of Intracellular ca^{2+} in Sinoatrial Arrhythmias

In the normal heart, pacemaker cells in the sinoatrial node (SAN) generate spontaneous membrane depolarizations that trigger action potentials, which then propagate through the conduction system to initiate atrial and ventricular cell depolarization and contraction. In contrast to normal pacemaker activity, abnormal arrhythmogenic electrical activity can arise in ectopic sites due to impulse re-entry or abnormal spontaneous membrane depolarizations (Nattel, 2002).

SAN and the surrounding atria form the SAN-Atrial pacemaker complex, which can provide substrates for re-entrant activity that can lead to AF (Sanders et al., 2004; Fedorov et al., 2010).

Dysfunction of pacemaker ion channels, including altered HCN4 channels, are associated with familial tachycardia-bradycardia syndrome and atrial fibrillation (Duhme et al., 2013). While it is clear that cardiac arrhythmias, including SAN dysfunction and atrial fibrillation (AF), are multifactorial there is increasing experimental evidence for abnormal Ca^{2+} handling being a key factor (Dobrev and Nattel, 2008; Yeh et al., 2008) and is the focus of this paper.

The most prominent Ca^{2+}-dependent ionic current during pacemaker activity is the Na/Ca exchange (NCX) current which not only contributes to pacemaker current(s) but may also produce arrhythmogenic electrical activity (Sipido et al., 2006) which is related to abnormalities in Ca^{2+} handling leading to abnormal NCX currents (Hove-Madsen et al., 2004; Vest et al., 2005). Spontaneous Ca^{2+} release events or "leak" via the ryanodine receptor (RyR), the major cardiac SR Ca^{2+} release channel, will produce depolarizing NCX current and contribute spontaneous membrane depolarization(s) to feed the genesis of AF (for review see Greiser et al., 2011; Wakili et al., 2011). In addition, AF has also been linked to Ca^{2+} release via a second class of SR Ca^{2+} release channel, inositol 1,4,5-*tris*phosphate receptor family (IP_3Rs) (Woodcock et al., 2000; Mackenzie et al., 2002; Li et al., 2005; Berridge, 2009). Activation of IP_3Rs by IP_3 is linked to the activation of G-protein coupled receptors (GPCRs) and the phospholipase C (PLC)-IP_3 signaling pathway (see **Figure 1**). Activation of GPCRs by agonists such as angiotensin II (Ang II) or endothelin-1 (ET-1) can cause SAN dysfunction (Neef et al., 2010) and AF (Woodcock et al., 2000; Mackenzie et al., 2002; Li et al., 2005).

Previously, we reported that in mouse SAN, there is a substantial sarcolemmal Ca^{2+} influx upon SR Ca^{2+} store depletion, a phenomenon known as "store-operated Ca^{2+} entry" (SOCE) (Ju et al., 2007; Ju and Allen, 2007). We also showed that type II IP_3R are functionally expressed and affect Ca^{2+} handling and pacemaker activity in the mouse SAN and whose activation would lead to store depletion (Ju et al., 2011, 2012). The linkage between IP_3R activation and SOCE has proven elusive, but a potential candidate, was found in HEK 293 cells expressing the Transient Receptor Potential Canonical-3 (TRPC3) channel (see below) (Kiselyov et al., 1998).

TRPC3, SOCE/ROCE, and STIM1

Studies on the transient receptor potential (TRP) gene from *Drosophila* showed that it encodes a PLC-activated Ca^{2+} permeable channel. Subsequently, seven homologs of TRP channels have been identified in mammals, termed TRPC1 to TRPC7 (Montell et al., 2002). TRPCs are thought to be strong candidates for the elusive SOCE pathway (for review see Salido et al., 2009). We have found that the SAN expresses all TRPC subtypes except TRPC5 (Ju et al., 2007). Among them, TRPC3 was the only subtype located in the surface membrane of pacemaker cells, making this isoform the strongest candidate for the SOCE channel in SAN (Ju et al., 2007).

Ca^{2+} influx can also be triggered as a direct consequence of PLC activation and production of diacylglycerol (DAG) that is independent of SR Ca^{2+} store depletion and forms a "receptor-operated Ca^{2+} entry" (ROCE) pathway (Mohl et al., 2011) (**Figure 1**). ROCE pathways may be closely related to SOCE

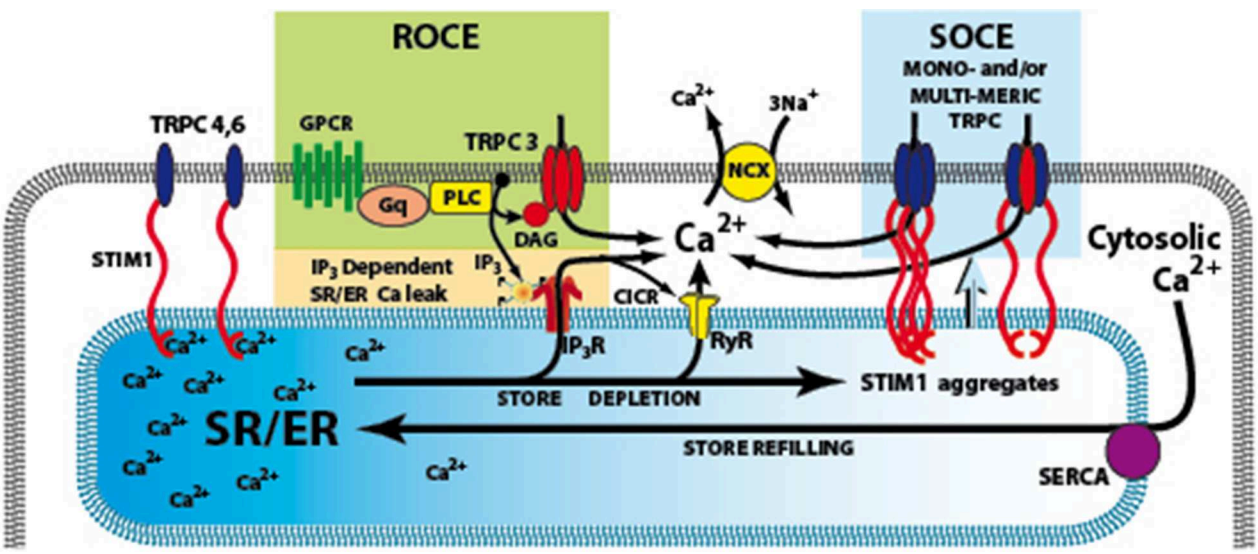

FIGURE 1 | Signaling pathways involved in the activation of TRPC3. The G-protein coupled receptor (GPCRs) activates phospholiase C (PLC), resulting in generation of IP3 and diacylglycerol (DAG). IP3 activates its receptor that leads to Ca^{2+} release from SR/ER and the depletion of SR/ER Ca^{2+} store. The Ca^{2+} content change in the store can be sensed by STIM1, the ER Ca^{2+} sensor and cause store-operated Ca^{2+} entry (SOCE) through TRPC3 channels. An additional or alternate possibility is that DAG can directly activate TRPC3, and produce receptor-operated Ca^{2+} entry (ROCE). GPCRs, G-protein coupled receptors; IP3R, inositol 1,4,5-trisphosphate receptors; PLC, Phospholipase C; ROCE, Receptor–operated Ca^{2+} entry; SOCE, store-operated Ca^{2+} entry; SR/ER, sarco- endo-plasmic reticulum; STIM1, stromal interacting molecule 1; TRPC3,4,6 canonical transient receptor potential channel types 3,4,6; NCX Na/Ca exchange.

because PLC activation can be enhanced by IP_3-induced store depletion. TRPC channels are non-selective Ca^{2+}-permeable cation channels which are activated by diacylglycerol (DAG) liberated from the plasma membrane, triggered by agonist binding to G protein—coupled receptors, such as angiotensin II and endothelin-1 receptors. Treatment with antisense RNA, to inhibit translation of endogenous TRPC3 mRNA, reduces Ca^{2+} influx activated either by receptor stimulation or passive store depletion (Wu et al., 2004; Worley et al., 2007). Therefore, it is possible that TRPC3 is involved in both SOCE and ROCE (see **Figure 1**) (for review see Birnbaumer, 2009).

Another important breakthrough in SOCE/ROCE research was the identification of a new component of SOCE called stromal interacting molecule 1 (STIM1) (Roos et al., 2005). STIM1 functions as an ER/SR Ca^{2+} sensor, probably via a STIM1 Ca^{2+} binding EF hand inside the SR/ER lumen. The activation of SOCE requires STIM1 migration in the SR/ER membrane where it interacts with other molecular components of the SOCE system (Lewis, 2007). In addition, conformation coupling between IP_3R and TRPC3 has been suggested as a mechanism of activation of TRPC3 (Kiselyov et al., 1998) and a region in the C terminus of TRPC3 has been shown to interact with IP_3 receptor as well as calmodulin (Calmodulin/IP_3 receptor-binding region (Zhang et al., 2001).

TRPC3 in cardiac cells provides a Ca^{2+} entry pathway that is connected to pathological signaling of the heart such as in cardiac hypertrophy (Onohara et al., 2006; Eder and Molkentin, 2011). However, there is little functional data on the role of TRPC3 in pacemaker and atrial cells to date. In the present study, we present new data suggesting that pacemaker cells expresses the molecular components of SOCE/ROCE pathways, including TRPC3, STIM1, and IP_3R2. We present preliminary experiments using TRPC3$^{-/-}$ mice and the specific TRPC3 channel blocker Pyr10 to show that TRPC3 appears to be able to contribute to sinoatrial and atrial arrhythmias induced by activation of GPCR Ca^{2+} signaling.

Material and Methods

Animals

Colonies of TRPC3$^{-/-}$ mice (Hartmann et al., 2008) and their wild-type litter mates were gifts from Prof. Housley's laboratory at University of New South Wales. The mice were deeply anesthetised with intra peritoneal pentobarbitone (1 ml/2 kg) before any procedures were carried out. All procedures on mice were performed according to the guidelines of the National Health and Medical Research Council of Australia and approved by the Institutional Ethics Committee.

Electrophysiological Studies in Langendorff-Perfused Hearts

Hearts were cannulated and perfused with a modified Tyrode's solution containing (in mM/L) 130 NaCl, 1.8 $CaCl_2$, 1.2 MgCl, 5.4 KCl, 1.2 NaH_2PO_4, 12 $NaHCO_3$, 11 glucose, 10 HEPES, with pH adjusted to 7.4 with NaOH. Perfusion was set at a constant flow rate of 2–2.5 ml/min and solutions were oxygenated with 95% O_2–5% CO_2. Electrical activity was recorded with two miniature monopolar ECG electrodes (Harvard Apparatus) placed on the atria and ventricle (Zhang et al., 2011). To determine the electrical conduction velocity of SAN and surrounding atrial tissue, custom-made electrode arrays were used to record the electrical activity from the isolated Langendorff-perfused hearts as described previously (Davies et al., 2014). To assess atrial arrhythmogenesis, Langendorff-perfused hearts from WT and KO mice were subjected to programmed electrical stimulation with three different pacing protocols as described elsewhere (Head et al., 2005; Zhang et al., 2011). Atrial tachycardia (AT) was defined as a sequence of three or more atrial depolarizations at the rate of 10 Hz or more than 10Hz. AF were characterized by irregular fibrillating waveforms. Sinus bradycardia was defined as a 30% reduction of baseline heart rate (HR) from the control condition. An arrhythmia index was calculated by the number of mice that have pacing induced arrhythmias events/the total number of mice in each group.

The Preparation of Intact SAN and Single Pacemaker Cells

Intact SANs were micro-dissected from right atria as described previously (Ju et al., 2007). The central SAN was identified from anatomical land marks, including the superior vena cava, the crista terminalis, and the interatrial septum (Marionneau et al., 2005). For physiological experiments, the intact SANs were continuously superfused with Tyrode's solution at 33°C.

Measurement of Intracellular Ca^{2+}, SOCE and ROCE

The isolated SANs were loaded with membrane-permeant fluorescent Ca^{2+} indicators, indo-1-AM or Fluo-4-AM (10 μM/L), using established methods (Ju and Allen, 1998; Ju et al., 2003). To measure Ca^{2+} influx through SOCE in sinoatrial tissue, preparations were exposed to a nominally Ca^{2+} free solution with the SR CaATPase pump inhibitor, cyclopiazonic acid (CPA, 10 μM) for 15 min to deplete the SR Ca^{2+} store. SOCE then occurs upon reintroduction of Ca^{2+} to the perfusate (Ju et al., 2007). ROCE was determined by measuring the agonist-mediated increases in $[Ca^{2+}]_i$ (Ang II, 1 μM/L and/or 1-oleoyl-2-acetyl-sn-glycerol - OAG, 100 μM/L) (Ikeda et al., 2013).

Immunohistochemistry

A rabbit polyclonal antibody was used to label type II IP_3Rs (1:200; Affinity Bioreagents) and TRPC3 (1:100, Alomone Lab) in single isolated pacemaker cells. A mouse antibody to STIM1 was also used (1:100, BD Biosciences). Anti-mouse or anti-rabbit secondary antibodies (Alexa-488 anti-mouse and Alexa-594 anti-rabbit (Molecular Probes) were used as secondary antibodies. Prolong gold antifade reagent with DAPI (Molecular Probes) was used as the mounting media and to provide nuclear staining.

Osmotic Mini-Pump Implantation

Alzet osmotic mini-pumps were implanted subcutaneously in WT, or TRPC3$^{-/-}$ mice. Ang II was delivered at the rate of 2 μg/g/day for 10–14 days.

Statistics

Data are expressed as mean ± SEM, with the number of preparations as n. Statistical tests were either Student's paired or unpaired t-tests, and $P < 0.05$ was used as the limit of statistical confidence.

Results

Evidence for TRPC3 Involvment in Atrial Arrhythmias

Ang II signaling pathways lead to a hypertrophy which seems to be related to TRPC3 expression (Onohara et al., 2006). To examine whether TRPC3 is involved in AF induced by Ang II, we induced AF in mice by pacing Langendorff-perfused hearts from WT and TRPC3$^{-/-}$ KO mice which had been treated with Ang II (See Methods) over of 10–14 days. **Figure 2A** shows the conduction of the AP across the SAN to the atria reconstructed from the timing of the recorded electrical signals (panel below) using a 36 mini electrode array placed on the right atrium. Atrial arrhythmic events are illustrated in **Figure 2B**, and were induced by using a pacing protocol that varied pacing voltage and frequency. To investigate the possible role of TRPC3 in these arrhythmias, we made ECG recordings from Langendorff-perfused hearts under control condition in WT and TRPC3$^{-/-}$ respectively, as shown in the selected recordings illustrated in **Figure 2C**. Electrical pacing induced AF, AT, and conduction block were recorded and analyzed in WT and TRPC3$^{-/-}$, respectively (exemplar data shown in **Figure 2D**). We found that atrial arrhythmias induced by Ang II and pacing were significantly reduced in the TRPC3$^{-/-}$ mice compared to the controls ($P = 0.004$, $n = 11$) (**Figure 2E**).

We previously reported that that pacemaker cells express TRPC3 and it is preferentially localized to the surface membrane (Ju et al., 2007). Therefore, the increased resistance to arrhythmias in TRPC3$^{-/-}$ mice supports the idea of a possible involvement of TRPC3 in arrhythmogenesis. As described above, Ca^{2+} entry through TRPC3 channel activated via a SOCE/ROCE signaling pathway and STIM1 could contribute arrhythmogenic current. To investigate this possibility, we examined expression and molecular localisation of STIM1, and the possibility of molecular interaction between TRPC3, STIM1, and IP$_3$R2 in isolated cardiac pacemaker cells.

Mouse Pacemaker Cells Express STIM1, a Molecular Component of SOCE /ROCE

Previously, we demonstrated that mouse SAN tissue expressing HCN4 mRNA also expressed TRPC3 (Ju et al., 2007). We also found that pacemaker tissue express STIM1 mRNA and protein (Liu et al., 2015). In the present study we wanted to extend these findings to the localisation of TRPC3 and STIM1 in single isolated pacemaker cells. **Figure 3** shows that isolated group (**Figure 3A**) and single pacemaker cells (**Figure 1B**) were positively labeled with a HCN4 antibody (which is a common selective molecular marker for pacemaker cells). The cells isolated from same SAN region were then double labeled with TRPC3 and STIM1 antibodies, and exemplar data is shown in **Figure 3C**. TRPC3 (red) showed both a sarcomeric pattern as well as membrane staining while STIM1 (green) displayed both cytosolic and near membrane labeling. A previous study examined the interaction of all mammalian TRPC channels with topically expressed STIM1 and found that that the STIM1 ERM domain binds to TRPC1, TRPC4, and TRPC5 but not TRPC3, TRPC6, and TRPC7 (Worley et al., 2007). However, knock down of STIM1 significantly reduced the current carried by TRPC3 (Yuan et al., 2007). The expression of both TRPC3 and STIM1 in cardiac pacemaker cells suggested to us that TRPC3 could be involved in Ca^{2+} influx through SOCE.

We have previously reported that pacemaker cells express Type II IP$_3$R (IP$_3$R2) which can modulate pacemaker activity. To examine if IP$_3$R and STIM1 form a signaling complex in SAN we double labeled isolated pacemaker cells with anti-IP3R2 and anti-STIM1 antibodies. **Figure 3D** shows that STIM1 labeling occurred both in cell periphery as well as inside the cell. IR$_3$R2 was similarly distributed and there was some co-localization between these labels (yellow dots at the cell periphery in merged image). To achieve higher resolution (∼100 nm), a N-SIM/N-STORM super resolution microscope was used. **Figure 3E** shows the higher resolution N-SIM microscope image, which revealed tighter areas of co-localization between STIM1 and IP$_3$R2. Given that the necessary molecular components of SOCE/ROCE (including TRPC3, and STIM1) as well as IP$_3$R are present in pacemaker cells, we next examined if SOCE can be modulated by IP$_3$R activation.

Evidence for Interaction between IP$_3$Rs and SOCE in Mouse Pacemaker Tissue

To clarify if TRPC3 is involved in AF associated with GPCR activation (**Figure 2**), we examined whether SOCE /ROCE could be modified by GPCR activation. While we previously reported that enhanced IP$_3$R Ca^{2+} signaling modulated pacemaker firing rate, it remains unknown whether IP$_3$R agonists and antagonists (which can modulate heart rate) also modulate SOCE activity in SAN. Previous work on cardiac myocytes showed that overexpression of TRPC3 enhanced Ca^{2+} entry through SOCE while knock down of TRPCs inhibited SOCE (Wu et al., 2010). We therefore used the intact mouse SAN preparation loaded with the ratiometric Ca^{2+} indicator indo-1 to study the interaction between IP$_3$Rs and SOCE.

After initial incubation of the SAN in Ca^{2+} free Tyrode's with the SR uptake blocked with CPA (10 μmol/L), reintroduction of Ca^{2+} (1.8 mmol/L) caused a significant Ca^{2+} influx (i.e., SOCE) as shown by an increase in Indo-1 ratio (**Figure 4A**). Importantly, peak SOCE was increased by 63 ± 10% ($n = 4$, $P < 0.05$) in the presence of ET-1, a representative trace of which is shown in **Figure 4A**. Addition of the membrane permeant IP$_3$ analog, IP$_3$-BM (10 μmol/L) was also able to increase SOCE by 31 ± 10% ($n = 3$, data not shown). To test whether ET-1 or IP$_3$-BM acted by opening IP$_3$R release channels and thereby causing a greater store depletion (and hence SOCE), we examined the effect of enhancing store depletion by increasing both the CPA concentration and the incubation time in Ca^{2+} free solution. When the CPA concentration was increased from 10 μmol/L to 20 μmol/L and the incubation time in Ca^{2+} free buffer increased from 15 min to 30 min ET-1 was no longer able to further increase SOCE (**Figure 4B**). Similar results were found in three other

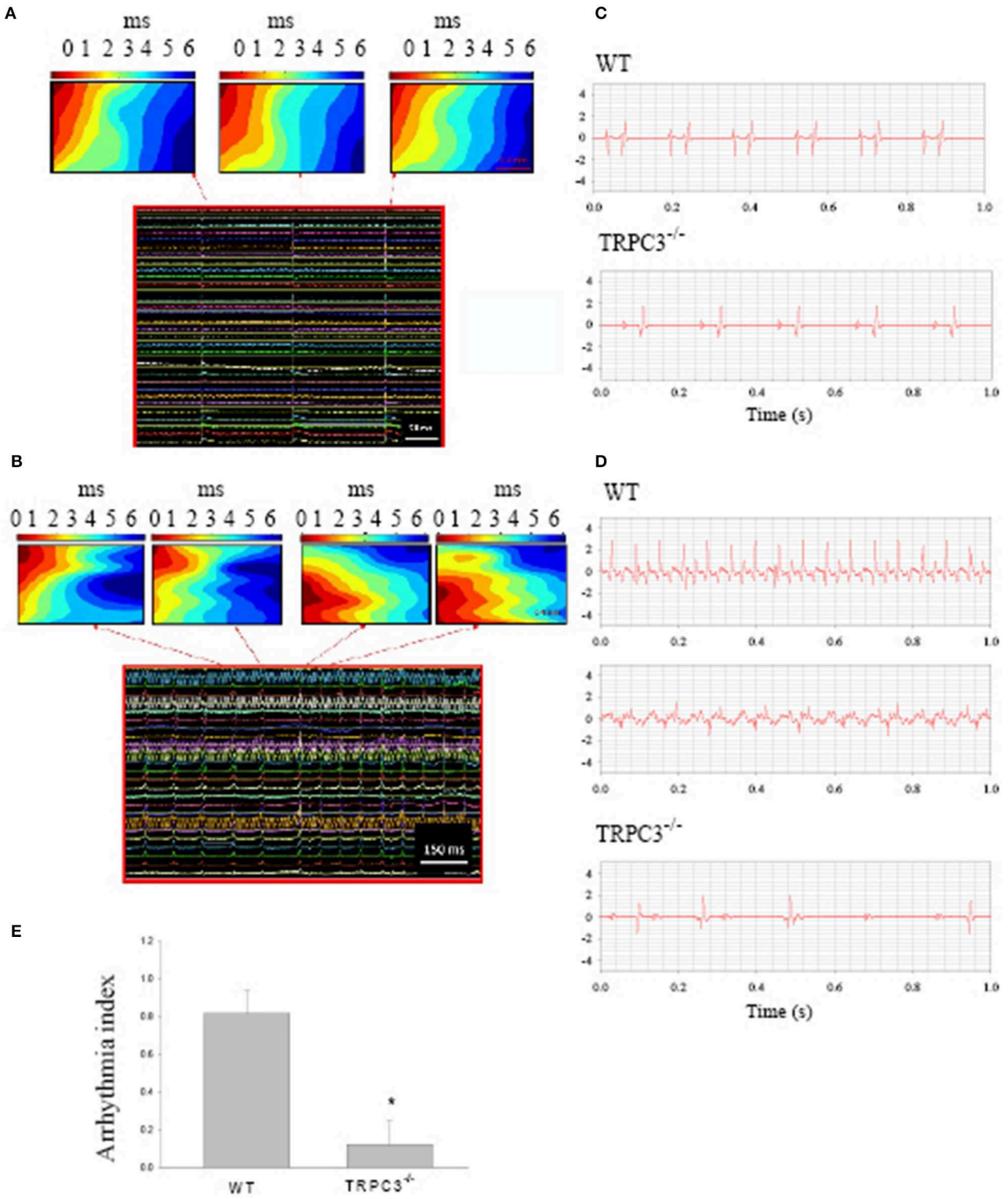

FIGURE 2 | Atrial arrhythmias induced by Ang II and pacing. Reconstructed excitation maps of data from multi-electrode array recordings (images below) from a Langendorff-perfused isolated heart. **(A)** sinus rhythm and **(B)** pacing induced atrial tachycardia. Note in AT, the ectopic beat starts from a different site to sinus rhythms. **(C)** Representative ECG recordings from isolated heart from WT and TRPC3 $^{-/-}$ mice under control conditions. **(D)** Atrial tachycardia and atrial fibrillation induced by burst pacing in WT mice and atrial-ventricular conduction block recorded from a TRPC$^{-/-}$ mouse heart respectively. **(E)** On average, the arrhythmia index was significant reduced in TRPC3KO mice ($n = 8$) compared to WT mice ($n = 11$, $P = 0.004$).

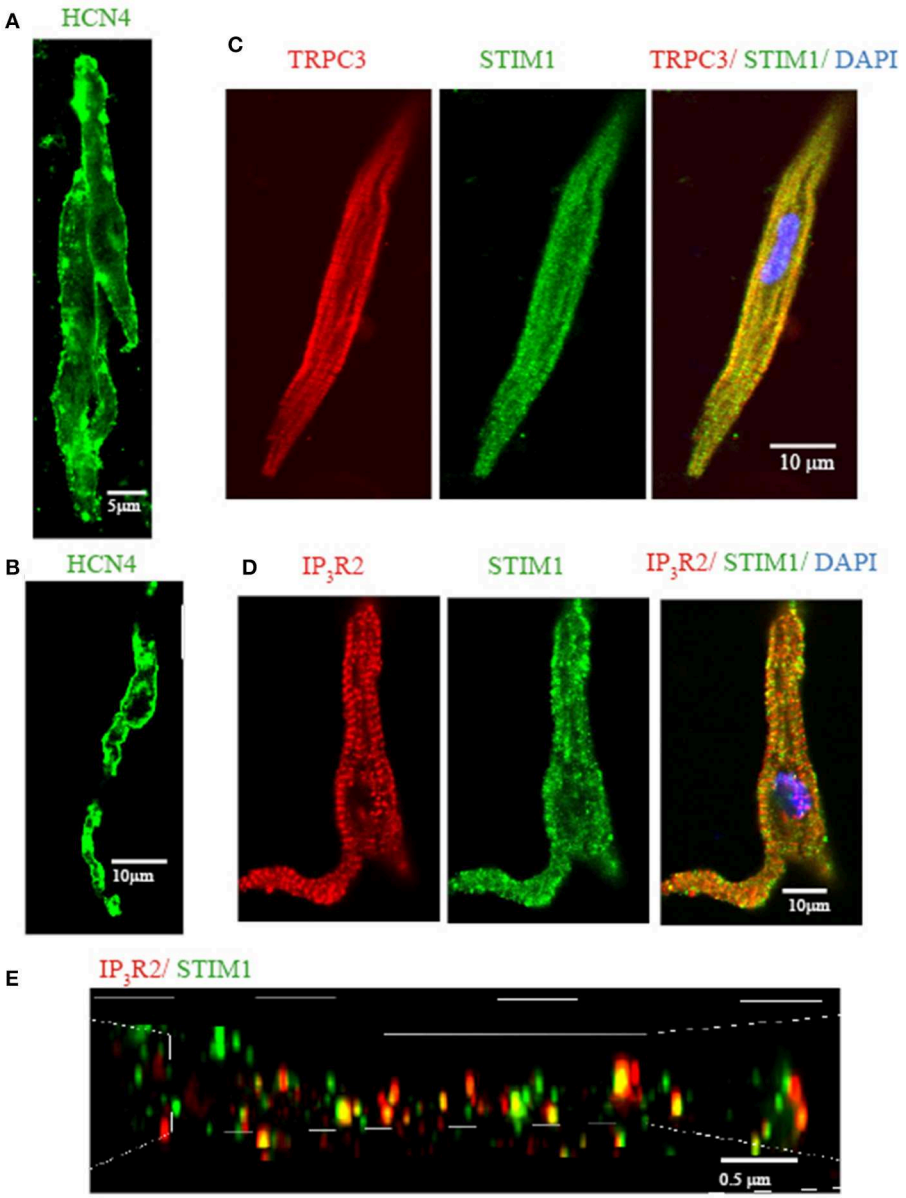

FIGURE 3 | Isolated single SAN cells express TRPC3, STIM1, and IP_3R2. Confocal immunofluorenscence images of isolated single pacemaker cells. Isolated group **(A)** and single **(B)** pacemaker cells were positively stained with anti HCN4 (in green). **(C)** Anti-TRPC3 in red, anti-STIM1 in green. **(D)** Anti-IP3R2 in red, anti-STIM1 in green. **(E)** 3D reconstruction image using N-SIM microscopy. Anti-IP_3R2 in red, anti-STIM1 in green. Areas of co-localisation appear yellow due to color mixing.

SAN preparations. These results suggest that ET-1 exerts its effects on SOCE via activation of IP_3Rs and caused Ca^{2+} release and store depletion rather than by direct stimulation of SOC channels.

Previous studies found that membrane permeant 2-APB has a direct effect on SOCE in some cell types, independent of its action as an IP_3R antagonist.(Bootman et al., 2002) We tested this possibility by adding 40 μmol/L 2-APB at the same time that Ca^{2+} was reintroduced to the solution (**Figure 4C**). Ca^{2+} influx through SOCE was not inhibited by 2-APB under these conditions, suggesting that 2-APB is not working as a direct SOCE channel blockers such as gadolinium or SKF-96365 (Ju et al., 2007). However, if 2-APB was added 15 min before reintroduction of Ca^{2+}, Ca^{2+} entry via SOCE was then significantly inhibited (**Figure 4D**). On average, Ca^{2+} entry through the SOCE channel with 2-APB decreased by 78 ± 8% ($n = 4$, $P < 0.01$). Thus, 2-APB does not serve as a classic SOCE channel blocker in pacemaker cells, but can inhibit SOCE by a slower mechanism which may involve IP_3R2 regulation as suggested previously (Ma et al., 2000). Although the specificity of 2-APB is questionable, we

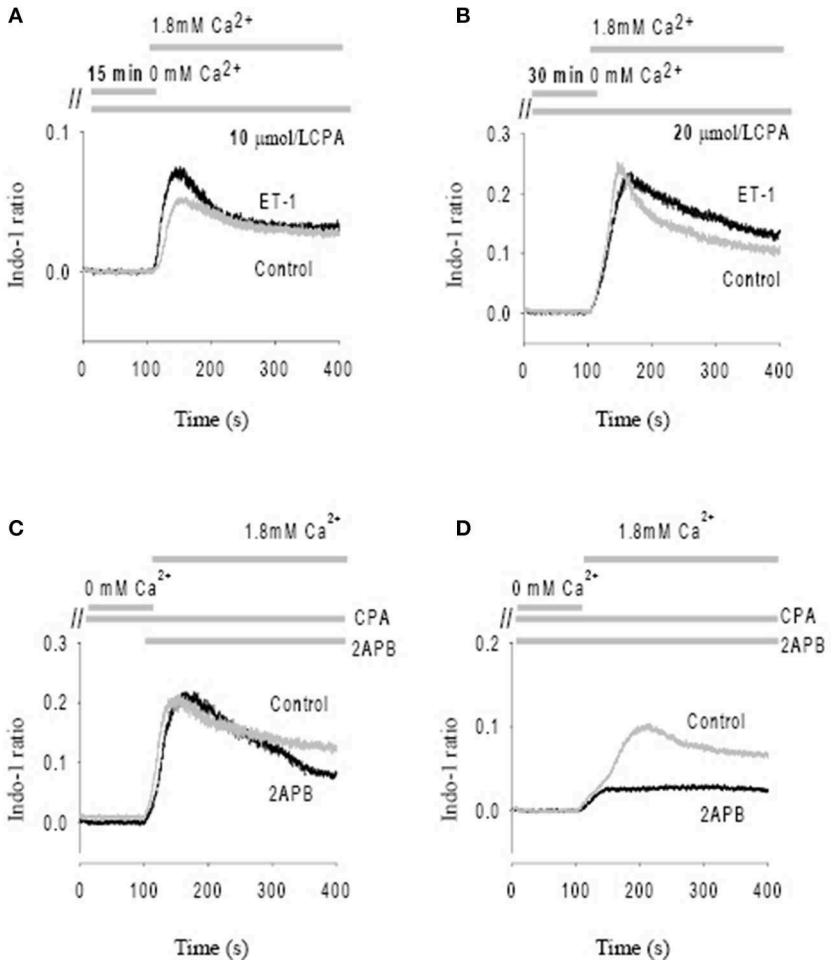

FIGURE 4 | Modulation of store-operated Ca entry (SOCE) by ET-1 and 2-APB. SOCE was induced by using cyclopiazonic acid (CPA) and low external Ca^{2+}. The addition timing of extracellular Ca^{2+} change is indicated in the top panels. **(A)** The effect of ET-1 on SOCE induced by 10 μM CPA with 15 min incubation in Ca^{2+} free Tyrode's solution. **(B)** The effect of ET-1 on SOCE induced by 20 μM CPA with 30 min incubation in Ca^{2+} free Tyrode's solution. **(C)** The effect of 40 μM 2-APB on SOCE. 2-APB was added in the same time of reintroduction of extracellular Ca^{2+} after perfusion of Ca^{2+} free Tyrode's Solution containing 10 μM CPA. **(D)** The effect of 40 μM 2-APB on SOCE. 2-APB was added into the Ca^{2+} free Tyrode's solution with 10 μM CPA during the 15 min incubation period. The gray traces represent controls; the black traces represent the treatments with ET-1 **(A,B)** or 2-APB **(C,D)**, respectively.

found that the effect of 2-APB was diminished in IP_3R2 KO, also supporting the involvement of IP_3R2 in the slower onset effects of 2-APB on SOCE. These data are consistent with a previous study that suggested 2-APB blocks activation of TRPC3 indirectly via disruption of the coupling process between SOCE, TRPC and IP_3R (Ma et al., 2002).

Evidence TRPC3 is Involved in ROCE in Intact Mouse Sinoatrial Node

TRPC3 has been implicated in not only SOCE but also ROCE (see Introduction) (for review see Birnbaumer, 2009). To further examine if Ca^{2+} influx through ROCE contributes to Ang II-induced arrhythmias we measured action potentials and Ca^{2+} influx in isolated SAN-atrial preparations treated with Ang II (1 μM) and/or OAG (100 μM), the agonists known to activate ROCE (Ikeda et al., 2013). Pyr3, a pyrazole derivative, has been suggested to be a blocker of TRPC3 (Kiyonaka et al., 2009) but it inhibits Orai1 mediated SOCE with similar potency (Salmon and Ahluwalia, 2010). Recently, a new selective blocker of TRPC3-ROCE blocker, Pyr10 has been developed and it displayed substantial selectivity for TRPC3-ROCE mediated responses over Orai1 mediated SOCE (Schleifer et al., 2012). We therefore studied the effect of Pyr10 on pacemaking and intracellular Ca^{2+} after application of Ang II and/or the DAG derivative, OAG.

Figure 5 shows action potentials recorded from an intact sinoatrial node preparation using conventional intracellular recording techniques. After application of 1 μM Ang II for 30 min, there was an increase in pacemaker firing rate associated with a depolarised membrane potential (**Figure 5B**). Application of 2 μM Pyr10 for 20 min, slowed pacemaker firing rate

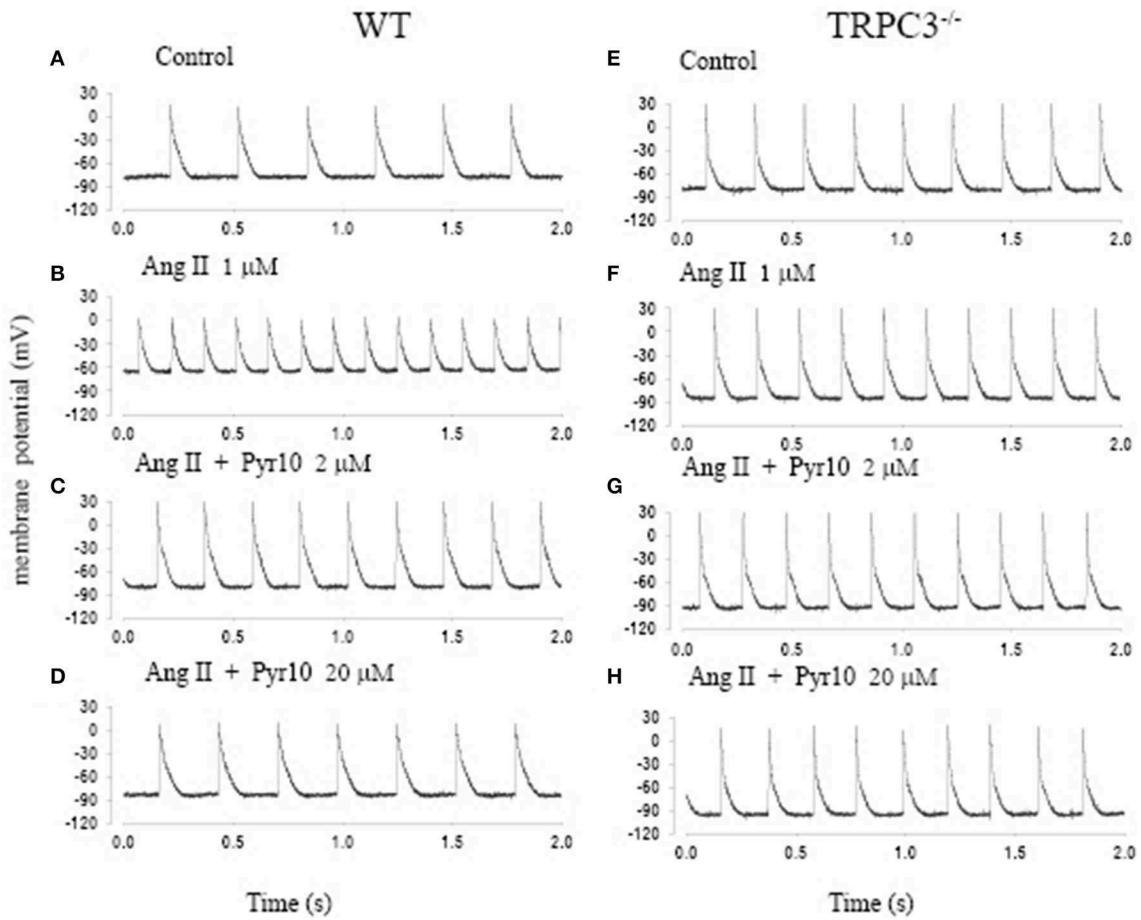

FIGURE 5 | The effect of angiotension II (Ang II) and a selective TRPC3 channel blocker Pyr10 on pacemaker action potential after application of Ang II. (A–D) Intracellular recordings from WT mice; **(E–H)** Intracellular recordings from TRPC3$^{-/-}$ mice with conditions as indicated in each panel.

with maximum diastolic potential returning to the control level (**Figure 5C**). Application of 20 μM Pyr10 further reduced firing rate within 7 min (**Figure 5D**). These results suggest that the membrane depolarization caused by Ang II could be reversed by the TRPC3 channel blocker. The results also support the idea that TRPC3 could be a channel that produces an inward current after GPCR activation by Ang II (Onohara et al., 2006). Importantly, and in contrast to WT mice, the pacemaker firing rate and action potential depolarization were not affected by Ang II and this response not significantly altered by application of Pyr10 to SAN from TRPC3 KO mice (**Figures 5E–H**). This is consistent with pacing induced AF in mice treated with Ang II being reduced in TRPC3$^{-/-}$ mice. (**Figure 2**) Therefore, these results strongly suggest that Pyr10 not only specifically blocked TRPC3 channels but that TRPC3 also contributes to pacemaker activity. To further investigate if the changes in pacemaker activity were related to Ca^{2+} entry through ROCE we examined intracellular Ca^{2+} changes caused by OAG and the effect of Pyr10. **Figure 6Aa** shows a representative intracellular Ca^{2+} signal recorded from a WT intact sinoatrial preparation loaded with the Ca^{2+} indicator indo-1. Both resting Ca^{2+} and Ca^{2+} transients were increased after 20 min application of 100 μM OAG (**Figure 6Ab**). Resting Ca^{2+} returned to the control level associated with a slowed firing rate after application of 2 μM Pyr10 for 15 min (**Figure 6Ac**). Further slowing and irregular pacemaker activity was apparent when the concentration of Pyr10 was increased to 20 μM for 15 min as shown in **Figure 6Ad**. On average, resting Ca^{2+} increased by 20.2 ± 6.9% ($P = 0.023$, $n = 5$); the Ca^{2+} transient also increased by 26.1 ± 5.6% ($p = 0.003$, $n = 5$) and was associated with a 13.9% increase in pacemaker firing rate ($p = 0.005$, $n = 5$,) in response to OAG treatment. There no significant changes by OAG in TRPC3 KO groups ($n = 4$) as shown in **Figure 6B**. The results further confirmed that TRPC3 was involved in OAG produced Ca^{2+} entry through ROCE upon GPCR activation. 2 μM Pyr10 significantly reduced the resting Ca^{2+} elevation produced by OAG treatment in WT but not in TRPC3 KO mice (**Figure 6C**). Unexpectedly, PyR10 produced no significant changes in Ca^{2+} transient amplitude and firing rate in both groups after exposure to OAG. The results indicated that Ca^{2+} entry through ROCE appeared to mainly influence resting Ca^{2+} in pacemaker cells and the lack of effect of PYR10 after OAG stimulation on the Ca^{2+} transient and pacemaker firing

rate may reflect additional effect(s) of PyR10 beyond TRPC3. In support of the latter idea, 20 μM Pyr10 reduced the amplitude of the Ca^{2+} transient in TRPC3 KO mice without significantly changing pacemaker firing rate or resting Ca^{2+} level (data not show).

Discussion

TRPC3 and Sino-Atrial Arrhythmias

In this study, we found that pacing-induced atrial fibrillation in angiotensin II treated mice was significantly reduced in mice lacking the TRPC3 gene ($TRPC3^{-/-}$ mice). This suggests that TRPC3 channels may be involved in Ang II induced changes in the electrical properties of sinoatrial tissue. Recent evidence has implicated Ca^{2+} entry through TRPC3 as a pro-arrhythmic pathway (Harada et al., 2012). TRPC3 is known to be up-regulated in AF patients and experimental goat and canine AF models and also mediates a non-selective cation current in atrial fibroblasts (Harada et al., 2012). TRPC3 has also been implicated in dysfunction of SAN (Yanni et al., 2011) and atrioventricular conduction block (Sabourin et al., 2012). Collectively, all of these studies point to a functional role for TRPC3 activation in cardiac tissue and linkage to arrhythmogenesis.

Some ryrazole derivatives have recently been suggested to be relatively selective blockers for TRPC channels (Schleifer et al., 2012). In WT mice, we showed that Pyr10, blocked the membrane depolarization of SAN cause by Ang II and attenuated the increase in pacemaker firing rate induced by Ang II (**Figure 5**). A higher concentration of Pyr10 (20 μM) induced slower and irregular pacemaker activity without changing the upstroke of the action potential (**Figure 5D**). The latter result suggests that Pyr10 did not block L-type Ca channels which provide the main cation current for the upstroke of pacemaker action potentials. (Irisawa et al., 1993) This effect of Pyr10 was similar to our previous observation using a different SOCE inhibitor (SKF-96365) (Ju et al., 2007). In contrast, Pyr10 did not cause any significant changes in slowing pacemaker action potentials recorded from sinoatrial tissue from $TRPC3^{-/-}$ mice (**Figure 5H**). These results suggest that Pyr10 is mainly active on a SAN diastolic membrane current, and is in accord with the idea that TRPC3 activation can provide a non-selective cation current in pacemaker cells (Eder and Molkentin, 2011). Intracellular Ca^{2+} measurements also showed that GPCR activation by Ang II or the DAG analog, OAG, caused an increase in both resting Ca^{2+} and Ca^{2+} transients that were associated with increased pacemaker firing rate in WT mice (**Figure 6**). The increased resting Ca^{2+} seemed directly related to ROCE as resting Ca^{2+} was significantly reduced in the presence of ROCE blocker, Pyr10 (**Figure 6C**). In contrast, such changes were absent in the $TRPC3^{-/-}$ group. These results provide further evidence that TRPC3 is involved in regulation of intracellular Ca^{2+} and ROCE mechanisms in SAN (**Figure 6**).

Interaction between IP_3R and SOCE in Cardiac Pacemaker Tissue

It has become generally accepted that Ca^{2+} release from the SR contributes to pacemaker activity through its influence on NCX currents (Ju and Allen, 2001; Vinogradova et al., 2005; Maltsev and Lakatta, 2008). Alterations in Ca^{2+} metabolism and consequent changes in Ca^{2+} dependent currents (such as NCX) have also been implicated in failure of pacemaker function and cardiac arrhythmias (Du and Nathan, 2007; Maltsev and Lakatta, 2007).

We previously reported that IP_3Rs are expressed in murine SAN and that the predominant isoform is the Type II IP_3R (IP_3R2) (Ju et al., 2011). Importantly, the modulation of pacemaker firing and intracellular Ca^{2+} by IP_3R-agonists and antagonists was abolished in IP_3R2 KO mice, demonstrating a clear functional, modulatory, role for IP_3R2 in SAN. The present study also supports the idea that Ca^{2+} release via IP_3Rs can modulate heart rate, depending on the activation of G-protein coupled receptors and the phospholipase C-IP_3 signaling pathway.

In non-excitable cells and smooth muscle, it has also been suggested that SOCE are coupled to IP_3Rs (Putney, 1986). Since the discovery of TRPC channels and their candidacy for the SOCE, interactions between IP_3Rs and members of the TRPC family have been reported (Vazquez et al., 2004). For example, it has been shown that IP_3R2 interacts with TRPC3 forming a protein complex that possibly underlies the enhanced SOCE activity seen in gravid uterine endothelium (Gifford et al., 2006). In the present study, we show that Ca^{2+} influx through SOCE in the SAN can be modulated by IP_3 agonists(ET-1, IP_3-BM) and IP_3R2 antagonists (2-APB) through mainly their effect on increasing Ca^{2+} release and hence reducing store content (see **Figure 4**). Since some IP_3Rs appear to be localized near the surface membrane, where TRPC3 is also located (Ju et al., 2007, 2011), it is possible that Ca^{2+} release via IP_3Rs could interact with these ion channels in the surface membrane (and/or affect their trafficking). IP_3R expression has been shown to increase in heart failure (Marks, 2000) and in atrial fibrillation (Yamada et al., 2002), which raises the possibility that this IP3-TRPC signaling system may become more important in pathological conditions (Worley et al., 2007; Ju et al., 2012).

SOCE over ROCE in Cardiac Tissue

As described above, SOCE and ROCE may be linked phenomena but the extent to which these mechanisms cross-communicate/activate is unclear -especially after GPCR activation of PLC which triggers formation of IP_3 and DAG (Liao et al., 2009). While it has been established that TRPC3 is involved in ROCE (Hofmann et al., 1999), it remains uncertain whether TRPC3 can also contribute to SOCE (for review see Cahalan, 2009) (Zagranichnaya et al., 2005; Dehaven et al., 2009).

We showed that TRPC3 expressing pacemaker cells also express the ER-Ca^{2+} sensor protein, STIM1. The latter may provide the missing molecular signaling link between Ca^{2+} release via IP_3Rs, store depletion and the activation of SOCE(Lewis, 2007; Yuan et al., 2007). However, it remains unclear whether STIM1 directly regulates the TRPC channels related to SOCE (Worley et al., 2007; Yuan et al., 2007; Dehaven et al., 2009). In addition to TRPCs, Orai1 is a protein that may produce a specific SOCE pathway and appears as a Ca^{2+} release activated Ca^{2+} current (Icrac). While we found that Orai1 is expressed in mouse pacemaker cells (not shown), TRPC3 was more dominant at both mRNA and protein levels (Ju et al., 2007). It has been suggested that TRPC3 and Orai1 may form a complex that

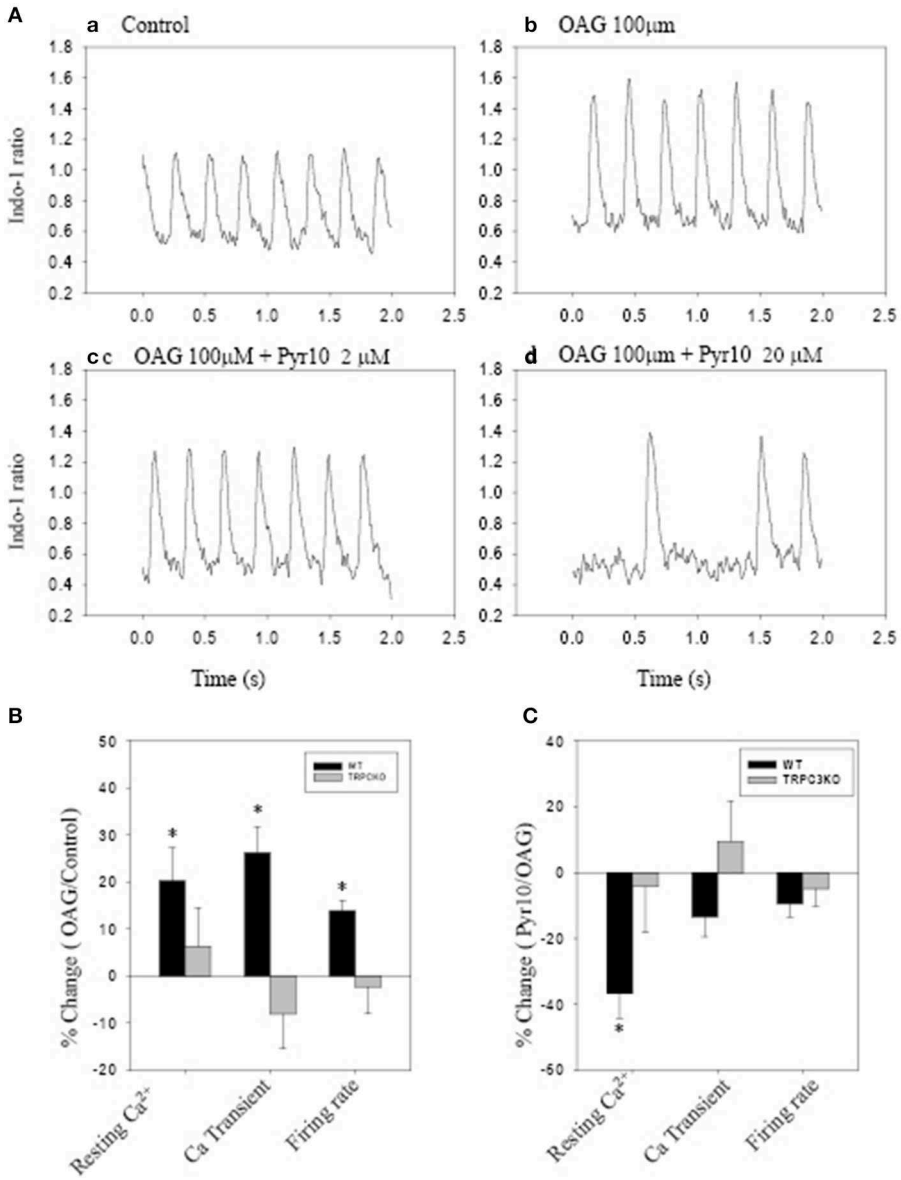

FIGURE 6 | The effect of Pyr10 on intracellular Ca^{2+} after application of 1-oleoy1-2-acyl-sn-glycerol (OAG) 100 μM. The intact SANs were loaded with Ca^{2+} indicator indo-1. **(A,B)** show intracellular Ca^{2+} recordings from a WT mouse. **(B,C)** The statistics pool data shows percentage changes in resting Ca^{2+}, Ca^{2+} transient and firing rate in WT and TRPC3 KO mice respectively. **(B)** OAG treatment against control. **(C)** 2 μM Pyr10 treatment against OAG treatment. $^{*}P < 0.05$.

mediates both SOCE and ROCE and the conversion from ROCE to SOCE may be mediated through STIM1 binding (Liao et al., 2008).

The Limitation of Current Study

The current study does not rule out the possibility that Pyr10 has effects on currents other than TRPC3, such as I_f. In addition, it would be desirable to examine if other molecular components, such as NCX, SERCA, etc. that regulate intracellular Ca^{2+} are changed in TRPC3$^{-/-}$ mice. Despite these limitations, we shown that Ca^{2+} entry through both SOCE and ROCE occurs in murine SAN and appears to be regulated by the GPCRs in a GPCR≫ PLC ≫ IP_3R/DAG ≫ Ca^{2+} signal transduction cascade. We suggest that TRPC3 channels might provide a potential target for future treatment of SAN dysfunction and AF as it links both receptor activation and intracellular Ca^{2+} signaling.

Acknowledgments

This study was supported by the National Health and Medical Research Council of Australia (program grant 354400, and project grant 570926).

References

Berridge, M. J. (2009). Inositol trisphosphate and calcium signalling mechanisms. *Biochim. Biophys. Acta* 1793, 933–940. doi: 10.1016/j.bbamcr.2008.10.005

Birnbaumer, L. (2009). The TRPC class of ion channels: a critical review of their roles in slow, sustained increases in intracellular Ca(2+) concentrations. *Annu. Rev. Pharmacol. Toxicol.* 49, 395–426. doi: 10.1146/annurev.pharmtox.48.113006.094928

Bootman, M. D., Collins, T. J., Mackenzie, L., Roderick, H. L., Berridge, M. J., and Peppiatt, C. M. (2002). 2-aminoethoxydiphenyl borate (2-APB) is a reliable blocker of store- operated Ca2+ entry but an inconsistent inhibitor of InsP3-induced Ca2+ release. *FASEB J.* 16, 1145–1150. doi: 10.1096/fj.02-0037rev

Cahalan, M. D. (2009). STIMulating store-operated Ca(2+) entry. *Nat. Cell Biol.* 11, 669–677. doi: 10.1038/ncb0609-669

Davies, L., Jin, J., Shen, W., Tsui, H., Shi, Y., Wang, Y., et al. (2014). Mkk4 is a negative regulator of the transforming growth factor beta 1 signaling associated with atrial remodeling and arrhythmogenesis with age. *J. Am. Heart Assoc.* 3:e000340. doi: 10.1161/JAHA.113.000340

Dehaven, W. I., Jones, B. F., Petranka, J. G., Smyth, J. T., Tomita, T., Bird, G. S., et al. (2009). TRPC channels function independently of STIM1 and Orai1. *J. Physiol.* 587, 2275–2298. doi: 10.1113/jphysiol.2009.170431

Dobrev, D., and Nattel, S. (2008). Calcium handling abnormalities in atrial fibrillation as a target for innovative therapeutics. *J. Cardiovasc. Pharmacol.* 52, 293–299. doi: 10.1097/FJC.0b013e318171924d

Du, Y. M., and Nathan, R. D. (2007). Ionic basis of ischemia-induced bradycardia in the rabbit sinoatrial node. *J. Mol. Cell. Cardiol.* 42, 315–325. doi: 10.1016/j.yjmcc.2006.10.004

Duhme, N., Schweizer, P. A., Thomas, D., Becker, R., Schroter, J., Barends, T. R., et al. (2013). Altered HCN4 channel C-linker interaction is associated with familial tachycardia-bradycardia syndrome and atrial fibrillation. *Eur. Heart J.* 34, 2768–2775. doi: 10.1093/eurheartj/ehs391

Eder, P., and Molkentin, J. D. (2011). TRPC channels as effectors of cardiac hypertrophy. *Circ. Res.* 108, 265–272. doi: 10.1161/CIRCRESAHA.110.225888

Fedorov, V. V., Chang, R., Glukhov, A. V., Kostecki, G., Janks, D., Schuessler, R. B., et al. (2010). Complex interactions between the sinoatrial node and atrium during reentrant arrhythmias in the canine heart. *Circulation* 122, 782–789. doi: 10.1161/CIRCULATIONAHA.109.935288

Gifford, S. M., Yi, F. X., and Bird, I. M. (2006). Pregnancy-enhanced store-operated Ca2+ channel function in uterine artery endothelial cells is associated with enhanced agonist-specific transient receptor potential channel 3-inositol 1,4,5-trisphosphate receptor 2 interaction. *J. Endocrinol.* 190, 385–395. doi: 10.1677/joe.1.06773

Greiser, M., Lederer, W. J., and Schotten, U. (2011). Alterations of atrial Ca(2+) handling as cause and consequence of atrial fibrillation. *Cardiovasc. Res.* 89, 722–733. doi: 10.1093/cvr/cvq389

Harada, M., Luo, X., Qi, X. Y., Tadevosyan, A., Maguy, A., Ordog, B., et al. (2012). Transient receptor potential canonical-3 channel-dependent fibroblast regulation in atrial fibrillation. *Circulation* 126, 2051–2064. doi: 10.1161/CIRCULATIONAHA.112.121830

Hartmann, J., Dragicevic, E., Adelsberger, H., Henning, H. A., Sumser, M., Abramowitz, J., et al. (2008). TRPC3 channels are required for synaptic transmission and motor coordination. *Neuron* 59, 392–398. doi: 10.1016/j.neuron.2008.06.009

Head, C. E., Balasubramaniam, R., Thomas, G., Goddard, C. A., Lei, M., Colledge, W. H., et al. (2005). Paced electrogram fractionation analysis of arrhythmogenic tendency in DeltaKPQ Scn5a mice. *J. Cardiovasc. Electrophysiol.* 16, 1329–1340. doi: 10.1111/j.1540-8167.2005.00200.x

Hofmann, T., Obukhov, A. G., Schaefer, M., Harteneck, C., Gudermann, T., and Schultz, G. (1999). Direct activation of human TRPC6 and TRPC3 channels by diacylglycerol. *Nature* 397, 259–263. doi: 10.1038/16711

Hove-Madsen, L., Llach, A., Bayes-Genis, A., Roura, S., Rodriguez, F. E., Aris, A., et al. (2004). Atrial fibrillation is associated with increased spontaneous calcium release from the sarcoplasmic reticulum in human atrial myocytes. *Circulation* 110, 1358–1363. doi: 10.1161/01.CIR.0000141296.59876.87

Ikeda, K., Nakajima, T., Yamamoto, Y., Takano, N., Tanaka, T., Kikuchi, H., et al. (2013). Roles of transient receptor potential canonical (TRPC) channels and reverse-mode Na+/Ca2+ exchanger on cell proliferation in human cardiac fibroblasts: effects of transforming growth factor beta1. *Cell Calcium* 54, 213–225. doi: 10.1016/j.ceca.2013.06.005

Irisawa, H., Brown, H. F., and Giles, W. (1993). Cardiac pacemaking in the sinoatrial node. *Physiol. Rev.* 73, 197–227.

Ju, Y. K., and Allen, D. G. (1998). Intracellular calcium and Na^+-Ca^{2+} exchange current in isolated toad pacemaker cells. *J. Physiol.* 508, 153–166. doi: 10.1111/j.1469-7793.1998.153br.x

Ju, Y. K., and Allen, D. G. (2001). Does Ca^{2+} release from the sarcoplasmic reticulum influence heart rate? *Clin. Exp. Pharmacol. Physiol.* 28, 703–708. doi: 10.1046/j.1440-1681.2001.03506.x

Ju, Y. K., and Allen, D. G. (2007). Store-operated Ca2+ entry and TRPC expression; possible roles in cardiac pacemaker tissue. *Heart Lung Circ.* 16, 349–355. doi: 10.1016/j.hlc.2007.07.004

Ju, Y. K., Chu, Y., Chaulet, H., Lai, D., Gervasio, O. L., Graham, R. M., et al. (2007). Store-operated Ca^{2+} influx and expression of TRPC genes in mouse sinoatrial node. *Circ. Res.* 100, 1605–1614. doi: 10.1161/CIRCRESAHA.107.152181

Ju, Y. K., Huang, W. B., Jiang, L., Barden, J. A., and Allen, D. G. (2003). ATP modulates intracellular Ca^{2+} and firing rate through a P2Y1 purinoceptor in cane toad pacemaker cells. *J. Physiol.* 552, 777–787. doi: 10.1113/jphysiol.2003.052258

Ju, Y. K., Liu, J., Lee, B. H., Lai, D., Woodcock, E. A., Lei, M., et al. (2011). Distribution and functional role of inositol 1,4,5-trisphosphate receptors in mouse sinoatrial node. *Circ. Res.* 109, 848–857. doi: 10.1161/CIRCRESAHA.111.243824

Ju, Y. K., Woodcock, E. A., Allen, D. G., and Cannell, M. B. (2012). Inositol 1,4,5-trisphosphate receptors and pacemaker rhythms. *J. Mol. Cell. Cardiol.* 53, 375–381. doi: 10.1016/j.yjmcc.2012.06.004

Kiselyov, K., Xu, X., Mozhayeva, G., Kuo, T., Pessah, I., Mignery, G., et al. (1998). Functional interaction between InsP3 receptors and store-operated Htrp3 channels. *Nature* 396, 478–482. doi: 10.1038/24890

Kiyonaka, S., Kato, K., Nishida, M., Mio, K., Numaga, T., Sawaguchi, Y., et al. (2009). Selective and direct inhibition of TRPC3 channels underlies biological activities of a pyrazole compound. *Proc. Natl. Acad. Sci. U.S.A.* 106, 5400–5405. doi: 10.1073/pnas.0808793106

Lewis, R. S. (2007). The molecular choreography of a store-operated calcium channel. *Nature* 446, 284–287. doi: 10.1038/nature05637

Li, X., Zima, A. V., Sheikh, F., Blatter, L. A., and Chen, J. (2005). Endothelin-1-induced arrhythmogenic Ca2+ signaling is abolished in atrial myocytes of inositol-1,4,5-trisphosphate(IP3)-receptor type 2-deficient mice. *Circ. Res.* 96, 1274–1281. doi: 10.1161/01.RES.0000172556.05576.4c

Liao, Y., Erxleben, C., Abramowitz, J., Flockerzi, V., Zhu, M. X., Armstrong, D. L., et al. (2008). Functional interactions among Orai1, TRPCs, and STIM1 suggest a STIM-regulated heteromeric Orai/TRPC model for SOCE/Icrac channels. *Proc. Natl. Acad. Sci. U.S.A.* 105, 2895–2900. doi: 10.1073/pnas.0712288105

Liao, Y., Plummer, N. W., George, M. D., Abramowitz, J., Zhu, M. X., and Birnbaumer, L. (2009). A role for Orai in TRPC-mediated Ca2+ entry suggests that a TRPC:Orai complex may mediate store and receptor operated Ca2+ entry. *Proc. Natl. Acad. Sci. U.S.A.* 106, 3202–3206. doi: 10.1073/pnas.0813346106

Liu, J., Xin, L., Benson, V. L., Allen, D. G., and Ju, Y.-K. (2015). Store-operated calcium entry and the localization of STIM1 and Orai1 proteins in isolated mouse sinoatrial node cells. *Front. Physiol.* 6:69. doi: 10.3389/fphys.2015.00069

Ma, H. T., Patterson, R. L., van Rossum, D. B., Birnbaumer, L., Mikoshiba, K., and Gill, D. L. (2000). Requirement of the inositol trisphosphate receptor for activation of store-operated Ca2+ channels. *Science* 287, 1647–1651. doi: 10.1126/science.287.5458.1647

Ma, H. T., Venkatachalam, K., Parys, J. B., and Gill, D. L. (2002). Modification of store-operated channel coupling and inositol trisphosphate receptor function by 2-aminoethoxydiphenyl borate in DT40 lymphocytes. *J. Biol. Chem.* 277, 6915–6922. doi: 10.1074/jbc.M107755200

Mackenzie, L., Bootman, M. D., Laine, M., Berridge, M. J., Thuring, J., Holmes, A., et al. (2002). The role of inositol 1,4,5-trisphosphate receptors in Ca^{2+} signalling and the generation of arrhythmias in rat atrial myocytes. *J. Physiol.* 541, 395–409. doi: 10.1113/jphysiol.2001.013411

Maltsev, V. A., and Lakatta, E. G. (2007). Cardiac pacemaker cell failure with preserved I(f), I(CaL), and I(Kr): a lesson about pacemaker function learned from ischemia-induced bradycardia. *J. Mol. Cell. Cardiol.* 42, 289–294. doi: 10.1016/j.yjmcc.2006.11.009

Maltsev, V. A., and Lakatta, E. G. (2008). Dynamic interactions of an intracellular Ca^{2+} clock and membrane ion channel clock underlie robust initiation and regulation of cardiac pacemaker function. *Cardiovasc. Res.* 77, 274–284. doi: 10.1093/cvr/cvm058

Marionneau, C., Couette, B., Liu, J., Li, H., Mangoni, M. E., Nargeot, J., et al. (2005). Specific pattern of ionic channel gene expression associated with pacemaker activity in the mouse heart. *J. Physiol.* 562, 223–234. doi: 10.1113/jphysiol.2004.074047

Marks, A. R. (2000). Cardiac intracellular calcium release channels—role in heart failure. *Circ. Res.* 87, 8–11. doi: 10.1161/01.RES.87.1.8

Mohl, M. C., Iismaa, S. E., Xiao, X. H., Friedrich, O., Wagner, S., Nikolova-Krstevski, V., et al. (2011). Regulation of murine cardiac contractility by activation of alpha(1A)-adrenergic receptor-operated Ca(2+) entry. *Cardiovasc. Res.* 91, 310–319. doi: 10.1093/cvr/cvr081

Montell, C., Birnbaumer, L., and Flockerzi, V. (2002). The TRP channels, a remarkably functional family. *Cell* 108, 595–598. doi: 10.1016/S0092-8674(02)00670-0

Nattel, S. (2002). New ideas about atrial fibrillation 50 years on. *Nature* 415, 219–226. doi: 10.1038/415219a

Neef, S., Dybkova, N., Sossalla, S., Ort, K. R., Fluschnik, N., Neumann, K., et al. (2010). CaMKII-dependent diastolic SR Ca2+ leak and elevated diastolic Ca2+ levels in right atrial myocardium of patients with atrial fibrillation. *Circ. Res.* 106, 1134–1144. doi: 10.1161/CIRCRESAHA.109.203836

Onohara, N., Nishida, M., Inoue, R., Kobayashi, H., Sumimoto, H., Sato, Y., et al. (2006). TRPC3 and TRPC6 are essential for angiotensin II-induced cardiac hypertrophy. *EMBO J.* 25, 5305–5316. doi: 10.1038/sj.emboj.7601417

Putney, J. W. Jr. (1986). A model for receptor-regulated calcium entry. *Cell Calcium* 7, 1–12. doi: 10.1016/0143-4160(86)90026-6

Roos, J., DiGregorio, P. J., Yeromin, A. V., Ohlsen, K., Lioudyno, M., Zhang, S., et al. (2005). STIM1, an essential and conserved component of store-operated Ca2+ channel function. *J. Cell Biol.* 169, 435–445. doi: 10.1083/jcb.200502019

Sabourin, J., Antigny, F., Robin, E., Frieden, M., and Raddatz, E. (2012). Activation of transient receptor potential canonical 3 (TRPC3)-mediated Ca2+ entry by A1 adenosine receptor in cardiomyocytes disturbs atrioventricular conduction. *J. Biol. Chem.* 287, 26688–26701. doi: 10.1074/jbc.M112.378588

Salido, G. M., Sage, S. O., and Rosado, J. A. (2009). TRPC channels and store-operated Ca(2+) entry. *Biochim. Biophys. Acta* 1793, 223–230. doi: 10.1016/j.bbamcr.2008.11.001

Salmon, M. D., and Ahluwalia, J. (2010). Discrimination between receptor- and store-operated Ca(2+) influx in human neutrophils. *Cell. Immunol.* 265, 1–5. doi: 10.1016/j.cellimm.2010.07.009

Sanders, P., Morton, J. B., Kistler, P. M., Spence, S. J., Davidson, N. C., Hussin, A., et al. (2004). Electrophysiological and electroanatomic characterization of the atria in sinus node disease: evidence of diffuse atrial remodeling. *Circulation* 109, 1514–1522. doi: 10.1161/01.CIR.0000121734.47409.AA

Schleifer, H., Doleschal, B., Lichtenegger, M., Oppenrieder, R., Derler, I., Frischauf, I., et al. (2012). Novel pyrazole compounds for pharmacological discrimination between receptor-operated and store-operated Ca(2+) entry pathways. *Br. J. Pharmacol.* 167, 1712–1722. doi: 10.1111/j.1476-5381.2012.02126.x

Sipido, K. R., Varro, A., and Eisner, D. (2006). Sodium calcium exchange as a target for antiarrhythmic therapy. *Handb. Exp. Pharmacol.* 159–199. doi: 10.1007/3-540-29715-4_6

Vazquez, G., Wedel, B. J., Aziz, O., Trebak, M., and Putney, J. W. Jr. (2004). The mammalian TRPC cation channels. *Biochim. Biophys. Acta* 1742, 21–36. doi: 10.1016/j.bbamcr.2004.08.015

Vest, J. A., Wehrens, X. H., Reiken, S. R., Lehnart, S. E., Dobrev, D., Chandra, P., et al. (2005). Defective cardiac ryanodine receptor regulation during atrial fibrillation. *Circulation* 111, 2025–2032. doi: 10.1161/01.CIR.0000162461.67140.4C

Vinogradova, T. M., Maltsev, V. A., Bogdanov, K. Y., Lyashkov, A. E., and Lakatta, E. G. (2005). Rhythmic Ca^{2+} oscillations drive sinoatrial nodal cell pacemaker function to make the heart tick. *Ann. N.Y. Acad. Sci.* 1047, 138–156. doi: 10.1196/annals.1341.013

Wakili, R., Voigt, N., Kaab, S., Dobrev, D., and Nattel, S. (2011). Recent advances in the molecular pathophysiology of atrial fibrillation. *J. Clin. Invest.* 121, 2955–2968. doi: 10.1172/JCI46315

Woodcock, E. A., Arthur, J. F., and Matkovich, S. J. (2000). Inositol 1,4,5-trisphosphate and reperfusion arrhythmias. *Clin. Exp. Pharmacol. Physiol.* 27, 734–737. doi: 10.1046/j.1440-1681.2000.03328.x

Worley, P. F., Zeng, W., Huang, G. N., Yuan, J. P., Kim, J. Y., Lee, M. G., et al. (2007). TRPC channels as STIM1-regulated store-operated channels. *Cell Calcium* 42, 205–211. doi: 10.1016/j.ceca.2007.03.004

Wu, X., Eder, P., Chang, B., and Molkentin, J. D. (2010). TRPC channels are necessary mediators of pathologic cardiac hypertrophy. *Proc. Natl. Acad. Sci. U.S.A.* 107, 7000–7005. doi: 10.1073/pnas.1001825107

Wu, X., Zagranichnaya, T. K., Gurda, G. T., Eves, E. M., and Villereal, M. L. (2004). A TRPC1/TRPC3-mediated increase in store-operated calcium entry is required for differentiation of H19-7 hippocampal neuronal cells. *J. Biol. Chem.* 279, 43392–43402. doi: 10.1074/jbc.M408959200

Yamada, J., Ohkusa, T., Nao, T., Ueyama, T., Yano, M., Kobayashi, S., et al. (2002). [Up-regulation of inositol 1, 4, 5-trisphosphate receptor expression in atrial tissue in patients with chronic atrial fibrillation]. *J. Cardiol.* 39, 57–58. doi: 10.1016/S0735-1097(01)01144-5

Yanni, J., Tellez, J. O., Maczewski, M., Mackiewicz, U., Beresewicz, A., Billeter, R., et al. (2011). Changes in ion channel gene expression underlying heart failure-induced sinoatrial node dysfunction. *Circ. Heart Fail.* 4, 496–508. doi: 10.1161/CIRCHEARTFAILURE.110.957647

Yeh, Y. H., Wakili, R., Qi, X. Y., Chartier, D., Boknik, P., Kaab, S., et al. (2008). Calcium-handling abnormalities underlying atrial arrhythmogenesis and contractile dysfunction in dogs with congestive heart failure. *Circ. Arrhythm. Electrophysiol.* 1, 93–102. doi: 10.1161/CIRCEP.107.754788

Yuan, J. P., Zeng, W., Huang, G. N., Worley, P. F., and Muallem, S. (2007). STIM1 heteromultimerizes TRPC channels to determine their function as store-operated channels. *Nat. Cell Biol.* 9, 636–645. doi: 10.1038/ncb1590

Zagranichnaya, T. K., Wu, X., and Villereal, M. L. (2005). Endogenous TRPC1, TRPC3, and TRPC7 proteins combine to form native store-operated channels in HEK-293 cells. *J. Biol. Chem.* 280, 29559–29569. doi: 10.1074/jbc.M505842200

Zhang, Y., Fraser, J. A., Jeevaratnam, K., Hao, X., Hothi, S. S., Grace, A. A., et al. (2011). Acute atrial arrhythmogenicity and altered Ca(2+) homeostasis in murine RyR2-P2328S hearts. *Cardiovasc. Res.* 89, 794–804. doi: 10.1093/cvr/cvq229

Zhang, Z., Tang, J., Tikunova, S., Johnson, J. D., Chen, Z., Qin, N., et al. (2001). Activation of Trp3 by inositol 1,4,5-trisphosphate receptors through displacement of inhibitory calmodulin from a common binding domain. *Proc. Natl. Acad. Sci. U.S.A.* 98, 3168–3173. doi: 10.1073/pnas.051632698

Conflict of Interest Statement: The authors declare that the research was conducted in the absence of any commercial or financial relationships that could be construed as a potential conflict of interest.

frontiers in Physiology

ORIGINAL RESEARCH
published: 20 March 2015
doi: 10.3389/fphys.2015.00078

Abnormal calcium homeostasis in heart failure with preserved ejection fraction is related to both reduced contractile function and incomplete relaxation: an electromechanically detailed biophysical modeling study

Ismail Adeniran[1]*, *David H. MacIver*[1,2], *Jules C. Hancox*[1,3] and *Henggui Zhang*[1,4]*

[1] Biological Physics Group, School of Physics and Astronomy, The University of Manchester, Manchester, UK, [2] Department of Cardiology, Taunton and Somerset Hospital, Musgrove Park, Taunton, UK, [3] School of Physiology and Pharmacology and Cardiovascular Research Laboratories, School of Medical Sciences, Bristol, UK, [4] School of Computer Science and Technology, Harbin Institute of Technology, Harbin, China

Heart failure with preserved ejection fraction (HFpEF) accounts for about 50% of heart failure cases. It has features of incomplete relaxation and increased stiffness of the left ventricle. Studies from clinical electrophysiology and animal experiments have found that HFpEF is associated with impaired calcium homeostasis, ion channel remodeling and concentric left ventricle hypertrophy (LVH). However, it is still unclear how the abnormal calcium homeostasis, ion channel and structural remodeling affect the electro-mechanical dynamics of the ventricles. In this study we have developed multiscale models of the human left ventricle from single cells to the 3D organ, which take into consideration HFpEF-induced changes in calcium handling, ion channel remodeling and concentric LVH. Our simulation results suggest that at the cellular level, HFpEF reduces the systolic calcium level resulting in a reduced systolic contractile force, but elevates the diastolic calcium level resulting in an abnormal residual diastolic force. In our simulations, these abnormal electro-mechanical features of the ventricular cells became more pronounced with the increase of the heart rate. However, at the 3D organ level, the ejection fraction of the left ventricle was maintained due to the concentric LVH. The simulation results of this study mirror clinically observed features of HFpEF and provide new insights toward the understanding of the cellular bases of impaired cardiac electromechanical functions in heart failure.

Keywords: heart failure, calcium, 3D model, ventricle

OPEN ACCESS

Edited by:
Ming Lei,
University of Oxford, UK

Reviewed by:
Michael Franz,
Georgetown University, USA
James Alastair Fraser,
University of Cambridge, UK

***Correspondence:**
Henggui Zhang,
Biological Physics Group, School of Physics and Astronomy, The University of Manchester, Room 3.07, Schuster Building, Brunswick Street, Manchester M13 9PL, UK
henggui.zhang@manchester.ac.uk;
Ismail Adeniran,
Biological Physics Group, School of Physics and Astronomy, The University of Manchester, Schuster Building, Brunswick Street, Manchester M13 9PL, UK
ismail.adeniran@manchester.ac.uk

Specialty section:
This article was submitted to Cardiac Electrophysiology, a section of the journal Frontiers in Physiology

Received: *25 November 2014*
Accepted: *26 February 2015*
Published: *20 March 2015*

Citation:
Adeniran I, MacIver DH, Hancox JC and Zhang H (2015) Abnormal calcium homeostasis in heart failure with preserved ejection fraction is related to both reduced contractile function and incomplete relaxation: an electromechanically detailed biophysical modeling study. Front. Physiol. 6:78. doi: 10.3389/fphys.2015.00078

Introduction

Heart failure (HF) is often categorized into two major types (Borlaug and Paulus, 2010; MacIver, 2010a; Phan et al., 2012; Liu et al., 2013; Zouein et al., 2013): HF with reduced ejection fraction (HFrEF) and HF with preserved ejection fraction (HFpEF). The main distinguishing criterion is an arbitrary cut-off value for the left ventricular ejection fraction of >50% for HFpEF

(Vasan and Levy, 2000; Zile et al., 2001; Yturralde and Gaasch, 2005; Asrar Ul Haq et al., 2014) and ≤ 50% for HFrEF (Borlaug and Paulus, 2010; Phan et al., 2012; Liu et al., 2013; Zouein et al., 2013). HFpEF and HFrEF are also commonly referred to as diastolic and systolic HF respectively and also share a variety of abnormalities (Borlaug and Paulus, 2010; Soma, 2011; MacIver and Dayer, 2012; Asrar Ul Haq et al., 2014). Currently, the prevalence of HFpEF is ∼50% (Konstantinou et al., 2013; Liu et al., 2013; Asrar Ul Haq et al., 2014), but it is predicted to become the dominant form of HF within the next decade (Liu et al., 2013; Asrar Ul Haq et al., 2014).

The leading cause of HFpEF is hypertension and the dominant pathophysiological mechanism is thought to involve impaired relaxation of the left ventricle (LV) (Liu et al., 2013; Asrar Ul Haq et al., 2014). Other distinguishing features cited are increased LV stiffness and elevated LV end-diastolic pressures (Liu et al., 2013; Asrar Ul Haq et al., 2014). In addition, abnormalities of systolic shortening are common with reduced global longitudinal strain, strain rate, reduced midwall fractional shortening, reduced systolic annular motion, increased isovolumetric contraction time and reduced systolic longitudinal shortening velocities in HFpEF (Sanderson, 2007; Wang et al., 2008; Kono et al., 2009; MacIver, 2010a). HFpEF is also characterized by dyspnoea, fluid retention, exercise intolerance, coronary artery disease and atrial fibrillation (Redfield et al., 2003; Bhatia et al., 2006; Owan et al., 2006; Konstantinou et al., 2013; Liu et al., 2013). It has a greater prevalence in older people and females (Liu et al., 2013). Patients also exhibit other comorbidities such as diabetes, obesity, peptic ulcer disease, cancer and chronic obstructive pulmonary disease (Liu et al., 2013).

As relaxation is an active energy-consuming process and dependent on intracellular Ca^{2+} homeostasis (Robertson et al., 1982; Ebashi, 1984; Barry and Bridge, 1993; Bers, 2001; Konstantinou et al., 2013), impaired relaxation in HFpEF may reflect abnormal intracellular Ca^{2+} homeostasis. Indeed, experimental data from clinical electrophysiology and animal model studies have shown that HFpEF is associated with abnormal Ca^{2+} handling, including an increased SR Ca^{2+} leak current (I_{leak}) and a decreased Ca^{2+} release from ryanodine receptors (Borbély et al., 2005; Selby et al., 2011; Zile and Gaasch, 2011; Trenor et al., 2012; Gomez et al., 2014). In addition, some ionic currents responsible for generating cardiac action potentials are also remodeled, including those carried by the late-sodium channel, the transient outward K^+ channel, the inward rectifier K^+ channel, the Na^+/K^+ pump (I_{NaK}), the background Ca^{2+} channel and the Na^+/Ca^{2+} exchanger (Borbély et al., 2005; Selby et al., 2011; Zile and Gaasch, 2011; Gomez et al., 2014; Trenor et al., 2012). Structurally, HFpEF is also associated with concentric LV hypertrophy with high LV mass/volume ratio, cardiomyocyte hypertrophy and interstitial fibrosis. This is different to HFrEF, where structural remodeling is characterized by progressive ventricular dilation, eccentric LV remodeling, low LV mass/volume ratio, cardiomyocyte loss along with replacement fibrosis (Borlaug and Paulus, 2010; Konstantinou et al., 2013; Asrar Ul Haq et al., 2014).

The functional impacts of HFpEF-related abnormal Ca^{2+} homeostasis, ion channel and structural remodeling on cardiac electro-mechanics are unclear. Thus, the present study was conducted in order: (1) to develop a novel HFpEF electromechanical single cell model based on extant experimental data; (2) to investigate the cellular mechanisms influencing myocardial calcium homeostasis in HFpEF using an electromechanical single cell model; and (3) to evaluate the functional impacts of impaired Ca^{2+} handling, ion channel remodeling and degrees of concentric LV hypertrophy on the electro-mechanical activity of the heart.

Materials and Methods

Electromechanical Single Cell Model

For electrophysiology (EP), we utilized the O'Hara-Rudy (ORd) human ventricular single cell model (O'Hara et al., 2011), which was developed from undiseased human ventricular data and recapitulates human ventricular cell electrical and membrane channel properties, as well as the transmural heterogeneity of ventricular action potential (AP) across the ventricular wall (O'Hara et al., 2011). The ORd model also reproduces Ca^{2+} vs. voltage-dependent inactivation of L-type Ca^{2+} current and Ca^{2+}/calmodulin-dependent protein kinase II (CaMK) modulated rate dependence of Ca^{2+} cycling. For simulating cellular mechanics properties, we used the Tran et al. myofilament (MM) model (Tran et al., 2010). This model was chosen as it is an extension of the well-established cross-bridge cycling model of cardiac muscle contraction model of Rice et al. (2008). In addition to its ability to replicate a wide range of experimental data including steady-state force-sarcomere length (F-SL), force-calcium and sarcomere length-calcium relationships (Rice et al., 2008; Tran et al., 2010), it also reproduces many of the observed effects of MgATP, MgADP, Pi, and H^+ on force development.

The intracellular calcium concentration from the EP model was used as the coupling link to the MM model. $[Ca^{2+}]_i$ produced as dynamic output from the EP model during the AP served as input to the MM model from which the amount of Ca^{2+} bound to troponin is calculated. The formulation of the myoplasmic Ca^{2+} concentration in the human ventricular myocyte electromechanical cell model is:

$$\frac{d[Ca^{2+}]_i}{dt} = \beta_{Cai} \cdot \left(-(I_{pCa} + I_{Cab} - 2 \cdot I_{NaCa,i}) \cdot \frac{A_{cap}}{2 \cdot F \cdot v_{myo}} - J_{up} \cdot \frac{v_{nsr}}{v_{myo}} + J_{diff,Ca} \cdot \frac{v_{ss}}{v_{myo}} - \frac{J_{Trop}}{1000} \right) \quad (1)$$

where β_{Cai} is the buffer factor for $[Ca^{2+}]_i$, I_{pCa} (μA/μF) is the sarcolemmal Ca^{2+} pump current, I_{Cab} (μA/μF) is the Ca^{2+} background current, $I_{NaCa,i}$ (μA/μF) is the myoplasmic component of Na^+/Ca^{2+} exchange current, A_{cap} (cm^2) is capacitive area, F (coul/mol) is the Faraday constant, v_{myo} (μL) is the volume of the myoplasmic compartment, v_{nsr} (μL)is the volume of the network sarcoplasmic reticulum compartment, v_{ss} (μL) is the volume of the subspace compartment, J_{up} (mM/ms) is the total Ca^{2+} uptake flux, via SERCA pump from myoplasm to the network sarcoplasmic reticulum, $J_{diff,Ca}$ (mM/ms) is the flux of the diffusion of Ca^{2+} from the subspace to the myoplasm and J_{Trop} (μM/ms)

is the flux of Ca^{2+} binding to troponin calculated via the MM model. β_{Cai} is formulated as:

$$\beta_{Cai} = \frac{1}{1 + \frac{[CMDN] \cdot K_{m,CMDN}}{(K_{m,CMDN} + [Ca^{2+}]_i)^2}} \quad (2)$$

where [CMDN] is the calmodulin Ca^{2+} buffer in the myoplasm and $K_{m,CMDN}$ is the half-saturation concentration of calmodulin.

HFpEF Electromechanical Single Cell Model

To develop the human electromechanical single cell model of a HFpEF cardiomyocyte, we first modified parameters of the ORd model based on HF experimental data following the work of Gomez et al. (2014), Trenor et al. (2012) on human HF. This resulted in a generic human HF model. We then made alterations based on the cellular and molecular properties of HFpEF (Zile and Gaasch, 2011) to obtain a biophysically detailed model of HFpEF. For the myofilament changes relative to control, we made modifications based on experimental data on HFpEF patients following the work of Borbély et al. (2005), Selby et al. (2011). **Table 1** summarizes the extensive modifications to the control ORd cardiomyocyte to produce the HFpEF cardiomyocyte model.

Parameter Sensitivity Analysis for Influential Cellular Processes on Relaxation in HFpEF

To our knowledge, only the work by Zile and Gaasch (2011) provides any data on the differences in the cellular and molecular processes that influence Ca^{2+} homeostasis in patients with systolic and diastolic HF. We based our HFpEF model on their work (Zile and Gaasch, 2011) as given in section HFpEF Electromechanical Single Cell Model. In simulations, the only difference between the HFrEF and HFpEF models is a reduction in NCX in the HFpEF condition (see **Table 1**) as compared to the HFrEF condition. In order to determine whether a reduction in NCX is responsible for the poor end-diastolic relaxation in HFpEF, we performed a parameter-dependent sensitivity analysis of the HFpEF model to NCX, by varying NCX from 70% (HFpEF) to 175% (HFrEF).

TABLE 1 | Changes in original ORd model to simulate HFpEF and HFrEF.

Parameter modified	% change in the HFrEF model compared to the normal model	% change in the HFpEF model compared to the normal model
I_{NaL}	180%	180%
τ_{hL}	180%	180%
I_{to}	40%	40%
I_{K1}	68%	68%
I_{NaK}	70%	70%
I_{Nab}	100%	100%
I_{NCX}	175%	70%
I_{leak}	130%	130%
CaMKa	150%	150%
$J_{rel,NP,\infty}$	80%	80%
	Myofilament (Borbély et al., 2005; Zile and Gaasch, 2011)	
PCon_titin	x1.00	x2.00
PCon_collagen	x2.36	x2.00
P_Exp_collagen	x0.42	x0.50

The modified parameters are: the late Na^+ current (I_{NaL}), the time constant of inactivation of the I_{NaL} (t_{hL}), the transient outward K^+ current (I_{to}), the inward rectifier K^+ current (I_{K1}), the Na^+/K^+ pump current (I_{NaK}), the background Ca^{2+} current (I_{CaB}), the Na^+/Ca^{2+} exchanger (I_{NCX}), the SR Ca^{2+} leak current (I_{leak}), the Ca^{2+}/calmodulin-dependent protein kinase II (CaMK), the nonphosphorylated Ca^{2+} release, via ryanodine receptors ($J_{rel,NP,\infty}$), passive force factor due to titin (PCon_titin), passive force (F_passive) and active force (F_active). Based on Borbély et al. (2005), Zile and Gaasch (2011), Trenor et al. (2012) and Gomez et al. (2014).

Protocols

The pacing protocols used to evaluate Ca^{2+} homeostasis were as follows:

Post-Rest Contractions

We used a post-rest contraction (PRC) protocol to evaluate sarcoplasmic reticulum (SR) Ca^{2+} content, retention, release, reuptake, and leak. After pacing the single cell for 10 min at 1 Hz to allow steady-conditions to be attained, resting intervals of 1, 2, 3, 5, and 10 s were introduced. The resting periods were then followed by a single stimulus. The varying developed indices such as active tension are a reflection of SR Ca^{2+} release.

Tissue Mechanics Model

We modeled cardiac tissue mechanics within the theoretical framework of nonlinear elasticity (Marsden and Hughes, 1994; Holzapfel, 2000) as an inhomogeneous, anisotropic, nearly incompressible nonlinear material similar to previous studies (Costa et al., 2001; Whiteley et al., 2007; Niederer and Smith, 2008; Pathmanathan and Whiteley, 2009; Adeniran et al., 2013a,b). We used a two-field variational principle with the deformation u and the hydrostatic pressure p as the two fields (Bonet and Wood, 2008; Adeniran et al., 2013a,b; Le Tallec). p is utilized as the Lagrange multiplier to enforce the near incompressibility constraint. Thus, the total potential energy function Π for the mechanics problem is formulated as:

$$\Pi(u, p) = \Pi_{\text{int}}(u, p) + \Pi_{ext}(u) \quad (3)$$

where $\Pi_{\text{int}}(u, p)$ is the internal potential energy or total strain energy of the body and $\Pi_{ext}(u)$ is the external potential energy or potential energy of the external loading of the body. As in previous studies (Niederer and Smith, 2008; Keldermann et al., 2009; Pathmanathan and Whiteley, 2009; Adeniran et al., 2013a,b), in the absence of body forces, and assuming that the body is always in instantaneous equilibrium and no inertia effects, the coordinates of the deformed body satisfies the steady-state equilibrium equation with near incompressibility enforced.

The values that minimize the total potential energy in Equation (3) are obtained by searching for its critical points in suitable admissible displacement and pressure spaces $\hat{U}$ and $\hat{P}$. The corresponding Euler-Lagrange equations resulting from Equation (3) lead to solving the problem (Braess and Ming, 2005; Auricchio et al., 2010; Boffi et al., 2013; Le Tallec):

Find (u, p) in $\hat{U} \times \hat{P}$ such that:

$$\int_\Omega \frac{\partial \hat{W}}{dF}(x, Id + \nabla u)\colon \nabla v dx - \int_\Omega p \frac{\partial \det}{dF}(x, Id + \nabla u)\colon \nabla v dx = \int_{\partial\Omega} g.v ds \quad \forall v, u \in \hat{U}$$

$$\int_\Omega q\left[\det(Id + \nabla u) - 1\right] dx = 0 \qquad \forall v, u \in \hat{P} \tag{4}$$

where $\hat{U}$ and $\hat{P}$ are the admissible variation spaces for the displacements and the pressures, respectively. $F = Id + \nabla u$ is the deformation gradient, v is a test function and $\hat{W}$ is the material stored energy function and corresponds to the density of elastic energy locally stored in the body during the deformation.

The deformation gradient F is a tensor that maps elements from the undeformed configuration to the deformed configuration (Marsden and Hughes, 1994; Holzapfel, 2000). Following Cherubini et al. (2008), Ambrosi et al. (2011), we multiplicatively decompose F into a microscopic (active) component and a macroscopic elastic (passive) component:

$$F = F_e F_0 \tag{5}$$

The active component F_o measures the length change of the tissue due to muscle contraction while the passive component F_e accounts for the passive mechanical response of the tissue and possible tension due to external loads.

With the vector fields *f, s, and n* denoting the unique direction of the fibers, sheets and sheet-normals in the undeformed state of the LV, the microscopic active component of the deformation tensor F takes the form:

$$F_o = I + \gamma_f f \otimes f + \gamma_s s \otimes s + \gamma n \otimes n \tag{6}$$

where I is the identity tensor and γ_x is a scalar field that represents the intensity of the contraction, i.e., the active strain in the appropriate direction. γ_f is defined as:

$$\gamma_f = \frac{SL - SL_0}{SL_0} \tag{7}$$

where SL is the new sarcomeric length and SL_0 is the resting sarcomere length of the electromechanical single cell. Following the work of (Rossi et al., 2014)

$$\gamma_n = K\gamma_f, \gamma_s = \frac{1}{(1 + \gamma_f)(1 + \gamma_n)} - 1$$

Thus, $\gamma > 0$ denotes elongation, and $\gamma < 0$ denotes contraction. The parameter K is the link between the microscopic and the macroscopic active deformations (Bogaert and Rademakers, 2001; Rossi et al., 2014) and in our simulations, we used $K = 4$, according to experimental observations (Rademakers et al., 1994; Rossi et al., 2014).

The elastic component F_e is formulated as:

$$F_e = FF_0^{-1} \tag{8}$$

and the corresponding Right Cauchy-Green strain tensor is:

$$C_e = F_e^T F_e \tag{9}$$

The associated Green-Lagrange strain tensor is:

$$E_e = \frac{1}{2}(C_e - I) \tag{10}$$

To characterize the constitutive behavior of cardiac tissue, we used a mixed formulation of the compressible neo-Hookean strain energy function W (Auricchio et al., 2010):

$$\hat{W} = \frac{\mu}{2}[I : \hat{C} - d] - \mu \ln\hat{J} + p\ln\hat{J} - \frac{p^2}{2\lambda} \tag{11}$$

where μ and λ are positive constants, ":" represents the usual inner product for second-order tensors, $\hat{C}$ is the right Cauchy-Green deformation tensor, d is the spatial dimension and $\hat{J} = \det\hat{F}$ is the Jacobian of the deformation gradient.

Tissue Electrophysiology Model

The monodomain representation (Colli Franzone et al., 2005; Keener and Sneyd, 2008; Adeniran et al., 2013a,b) of cardiac tissue was used for the electrophysiology model:

$$C_m \frac{dv}{dt} = -(I_{ion} + I_{stim}) + \nabla \cdot (D\nabla V) \tag{12}$$

where C_m is the cell capacitance per unit surface area, V is the membrane potential, I_{ion} is the sum of all transmembrane ionic currents from the electromechanics single cell model, I_{stim} is an externally applied stimulus and D is the anisotropic diffusion tensor given by:

$$D = \sigma_f(f \otimes f) + \sigma_s(s \otimes s) + \sigma_n(n \otimes n) \tag{13}$$

σ_f, σ_f, and σ_f are the intracellular conductivities in the fiber, sheet and cross-sheet directions respectively. These were set to 3.0, 0.1, and 0.31525 $\text{ms}\cdot\text{mm}^{-1}$ respectively. These gave a conduction velocity of 65 $\text{cm}\cdot\text{s}^{-1}$ in the fiber direction along multiple cells, which is close to the value 70 $\text{cm}\cdot\text{s}^{-1}$ observed in the fiber direction in human myocardium (Taggart et al., 2000). To guard against any drift in the steady state values of the ion concentrations in the model, the electromechanical single cell models described in sections Electromechanical Single Cell Model to HFpEF Electromechanical Single Cell Model were pre-paced for a 1000 beats before being incorporated into the tissue model.

Geometry and Meshes

For unbiased comparison between increasing severity of concentric LV hypertrophy in HFpEF, we used truncated ellipsoids for the 3D simulations (**Figure 1A**). Each LV geometry was segmented into distinct endocardial (60%), mid-myocardial (30%), and epicardial (10%) regions. The chosen cell proportion in each region reflects experimental data for cells spanning the left ventricular wall of the human heart (Drouin et al., 1995). There exists some controversy on the existence and functional role of

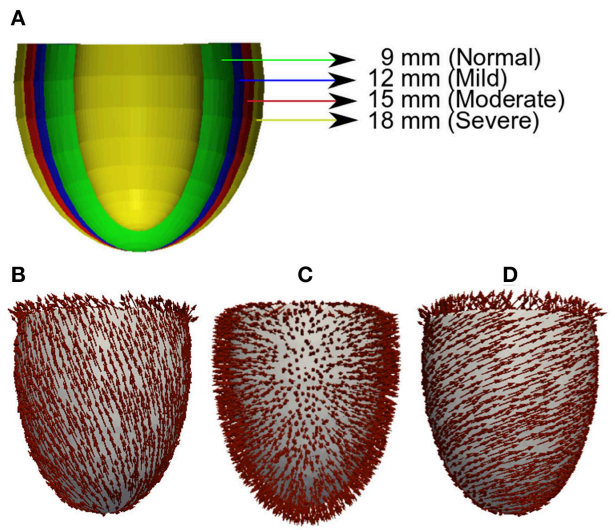

FIGURE 1 | Geometry and fiber directions in 3D left ventricle with varied wall thickness. (A) Control and HFpEF concentric hypertrophic geometries—NORMAL (green, 9 mm), MILD (red, 12 mm), MODERATE (blue, 15 mm) and SEVERE (yellow, 18 mm). **(B)** Fiber direction. **(C)** Sheet direction. **(D)** Sheet-normal or cross-sheet direction.

MCELLs in the human heart (Wilson et al., 2011). However, we included MCELLs in our model on the basis of studies that give evidence of their existence in cells isolated from the right ventricle of patients with heart failure (Li et al., 1998) and in a perfused piece of left ventricular wall ("wedge preparation") (Drouin et al., 1995). The conditional activation sites were projected from those of a healthy 34-year old male determined empirically across the ventricle wall and were validated by reproducing the activation sequence and QRS complex in the measured 64-channel ECG (Keller et al., 2009) of that person. **Figures 1B–D** shows the anisotropic fiber fields reconstructed by the algorithm in Rossi et al. (2014) for the fiber (**Figure 1B**), sheet (**Figure 1C**), and cross-sheet (**Figure 1D**) directions.

Solving the Electromechanics Problem

The electromechanics problem consists of two sub-problems: the electrophysiology problem and the mechanics problem. The electrophysiology problem (Equation 14) was solved with a Strang splitting method (Sundnes et al., 2005) ensuring that the solution is second-order accurate. It was discretized in time using the Crank-Nicholson method (Burnett, 1987), which is also second-order accurate and discretized in space with Finite Elements (Ciarlet, 2002; Braess, 2007; Brenner and Scott, 2010). I_{ion} in Equation (14) represents the single cell electromechanics model from which the active strain input to the 3D mechanics model for contraction is obtained. The system of ordinary differential equations (ODE) composing I_{ion} was solved with a combination of the Rush-Larsen scheme (Rush and Larsen, 1978) and the CVODE solver (Cohen and Hindmarsh, 1996; Alan and Hindmarsh, 2005).

The mechanics problem (Equation 2) was also solved using the Finite element Method using the automated scientific computing library, FEniCS (Logg et al., 2012). The resulting nonlinear system of equations was solved iteratively using Newton's method to determine the equilibrium configuration of the system. Over a typical finite element domain, P_2 elements (Braess, 2007; Brenner and Scott, 2010; Ern and Guermond, 2010; Boffi et al., 2013) were used to discretize the displacement variable u, while the pressure variable p was discretized with P_1 elements (Braess, 2007; Brenner and Scott, 2010; Ern and Guermond, 2010; Boffi et al., 2013). This P_2–P_1 mixed finite element has been proven to ensure stability (Chamberland et al., 2010; Haga et al., 2012; Logg et al., 2012) and an optimal convergence rate (Hughes, 2000; Chamberland et al., 2010; Ern and Guermond, 2010).

The algorithm for solving the full electromechanics problem is as follows:

(1) While time < tend:

  (a) Solve the electrophysiology problem for $\Delta t_{\text{mechanics}} = 1$ ms with active strain γ as output ($\Delta t_{\text{electrophysiology}} = 0.01$ ms).
  (b) Project γ from the electrophysiology mesh onto the mechanics mesh.

(2) Solve the mechanics problem with γ as input.

Results

Model Validation

To validate the HFpEF model, we computed a steady-state force-calcium (F-pCa) relation for a sarcomere length (SL) of 2.2 μm for comparison with prior experimental data (Borbély et al., 2005). Results are shown in **Figure 2**. The model reproduced the differences in total and passive forces between control and HFpEF, which matched experimental data (inset).

Functional Consequences of HFpEF Transmurally in the LV

Figure 3 shows the electromechanical consequences of HFpEF in a free-running cell from each of the epicardium (EPI) (**Figures 3Ai–Aiv**), mid-myocardium (MCELL) (**Figures 3Bi–Biv**) and endocardium (ENDO) (**Figures 3Ci–Civ**). HFpEF increased the action potential duration (APD_{90}) in each of the EPI (**Figure 3Bi**), MCELL (**Figure 3Bii**) and ENDO (**Figure 3Bi**) cell types. APD_{90} was increased from 233 to 262 ms in EPI, 357 to 439 ms in MCELL and 274 to 348 ms in ENDO. These differences in APD_{90} across the ventricular wall are suggestive of possible T-wave changes and altered dispersion of repolarization in HFpEF. The cytosolic Ca^{2+} concentration $[Ca^{2+}]_i$ was reduced in amplitude in all the cell types (**Figures 3Aii–Cii**), which led to a decrease in the SL shortening (**Figures 3Aiii–Ciii**) and consequently, a reduction in the active force (**Figures 3Aiv–Civ**). Of note is that the diastolic $[Ca^{2+}]_i$ level was increased in HFpEF compared to control (**Figures 3Aii–Cii**) leading to incomplete relaxation (**Figures 3Aiv–Civ**). This electromechanical model predicted a combination of reduced contractile force and stress generation and incomplete relaxation as the pathophysiological mechanism of HFpEF (Zile et al., 2004; Borlaug and Paulus, 2010; Phan et al.,

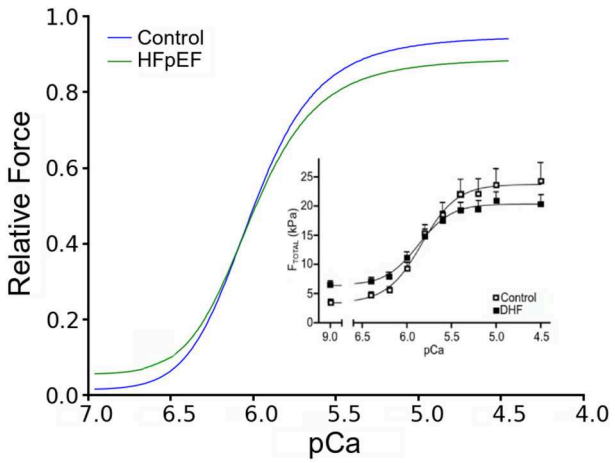

FIGURE 2 | Force-pCa relationship. Simulated Force-pCa relation of control and HFpEF. Relative force is normalized to maximum value in control. Inset: Experimental force-pCa relation from human patients adopted from Borbély et al. (2005).

2012; Konstantinou et al., 2013; Liu et al., 2013; Zouein et al., 2013; Asrar Ul Haq et al., 2014).

Functional Consequences of HFpEF on Ionic Currents Compared with HFrEF

Figure 4 shows action potentials in control, HFrEF and HFpEF conditions (**Figure 4A**) computed from the EPI cell model, together with the corresponding ionic currents of I_{CaL} (**Figure 4B**), I_{NaCa} (**Figure 4C**), the SR content (**Figure 4D**), I_{pCa} (**Figure 4E**), intracellular Na^+ ($[Na^+]_i$; **Figure 4F**) and K^+ ($[K^+]_i$; **Figure 4G**) concentrations and $I_{Na,K}$. In comparison to the control condition, HFpEF and HFrEF increased the APD, which can be attributable to the increased inward Na^+ current (I_{NaL}) and decreased outward K^+ current (I_{K1} and I_{NaK}; see **Table 1**) (**Figure 4H**) (Glitsch, 2001; Workman et al., 2003; Bueno-Orovio et al., 2014). Accompanying these changes were increased $[Na^+]_i$ (**Figure 4F**) and reduced $[K^+]_i$ (**Figure 4G**). The difference in the amplitude of I_{CaL} among control, HFpEF and HFrEF was small, but its duration was longer in HFpEF and longest in HFrEF (**Figure 4B**), possibly due to a secondary effect of a prolonged APD. In the HFpEF condition, a decreased I_{NaCa} was observed, partially due to reduced Na^+-Ca^{2+} exchanger (NCX) (see **Table 1**) and partially due to the reduction in the Na^+-K^+ pump activity as it indirectly regulated Ca^{2+} extrusion by the NCX (Barry et al., 1985; Bueno-Orovio et al., 2014). This resulted in a reduced sarcoplasmic reticulum (SR) content in HFpEF (**Figure 4D**), and consequently leading to a smaller SR Ca^{2+} release as demonstrated by the reduced amplitude of the SR content (**Figure 4D**). The activity of the sarcolemmal Ca^{2+} pump was increased during the diastolic period, but reduced in the systolic period (**Figure 4E**). These simulation results provided a cellular basis for the abnormal Ca^{2+} handling in HFpEF. Results from the MCELL and ENDO cell models showed similar behavior (these are shown in the Supplementary Material).

Unlike in HFpEF, there was an increased I_{NaCa} (**Figure 4C**) due to the HFrEF model formulation involved a 175% NCX increase (**Table 1**). **Figure 4C** shows that NCX removed an excessive amount of Ca^{2+} from the cell in its forward mode compared to control, leading to a deficit in the SR Ca^{2+} content (**Figure 4D**), a greater reduction in $[Ca^{2+}]_i$ compared to HFpEF (**Figure 4J**) and consequently a lower active force (**Figure 4L**).

Post-Rest Contraction Properties of HFpEF

Further simulations were performed to investigate the rate-dependent impact of HEpEF on Ca^{2+} handling. Results are shown in **Figure 5**, which shows the outcome of the PRC protocol at a pacing rate of 1 Hz (**Figures 5Ai–Av**) and 2 Hz (**Figures 5Bi–Bv**). Diastolic $[Ca^{2+}]_i$ level in HFpEF increased by ∼75% relative to control at all resting intervals (**Figures 5Ai,Bi**). This led to an increase in resting tension (**Figures 5Aiii,Biii**). Though there was a significant increase in diastolic $Ca^{2+}]_i$ level, the SR content was lower in HFpEF than in control (**Figures 5Aii,Bii**) as was peak systolic tension (**Figures 5Aiv,Biv**). This is counter-intuitive as with an increased diastolic concentration of Ca^{2+} in the cytosol, one would expect greater Ca^{2+} sequestration into the SR, and therefore an increased Ca^{2+} content leading to an increased Ca^{2+} release from the SR, resulting in a greater Ca^{2+} transient amplitude and a greater systolic tension. The reduction in the peak systolic Ca^{2+} level and the corresponding tension and inefficient SR Ca^{2+} activity was due to excessive leak of Ca^{2+} from the SR (**Figures 5Av,Bv**). These results were more pronounced at a pacing rate of 2 Hz (**Figures 5Bi–Bv**) because of the shorter duration between beats allowing less recovery time for Ca^{2+} cycling processes.

Sensitivity of Diastolic Relaxation to NCX

In **Figure 6**, effects of a systematic change of NCX in HFpEF model from 70% (HEpEF) to 175% (HFrEF) on the action potentials (**Figure 6A**), I_{NaCa} (**Figure 6B**), $[Ca^{2+}]_i$ (**Figure 6C**) and active force (**Figure 6D**) are shown. Diastolic relaxation was impaired when NCX was at 70% of the control value (e.g., for HFpEF), but gradually improved with increasing NCX activity to 100 and 150% of the control value. It became normal at 175% (e.g., for HFrEF; **Figure 6D**) of the control value. Peak relative force during systole occurred later and with lower amplitude with increasing NCX activity.

3D Electromechanical Consequences of HFpEF in Hypertrophic Geometries

Figure 7 shows the results of incorporating the cellular HFpEF electromechanical models into three-dimensional truncated ellipsoid representations of the LV. Effects of varying degrees of left ventricular hypertrophy on the ejection fraction are also shown. The LV was at rest before activation (0 ms). At about 200 ms, the LV was completely activated and contraction was underway in the NORMAL, MILD, MODERATE, and SEVERE conditions of hypertrophy. By 300 ms, repolarization had commenced and the LV in all conditions was undergoing relaxation. At 700 ms, repolarization was completed in all the conditions; however, relaxation was still on going in the hypertrophic cases but was complete in the NORMAL condition. The LVEF in NORMAL, MILD, MODERATE, and SEVERE was 58, 57, 63, and 71% respectively showing that LVEF was increased with increasing

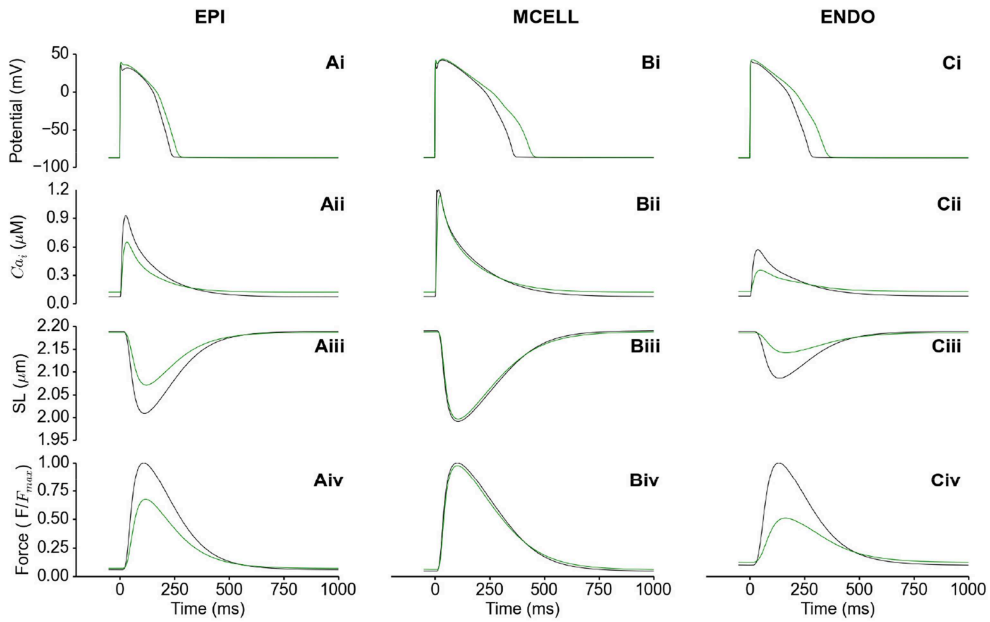

FIGURE 3 | Single cell simulations of HFpEF. (Ai–Ci) Control (black) and HFpEF (green) action potentials in the EPI **(Ai)**, MCELL **(Bi)**, and ENDO **(Ci)** cell models. **(Aii–Cii)** Control (black) and HFpEF (green) cytosolic Ca^{2+} concentration in the EPI **(Aii)**, MCELL **(Bii)**, and ENDO **(Cii)** cell models. **(Aiii–Ciii)** Control (black) and HFpEF (green) sarcomere length (SL) in the EPI **(Aiii)**, MCELL **(Biii)**, and ENDO **(Ciii)** cell models. **(Aiv–Civ)** Control (black) and HFpEF (green) active force in the EPI **(Aiv)**, MCELL **(Biv)**, and ENDO **(Civ)** cell models. Values are normalized to Control maximum active force for each cell type.

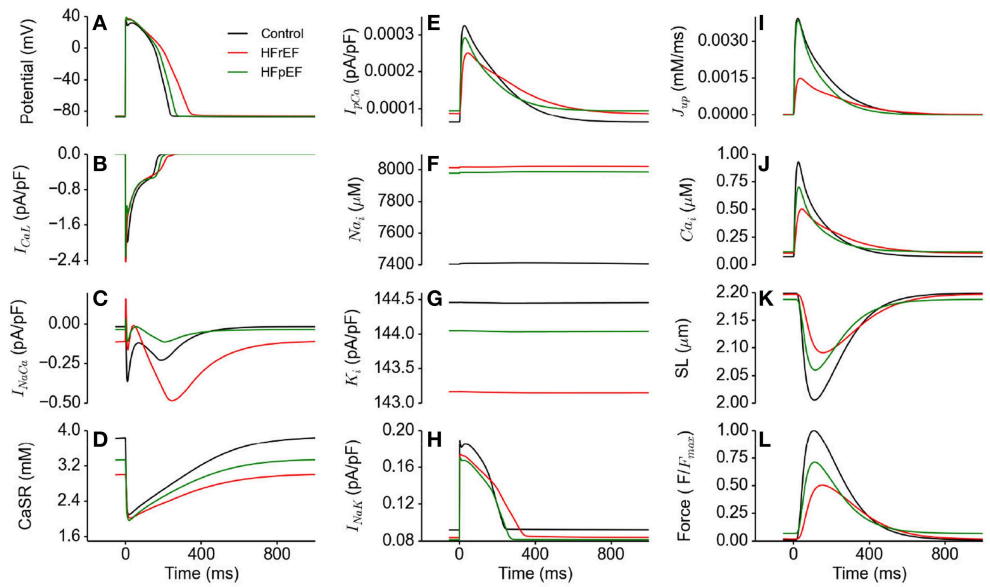

FIGURE 4 | Effects of HFpEF and HFrEF on underlying ion channel currents, concentrations and force generation. (A) Control (black), HFpEF (green), and HFrEF (red) action potentials. **(B)** I_{CaL} current profile in control (black), HFpEF (green), and HFrEF (red). **(C)** I_{NaCa} current profile in control (black), HFpEF (green), and HFrEF (red). **(D)** SR Ca^{2+} content profile in control (black), HFpEF (green), and HFrEF (red). **(E)** I_{pCa} current profile in control (black), HFpEF (green), and HFrEF (red). **(F)** $[Na]_i$ time course in control (black), HFpEF (green), and HFrEF (red). **(G)** $[K]_i$ time course in control (black), HFpEF (green), and HFrEF (red). **(H)** I_{NaK} current profile in control (black) HFpEF (green), and HFrEF (red). **(I)** J_{up} (Ca^{2+} uptake via SERCA pump) profile in control (black), HFpEF (green), and HFrEF (red). **(J)** Ca^{2+} concentration in Control (black) HFpEF (green), and HFrEF (red) cytosolic. **(K)** Sarcomere length (SL) in control (black), HFpEF (green), and HFrEF (red). **(L)** Active force in control (black), HFpEF (green), and HFrEF (red). Values are normalized to Control maximum active force.

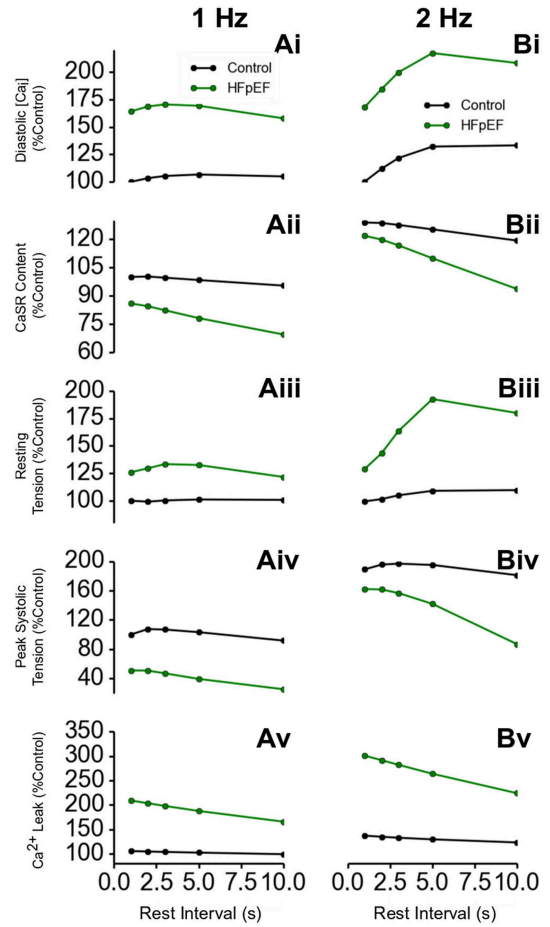

FIGURE 5 | Ca^{2+} handling and post-rest properties in HFpEF. (Ai,Bi) Diastolic Ca^{2+} level in HFpEF relative to control at 1 Hz **(Ai)** and 2 Hz **(Bi)** pacing rates. **(Aii,Bii)** SR Ca^{2+} content level in HFpEF relative to control at 1 Hz **(Aii)** and 2 Hz **(Bii)** pacing rates. **(Aiii,Biii)** Resting tension in HFpEF relative to control at 1 Hz **(Aiii)** and 2 Hz **(Biii)** pacing rates. **(Aiv,Biv)** Peak systolic tension in HFpEF relative to control at 1 Hz **(Aiv)** and 2 Hz **(Biv)** pacing rates. **(Av,Bv)** SR Ca^{2+} Ca leak in HFpEF relative to control at 1 Hz **(Av)** and 2 Hz **(Bv)** pacing rates.

the end-diastolic wall thickness. These simulation results can account for incomplete relaxation and preserved LVEF at the 3D organ level, whilst at the cellular level, the activation force and cell sarcolemmal shortening are dramatically impaired in the HFpEF condition. This is attributable to the hypertrophied ventricle wall.

Stress Distribution in HFpEF

Effects of LV wall thickness on the spatial distribution of stress was investigated. **Figure 8** shows a 4-chamber view of the magnitude of the stress distribution across the LV in control and varied hypertrophic conditions (**Figures 8A–G**). At 0 ms, the stress magnitude across the ventricle was low in all the conditions as excitation had yet to commence (**Figure 8A**). By 100 ms, when the LV was electrically activated, there was developed stress in all cases with the greatest stress in apex of the MODERATE LV (**Figure 8B**). At 200 ms (**Figure 8C**), there was considerable stress in the LV in all conditions with the greatest stress intensity in SEVERE. The hypertrophic LV also had greater stress intensity in the LV apex and epicardium compared to NORMAL. The situation was similar at 300 ms (**Figure 8D**) and 400 ms (**Figure 8E**) except that there was progressive relaxation and the stress intensity was less than at 200 ms. By 600 ms (**Figure 8F**), stress in most of the NORMAL LV had reduced considerably while the hypertrophic LVs still showed ∼25% stress. At 700 ms, stress in the NORMAL LV was negligible but still about ∼20% in the hypertrophic cases. These simulation results showed that increased wall thickness led to increased tissue stress though, at the cellular level, the active force was reduced during the time course of action potentials in HEpEF condition.

Strain Distribution in HFpEF

Effects of wall thickness on the spatial distribution of strain was also analyzed. **Figure 9** also shows a 4-chamber view of the magnitude of the strain distribution across the LV in control and hypertrophic conditions during the time course cardiac excitation (**Figures 9A–G**). Strain developed from the rest state (**Figure 9A**) to ∼50% at 100 ms (**Figure 9B**) in all cases with the smallest strain magnitude in SEVERE. By 200 ms (**Figure 9C**), strain magnitude had reached a distribution of between 50 and 100% in all cases with SEVERE having the highest strain intensity. This was concentrated in the epicardial to mid-wall regions and the middle segment of the LV. The situation was similar at 300 ms (**Figure 9D**) and 400 ms (**Figure 9E**) except that the strain intensity was reduced as relaxation was underway. The strain magnitude reduced further at 600 ms (**Figure 9F**) to ∼10–15% in NORMAL, ∼25% in MILD, ∼25–30% in MODERATE and ∼30–35% in SEVERE. The strain was mainly concentrated in the LV apex in all cases. By 700 ms (**Figure 9G**), strain magnitude was ∼5% in NORMAL, 10–25% in all the hypertrophic cases. These simulation results showed an increased residual of strain in cardiac tissue due to elevated diastolic Ca^{2+} level, which was consistent with observed incomplete relaxation of the LV in HEpEF condition.

Discussion

Summary of Major Findings

In this study we have developed, for the first time, a family of multilevel models for the electro-mechanics of the left ventricle in the setting of HFpEF, at the cellular and 3D organ levels. These models incorporated detailed HFpEF-related ion channel remodeling and impaired Ca^{2+} homeostasis at the cellular level, and concentric hypertrophy of the left ventricle wall at the organ level. Our major findings are: (i) with impaired Ca^{2+} handling and ion channel remodeling in HFpEF, the action potential duration of ventricular cells are prolonged, together with an elevated diastolic Ca^{2+} concentration, but a decreased systolic Ca^{2+} level. Such an elevated diastolic Ca^{2+} concentration provides a cellular basis for incomplete ventricular relaxation at the organ level; (ii) at the cellular level the active force and sarcomere length shortening is reduced during the time course of action potentials in HFpEF. However, at the organ level, tissue stress and strain is increased due to the increased wall thickness of

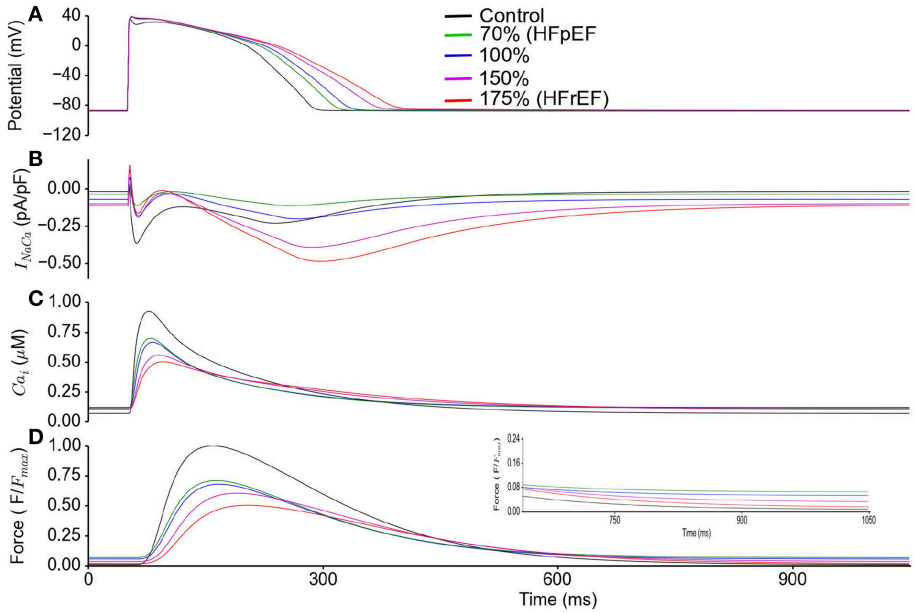

FIGURE 6 | HFpEF Model sensitivity to increasing NCX activity and its influence on incomplete relaxation in the cellular model. Simulation results were compared between control (in absence of ionic current remodeling) and HFpEF condition. HFpEF simulations were performed with parameters as listed in **Table 1**, but with NCX activity changing from 70% (HFpEF condition) to 100, 150, and 175% (HFrEF condition) of the control value. **(A)** Action potential **(B)** I_{NaCa} current profile. **(C)** Ca^{2+} concentration. **(D)** Active force. Values are normalized to maximum active force in control. (Inset: magnified diastolic phase).

concentric LV hypertrophy; (iii) the impaired Ca^{2+} homeostasis becomes more pronounced at high stimulation rates; and (iv) reduction of I_{NaCa} in the HEpEF model is the most influential factor on impaired relaxation dynamics. Collectively, these simulations predict the key features of HFpEF observed clinically, and also provide insights for understanding the cellular and tissue bases of impaired electro-mechanics of the heart in HFpEF.

Cellular Basis of Impaired Cardiac Electro-Mechanics

The results of our study suggest that at the cellular level the observed impaired cardiac electro-mechanics (such as reduced cell length shortening and active force) are attributable to alterations in cellular Ca^{2+} homeostasis and action potentials. In simulations, we observed an elevated diastolic intracellular Ca^{2+} concentration, but a reduced systolic Ca^{2+} concentration. The elevated diastolic Ca^{2+} concentration is due to an increased Ca^{2+} leak from the SR (see **Table 1**), and the reduced systolic Ca^{2+} concentration can be explained by a reduced Ca^{2+} release from the SR as a consequence of a decreased SR content (**Figure 4D**). The observed APD prolongation is attributable to the augmented late-Na^+ current, reduced potassium channel currents and I_{NaK} as seen in the heart failure condition (see **Table 1**). These results were more pronounced at a pacing rate of 2 Hz (**Figures 5Bi–Bv**) because of the shorter duration between beats allowing less recovery time for Ca^{2+} cycling processes. This is related to changes in mechanical and relaxation restitution, which correlate physiologically to the recovery kinetics of Ca^{2+} release mechanisms and sequestration capacity of the SR (Franz et al., 1983; Burkhoff et al., 1984; Prabhu and Freeman, 1995; Zaugg et al., 1995; Kjørstad et al., 2007).

In simulations, we also observed an increased intracellular Na^+ concentration and a reduced intracellular K^+ concentration (**Figures 4F,G**), which may be attributable to the augmented I_{NaL} and reduced I_{NaK} (see **Table 1**). The altered Na^+ and K^+ homeostasis may also impair Ca^{2+} homeostasis. During the time course of an action potential, there was a reduced I_{NaK}, which also contributed partially to an increase of $[Na^+]_i$ and a decrease in $[K^+]_i$ within the cytosol. NCX extrudes Ca^{2+} from the cytoplasm and imports Na^+ into it. However, with the build-up of Na^+ in the cytoplasm as a result of the reduced activity of the Na^+-K^+ pump, the forward mode activity of NCX was reduced, but its reverse mode activity was enhanced. This led to an increase in Na^+ extrusion coupled to Ca^{2+} import (see **Figure 4C**) leading to an increased Ca^{2+} concentration at diastolic phase but a reduced Ca^{2+} concentration at systolic phase. Consequently, this led to a decreased cell length shortening and active force in the systolic phase.

In addition, our simulation results showed that the SR Ca^{2+} content was reduced compared to control condition, though the Ca^{2+} release from the SR was compromised. This is attributable to an excessive Ca^{2+} leak from the SR. It was shown that SR Ca^{2+} leak was ∼100% greater in HFpEF as compared to control (**Figure 5**). The excessive Ca^{2+} leak from the SR and the reduced activity of NCX produced an increased diastolic Ca^{2+} level, leading to incomplete relaxation and an increase in the active resting tone. This implies that complete relaxation will never be achieved regardless of the duration of diastole.

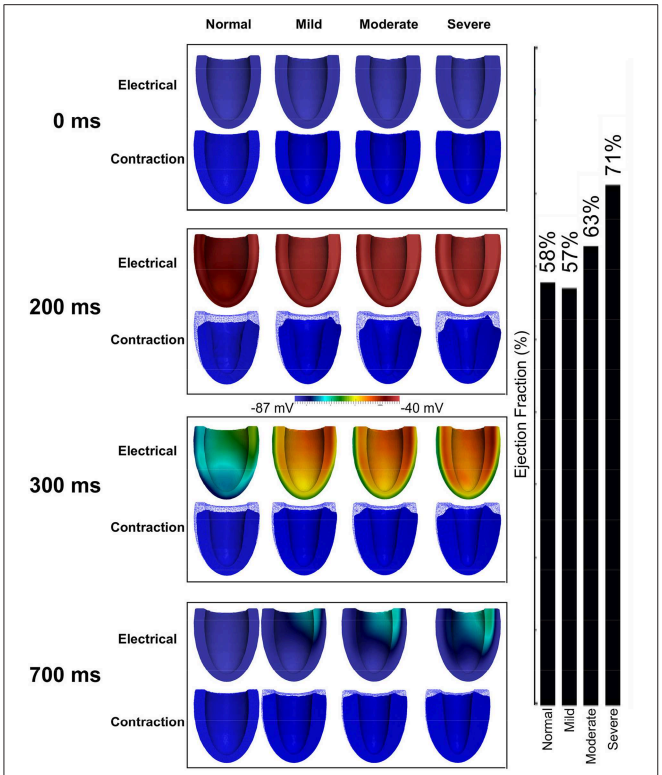

FIGURE 7 | Effects of HFpEF on 3D electro-mechanics. Electrical wave propagation and mechanical contraction at 0, 200, 300, and 700 ms in NORMAL, MILD, MODERATE, and SEVERE HFpEF hypertrophic cases. (Far right) Ejection fraction in NORMAL, MILD, MODERATE, and SEVERE HFpEF hypertrophic cases.

The simulation results discussed above were based on our HFpEF model developed from work by Zile and Gaasch (2011) and Selby et al. (2011). To our knowledge these are the only two studies that provide any notion of electrophysiological changes in HFpEF relative to control conditions. As the only difference between the HFpEF and the HFrEF models is a 30% NCX reduction in the former compared to control and a 175% increase in the latter (**Table 1**), we investigated whether changes in NCX activity could convert HFpEF to HFrEF and vice-versa, and therefore affect myocyte relaxation dynamics (**Figure 6**). This indeed proved to be the case. The results imply that a change in NCX activity is the dominant factor leading to impaired diastolic relaxation in HFpEF.

Effects of Concentric Hypertrophy of the Ventricle Wall on Cardiac Electro-Mechanics

Increased ventricular wall thickness has dramatic impacts on cardiac electro-mechanics. This is illustrated by the effects of varied degrees of hypertrophy on the ejection fraction in HFpEF condition (**Figure 9**). In simulations, the wall thickness of the LV varied from 9 mm (normal) to 12, 15, and 18 mm, mimicking varying degrees of hypertrophy. Though at the cellular level, cell length shortening and active force was decreased in HFpEF condition, the LVEF was preserved and increased with the increase of LV wall thickness. This agrees with what is seen clinically (Borlaug and Paulus, 2010; Phan et al., 2012; Liu et al., 2013; Zouein et al., 2013) and with previous modeling data (MacIver and Townsend, 2008; MacIver, 2010b, 2011). Our simulations confirm that the preserved LVEF in HFpEF is due to the thicker wall of the ventricle arising from concentric hypertrophy.

Taken together, our simulations suggest a possible pathway and mechanism underlying cardiac dysfunction in HFpEF. Any co-morbidities such as diabetes, hypertension, inflammation and/or hypertrophy may cause the ion channel and myofilament remodeling in myocardial cells. Cellular remodeling results in abnormal Ca^{2+} homeostasis, which in turn lead to abnormalities of contraction and incomplete relaxation of the LV with a persistent active resting tone. These abnormalities combine to increase the length of time to which the myocardium is subjected to stress prolonging systole and resulting in abnormal energy utilization and less efficient ejection of the stroke volume.

Relevance to Previous Studies

Lacombe et al. (2007) investigated the underlying mechanisms of diastolic dysfunction in type 1 diabetic rats. They observed no significant change in I_{CaL}, a reduction in Ca^{2+} transient amplitude and prolongation in its decay, a reduction in SR Ca^{2+} load and a decrease in the expression of sarco(endo)plasmic reticulum Ca^{2+}-ATPase-2a (SERCa) protein levels. They concluded that impairment of Ca^{2+} reuptake during myocyte relaxation contributed to diastolic dysfunction, with preserved global systolic function.

Selby et al. (2011) carried out a study to evaluate tachycardia-induced relaxation abnormalities in myocardium from patients with a normal ejection fraction. They observed incomplete relaxation with increased diastolic tension development at increasing pacing rates, significant resting tone and disproportionately elevated Ca^{2+} loads due to reduced sarcolemmal Ca^{2+} extrusion reserve. However, their patients did not carry a clinical diagnosis of heart failure.

MacIver and Townsend (2008) performed a mathematical study on HFpEF to determine the effect of changes in LV hypertrophy on stroke volume and LVEF. They concluded from their model that the preserved LVEF in HFpEF patients was a result of LV hypertrophy, which amplified absolute radial wall thickening in the setting of reduced long-axis shortening. MacIver also showed, using a simple abstract model, that remodeling was necessary to normalize stroke volume and suggested that regulation of end-diastolic volume was a primary compensatory mechanism in heart failure (MacIver, 2010b). However, their models did not consider the contribution of cardiomyocytes, coupled electrical wave propagation or nonlinear anisotropic cardiac mechanics.

Our simulation results are in agreement with and extend the findings of these previous studies (Lacombe et al., 2007; MacIver and Townsend, 2008; Selby et al., 2011), adding new evidence that impaired Ca^{2+} homeostasis (such as reduced systolic Ca^{2+} concentration and elevated diastolic Ca^{2+} concentration) together with hypertrophied wall underlie the key features of HFpEF with preserved ejection fraction and incomplete end-diastolic relaxation.

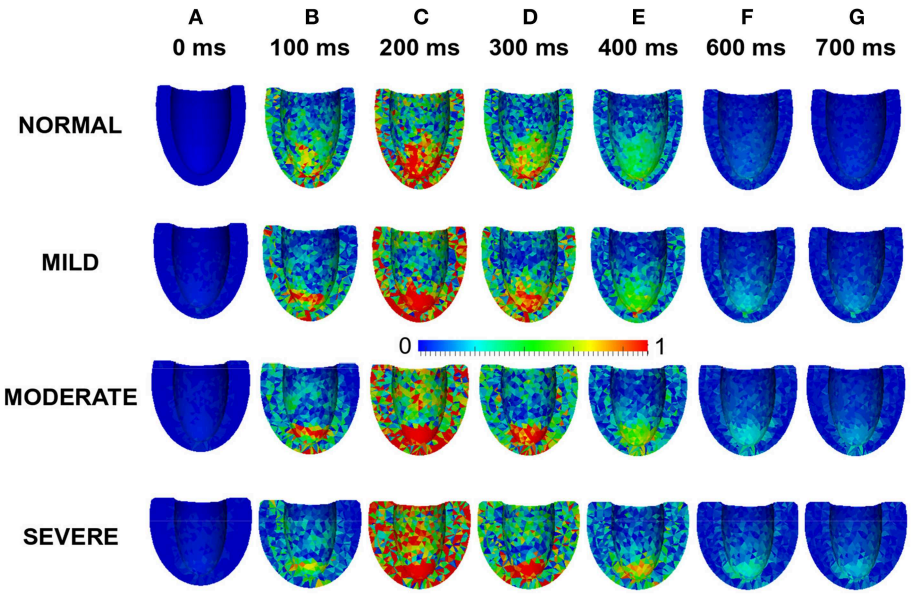

FIGURE 8 | Effects of HFpEF on stress magnitude distribution. Stress magnitude distribution at 0 ms **(A)**, 100 ms **(B)**, 200 ms **(C)**, 300 ms **(D)**, 400 ms **(E)** 600 ms **(F)**, and 700 ms **(G)** in NORMAL, MILD, MODERATE, and SEVERE hypertrophic HFpEF cases.

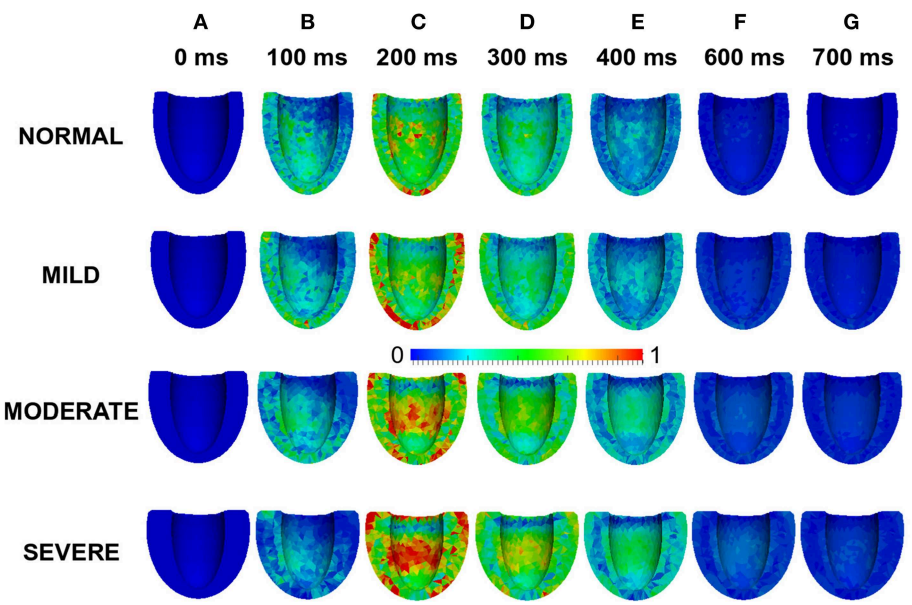

FIGURE 9 | Effects of HFpEF on strain magnitude distribution. Strain magnitude distribution at 0 ms **(A)**, 100 ms **(B)**, 200 ms **(C)**, 300 ms **(D)**, 400 ms **(E)** 600 ms **(F)**, and 700 ms **(G)** in NORMAL, MILD, MODERATE, and SEVERE hypertrophic HFpEF cases.

Limitations

In addition to acknowledged limitations of both the ORd electrophysiology model (O'Hara et al., 2011) and the (Tran et al., 2010) myofilament model, as experimental data show a reduction in NCX activity in diastolic dysfunction compared to control (Zile and Gaasch, 2011), we made a 30% reduction in NCX activity in our HFpEF model as there was no quantitative data available at the time of this study. In HFpEF patients, collagen production results in interstitial fibrosis (Heymans et al., 2005; Konstantinou et al., 2013), which we considered by reducing the intracellular electrical conductivities by 20% due to a lack of quantitative data. The HFpEF model also relaxes somewhat faster than the experimental data, which would imply that the effects of incomplete relaxation would be even greater than we have shown. As there

are no data available, we assumed the same degree of ion channel remodeling for the hypertrophied ventricles and also assumed the same distribution of ENDO, MCELL, and EPI cell types across the ventricular wall. We also did not consider electromechanical feedback between the electrical wave propagation and mechanically contracting ventricles. Finally, the use of a fluid-structure interaction model with the interaction of blood and the myocardial wall to determine pressure boundary conditions would allow a more realistic pressure profile. Whilst it is important that these potential limitations are stated, they do not fundamentally alter the principal conclusions of this study.

Conclusion

We have developed a novel, biophysically detailed model of HFpEF and used it to investigate the cellular mechanisms underlying myocardial Ca^{2+} homeostasis in HFpEF. We observed an elevated diastolic $[Ca^{2+}]_i$ level, a reduction in SR Ca^{2+} content and reduced SR Ca^{2+} release, a reduction in SR Ca^{2+} sequestration, an increase in resting tension, incomplete relaxation, reduced systolic stress and prolonged stress and strain durations. These mechanisms suggest that in HFpEF patients, impaired Ca^{2+} handling principally caused by reduction in NCX activity is a dominant abnormality in the condition that explains the mechanisms for impaired cardiac electro-mechanics in HFpEF.

Acknowledgments

This work was supported by project grants from Engineering and Physical Science Research Council UK (EP/J00958X/1; EP/I029826/1).

Supplementary Material

The Supplementary Material for this article can be found online at: http://www.frontiersin.org/journal/10.3389/fphys.2015.00078/abstract

References

Adeniran, I., Hancox, J. C., and Zhang, H. (2013a). Effect of cardiac ventricular mechanical contraction on the characteristics of the ECG: a simulation study. *J. Biomed. Sci. Eng.* 6, 47–60. doi: 10.4236/jbise.2013.612A007

Adeniran, I., Hancox, J., and Zhang, H. (2013b). *In silico* investigation of the short QT syndrome, using human ventricle models incorporating electromechanical coupling. *Front. Physiol.* 4:166. doi: 10.3389/fphys.2013.00166

Alan, C., and Hindmarsh, P. N. B. (2005). SUNDIALS: suite of nonlinear and differential/algebraic equation solvers. *ACM Trans. Math. Softw.* 31, 363–396. doi: 10.1145/1089014.1089020

Ambrosi, D., Arioli, G., Nobile, F., and Quarteroni, A. (2011). Electromechanical coupling in cardiac dynamics: the active strain approach. *SIAM J. Appl. Math.* 71, 605–621. doi: 10.1137/100788379

Asrar Ul Haq, M., Mutha, V., Rudd, N., Hare, D. L., and Wong, C. (2014). Heart failure with preserved ejection fraction—unwinding the diagnosis mystique. *Am. J. Cardiovasc. Dis.* 4, 100–113.

Auricchio, F., Beirão da Veiga, L., Lovadina, C., and Reali, A. (2010). The importance of the exact satisfaction of the incompressibility constraint in nonlinear elasticity: mixed FEMs versus NURBS-based approximations. *Comput. Methods Appl. Mech. Eng.* 199, 314–323. doi: 10.1016/j.cma.2008.06.004

Barry, W. H., and Bridge, J. H. (1993). Intracellular calcium homeostasis in cardiac myocytes. *Circulation* 87, 1806–1815. doi: 10.1161/01.CIR.87.6.1806

Barry, W. H., Hasin, Y., and Smith, T. W. (1985). Sodium pump inhibition, enhanced calcium influx via sodium-calcium exchange, and positive inotropic response in cultured heart cells. *Circ. Res.* 56, 231–241. doi: 10.1161/01.RES.56.2.231

Bers, D. (2001). *Excitation-Contraction Coupling and Cardiac Contractile Force, 2nd Edn.* Dordrecht: Springer.

Bhatia, R. S., Tu, J. V., Lee, D. S., Austin, P. C., Fang, J., Haouzi, A., et al. (2006). Outcome of heart failure with preserved ejection fraction in a population-based study. *N. Engl. J. Med.* 355, 260–269. doi: 10.1056/NEJMoa051530

Boffi, D., Brezzi, F., and Fortin, M. (2013). *Mixed Finite Element Methods and Applications, 2013 Edn*. New York, NY: Springer.

Bogaert, J., and Rademakers, F. E. (2001). Regional nonuniformity of normal adult human left ventricle. *Am. J. Physiol. Heart Circ. Physiol.* 280, H610–H620.

Bonet, J., and Wood, R. D. (2008). *Nonlinear Continuum Mechanics for Finite Element Analysis, 2nd Edn*. New York, NY: Cambridge University Press.

Borbély, A., van der Velden, J., Papp, Z., Bronzwaer, J. G., Edes, I., Stienen, G. J., et al. (2005). Cardiomyocyte stiffness in diastolic heart failure. *Circulation* 111, 774–781. doi: 10.1161/01.CIR.0000155257.33485.6D

Borlaug, B. A., and Paulus, W. J. (2010). Heart failure with preserved ejection fraction: pathophysiology, diagnosis, and treatment. *Eur. Heart J.* 32, 670–679. doi: 10.1093/eurheartj/ehq426

Braess, D. (2007). *Finite Elements: Theory, Fast Solvers, and Applications in Solid Mechanics, 3rd Edn*. New York, NY: Cambridge University Press.

Braess, D., and Ming, P. (2005). A finite element method for nearly incompressible elasticity problems. *Math. Comput.* 74, 25–52. doi: 10.1090/S0025-5718-04-01662-X

Brenner, S. C., and Scott, R. (2010). *The Mathematical Theory of Finite Element Methods, 3rd Edn. 2008*. New York, NY: Springer.

Bueno-Orovio, A., Sánchez, C., Pueyo, E., and Rodriguez, B. (2014). Na/K pump regulation of cardiac repolarization: insights from a systems biology approach. *Pflügers. Arch. Eur. J. Physiol.* 466, 183–193. doi: 10.1007/s00424-013-1293-1

Burkhoff, D., Yue, D. T., Franz, M. R., Hunter, W. C., and Sagawa, K. (1984). Mechanical restitution of isolated perfused canine left ventricles. *Am. J. Physiol.* 246, H8–H16.

Burnett, D. S. (1987). *Finite Element Analysis: From Concepts to Applications, 1st Edn*. Reading, MA: Addison Wesley.

Chamberland, E., Fortin, A., and Fortin, M. (2010). Comparison of the performance of some finite element discretizations for large deformation elasticity problems. *Comput. Struct.* 88, 664–673. doi: 10.1016/j.compstruc.2010.02.007

Cherubini, C., Filippi, S., Nardinocchi, P., and Teresi, L. (2008). An electromechanical model of cardiac tissue: constitutive issues and electrophysiological effects. *Prog. Biophys. Mol. Biol.* 97, 562–573. doi: 10.1016/j.pbiomolbio.2008.02.001

Ciarlet, P. G. (2002). *The Finite Element Method for Elliptic Problems, 2nd Edn*. New York, NY: Society for Industrial and Applied Mathematics.

Cohen, S., and Hindmarsh, A. C. (1996). "Cvode, a stiff/nonstiff ode solver in C," in *C. Computers in Physics*, ed L. M. Holmes (New York, NY: American Institute of Physics Inc.), 138–143.

Colli Franzone, P., Pavarino, L. F., and Taccardi, B. (2005). Simulating patterns of excitation, repolarization and action potential duration with cardiac Bidomain and Monodomain models. *Math. Biosci.* 197, 35–66. doi: 10.1016/j.mbs.2005.04.003

Costa, K. D., Holmes, J. W., and McCulloch, A. D. (2001). Modelling cardiac mechanical properties in three dimensions. *Philos. Trans. R. Soc. Lond. Ser. Math. Phys. Eng. Sci.* 359, 1233–1250. doi: 10.1098/rsta.2001.0828

Drouin, E., Charpentier, F., Gauthier, C., Laurent, K., and Le Marec, H. (1995). Electrophysiologic characteristics of cells spanning the left ventricular wall of human heart: evidence for presence of M cells. *J. Am. Coll. Cardiol.* 26, 185–192. doi: 10.1016/0735-1097(95)00167-X

Ebashi, S. (1984). Ca^{2+} and the contractile proteins. *J. Mol. Cell. Cardiol.* 16, 129–136. doi: 10.1016/S0022-2828(84)80701-4

Ern, A., and Guermond, J.-L. (2010). *Theory and Practice of Finite Elements, 1st Edn. 2004*. New York, NY: Springer.

Franz, M. R., Schaefer, J., Schöttler, M., Seed, W. A., and Noble, M. I. (1983). Electrical and mechanical restitution of the human heart at different rates of stimulation. *Circ. Res.* 53, 815–822. doi: 10.1161/01.RES.53.6.815

Glitsch, H. G. (2001). Electrophysiology of the sodium-potassium-ATPase in cardiac cells. *Physiol. Rev.* 81, 1791–1826.

Gomez, J. F., Cardona, K., Romero, L., Ferrero, J. M., and Trenor, B. (2014). Electrophysiological and structural remodeling in heart failure modulate arrhythmogenesis. 1D simulation study. *PLoS ONE* 9:e106602. doi: 10.1371/journal.pone.0106602

Haga, J. B., Osnes, H., and Langtangen, H. P. (2012). On the causes of pressure oscillations in low-permeable and low-compressible porous media. *Int. J. Numer. Anal. Methods Geomech.* 36, 1507–1522. doi: 10.1002/nag.1062

Heymans, S., Schroen, B., Vermeersch, P., Milting, H., Gao, F., Kassner, A., et al. (2005). Increased cardiac expression of tissue inhibitor of metalloproteinase-1 and tissue inhibitor of metalloproteinase-2 is related to cardiac fibrosis and dysfunction in the chronic pressure-overloaded human heart. *Circulation* 112, 1136–1144. doi: 10.1161/CIRCULATIONAHA.104.516963

Holzapfel, G. A. (2000). *Nonlinear Solid Mechanics: A Continuum Approach for Engineering, 1st Edn*. Chichester: Wiley.

Hughes, T. J. R. (2000). *The Finite Element Method: Linear Static and Dynamic Finite Element Analysis*. New York, NY: Dover Publications.

Keener, J., and Sneyd, J. (2008). *Mathematical Physiology: II: Systems Physiology, 2nd Edn*. New York, NY: Springer.

Keldermann, R. H., Nash, M. P., and Panfilov, A. V. (2009). Modeling cardiac mechano-electrical feedback using reaction-diffusion-mechanics systems. *Phys. Nonlinear Phenom.* 238, 1000–1007. doi: 10.1016/j.physd.2008.08.017

Keller, D. U. J., Kalayciyan, R., Dössel, O., and Seemann, G. (2009). "Fast creation of endocardial stimulation profiles for the realistic simulation of body surface ECGs," in *IFMBE Proceedings*, 145–148. Available online at: http://www.scopus.com/inward/record.url?eid=2-s2.0-77950134835&partnerID=40&md5=2db2b89cc19de5e28ec01ebbf0dffff0 (Accessed July 20, 2011).

Kjørstad, K. E., Nordhaug, D. O., Korvald, C., Müller, S., Steensrud, T., and Myrmel, T. (2007). Mechanical restitution curves: a possible load independent assessment of contractile function. *Eur. J. Cardio-Thorac. Surg.* 31, 677–684. doi: 10.1016/j.ejcts.2007.01.013

Kono, M., Kisanuki, A., Takasaki, K., Nakashiki, K., Yuasa, T., Kuwahara, E., et al. (2009). Left ventricular systolic function is abnormal in diastolic heart failure: re-assessment of systolic function using cardiac time interval analysis. *J. Cardiol.* 53, 437–446. doi: 10.1016/j.jjcc.2009.02.014

Konstantinou, D. M., Chatzizisis, Y. S., and Giannoglou, G. D. (2013). Pathophysiology-based novel pharmacotherapy for heart failure with preserved ejection fraction. *Pharmacol. Ther.* 140, 156–166. doi: 10.1016/j.pharmthera.2013.05.012

Lacombe, V. A., Viatchenko-Karpinski, S., Terentyev, D., Sridhar, A., Emani, S., Bonagura, J. D., et al. (2007). Mechanisms of impaired calcium handling underlying subclinical diastolic dysfunction in diabetes. *Am. J. Physiol. Regul. Integr. Comp. Physiol.* 293, R1787–R1797. doi: 10.1152/ajpregu.00059.2007

Le Tallec, P. (1994). "Numerical methods for nonlinear three-dimensional elasticity," in *Handbook of Numerical Analysis*, Vol. III, eds P. G. Ciarlet and J. L. Lions (North-Holland: Amsterdam), 465–622.

Li, G. R., Feng, J., Yue, L., and Carrier, M. (1998). Transmural heterogeneity of action potentials and Ito1 in myocytes isolated from the human right ventricle. *Am. J. Physiol.* 275, H369–H377.

Liu, Y., Haddad, T., and Dwivedi, G. (2013). Heart failure with preserved ejection fraction: current understanding and emerging concepts. *Curr. Opin. Cardiol.* 28, 187–196. doi: 10.1097/HCO.0b013e32835c5492

Logg, A., Mardal, K.-A., and Wells, G. (eds.) (2012). *Automated Solution of Differential Equations by the Finite Element Method: The FEniCS Book, 2012th Edn*. Heidelberg: Springer.

MacIver, D. H. (2010a). Current controversies in heart failure with a preserved ejection fraction. *Future Cardiol.* 6, 97–111. doi: 10.2217/fca.09.56

MacIver, D. H. (2010b). Is remodeling the dominant compensatory mechanism in both chronic heart failure with preserved and reduced left ventricular ejection fraction? *Basic Res. Cardiol.* 105, 227–234. doi: 10.1007/s00395-009-0063-x

MacIver, D. H. (2011). A new method for quantification of left ventricular systolic function using a corrected ejection fraction. *Eur. J. Echocardiogr.* 12, 228–234. doi: 10.1093/ejechocard/jeq185

MacIver, D. H., and Dayer, M. J. (2012). An alternative approach to understanding the pathophysiological mechanisms of chronic heart failure. *Int. J. Cardiol.* 154, 102–110. doi: 10.1016/j.ijcard.2011.05.075

MacIver, D. H., and Townsend, M. (2008). A novel mechanism of heart failure with normal ejection fraction. *Heart Br. Card. Soc.* 94, 446–449. doi: 10.1136/hrt.2006.114082

Marsden, J. E., and Hughes, T. J. R. (1994). *Mathematical Foundations of Elasticity*. New Jersey: Dover Publications.

Niederer, S. A., and Smith, N. P. (2008). An improved numerical method for strong coupling of excitation and contraction models in the heart. *Prog. Biophys. Mol. Biol.* 96, 90–111. doi: 10.1016/j.pbiomolbio.2007.08.001

O'Hara, T., Virág, L., Varró, A., and Rudy, Y. (2011). Simulation of the undiseased human cardiac ventricular action potential: model formulation and experimental validation. *PLoS Comput. Biol.* 7:e1002061. doi: 10.1371/journal.pcbi.1002061

Owan, T. E., Hodge, D. O., Herges, R. M., Jacobsen, S. J., Roger, V. L., and Redfield, M. M. (2006). Trends in prevalence and outcome of heart failure with preserved ejection fraction. *N. Engl. J. Med.* 355, 251–259. doi: 10.1056/NEJMoa052256

Pathmanathan, P., and Whiteley, J. P. (2009). A numerical method for cardiac mechanoelectric simulations. *Ann. Biomed. Eng.* 37, 860–873. doi: 10.1007/s10439-009-9663-8

Phan, T. T., Shivu, G. N., Abozguia, K., Sanderson, J. E., and Frenneaux, M. (2012). The pathophysiology of heart failure with preserved ejection fraction: from molecular mechanisms to exercise haemodynamics. *Int. J. Cardiol.* 158, 337–343. doi: 10.1016/j.ijcard.2011.06.113

Prabhu, S. D., and Freeman, G. L. (1995). Effect of tachycardia heart failure on the restitution of left ventricular function in closed-chest dogs. *Circulation* 91, 176–185. doi: 10.1161/01.CIR.91.1.176

Rademakers, F. E., Rogers, W. J., Guier, W. H., Hutchins, G. M., Siu, C. O., Weisfeldt, M. L., et al. (1994). Relation of regional cross-fiber shortening to wall thickening in the intact heart. Three-dimensional strain analysis by NMR tagging. *Circulation* 89, 1174–1182. doi: 10.1161/01.CIR.89.3.1174

Redfield, M. M., Jacobsen, S. J., Burnett, J. C., Mahoney, D. W., Bailey, K. R., and Rodeheffer, R. J. (2003). Burden of systolic and diastolic ventricular dysfunction in the community: appreciating the scope of the heart failure epidemic. *JAMA* 289, 194–202. doi: 10.1001/jama.289.2.194

Rice, J. J., Wang, F., Bers, D. M., and de Tombe, P. P. (2008). Approximate model of cooperative activation and crossbridge cycling in cardiac muscle using ordinary differential equations. *Biophys. J.* 95, 2368–2390. doi: 10.1529/biophysj.107.119487

Robertson, S. P., Johnson, J. D., Holroyde, M. J., Kranias, E. G., Potter, J. D., and Solaro, R. J. (1982). The effect of troponin I phosphorylation on the Ca^{2+}-binding properties of the Ca^{2+}-regulatory site of bovine cardiac troponin. *J. Biol. Chem.* 257, 260–263.

Rossi, S., Lassila, T., Ruiz-Baier, R., Sequeira, A., and Quarteroni, A. (2014). Thermodynamically consistent orthotropic activation model capturing ventricular systolic wall thickening in cardiac electromechanics. *Eur. J. Mech. ASolids.* 48, 129–142. doi: 10.1016/j.euromechsol.2013.10.009

Rush, S., and Larsen, H. (1978). A practical algorithm for solving dynamic membrane equations. *IEEE Trans. Biomed. Eng.* 25, 389–392. doi: 10.1109/TBME.1978.326270

Sanderson, J. E. (2007). Heart failure with a normal ejection fraction. *Heart* 93, 155–158. doi: 10.1136/hrt.2005.074187

Selby, D. E., Palmer, B. M., LeWinter, M. M., and Meyer, M. (2011). Tachycardia-induced diastolic dysfunction and resting tone in myocardium from patients with a normal ejection fraction. *J. Am. Coll. Cardiol.* 58, 147–154. doi: 10.1016/j.jacc.2010.10.069

Soma, J. (2011). Heart failure with preserved left ventricular ejection fraction: concepts, misconceptions and future directions. *Blood Press.* 20, 129–133. doi: 10.3109/08037051.2010.542642

Sundnes, J., Lines, G. T., and Tveito, A. (2005). An operator splitting method for solving the bidomain equations coupled to a volume conductor model for the torso. *Math. Biosci.* 194, 233–248. doi: 10.1016/j.mbs.2005.01.001

Taggart, P., Sutton, P. M., Opthof, T., Coronel, R., Trimlett, R., Pugsley, W., et al. (2000). Inhomogeneous transmural conduction during early ischaemia

in patients with coronary artery disease. *J. Mol. Cell. Cardiol.* 32, 621–630. doi: 10.1006/jmcc.2000.1105

Tran, K., Smith, N. P., Loiselle, D. S., and Crampin, E. J. (2010). A metabolite-sensitive, thermodynamically constrained model of cardiac cross-bridge cycling: implications for force development during ischemia. *Biophys. J.* 98, 267–276. doi: 10.1016/j.bpj.2009.10.011

Trenor, B., Cardona, K., Gomez, J. F., Rajamani, S., Ferrero, J. M., Belardinelli, L., et al. (2012). Simulation and mechanistic investigation of the arrhythmogenic role of the late sodium current in human heart failure. *PLoS ONE* 7:e32659. doi: 10.1371/journal.pone.0032659

Vasan, R. S., and Levy, D. (2000). Defining diastolic heart failure: a call for standardized diagnostic criteria. *Circulation* 101, 2118–2121. doi: 10.1161/01.CIR.101.17.2118

Wang, J., Khoury, D. S., Yue, Y., Torre-Amione, G., and Nagueh, S. F. (2008). Preserved left ventricular twist and circumferential deformation, but depressed longitudinal and radial deformation in patients with diastolic heart failure. *Eur. Heart J.* 29, 1283–1289. doi: 10.1093/eurheartj/ehn141

Whiteley, J. P., Bishop, M. J., and Gavaghan, D. J. (2007). Soft tissue modelling of cardiac fibres for use in coupled mechano-electric simulations. *Bull. Math. Biol.* 69, 2199–2225. doi: 10.1007/s11538-007-9213-1

Wilson, L. D., Jennings, M. M., and Rosenbaum, D. S. (2011). Point: M cells are present in the ventricular myocardium. *Heart Rhythm* 8, 930–933. doi: 10.1016/j.hrthm.2011.01.026

Workman, A. J., Kane, K. A., and Rankin, A. C. (2003). Characterisation of the Na, K pump current in atrial cells from patients with and without chronic atrial fibrillation. *Cardiovasc. Res.* 59, 593–602. doi: 10.1016/S0008-6363(03)00466-8

Yturralde, R. F., and Gaasch, W. H. (2005). Diagnostic criteria for diastolic heart failure. *Prog. Cardiovasc. Dis.* 47, 314–319. doi: 10.1016/j.pcad.2005.02.007

Zaugg, C. E., Kojima, S., Wu, S. T., Wikman Coffelt, J., Parmley, W. W., and Buser, P. T. (1995). 997-86 intracellular calcium transients underlie mechanical restitution in whole rat hearts. *J. Am. Coll. Cardiol.* 25, 325A. doi: 10.1016/0735-1097(95)92811-I

Zile, M. R., Baicu, C. F., and Gaasch, W. H. (2004). Diastolic heart failure—abnormalities in active relaxation and passive stiffness of the left ventricle. *N. Engl. J. Med.* 350, 1953–1959. doi: 10.1056/NEJMoa032566

Zile, M. R., and Gaasch, W. H. (2011). Abnormal calcium homeostasis: one mechanism in diastolic heart failure. *J. Am. Coll. Cardiol.* 58, 155–157. doi: 10.1016/j.jacc.2010.10.068

Zile, M. R., Gaasch, W. H., Carroll, J. D., Feldman, M. D., Aurigemma, G. P., Schaer, G. L., et al. (2001). Heart failure with a normal ejection fraction: is measurement of diastolic function necessary to make the diagnosis of diastolic heart failure? *Circulation* 104, 779–782. doi: 10.1161/hc3201.094226

Zouein, F. A., de Castro Brás, L. E., da Costa, D. V., Lindsey, M. L., Kurdi, M., and Booz, G. W. (2013). Heart failure with preserved ejection fraction: emerging drug strategies. *J. Cardiovasc. Pharmacol.* 62, 13–21. doi: 10.1097/FJC.0b013e31829a4e61

Conflict of Interest Statement: The authors declare that the research was conducted in the absence of any commercial or financial relationships that could be construed as a potential conflict of interest.

frontiers in Physiology

MINI REVIEW
published: 17 March 2015
doi: 10.3389/fphys.2015.00076

Novel insights into mechanisms for Pak1-mediated regulation of cardiac Ca^{2+} homeostasis

Yanwen Wang[1], Hoyee Tsui[2], Emma L. Bolton[1], Xin Wang[2], Christopher L.-H. Huang[3], R. John Solaro[4], Yunbo Ke[4] and Ming Lei[1]**

[1] Department of Pharmacology, University of Oxford, Oxford, UK, [2] Faculty of Life Science, University of Manchester, Manchester, UK, [3] Physiological Laboratory, University of Cambridge, Cambridge, UK, [4] Department of Physiology and Biophysics, University of Illinois, Chicago, IL, USA

OPEN ACCESS

Edited by:
Zhilin Qu, University of California, Los Angeles, USA

Reviewed by:
David R. Van Wagoner, Cleveland Clinic Lerner College of Medicine of Case Western Reserve University, USA
Przemyslaw Radwanski, Ohio State University, USA

***Correspondence:**
Yunbo Ke, Department of Physiology and Biophysics, University of Illinois, 835 S. Wolcott Ave., M/C 901, Chicago, IL 60612, USA
yke@uic.edu;
Ming Lei, Department of Pharmacology, University of Oxford, Mansfield Road, Oxford OX1 3QT, UK
ming.lei@pharm.ox.ac.uk

Specialty section:
This article was submitted to Cardiac Electrophysiology, a section of the journal Frontiers in Physiology

Received: *20 December 2014*
Accepted: *25 February 2015*
Published: *17 March 2015*

Citation:
Wang Y, Tsui H, Bolton EL, Wang X, Huang CL-H, Solaro RJ, Ke Y and Lei M (2015) Novel insights into mechanisms for Pak1-mediated regulation of cardiac Ca^{2+} homeostasis. Front. Physiol. 6:76. doi: 10.3389/fphys.2015.00076

A series of recent studies report novel roles for Pak1, a key member of the highly conserved family of serine-threonine protein kinases regulated by Ras-related small G-proteins, Cdc42/Rac1, in cardiac physiology and cardioprotection. Previous studies had identified Pak1 in the regulation of hypertrophic remodeling that could potentially lead to heart failure. This article provides a review of more recent findings on the roles of Pak1 in cardiac Ca^{2+} homeostasis. These findings identified crucial roles for Pak1 in cardiomyocyte Ca^{2+} handling and demonstrated that it functions through unique mechanisms involving regulation of the post-transcriptional activity of key Ca^{2+}-handling proteins, including the expression of Ca^{2+}-ATPase SERCA2a, along with the speculative possibility of an involvement in the maintenance of transverse (T)-tubular structure. They highlight important regulatory functions of Pak1 in Ca^{2+} homeostasis in cardiac cells, and identify novel potential therapeutic strategies directed at manipulation of Pak1 signaling for the management of cardiac disease, particularly heart failure.

Keywords: Pak1, Ca^{2+} homeostasis, heart

Introduction

Protein kinases are versatile signaling molecules involved in the regulation of a wide range of physiological processes. Of these, the p21-activated kinases (Paks) form a group of serine/threonine protein kinases activated by Cdc42 and Rac1, and were first discovered in rat brain tissue two decades ago (Manser et al., 1994). The structure, substrate-specificity and functional role of Paks are evolutionarily conserved from protozoa to mammals. Vertebrate Paks are particularly important in cytoskeletal remodeling and the assembly of focal adhesion structures, thereby contributing to the modulation of dynamic processes such as cell migration and synaptic plasticity (Manser and Lim, 1999; Hofmann et al., 2004; Zhao and Manser, 2005). Over the past decade, significant progress has been made in understanding the functions of Pak1, a key member of the Pak family, in particular, its roles in the regulation of excitability and contractility of the heart (Ke et al., 2004, 2007, 2009). The present review now provides an updated account of these recent findings regarding additional roles of Pak1 in Ca^{2+} homeostasis and Ca^{2+} handling in cardiac cells.

Regulation of L-Type Ca^{2+} Channels in Sinoatrial Node Pacemaker Cells

The role of pak1 in the regulation of ion channel activity in cardiomyocytes was first demonstrated in isolated guinea pig sinoatrial node (SAN) pacemaker cells (Ke et al., 2007). In cultured guinea pig SAN cells, where active Pak1 expression was induced through infection with recombinant adenovirus expressing constitutively active Pak1 (CA-Pak1), responses of both L-type Ca^{2+} channel (LTCC) and delayed rectifier K^+ channel currents to β-adrenergic stimulation by isoproterenol were depressed in comparison to SAN cells infected with control virus, Ad-LacZ. Similarly chronotropic responses to isoproterenol stimulation, reflected in repetitive action potential frequency were depressed in both intact SAN tissue and isolated SAN cells expressing active Pak1, when compared to controls expressing Ad-LacZ (Ke et al., 2007). In contrast, Pak1 deletion in cardiac specific conditional knockout (Pak1cko) or in total knockout mice resulted in an increased SAN driven heart rate (Wang et al., 2014a). These modified responses to isoproterenol stimulation in SAN tissue and cells infected by CA-Pak1 likely reflect alterations in protein phosphorylation which modulate LTCC and delayed rectifier K^+ channel activity, and their responses to β-adrenergic stimulation.

Our further studies focussing on LTCC regulation in SAN cells implicated Pak1 as a regulator of protein phosphatase 2A (PP2A). Immunoprecipitation studies indicated that Pak1 and PP2A form a complex, leading to the hypothesis that Pak1 may regulate LTCC activity through PP2A action (Ke et al., 2007). This hypothesis was substantiated by studying the influence of the PP2A inhibitor okadaic acid (OA) on the effects of isoproterenol on LTCC activity in Ad-Pak1–infected cells. OA partially reversed the suppressant effect of active Pak1 on the response of LTCCs to isoproterenol in Ad-Pak1–infected cells. This suggests that Pak1 acts by increasing PP2A activity. Conversely, our recent study demonstrated that mice with a cardiomyocyte-specific Pak1 deletion (Pak1cko) showed higher heart rates than their control littermates (Pak1f/f), although Pak1cko and control Pak1f/f mice showed similar baseline electrocardiographic P wave durations and P-R, QRS and QT intervals (Wang et al., 2014a).

Accumulating evidence implicates a coordinated interplay between the activities of kinases and phosphatases in modulation of LTCC-mediated Ca^{2+} influx even in the absence of humoral stimulation. For example, in the well-known β-adrenergic receptor/protein kinase A (PKA) cascade, inhibitor-1 is a downstream PKA target whose activation results in an attenuation of protein phosphatase 1 (PP1) activity (Gupta et al., 1996). Santana et al. (2002) showed that the phosphatase calcineurin opposes PKA action in mouse ventricular myocytes. Application of the PP2A inhibitor OA can activate LTCC (duBell and Rogers, 2004). Calyculin A, which inhibits both PP1 and PP2A, increases contractility in ventricular myocytes by increasing LTCC activity (duBell et al., 2002). A complementary study by duBell et al reported that addition of exogenous PP2A decreased LTCC currents in rat ventricular myocytes (duBell et al., 1996).

These results together suggested an existence of a dynamic regulatory balance between kinase and phosphatase activity in regulating the LTCC and delayed rectifier K^+ channel activity in cardiac cells that may be important in controlling cardiac pacemaker activity in response to autonomic and humoral stimulation.

Regulation of Ca^{2+} Handling and Ca^{2+} Homeostasis in Ventricular Myocytes

In parallel with Pak1 action in SAN myocytes, enhanced Pak1 function brought about by Pak1 activating peptide, PAP (Wang et al., 2014b) in ventricular tissue prevented hypertrophic associated ventricular arrhythmias, and Pak1 deletion in *Pak1*^{cko} or in knockout mice increased the risks of ventricular alternans and arrhythmias compared to WT mice. These findings went with a co-immunoprecipitation of Pak1 and PP2A suggesting a complex formation in ventricular myocytes, in common with SAN cells (Ke et al., 2007). Recent studies have also suggested regulatory roles of Pak1 in Ca^{2+} homeostasis in ventricular myocytes (Sheehan et al., 2009; DeSantiago et al., 2013; Wang et al., 2014a). CA-Pak1 over-expression altered Ca^{2+} transient decay constants (τ_{Ca}) (Sheehan et al., 2009) and antagonized adrenergic signaling by attenuating isoproterenol-induced increases in the activity ofLTCCs and other proteins regulating Ca^{2+} handling (Sheehan et al., 2009). In contrast, ventricular myocytes from *Pak1*^{cko} mice with a cardiomyocyte-specific *Pak1* knockout showed abnormal Ca^{2+} homeostasis including increased diastolic $[Ca^{2+}]_i$, as well as decreased sarcoplasmic reticular (SR) Ca^{2+} content and decreased SERCA function, particularly during β-adrenergic stress (Wang et al., 2014a). Significant differences in Ca^{2+} homeostasis were observed between isolated *Pak1*^{cko} and wild type, *Pak1*$^{f/f}$, ventricular myocytes. Diastolic $[Ca^{2+}]_i$ was higher in *Pak1*^{cko} than *Pak1*$^{f/f}$ myocytes under both baseline and chronic β-adrenergic stress conditions. *Pak1*^{cko} myocytes showed more frequent irregular, alternating Ca^{2+} transients and/or Ca^{2+} waves at increased stimulation frequencies than *Pak1*$^{f/f}$ myocytes under both baseline and chronic β-adrenergic stress conditions during 0.5, 1, and 3 Hz field stimulation. This abnormal Ca^{2+} homeostasis in *Pak1*^{cko} myocytes correlated with differences in evoked cytosolic and SR Ca^{2+} responses between *Pak1*$^{f/f}$ and *Pak1*^{cko} myocytes, in both the absence and presence of chronic β-adrenergic stress (Wang et al., 2014a). Thus, time constants for decays of the Na^+-Ca^{2+} exchange (NCX) current (I_{NCX}) following I_{NCX} induction by 10 mM caffeine were significantly greater in *Pak1*^{cko} than *Pak1*$^{f/f}$ myocytes under chronic β-adrenergic stress. SR Ca^{2+}content, measured by integration of the I_{NCX} records, was reduced in *Pak1*^{cko} compared to *Pak1*$^{f/f}$ myocytes in both the absence and presence of chronic β-adrenergic stress. The decay rate constants of systolic Ca^{2+} transients in *Pak1*^{cko} myocytes k_{SERCA}, representing the kinetics of cytosolic Ca^{2+} removal brought about by both SERCA and NCX, was significantly lower than that shown by *Pak1*$^{f/f}$ myocytes in both the absence and presence of chronic β-adrenergic stress (Wang et al., 2014a). The rate constant k_{SERCA} was reduced by chronic β-adrenergic stress in both the *Pak1*$^{f/f}$ and *Pak1*^{cko} myocytes but more severely so in the *Pak1*^{cko} myocytes. Finally,

peak systolic $[Ca^{2+}]_i$, estimated from the differences between peaks and baselines of systolic Ca^{2+} transients obtained during regular stimulation, was indistinguishable between *Pak1*$^{f/f}$ and *Pak1*^{cko} under baseline conditions, but was significantly reduced by chronic β-adrenergic stress in both *Pak1*$^{f/f}$ and *Pak1*^{cko}, and again more severely so in the *Pak1*^{cko} (Wang et al., 2014a). In contrast, LTCC activity was indistinguishable between *Pak1*^{cko} and *Pak1*$^{f/f}$ under both baseline and chronic β-adrenergic stress conditions, but chronic β-adrenergic stress reduced LTCC current in both *Pak1*^{cko} and *Pak1*$^{f/f}$ ventricular myocytes, which suggests that genetic deletion of Pak1 did not alter the expression and activity of LTCC in these cells. This result contrasts with the effect of CA-Pak1 in SAN cells, and may reflect differing effects of Pak1 on ion channels in different cell types or physiological conditions, and requires further investigation (Wang et al., 2014a). These alterations in Ca^{2+} homeostasis were associated with an increased incidence of ventricular arrhythmias and electrophysiological instability during either acute or chronic β-adrenergic challenge induced by isoproterenol in *Pak1*^{cko} hearts. Hence modulation of Pak1 activity modified Ca^{2+} handling under both physiological and β-adrenergic challenge conditions.

Our further molecular studies associated these physiological findings with an impaired SERCA2a function and down-regulation of SERCA2a mRNA and protein expression in *Pak1*^{cko} hearts (Wang et al., 2014a). Further exploration of this altered transcriptional regulation in cultured neonatal rat cardiomyocytes (NRCMs) demonstrated that exposure to control Ad-shC2 virus infection increased SERCA2a protein and mRNA levels following phenylephrine challenge (Wang et al., 2014a). This was abolished by the Pak1-knockdown in Ad-shPak1-infected NRCMs and increased by constitutive over-expression of active Pak1 (Ad-CAPak1) (Wang et al., 2014a). This regulation appeared to involve activation of serum response factor (SRF), a transcriptional factor well-known for its vital role in regulation of cardiogenesis genes in the Pak1-dependent regulation of SERCA2a (Wang et al., 2014a).

The above results indicate that modulation of Pak1 activity in ventricular myocytes can have a significant impact on Ca^{2+} handling in these cells under both baseline physiological and β-adrenergic challenge conditions.

Possible Roles in Maintaining Transverse (T)-Tubular Structure

Preliminary evidence (DeSantiago et al., 2013) suggests structural roles of Pak1, in addition to the above functional role of Pak1 in maintaining transverse (T)-tubular structure, which is altered in hypertrophic remodeling. Pak1$^{-/-}$ ventricular myocytes showed decreased cell capacitances compared to WT suggesting decreased T-tubular density. Under these conditions, cells showed comparable SR Ca loads and phospholamban phosphorylation, while their systolic Ca^{2+} transients showed decreased amplitudes and delayed rise times, consistent with a reduced coupling between LTCC-mediated Ca^{2+} influx and RyR2-mediated Ca^{2+}-induced Ca^{2+} release (CICR); changes which were not observed in Pak1$^{-/-}$ atrial myocytes. Such findings are consistent with the central role of T-tubules in triggering and synchronizing excitation–contraction coupling, and merit

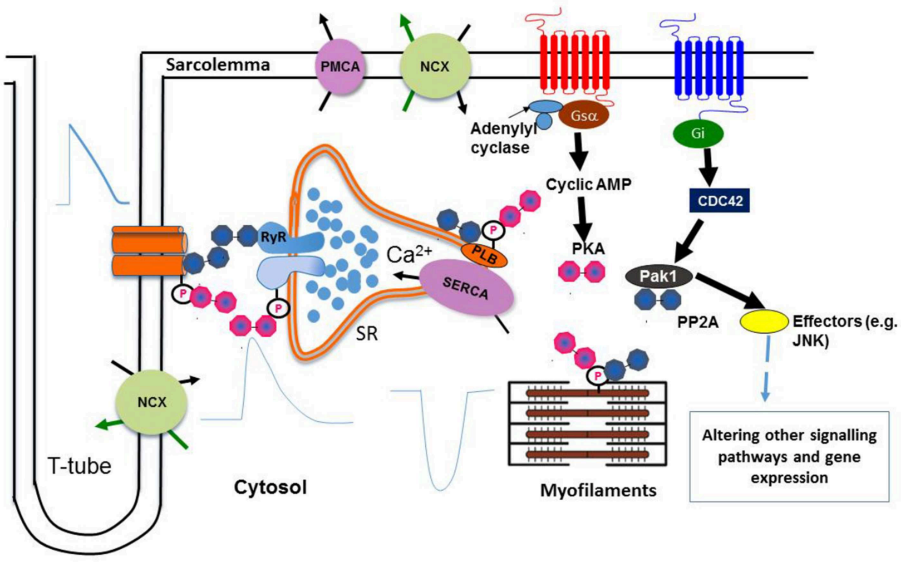

FIGURE 1 | Regulation of Ca^{2+} homeostasis by Pak1. Protein kinase PKA and phosphatase PP2A are associated with key Ca^{2+} handling and regulatory proteins, which in turn are linked to upstream signaling cascades. A balance of protein kinase and phosphatase activities is required to maintain normal cardiac functions. Pak1 also regulates hypertrophic signaling and gene expression of SERCA2a through other signaling pathways by activating its downstream effectors (e.g., JNK). (Liu et al., 2011; Wang et al., 2014a) (NCX: Na^+-Ca^{2+} exchanger, PMCA: Plasma membrane Ca^{2+} ATPase, JNK: c-Jun N-terminal Kinase).

further exploration. T-tubular remodeling has been reported in other cardiac pathologies, and could well be involved in the associated alterations in cellular processes, and hence cardiac function.

In summary, as illustrated in **Figure 1**, these novel Pak1 effects on Ca^{2+} homestasis complement previously established actions upon PP2A and the resulting balance between kinase and phosphatase activity in controlling cardiac ion channel activity and rhythmic Ca^{2+} cycling.

Earlier reports (Liu et al., 2011) had identified Pak1 as a novel regulator of hypertrophic remodeling whose cardiomyocyte-specific deletion exacerbated cardiac hypertrophy leading to heart failure, following transverse aortic constriction. These features were prevented by the non-selective Pak1 activator FTY720 in wild-type but not $Pak1^{cko}$ mice (Liu et al., 2013). Such cardiac hypertrophy, with improved cardiac function and decreased myocyte apoptosis compared to WT, was reduced in mice overexpressing Pak1, with improved cardiac function and decreased myocyte apoptosis compared to WT (Mao et al., 2009). A recent study identified Pak1 as one of the significant genes on the core networks for dilated cardiomyopathies by pathway analyses in a Genome wide association study (GWAS) dataset of patients suffering from DCM (Backes et al., 2014). Over the past decade, significant progress has also been made in understanding of additional roles of Pak1 in the regulation of Ca^{2+} homeostasis and Ca^{2+} handling in turn regulating cardiomyocyte excitability and contractility (Ke et al., 2004, 2007, 2009). There have also been speculative suggestions for a role of Pak1 in the maintenance of transverse (T) tubule structure. The present review now provides an updated account of these recent findings. Thus, Pak1 may thus offer a novel therapeutic target for modulation of Ca^{2+} handling in cardiac disease conditions.

Source of Funding

The work was supported by the Medical Research Council (G10002647:ML, XW, EJC, JRS, YBK), the British Heart Foundation (PG/11/59/29006; PG/12/21/29473: ML, XW), The MacVeigh benefaction (CLH)" and a Chinese Nature Science Foundation Grant (31171085: ML), NIH Grant HL 064035 (JRS), PO1 HL 062426 (JRS).

References

Backes, C., Ruhle, F., Stoll, M., Haas, J., Frese, K., Franke, A., et al. (2014). Systematic permutation testing in gwas pathway analyses: identification of genetic networks in dilated cardiomyopathy and ulcerative colitis. *BMC Genomics*15:622. doi: 10.1186/1471-2164-15-622

DeSantiago, J., Bare, D. J., Ke, Y., Sheehan, K. A., Solaro, R. J., and Banach, K. (2013). Functional integrity of the t-tubular system in cardiomyocytes depends on p21-activated kinase 1. *J. Mol. Cell. Cardiol.* 60, 121–128. doi: 10.1016/j.yjmcc.2013.04.014

duBell, W. H., Gigena, M. S., Guatimosim, S., Long, X., Lederer, W. J., and Rogers, T. B. (2002). Effects of pp1/pp2a inhibitor calyculin a on the e-c coupling cascade in murine ventricular myocytes. *Am. J. Physiol. Heart Circ. Physiol.* 282, H38–H48. doi: 10.1152/ajpheart.00536.2001

duBell, W. H., and Rogers, T. B. (2004). Protein phosphatase 1 and an opposing protein kinase regulate steady-state l-type Ca^{2+} current in mouse cardiac myocytes. *J. Physiol.* 556, 79–93. doi: 10.1113/jphysiol.2003.059329

duBell, W., Lederer, W., and Rogers, T. (1996). Dynamic modulation of excitation-contraction coupling by protein phosphatases in rat ventricular myocytes. *J. Physiol.* 493, 793–800. doi: 10.1113/jphysiol.1996.sp021423

Gupta, R. C., Neumann, J., Watanabe, A. M., Lesch, M., and Sabbah, H. N. (1996). Evidence for presence and hormonal regulation of protein phosphatase inhibitor-1 in ventricular cardiomyocyte. *Am. J. Physiol. Heart Circ. Physiol.* 270, H1159–H1164.

Hofmann, C., Shepelev, M., and Chernoff, J. (2004). The genetics of pak. *J. Cell Sci.* 117, 4343–4354. doi: 10.1242/jcs.01392

Ke, Y., Lei, M., Collins, T. P., Rakovic, S., Mattick, P. A., Yamasaki, M., et al. (2007). Regulation of l-type calcium channel and delayed rectifier potassium channel activity by p21-activated kinase-1 in guinea pig sinoatrial node pacemaker cells. *Circ. Res.* 100, 1317–1327. doi: 10.1161/01.RES.0000266742.51389.a4

Ke, Y., Lei, M., and Solaro, R. J. (2009). Regulation of cardiac excitation and contraction by p21 activated kinase-1. *Prog. Biophys. Mol. Biol.* 98, 238–250. doi: 10.1016/j.pbiomolbio.2009.01.007

Ke, Y., Wang, L., Pyle, W. G., de Tombe, P. P., and Solaro, R. J. (2004). Intracellular localization and functional effects of p21-activated kinase-1 (pak1) in cardiac myocytes. *Circ. Res.* 94, 194–200. doi: 10.1161/01.RES.0000111522.02730.56

Liu, W., Zi, M., Naumann, R., Ulm, S., Jin, J., Taglieri, D. M., et al. (2011). Pak1 as a novel therapeutic target for antihypertrophic treatment in the heart. *Circulation* 124, 2702–2715. doi: 10.1161/CIRCULATIONAHA.111.048785

Liu, W., Zi, M., Tsui, H., Chowdhury, S. K., Zeef, L., Meng, Q.-J., et al. (2013). A novel immunomodulator, fty-720 reverses existing cardiac hypertrophy and fibrosis from pressure overload by targeting nfat (nuclear factor of activated t-cells) signaling and periostin. *Circ. Heart Fail.* 6, 833–844. doi: 10.1161/CIRCHEARTFAILURE.112.000123

Manser, E., Leung, T., Salihuddin, H., Zhao, Z.-S., and Lim, L. (1994). A brain serine/threonine protein kinase activated by cdc42 and rac1. *Nature* 367, 40–46. doi: 10.1038/367040a0

Manser, E., and Lim, L. (1999). Roles of pak family kinases. *Prog. Mol. Subcell. Biol.* 22, 115–133. doi: 10.1007/978-3-642-58591-3_6

Mao, K., Healy, C., Timm, D., Kobayashi, S., Volden, P., Chernoff, J., et al. (2009). P21 activated kinase 1 (pak1) protects heart from pressure overload induced pathological cardiac remodeling. *FASEB J.* 23(Meeting Abstract Supplement), 362.5.

Santana, L. F., Chase, E. G., Votaw, V. S., Nelson, M. T., and Greven, R. (2002). Functional coupling of calcineurin and protein kinase a in mouse ventricular myocytes. *J. Physiol.* 544, 57–69. doi: 10.1113/jphysiol.2002.020552

Sheehan, K. A., Ke, Y., Wolska, B. M., and Solaro, R. J. (2009). Expression of active p21-activated kinase-1 (pak1) induces ca2+-flux modification with altered regulatory protein phosphorylation in cardiac myocytes. *Am. J. Physiol. Cell Physiol.* 296, C47–C58. doi: 10.1152/ajpcell.00012.2008

Wang, R., Wang, Y., Lin, K., Zhang, Y., Liu, W., Huang, K., et al. (2014b). Inhibition of angiotensin ii-induced cardiac hypertrophy and associated ventricular arrhythmias by a p21 activated kinase 1 bioactive peptide. *PLoS ONE* 9:e101974. doi: 10.1371/journal.pone.0101974

Wang, Y., Tsui, H., Ke, Y., Shi, Y., Li, Y., Davies, L., et al. (2014a). Pak1 is required to maintain ventricular Ca^{2+} homeostasis and electrophysiological stability through serca2a regulation in mice. *Circ. Arrhythm. Electrophysiol.* 7, 938–948. doi: 10.1161/CIRCEP.113.001198

Zhao, Z., and Manser, E. (2005). Pak and other rho-associated kinases–effectors with surprisingly diverse mechanisms of regulation. *Biochem. J.* 386, 201–214. doi: 10.1042/BJ20041638

Conflict of Interest Statement: The authors declare that the research was conducted in the absence of any commercial or financial relationships that could be construed as a potential conflict of interest.

frontiers in Physiology

ORIGINAL RESEARCH
published: 09 March 2015
doi: 10.3389/fphys.2015.00069

Store-operated calcium entry and the localization of STIM1 and Orai1 proteins in isolated mouse sinoatrial node cells

Jie Liu[1], Li Xin[2], Victoria L. Benson[1], David G. Allen[1]* and Yue-Kun Ju[1]**

[1] School of Medical Sciences and Bosch Institute, University of Sydney, Sydney, NSW, Australia, [2] Victor Chang Cardiac Research Institute, Sydney, NSW, Australia

In many non-excitable and excitable cells, store-operated calcium entry (SOCE) represents an additional pathway for calcium entry upon Ca^{2+} store depletion. In a previous study, we demonstrated SOCE activity in intact mouse cardiac pacemaker tissue, specifically from sinoatrial node (SAN) tissue. However, store content as a key determinant of SOCE activity is difficult to measure in intact SAN tissue. Therefore, to investigate the interaction between SOCE and store content and its role in cardiac pacemaking, it is necessary to investigate SOCE activity in single cardiac pacemaker cells. Furthermore, recent studies in other tissues have identified two new proteins involved in SOCE, stromal interacting molecule (STIM), which is an ER Ca^{2+} sensor, and the surface membrane channel Orai, a prototypic gene encoding for SOCE. However, whether STIM and Orai are expressed in native pacemaker cells is still unknown. In this current study, we examined SOCE activity in single firing pacemaker cells isolated from mouse sinoatrial node tissue. We found a significant rise in Ca^{2+} entry in response to Ca^{2+} store depletion. SOCE blockers reduced the amplitude and frequency of spontaneous Ca^{2+} transients and reduced Ca^{2+} store content. We demonstrated for the first time that STIM and Orai are expressed in pacemaker cells. After store depletion, STIM1 redistributed to the cell periphery and showed increased co-localization with surface membrane located Orai1, indicating a possible involvement of these proteins in SOCE activity in native cardiac pacemaker cells. These results suggest the novel concept that SOCE plays a functional role in regulating intracellular Ca^{2+} of cardiac pacemaker cells.

Keywords: store-operated Ca^{2+} entry, STIM1, Orai1, sinoatrial node

OPEN ACCESS

Edited by:
Ming Lei,
University of Oxford, UK

Reviewed by:
Wayne Rodney Giles,
The University of Calgary, Canada
Derek Anthony Terrar,
University of Oxford, UK

****Correspondence:***
Jie Liu, David G. Allen and Yue-Kun Ju, School of Medical Sciences (F13), University of Sydney, Anderson Stuart Building, Eastern Ave., Sydney, NSW 2006, Australia
liujie@physiol.usyd.edu.au; david.allen@sydney.edu.au; yue-kun.ju@sydney.edu.au

Specialty section:
This article was submitted to Cardiac Electrophysiology, a section of the journal Frontiers in Physiology

Received: *20 November 2014*
Accepted: *19 February 2015*
Published: *09 March 2015*

Citation:
Liu J, Xin L, Benson VL, Allen DG and Ju Y-K (2015) Store-operated calcium entry and the localization of STIM1 and Orai1 proteins in isolated mouse sinoatrial node cells. Front. Physiol. 6:69. doi: 10.3389/fphys.2015.00069

Introduction

Cardiac contraction originates in the spontaneous firing of pacemaker cells in the sinoatrial node (SAN) of the heart. Originally it was thought that the spontaneous firing of pacemaker cells was driven purely by voltage-dependent membrane currents (Noble, 1960) but subsequently it has been found that intracellular Ca^{2+} cycling also plays an important role (Rigg and Terrar, 1996; Ju and Allen, 1998, 1999; Rigg et al., 2000; Lakatta et al., 2010). During each spontaneous cycle, Ca^{2+} influx through L-type Ca^{2+} channels triggers sarcoplasmic reticulum (SR)

Ca^{2+} release and produces a global Ca^{2+} transient. The loss of Ca^{2+} from the SR causes partial depletion which recovers as the SR Ca^{2+} pump (SERCA) returns Ca^{2+} to the SR. Ca^{2+} extrusion through the Na^{+}/Ca^{2+} exchanger generates an inward current that contributes to pacemaker diastolic depolarization.(Rigg and Terrar, 1996; Ju and Allen, 1998, 2000; Rigg et al., 2000; Vinogradova et al., 2000, 2006). Although controversies still exist about the relative importance of intracellular Ca^{2+} cycling over membrane currents (Lakatta and DiFrancesco, 2009; Himeno et al., 2011), it is now generally accepted that pacemaker activity is orchestrated by the coupled system of membrane ionic currents (the "membrane clock") and intracellular SR calcium cycling (the "calcium clock") (for review see, Lakatta et al., 2010).

In many non-excitable and excitable cells, store-operated calcium entry (SOCE) represents an additional pathway for calcium entry into the cell to refill the SR calcium store. SOCE is activated by the decline of Ca^{2+} concentration within the lumen of the endoplasmic reticulum (ER) or SR. Activation of SOCE produces Ca^{2+} influx which provides a regulatory link between SR Ca^{2+} level and membrane calcium entry, thereby helping to maintain SR calcium homeostasis (Parekh and Putney, 2005). In a previous study, we demonstrated SOCE in an intact SAN tissue preparation based on a rise of intracellular Ca^{2+} ($[Ca^{2+}]_i$) when extracellular Ca^{2+} was replenished after store depletion (Ju et al., 2007). However, SAN tissue contains pacemaker cells intermingled with fibroblasts, atrial myocytes and endothelium cells, all of which are capable of expressing SOCE (Camelliti et al., 2004; Chen et al., 2010; Li et al., 2011). Additionally, store content as a key determinant of SOCE activity is difficult to measure in intact SAN tissue. Therefore, to rule out possible endogenous cell contamination and investigate store content, it is necessary to investigate SOCE activity in single pacemaker cells.

In the present study, we examined SOCE in single firing pacemaker cells, by measuring the changes in intracellular Ca^{2+} in response to SR Ca^{2+} store depletion. Using two different blockers of SOCE, SKF96365, and BTP-2, we estimated the contribution of SOCE to pacemaker activity and the refilling of the SR Ca^{2+} store.

The genes encoding SOCE in pacemaker cells remain to be identified. We previously found that TRPC channel genes are expressed in pacemaker cells isolated from mouse SAN. Because the involvement of TRPC channels in SOCE has also been reported in many other cell types (Clapham, 2003; Birnbaumer, 2009), this result suggests that TRPC channels could be encoding SOCE in pacemaker cells. Ca^{2+} influx through TRPC channels has also been implicated in cardiac hypertrophy (Wu et al., 2010; Eder and Molkentin, 2011) and cardiac arrhythmias (Harada et al., 2012). However, despite the large numbers of reports implicating TRPCs as store-operated channels, whether activation of TRPC channels requires depletion of SR Ca^{2+} store remain debatable (Lewis, 2007; Birnbaumer, 2009; Putney, 2009). Accumulated evidence suggests that activation of certain isoforms of TRPC channels, especially TRPC3 and TRPC6, are directly related to G-protein coupled receptor activation and phospholipase C mediated production of diacylglycerol, referred to as receptor-operated Ca^{2+} entry (ROCE) (Hofmann et al., 1999; Onohara et al., 2006; Mohl et al., 2011). Such Ca^{2+} entry is independent of SR store depletion.

In recent years, studies using genetic approaches have identified genes encoding the ER Ca^{2+} sensor, namely the stromal interaction molecule (STIM) (Liou et al., 2005; Zhang et al., 2005, also for review see Cahalan, 2009). Subsequently, the Orai family of membrane proteins was identified as forming a prototypic SOCE, the Ca^{2+} release activated Ca^{2+} channel (CRAC) (Feske et al., 2006; Vig et al., 2006; Zhang et al., 2006). CRAC channels are Ca^{2+}-selective channels located in the cell membrane and fulfill the criteria for being store-operated (Feske et al., 2006; Vig et al., 2006). In response to decreased ER Ca^{2+} concentration, STIM1 translocates within the ER membrane to form discrete surface membrane-associated aggregates where it activates Orai channels (Lewis, 2007; Penna et al., 2008; Wang et al., 2010b). A recent study using high resolution nuclear magnetic resonance determined the structure of protein segments from STIM1 and Orai1 confirmed their interaction and possible role in Orai1 activation (Stathopulos et al., 2013). There is now substantial evidence that SOCE plays a key role in mediating cardiomyocyte hypertrophy, both *in vitro* and *in vivo*, and there is growing support for the contribution of SOCE to Ca^{2+} overload associated with ischemia/reperfusion injury (Collins et al., 2013). However, the expression and cellular distribution of STIM and Orai molecules have not been determined in cardiac pacemaker cells.

In this study, we examined the expression of STIM and Orai isoforms in pacemaker cells, their cellular localization under physiological conditions, and redistribution after store depletion.

Materials and Methods

Single SAN Cell Isolation

Cardiac cells were harvested from male Balb/c mice (2–4 months old) under a protocol approved by the Animal Ethics Committee of the University of Sydney.

Single SAN cells were isolated using a modified protocol as described previously (Liu et al., 2011). Briefly, hearts were removed from animals and microdissection of the SAN region was performed with constant perfusion of Tyrode solution with 1.8 mmol/L Ca^{2+} using a dissecting microscope. A strip of tissue containing the SAN region, measuring ~0.5 mm × ~1 mm, was identified by anatomic landmarks and dissected out. The SAN strips were cut into 3–5 smaller strips and rinsed in a "Ca^{2+} free" solution containing (in mmol/L) 120 NaCl, 5.4 KCl, 0.5 $MgCl_2$, 1.2 KH_2PO_4, 20 taurine, 11.1 glucose, 10 HEPES, 0.3 EGTA, 10 Na-Pyruvic acid, 5 Creatine, 5 μmol/L Blebbistatin, 2 mg/ml bovine serum albumin (BSA), pH 7.0. The rinsed SAN tissue strips were digested in the same "Ca^{2+} free" solution containing collagenase (229 u/ml, type II, Worthington Biochemical Corporation), elastase (1.9 u/ml) and protease (0.9 u/ml, type XIV) for 30–40 min at 35 ± 0.5°C and bubbled with pure oxygen. After enzyme digestion, the tissue was then washed and stored in Kruftbrühe (KB) solution which contains (in mmol/L), 30 KCl, 10 KH_2PO_4, 2 $MgCl_2$, 70 L-glutamic acid, 10 HEPES, 20 taurine, 5 creatine, 0.3 EGTA, 10 Na-Pyruvic acid, 5 Creatine, 5 μmol/L Blebbistatin, 80 KOH, 11.1 glucose and 10 HEPES, with pH adjusted to 7.2 with KOH. Single SAN cells were released by gentle pipetting of the digested tissue strips. SAN cells were identified under light microscopy by their spindle shape and small size with

centered single nuclei. Atrial myocytes were dissociated following the same isolation protocol while ventricular myocytes were dissociated by the collagenase-based coronary perfusion method as described elsewhere (Zhou et al., 2000). All chemicals were purchased from Sigma unless otherwise specified.

Intracellular Ca^{2+} Recording

Isolated single mouse SAN cells were placed on laminin-coated (20 μg/ml) 35 mm glass bottom petri dishes (MatTek Cultureware) for 20 min to attach. Fluo-4-AM (FluoroPure grade, Invitrogen. USA) was mixed with Pluronic F-127 by sonication and diluted to a final concentration of 5 μmol/L in Tyrode solution. This solution was used to load single pacemaker cells (20 min at room temperature). After superfusion with normal Tyrode solution (with 1.8 mmol/L Ca^{2+}) for 20 min to de-esterify Fluo-4-AM, spontaneously beating pacemaker cells were selected for study. A LSM 510 META confocal microscope (Carl Zeiss Inc., Germany) equipped with an argon laser provided excitation at 488 nm and the fluorescence signal was collected at wavelengths of >515 nm. A heated microscope stage and a 63 × /1.4 oil objective heater (PeCon GmbH, Germany) were attached to maintain cells at 37°C throughout the experiment. Cell shortening was recorded by line scan mode and analyzed offline with ImageJ software (NIH, USA). Intracellular Ca^{2+} was recorded using either line scan mode (xt mode) or frame mode (xy mode) with time series. Results were recorded at Zeiss LSM scan speed 8 (3.07 ms/line) and 10 s intervals exist between two consecutive frames in frame mode. Data were analyzed with Zeiss LSM image examiner (version 4.2, Carl Zeiss Inc., Germany) and imageJ (NIH, USA). Global intracellular Ca^{2+} levels were translated into relative fluorescence levels, F/F0, where F and F0 represent the fluorescence intensities at a given time and at minimum resting level, respectively. Maximum change in F/F_0 (in frame mode) was calculated as the change in the peak value after Ca^{2+} re-admission relative to initial level before Ca^{2+} removal.

Reverse Trascriptase-Polymerase Chain Reaction (RT-PCR) Analysis

Total mRNA from isolated cardiac myocytes (SAN cells, atrial and ventricular myocytes) and spleen cells were extracted with TRIzol (Invitrogen. USA) following manufacturer's protocol. Reverse transcription was carried out with 1 μg total RNA using the Superscript First-Strand Synthesis System for RT-PCR (Invitrogen), according to the manufacturer's instructions. RT-PCR was performed with Platinum Taq (Invitrogen) under the following conditions as described by Wissenbach et al. (2007): one cycle 50°C/30 min; one cycle 94°C/2 min; 40–45 cycles 94°C/15 s, 56°C/30 s, 72°C/30 s; one cycle 72°C/5 min. The following primer pairs, deduced from cDNA sequences and flanking at least one intron were used: 5′ GAT CGG CCA GAG TTA CTC C and 5′ CGA TGC ATG CGC TCG TGG (ORAI1); 5′ AA GAA GGG AGA GAC ACA CAG and 5′ ACT CGC TGA TGG AGT TGAG G (ORAI2); 5′ GCC AGT CAG CAC TCT CTG C and 5′ CCA CCA GAA CAA CTT CAG CC (ORAI3); 5′ GCC ACA GCT TGG CCT GG and 5′ GCT CCA TCA GG CTG TGG (STIM1); 5′ TGA GGA TAC CCT GCA GTG G and 5′ CAG TCT GCA GAC TCT CTA AG (STIM2); 5′ GCT CGA GAT GTC ATG AAG G and 5′ GGC TGT ACT GCT TAA CCA GG (HPRT1).

Immunostaining and Western Blots

Immunostaining of single SAN cells was carried out using standard protocols as described previously (Liu et al., 2011). Briefly, isolated pacemaker cells were plated onto laminin-treated slides and allowed to settle for 30 min before being fixed with 2% paraformaldehyde (Sigma) for 5 min. A subset of cells was incubated with Ca^{2+} free Tyrode Solution with either 5 μmol/L cyclopiazonic acid (CPA) or 1 μmol/L thapsigargin (TG) for 30 min at room temperature before fixation. Fixed cells were washed three times with phosphate buffer solution (PBS) over 30 min, permeabilized by 0.1% Triton X-100 (Sigma) for 5 min, washed three times with PBS over 30 min, and blocked with 1% bovine serum albumin (BSA; Sigma) and 4% normal Goat serum (invitrogen, USA) in PBS for 1–2 h before application of primary antibody. Primary antibodies were diluted in 1% BSA and 4% normal goat serum in PBS. Cells were incubated with primary antibodies at an appropriate concentration (see **Table 1**) at 4°C overnight, briefly washed in PBS and then Alexa Fluo-488 goat anti-rabbit or Alexa Fluo-561 goat anti-mouse secondary antibodies (both at 1:200 dilution, Invitrogen, USA) were applied. Cells were washed three times with PBS and then mounted with Prolong Gold mounting media with DAPI (Invitrogen, USA) and cover slips were sealed with nail polish. In negative control experiments, no primary antibody was used and no labeling was detected. Confocal images were acquired with LSM 510 META confocal microscope (Carl Zeiss Inc., Germany) and analyzed with LSM image examiner.

For Western blot, strips of SAN (restricted by Crista terminalis, atrial septum, superior and inferior vena cava), atrium (from left atrium wall) and ventricle (left ventricle free wall) were freshly dissected and snap frozen in liquid nitrogen. Spleen tissue was collected in the same way and served as positive control protein. Total protein extracts were prepared with Mammalian Cell Lysis Kit (Sigma, Cat no: MCL1) containing RIPA buffer and protease inhibitor cocktail. Tissue samples were homogenized on ice using a Polytron homogenizer (PT900 CL) and cleared by centrifugation at 12,000 g for 10 min. Protein extracts were separated on 8% SDS-PAGE gel and transferred to a nitrocellulose membrane (Whatman). The membranes were immunoblotted with the appropriate antibodies (**Table 1**) following standard procedures published elsewhere (Nishiyama et al., 2009). Immunoblots were probed with antibodies against STIM1, STIM2, Orai1, and Orai3 but not Orai2 due to lack of Orai2 mRNA expression in cardiac cells.

Drugs

Thapsigargin (TG, 1 μmol/L) and Cyclopiazonic acid (CPA, 5 μmol/L) which are SR Ca^{2+}-ATPase (SERCA) inhibitors were used to deplete store content. The imidazole compound SKF-96365 (1-[2-(4-methoxyphenyl)-2-[3-(4-methoxyphenyl) propoxy]ethyl-1H-imidazole hydrochloride) has been shown to target the STIM1-Orai1 pathway and inhibit SOCE in cell lines (Liou et al., 2005; Huang et al., 2006). BTP-2, a bistrifluoromethyl-pyrazole derivative, is a potent and fast-acting

TABLE 1 | List of antibody used in the study.

Antibody	Company (cat #)	Clone	Ab isoform	Dilution staining	Dilution western
ORAI1	Sigma (O8264)	NA	Rabbit	1:100	
ORAI1	ProSci (PM-5207)	NA	Mouse	1:500	1:1000
ORAI3	ProSci (4117)	Polyclone	Rabbit	1:200	1:1000
STIM1	BD transduction	44/stim1	Mouse IgG2a	1:100	1:1000
STIM2	ProSci (4123)	Polyclone	Rabbit	1:400	1:1000
HCN4	Abcam (ab32675)	SHG 1E5	Rat	1:800	
Caveolin-3	BD transduction	26/cav-3	Mouse IgG1	1:500	
SERCA2	Abcam (ab2861)	2A7-A1	Mouse IgG2a	1:500	
RyR2	ABR (MA3-916)	C3-33	Mouse IgG1	1:200	
NCX1	Swant (R3F1)	R3F1	Mouse IgG1	1:200	

SOCE blocker in a number of immortal cell lines and immune cells (He et al., 2005; Yonetoku et al., 2008). SKF-96365 and BTP-2 (both at 10 μmol/L) were used as SOCE blockers in this study. All drugs were dissolved in DMSO as stock solution stored at − 20°C and diluted in Tyrode solution at working concentration before applying to cells.

Statistical Analysis

Data were presented as means ± SEM. The statistical significance of effects was evaluated by Student's *t*-test or ANOVA and a value of $P < 0.05$ was considered statistically significant.

Results

SOCE Activities in Single Isolated Pacemaker Cells

To investigate whether SOCE exists in isolated single pacemaker cells, we studied the changes in $[Ca^{2+}]_i$ in response to an intervention protocol which involves removing extracellular Ca^{2+} in addition to the application of SR Ca^{2+}-ATPase (SERCA) inhibitor. We previously showed that this protocol caused activation of SOCE in intact mouse SAN tissue (Ju et al., 2007). **Figure 1A** shows serial confocal Ca^{2+} images collected from an isolated single isolated pacemaker cell undergoing the SOCE activation protocol. Under control conditions (1.8 mM $[Ca^{2+}]_o$), the cell exhibited spontaneous firing and regular Ca^{2+} transients **Figure 1A**(1) (xy plot, duration 1.5 s). The cell stopped firing when the SERCA inhibitor, cyclopiazonic acid (CPA, 5 μmol/L) was applied along with extracellular Ca^{2+} withdrawal from the solution for 5 min, which was associated with a significantly reduced $[Ca^{2+}]_i$ [**Figure 1A**(2)]. A marked global rise in $[Ca^{2+}]_i$ upon Ca^{2+} re-admission is demonstrated in **Figure 1A**(3) associated with visible cell shortening (hypercontraction). $[Ca^{2+}]_i$ rapid declined after an initial transient overshoot [**Figure 1A**(4)]. Spontaneous Ca^{2+} transients associated with pacemaker firing reappeared as $[Ca^{2+}]_i$ gradually returned to control level after wash off of CPA [**Figure 1A**(5)]. **Figure 1B** demonstrated the time course of Ca^{2+} fluorescence intensity changes deduced from 60 consecutively collected Ca^{2+} images in response to the SOCE activation protocol. The top panel showed the timing of extracellular $[Ca^{2+}]$ withdrawal and readmission. A large Ca^{2+} influx reached its maximum within 30 s after Ca^{2+} re-admission and lasted for 1–2 min (**Figure 1B** top trace). In contrast, only a small Ca^{2+} influx was seen in the presence of the selective SOCE blocker BTP-2 (Yonetoku et al., 2008; Singh et al., 2010) (**Figure 1B** bottom trace). We found that SKF-96365 has similar effect to BTP-2 in single pacemaker cells and the results were similar to that previously reported in intact SAN preparations (Ju et al., 2007). Both SOCE blockers also significantly reduced CPA or TG -induced SOCE in single pacemaker cells. In addition, Ca^{2+} influx was not seen upon reintroducing extracellular Ca^{2+} after removal of extracellular Ca^{2+} without using SERCA inhibitors. **Figure 1C** compares the amplitude of the $[Ca^{2+}]_i$ rise upon Ca^{2+} re-admission relative to initial levels for each treatment. These results confirm there is significant Ca^{2+} influx in isolated single mouse pacemaker cells in response to a SOCE activation protocol that presumably causes store depletion.

To confirm that the large $[Ca^{2+}]_i$ rise was indeed associated with a store Ca^{2+} depletion, the store Ca^{2+} content was assessed using rapid caffeine application (**Figure 2**). Rapid application of caffeine causes a large and rapid rise in $[Ca^{2+}]_i$ that has been widely used to measure SR Ca^{2+} content (Bers, 1987). Caffeine-induced Ca^{2+} transients were compared under control conditions [**Figure 2A**(i)], after 5 min. of extracellular Ca^{2+} removal [**Figure 2A**(ii)], and after Ca^{2+} removal combined with SERCA inhibition by TG [**Figure 2A**(iii)]. Three superimposed spatially-averaged traces of caffeine-induced Ca^{2+} transients are shown in **Figure 2B**. Note that regular spontaneous Ca^{2+} transients were seen only in control conditions before the application of caffeine (black line, **Figure 2B**), but not in extracellular Ca^{2+} free (red line) and extracellular Ca^{2+} free plus thapsigargin (green line). SR Ca^{2+} store content indicated by caffeine induced Ca^{2+} transients (quantified by maximum $\Delta F/F_0$) showed a small but non-significant reduction after extracellular Ca^{2+} removal (**Figure 2C**, $n = 4$ cells from 3 mice, $P = 0.81$) but exhibited a large and significant fall when extracellular Ca^{2+} removal was combined with SERCA inhibition (**Figure 2C**, $n = 5$ cells from 3 mice, $P < 0.05$). These data confirm that the combination of extracellular Ca^{2+} removal and application of a SERCA blocker cause store depletion. The large Ca^{2+} influx is dependent on SR Ca^{2+} store content and is store-operated Ca^{2+} entry.

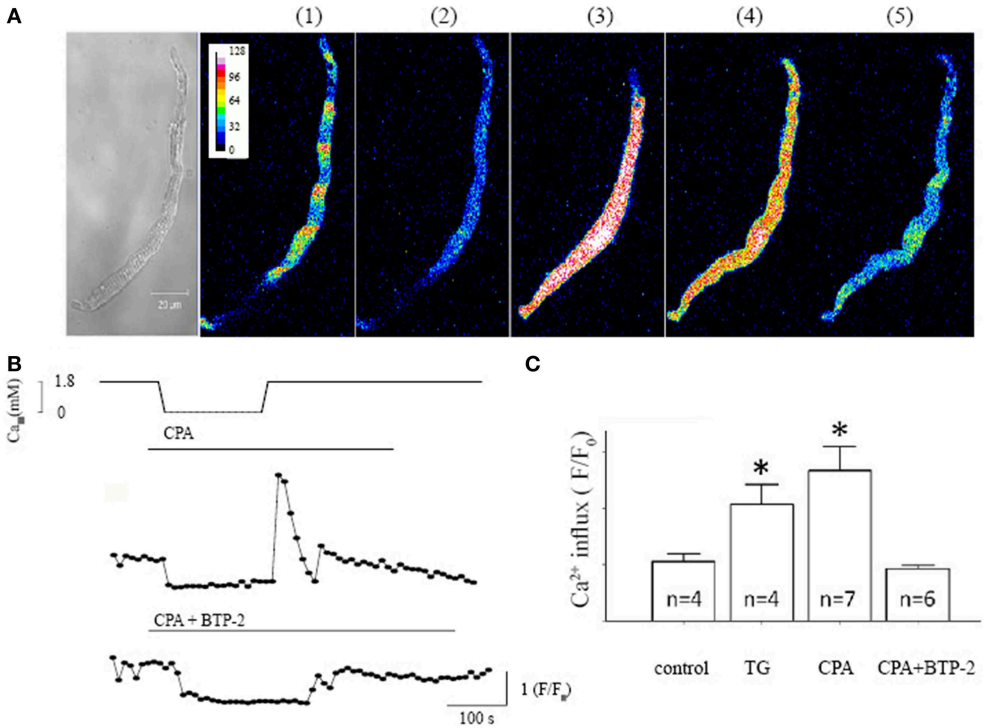

FIGURE 1 | Characteristic store operated Ca^{2+} entry (SOCE) induced in isolated pacemaker cells. (A) The left panel shows a transmitted light image of a spontaneously firing pacemaker cell loaded with Ca^{2+} indicator Fluo-4 AM. The regular spontaneous Ca^{2+} transients were detected as regular fluctuations in fluorescence intensity during a single xy frame recorded over a period of 1.5 s, (during which there were ~5 beats under control condition as shown next image (1). There are five selected fluorescent images representing intracellular Ca^{2+} changes under 5 different experimental conditions in the same cell; (1) control, (2) after store depletion with 0 mmol/L Ca^{2+} and the SERCA inhibitor cyclopiazonic acid (CPA, 5 μmol/L), (3 and 4) upon Ca^{2+} re-admission, and (5) wash off respectively. **(B)** The time course of Ca^{2+} fluorescent intensity changes deduced from 60 Ca^{2+} images consecutively collected at 10 s intervals. The top panel shows the course of SOCE activation protocol, i.e., timing of extracellular $[Ca^{2+}]$ withdrawal and readmission and time of application of CPA. The bottom trace shows the intracellular Ca^{2+} changes in the presence of SOCE blocker BTP-2 during the course of SOCE activation. **(C)** Summary data (mean ± SEM) represents the maximum amplitude of $[Ca^{2+}]_i$ rise upon Ca^{2+} re-admission, relative to the initial $[Ca^{2+}]_i$ level before Ca^{2+} removal. Control experiments were done with Ca^{2+} removal and re-admission only. N equals number of cells for each group, $^*P < 0.05$.

SOCE Blockers Reduce Store Content

The important physiological function of SOCE is to refill the SR Ca^{2+} store (Seth et al., 2012). Thus, it would be expected that SOCE blockers would cause decreased SR Ca store content.

To test this idea, we examined the effect of a SOCE blocker on SR Ca^{2+} store content, estimated by caffeine-induced Ca^{2+} release (Bers, 1987). **Figure 3A** shows Ca^{2+} transients recorded from a spontaneously beating pacemaker cell. Rapid application of caffeine induced a large and rapid rise in $[Ca^{2+}]_I$ under control conditions. BTP-2 slowed the spontaneous firing rate and reduced the amplitude of both the spontaneous Ca^{2+} transient and the caffeine-induced transient. Both these observations are clearly shown in **Figure 3B** which shows superimposed, spatially-averaged records. On average BTP-2 reduced the amplitude of the spontaneous Ca^{2+} transient by 24% ($n = 6$, $P = 0.018$, **Figure 3C**). BTP-2 also reduced the amplitude of the caffeine-induced Ca^{2+} signal—which is indicative of SR Ca^{2+} store content—by 22% ($n = 6$ cells from 4 mice, $P = 0.026$) (**Figure 3D**). These data demonstrate SOCE inhibition reduced store content and firing rate, which suggests that SOCE may participate in maintaining store content and pacemaker function. To estimate how much SOCE might be involved in normal pacemaker activity, we investigated the effect of SOCE blockers on pacemaker firing rate. When applied to normally firing pacemaker cells, BTP-2 reduced the firing rate by 16.0 ± 1.4% ($n = 6$ cells in each group, $P < 0.01$ as shown in **Figure 3E**). SKF-96365 also reduced pacemaker firing rate by 12.3 ± 1.8%. The negative chronotropic effects caused by inhibition of SOCE may indicate that SOCE might be involved in the regulation of pacemaker activity.

Expression of STIM/Orai in Pacemaker Cells

Although we found SOCE activity in pacemaker cells as described above, the genes encoding SOCE in pacemaker cells remain to be identified. In recent years, Orai proteins have emerged as new molecular candidates for the channels that underlie the store depletion activated Ca^{2+} current, I_{CRAC} (Huang et al., 2006; Zhou et al., 2010). Before the discovery of

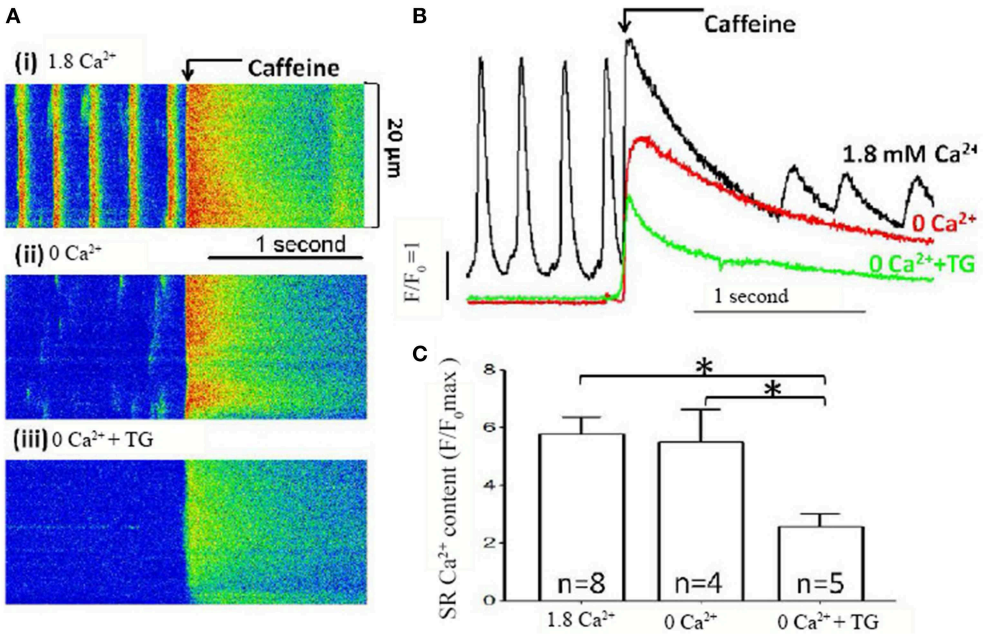

FIGURE 2 | SR Ca^{2+} store content measured in pacemaker cells. **(A)** Representative line scan recording of $[Ca^{2+}]_i$ and caffeine induced Ca^{2+} transients, as the measurement of SR Ca^{2+} store content, in SAN cells; (i) under control conditions with 1.8 mmol/L Ca^{2+}, (ii) with removal of external Ca^{2+} only and (iii) with removal of Ca^{2+} in the presence of TG. **(B)** Overlapping representative line plot traces of Ca^{2+} images shown in **(A)**. The associated line colors represented $[Ca^{2+}]_i$ under control conditions (black), removal of external Ca^{2+} only (red) and removal of Ca^{2+} in the presence of TG (green), respectively. **(C)** Summary data (mean ± SEM) of store content indicated by maximal rise of F/F_0 measured by caffeine induced Ca^{2+} release. N equals number of cells for each group, $^*P < 0.05$.

Orai genes, the TRPC channels were regarded as the most likely candidates for SOCE. We previously found that pacemaker cells express all TRPC isoforms, except TRPC5 (Ju et al., 2007). However, it is still debatable whether the activation of TRPC channels is dependent on Ca^{2+} depletion from SR Ca^{2+} store (SOCE) or is dependent on G-protein coupled receptor activation (ROCE) (Hofmann et al., 1999). In addition, stromal interacting molecular 1 (STIM1) has been identified as the ER sensor. It is known that activation of SOCE requires STIM1 migration and interaction with other molecular components of SOCE (Lewis, 2007). Given the importance of STIM1 and Orai, we wanted to establish their expression in pacemaker tissue. RT-PCR was performed with mRNA extracted from isolated SAN, atrial and ventricular myocytes, respectively. Spleen tissue was used as a positive control sample, as there is abundant expression of these genes in immune cells. The housekeeping gene Hypoxanthine–Guanine Phosphoribosyltransferase (HPRT) was used as an internal control. **Figure 4A** shows gel images of amplified PCR products. SAN and other cardiac myocytes expressed mRNA transcripts of STIM1, STIM2, Orai1, and Orai3, but not Orai2. In contrast, spleen tissue expressed all STIM and Orai isoforms as reported by others (Wissenbach et al., 2007).

Expression of STIM and Orai proteins in SAN and other cardiac tissue were also examined by immunoblot with specific antibodies against each isoform. **Figure 4B** shows bands of STIM1, STIM2, Orai1, and Orai3 in cardiac tissues at their predicted molecular weight. The antibodies recognize proteins with appropriate molecular weight and confirm the expression of STIM1, STIM2, Orai1, and Orai3 in the heart tissues, including SAN, atrial and ventricular tissue. **Figure 4C** shows quantitative western blot analysis of STIM1 protein levels in spleen and heart with heart samples normalized to spleen.

Among the different isoforms of STIM and Orai, the STIM1 and Orai1 have been considered to be the most relevant components of SOCE (Lewis, 2007; Stathopulos et al., 2013). To explore the possibility that STIM1 and Orai1 in pacemaker cells are functioning in SOCE, we investigated the localization of STIM1 and Orai1 proteins in isolated SAN cells using immunohistochemistry. It is known that pacemaker cells express HCN4 (hyperpolarization-activated, cyclic nucleotide-gate cation channels, type 4) (Marionneau et al., 2005; Liu et al., 2007), a channel carrying I_f current in these cells (Herrmann et al., 2007). **Figure 4D** shows that a HCN4 positive cell (green in color) isolated from mouse SAN tissue also demonstrates positive labeling of Orai1 (red in color). The distribution of Orai1 labeling is enhanced in the surface membrane where HCN4 is also located (yellow color showed in merged images). This result suggests that Orai1 could form functional channels in pacemaker cells. We found that positive HCN4 labeled cells can be also positively labeled with anti-STIM1 antibody (data not shown). STIM1 is an SR/ER Ca^{2+} sensor protein located predominantly within the ER/SR, but also to a limited extent in the plasma membrane (Liou et al., 2005; Wu et al., 2006). When perfused with normal Ca^{2+} containing solution, the distribution of STIM1 staining was

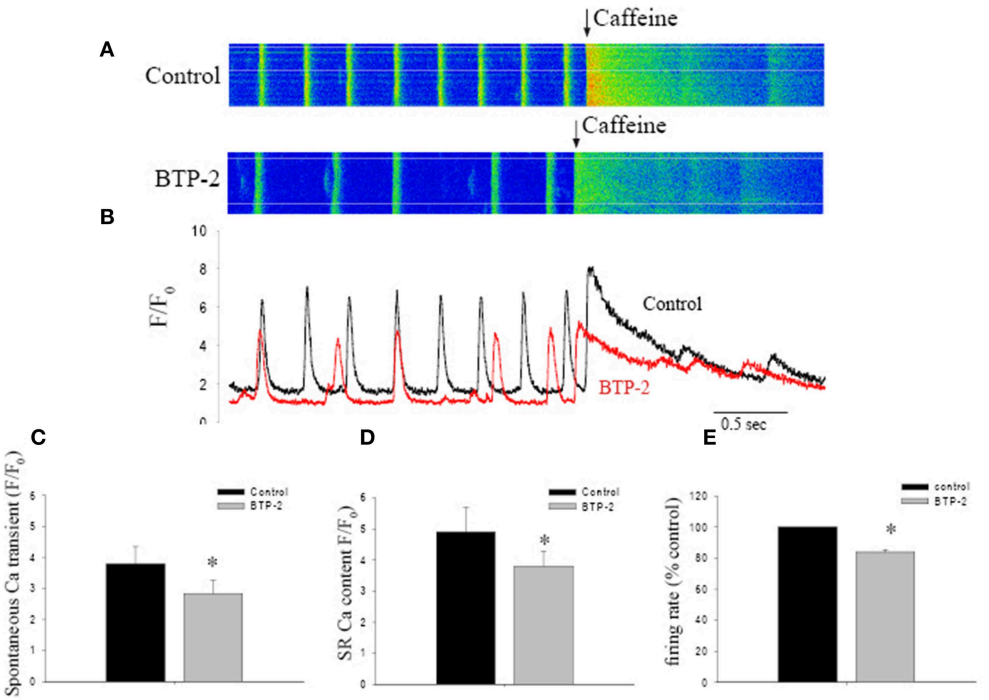

FIGURE 3 | The effect of BTP-2, a SOCE inhibitor on the spontaneous firing rate, Ca^{2+} transient amplitude and SR Ca^{2+} content in pacemaker cells. (A) Confocal Ca^{2+} images show the changes in firing rate and $[Ca^{2+}]_i$ before and after BTP-2 application. **(B)** The line plots deduced from images in **(A)** that compare spontaneous Ca^{2+} transients and SR store content (caffeine induced Ca^{2+} transients) before and after BTP-2 application. **(C)** Summary data (mean ± SEM) represents average change of $\Delta F/F_{0max}$ of spontaneous Ca^{2+} transients, SR Ca^{2+} content and pacemaker firing rate in control, BTP-2, respectively. $^*P < 0.05$.

mainly intracellular as showed in two isolated SAN pacemaker cells (**Figure 4E** top panel). It has been reported that STIM1 can be translocated toward the plasma membrane upon SR Ca^{2+} store depletion in transfected RBL cells (Liou et al., 2007). After treating pacemaker cells with thapsigargin, we found that the STIM1 staining was redistributed and became predominately located at the cell membrane as shown in **Figure 4E**, bottom panel.

Peripheral Redistribution of STIM1 upon Depletion of SR Ca^{2+} Store

Store-dependent translocation of STIM1 appears to be a prerequisite for the physical interaction with Orai1, which is followed by Orai1 activation and Ca^{2+} influx (Liou et al., 2007). To further investigate whether such STIM1 translocation can form a functional interaction with Orai1 in pacemaker cells, we examined the localization of Orai1 and STIM1 under control and store depleted conditions. **Figure 5A** shows a pacemaker cell that was immersed in Ca^{2+} free solution containing thapsigargin before labeling with Orai1 (red) and STIM1 (green). Orai1 labeling appears closer to the cell membrane, while STIM1 labeling also appears along the surface membrane where Orai1 is located. The colocalization of two proteins is demonstrated by the yellow staining as showed in an enlarged panel (arrows) [**Figure 5A**(ii)]. We examined two separate groups of pacemaker cells, the control group cells that were kept in normal Tyrode solution (Ca^{2+} 1.8 mmol/L) whereas the store depleted cells were kept in Ca^{2+} free solution containing the SERCA blockers CPA or TG for 30 min. The translocation after store depletion was quantified by dividing the diameter of cells into 4 equal regions (**Figure 5B**) and the ratio of two outer quartiles (including cell membrane) to two inner quartiles (cell interior) was calculated (**Figure 5B**). For Orai1, this ratio is around 2–3, indicating substantial concentration in the cell membrane, and does not change with store depletion (data not shown). Conversely for STIM1, the ratio in control cells is 1.25 ± 0.12 ($n = 9$ cells in 1.8 mM Ca^{2+}), indicating very little concentration in the cell membrane, but changed significantly to 4.16 ± 0.56 ($n = 9$ in the presence of CPA) or 4.35 ± 1.38 ($n = 9$ in the presence of TG) ($P < 0.05$) when the store was depleted (**Figure 5C**). This data shows increased peripheral localization of STIM1 and increased colocalization of STIM1 and Orai1 upon store depletion. Under the same conditions, images of these antibody-stained cells were analyzed for colocalization, utilizing the colocalization coefficient (the ratio of colocalized STIM1 pixels to total STIM1 pixels). Colocalization coefficients for both STIM1 increased significantly after store depletion (**Figure 5D**, $n \geq 9$ cells per group, $P < 0.05$). Similar results were obtained for the colocalization of Orai1 with STIM1 (not shown). This increased colocalization resulting from the peripheral redistribution of STIM1 is expected to increase the opportunity for physical interaction between STIM1

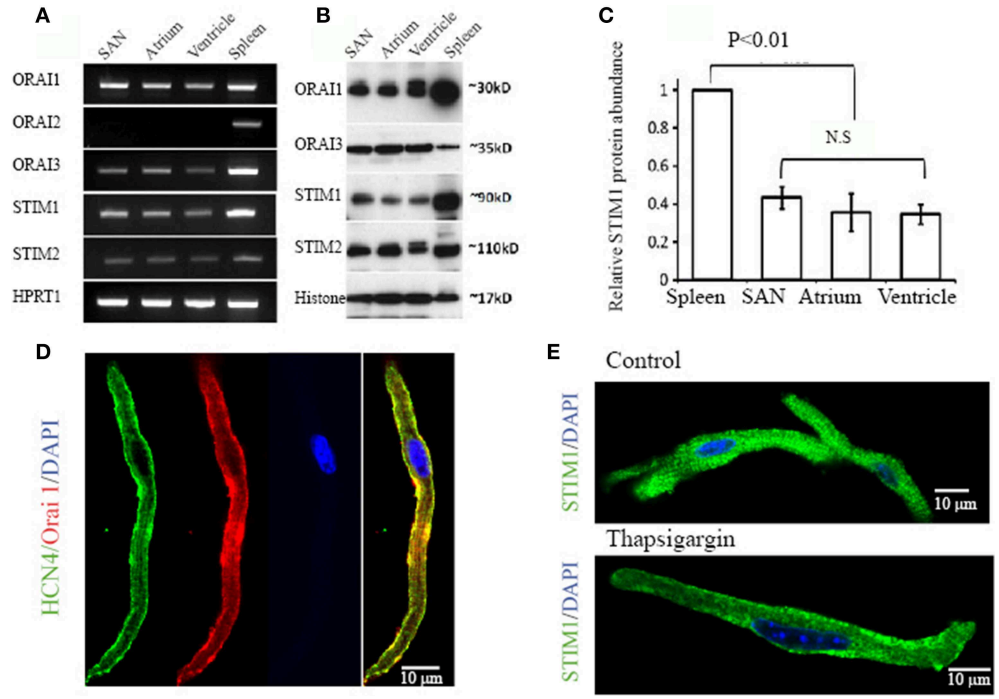

FIGURE 4 | Expression of STIM and Orai molecules in mouse cardiac myocytes. (A) Total RNA was isolated from pacemaker cells (SAN), atrial myocytes (Atrium), ventricular myocytes (Ventricle) and spleen. Transcripts of Stim1, Stim2, Orai1, Orai2, and Orai3 in cardiac myocytes were compared with the spleen as positive control. The housekeeping gene Hypoxanthine–Guanine Phosphoribosyltransferase (HPRT1) was used as an internal control. **(B)** Protein levels of STIM1, STIM2, Orai1, and Orai3 were examined in total protein extracts from SAN region (SAN), atrium (Atrium), ventricle (Ventricle) and spleen and determined by Western Blot analysis. The nuclear protein histone was used as loading control. **(C)** Bar graph showing quantitative western blot analysis of STIM1 protein levels in spleen and heart with heart samples normalized to spleen as 1 ($n = 3$ gels, $P < 0.05$, ANOVA). **(D)** Confocal images of an isolated pacemaker cell shows expression of HCN4 (green in color), a positive marker for pacemaker cells. The cell also positively stained with anti-Orai1 antibody (red in color). The nucleus is stained blue with DAPI. A merged image on the left shows the co-localization of HCN4 and Orai1 along the surface membrane (color in yellow). **(E)** Representative confocal images of an isolated pacemaker cell labeled with STIM1 (green in color) and DAPI (blue in color). When perfused with normal Ca^{2+} containing solution, positive STIM1 staining was distributed both intracellularly and in the cell periphery as showed in the top panel. When perfused with Ca^{2+}-free solution containing thapsigargin, STIM1 peripheral localization was enhanced, as shown in the bottom panel.

and Orai1, resulting in activation of calcium influx through Orai1.

Discussion

SOCE and Pacemaker Function

In the present study, we examined both the functional consequences of SOCE and molecular components of SOCE in isolated pacemaker cells. The study strengthens our earlier identification of SOCE in intact mouse SAN (Ju et al., 2007).

Given that pacemaker cells generate robust spontaneous firing by a combination of voltage-dependent channels and Ca^{2+} cycling, one might question what functional role SOCE can play in pacemaker cells. Application of the blockers to the normally firing pacemaker cells caused only modest reductions of the firing rate, though the fact that they were accompanied by a reduction in store level strengthens the case for the effect arising from blocking SOCE. Reduced SR store Ca^{2+} content would influence both diastolic and systolic SR Ca^{2+} release and hence influence pacemaker activity (Bassani et al., 1995; Vinogradova et al., 2004, 2006). However, we could not eliminate the possible effect of these blockers on other pacemaker currents such as voltage-gated Ca^{2+} current or potassium currents, which might prevent us from accurately estimating the contribution of SOCE to pacemaker electrical activity.

From an evolutionary perspective, survival of an animal depends critically on the activity of several small groups of pacemaker cells. No doubt this is the reason why pacemaker cells contain several independent pacing mechanisms so that the loss of one through ingested toxin, injury or genetic mutation is not necessarily lethal. The experimental data presented here demonstrated a small change (~15% decrease) in firing rate when SOCE was blocked, and thus supports a possible role of SOCE in regulating the firing rate under physiological conditions. Using computer simulation, we recently found that an additional inward SOCE current with a long time constant of activation (e.g., 800 ms) could lead to a small increase (~11%) in firing rate. With such a long activation time constant, SOCE current effectively becomes a background current whose level changes little over the cardiac cycle and whose magnitude depends on the mean level of Ca^{2+} in the SR over the cardiac cycle, providing a calcium influx regulated by mean store size (Allen et al., 2012).

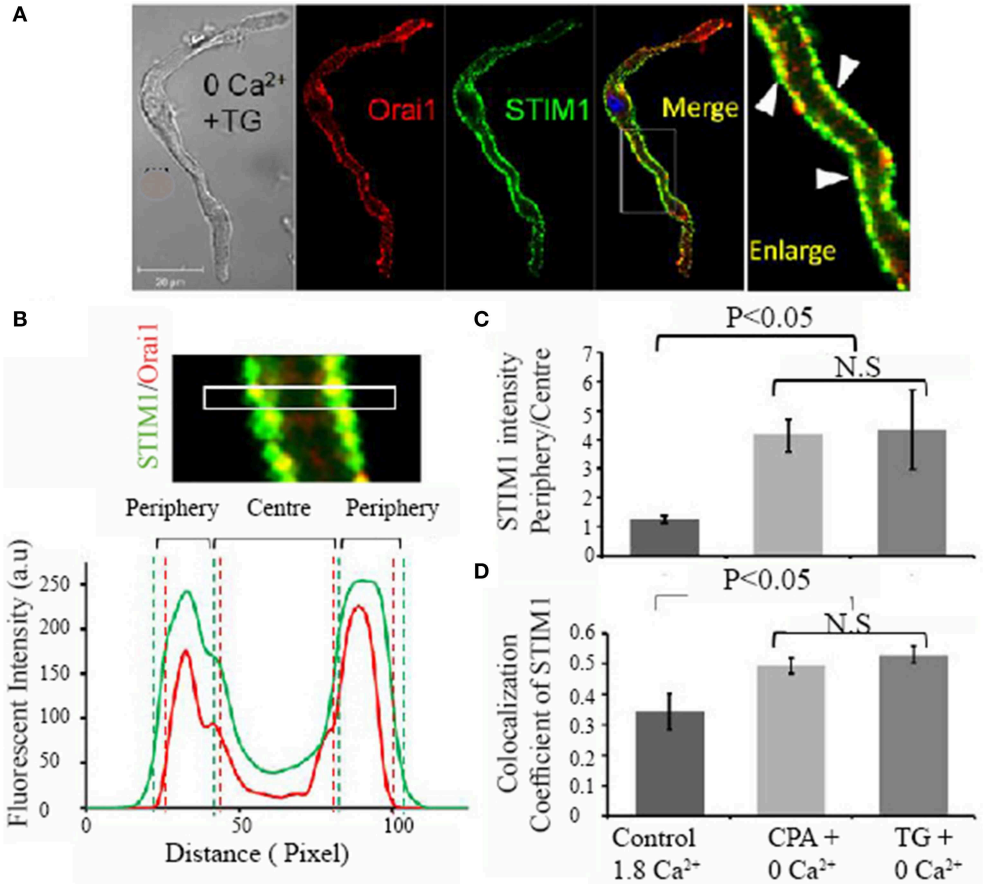

FIGURE 5 | Evidence of migration of STIM1 proteins to the cell membrane region after store depletion. Ca^{2+} store was depleted by treating cells with Ca^{2+} free solution plus 10 μmol/L thapsigargin. **(A)** The colocalization of STIM1 and Orai1 is demonstrated by membrane staining of STIM1 in the merged image (yellow in color) and is also indicated by white triangle arrows in the enlarged image (far right panel). To determine the region of a cell, the confocal image of a cell was equally divided into peripheral quarters and center quarters across cell width, and fluorescent intensity in each quarter was plotted against distance as demonstrated in **(B)**. **(C)** Summary data of the fluorescent intensity ratio of peripheral quarters to center quarters of STIM1 under three conditions; control, CPA + 0 Ca^{2+}, thapsigargin (TG) + 0 Ca^{2+} ($n = 9$ cells in each group, $P < 0.05$, ANOVA). **(D)** Summary data (mean ± SEM) of the colocalization coefficiency, a ratio of STIM1 and Orai1 colocalized pixels (Colocal) over total STIM1 pixels under three conditions. ($n = 9$ cells in each group, $P < 0.05$, ANOVA).

Background currents of this sort have been previously recognized in rabbit pacemaker cells (Hagiwara et al., 1992). In this context, it would be of interest to determine whether the background current in pacemaker cells is dependent on SR Ca^{2+} store depletion.

Distribution and Localization of STIM and Orai in Pacemaker Cells

In the present study we demonstrate that SOCE activity is present in single pacemaker cells. We also demonstrate that several new SOCE proteins, including STIM1, STIM2, Orai1, and Orai3, but not Orai2, are expressed in pacemaker cells of mouse SAN tissue. Using immunohistochemistry, we show that while Orai1 proteins are predominantly located in the sarcolemma, STIM1 proteins under control conditions are distributed across the cell. It has been reported that STIM activation induces conformational changes of Orai proteins and subsequent STIM-Orai colocalization, which forms the active store-operated calcium channel (Lewis, 2007; Stathopulos et al., 2013). We also found that there was a certain proportion of STIM1 and Orai1 clustered and co-localized at the periphery of pacemaker cells in response to the store depletion. These results suggest a possible interaction between STIM1 and Orai1 and how they might play a functional role related to SOCE. However, to further quantify the involvement of STIM1 and Orai1 in SOCE activities in native pacemaker cells would require the use of tissue specific/conditional knock out related genes and proteins and then record associated changes of the amplitude of Ca^{2+} release activated current (I_{CRAC}).

While the molecular mechanism of STIM1/Orai1 activity and their functional importance have been studied in great detail, the functional relevance of other isoforms of STIM and Orai still remain speculative (Hoth and Niemeyer, 2013). STIM2 and STIM1 share 60% homology in their amino acid sequence.

Although we also found the presence of STIM2, the role of STIM2 in pacemaker cells might be less significant as we did not observe the translocation of STIM2 in response to store depletion (data not shown).

We also found that in addition to Orai1, Orai3 was also expressed in cardiac myocytes, including pacemaker cells, a result consistent with a recent finding in rat ventricular myocardium (Wolkowicz et al., 2011). In addition to forming functional SOCE channels, STIM1 and Orai1 have been shown to interact with many other Ca^{2+} handling proteins, including TRPC (Liao et al., 2008, 2009), the L-type Ca channel (Wang et al., 2010a), the sodium-calcium exchanger (Liu et al., 2010), the plasma membrane Ca^{2+} ATPase (Ritchie et al., 2012), and the sarcoplasmic reticulum Ca^{2+} ATPase (Lopez et al., 2008). Given that all these potential pathways could contribute to Ca^{2+} handling and therefore pacemaker function, these offer multiple possible directions for future research.

In our earlier work we identified that TRPC1, 3, 4, and 6 are all expressed in pacemaker cells (Ju et al., 2007). The current study demonstrates the presence of two of the best characterized SOCE components, STIM1 and Orai1, in pacemaker cells and in addition demonstrates translocation of STIM1 to the sites of Orai1 on store depletion, as characterized in many other cell types. It has been suggested that Orai and TRPC protein form complexes that participate in Ca^{2+} entry with or without activation of store depletion (Liao et al., 2009). Since these SOCE related proteins are all expressed in the pacemaker cells, it is possible that SOCE or related Ca^{2+} signaling pathways such as receptor operated Ca^{2+} entry (ROCE) (Hofmann et al., 1999) might contribute to pacemaker activity under physiological or pathophysiological conditions.

Limitations of the Current Study

A patch clamp study is needed to further establish whether SOCE is accompanied by an inward current (Potier et al., 2009) which directly contributes to diastolic pacemaker potential.

Acknowledgments

This study was supported by grants from the National Health and Medical Research Council. The confocal imaging was carried out at the Bosch Institute Advanced Microscopy Facility at the University of Sydney.

References

Allen, D. G., Ju, Y. K., Liu, J., and Imtiaz, M. (2012). "SOCE as a determinant of cardiac pacemaker function," in *Store-Operated Ca^{2+} Entry Pathways*, eds K. Groschner, W. F. Graier, and C. Romanin (Wien: Springer), 363–376.

Bassani, J. W., Yuan, W., and Bers, D. M. (1995). Fractional SR Ca release is regulated by trigger Ca and SR Ca content in cardiac myocytes. *Am. J. Physiol.* 268, C1313–C1319.

Bers, D. M. (1987). Ryanodine and the calcium content of cardiac SR assessed by caffeine and rapid cooling contractures. *Am. J. Physiol. Cell Physiol.* 253, C408–C415.

Birnbaumer, L. (2009). The TRPC class of ion channels: a critical review of their roles in slow, sustained increases in intracellular Ca(2+) concentrations. *Annu. Rev. Pharmacol. Toxicol.* 49, 395–426. doi: 10.1146/annurev.pharmtox.48.113006.094928

Cahalan, M. D. (2009). STIMulating store-operated Ca(2+) entry. *Nat. Cell. Biol.* 11, 669–677. doi: 10.1038/ncb0609-669

Camelliti, P., Green, C. R., LeGrice, I., and Kohl, P. (2004). Fibroblast network in rabbit sinoatrial node - structural and functional identification of homogeneous and heterogeneous cell coupling. *Circ. Res.* 94, 828–835. doi: 10.1161/01.RES.0000122382.19400.14

Chen, J. B., Tao, R., Sun, H. Y., Tse, H. F., Lau, C. P., and Li, G. R. (2010). Multiple Ca^{2+} signaling pathways regulate intracellular Ca^{2+} activity in human cardiac fibroblasts. *J. Cell. Physiol.* 223, 68–75. doi: 10.1002/jcp.22010

Clapham, D. E. (2003). TRP channels as cellular sensors. *Nature* 426, 517–524. doi: 10.1038/nature02196

Collins, H. E., Zhu-Mauldin, X., Marchase, R. B., and Chatham, J. C. (2013). STIM1/Orai1-mediated SOCE: current perspectives and potential roles in cardiac function and pathology. *Am. J. Physiol. Heart Circ. Physiol.* 305, H446–H458. doi: 10.1152/ajpheart.00104.2013

Eder, P., and Molkentin, J. D. (2011). TRPC channels as effectors of cardiac hypertrophy. *Circ. Res.* 108, 265–272. doi: 10.1161/CIRCRESAHA.110.225888

Feske, S., Gwack, Y., Prakriya, M., Srikanth, S., Puppel, S. H., Tanasa, B., et al. (2006). A mutation in Orai1 causes immune deficiency by abrogating CRAC channel function. *Nature* 441, 179–185. doi: 10.1038/nature04702

Hagiwara, N., Irisawa, H., Kasanuki, H., and Hosoda, S. (1992). Background current in sino-atrial node cells of the rabbit heart. *J. Physiol.* 448, 53–72. doi: 10.1113/jphysiol.1992.sp019029

Harada, M., Luo, X., Qi, X. Y., Tadevosyan, A., Maguy, A., Ordog, B., et al. (2012). Transient receptor potential canonical-3 channel-dependent fibroblast regulation in atrial fibrillation. *Circulation* 126, 2051–2064. doi: 10.1161/CIRCULATIONAHA.112.121830

He, L. P., Hewavitharana, T., Soboloff, J., Spassova, M. A., and Gill, D. L. (2005). A functional link between store-operated and TRPC channels revealed by the 3,5-Bis(trifluoromethyl)pyrazole derivative, BTP2. *J. Biol. Chem.* 280, 10997–11006. doi: 10.1074/jbc.M411797200

Herrmann, S., Stieber, J., Stockl, G., Hofmann, F., and Ludwig, A. (2007). HCN4 provides a 'depolarization reserve' and is not required for heart rate acceleration in mice. *EMBO J.* 26, 4423–4432. doi: 10.1038/sj.emboj.7601868

Himeno, Y., Toyoda, F., Satoh, H., Amano, A., Cha, C. Y., Matsuura, H., et al. (2011). Minor contribution of cytosolic Ca^{2+} transients to the pacemaker rhythm in guinea pig sinoatrial node cells. *Am. J. Physiol.Heart. Circul. Physiol.* 300, H251–H261. doi: 10.1152/ajpheart.00764.2010

Hofmann, T., Obukhov, A. G., Schaefer, M., Harteneck, C., Gudermann, T., and Schultz, G. (1999). Direct activation of human TRPC6 and TRPC3 channels by diacylglycerol. *Nature* 397, 259–263. doi: 10.1038/16711

Hoth, M., and Niemeyer, B. A. (2013). The neglected CRAC proteins: Orai2, Orai3, and STIM2. *Curr. Top. Membr.* 71, 237–271. doi: 10.1016/B978-0-12-407870-3.00010-X

Huang, G. N., Zeng, W. Z., Kim, J. Y., Yuan, J. P., Han, L. H., Muallem, S., et al. (2006). STIM1 carboxyl-terminus activates native SOC, I-crac and TRPC1 channels. *Nat. Cell Biol.* 8, 1003. doi: 10.1038/ncb1454

Ju, Y. K., and Allen, D. G. (1998). Intracellular calcium and Na^{+}-Ca^{2+} exchange current in isolated toad pacemaker cells. *J. Physiol.* 508, 153–166. doi: 10.1111/j.1469-7793.1998.153br.x

Ju, Y. K., and Allen, D. G. (1999). How does β-adrenergic stimulation increase heart rate? the role of intracellular Ca^{2+} release in amphibian pacemaker cells. *J. Physiol.* 516, 793–804. doi: 10.1111/j.1469-7793.1999.0793u.x

Ju, Y. K., and Allen, D. G. (2000). The mechanisms of sarcoplasmic reticulum Ca^{2+} release in toad pacemaker cells. *J. Physiol.* 525, 695–705. doi: 10.1111/j.1469-7793.2000.t01-1-00695.x

Ju, Y. K., Chu, Y., Chaulet, H., Lai, D., Gervasio, O. L., Graham, R. M., et al. (2007). Store-operated Ca^{2+} influx and expression of TRPC genes in mouse sinoatrial node. *Circ. Res.* 100, 1605–1614. doi: 10.1161/CIRCRESAHA.107.152181

Lakatta, E. G., and DiFrancesco, D. (2009). What keeps us ticking: a funny current, a calcium clock, or both? *J. Mol. Cell. Cardiol.* 47, 157–170. doi: 10.1016/j.yjmcc.2009.03.022

Lakatta, E. G., Maltsev, V. A., and Vinogradova, T. M. (2010). A Coupled SYSTEM of Intracellular Ca^{2+} clocks and surface membrane voltage clocks controls the timekeeping mechanism of the Heart's Pacemaker. *Circ. Res.* 106, 659–673. doi: 10.1161/CIRCRESAHA.109.206078

Lewis, R. S. (2007). The molecular choreography of a store-operated calcium channel. *Nature* 446, 284–287. doi: 10.1038/nature05637

Li, J., Cubbon, R. M., Wilson, L. A., Amer, M. S., McKeown, L., Hou, B., et al. (2011). Orai1 and CRAC channel dependence of VEGF-Activated Ca^{2+} entry and endothelial tube formation/novelty and significance. *Circ. Res.* 108, 1190–1198. doi: 10.1161/CIRCRESAHA.111.243352

Liao, Y., Erxleben, C., Abramowitz, J., Flockerzi, V., Zhu, M. X., Armstrong, D. L., et al. (2008). Functional interactions among Orai1, TRPCs, and STIM1 suggest a STIM-regulated heteromeric Orai/TRPC model for SOCE/Icrac channels. *Proc. Natl. Acad. Sci. U.S.A.* 105, 2895–2900. doi: 10.1073/pnas.0712288105

Liao, Y., Plummer, N. W., George, M. D., Abramowitz, J., Zhu, M. X., and Birnbaumer, L. (2009). A role for Orai in TRPC-mediated Ca2+ entry suggests that a TRPC:Orai complex may mediate store and receptor operated Ca2+ entry. *Proc. Natl. Acad. Sci. U.S.A.* 106, 3202–3206. doi: 10.1073/pnas.0813346106

Liou, J., Fivaz, M., Inoue, T., and Meyer, T. (2007). Live-cell imaging reveals sequential oligomerization and local plasma membrane targeting of stromal interaction molecule 1 after Ca^{2+} store depletion. *Proc. Natl. Acad. Sci. U.S.A.* 104, 9301–9306. doi: 10.1073/pnas.0702866104

Liou, J., Kim, M. L., Do Heo, W., Jones, J. T., Myers, J. W., Ferrell, J., et al. (2005). STIM Is a Ca^{2+} sensor essential for Ca^{2+}-store-depletion-triggered Ca^{2+} Influx. *Curr. Biol.* 15, 1235–1241. doi: 10.1016/j.cub.2005.05.055

Liu, B., Peel, S. E., Fox, J., and Hall, I. P. (2010). Reverse mode Na+/Ca2+ exchange mediated by STIM1 contributes to Ca2+ influx in airway smooth muscle following agonist stimulation. *Respir. Res.* 11:168. doi: 10.1186/1465-9921-11-168

Liu, J., Dobrzynski, H., Yanni, J., Boyett, M. R., and Lei, M. (2007). Organisation of the mouse sinoatrial node: structure and expression of HCN channels. *Cardiovas. Res.* 73, 729–738. doi: 10.1016/j.cardiores.2006.11.016

Liu, J., Sirenko, S., Juhaszova, M., Ziman, B., Shetty, V., Rain, S., et al. (2011). A full range of mouse sinoatrial node AP firing rates requires protein kinase A-dependent calcium signaling. *J. Mol. Cell. Cardiol.* 51, 730–739. doi: 10.1016/j.yjmcc.2011.07.028

Lopez, J. J., Jardin, I., Bobe, R., Pariente, J. A., Enouf, J., Salido, G. M., et al. (2008). STIM1 regulates acidic Ca2+ store refilling by interaction with SERCA3 in human platelets. *Biochem. Pharmacol.* 75, 2157–2164. doi: 10.1016/j.bcp.2008.03.010

Marionneau, C., Couette, B., Liu, J., Li, H., Mangoni, M. E., Nargeot, J., et al. (2005). Specific pattern of ionic channel gene expression associated with pacemaker activity in the mouse heart. *J. Physiol.* 562, 223–234. doi: 10.1113/jphysiol.2004.074047

Mohl, M. C., Iismaa, S. E., Xiao, X. H., Friedrich, O., Wagner, S., Nikolova-Krstevski, V., et al. (2011). Regulation of murine cardiac contractility by activation of alpha(1A)-adrenergic receptor-operated Ca(2+) entry. *Cardiovasc. Res.* 91, 310–319. doi: 10.1093/cvr/cvr081

Nishiyama, A., Xin, L., Sharov, A. A., Thomas, M., Mowrer, G., Meyers, E., et al. (2009). Uncovering early response of gene regulatory networks in ESCs by systematic induction of transcription factors. *Cell Stem Cell* 5, 420–433. doi: 10.1016/j.stem.2009.07.012

Noble, D. (1960). Cardiac action and pace-maker potentials based on the Hodgkin-Huxley equations. *Nature* 188, 495–497. doi: 10.1038/188495b0

Onohara, N., Nishida, M., Inoue, R., Kobayashi, H., Sumimoto, H., Sato, Y., et al. (2006). TRPC3 and TRPC6 are essential for angiotensin II-induced cardiac hypertrophy. *EMBO J.* 25, 5305–5316. doi: 10.1038/sj.emboj.7601417

Parekh, A. B., and Putney, J. W. Jr. (2005). Store-operated calcium channels. *Physiol. Rev.* 85, 757–810. doi: 10.1152/physrev.00057.2003

Penna, A., Demuro, A., Yeromin, A. V., Zhang, S. L., Safrina, O., Parker, I., et al. (2008). The CRAC channel consists of a tetramer formed by Stim-induced dimerization of Orai dimers. *Nature* 456, 116–120. doi: 10.1038/nature07338

Potier, M., Gonzalez, J. C., Motiani, R. K., Abdullaev, I. F., Bisaillon, J. M., Singer, H. A., et al. (2009). Evidence for STIM1- and Orai1-dependent store-operated calcium influx through ICRAC in vascular smooth muscle cells: role in proliferation and migration. *FASEB J.* 23, 2425–2437. doi: 10.1096/fj.09-131128

Putney, J. W. (2009). Capacitative calcium entry: from concept to molecules. *Immunol. Rev.* 231, 10–22. doi: 10.1111/j.1600-065X.2009.00810.x

Rigg, L., Heath, B. M., Cui, Y., and Terrar, D. A. (2000). Localisation and functional significance of ryanodine receptors during beta-adrenoceptor stimulation in the guinea-pig sino-atrial node. *Cardiovasc. Res.* 48, 254–264. doi: 10.1016/S0008-6363(00)00153-X

Rigg, L., and Terrar, D. A. (1996). Possible role of calcium release from the sarcoplasmic reticulum in pacemaking in guinea-pig sino-atrial node. *Exp. Physiol.* 81, 877–880. doi: 10.1113/expphysiol.1996.sp003983

Ritchie, M. F., Samakai, E., and Soboloff, J. (2012). STIM1 is required for attenuation of PMCA-mediated Ca2+ clearance during T-cell activation. *EMBO J.* 31, 1123–1133. doi: 10.1038/emboj.2011.495

Seth, M., Li, T., Graham, V., Burch, J., Finch, E., Stiber, J. A., et al. (2012). Dynamic regulation of sarcoplasmic reticulum Ca(2+) stores by stromal interaction molecule 1 and sarcolipin during muscle differentiation. *Dev. Dyn.* 241, 639–647. doi: 10.1002/dvdy.23760

Singh, A., Hildebrand, M. E., Garcia, E., and Snutch, T. P. (2010). The transient receptor potential channel antagonist SKF96365 is a potent blocker of low-voltage-activated T-type calcium channels. *Br. J. Pharmacol.* 160, 1464–1475. doi: 10.1111/j.1476-5381.2010.00786.x

Stathopulos, P. B., Schindl, R., Fahrner, M., Zheng, L., Gasmi-Seabrook, G. M., Muik, M., et al. (2013). STIM1/Orai1 coiled-coil interplay in the regulation of store-operated calcium entry. *Nat. Commun.* 4, 2963. doi: 10.1038/ncomms3963

Vig, M., Peinelt, C., Beck, A., Koomoa, D. L., Rabah, D., Koblan-Huberson, M., et al. (2006). CRACM1 is a plasma membrane protein essential for store-operated Ca^{2+} entry. *Science* 312, 1220–1223. doi: 10.1126/science.1127883

Vinogradova, T. M., Lyashkov, A. E., Zhu, W., Ruknudin, A. M., Sirenko, S., Yang, D., et al. (2006). High basal protein kinase A-dependent phosphorylation drives rhythmic internal Ca^{2+} store oscillations and spontaneous beating of cardiac pacemaker cells. *Circ. Res.* 98, 505–514. doi: 10.1161/01.RES.0000204575.94040.d1

Vinogradova, T. M., Zhou, Y. Y., Bogdanov, K. Y., Yang, D., Kuschel, M., Cheng, H., et al. (2000). Sinoatrial node pacemaker activity requires Ca^{2+}/calmodulin-dependent protein kinase II activation. *Circ. Res.* 87, 760–767. doi: 10.1161/01.RES.87.9.760

Vinogradova, T. M., Zhou, Y. Y., Maltsev, V., Lyashkov, A., Stern, M., and Lakatta, E. G. (2004). Rhythmic ryanodine receptor Ca2+ releases during diastolic depolarization of sinoatrial pacemaker cells do not require membrane depolarization. *Circ. Res.* 94, 802–809. doi: 10.1161/01.RES.0000122045.55331.0F

Wang, Y., Deng, X., and Gill, D. L. (2010b). Calcium signaling by STIM and orai: intimate coupling details revealed. *Sci. Signal.* 3:e42. doi: 10.1126/scisignal.3148pe42

Wang, Y., Deng, X., Mancarella, S., Hendron, E., Eguchi, S., Soboloff, J., et al. (2010a). The calcium store sensor, STIM1, reciprocally controls Orai and CaV1.2 channels. *Science* 330, 105–109. doi: 10.1126/science.1191086

Wissenbach, U., Philipp, S. E., Gross, S. A., Cavalie, A., and Flockerzi, V. (2007). Primary structure, chromosomal localization and expression in immune cells of the murine ORAI and STIM genes. *Cell Calcium* 42, 439–446. doi: 10.1016/j.ceca.2007.05.014

Wolkowicz, P. E., Huang, J., Umeda, P. K., Sharifov, O. F., Tabengwa, E., Halloran, B. A., et al. (2011). Pharmacological evidence for Orai channel activation as a source of cardiac abnormal automaticity. *Europ. J. Pharmacol.* 668, 208–216. doi: 10.1016/j.ejphar.2011.06.025

Wu, M. M., Buchanan, J., Luik, R. M., and Lewis, R. S. (2006). Ca2+ store depletion causes STIM1 to accumulate in ER regions closely associated with the plasma membrane. *J. Cell Biol.* 174, 803–813. doi: 10.1083/jcb.200604014

Wu, X., Eder, P., Chang, B., and Molkentin, J. D. (2010). TRPC channels are necessary mediators of pathologic cardiac hypertrophy. *Proc. Natl. Acad. Sci. U.S.A.* 107, 7000–7005. doi: 10.1073/pnas.1001825107

Yonetoku, Y., Kubota, H., Miyazaki, Y., Okamoto, Y., Funatsu, M., Yoshimura-Ishikawa, N., et al. (2008). Novel potent and selective Ca2+ release-activated Ca2+ (CRAC) channel inhibitors. Part 3: synthesis and CRAC channel inhibitory activity of 4'-[(trifluoromethyl)pyrazol-1-yl]carboxanilides. *Bioorg. Med. Chem.* 16, 9457–9466. doi: 10.1016/j.bmc.2008.09.047

Zhang, S. L., Yeromin, A. V., Zhang, X. H., Yu, Y., Safrina, O., Penna, A., et al. (2006). Genome-wide RNAi screen of Ca(2+) influx identifies genes that regulate Ca(2+) release-activated Ca(2+) channel activity. *Proc. Natl. Acad. Sci. U.S.A.* 103, 9357–9362. doi: 10.1073/pnas.0603161103

Zhang, S. L., Yu, Y., Roos, J., Kozak, J. A., Deerinck, T. J., Ellisman, M. H., et al. (2005). STIM1 is a Ca2+ sensor that activates CRAC channels and migrates from the Ca2+ store to the plasma membrane. *Nature* 437, 902–905. doi: 10.1038/nature04147

Zhou, Y., Meraner, P., Kwon, H. T., Machnes, D., Oh-hora, M., Zimmer, J., et al. (2010). STIM1 gates the store-operated calcium channel ORAI1 *in vitro*. *Nat. Struct. Mol. Biol.* 17, 112–116. doi: 10.1038/nsmb.1724

Zhou, Y. Y., Wang, S. Q., Zhu, W. Z., Chruscinski, A., Kobilka, B. K., Ziman, B., et al. (2000). Culture and adenoviral infection of adult mouse cardiac myocytes: methods for cellular genetic physiology. *Am. J. Physiol. Heart Circ. Physiol.* 279, H429–H436.

Conflict of Interest Statement: The authors declare that the research was conducted in the absence of any commercial or financial relationships that could be construed as a potential conflict of interest.

frontiers in
PHYSIOLOGY

REVIEW ARTICLE
published: 19 February 2015
doi: 10.3389/fphys.2015.00046

SR calcium handling dysfunction, stress-response signaling pathways, and atrial fibrillation

Xun Ai*

Department of Cell and Molecular Physiology, Loyola University Chicago, Maywood, IL, USA

Edited by:
Ming Lei, University of Oxford, UK

Reviewed by:
Andrew F. James, University of Bristol, UK
Jin O-Uchi, Thomas Jefferson University, USA

****Correspondence:***
Xun Ai, Department of Cell and Molecular Physiology, Loyola University Chicago, 2160 South First Avenue, Maywood, IL 60153, USA
e-mail: xai1@luc.edu

Atrial fibrillation (AF) is the most common sustained arrhythmia. It is associated with a markedly increased risk of premature death due to embolic stroke and also complicates co-existing cardiovascular diseases such as heart failure. The prevalence of AF increases dramatically with age, and aging has been shown to be an independent risk of AF. Due to an aging population in the world, a growing body of AF patients are suffering a diminished quality of life and causing an associated economic burden. However, effective pharmacologic treatments and prevention strategies are lacking due to a poor understanding of the molecular and electrophysiologic mechanisms of AF in the failing and/or aged heart. Recent studies suggest that altered atrial calcium handling contributes to the onset and maintenance of AF. Here we review the role of stress-response kinases and calcium handling dysfunction in AF genesis in the aged and failing heart.

Keywords: atrial fibrillation, calcium handling, arrhythmogenesis, stress-response kinases, heart failure, aging

INTRODUCTION

Clinical studies have shown that atrial fibrillation (AF) is the most common cardiac arrhythmia and has an associated high risk of mortality and morbidity (such as stroke and heart failure) in the aging population (Benjamin et al., 1994; Psaty et al., 1997; Podrid, 1999; Go et al., 2001; Miyasaka et al., 2006; Rich, 2009). Both heart failure (HF) and aging have been shown to be independent risk factors for AF (Benjamin et al., 1994; Kannel et al., 1998; Ehrlich et al., 2002; Neuberger et al., 2007). HF affects nearly 15 million people worldwide (Cowie et al., 1997; Hershberger et al., 2003). One third to one half of patients with HF develop AF (Markides and Peters, 2002). New-onset AF among HF patients has consistently been associated with a 2-fold increase in all-cause mortality. Due to an aging population, the prevalence of both AF and HF is predicted to more than double by 2050 (Linne et al., 2000; Di Lenarda et al., 2003). The high prevalence of these multiple co-morbidities (Wang et al., 2003) (e.g., very frequent co-existence of HF, AF, with aging) has tremendous impact on the quality of life and daily functioning of elderly individuals, and is a significant financial burden worldwide (Linne et al., 2000; Di Lenarda et al., 2003). However, pharmacological treatment and prevention strategies remain ineffective due to the incomplete understanding of the underlying molecular and electrophysiologic mechanisms of AF genesis and development.

Accumulating evidence suggests that intrinsic stress (e.g., oxidative stress and chronic inflammatory stress) are markedly enhanced in aging, HF, and AF, while the aged and pathologically altered hearts have been shown to exhibit a higher susceptibility to extrinsic stress stimuli (Belmin et al., 1995; Beckman and Ames, 1998; Juhaszova et al., 2005; Neuman et al., 2007; He et al., 2011; Ismahil et al., 2014). The mitogen-activated protein kinase (MAPK) cascade is composed of a family of signaling cascades, which act as critical regulators of cell survival and growth in response to both intrinsic and extrinsic stress challenges. The three MAPK subfamilies c-Jun N-terminal kinase (JNK), extracellular signal-regulated kinases (ERKs), and p38 MAPKs have been the focus of extensive studies to uncover their roles in cardiac disease development (Davis, 2000; Karin and Gallagher, 2005; Ramos, 2008; Rose et al., 2010). The impacts of these stress-response kinases on sarcoplasmic reticulum (SR) calcium (Ca) handling proteins have begun to be revealed (Ho et al., 1998, 2001; Takahashi et al., 2004; Hagiwara et al., 2007; Scharf et al., 2013; Huang et al., 2014). Extensive studies suggest that alterations of Ca handling proteins including RyR2, phospholamban [PLB, an inhibitory protein of SR Ca pump (SERCA2)], and L-type Ca channels (Cav1.2) contribute to changed intracellular Ca transients and diastolic SR Ca release that in turn lead to Ca-triggered ventricular and atrial arrhythmogenesis (Schulman et al., 1992; Wu et al., 1999; DeSantiago et al., 2002). Thus, this review focuses on the recent progress in understanding the role of stress-response kinases and calcium signaling dysfunction in AF genesis in the aged and failing heart.

ELECTRICAL REMODELING PRECEDES AF ONSET AND DEVELOPMENT

It is generally believed that abnormal triggers initiate AF, while an arrhythmogenic substrate sustains it (Nattel et al., 2008). While reentry circuits due to the formation of arrhythmogenic substrate including molecular and structural remodeling have been demonstrated to be important in AF development (Allessie et al., 1976; Mandapati et al., 2000), the underlying mechanisms of AF initiated by abnormal ectopic trigger activities remain unclear. Extensive studies in ventricular myocytes have shown that ectopic activities can occur by prolonged action potential duration (APD) causing early afterdepolarizations (EADs) and by spontaneous SR Ca releases leading to delayed afterdepolarizations (DADs)

(Nattel et al., 2008). EADs normally occur with abnormal depolarization during phase 2 or phase 3 of the action potential (AP). While ventricular myocytes can only develop phase 2 EADs, atrial myocytes do not produce phase 2 EAD but may produce late phase 3 EADs with an abbreviation of the atrial APD (Burashnikov and Antzelevitch, 2003; Patterson et al., 2005). Studies suggest that electrical remodeling of atrial membrane ion channels (e.g., Ca and potassium channels) leads to altered APD and atrial effective refractory period (AERP); both have been found to be associated with the development of AF (Marx et al., 2000; Christ et al., 2004; Nattel et al., 2007). Before the onset of AF, shorter AERPs were associated with a higher inducibility of AF, while longer AERPs and slowing atrial conduction velocity, which may cause a pro-arrhythmogeinc shortening of the conduction wavelength, Rensma et al. (1988) were found to be linked to AF development in HF patients and animals (Huang et al., 2003; Sanders et al., 2003). In aged rabbit left atrium, we found that a slight reduction in AERP and unchanged action potential duration (APD_{30} and APD_{60}; pacing cycle length = 200 ms) were associated with slowed conduction velocity and a markedly increased pacing induced AF compared to that of young controls (**Figure 1**)(Yan et al., 2013). Although similar results of slightly altered APD and AERP were also reported in aged canine and rat atria, Anyukhovsky et al. (2005) and Huang et al. (2006) studies from coronary artery bypass graft (CABG) surgery patients suggest that AERP was positively correlated with age (Sakabe et al., 2003). However, the molecular and electrophysiological properties of human hearts are known to be varied and complicated, especially when co-existing pathological conditions (such as HF or myocardial infarction) are present. While these results need to be further confirmed in healthy aging human donor hearts and further validated in other animal aging models, studies suggest that atrial electrical remodeling was found to occur long before the first occurrence of AF, and was not always correlated with the occurrence of sustained AF in patients and animal models (van der Velden et al., 2000; Kanagaratnam et al., 2008). In addition, late-phase 3 EADs have only been shown to be responsible for the immediate initiation of AF following termination of paroxysmal AF, but not in the case of newly onset AF or reoccurrence of AF that has been terminated for a long time (Timmermans et al., 1998; Oral et al., 2003). Thus, other features of the arrhythmogenic substrate such as SR Ca handling dysfunction, a generally acknowledged arrhythmogenic factor of generating DADs, could play an important role in failing or age-related enhancement of atrial arrhythmogenicity.

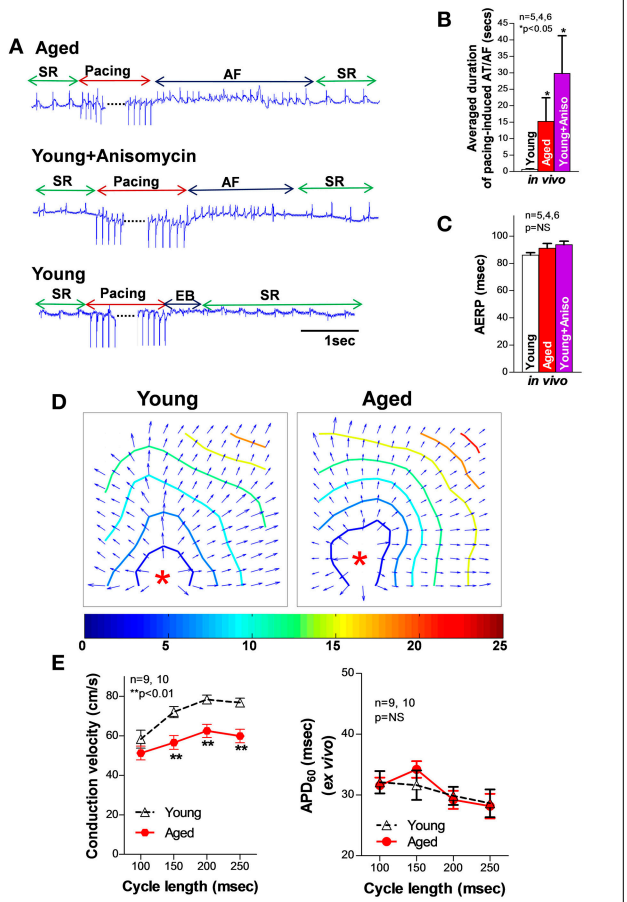

FIGURE 1 | (A) Representative electrograms (EG) of burst pacing (for 30 s at 6× diastolic threshold, CL = ±5 ms of atrial effective refractory period (AERP) induced AF followed by self-reversion to sinus rhythm (SR) in open-chest aged (top row) and anisomycin-challenged young rabbit LA (middle row), and self-restored SR after burst pacing induced extra beats (EB) in sham control young rabbit LA (bottom row). **(B–C)** Summarized data of average duration of pacing-induced AT/AF as well as AERP in open-chest aged rabbit LA and young rabbit LA with or without anisomycin treatment (*$p < 0.05$ and p = NS, respectively). **(D)** Representative isochronal maps from young and aged rabbit hearts subjected to pacing at a CL of 200 ms (π indicates the pacing sites). **(E)** Summarized optical mapping CV data show that aged rabbits exhibited a CL-dependent, slower conduction but unchanged AERP vs. young controls. This figure is modified from Yan et al. (2013).

ATRIAL SR Ca HANDLING IN AF GENESIS

Although Ca handling in atrial myocytes is similar to that of ventricular myocytes, there are some important structural and cellular signal differences between atrial and ventricular myocytes. Atrial myocytes are thinner and longer, Walden et al. (2009) which may lead to a longer delay between APs and Ca transients at the center of the cells. This property of the atrial cell can increase the instability of Ca propagation, which is pro-arrhythmogenic. In addition, atrial myocytes exhibit a different Transverse tubules (T-tubules) structure compared to ventricular myocytes. T-tubules are an important sub-cellular network involved in SR Ca dynamics in ventricular myocytes (Wang et al., 2001; Brette and Orchard, 2003; Franzini-Armstrong et al., 2005; Ibrahim et al., 2010). T-tubules are located at the z-line of the myocyte and provide close coupling of L-type Ca channels to ryanodine receptors (RyRs) on the SR membrane. This structure allows rapid intracellular Ca triggered SR Ca release in response to electrical excitation (Franzini-Armstrong et al., 2005). Emerging evidence suggests that an atrial T-tubule network is present in large mammalian species including humans, sheep, dogs, cows, and horses (Dibb et al., 2009; Lenaerts et al., 2009; Wakili et al., 2010; Richards et al., 2011) although atrial T-tubular networks are less abundant and less organized compared to that in the

ventricles. While it was previously believed that atrial T-tubules were virtually absent in the small rodents,(Forbes et al., 1990; Berlin, 1995) a recent report by Frisk et al. (2014) showed similar structural organization and density of the T-tubules in pig and rat atria. A disorganized T-tubule network has been found to contribute to SR Ca release dysfunction in failing ventricular myocytes from both human and HF animal models (Balijepalli et al., 2003; Louch et al., 2006; Heinzel et al., 2008; Lyon et al., 2009). In rapid pacing-induced failing dog atria, reduced T-tubular abundance was also found to be linked to altered subcellular Ca dynamics and AF development (Yeh et al., 2008; Dibb et al., 2009; Lenaerts et al., 2009). While accumulating evidence suggests that atrial T-tubular structure is present in most mammalian species, further investigations are clearly needed to understand whether there is remodeling in the failing and aged heart and its functional role in atrial SR Ca handling and AF development.

It is known that the cardiac Ca current during the normal AP contributes to the AP plateau and is involved in myocyte contraction. The voltage-gated L-type Ca channels (I_{Ca}) are activated by membrane depolarization that leads to a small amount of inward Ca flux (I_{Ca}) (Rougier et al., 1969). Ca entry via Ca current (I_{Ca}) along with a much smaller amount of Ca influx via Na-Ca exchange (NCX) activates large quantities of Ca release from SR via ryanodine receptor channels (RyR; also called Ca triggered SR Ca release channels). This Ca triggered SR Ca release involves a transient increase in intracellular Ca $[Ca]_i$ that initiates myocyte contraction as free Ca binds to the myofilaments (Bers, 2000). During the relaxation phase of the cells, intracellular free Ca ions will be removed from cytosol via: (1) pumping back to SR via a Ca pump SERCA2 (SR Ca-ATPase); (2) expulsion from the cell by NCXs; and (3) uptake by mitochondria via mitochondrial Ca uniporters (Bers, 2000).

Compared to ventricular myocytes, atrial myocytes have smaller Ca transient amplitude and a higher rate of intracellular Ca decay. This is due to an increased SERCA uptake and enhanced function of NCX to remove cytosolic Ca during the diastolic phase (Walden et al., 2009). The increased SERCA-dependent intracellular Ca removal is attributed to the greater amount of SERCA2 and less expression of SERCA inhibitory protein phospholamban (PLB) (Freestone et al., 2000; Walden et al., 2009). Another important feature of atrial myocytes is that atrial SR Ca content is greater than that of ventricular myocytes (Walden et al., 2009). With the greater atrial SR Ca content, atrial myocytes are prone to spontaneous diastolic SR Ca release when RyR channels are sensitized under pathological conditions (Venetucci et al., 2008; Bers, 2014).

We and others have previously discovered that increased diastolic SR Ca release causes abnormal ectopic activities, which lead to ventricular arrhythmogenesis in the failing heart (Ai et al., 2005; Yeh et al., 2008; Respress et al., 2012). During the diastolic phase, SR Ca release normally shuts off almost completely (∼99%). However, increased diastolic RyR Ca release could be responsible for increased diastolic SR Ca leak and reduced systolic $[Ca]_{FR}$ for a given L-type voltage-gated Ca current (I_{ca}) as the release trigger (Bassani et al., 1995; Shannon et al., 2000; Bers, 2014). The increased diastolic SR Ca leakage along with an impaired function of Ca uptake due to altered SERCA2 elevates the amount of $[Ca]_i$ and prolongs the $[Ca]_i$ decay phase in HF (Bers, 2000, 2014). Then, increased Na influx via NCX for $[Ca]_i$ removal can produce abnormal triggered activities (e.g., DADs) and initiate atrial arrhythmias (Bers, 2000, 2014). Studies suggest that alterations of Ca handling proteins including RyR2, PLB, and Cav1.2 contribute to changed intracellular Ca transients and diastolic SR Ca release (Schulman et al., 1992; DeSantiago et al., 2002; Wu et al., 1999). Others and we have previously demonstrated that activated CaMKII, a pro-arrhythmic signaling molecule, is critically involved in phosphorylation of RyR2-2815 and PLB-Thr17 (RyR2815-P, PLB17-P), which results in sensitized RyR channels that in turn leads to triggered activities and arrhythmia initiation due to diastolic SR Ca leak in pathologically altered ventricles (Hoch et al., 1999; Maier et al., 2003; Zhang et al., 2003; Ai et al., 2005; Yeh et al., 2008; Greiser et al., 2009; Sossalla et al., 2010; Respress et al., 2012). Recent studies indicate that alterations of CaMKII-dependent RyR phosphorylation are also exhibited in the atrium of chronic AF patients (Chelu et al., 2009; Neef et al., 2010). Results from several animal models have shown that these altered SR Ca handling proteins contribute to enhanced SR Ca leak and AF development (Chelu et al., 2009; Chiang et al., 2014). Although alteration of I_{Ca} could also contribute to abnormal SR Ca release, studies indicate that reduced I_{Ca} is a hallmark of AF induced electrical remodeling (Van Wagoner et al., 1999; Christ et al., 2004). CaMKII inhibition has been shown to improve the function of L-type Ca channel in mouse ventricular myocytes and cultured HL-1 atrial myocytes, which could be due to up-regulated expression of L-type Ca channel proteins (Zhang et al., 2005; Ronkainen et al., 2011). These results indicate that abnormal diastolic RyR Ca release could be the major cause of abnormal Ca handling in HF and chronic AF (Ai et al., 2005; Yeh et al., 2008 and Respress et al., 2012). However, other studies have reported inconsistent results of increased, reduced, or unchanged I_{ca} preceding the onset of AF in postoperative patients compared to that of patients at low risk for AF (Van Wagoner et al., 1999; Christ et al., 2004; Dinanian et al., 2008; Workman et al., 2009). Thus, the underlying mechanisms of abnormal Ca handling in AF onset and maintenance in the pathologically altered heart require further investigation.

In addition to altered phosphorylation of Ca handling proteins regulated by kinases, some protein phosphatases (PP1, PP2A) have also been found to play roles in regulating the phosphorylation state of channel proteins in failing ventricular myocytes (Ai et al., 2005, 2011; Ai and Pogwizd, 2005). However, contradictory results of the expression and activity of protein phosphatases have been reported in humans and animal models with chronic AF or paroxysmal AF (Christ et al., 2004; Chelu et al., 2009; Heijman et al., 2013; Voigt et al., 2014). It is clear that the functional role of protein phosphatases in atrial Ca handling and AF genesis need to be further explored.

STRESS SIGNALING PATHWAYS IN ABNORMAL SR Ca HANDLING AND AF DEVELOPMENT IN THE FAILING OR AGED HEART

It has been shown that failing and aged hearts exhibit increased intrinsic stress and higher susceptibility to extrinsic stress stimuli (Belmin et al., 1995; Beckman and Ames, 1998; Juhaszova et al.,

2005; Li et al., 2005a; Yang et al., 2005; Judge and Leeuwenburgh, 2007; Neuman et al., 2007; He et al., 2011; Ismahil et al., 2014). JNK, a family member of the MAPKs, was discovered by Davis in the early of 90s (Davis, 2000). And then JNK was found to be activated in response to stress challenges to regulate cell proliferation, differentiation, apoptosis, cell survival, cell mobility and cytokine production (Davis, 2000; Bogoyevitch and Kobe, 2006; Raman et al., 2007). It is known that the JNK signaling pathway is critical in the development of cancer, diabetes, and cardiovascular diseases (CVD; e.g., HF, myocardial infarction, atherosclerosis) (Davis, 2000; Karin and Gallagher, 2005; Rose et al., 2010). Emerging evidence suggests that enhanced JNK activation is also linked to significantly elevated intrinsic stress (e.g., oxidative stress or inflammatory stress) (Liu et al., 2014; Sun et al., 2014). Studies have shown that rapid transient JNK activation appears in cultured myocytes and animals that are subjected to exercise or severe pressure overload, Boluyt et al. (2003), Nadruz et al. (2004, 2005) and Pan et al. (2005) while 24 h mechanically stretched myocytes or exercise trained animals showed reduced or unchanged JNK activity (Boluyt et al., 2003; Miyamoto et al., 2004; Roussel et al., 2008). These results indicate that JNK activation could be a dynamic response to the stress stimuli. Our laboratory recently discovered and reported for the first time (Yan et al., 2013) that activated JNK plays an important role in reduced gap junction channels and slowed conduction (**Figure 2**) that is associated with markedly increased pacing-induced AF *in vivo* in aged rabbits. Young rabbits subjected to a JNK activator (anisomycin) (Hazzalin et al., 1998; Petrich et al., 2004) challenge *in vivo* also exhibited dramatically increased incidence and duration of pacing-induced AT/AF, which is comparable to that found in aged hearts (**Figure 1**). While a significantly increased propensity for AF in aged humans has been well-recorganized, Benjamin et al. (1994), Go et al. (2001) and Rich (2009) our recent observations (Wu et al., 2014) suggest an increase in activated JNK in aging human atrium from healthy donor hearts (which were rejected for heart transplant due to technical reasons). Moreover, we demonstrated that JNK-induced gap junction remodeling impairs atrial conduction and causes formation of reentrant circuits in cultured atrial myocytes (**Figures 2C,D**) (Yan et al., 2013). However, previous studies suggest that gap junction remodeling is most likely to contribute to stabilization and maintenance of AF (Elvan et al., 1997; van der

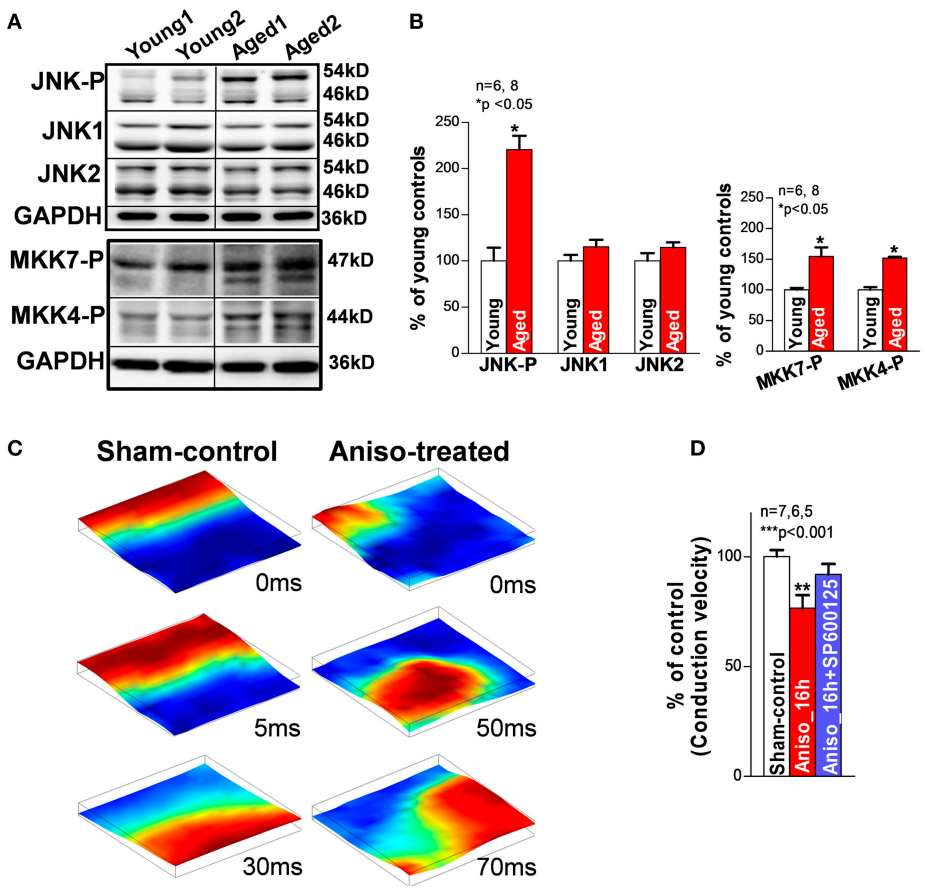

FIGURE 2 | (A,B) Immunoblotting images and summarized data of phosphorylated JNK (JNK-P), JNK1, JNK2, and phosphorylated MKK7 and MKK4 (MKK7-P, MKK4-P) in young and aged rabbit LA. **(C)** Representative sequential images of uniformly propagated action potentials (CL = 200 ms) in sham-control HL-1 monolayers and broken and reentrant AP wave in an anisomycin-treated (24 h) monolayer. **(D)** Summarized data of conduction velocity between the three groups (**$p < 0.01$ vs. sham-control). This figure is modified from Yan et al. (2013).

Velden et al., 1998, 2000; Dupont et al., 2001; Polontchouk et al., 2001; Kostin et al., 2002; Nao et al., 2003; Kanagaratnam et al., 2004; Sakabe et al., 2004; Wetzel et al., 2005; Nattel et al., 2008). Therefore, other mechanisms such as SR Ca handling dysfunction could be responsible for the initiation of atrial arrhythmias in aged hearts. To date, the role of JNK in SR Ca handling and AF development in the failing and aged heart remains unknown. Our recent results suggest that activated JNK plays an important role in SR Ca leak and AF development in aged animals as well as young animals with manipulated JNK activity. A computer simulation study (Xie et al., 2010) suggested that generating an ectopic beat in heart tissue with poorly coupled neighboring myocytes (slowed AP conduction) requires much fewer EAD or DAD-producing myocytes than in normal tissue composed of well-coupled cells. In another words, impaired intercellular coupling could make cardiac tissue more vulnerable for generating ectopic triggers that may initiate arrhythmias. Therefore, JNK-induced slowed conduction in the aged atria may create a favorable environment for JNK-induced abnormal Ca activities to form ectopic beats and even to initiate AF. Many questions regarding the underlying mechanisms of JNK-induced AF genesis remain unanswered. Further investigations are clearly needed in this important research area.

ERKs and p38 MAPKs are the other two important stress-response signaling pathways in cellular biology (Ramos, 2008; Rose et al., 2010). At the cellular level, the two stress signaling pathways modulate cell proliferation and differentiation, cytokinesis, transcription, cell death, and cell adhesion. Like JNK, both ERK and p38 are involved in various pathologies such as cardiovascular diseases, diabetes, and cancers (Davis, 2000; Kyriakis and Avruch, 2001; Karin and Gallagher, 2005; Kyoi et al., 2006; Yoon and Seger, 2006; Rose et al., 2010). While enhanced activity of ERK or p38 alone may or may not be required or sufficient for facilitating cardiac hypertrophy, both ERK and p38 were found to be activated in HF and these activated stress kinases are involved in pathological remodeling and AF development in the failing heart (Zechner et al., 1997; Wang et al., 1998; Li et al., 2001, 2005b; Cardin et al., 2003; Nishida et al., 2004; Purcell et al., 2007). Studies suggest that hypertrophic stimuli lead to an increase in L-type Ca transients and down-regulation of SERCA2 expression via activated ERK (Takahashi et al., 2004; Hagiwara et al., 2007; Huang et al., 2014). Ras, a GTPase, is able to activate ERK through a Ras-Raf-MEK cascade (Avruch et al., 2001). Ras signaling activated ERK was found to contribute to down-regulation of L-type Ca channels and reduced channel activity along with reduced SERCA2 protein expression in cultured myocytes (Ho et al., 1998, 2001; Huang et al., 2014). It was also found that Ras-ERK-modulated molecular remodeling led to decreased intracellular Ca transients and impaired SR Ca uptake, which could lead to enhanced arrhythmogenicity (Zheng et al., 2004). Moreover, recent work reported by Scharf et al. (2013) suggests that p38 directly regulates SERCA2 mRNA and protein expression via transcription factors Egr-1 and SP1. Taken together, emerging evidence indicates that the stress-response MAP kinases signaling cascades could be involved in cardiac Ca handling and AF development (**Figure 3**). However, more work needs to be done to further understand the underlying molecular and electrophysiological mechanisms of altered stress signaling cascades and their crosstalking in AF development in the failing and aged heart.

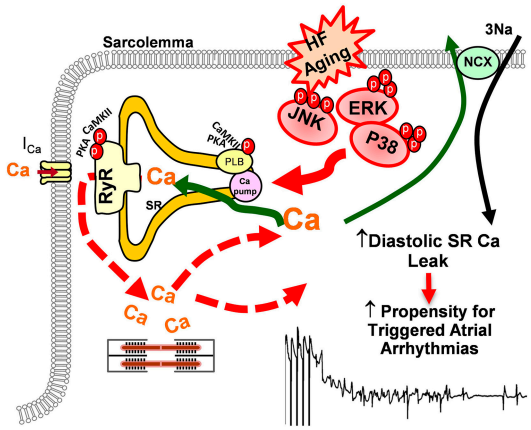

FIGURE 3 | Schematic outline of the potential impact of stress-response MAP kinases on sarcolemma reticulum (SR) Ca handling that may increase AF propensity in failing and/or aged atria.

CONCLUSION

Accumulating evidence suggests that abnormal SR Ca handling is associated with the initiation and development of AF. However, much work still needs to be done to further uncover the underlying molecular and electrophysiological mechanisms of AF initiation and maintenance in diseased and aged hearts. To date, most of the mechanistic studies of SR Ca dynamics have been performed in isolated myocytes. However, isolated myocytes provide limited information regarding the spatial complexity of SR Ca kinetics in the 3-dimensional myocardial structure, which is completely disrupted by the enzymatic dissociation procedure of cell isolation. Thus, measuring Ca dynamics in intact atria using high-resolution Ca imaging should be considered in future studies to obtain important information about the relationship of SR Ca handling and APs, as well as their role in arrhythmogenesis. At present, emerging evidence indicates a link between altered stress signaling cascades and abnormal Ca handling in pathologically altered atrium. Further understanding of the underlying mechanisms of stress-induced AF development in the failing and/or aged heart could reveal potential effective therapeutic strategies for AF prevention and treatment.

ACKNOWLEDGMENT

This research was supported by American Heart Association (10GRNT3770030 & 12GRNT12050478 to XA) and National Institutes of Health (HL113640 to XA).

REFERENCES

Ai, X., and Pogwizd, S. M. (2005). Connexin 43 downregulation and dephosphorylation in nonischemic heart failure is associated with enhanced colocalized protein phosphatase type 2a. *Circ. Res.* 96, 54–63. doi: 10.1161/01.RES.0000152325.07495.5a

Ai, X., Curran, J. W., Shannon, T. R., Bers, D. M., and Pogwizd, S. M. (2005). Ca2+/calmodulin-dependent protein kinase modulates cardiac ryanodine

receptor phosphorylation and sarcoplasmic reticulum ca2+ leak in heart failure. *Circ. Res.* 97, 1314–1322. doi: 10.1161/01.RES.0000194329.41863.89

Ai, X., Jiang, A., Ke, Y., Solaro, R. J., and Pogwizd, S. M. (2011). Enhanced activation of p21-activated kinase 1 in heart failure contributes to dephosphorylation of connexin 43. *Cardiovasc. Res.* 92, 106–114. doi: 10.1093/cvr/cvr163

Allessie, M. A., Bonke, F. I., and Schopman, F. J. (1976). Circus movement in rabbit atrial muscle as a mechanism of tachycardia. Ii. The role of nonuniform recovery of excitability in the occurrence of unidirectional block, as studied with multiple microelectrodes. *Circ. Res.* 39, 168–177. doi: 10.1161/01.RES.39.2.168

Anyukhovsky, E. P., Sosunov, E. A., Chandra, P., Rosen, T. S., Boyden, P. A., Danilo, P. Jr., et al. (2005). Age-associated changes in electrophysiologic remodeling: a potential contributor to initiation of atrial fibrillation. *Cardiovasc. Res.* 66, 353–363. doi: 10.1016/j.cardiores.2004.10.033

Avruch, J., Khokhlatchev, A., Kyriakis, J. M., Luo, Z., Tzivion, G., Vavvas, D., et al. (2001). Ras activation of the raf kinase: tyrosine kinase recruitment of the map kinase cascade. *Recent Prog. Horm. Res.* 56, 127–155. doi: 10.1210/rp.56.1.127

Balijepalli, R. C., Lokuta, A. J., Maertz, N. A., Buck, J. M., Haworth, R. A., Valdivia, H. H., et al. (2003). Depletion of t-tubules and specific subcellular changes in sarcolemmal proteins in tachycardia-induced heart failure. *Cardiovasc. Res.* 59, 67–77. doi: 10.1016/S0008-6363(03)00325-0

Bassani, J. W., Yuan, W., and Bers, D. M. (1995). Fractional sr ca release is regulated by trigger ca and sr ca content in cardiac myocytes. *Am. J. Physiol.* 268, C1313–C1319.

Beckman, K. B., and Ames, B. N. (1998). The free radical theory of aging matures. *Physiol. Rev.* 78, 547–581.

Belmin, J., Bernard, C., Corman, B., Merval, R., Esposito, B., and Tedgui, A. (1995). Increased production of tumor necrosis factor and interleukin-6 by arterial wall of aged rats. *Am. J. Physiol.* 268, H2288–H2293.

Benjamin, E. J., Levy, D., Vaziri, S. M., D'Agostino, R. B., Belanger, A. J., and Wolf, P. A. (1994). Independent risk factors for atrial fibrillation in a population-based cohort. The framingham heart study. *JAMA* 271, 840–844.

Berlin, J. R. (1995). Spatiotemporal changes of ca2+ during electrically evoked contractions in atrial and ventricular cells. *Am. J. Physiol.* 269, H1165–H1170.

Bers, D. M. (2000). Calcium fluxes involved in control of cardiac myocyte contraction. *Circ. Res.* 87, 275–281. doi: 10.1161/01.RES.87.4.275

Bers, D. M. (2014). Cardiac sarcoplasmic reticulum calcium leak: basis and roles in cardiac dysfunction. *Annu. Rev. Physiol.* 76, 107–127. doi: 10.1146/annurev-physiol-020911-153308

Bogoyevitch, M. A., and Kobe, B. (2006). Uses for jnk: the many and varied substrates of the c-jun n-terminal kinases. *Microbiol. Mol. Biol. Rev.* 70, 1061–1095. doi: 10.1128/MMBR.00025-06

Boluyt, M. O., Loyd, A. M., Roth, M. H., Randall, M. J., and Song, E. Y. (2003). Activation of jnk in rat heart by exercise: effect of training. *Am. J. Physiol. Heart Circ. Physiol.* 285, H2639–H2647. doi: 10.1152/ajpheart.00596.2003

Brette, F., and Orchard, C. (2003). T-tubule function in mammalian cardiac myocytes. *Circ. Res.* 92, 1182–1192. doi: 10.1161/01.RES.0000074908.17214.FD

Burashnikov, A., and Antzelevitch, C. (2003). Reinduction of atrial fibrillation immediately after termination of the arrhythmia is mediated by late phase 3 early afterdepolarization-induced triggered activity. *Circulation* 107, 2355–2360. doi: 10.1161/01.CIR.0000065578.00869.7C

Cardin, S., Li, D., Thorin-Trescases, N., Leung, T. K., Thorin, E., and Nattel, S. (2003). Evolution of the atrial fibrillation substrate in experimental congestive heart failure: angiotensin-dependent and -independent pathways. *Cardiovasc. Res.* 60, 315–325. doi: 10.1016/j.cardiores.2003.08.014

Chelu, M. G., Sarma, S., Sood, S., Wang, S., van Oort, R. J., Skapura, D. G., et al. (2009). Calmodulin kinase ii-mediated sarcoplasmic reticulum ca2+ leak promotes atrial fibrillation in mice. *J. Clin. Invest.* 119, 1940–1951. doi: 10.1172/JCI37059

Chiang, D. Y., Kongchan, N., Beavers, D. L., Alsina, K. M., Voigt, N., Neilson, J. R., et al. (2014). Loss of microrna-106b-25 cluster promotes atrial fibrillation by enhancing ryanodine receptor type-2 expression and calcium release. *Circ. Arrhythm. Electrophysiol.* 7, 1214–1222. doi: 10.1161/CIRCEP.114.001973

Christ, T., Boknik, P., Wohrl, S., Wettwer, E., Graf, E. M., Bosch, R. F., et al. (2004). L-type ca2+ current downregulation in chronic human atrial fibrillation is associated with increased activity of protein phosphatases. *Circulation* 110, 2651–2657. doi: 10.1161/01.CIR.0000145659.80212.6A

Cowie, M. R., Mosterd, A., Wood, D. A., Deckers, J. W., Poole-Wilson, P. A., Sutton, G. C., et al. (1997). The epidemiology of heart failure. *Eur. Heart J.* 18, 208–225. doi: 10.1093/oxfordjournals.eurheartj.a015223

Davis, R. J. (2000). Signal transduction by the jnk group of map kinases. *Cell* 103, 239–252. doi: 10.1016/S0092-8674(00)00116-1

DeSantiago, J., Maier, L. S., and Bers, D. M. (2002). Frequency-dependent acceleration of relaxation in the heart depends on camkii, but not phospholamban. *J. Mol. Cell. Cardiol.* 34, 975–984. doi: 10.1006/jmcc.2002.2034

Di Lenarda, A., Scherillo, M., Maggioni, A. P., Acquarone, N., Ambrosio, G. B., Annicchiarico, M., et al. (2003). Current presentation and management of heart failure in cardiology and internal medicine hospital units: a tale of two worlds–the temistocle study. *Am. Heart J.* 146, E12. doi: 10.1016/S0002-8703(03)00315-6

Dibb, K. M., Clarke, J. D., Horn, M. A., Richards, M. A., Graham, H. K., Eisner, D. A., et al. (2009). Characterization of an extensive transverse tubular network in sheep atrial myocytes and its depletion in heart failure. *Circ. Heart Fail.* 2, 482–489. doi: 10.1161/CIRCHEARTFAILURE.109.852228

Dinanian, S., Boixel, C., Juin, C., Hulot, J. S., Coulombe, A., Rucker-Martin, C., et al. (2008). Downregulation of the calcium current in human right atrial myocytes from patients in sinus rhythm but with a high risk of atrial fibrillation. *Eur. Heart J.* 29, 1190–1197. doi: 10.1093/eurheartj/ehn140

Dupont, E., Ko, Y., Rothery, S., Coppen, S. R., Baghai, M., Haw, M., et al. (2001). The gap-junctional protein connexin40 is elevated in patients susceptible to postoperative atrial fibrillation. *Circulation* 103, 842–849. doi: 10.1161/01.CIR.103.6.842

Ehrlich, J. R., Nattel, S., and Hohnloser, S. H. (2002). Atrial fibrillation and congestive heart failure: specific considerations at the intersection of two common and important cardiac disease sets. *J. Cardiovasc. Electrophysiol.* 13, 399–405. doi: 10.1046/j.1540-8167.2002.00399.x

Elvan, A., Huang, X. D., Pressler, M. L., and Zipes, D. P. (1997). Radiofrequency catheter ablation of the atria eliminates pacing-induced sustained atrial fibrillation and reduces connexin 43 in dogs. *Circulation* 96, 1675–1685. doi: 10.1161/01.CIR.96.5.1675

Forbes, M. S., Van Niel, E. E., and Purdy-Ramos, S. I. (1990). The atrial myocardial cells of mouse heart: a structural and stereological study. *J. Struct. Biol.* 103, 266–279. doi: 10.1016/1047-8477(90)90045-E

Franzini-Armstrong, C., Protasi, F., and Tijskens, P. (2005). The assembly of calcium release units in cardiac muscle. *Ann. N. Y. Acad. Sci.* 1047, 76–85. doi: 10.1196/annals.1341.007

Freestone, N. S., Ribaric, S., Scheuermann, M., Mauser, U., Paul, M., and Vetter, R. (2000). Differential lusitropic responsiveness to beta-adrenergic stimulation in rat atrial and ventricular cardiac myocytes. *Pflugers Arch.* 441, 78–87. doi: 10.1007/s004240000397

Frisk, M., Koivumaki, J. T., Norseng, P. A., Maleckar, M. M., Sejersted, O. M., and Louch, W. E. (2014). Variable t-tubule organization and ca2+ homeostasis across the atria. *Am. J. Physiol. Heart Circ. Physiol.* 307, H609–H620. doi: 10.1152/ajpheart.00295.2014

Go, A. S., Hylek, E. M., Phillips, K. A., Chang, Y., Henault, L. E., Selby, J. V., et al. (2001). Prevalence of diagnosed atrial fibrillation in adults: national implications for rhythm management and stroke prevention: the anticoagulation and risk factors in atrial fibrillation (atria) study. *JAMA* 285, 2370–2375. doi: 10.1001/jama.285.18.2370

Greiser, M., Neuberger, H. R., Harks, E., El-Armouche, A., Boknik, P., de Haan, S., et al. (2009). Distinct contractile and molecular differences between two goat models of atrial dysfunction: AV block-induced atrial dilatation and atrial fibrillation. *J. Mol. Cell. Cardiol.* 46, 385–394. doi: 10.1016/j.yjmcc.2008.11.012

Hagiwara, Y., Miyoshi, S., Fukuda, K., Nishiyama, N., Ikegami, Y., Tanimoto, K., et al. (2007). Shp2-mediated signaling cascade through gp130 is essential for lif-dependent i cal, [ca2+]i transient, and apd increase in cardiomyocytes. *J. Mol. Cell. Cardiol.* 43, 710–716. doi: 10.1016/j.yjmcc.2007.09.004

Hazzalin, C. A., Le Panse, R., Cano, E., and Mahadevan, L. C. (1998). Anisomycin selectively desensitizes signalling components involved in stress kinase activation and fos and jun induction. *Mol. Cell. Biol.* 18, 1844–1854.

He, B. J., Joiner, M. L., Singh, M. V., Luczak, E. D., Swaminathan, P. D., Koval, O. M., et al. (2011). Oxidation of camkii determines the cardiotoxic effects of aldosterone. *Nat. Med.* 17, 1610–1618. doi: 10.1038/nm.2506

Heijman, J., Dewenter, M., El-Armouche, A., and Dobrev, D. (2013). Function and regulation of serine/threonine phosphatases in the healthy and diseased heart. *J. Mol. Cell. Cardiol.* 64, 90–98. doi: 10.1016/j.yjmcc.2013.09.006

Heinzel, F. R., Bito, V., Biesmans, L., Wu, M., Detre, E., von Wegner, F., et al. (2008). Remodeling of t-tubules and reduced synchrony of ca2+ release in

myocytes from chronically ischemic myocardium. *Circ. Res.* 102, 338–346. doi: 10.1161/CIRCRESAHA.107.160085

Hershberger, R. E., Nauman, D., Walker, T. L., Dutton, D., and Burgess, D. (2003). Care processes and clinical outcomes of continuous outpatient support with inotropes (cosi) in patients with refractory endstage heart failure. *J. Card. Fail.* 9, 180–187. doi: 10.1054/jcaf.2003.24

Ho, P. D., Fan, J. S., Hayes, N. L., Saada, N., Palade, P. T., Glembotski, C. C., et al. (2001). Ras reduces l-type calcium channel current in cardiac myocytes. Corrective effects of l-channels and serca2 on [ca(2+)](i) regulation and cell morphology. *Circ. Res.* 88, 63–69. doi: 10.1161/01.RES.88.1.63

Ho, P. D., Zechner, D. K., He, H., Dillmann, W. H., Glembotski, C. C., and McDonough, P. M. (1998). The raf-mek-erk cascade represents a common pathway for alteration of intracellular calcium by ras and protein kinase c in cardiac myocytes. *J. Biol. Chem.* 273, 21730–21735. doi: 10.1074/jbc.273.34.21730

Hoch, B., Meyer, R., Hetzer, R., Krause, E. G., and Karczewski, P. (1999). Identification and expression of delta-isoforms of the multifunctional ca2+/calmodulin-dependent protein kinase in failing and nonfailing human myocardium. *Circ. Res.* 84, 713–721. doi: 10.1161/01.RES.84.6.713

Huang, C., Ding, W., Li, L., and Zhao, D. (2006). Differences in the aging-associated trends of the monophasic action potential duration and effective refractory period of the right and left atria of the rat. *Circ. J.* 70, 352–357. doi: 10.1253/circj.70.352

Huang, H., Joseph, L. C., Gurin, M. I., Thorp, E. B., and Morrow, J. P. (2014). Extracellular signal-regulated kinase activation during cardiac hypertrophy reduces sarcoplasmic/endoplasmic reticulum calcium atpase 2 (serca2) transcription. *J. Mol. Cell. Cardiol.* 75, 58–63. doi: 10.1016/j.yjmcc.2014.06.018

Huang, J. L., Tai, C. T., Chen, J. T., Ting, C. T., Chen, Y. T., Chang, M. S., et al. (2003). Effect of atrial dilatation on electrophysiologic properties and inducibility of atrial fibrillation. *Basic Res. Cardiol.* 98, 16–24. doi: 10.1007/s00395-003-0385-z

Ibrahim, M., Al Masri, A., Navaratnarajah, M., Siedlecka, U., Soppa, G. K., Moshkov, A., et al. (2010). Prolonged mechanical unloading affects cardiomyocyte excitation-contraction coupling, transverse-tubule structure, and the cell surface. *FASEB J.* 24, 3321–3329. doi: 10.1096/fj.10-156638

Ismahil, M. A., Hamid, T., Bansal, S. S., Patel, B., Kingery, J. R., and Prabhu, S. D. (2014). Remodeling of the mononuclear phagocyte network underlies chronic inflammation and disease progression in heart failure: critical importance of the cardiosplenic axis. *Circ. Res.* 114, 266–282. doi: 10.1161/CIRCRESAHA.113.301720

Judge, S., and Leeuwenburgh, C. (2007). Cardiac mitochondrial bioenergetics, oxidative stress, and aging. *Am. J. Physiol. Cell Physiol.* 292, C1983–C1992. doi: 10.1152/ajpcell.00285.2006

Juhaszova, M., Rabuel, C., Zorov, D. B., Lakatta, E. G., and Sollott, S. J. (2005). Protection in the aged heart: preventing the heart-break of old age? *Cardiovasc. Res.* 66, 233–244. doi: 10.1016/j.cardiores.2004.12.020

Kanagaratnam, P., Cherian, A., Stanbridge, R. D., Glenville, B., Severs, N. J., and Peters, N. S. (2004). Relationship between connexins and atrial activation during human atrial fibrillation. *J. Cardiovasc. Electrophysiol.* 15, 206–216. doi: 10.1046/j.1540-8167.2004.03280.x

Kanagaratnam, P., Kojodjojo, P., and Peters, N. S. (2008). Electrophysiological abnormalities occur prior to the development of clinical episodes of atrial fibrillation: observations from human epicardial mapping. *Pacing Clin. Electrophysiol.* 31, 443–453. doi: 10.1111/j.1540-8159.2008.01014.x

Kannel, W. B., Wolf, P. A., Benjamin, E. J., and Levy, D. (1998). Prevalence, incidence, prognosis, and predisposing conditions for atrial fibrillation: population-based estimates. *Am. J. Cardiol.* 82, 2N–9N. doi: 10.1016/S0002-9149(98)00583-9

Karin, M., and Gallagher, E. (2005). From jnk to pay dirt: jun kinases, their biochemistry, physiology and clinical importance. *IUBMB Life* 57, 283–295. doi: 10.1080/15216540500097111

Kostin, S., Klein, G., Szalay, Z., Hein, S., Bauer, E. P., and Schaper, J. (2002). Structural correlate of atrial fibrillation in human patients. *Cardiovasc. Res.* 54, 361–379. doi: 10.1016/S0008-6363(02)00273-0

Kyoi, S., Otani, H., Matsuhisa, S., Akita, Y., Tatsumi, K., Enoki, C., et al. (2006). Opposing effect of p38 map kinase and jnk inhibitors on the development of heart failure in the cardiomyopathic hamster. *Cardiovasc. Res.* 69, 888–898. doi: 10.1016/j.cardiores.2005.11.015

Kyriakis, J. M., and Avruch, J. (2001). Mammalian mitogen-activated protein kinase signal transduction pathways activated by stress and inflammation. *Physiol. Rev.* 81, 807–869.

Lenaerts, I., Bito, V., Heinzel, F. R., Driesen, R. B., Holemans, P., D'Hooge, J., et al. (2009). Ultrastructural and functional remodeling of the coupling between ca2+ influx and sarcoplasmic reticulum ca2+ release in right atrial myocytes from experimental persistent atrial fibrillation. *Circ. Res.* 105, 876–885. doi: 10.1161/CIRCRESAHA.109.206276

Li, D., Shinagawa, K., Pang, L., Leung, T. K., Cardin, S., Wang, Z., et al. (2001). Effects of angiotensin-converting enzyme inhibition on the development of the atrial fibrillation substrate in dogs with ventricular tachypacing-induced congestive heart failure. *Circulation* 104, 2608–2614. doi: 10.1161/hc4601.099402

Li, M., Georgakopoulos, D., Lu, G., Hester, L., Kass, D. A., Hasday, J., et al. (2005b). P38 map kinase mediates inflammatory cytokine induction in cardiomyocytes and extracellular matrix remodeling in heart. *Circulation* 111, 2494–2502. doi: 10.1161/01.CIR.0000165117.71483.0C

Li, S. Y., Du, M., Dolence, E. K., Fang, C. X., Mayer, G. E., Ceylan-Isik, A. F., et al. (2005a). Aging induces cardiac diastolic dysfunction, oxidative stress, accumulation of advanced glycation endproducts and protein modification. *Aging Cell* 4, 57–64. doi: 10.1111/j.1474-9728.2005.00146.x

Linne, A. B., Liedholm, H., Jendteg, S., and Israelsson, B. (2000). Health care costs of heart failure: results from a randomised study of patient education. *Eur. J. Heart Fail.* 2, 291–297. doi: 10.1016/S1388-9842(00)00089-1

Liu, Y., Wang, J., Qi, S. Y., Ru, L. S., Ding, C., Wang, H. J., et al. (2014). Reduced endoplasmic reticulum stress might alter the course of heart failure via caspase-12 and jnk pathways. *Can. J. Cardiol.* 30, 368–375. doi: 10.1016/j.cjca.2013.11.001

Louch, W. E., Mork, H. K., Sexton, J., Stromme, T. A., Laake, P., Sjaastad, I., et al. (2006). T-tubule disorganization and reduced synchrony of ca2+ release in murine cardiomyocytes following myocardial infarction. *J. Physiol.* 574, 519–533. doi: 10.1113/jphysiol.2006.107227

Lyon, A. R., MacLeod, K. T., Zhang, Y., Garcia, E., Kanda, G. K., Lab, M. J., et al. (2009). Loss of t-tubules and other changes to surface topography in ventricular myocytes from failing human and rat heart. *Proc. Natl. Acad. Sci. U.S.A.* 106, 6854–6859. doi: 10.1073/pnas.0809777106

Maier, L. S., Zhang, T., Chen, L., DeSantiago, J., Brown, J. H., and Bers, D. M. (2003). Transgenic camkiideltac overexpression uniquely alters cardiac myocyte ca2+ handling: reduced sr ca2+ load and activated sr ca2+ release. *Circ. Res.* 92, 904–911. doi: 10.1161/01.RES.0000069685.20258.F1

Mandapati, R., Skanes, A., Chen, J., Berenfeld, O., and Jalife, J. (2000). Stable microreentrant sources as a mechanism of atrial fibrillation in the isolated sheep heart. *Circulation* 101, 194–199. doi: 10.1161/01.CIR.101.2.194

Markides, V., and Peters, N. S. (2002). Mechanisms underlying the development of atrial arrhythmias in heart failure. *Heart Fail. Rev.* 7, 243–253. doi: 10.1023/A:1020077206796

Marx, S. O., Reiken, S., Hisamatsu, Y., Jayaraman, T., Burkhoff, D., Rosemblit, N., et al. (2000). Pka phosphorylation dissociates fkbp12.6 from the calcium release channel (ryanodine receptor): defective regulation in failing hearts. *Cell* 101, 365–376. doi: 10.1016/S0092-8674(00)80847-8

Miyamoto, T., Takeishi, Y., Takahashi, H., Shishido, T., Arimoto, T., Tomoike, H., et al. (2004). Activation of distinct signal transduction pathways in hypertrophied hearts by pressure and volume overload. *Basic Res. Cardiol.* 99, 328–337. doi: 10.1007/s00395-004-0482-7

Miyasaka, Y., Barnes, M. E., Gersh, B. J., Cha, S. S., Bailey, K. R., Abhayaratna, W. P., et al. (2006). Secular trends in incidence of atrial fibrillation in olmsted county, minnesota, 1980 to 2000, and implications on the projections for future prevalence. *Circulation* 114, 119–125. doi: 10.1161/CIRCULATIONAHA.105.595140

Nadruz, W. Jr., Corat, M. A., Marin, T. M., Guimaraes Pereira, G. A., and Franchini, K. G. (2005). Focal adhesion kinase mediates mef2 and c-jun activation by stretch: role in the activation of the cardiac hypertrophic genetic program. *Cardiovasc. Res.* 68, 87–97. doi: 10.1016/j.cardiores.2005.05.011

Nadruz, W. Jr., Kobarg, C. B., Kobarg, J., and Franchini, K. G. (2004). C-jun is regulated by combination of enhanced expression and phosphorylation in acute-overloaded rat heart. *Am. J. Physiol. Heart Circ. Physiol.* 286, H760–H767. doi: 10.1152/ajpheart.00430.2003

Nao, T., Ohkusa, T., Hisamatsu, Y., Inoue, N., Matsumoto, T., Yamada, J., et al. (2003). Comparison of expression of connexin in right atrial myocardium in patients with chronic atrial fibrillation versus those in sinus rhythm. *Am. J. Cardiol.* 91, 678–683. doi: 10.1016/S0002-9149(02)03403-3

Nattel, S., Burstein, B., and Dobrev, D. (2008). Atrial remodeling and atrial fibrillation: mechanisms and implications. *Circ. Arrhythm. Electrophysiol.* 1, 62–73. doi: 10.1161/CIRCEP.107.754564

Nattel, S., Maguy, A., Le Bouter, S., and Yeh, Y. H. (2007). Arrhythmogenic ion-channel remodeling in the heart: heart failure, myocardial infarction, and atrial fibrillation. *Physiol. Rev.* 87, 425–456. doi: 10.1152/physrev.00014.2006

Neef, S., Dybkova, N., Sossalla, S., Ort, K. R., Fluschnik, N., Neumann, K., et al. (2010). Camkii-dependent diastolic sr ca2+ leak and elevated diastolic ca2+ levels in right atrial myocardium of patients with atrial fibrillation. *Circ. Res.* 106, 1134–1144. doi: 10.1161/CIRCRESAHA.109.203836

Neuberger, H. R., Mewis, C., van Veldhuisen, D. J., Schotten, U., van Gelder, I. C., Allessie, M. A., et al. (2007). Management of atrial fibrillation in patients with heart failure. *Eur. Heart J.* 28, 2568–2577. doi: 10.1093/eurheartj/ehm341

Neuman, R. B., Bloom, H. L., Shukrullah, I., Darrow, L. A., Kleinbaum, D., Jones, D. P., et al. (2007). Oxidative stress markers are associated with persistent atrial fibrillation. *Clin. Chem.* 53, 1652–1657. doi: 10.1373/clinchem.2006.083923

Nishida, K., Yamaguchi, O., Hirotani, S., Hikoso, S., Higuchi, Y., Watanabe, T., et al. (2004). P38alpha mitogen-activated protein kinase plays a critical role in cardiomyocyte survival but not in cardiac hypertrophic growth in response to pressure overload. *Mol. Cell. Biol.* 24, 10611–10620. doi: 10.1128/MCB.24.24.10611-10620.2004

Oral, H., Ozaydin, M., Sticherling, C., Tada, H., Scharf, C., Chugh, A., et al. (2003). Effect of atrial fibrillation duration on probability of immediate recurrence after transthoracic cardioversion. *J. Cardiovasc. Electrophysiol.* 14, 182–185. doi: 10.1046/j.1540-8167.2003.02415.x

Pan, J., Singh, U. S., Takahashi, T., Oka, Y., Palm-Leis, A., Herbelin, B. S., et al. (2005). Pkc mediates cyclic stretch-induced cardiac hypertrophy through rho family gtpases and mitogen-activated protein kinases in cardiomyocytes. *J. Cell. Physiol.* 202, 536–553. doi: 10.1002/jcp.20151

Patterson, E., Po, S. S., Scherlag, B. J., and Lazzara, R. (2005). Triggered firing in pulmonary veins initiated by *in vitro* autonomic nerve stimulation. *Heart Rhythm* 2, 624–631. doi: 10.1016/j.hrthm.2005.02.012

Petrich, B. G., Eloff, B. C., Lerner, D. L., Kovacs, A., Saffitz, J. E., Rosenbaum, D. S., et al. (2004). Targeted activation of c-jun n-terminal kinase *in vivo* induces restrictive cardiomyopathy and conduction defects. *J. Biol. Chem.* 279, 15330–15338. doi: 10.1074/jbc.M314142200

Podrid, P. J. (1999). Atrial fibrillation in the elderly. *Cardiol. Clin.* 17, 173–188, ix-x. doi: 10.1016/S0733-8651(05)70063-1

Polontchouk, L., Haefliger, J. A., Ebelt, B., Schaefer, T., Stuhlmann, D., Mehlhorn, U., et al. (2001). Effects of chronic atrial fibrillation on gap junction distribution in human and rat atria. *J. Am. Coll. Cardiol.* 38, 883–891. doi: 10.1016/S0735-1097(01)01443-7

Psaty, B. M., Manolio, T. A., Kuller, L. H., Kronmal, R. A., Cushman, M., Fried, L. P., et al. (1997). Incidence of and risk factors for atrial fibrillation in older adults. *Circulation* 96, 2455–2461. doi: 10.1161/01.CIR.96.7.2455

Purcell, N. H., Wilkins, B. J., York, A., Saba-El-Leil, M. K., Meloche, S., Robbins, J., et al. (2007). Genetic inhibition of cardiac erk1/2 promotes stress-induced apoptosis and heart failure but has no effect on hypertrophy *in vivo*. *Proc. Natl. Acad. Sci. U.S.A.* 104, 14074–14079. doi: 10.1073/pnas.0610906104

Raman, M., Chen, W., and Cobb, M. H. (2007). Differential regulation and properties of mapks. *Oncogene* 26, 3100–3112. doi: 10.1038/sj.onc.1210392

Ramos, J. W. (2008). The regulation of extracellular signal-regulated kinase (erk) in mammalian cells. *Int. J. Biochem. Cell Biol.* 40, 2707–2719. doi: 10.1016/j.biocel.2008.04.009

Rensma, P. L., Allessie, M. A., Lammers, W. J., Bonke, F. I., and Schalij, M. J. (1988). Length of excitation wave and susceptibility to reentrant atrial arrhythmias in normal conscious dogs. *Circ. Res.* 62, 395–410. doi: 10.1161/01.RES.62.2.395

Respress, J. L., van Oort, R. J., Li, N., Rolim, N., Dixit, S. S., deAlmeida, A., et al. (2012). Role of ryr2 phosphorylation at s2814 during heart failure progression. *Circ. Res.* 110, 1474–1483. doi: 10.1161/CIRCRESAHA.112.268094

Rich, M. W. (2009). Epidemiology of atrial fibrillation. *J. Interv. Card. Electrophysiol.* 25, 3–8. doi: 10.1007/s10840-008-9337-8

Richards, M. A., Clarke, J. D., Saravanan, P., Voigt, N., Dobrev, D., Eisner, D. A., et al. (2011). Transverse tubules are a common feature in large mammalian atrial myocytes including human. *Am. J. Physiol. Heart Circ. Physiol.* 301, H1996–H2005. doi: 10.1152/ajpheart.00284.2011

Ronkainen, J. J., Hanninen, S. L., Korhonen, T., Koivumaki, J. T., Skoumal, R., Rautio, S., et al. (2011). Ca2+-calmodulin-dependent protein kinase ii represses cardiac transcription of the l-type calcium channel alpha(1c)-subunit gene (cacna1c) by dream translocation. *J. Physiol.* 589, 2669–2686. doi: 10.1113/jphysiol.2010.201400

Rose, B. A., Force, T., and Wang, Y. (2010). Mitogen-activated protein kinase signaling in the heart: angels versus demons in a heart-breaking tale. *Physiol. Rev.* 90, 1507–1546. doi: 10.1152/physrev.00054.2009

Rougier, O., Vassort, G., Garnier, D., Gargouil, Y. M., and Coraboeuf, E. (1969). Existence and role of a slow inward current during the frog atrial action potential. *Pflugers Arch.* 308, 91–110. doi: 10.1007/BF00587018

Roussel, E., Gaudreau, M., Plante, E., Drolet, M. C., Breault, C., Couet, J., et al. (2008). Early responses of the left ventricle to pressure overload in wistar rats. *Life Sci.* 82, 265–272. doi: 10.1016/j.lfs.2007.11.008

Sakabe, K., Fukuda, N., Nada, T., Shinohara, H., Tamura, Y., Wakatsuki, T., et al. (2003). Age-related changes in the electrophysiologic properties of the atrium in patients with no history of atrial fibrillation. *Jpn. Heart J.* 44, 385–393. doi: 10.1536/jhj.44.385

Sakabe, M., Fujiki, A., Nishida, K., Sugao, M., Nagasawa, H., Tsuneda, T., et al. (2004). Enalapril prevents perpetuation of atrial fibrillation by suppressing atrial fibrosis and over-expression of connexin43 in a canine model of atrial pacing-induced left ventricular dysfunction. *J. Cardiovasc. Pharmacol.* 43, 851–859. doi: 10.1097/00005344-200406000-00015

Sanders, P., Morton, J. B., Davidson, N. C., Spence, S. J., Vohra, J. K., Sparks, P. B., et al. (2003). Electrical remodeling of the atria in congestive heart failure: electrophysiological and electroanatomic mapping in humans. *Circulation* 108, 1461–1468. doi: 10.1161/01.CIR.0000090688.49283.67

Scharf, M., Neef, S., Freund, R., Geers-Knorr, C., Franz-Wachtel, M., Brandis, A., et al. (2013). Mitogen-activated protein kinase-activated protein kinases 2 and 3 regulate serca2a expression and fiber type composition to modulate skeletal muscle and cardiomyocyte function. *Mol. Cell. Biol.* 33, 2586–2602. doi: 10.1128/MCB.01692-12

Schulman, H., Hanson, P. I., and Meyer, T. (1992). Decoding calcium signals by multifunctional cam kinase. *Cell Calcium* 13, 401–411. doi: 10.1016/0143-4160(92)90053-U

Shannon, T. R., Ginsburg, K. S., and Bers, D. M. (2000). Potentiation of fractional sarcoplasmic reticulum calcium release by total and free intra-sarcoplasmic reticulum calcium concentration. *Biophys. J.* 78, 334–343. doi: 10.1016/S0006-3495(00)76596-9

Sossalla, S., Fluschnik, N., Schotola, H., Ort, K. R., Neef, S., Schulte, T., et al. (2010). Inhibition of elevated ca2+/calmodulin-dependent protein kinase ii improves contractility in human failing myocardium. *Circ. Res.* 107, 1150–1161. doi: 10.1161/CIRCRESAHA.110.220418

Sun, A., Zou, Y., Wang, P., Xu, D., Gong, H., Wang, S., et al. (2014). Mitochondrial aldehyde dehydrogenase 2 plays protective roles in heart failure after myocardial infarction via suppression of the cytosolic jnk/p53 pathway in mice. *J. Am. Heart Assoc.* 3:e000779. doi: 10.1161/JAHA.113.000779

Takahashi, E., Fukuda, K., Miyoshi, S., Murata, M., Kato, T., Ita, M., et al. (2004). Leukemia inhibitory factor activates cardiac l-type ca2+ channels via phosphorylation of serine 1829 in the rabbit cav1.2 subunit. *Circ. Res.* 94, 1242–1248. doi: 10.1161/01.RES.0000126405.38858.BC

Timmermans, C., Rodriguez, L. M., Smeets, J. L., and Wellens, H. J. (1998). Immediate reinitiation of atrial fibrillation following internal atrial defibrillation. *J. Cardiovasc. Electrophysiol.* 9, 122–128. doi: 10.1111/j.1540-8167.1998.tb00893.x

van der Velden, H. M., Ausma, J., Rook, M. B., Hellemons, A. J., van Veen, T. A., Allessie, M. A., et al. (2000). Gap junctional remodeling in relation to stabilization of atrial fibrillation in the goat. *Cardiovasc. Res.* 46, 476–486. doi: 10.1016/S0008-6363(00)00026-2

van der Velden, H. M., van Kempen, M. J., Wijffels, M. C., van Zijverden, M., Groenewegen, W. A., Allessie, M. A., et al. (1998). Altered pattern of connexin40 distribution in persistent atrial fibrillation in the goat. *J. Cardiovasc. Electrophysiol.* 9, 596–607. doi: 10.1111/j.1540-8167.1998.tb00940.x

Van Wagoner, D. R., Pond, A. L., Lamorgese, M., Rossie, S. S., McCarthy, P. M., and Nerbonne, J. M. (1999). Atrial l-type ca2+ currents and human atrial fibrillation. *Circ. Res.* 85, 428–436. doi: 10.1161/01.RES.85.5.428

Venetucci, L. A., Trafford, A. W., O'Neill, S. C., and Eisner, D. A. (2008). The sarcoplasmic reticulum and arrhythmogenic calcium release. *Cardiovasc. Res.* 77, 285–292. doi: 10.1093/cvr/cvm009

Voigt, N., Heijman, J., Wang, Q., Chiang, D. Y., Li, N., Karck, M., et al. (2014). Cellular and molecular mechanisms of atrial arrhythmogenesis in

patients with paroxysmal atrial fibrillation. *Circulation* 129, 145–156. doi: 10.1161/CIRCULATIONAHA.113.006641

Wakili, R., Yeh, Y. H., Yan Qi, X., Greiser, M., Chartier, D., Nishida, K., et al. (2010). Multiple potential molecular contributors to atrial hypocontractility caused by atrial tachycardia remodeling in dogs. *Circ. Arrhythm. Electrophysiol.* 3, 530–541. doi: 10.1161/CIRCEP.109.933036

Walden, A. P., Dibb, K. M., and Trafford, A. W. (2009). Differences in intracellular calcium homeostasis between atrial and ventricular myocytes. *J. Mol. Cell. Cardiol.* 46, 463–473. doi: 10.1016/j.yjmcc.2008.11.003

Wang, S. Q., Song, L. S., Lakatta, E. G., and Cheng, H. (2001). Ca2+ signalling between single l-type ca2+ channels and ryanodine receptors in heart cells. *Nature* 410, 592–596. doi: 10.1038/35069083

Wang, T. J., Larson, M. G., Levy, D., Vasan, R. S., Leip, E. P., Wolf, P. A., et al. (2003). Temporal relations of atrial fibrillation and congestive heart failure and their joint influence on mortality: the framingham heart study. *Circulation* 107, 2920–2925. doi: 10.1161/01.CIR.0000072767.89944.6E

Wang, Y., Huang, S., Sah, V. P., Ross, J. Jr., Brown, J. H., Han, J., et al. (1998). Cardiac muscle cell hypertrophy and apoptosis induced by distinct members of the p38 mitogen-activated protein kinase family. *J. Biol. Chem.* 273, 2161–2168. doi: 10.1074/jbc.273.10.5423

Wetzel, U., Boldt, A., Lauschke, J., Weigl, J., Schirdewahn, P., Dorszewski, A., et al. (2005). Expression of connexins 40 and 43 in human left atrium in atrial fibrillation of different aetiologies. *Heart* 91, 166–170. doi: 10.1136/hrt.2003.024216

Workman, A. J., Pau, D., Redpath, C. J., Marshall, G. E., Russell, J. A., Norrie, J., et al. (2009). Atrial cellular electrophysiological changes in patients with ventricular dysfunction may predispose to af. *Heart Rhythm* 6, 445–451. doi: 10.1016/j.hrthm.2008.12.028

Wu, X., Zhao, W., Corrillo, E., Chen, W., Yan, J., Bers, D. M., et al. (2014). "Novel stress signaling jnk regulates camkiiδ activity and expression in aged human atrium," in *AHA Annual Meeting* (Chicago).

Wu, Y., MacMillan, L. B., McNeill, R. B., Colbran, R. J., and Anderson, M. E. (1999). Cam kinase augments cardiac l-type ca2+ current: a cellular mechanism for long q-t arrhythmias. *Am. J. Physiol.* 276, H2168–H2178.

Xie, Y., Sato, D., Garfinkel, A., Qu, Z., and Weiss, J. N. (2010). So little source, so much sink: requirements for afterdepolarizations to propagate in tissue. *Biophys. J.* 99, 1408–1415. doi: 10.1016/j.bpj.2010.06.042

Yan, J., Kong, W., Zhang, Q., Beyer, E. C., Walcott, G., Fast, V. G., et al. (2013). C-jun n-terminal kinase activation contributes to reduced connexin43 and development of atrial arrhythmias. *Cardiovasc. Res.* 97, 589–597. doi: 10.1093/cvr/cvs366

Yang, Z., Shen, W., Rottman, J. N., Wikswo, J. P., and Murray, K. T. (2005). Rapid stimulation causes electrical remodeling in cultured atrial myocytes. *J. Mol. Cell. Cardiol.* 38, 299–308. doi: 10.1016/j.yjmcc.2004.11.015

Yeh, Y. H., Wakili, R., Qi, X. Y., Chartier, D., Boknik, P., Kaab, S., et al. (2008). Calcium-handling abnormalities underlying atrial arrhythmogenesis and contractile dysfunction in dogs with congestive heart failure. *Circ. Arrhythm. Electrophysiol.* 1, 93–102. doi: 10.1161/CIRCEP.107.754788

Yoon, S., and Seger, R. (2006). The extracellular signal-regulated kinase: multiple substrates regulate diverse cellular functions. *Growth Factors* 24, 21–44. doi: 10.1080/02699050500284218

Zechner, D., Thuerauf, D. J., Hanford, D. S., McDonough, P. M., and Glembotski, C. C. (1997). A role for the p38 mitogen-activated protein kinase pathway in myocardial cell growth, sarcomeric organization, and cardiac-specific gene expression. *J. Cell Biol.* 139, 115–127. doi: 10.1083/jcb.139.1.115

Zhang, R., Dzhura, I., Grueter, C. E., Thiel, W., Colbran, R. J., and Anderson, M. E. (2005). A dynamic alpha-beta inter-subunit agonist signaling complex is a novel feedback mechanism for regulating l-type ca2+ channel opening. *FASEB J.* 19, 1573–1575. doi: 10.1096/fj.04-3283fje

Zhang, T., Maier, L. S., Dalton, N. D., Miyamoto, S., Ross, J. Jr., Bers, D. M., et al. (2003). The deltac isoform of camkii is activated in cardiac hypertrophy and induces dilated cardiomyopathy and heart failure. *Circ. Res.* 92, 912–919. doi: 10.1161/01.RES.0000069686.31472.C5

Zheng, M., Dilly, K., Dos Santos Cruz, J., Li, M., Gu, Y., Ursitti, J. A., et al. (2004). Sarcoplasmic reticulum calcium defect in ras-induced hypertrophic cardiomyopathy heart. *Am. J. Physiol. Heart Circ. Physiol.* 286, H424–H433. doi: 10.1152/ajpheart.00110.2003

Conflict of Interest Statement: The author declares that the research was conducted in the absence of any commercial or financial relationships that could be construed as a potential conflict of interest.

Received: 02 December 2014; accepted: 30 January 2015; published online: 19 February 2015.

Citation: Ai X (2015) SR calcium handling dysfunction, stress-response signaling pathways, and atrial fibrillation. Front. Physiol. ***6****:46. doi: 10.3389/fphys.2015.00046*

This article was submitted to Cardiac Electrophysiology, a section of the journal Frontiers in Physiology.

frontiers in
PHYSIOLOGY

ORIGINAL RESEARCH ARTICLE
published: 10 February 2015
doi: 10.3389/fphys.2015.00023

Cytosolic calcium ions exert a major influence on the firing rate and maintenance of pacemaker activity in guinea-pig sinus node

Rebecca A. Capel and Derek A. Terrar*

Department of Pharmacology, University of Oxford, Oxford, UK

Edited by:
Ruben Coronel, Academic Medical Center, Netherlands

Reviewed by:
Christopher Huang, University of Cambridge, UK
Jules Hancox, University of Bristol, UK

****Correspondence:***
Derek A. Terrar, Department of Pharmacology, University of Oxford, Mansfield Road, Oxford, Oxon OX1 3QT, UK
e-mail: derek.terrar@pharm.ox.ac.uk

The sino-atrial node (SAN) provides the electrical stimulus to initiate every heart beat. Cellular processes underlying this activity have been debated extensively, especially with regards to the role of intracellular calcium. We have used whole-cell application of 1,2-bis(o-aminophenoxy)ethane-N,N,N′,N′-tetraacetic acid (BAPTA), a rapid calcium chelator, to guinea pig isolated SAN myocytes to assess the effect of rapid reduction of intracellular calcium on SAN cell electrical activity. High-dose (10 mM) BAPTA induced rapid and complete cessation of rhythmic action potential (AP) firing (time to cessation 5.5 ± 1.7 s). Over a range of concentrations, BAPTA induced slowing of action potential firing and disruption of rhythmic activity, which was dose-dependent in its time of onset. Exposure to BAPTA was associated with stereotyped action potential changes similar to those previously reported in the presence of ryanodine, namely depolarization of the most negative diastolic potential, prolongation of action potentials and a reduction in action potential amplitude. These experiments are consistent with the view that cytosolic calcium is essential to the maintenance of rhythmic pacemaker activity.

Keywords: sino-atrial node, heart rate, pacemaking, cytosolic calcium, calcium chelation

INTRODUCTION

It has been proposed that cytosololic calcium including that released from the sarcoplasmic reticulum (SR) plays an important role in the generation of pacemaker activity in both mammalian and amphibian pacemaker tissue (Rigg and Terrar, 1996; Ju and Allen, 1998, 1999; Rigg et al., 2000), as well as in subsidiary pacemaker (Zhou and Lipsius, 1993) and atrioventricular cells (Hancox et al., 1994). It has been suggested that uptake and release of calcium by the SR could provide a timing mechanism for pacemaking that is referred to as the "calcium clock" (Vinogradova et al., 2004), and in recent years there has been vigorous debate concerning the relative importance of such a "calcium clock" and the more conventional "membrane clock" dependent on activation and de-activation of membrane ion channels (Lakatta and Difrancesco, 2009; DiFrancesco and Noble, 2012; Maltsev and Lakatta, 2012).

An important challenge to the possible importance of cytosolic calcium for pacemaking was provided by the work of Himeno et al. (2011) who recorded spontaneous electrical activity in guinea pig isolated pacemaker myocytes under perforated patch conditions, and then ruptured the membrane beneath the patch to apply the calcium chelator BAPTA to the cytosol from the patch pipette solution. Under these conditions, spontaneous action potentials were observed to continue at least for 30 s in the presence of cytosolic BAPTA, although pacemaker activity did become erratic or stop after several minutes. The observations were thought not to be consistent with a major role for cytosolic calcium in controlling pacemaker activity, at least for short term (ms or seconds) mechanisms. These observations have in turn been challenged, at least in part on the basis of arguments concerning possible changes in the seal resistance (Maltsev et al., 2011; Yaniv et al., 2013).

The aim of the experiments presented here was to further examine this question in guinea pig pacemaker myocytes isolated from sino-atrial node. We have used techniques similar to those of Himeno et al. (2011), as well as conventional ruptured patch approaches with several concentrations of BAPTA applied from the patch pipette.

MATERIALS AND METHODS

Guinea pig sino-atrial node myocytes were isolated as described previously (Rigg et al., 2000). Briefly, guinea-pigs were killed by concussion followed by cervical dislocation, the heart rapidly removed, placed into heparin-containing zero-calcium modified Tyrode solution (in mM: NaCl 136, KCl 5.4, NaHCO3 12, Na^+ pyruvate 1, NaH_2PO_4 1, $MgCl_2$ 1, glucose 5, ethylene glycol tetraacetic acid (EGTA) 0.04; gassed with 95% O_2/5% CO_2 to maintain a pH of 7.4) and then mounted on a Langendorff apparatus for retrograde perfusion (zero-calcium modified Tyrode without addition of EGTA). The heart was enzymatically digested (Worthington Type II Collagenase, Worthington Biochemical Corp), atria removed and the SAN dissected into small strips under a microscope. Single cells were isolated by trituration in warmed, oxygenated high-potassium storage solution (in mM: KCl 70, $MgCl_2$ 5, K^+-glutamine 5, taurine 20, EGTA 0.04, succinic acid 5, KH_2PO_4 20, HEPES 5, glucose 10; pH to 7.2 with

KOH) and then transferred directly to 4°C for storage in the same solution until use.

Standard whole-cell patch solution contained (in mM): K^+-aspartate 110, KCl 10, NaCl 5, $MgCl_2$ 5.2, HEPES 5, K_2ATP 5, pH to 7.2 with KOH. Amphotericin was dissolved in dimethyl sulphoxide (DMSO) to form a stock solution (20 mg ml^{-1}) and then diluted into patch solution to achieve a final concentration of 240 $\mu g\ ml^{-1}$. 1,2-Bis(2-aminophenoxy)ethane-N,N,N′,N′-tetraacetic acid tetrapotassium salt (BAPTA) was dissolved in double-distilled water and diluted into whole-cell patch solution as appropriate.

During experiments, cells were superfused with physiological saline solution (PSS) at 35 ± 2°C (in mM: NaCl 125, $NaHCO_3$ 25, KCl 5.4, NaH_2PO_4 1.2, $MgCl_2$ 1, glucose 5.5, $CaCl_2$ 1.8, pH to 7.4 with NaOH and oxygenated with 95% O_2/5% CO_2). Within a given experiment, temperature fluctuation was < 0.5°C.

For perforated patch recording, micropipettes of 3–6 MΩ were manufactured from borosilicate glass (GC100F, Harvard Apparatus) using a two-step gravity-driven puller (PP-83, Narishige, Japan). Pipettes were mounted on a CV203BU headstage and recordings made using an AxoPatch200B amplifier with pClamp7 software. GΩ seals were formed using manual suction and up to 15 min allowed for stable perforation. Action potentials were recorded in current clamp mode, cells were switched to voltage clamp in order to monitor seal integrity and whole-cell access achieved by manual suction. A holding potential of −60 mV was used during this process. Upon whole-cell access, judged by appearance of capacitative transients, the amplifier was rapidly switched back to current clamp mode and cellular action potentials were monitored until cessation of rhythmic activity. A representative control trace to demonstrate this method is presented in **Figure 1A**. A representative section of action potentials recorded during perforated patch, the transition from perforated to whole-cell patch and a representative section of action potentials in whole-cell configuration are shown expanded in **Figures 1B–D** respectively.

During experiments in which only whole-cell recordings were carried out, the same method was followed without the addition of amphotericin to the whole-cell patch solution. A holding voltage of −40 mV was used during confirmation of whole-cell access in these experiments since this was found to minimize damage to the seal during rupture of the patch. Where Fluo-5F was used for illustration of rhythmic firing before patch rupture this was applied as 3 μM of the cell-permeant form Fluo-5F-AM (Invitrogen, UK) by incubation at room temperature for 10 min followed by a further 10 min of superfusion with PSS to allow de-esterification.

RESULTS

INTRACELLULAR CALCIUM IS A REQUIREMENT FOR PACEMAKING ACTIVITY

Our first aim was to repeat the experiments of Himeno et al. (2011). We reasoned that, if cytosolic calcium has no effect on cellular beating rate, then carrying out experiments in the absence of amphotericin would allow us to confirm that the perforation technique itself was not causing any confounding effects.

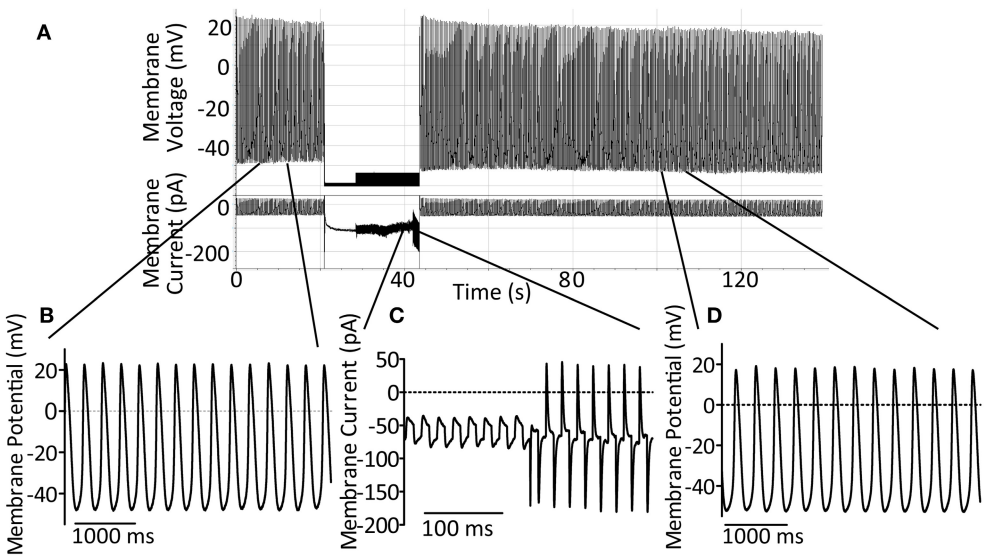

FIGURE 1 | (A) Demonstration of the perforated-to-whole-cell patch method with control patch solution. After formation of a GΩ seal, up to 15 min is allowed for perforation of the membrane (amphorericin B, 240 $\mu g\ ml^{-1}$). Action potentials are recorded in the perforated patch configuration for at least 10 s before switch to voltage clamp at −60 mV using an AxoPatch200B amplifier. Seal integrity can then be monitored and recorded using the amplifier-controlled seal test. Whole-cell access is achieved by rapid suction and confirmed by the onset of large capacitative transients. After gaining whole-cell access the amplifier is rapidly switched back to current clamp mode in order to follow spontaneous action potential firing once again. **(B)** An expanded section of trace, as indicated, to demonstrate control action potentials in the perforated patch configuration. **(C)** An expanded section of trace, as indicated, to demonstrate the seal test signal during patch rupture to achieve whole-cell access. **(D)** An expanded section of trace, as indicated, to demonstrate the maintenance of spontaneous action potential firing and expected action potential shape 60 s after patch rupture under control conditions.

Under these conditions the addition of 10 mM BAPTA to the patch pipette led to rapid cessation of rhythmic cellular activity with an average time to cessation of 5.5 ± 1.7 s from patch rupture ($n = 6$). In contrast, although control cells showed a gentle rate decline (9 ± 4% reduction after 60 s, $n = 3$) which was statistically-significant at 90 s post access (20 ± 3% reduction, $n = 3$), cells exposed to our standard whole-cell patch solution maintained rhythmic activity for over 5 min.

We performed some of these experiments after loading cells with the calcium indicator Fluo5F to demonstrate that rhythmic cellular activity was indeed present before rapid chelation of calcium, as it was common that cells stopped before the switch to current clamp could be completed. There was no difference in the response to BAPTA under these conditions. A representative trace of 10 mM BAPTA exposure with preceding calcium signal is presented in **Figure 2A**. The response of a cell to 10 mM BAPTA

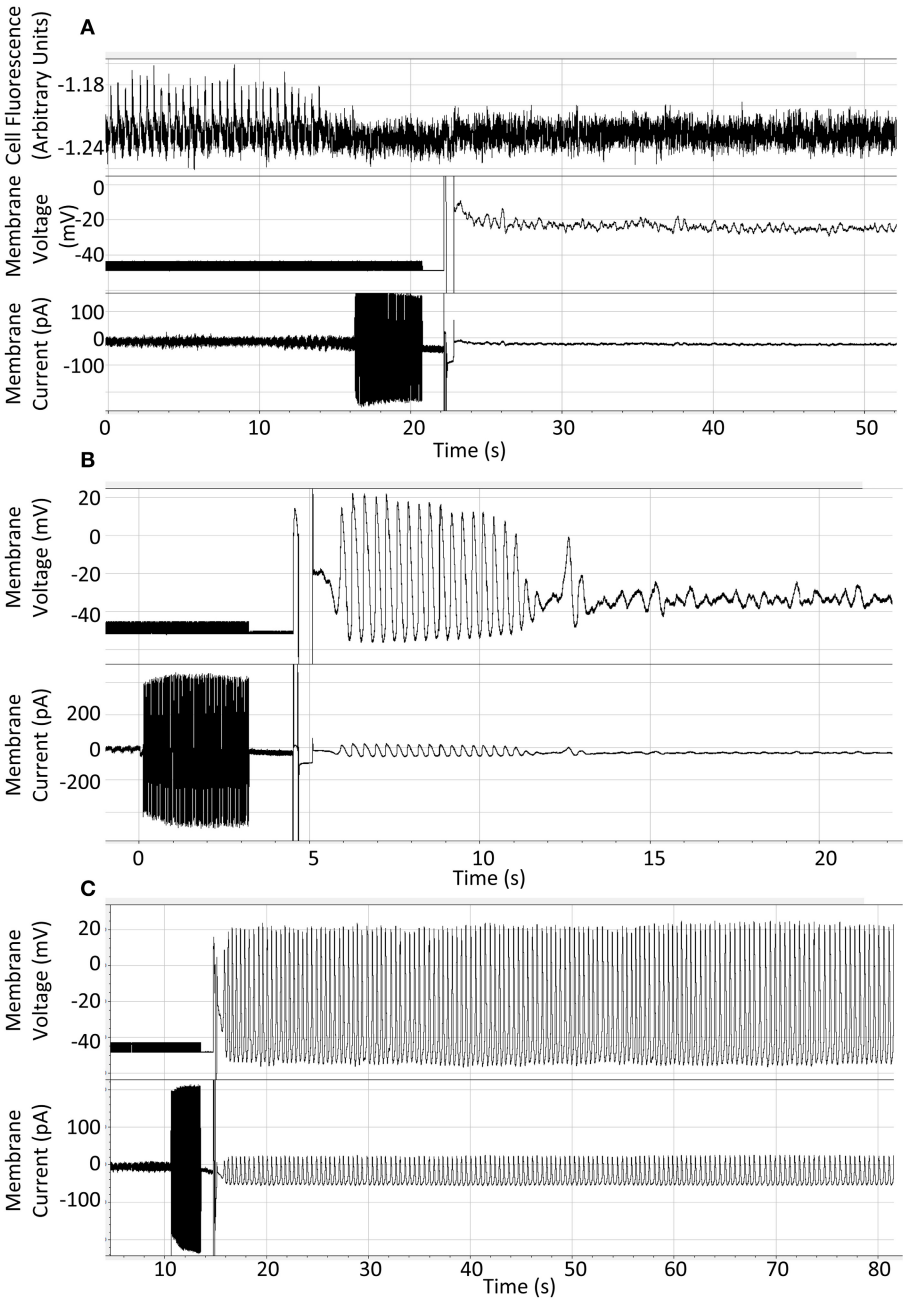

FIGURE 2 | (A) Representative recording to show result of patch-application of 10 mM BAPTA to an isolated guinea pig SAN cell with fluo5F included to demonstrate rhythmic activity under control conditions. **(B)** Representative recording to show rapid cessation of spontaneous activity on application of 10 mM BAPTA from the patch pipette solution. **(C)** Representative recording to show continuation of expected spontaneous rhythmic action potential generation when whole-cell access is gained using standard whole-cell patch solution. Cells were superfused with Physiological Saline Solution at 35 ± 2°C throughout.

in the absence of Fluo5F, which maintained action potentials for several seconds after patch rupture, is presented in **Figure 2B** and can be compared to that of a control cell shown in **Figure 2C**.

EFFECT OF INTRACELLULAR CALCIUM CHELATION ON ACTION POTENTIAL WAVEFORMS

The rapid cessation of action potential firing witnessed in our first set of recordings did not allow us to compare action potential waveforms seen over time. We therefore reverted to a direct repetition of the Himeno et al. (2011), experiments, recording control action potentials by perforated patch before BAPTA application by patch rupture and whole-cell access.

After exposure to amphotericin/DMSO by whole-cell access, SAN cell appearance became markedly changed over the course of 5 min, exhibiting cell swelling or membrane bulging. To minimize any confounding effects of these phenomena we assessed cellular rate over the first 90 s post whole-cell break-in only and then followed activity until perturbation of rhythmic action potential firing. Action potentials fired in each 10 s timebin from patch rupture were analyzed for morphology regardless of whether cell firing at the time was rhythmic or sporadic. Representative traces of the 0 and 10 mM BAPTA conditions presented in **Figures 3A,B.**

During BAPTA-induced cell slowing ($n = 5$) several changes were observed in action potential waveforms. BAPTA induced a significant reduction in action potential amplitude over time ($p < 0.05$, One-Way repeated measures ANOVA, **Figure 3C**), and prolongation of action potential half-width ($p < 0.05$, One-Way ANOVA, **Figure 3D**) whilst these values were unchanged in control cells (both $p > 0.05$, One-Way ANOVA with repeated measures, $n = 4$). Further, whilst exposure of cells to our standard whole-cell patch solution led to a significant hyperpolarization of the most negative diastolic potential over time ($p < 0.05$, One-Way ANOVA, $n = 4$), inclusion of 10 mM BAPTA in the patch solution led to a significant depolarization of this measure ($p < 0.05$, One-Way ANOVA, **Figure 3E**). No change was seen in the maximum rate of action potential upstroke under either condition (both, $p > 0.05$, separate One-Way ANOVA analyses, data not shown).

CELLULAR FIRING IS DOSE-DEPENDENTLY AFFECTED BY INTRACELLULAR CALCIUM CHELATION

During control recordings using our standard intracellular patch solution, conversion of cells from perforated patch to whole-cell patch led to in initial increase in rate followed by gentle slowing

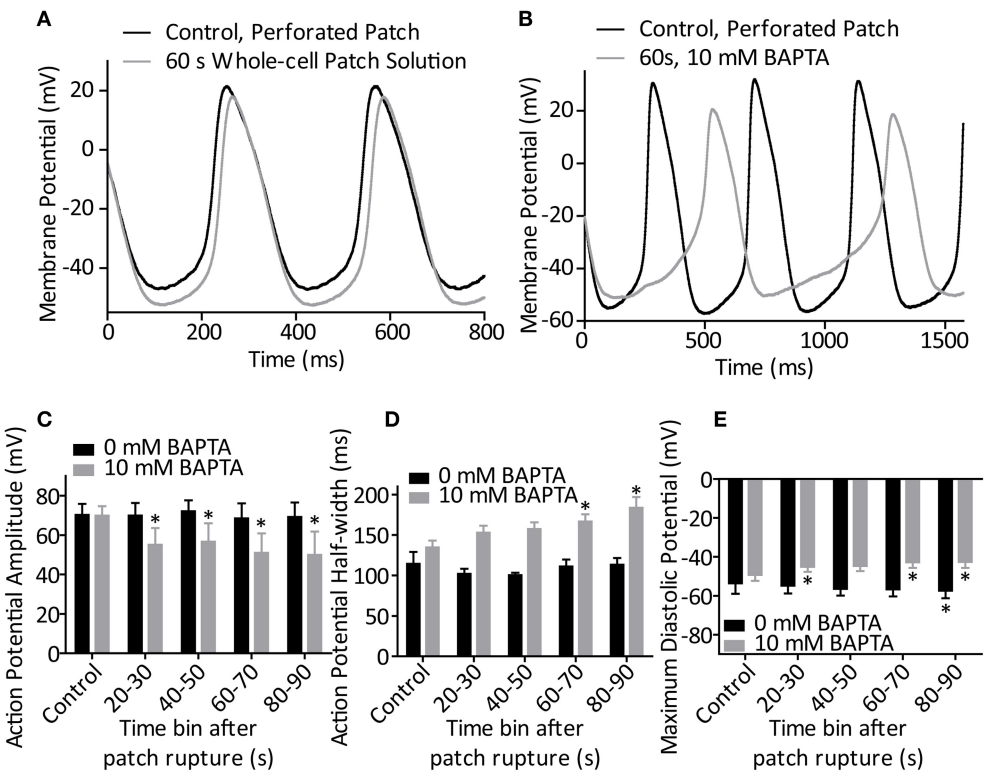

FIGURE 3 | (A) Representative action potentials recorded during perforated patch control and 60 s after patch rupture with standard whole-cell patch solution (0 mM BAPTA). **(B)** Representative action potentials recorded during perforated patch control and 60 s after patch rupture to apply 10 mM BAPTA. **(C)** Effect of patch rupture on action potential amplitude over the course of 90 s. 10 mM BAPTA significantly reduced AP amplitude ($p < 0.05$, One-Way ANOVA with repeated measures). **(D)** Effect of patch rupture on half-width of the action potential. 10 mM BAPTA significantly lengthened the action potential half-width ($p < 0.05$, One-Way ANOVA with repeated measures). **(E)** Effect of patch rupture on most negative diastolic potential over the course of 90 s. 10 mM BAPTA significantly depolarized the MDP ($p < 0.05$, One-Way ANOVA with repeated measures) *Denotes significant difference from control, during perforated patch recording ($p < 0.05$ by *post-hoc* test with Dunnett's multiple comparison performed after One-Way ANOVA). $n = 4$ for 0 mM and $n = 5$ for 10 mM recordings.

($p < 0.05$, One-Way repeated measures ANOVA, $n = 4$). *Post-hoc* testing with Tukey correction revealed that action potential firing only became significantly less frequent than that during the perforated patch at 90 s after patch rupture.

We next carried out action potential recordings by the perforated-to-whole-cell patch method at a range of BAPTA concentrations. Whole-cell application of BAPTA led to a dose-dependent perturbation of rhythmic activity. The time taken for a given cell to miss the expected firing of an action potential was longer than 3 min in all but one control cell (which missed one AP at 75 s post patch rupture and then returned to rhythmic firing and continued for longer than 3 min). In the presence of 0.1 mM BAPTA average time to miss a beat was 169 ± 55 s ($n = 3$). For the 1 mM condition, this shortened to 62 ± 19 s ($n = 5$) and for the 10 mM condition to 24 ± 9 s ($n = 5$). A "survival" plot of time to first pause in activity is presented in **Figure 4**. There is a significant effect of BAPTA concentration ($P < 0.0001$) as assessed by Log-Rank comparison of survival curves.

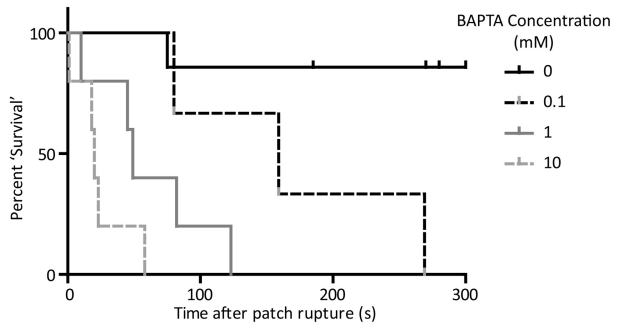

FIGURE 4 | "Survival" curve to show cessation of rhythmic activity on application of BAPTA by the perforated-to-whole-cell patch method. Time taken for cells to miss the firing of an expected action potential was significantly associated with the concentration of BAPTA included in the patch solution ($p < 0.05$, Log-rank comparison of survival curves). $n = 5$ for 0 mM, 3 for 0.1 mM, 5 for 1 mM, and 5 for 10 mM conditions.

Data are presented as time taken to miss an action potential because cellular behavior observed after this point was variable. In all cases cells ceased true rhythmic activity after missing one or more APs. Some cells rapidly fell into complete cessation, with membrane potential fluctuating in the region of −30 to −40 mV (See **Figure 5A**). In these cells, regardless of BAPTA concentration, application of hyperpolarizing voltage clamp to −60 mV and subsequent relief was able to induce firing of one or more action potentials by anode-break excitation (rebound excitation seen after injection of hyperpolarizing current), demonstrating that membrane currents associated with normal activity remained functional (**Figure 5B**). During quiescent periods it was common for cells to achieve a rhythmic fluctuation in cellular membrane potential which did not induce full action potential firing (**Figure 5C**). Further cells were seen to fire single action potentials at random or else commenced burst-like activity in which short trains of 3–5 action potentials could be observed occurring with little predictability (**Figure 5D**). Cells were not necessarily limited to a single one of these behaviors.

Due to the propensity of cells to continue sporadic firing after cessation of "normal" activity, or to exhibit membrane potential fluctuations which did not stimulate a full action potential, analysis of rate using our usual method (determination of

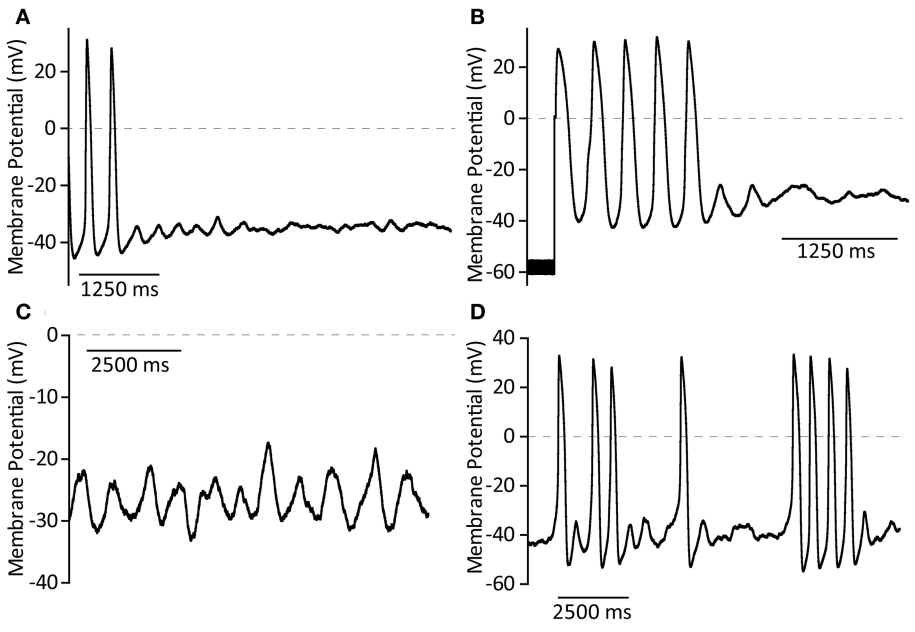

FIGURE 5 | Representative examples of membrane potential phenomena after cessation of true cell rhythmicity caused by exposure to BAPTA in the patch solution. (A) Complete cessation of action potential firing and quiescence around −35 mV. **(B)** Stimulation of a short train of action potentials by anode break excitation followed by return to quiescence. **(C)** Rhythmic membrane potential fluctuations which fail to convert to full action potential firing. **(D)** Sporadic burst firing activity.

dominant firing frequency by spectral analysis) was not deemed accurate for this purpose. Instead, we assessed the number of full action potentials fired over each 10 s period from patch rupture, where an action potential was defined as a spontaneously-fired event which overshot −10 mV or reached 50% of control action potential amplitude. As with data presented in **Figure 3**, action potentials included in this analysis were those considered to have fired regardless of rhythmic cell behavior or otherwise.

The effect of BAPTA on the number of fired action potentials over time is presented in **Figure 6**. Two-Way ANOVA analysis showed a significant effect of BAPTA concentration and of exposure time on cell firing frequency (both $p < 0.05$). However, there was also an interaction effect which suggests that the timecourse of BAPTA-mediated slowing differs between concentrations ($p < 0.05$). *Post-hoc* testing with Bonferroni corrections reveals a significant effect of both the 1 and 10 mM BAPTA concentrations in comparison to control, but no difference between these two concentrations over all time bins.

CONFOUNDING EFFECTS OF PATCH METHOD ON RESULTS OF BAPTA APPLICATION

Direct comparison of the effect of 10 mM BAPTA on cell firing by the whole-cell only and the perforated-to-whole-cell patch method show that cell "survival" is much more pronounced in the presence of the ionophore and its solvent ($p < 0.05$, Log-Rank test of "survival" time to first missed beat, **Figure 7**). Cells exposed to 10 mM BAPTA alone succumbed to the effects of chelation in 5.5 ± 1.7 s and were most likely to reach a quiescent or sub-threshold firing state. When amphotericin and DMSO were also included in the patch solution, perturbation of rhythm was seen at 24 ± 9 s and cells demonstrated the full range of behaviors described above.

DISCUSSION

The data presented in this paper are consistent with the proposal that the presence of intracellular calcium is an essential condition for the maintenance of rhythmic action potential firing in guinea pig sino-atrial node cells. All cells exposed to BAPTA, at a range of concentrations, experienced a derangement of rhythmic action potential firing which was not seen under control conditions. The time taken for cells to miss firing an expected action potential was dose-dependently related to BAPTA exposure. Although there is a time-dependent effect of BAPTA applied via the patch pipette, it would seem that there is not a distinct dose-response curve when the number of action potentials fired during each 10 s time bin is considered. The interpretation of these rate data is not straightforward since a range of cell firing characteristics was seen on cessation of true rhythmic activity. Taken together, these observations may suggest the gradual reduction of cytosolic calcium to a threshold level at which the cell no longer supports rhythmic activity as opposed to an effect of different chelation levels on different signaling pathways.

Rapid chelation of intracellular calcium during our whole-cell only experiments often resulted in cessation of rhythmic firing activity before the amplifier could be switched away from the seal-test mode and into current clamp. Previous work from this laboratory has shown that rapid switch (<1 s transition) of guinea pig SAN cells into BAPTA-AM leads to very rapid cessation of action potential firing. There is evidence that BAPTA-AM is capable of blocking voltage-gated potassium channels (Tang et al., 2007) which is the major reason why the effect of BAPTA application by whole-cell access is important to test. The data presented in this paper are therefore in agreement with previous studies which have used membrane-permeant chelators to investigate cell dependence on cytosolic calcium (Vinogradova et al., 2000; Sanders et al., 2006).

The action potential shape after exposure to BAPTA is distinctly different from those seen in control. In the absence of calcium directly beneath the membrane it would be expected that L-type calcium channels open for longer due to a reduced stimulus for calcium-dependent inactivation (Himeno et al., 2011). In this regard, our data are in agreement with the observations

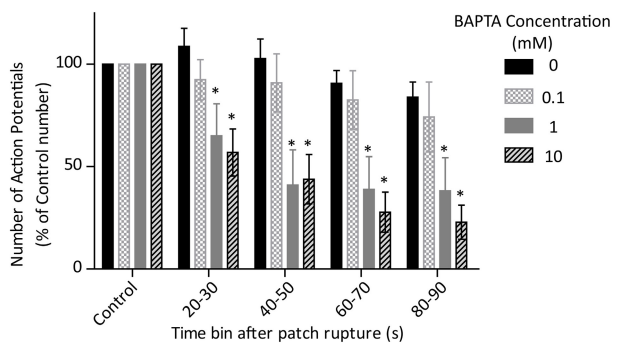

FIGURE 6 | Effects of control (0 mM, $n = 4$) and 0.1 ($n = 3$), 1 ($n = 5$) and 10 ($n = 5$) mM BAPTA on cell firing rate, measured as the number of action potentials fired during each 10 s time bin after rupture of the cell membrane and conversion of perforated patch to whole-cell access. There is a significant effect of BAPTA, time and also an interaction (all $p < 0.05$ by Two-Way ANOVA). *Denotes significant difference ($p < 0.05$) from 0 mM by *post-hoc* comparison with Bonferoni correction

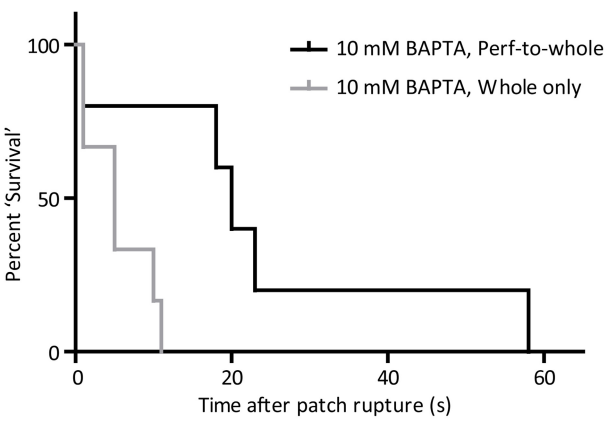

FIGURE 7 | "Survival" curve to show the difference in effect of 10 mM BAPTA when applied from the perforated patch ($n = 5$) and whole-cell ($n = 6$) only configurations. Time taken for cells to miss the firing of an expected action potential was significantly longer when BAPTA was applied in the whole-cell patch solution during the perforated patch method ($p < 0.05$, Log-rank comparison of survival curves).

of Noma's group (Himeno et al., 2011) in exhibiting significant action potential prolongation. Cytosolic calcium also enhances delayed rectifier potassium currents, particularly I_{Ks} (Xie et al., 2015). Cytosolic calcium chelation would therefore be expected to reduce the repolarizing potassium current and both prolong action potential duration and lead to depolarization of the most negative diastolic potential, which is indeed seen in our cells.

Chelation of intracellular calcium is also likely to inhibit activation of the funny current I_f (Rigg et al., 2003) and lead to slowing of rhythmic AP firing. Sino-atrial node cells are thought to maintain a diastolic cAMP (Vinogradova et al., 2006) and calcium (Sanders et al., 2006) level significantly above that of ventricular cells. Calcium-stimulated adenylyl cyclases, AC1 and AC8 are known to be present in guinea pig sino-atrial node cells and our group has previously provided evidence that calcium-dependent cAMP generation contributes to the I_f current measured in guinea pig sino-atrial node cells (Mattick et al., 2007).

Subjectively, conversion of cells from the linear, spontaneous, phase 4 action potential decay to the exponential rise which begets L-type calcium channel opening is slowed in cells after BAPTA exposure. This "saw-toothed" action potential shape (**Figure 3B**) in the presence of BAPTA is very similar to those presented as stereotyped during exposure to ryanodine in previous publications from this group which first proposed a calcium-dependence of SAN pacemaker activity (Rigg and Terrar, 1996; Rigg et al., 2000). If the "calcium clock" mechanism is dominant (Vinogradova et al., 2005) then the chelation of cytosolic calcium with a rapid and high affinity chelator such as BAPTA would be expected to effectively buffer calcium in the cleft between ryanodine receptors and the sodium-calcium exchange protein, and have effects that include suppression of local calcium release events (Bogdanov et al., 2006). Further, chelation with BAPTA may suppress other calcium-dependent events for which local calcium release events are not a requirement. For instance, the heightened diastolic calcium measured in SAN cells could itself drive a consistent inward current through NCX during all phases of the action potential (Sanders et al., 2006). Under either of these theories, chelation of cytosolic calcium would lead to a significant slowing of spontaneous diastolic depolarization before the opening of voltage-gated calcium channels by removing the depolarizing drive of NCX current.

Upon cessation of rhythmic action potential firing, we have also observed some interesting phenomena in cell membrane potential behavior. Cells which are rendered quiescent fluctuate gradually around a membrane potential in the region of −35 mV. This is very similar to the "zero-current" level previously described for the as yet unidentified background conductance of SAN myocytes (Noma and Irisawa, 1975). From this quiescent state, cells are often seen to undergo a significant membrane depolarization toward action potential threshold without actually reaching successful initiation of a complete depolarization. These events can occur as trains of distinct membrane fluctuations but are most often noted in lieu of an action potential when the cell misses one or several beats, just before firing of a sporadic action potential or burst of action potentials and during transition from any form of action potential firing back to a quiescent state. It has been shown that rapid voltage clamp of SAN myocytes is followed by several seconds of rhythmic cellular calcium transients (Vinogradova et al., 2004). The membrane potential fluctuations described here are very similar to those observed in the presence of ryanodine, which were also associated with spontaneous cellular calcium signals (Rigg et al., 2000). Whether one or a set of highly localized calcium signals are being spontaneously generated to lead to a partial depolarization by inward current through NCX, or whether these partial depolarization's themselves cause the calcium fluctuations seen by Rigg and colleagues will be interesting to discuss following future experimental work.

Data presented by Himeno et al. (2011) note that spontaneous action potential firing shows minimal interference over at least the first 30 s after patch rupture. These data have been challenged on the basis of possible changes in "seal" resistance around the patch electrode (Maltsev et al., 2011). Of particular interest in this regard is our finding that 10 mM BAPTA takes significantly longer to cause rhythm perturbations in perforated-to-whole-cell experiments than when BAPTA is applied in the absence of amphotericin/DMSO. Although it would be expected that amphotericin will not immediately compromise the SAN cell outer membrane in its entirety (it is standard practice to wait up to 15 min to achieve patch perforation for normal perforated patch recordings), the high membrane resistance of a healthy sino-atrial node cell means that the introduction of small conducting pathways can have a major influence. It cannot be ruled out that some of the changes in action potential waveforms are contributed to by this mechanism, but the similarity of these changes and the resulting action potentials to data presented during exposure of cells (Rigg et al., 2000) or tissue (Rigg and Terrar, 1996) to ryanodine supports the notion that these are attributable to a reduced contribution of calcium-dependent pathways.

In conclusion, our recordings suggest that the presence of cytosolic calcium is essential for the maintenance of normal rhythmic activity in isolated guinea pig SAN myocytes. The exact mechanism(s) which require this cytosolic calcium in order to maintain physiological function are still a matter for future investigation.

ACKNOWLEDGMENTS

Derek A. Terrar is supported by The British Heart Foundation. Rebecca A. Capel was supported in this work by a British Heart Foundation Graduate Studentship and, thereafter, a British Heart Foundation research grant.

REFERENCES

Bogdanov, K. Y., Maltsev, V. A., Vinogradova, T. M., Lyashkov, A. E., Spurgeon, H. A., Stern, M. D., et al. (2006). Membrane potential fluctuations resulting from submembrane Ca^{2+} releases in rabbit sinoatrial nodal cells impart an exponential phase to the late diastolic depolarization that controls their chronotropic state. *Circ. Res.* 99, 979–987. doi: 10.1161/01.RES.0000247933.66532.0b

DiFrancesco, D., and Noble, D. (2012). The funny current has a major pacemaking role in the sinus node. *Heart Rhythm* 9, 299–301. doi: 10.1016/j.hrthm.2011.09.021

Hancox, J. C., Levi, A. J., and Brooksby, P. (1994). Intracellular calcium transients recorded with Fura-2 in spontaneously active myocytes isolated from the atrioventricular node of the rabbit heart. *Proc. Biol. Sci.* 255, 99–105. doi: 10.1098/rspb.1994.0014

Himeno, Y., Toyoda, F., Satoh, H., Amano, A., Cha, C. Y., Matsuura, H., et al. (2011). Minor contribution of cytosolic Ca^{2+} transients to the pacemaker rhythm in guinea pig sinoatrial node cells. *Am. J. Physiol. Heart Circ. Physiol.* 300, H251–H261. doi: 10.1152/ajpheart.00764.2010

Ju, Y. K., and Allen, D. G. (1998). Intracellular calcium and Na^{+}-Ca^{2+} exchange current in isolated toad pacemaker cells. *J. Physiol.* 508(Pt 1), 153–166. doi: 10.1111/j.1469-7793.1998.153br.x

Ju, Y.-K., and Allen, D. G. (1999). How does β-adrenergic stimulation increase the heart rate? The role of intracellular Ca^{2+} release in amphibian pacemaker cells. *J. Physiol.* 516, 793–804. doi: 10.1111/j.1469-7793.1999.0793u.x

Lakatta, E. G., and Difrancesco, D. (2009). What keeps us ticking: a funny current, a calcium clock, or both? *J. Mol. Cell. Cardiol.* 47, 157–170. doi: 10.1016/j.yjmcc.2009.03.022

Maltsev, V. A., and Lakatta, E. G. (2012). The funny current in the context of the coupled-clock pacemaker cell system. *Heart Rhythm* 9, 302–307. doi: 10.1016/j.hrthm.2011.09.022

Maltsev, V. A., Vinogradova, T. M., Stern, M. D., and Lakatta, E. G. (2011). Letter to the editor:"Validating the requirement for beat-to-beat coupling of the Ca^{2+} clock and M clock in pacemaker cell normal automaticity." *Am. J. Physiol. Heart Circ. Physiol.* 300, H2323–H2324. doi: 10.1152/ajpheart.00110.2011

Mattick, P., Parrington, J., Odia, E., Simpson, A., Collins, T., and Terrar, D. (2007). Ca^{2+}-stimulated adenylyl cyclase isoform AC1 is preferentially expressed in guinea-pig sino-atrial node cells and modulates the I(f) pacemaker current. *J. Physiol.* 582, 1195–1203. doi: 10.1113/jphysiol.2007.133439

Noma, A., and Irisawa, H. (1975). Effects of Na^{+} and K^{+} on the resting membrane potential of the rabbit sinoatrial node cell. *Jpn. J. Physiol.* 25, 207–302. doi: 10.2170/jjphysiol.25.287

Rigg, L., Heath, B. M., Cui, Y., and Terrar, D. A. (2000). Localisation and functional significance of ryanodine receptors during beta-adrenoceptor stimulation in the guinea-pig sino-atrial node. *Cardiovasc. Res.* 48, 254–264. doi: 10.1016/S0008-6363(00)00153-X

Rigg, L., Mattick, P. A., Heath, B. M., and Terrar, D. A. (2003). Modulation of the hyperpolarization-activated current (I(f)) by calcium and calmodulin in the guinea-pig sino-atrial node. *Cardiovasc. Res.* 57, 497–504. doi: 10.1016/S0008-6363(02)00668-5

Rigg, L., and Terrar, D. A. (1996). Possible role of calcium release from the sarcoplasmic reticulum in pacemaking in guinea-pig sino-atrial node. *Exp. Physiol.* 81, 877–880. doi: 10.1113/expphysiol.1996.sp003983

Sanders, L., Rakovic, S., Lowe, M., Mattick, P. A., and Terrar, D. A. (2006). Fundamental importance of Na+-Ca2+ exchange for the pacemaking mechanism in guinea-pig sino-atrial node. *J. Physiol.* 571, 639–649. doi: 10.1113/jphysiol.2005.100305

Tang, Q., Jin, M. W., Xiang, J. Z., Dong, M. Q., Sun, H. Y., Lau, C. P., et al. (2007). The membrane permeable calcium chelator BAPTA-AM directly blocks human ether a-go-go-related gene potassium channels stably expressed in HEK 293 cells. *Biochem. Pharmacol.* 74, 1596–1607. doi: 10.1016/j.bcp.2007.07.042

Vinogradova, T. M., Lyashkov, A. E., Zhu, W., Ruknudin, A. M., Sirenko, S., Yang, D., et al. (2006). High basal protein kinase A-dependent phosphorylation drives rhythmic internal Ca^{2+} store oscillations and spontaneous beating of cardiac pacemaker cells. *Circ. Res.* 98, 505–514. doi: 10.1161/01.RES.0000204575.94040.d1

Vinogradova, T. M., Maltsev, V. A., Bogdanov, K. Y., Lyashkov, A. E., and Lakatta, E. G. (2005). Rhythmic Ca^{2+} oscillations drive sinoatrial nodal cell pacemaker function to make the heart tick. *Ann. N.Y. Acad. Sci.* 1047, 138–156. doi: 10.1196/annals.1341.013

Vinogradova, T. M., Zhou, Y. Y., Bogdanov, K. Y., Yang, D., Kuschel, M., Cheng, H., et al. (2000). Sinoatrial node pacemaker activity requires $Ca^{(2+)}$/calmodulin-dependent protein kinase II activation. *Circ. Res.* 87, 760–767. doi: 10.1161/01.RES.87.9.760

Vinogradova, T. M., Zhou, Y. Y., Maltsev, V., Lyashkov, A., Stern, M., and Lakatta, E. G. (2004). Rhythmic ryanodine receptor Ca^{2+} releases during diastolic depolarization of sinoatrial pacemaker cells do not require membrane depolarization. *Circ. Res.* 94, 802–809. doi: 10.1161/01.RES.0000122045.55331.0F

Xie, Y., Ding, W. G., and Matsuura, H. (2015). Ca(2+)/calmodulin potentiates I Ks in sinoatrial node cells by activating Ca(2+)/calmodulin-dependent protein kinase II. *Pflugers Arch.* 467, 241–251. doi: 10.1007/s00424-014-1507-1

Yaniv, Y., Stern, M. D., Lakatta, E. G., and Maltsev, V. A. (2013). Mechanisms of beat-to-beat regulation of cardiac pacemaker cell function by $Ca^{(2)(+)}$ cycling dynamics. *Biophys. J.* 105, 1551–1561. doi: 10.1016/j.bpj.2013.08.024

Zhou, Z., and Lipsius, S. L. (1993). $Na^{(+)}$-Ca^{2+} exchange current in latent pacemaker cells isolated from cat right atrium. *J. Physiol.* 466, 263–285.

Conflict of Interest Statement: The authors declare that the research was conducted in the absence of any commercial or financial relationships that could be construed as a potential conflict of interest.

Received: 18 December 2014; paper pending published: 22 December 2014; accepted: 14 January 2015; published online: 10 February 2015.

*Citation: Capel RA and Terrar DA (2015) Cytosolic calcium ions exert a major influence on the firing rate and maintenance of pacemaker activity in guinea-pig sinus node. Front. Physiol. **6**:23. doi: 10.3389/fphys.2015.00023*

This article was submitted to Cardiac Electrophysiology, a section of the journal Frontiers in Physiology.

frontiers in
PHYSIOLOGY

MINI REVIEW ARTICLE
published: 13 February 2015
doi: 10.3389/fphys.2015.00028

From two competing oscillators to one coupled-clock pacemaker cell system

Yael Yaniv[1]*, Edward G. Lakatta[2]* and Victor A. Maltsev[2]

[1] *Biomedical Engineering Faculty, Technion-IIT, Haifa, Israel*
[2] *Laboratory of Cardiovascular Science, Biomedical Research Center, Intramural Research Program, National Institute on Aging, National Institutes of Health, Baltimore, MD, USA*

Edited by:
Ming Lei, University of Oxford, UK

Reviewed by:
Sandeep Pandit, University of Michigan, USA
Oleg Aslanidi, King's College London, UK

****Correspondence:***
Yael Yaniv, Biomedical Engineering Faculty, Technion-IIT, Technion City, Haifa 3200003, Israel
e-mail: yaely@bm.technion.ac.il;
Edward G. Lakatta, Laboratory of Cardiovascular Science, Biomedical Research Center, Intramural Research Program, National Institute on Aging, National Institutes of Health, 251 Bayview Blvd, Baltimore 21224, MD, USA,
e-mail: lakattae@grc.nia.nih.gov

At the beginning of this century, debates regarding "what are the main control mechanisms that ignite the action potential (AP) in heart pacemaker cells" dominated the electrophysiology field. The original theory which prevailed for over 50 years had advocated that the ensemble of surface membrane ion channels (i.e., "M-clock") is sufficient to ignite rhythmic APs. However, more recent experimental evidence in a variety of mammals has shown that the sarcoplasmic reticulum (SR) acts as a "Ca^{2+}-clock" rhythmically discharges diastolic local Ca^{2+} releases (LCRs) beneath the cell surface membrane. LCRs activate an inward current (likely that of the Na^+/Ca^{2+} exchanger) that prompts the surface membrane "M-clock" to ignite an AP. Theoretical and experimental evidence has mounted to indicate that this clock "crosstalk" operates on a beat-to-beat basis and determines both the AP firing rate and rhythm. Our review is focused on the evolution of experimental definition and numerical modeling of the coupled-clock concept, on how mechanisms intrinsic to pacemaker cell determine both the heart rate and rhythm, and on future directions to develop further the coupled-clock pacemaker cell concept.

Keywords: arrhythmias, coupled-clock pacemaker system, heart rate variability, mathematical modeling, sinoatrial node

INTRODUCTION

Under normal conditions, specialized, self-excitable pacemaker cells within the sinoatrial node (SAN) initiate the spontaneous action potentials (AP) that are conducted to the ventricle to entrain the rate and rhythm of ventricular myocytes contractions. The identities and the relative roles of the control mechanisms within heart pacemaker cells that ignite the AP have been debated for more than 50 years. The predominant theory later named "M-clock" advocated that the ensemble of surface membrane ion channels was sufficient to ignite spontaneous AP (reviewed in Maltsev et al., 2006). This concept promoted decades of extensive voltage-clamp studies that have led to identification of numerous ion-current components in pacemaker cells (reviewed in Wilders, 2007): L-type Ca^{2+} current ($I_{Ca,L}$), outward-K^+ currents (I_K), etc. Importantly, some but not all investigators concluded that a hyperpolarization-activated "funny" current (I_f), is the dominant M-clock current driving early diastolic depolarization. However, since the time of I_f discovery its major role in cardiac pacemaking was challenged (Vassalle, 1995) and further experimental and theoretical results led to an extensive debate on the role of I_f (reviewed in Maltsev and Lakatta, 2012). In the late 1980s, experimental evidence began to emerge on the role of Ca^{2+} in pacemaker function under normal physiologic conditions (for more details see Maltsev et al., 2006). Subsequent studies discovered that sarcoplasmic reticulum (SR), a major Ca^{2+} store, can spontaneously and rhythmically oscillate Ca^{2+} uptake and release forming additional oscillator mechanism in pacemaker cells, termed Ca^{2+}-clock. Ca^{2+}-clock together with the M-clock form the modern concept that coupled-clock pacemaker system controls the cardiac pacemaker cell function.

To ignite an AP, the Ca^{2+}-clock communicates with the M-clock via multiple Ca^{2+} and voltage-dependent mechanisms (discussed below). Nevertheless, one approach to gain further insights into the systems operation has been to artificially split the two clocks into two separate competing mechanisms (see for example Noble et al., 2010). A major consequence of such approach let to a continuing debate about which clock or pacemaker mechanism is dominant, and which one is minor (i.e., being a follower or entrained) (Lakatta and Difrancesco, 2009; Rosen et al., 2012). An alternative view is that both intracellular and sarcolemmal mechanisms are dynamically and synergistically coupled to each other (**Figure 1**), and the degree of the coupling determines the normal pacemaker function (Lakatta et al., 2010). This view, known as a coupled-clock theory, is based on the results of numerical modeling (Maltsev and Lakatta, 2009, 2010, 2013) and verified by experimental data (Yaniv et al., 2013a, 2014b). Therefore, a modern view on the cardiac pacemaker cell function is that neither clock is dominant; rather it is the coupled-clock system that controls the pacemaker cell AP firing rate and rhythm.

MECHANISMS INTRINSIC TO PACEMAKER CELL DETERMINE THE COUPLED-CLOCK RATE

After more than 50 years of research it is apparent that the pacemaker function is orchestrated via intrinsic signaling mechanisms originating at multiple levels of organization, including subcellular (e.g., phosphorylation cascades, SR, mitochondria), cellular

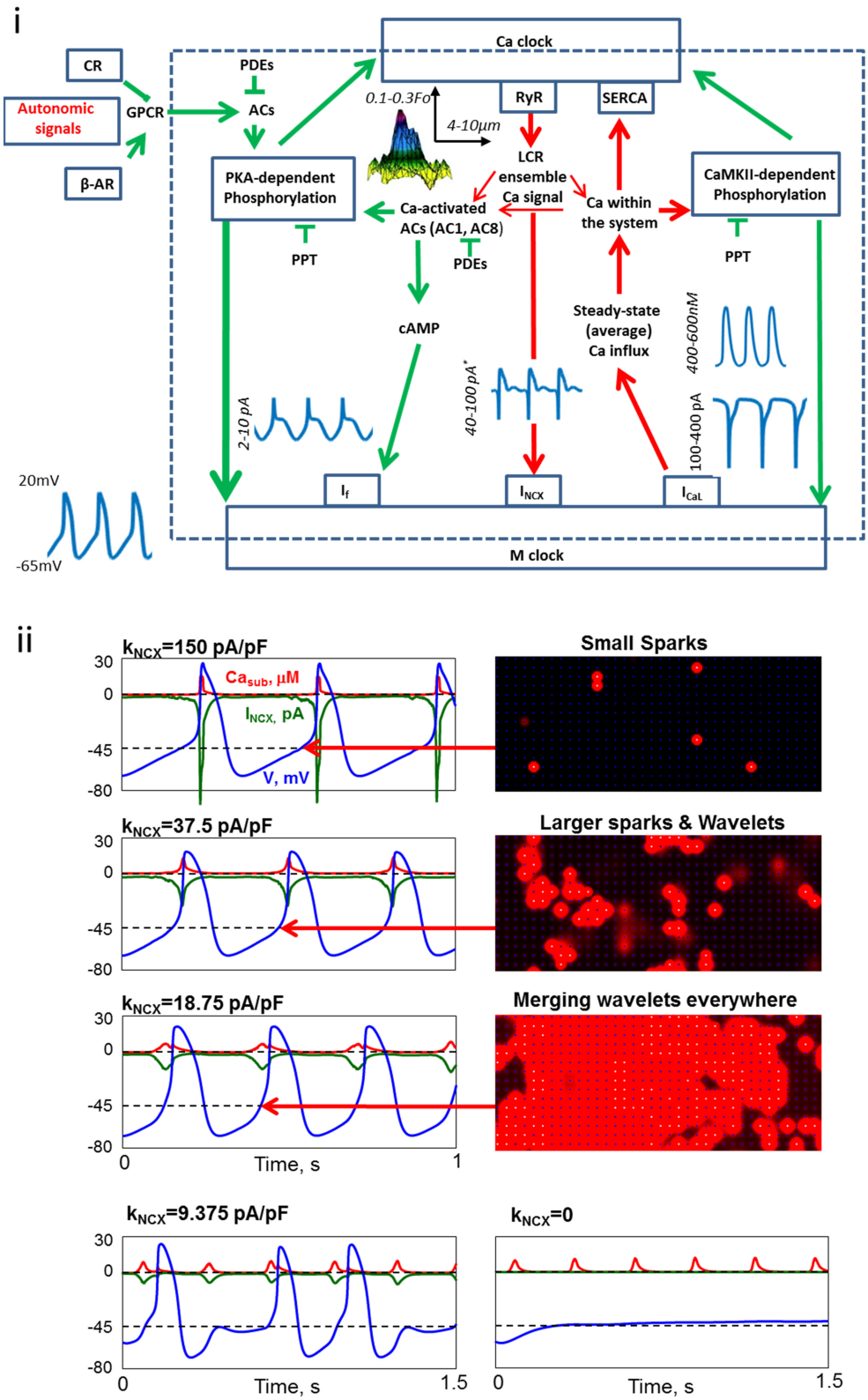

FIGURE 1 | Coupled-clock molecules and brain-heart signaling receptors that drive basal automaticity of SANC. (i) The neurotransmitters noradrenaline (NE) and acetylcholine (ACh) released from sympathetic or parasympathetic nerve terminals bind to β-adrenergic receptors (β-AR) or cholinergic receptors (CR), respectively. Autonomic receptor signaling couples to G-proteins (GPCR) and leads to modulation of the same coupled-clock molecules that drive basal automaticity of SANC.

(Continued)

FIGURE 1 | Continued
Basal Ca^{2+}-calmodulin activation of adenylyl cyclases (AC), which produce cAMP-PKA-dependent phosphorylation and calmodulin-dependent kinase II (CaMKII)-dependent phosphorylation signaling. cAMP positively shifts the f-channel activation curve. Phosphodiesterases (PDE) degrade cAMP production, while protein phosphatase (PPT) degrades phosphorylation activity. PKA and CaMKII signaling phosphorylate SR Ca^{2+} cycling proteins (RyR, phospholamban, which bind to and inhibit SERCA) and surface membrane ion channels.*The values are for I_{NCX} amplitude (within the cycle) achieved during systole, however the diastolic amplitude is almost an order of magnitude lower. **(ii)** Numerical model simulations of membrane potential (blue), I_{NCX} (green) and subspace Ca^{2+} (Ca_{sub}, red) in response to reduction in NCX expression. As NCX expression becomes reduced the spread of Ca^{2+} release between RyRs via Ca^{2+} induced Ca^{2+} release is enhanced, resulting in a more effective activation of the remaining NCX molecules by LCRs. Further reduction in NCX uncoupled (partially or fully) LCR from AP generation. Specifically, NCX current becomes too small to depolarize the membrane and AP generation fail (modified from Maltsev et al., 2013).

(i.e., surface membrane), hierarchical brain-heart signaling (i.e., neurotransmitter or hormonal stimulation of surface membrane receptors) and modulated by environmental mechanical, chemical and thermal factors (**Figure 1**). The SR rhythmically discharges local diastolic Ca^{2+} releases (LCRs) beneath the cell surface membrane; LCRs activate an inward Na^+/Ca^{2+} exchange (NCX) current that prompts the surface membrane clock (M clock), an ensemble of sarcolemmal electrogenic molecules, to generate an AP. LCR Ca^{2+} signal is regulated not only by the SR Ca^{2+} pumping, which depends not only on SR proteins (phospholamban and RyR), and their phosphorylation status, but also by functions and phosphorylation status of M-clock proteins, e.g., L-type Ca^{2+} channels that regulate cell Ca^{2+} available for SR pumping, i.e., Ca^{2+}-clock's substrate or "fuel." LCR signals affect Ca^{2+} -dependent electrogenic processes (such as Na^+/Ca^{2+} exchange) and voltage-dependent Ca^{2+} fluxes (such as via Ca^{2+}-dependent inactivation of L-type Ca^{2+} channels). Therefore, the amplitude and phase of the LCR Ca^{2+} signal sensed by M-clock proteins reports the degree of synchronization and coupling of pacemaker mechanisms of both clocks, i.e., a stronger, more synchronized, and earlier LCR signal to M-clock proteins reports more efficient clock coupling that results in further shortening of the AP-beating interval (BI).

The coupled-clock theory predicts that extremely complex crosstalk between the two clocks via signaling pathways can amplify each other via secondary (indirect) mechanisms (reviewed in Maltsev and Lakatta, 2012), e.g., the crosstalk determines cell Ca^{2+} which, in turn, activates calmodulin-adenylyl cyclase (AC)-dependent protein kinase A (PKA) and Ca^{2+}/calmodulin-dependent protein kinase II (CaMKII) (Mattick et al., 2007; Younes et al., 2008; Yaniv et al., 2013b). These phosphorylation signaling cascades act on both SR (phospholamban and RyR) and M-clock proteins (such as L type Ca^{2+} channels and K^+ channels). Numerical model simulations predict that the diastolic LCR signal is also regulated both by the level of Ca^{2+} cycling, and by the phosphorylation states of coupled-clock proteins (Maltsev and Lakatta, 2009; Yaniv et al., 2013a; Stern et al., 2014). Indeed, the LCR period (i.e., the time period of an LCR occurrence following the prior AP) reports the degree of synchronization of the coupled-clock mechanisms (Monfredi et al., 2013; Yaniv et al., 2013a, 2014b). Thus, during higher degrees of clock coupling AP BI and LCR period are shorter and vice versa. LCRs affect Ca^{2+} dependent mechanisms, specifically NCX, whereas the M-clock effects Ca^{2+} clock primarily via $I_{Ca,L}$. Phosphorylation signaling acts on both clocks and a decrease in its level is correlated with a decrease in the degree of synchronization of the coupled-clock mechanisms (Yaniv et al., 2014b). Numerical evidence has shown the essential roles of both mechanisms to couple clock functions (see below).

Although majority of the original experiments supporting the coupled-clock concept were performed in rabbit pacemaker cells, recent experimental results from mouse genetic models have clarified the role of many coupled-clock components: NCX (Groenke et al., 2013; Herrmann et al., 2013), I_f(Ludwig et al., 1998; Stieber et al., 2004; Herrmann et al., 2007), T-type channels (Mesirca et al., 2014), G protein signaling (Yang et al., 2010; Wydeven et al., 2014), Cav1.3 (Christel et al., 2012), CaMKII activity (Zhang et al., 2005; Gao et al., 2011) and ankyrin-B function (Le Scouarnec et al., 2008). In this regard mice pacemaker cell model provides evidence for the role of TRP channels and IP3 receptors; TRPM4 channels conduct both Na^+ and K^+, but does not conduct Ca^{2+}. TRPM has been recognized as the Ca^{2+}-activated nonselective cation channel (Demion et al., 2007) and its role in modulating AP firing rate has been shown recently (Hof et al., 2013). Specifically, TRPM7 has been shown as a dominant channel-kinase that influences diastolic membrane depolarization (Sah et al., 2013). 1,4,5-trisphosphate (IP3) receptors exist in mice pacemaker and can release Ca^{2+} from the SR contributing to the intracellular Ca^{2+} that couples both clocks (Ju et al., 2011, 2012). Note that the relevant of studies in mice to other species with much lower hear rate has to be proven.

MECHANISMS INTRINSIC TO PACEMAKER CELLS CONTROL AP FIRING RATE AND RHYTHM

The spontaneous AP BI of single isolated pacemaker cells and SAN tissue are roughly periodic, i.e., this period varies on a beat-to-beat basis (Verheijck et al., 1998; Rocchetti et al., 2000; Zaza and Lombardi, 2001; Monfredi et al., 2011; Papaioannou et al., 2013; Yaniv et al., 2014a,b). Recent experimental evidence shows that the degree of clock coupling determines not only the average pacemaker cell AP BI, but also the AP beating interval variability (BIV) (Yaniv et al., 2014b) (**Figure 2**). LCR periods vary among individual LCRs occurring within each spontaneous AP cycle and, similar to AP BI variability, among different cycles (Monfredi et al., 2013; Stern et al., 2014; Yaniv et al., 2014b). The ensemble LCR period and size report the extent of synchronization of the coupled-clock mechanisms. Indeed, the variability in the average LCR period in each cycle is correlated with the variability of the AP BI (Monfredi et al., 2013; Yaniv et al., 2014b) (**Figure 2**) and beat-to-beat variation in periodicity of LCRs is associated with intrinsic variations of spontaneous AP BI (Monfredi et al., 2013). Based on the coupled-clock theory, the stochasticity of LCR Ca^{2+} signal depends on stochastic RyR activation (Stern et al., 2014) and the cell Ca^{2+} balance that in turn is determined, in part, by

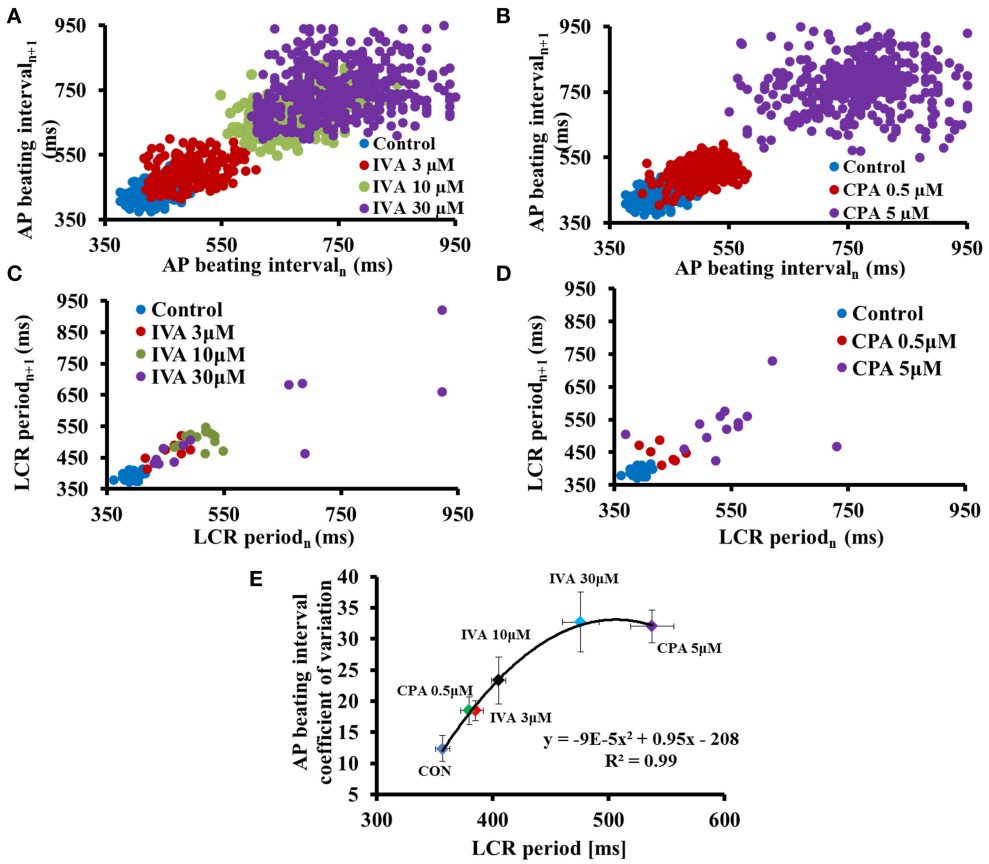

FIGURE 2 | Reduced synchronization of coupled-clock mechanisms prolongs AP beating interval variability and LCR period variability. To unravel clock-crosstalk effects on AP BIV and LCR period variability, clock function was perturbed by directly inhibiting either the M or Ca^{2+}-clock. To inhibit the M-clock, a range of concentrations of ivabradine (IVA), an I_f inhibitor were employed. To inhibit the Ca^{2+}-clock, a range of concentrations of cyclopiazonic acid (CPA), a SR Ca^{2+} pump inhibitor were employed. Poincaré plots of the beating interval in control and in response to **(A)** IVA or **(B)** CPA. Poincaré plots of LCR period in control and in response to **(C)** IVA or **(D)** CPA. **(E)** The relationship between the average AP BIV, quantified by coefficient of variation to the LCR period prior to and in response to different concentrations of either IVA or CPA (modified from Yaniv et al., 2014b).

stochastic sarcolemmal ion channel openings and closings. The occurrence of an AP synchronizes global stochastic RyR activation, and therefore synchronizes subsequent generation of LCRs by the RyRs during the diastolic depolarization phase. The amplitude of LCR Ca^{2+} signal to M-clock proteins reports the efficiency of clock coupling, i.e., a weaker LCR signal to M-clock proteins reports less-efficient clock coupling. At steady state, increase in LCR variability is also linked to reduced peak ensemble LCR Ca^{2+} signal amplitude that occurs later in diastole (i.e., prolonged next AP ignition). Therefore, the extent to which intrinsic clock mechanisms regulates the coupled-clock determines both the steady state BI and BIV in isolated pacemaker cells.

BRAIN MODULATION OF THE INTRINSIC MECHANISMS TO PACEMAKER CELL

The brain imparts flexibility to intrinsic clock mechanisms by concomitant activation of two types of receptors: β-adrenergic receptors (β-AR) that increases the heart rate and cholinergic receptors (CR) that decreases the heart rate (**Figure 1**). In humans, change in receptor activation can change the heart rate from 60 to 240 bpm. Receptor stimulation within pacemaker cells couples the signaling of G-proteins to AC (likely type 5 or 6), leading to activation or suppression of PKA and CaMKII- dependent phosphorylation signaling to key functional proteins of both clocks that regulate pacemaker cell automaticity. Therefore, both brain-heart signaling and intrinsic-pacemaker cell mechanisms signal to the very same nodes (coupling factors, such as PKA and CaMKII, **Figure 1**) of the coupled-clock system

β-AR stimulation in single pacemaker cell not only markedly decreases the average AP BI, but also decreases the AP BIV indices (Zaza et al., 1996; Yaniv et al., 2014a) and increases the likelihood that pacemaker cell BIs exhibit fractal-like behavior (Yaniv et al., 2014a). β-AR stimulation increases the efficiency of the coupled-clock system (Yaniv et al., 2014a). A reduction in LCR variability is associated with increased peak ensemble LCR Ca^{2+} signal that occurs early in diastole (Monfredi et al., 2012; Yaniv et al., 2014b). β-AR stimulation decreases the beating-interval entropy, which in isolated pacemaker cells is within a range that has been documented in random systems. Therefore, β-AR stimulation confers beating interval complexity. CR stimulation, in

contrast, not only markedly increases both the average AP BI and AP BIV indices of single isolated pacemaker cells, but also impairs beating interval complexity (Rocchetti et al., 2000; Zaza and Lombardi, 2001; Yaniv et al., 2014a). Therefore, CR stimulation reduces the efficiency of the clocks coupling (Yaniv et al., 2014a).

THE COUPLED CLOCK SYSTEM OPERATES ON A BEAT-TO-BEAT BASIS

While a mutual entrainment exists between the M and Ca^{2+}-clocks, it was not known if this entrainment happens on a beat-to-beat basis. Patch clamp experiments in single SAN cells (SANC) appeared to show a minor role of Ca^{2+} dynamics in SANC function (Himeno et al., 2011). The spontaneous AP rate was little changed when BAPTA, a Ca^{2+} chelator, was acutely infused via a patch pipette into SANC. These results, however, were later refuted on technical grounds (Maltsev et al., 2011b), taking into account that whole cell configuration generates artificial leak currents that substitute the pacemaker currents.

In contrast to these results, three sets of experiments that rapidly perturb the Ca^{2+}-clock in intact SANC have demonstrated the time-dependent beat-to-beat mutual entrainment between the two clocks. In the first experiment set single isolated rabbit SANC were loaded with a caged Ca^{2+} buffer, NP-EGTA, which induced an increase in AP BI and markedly suppressed LCR Ca^{2+} signals and uncoupled them from AP generation (Yaniv et al., 2011). Flash photolysis released Ca^{2+} from the caged compound, immediately restored Ca^{2+} dynamics and within the same AP cycle. In the second experiment set low concentrations of caffeine (2-4 mM) were rapidly applied to single isolated rabbit SANC (Yaniv et al., 2013c). Caffeine induced immediate Ca^{2+} release from the SR and immediately reduced the AP cycle. Lastly, in each given cycle the phase of the entire ensemble LCR signal (i.e. the average LCR period) is linked to that length of that cycle (Monfredi et al., 2013). Therefore, mutual clock entrainment exists on a beat-to-beat basis.

NUMERICAL MODELING: FROM ONE CLOCK TO ONE COUPLED SYSTEM

The shift from numerical models that describe only the M-clock to the new paradigm of the coupled-clock system occurred in several stages, as new data became available and new respective models were generated. The first model that attempted to explore the importance of Ca^{2+} levels in sub-membrane space with respect to M-clock molecules (specifically the NCX) was formulated by Kurata (Kurata et al., 2002). While this modeling approach reproduced, in part, bradycardic effects of intracellular Ca^{2+} buffering reported earlier in experimental studies (Vinogradova et al., 2000), it remained essentially naive and did not embrace a numerical mechanism of Ca^{2+} "clocking."

The coupled-clock mechanism was established in 2009 (Maltsev and Lakatta, 2009) by a detailed sensitivity analysis of a new pacemaker cell model originated from Kurata et al. model (Kurata et al., 2002). This new model (often referred to as Maltsev-Lakatta model or ML model) included, in addition to the formulations of the M-clock molecules, new formulations of the SR function, predicting oscillatory LCR ensemble Ca^{2+} signals, driven by SR Ca^{2+} pumping and Ca^{2+} release kinetics. The two clocks are coupled in the ML model via multiple coupling factors, such as Ca^{2+}, cAMP, PKA, and CaMKII. Therefore, the SR Ca^{2+}-clock not only modulates the M-clock, but the M-clock, in turn, also affects Ca^{2+}-clock.

This coupled-clock model made important predictions that prompted further studies:

(i) Importance of SR Ca^{2+} refilling kinetics for AP firing rate (confirmed experimentally in Vinogradova et al., 2010)
(ii) Both "biophysical" and "biochemical" entrainments are required to explain complex effects of clock's-specific perturbations (Yaniv et al., 2013a), e.g., by either ivabradine, a specific I_f blocker or cyclopiazonic acid, a specific SR Ca^{2+}-ATPase (SERCA) pump blocker. It was shown that a direct perturbation of one clock inevitably affects the other due to subsequent indirect effects, resulting in mutual entrainment, i.e., clocks coupling, predicted by the theory.
(iii) The entire range of physiological chronotropic modulation of SANC by activation of β-AR or CR can be achieved in simulations of the ML model only when their effect on both sarcolemmal ion channels and SR Ca^{2+} pumping capability are taking into account (Maltsev and Lakatta, 2010).

Of note, other numerical models with unbalanced mutual entrainment between the clocks have been developed (Zhang et al., 2000; Butters et al., 2010; Inada et al., 2014). Specifically, recent numerical model has applied to explain the relationship between heart rate and rhythm (Monfredi et al., 2014). Although these models have some merit and can explain some experimental results, the real test or value of numerical models is to reproduce the experimental data of mutual entrainment on a beat-to-beat basis, which these simplistic models cannot achieve.

Mutual entrainment of the Ca^{2+} and M-clock exists on a beat-to-beat basis (see above). Numerical simulations, using a modified ML "coupled-clock" model, faithfully reproduced experimentally reported prolongation of the AP BI and associated dys-rhythmic spontaneous beating in the presence of cytosolic Ca^{2+} buffering (Yaniv et al., 2013c). However, three contemporary numerical models (Kurata et al., 2002; Severi et al., 2012) and the original ML model (Maltsev and Lakatta, 2009), failed to reproduce the effects of severe and acute perturbations of the system, e.g., the transient reduction in AP BI induced by both caffeine and flash-induced Ca^{2+} release (Yaniv et al., 2013c).

The modified ML model provided new insights into the nature of beat-to-beat clock entrainment (Yaniv et al., 2013c): (i) The major mechanisms that couple the beat-to-beat changes in Ca^{2+}-clock to M-clock mechanisms is LCR-activation of the NCX current. (ii) The systems has a "memory" for several beats: after flash-induced Ca^{2+} release the temporal rate increase are linked to changes in Ca^{2+} available for pumping into the SR that ultimately results in a temporal increase in diastolic NCX current driving the AP firing rate increase.

Recognition of the limitations of the traditional common-pool model approach have led to novel pacemaker cell models featuring local Ca^{2+} control mechanisms (for review see Maltsev et al., 2014). Thus, newer local control models are more accurate vs. old

common pool models: the scale of amplitudes for Ca^{2+} dynamics attained locally is higher by as much as two orders of magnitude vs. that predicted by the old models. The common pool models also lack crucial mechanisms of Ca^{2+} dynamics, such as diffusion-reaction for the Ca^{2+} release, local Ca^{2+} pumping and local NCX activity. The first model (Maltsev et al., 2011a) generated LCRs via stochastic recruitment of the neighboring CRUs. This model was later updated to include LCR regulation by local interactions with M-clock driving by NCX (Maltsev et al., 2013). The model predicted that when the RyR sensitivity is very high or the NCX density is low, synchronization between the clocks is lost, leading to dysrhythmic AP BI (Maltsev et al., 2013). The most recent and advanced formulations of local Ca^{2+} mechanisms in pacemaker cells include stochastic gating of individual RyR and L-type Ca^{2+} channels in Ca^{2+} diffusion and buffering in 3 dimensions (Stern et al., 2014). The model succeeded in reproducing observed propagating local Ca^{2+} releases and realistic pacemaker rates only when RyR locations were assigned taking into account irregular, hierarchical distribution of RyR clusters (small and large) observed in 3D confocal scan sections of immunofluorescence staining.

A new generation of model featuring local Ca^{2+} dynamics within a coupled-clock system is being developed and will provide novel insights into pacemaker cell mechanisms. A "multi-scale" modeling has been put forward by James Weiss group that modeled Ca^{2+} dynamics in cardiac cells (Qu et al., 2011). This approach develops formulations for Ca^{2+} dynamics at each level or scale of integration. This, in turn, represents a substantial challenge and requires a detailed knowledge of the previous layer to avoid simply phenomenological or arbitrary descriptions. In this regard, the recent Stern et al. model (2014), describing states of all individual RyR and L-type Ca^{2+} channel will be helpful to approach the next level integration at the whole cell Ca^{2+} dynamics.

SUMMARY

Mechanisms intrinsic to pacemaker cells and their modulation by the brain-heart receptor signaling determine both the heart rate and heart rate variability. Crosstalk exists between M and Ca^{2+}-clock and the tightness of this crosstalk, informed by the LCR period, determines the rate and rhythm of spontaneous AP generation. Indeed, both theoretical and experimental evidence has mounted to indicate that this clock "crosstalk" operates on a beat-to-beat basis.

In the level of pacemaker cells, future experiments are needed to quantify beat-to-beat regulation of cAMP/PKA signaling that drives clock coupling in order to speculate whether they take part in the mutual entrainment between the clocks in a beat-to-beat basis. Moreover, the extent to which reduction in synchronization of intrinsic clock periods within pacemaker cells is associated with cardiac diseases and aging awaits further elucidation. Finally, novel mathematical models that quantify not only the average AP firing, but also determine its rhythm await further development.

Similar contribution of coupled-clock mechanisms to membrane firing rate and rhythm can exist in other heart tissues. In this regard, crosstalk between Ca^{2+} leak from the SR and NCX current can trigger an arrhythmia in atrial fibrillation patients (Lakatta and Guarnieri, 1993; Voigt et al., 2014). Future work is needed to determine if pacemaking-like behavior exist in atrial cell during normal and abnormal conditions.

ACKNOWLEDGMENTS

This research was partially supported by the Intramural Research Program of the NIH, National Institute on Aging, by Technion V.P.R Fund-Mallat Family Research Fund (YY) and by NSFC-ISF joint research program, No. 398/14 (YY).

REFERENCES

Butters, T. D., Aslanidi, O. V., Inada, S., Boyett, M. R., Hancox, J. C., Lei, M., et al. (2010). Mechanistic links between Na^+ channel (SCN5A) mutations and impaired cardiac pacemaking in sick sinus syndrome. *Circ. Res.* 107, 126–137. doi: 10.1161/CIRCRESAHA.110.219949

Christel, C. J., Cardona, N., Mesirca, P., Herrmann, S., Hofmann, F., Striessnig, J., et al. (2012). Distinct localization and modulation of Cav1.2 and Cav1.3 L-type Ca^{2+} channels in mouse sinoatrial node. *J. Physiol.* 590, 6327–6342. doi: 10.1113/jphysiol.2012.239954

Demion, M., Bois, P., Launay, P., and Guinamard, R. (2007). TRPM4, a Ca2+-activated nonselective cation channel in mouse sino-atrial node cells. *Cardiovasc. Res.* 73, 531–538. doi: 10.1016/j.cardiores.2006.11.023

Gao, Z., Singh, M. V., Hall, D. D., Koval, O. M., Luczak, E. D., Joiner, M. L., et al. (2011). Catecholamine-independent heart rate increases require Ca^{2+}/calmodulin-dependent protein kinase II. *Circ. Arrhythm. Electrophysiol.* 4, 379–387. doi: 10.1161/CIRCEP.110.961771

Groenke, S., Larson, E. D., Alber, S., Zhang, R., Lamp, S. T., Ren, X., et al. (2013). Complete atrial-specific knockout of sodium-calcium exchange eliminates sinoatrial node pacemaker activity. *PLoS ONE* 8:e81633. doi: 10.1371/journal.pone.0081633

Herrmann, S., Lipp, P., Wiesen, K., Stieber, J., Nguyen, H., Kaiser, E., et al. (2013). The cardiac sodium-calcium exchanger NCX1 is a key player in the initiation and maintenance of a stable heart rhythm. *Cardiovasc. Res.* 99, 780–788. doi: 10.1093/cvr/cvt154

Herrmann, S., Stieber, J., Stockl, G., Hofmann, F., and Ludwig, A. (2007). HCN4 provides a 'depolarization reserve' and is not required for heart rate acceleration in mice. *EMBO J.* 26, 4423–4432. doi: 10.1038/sj.emboj.7601868

Himeno, Y., Toyoda, F., Satoh, H., Amano, A., Cha, C. Y., Matsuura, H., et al. (2011). Minor contribution of cytosolic Ca^{2+} transients to the pacemaker rhythm in guinea pig sinoatrial node cells. *Am. J. Physiol. Heart Circ. Physiol.* 300, H251–H261. doi: 10.1152/ajpheart.00764.2010

Hof, T., Simard, C., Rouet, R., Salle, L., and Guinamard, R. (2013). Implication of the TRPM4 nonselective cation channel in mammalian sinus rhythm. *Heart Rhythm* 10, 1683–1689. doi: 10.1016/j.hrthm.2013.08.014

Inada, S., Zhang, H., Tellez, J. O., Shibata, N., Nakazawa, K., Kamiya, K., et al. (2014). Importance of gradients in membrane properties and electrical coupling in sinoatrial node pacing. *PLoS ONE* 9:e94565. doi: 10.1371/journal.pone.0094565

Ju, Y. K., Liu, J., Lee, B. H., Lai, D., Woodcock, E. A., Lei, M., et al. (2011). Distribution and functional role of inositol 1,4,5-trisphosphate receptors in mouse sinoatrial node. *Circ. Res.* 109, 848–857. doi: 10.1161/CIRCRESAHA.111.243824

Ju, Y. K., Woodcock, E. A., Allen, D. G., and Cannell, M. B. (2012). Inositol 1,4,5-trisphosphate receptors and pacemaker rhythms. *J. Mol. Cell. Cardiol.* 53, 375–381. doi: 10.1016/j.yjmcc.2012.06.004

Kurata, Y., Hisatome, I., Imanishi, S., and Shibamoto, T. (2002). Dynamical description of sinoatrial node pacemaking: improved mathematical model for primary pacemaker cell. *Am. J. Physiol. Heart Circ. Physiol.* 283, H2074–H2101. doi: 10.1152/ajpheart.00900.2001

Lakatta, E. G., and Difrancesco, D. (2009). What keeps us ticking: a funny current, a calcium clock, or both? *J. Mol. Cell. Cardiol.* 47, 157–170. doi: 10.1016/j.yjmcc.2009.03.022

Lakatta, E. G., and Guarnieri, T. (1993). Spontaneous myocardial calcium oscillations: are they linked to ventricular fibrillation? *J. Cardiovasc. Electrophysiol.* 4, 473–489. doi: 10.1111/j.1540-8167.1993.tb01285.x

Lakatta, E. G., Maltsev, V. A., and Vinogradova, T. M. (2010). A coupled SYSTEM of intracellular Ca^{2+} clocks and surface membrane voltage clocks controls the timekeeping mechanism of the heart's pacemaker. *Circ. Res.* 106, 659–673. doi: 10.1161/CIRCRESAHA.109.206078

Le Scouarnec, S., Bhasin, N., Vieyres, C., Hund, T. J., Cunha, S. R., Koval, O., et al. (2008). Dysfunction in ankyrin-B-dependent ion channel and transporter targeting causes human sinus node disease. *Proc. Natl. Acad. Sci. U.S.A.* 105, 15617–15622. doi: 10.1073/pnas.0805500105

Ludwig, A., Zong, X., Jeglitsch, M., Hofmann, F., and Biel, M. (1998). A family of hyperpolarization-activated mammalian cation channels. *Nature* 393, 587–591. doi: 10.1038/31255

Maltsev, A. V., Maltsev, V. A., Mikheev, M., Maltseva, L. A., Sirenko, S. G., Lakatta, E. G., et al. (2011a). Synchronization of stochastic $Ca^{(2)(+)}$ release units creates a rhythmic $Ca^{(2)(+)}$ clock in cardiac pacemaker cells. *Biophys. J.* 100, 271–283. doi: 10.1016/j.bpj.2010.11.081

Maltsev, A. V., Yaniv, Y., Stern, M. D., Lakatta, E. G., and Maltsev, V. A. (2013). RyR-NCX-SERCA local cross-talk ensures pacemaker cell function at rest and during the fight-or-flight reflex. *Circ. Res.* 113, e94–e100. doi: 10.1161/CIRCRESAHA.113.302465

Maltsev, V. A., and Lakatta, E. G. (2009). Synergism of coupled subsarcolemmal Ca^{2+} clocks and sarcolemmal voltage clocks confers robust and flexible pacemaker function in a novel pacemaker cell model. *Am. J. Physiol. Heart Circ. Physiol.* 296, H594–H615. doi: 10.1152/ajpheart.01118.2008

Maltsev, V. A., and Lakatta, E. G. (2010). A novel quantitative explanation for the autonomic modulation of cardiac pacemaker cell automaticity via a dynamic system of sarcolemmal and intracellular proteins. *Am. J. Physiol. Heart Circ. Physiol.* 298, H2010–H2023. doi: 10.1152/ajpheart.00783.2009

Maltsev, V. A., and Lakatta, E. G. (2012). The funny current in the context of the coupled-clock pacemaker cell system. *Heart Rhythm* 9, 302–307. doi: 10.1016/j.hrthm.2011.09.022

Maltsev, V. A., and Lakatta, E. G. (2013). Numerical models based on a minimal set of sarcolemmal electrogenic proteins and an intracellular $Ca^{(2+)}$ clock generate robust, flexible, and energy-efficient cardiac pacemaking. *J. Mol. Cell. Cardiol.* 59, 181–195. doi: 10.1016/j.yjmcc.2013.03.004

Maltsev, V. A., Vinogradova, T. M., and Lakatta, E. G. (2006). The emergence of a general theory of the initiation and strength of the heartbeat. *J. Pharmacol. Sci.* 100, 338–369. doi: 10.1254/jphs.CR0060018

Maltsev, V. A., Vinogradova, T. M., Stern, M. D., and Lakatta, E. G. (2011b). Letter to the editor: "Validating the requirement for beat-to-beat coupling of the Ca2+ clock and M clock in pacemaker cell normal automaticity." *Am. J. Physiol. Heart Circ. Physiol.* 300, H2323–H2324; author reply H2325–H2326.

Maltsev, V. A., Yaniv, Y., Maltsev, A. V., Stern, M. D., and Lakatta, E. G. (2014). Modern perspectives on numerical modeling of cardiac pacemaker cell. *J. Pharmacol. Sci.* 125, 6–38. doi: 10.1254/jphs.13R04CR

Mattick, P., Parrington, J., Odia, E., Simpson, A., Collins, T., and Terrar, D. (2007). Ca^{2+}-stimulated adenylyl cyclase isoform AC1 is preferentially expressed in guinea-pig sino-atrial node cells and modulates the I(f) pacemaker current. *J. Physiol.* 582, 1195–1203. doi: 10.1113/jphysiol.2007.133439

Mesirca, P., Torrente, A. G., and Mangoni, M. E. (2014). T-type channels in the sino-atrial and atrioventricular pacemaker mechanism. *Pflugers Arch.* 466, 791–799. doi: 10.1007/s00424-014-1482-6

Monfredi, O. J., Maltseva, L. A., Boyett, M. R., Lakatta, E. G., and Maltsev, V. A. (2011). Stochastic beat-to-beat variation in periodicity of local calcium releases predicts intrinsic cycle length variability in single sinoatrial node cells. *Biophys. J.* 100, 558a. doi: 10.1016/j.bpj.2010.12.3243

Monfredi, O., Lakatta, E. G., and Maltsev, A. V. (2012). Synchronization of local calcium releases by beta-adrenergic stimulation in cardiac pacemaker cells. *Biophys. J.* 102, 103a. doi: 10.1016/j.bpj.2011.11.581

Monfredi, O., Lyashkov, A. E., Johnsen, A. B., Inada, S., Schneider, H., Wang, R., et al. (2014). Biophysical characterization of the underappreciated and important relationship between heart rate variability and heart rate. *Hypertension* 64, 1334–1343. doi: 10.1161/HYPERTENSIONAHA.114.03782

Monfredi, O., Maltseva, L. A., Spurgeon, H. A., Boyett, M. R., Lakatta, E. G., and Maltsev, V. A. (2013). Beat-to-beat variation in periodicity of local calcium releases contributes to intrinsic variations of spontaneous cycle length in isolated single sinoatrial node cells. *PLoS ONE* 8:e67247. doi: 10.1371/journal.pone.0067247

Noble, D., Noble, P. J., and Fink, M. (2010). Competing oscillators in cardiac pacemaking: historical background. *Circ. Res.* 106, 1791–1797. doi: 10.1161/CIRCRESAHA.110.218875

Papaioannou, V. E., Verkerk, A. O., Amin, A. S., and De Bakker, J. M. (2013). Intracardiac origin of heart rate variability, pacemaker funny current and their possible association with critical illness. *Curr. Cardiol. Rev.* 9, 82–96. doi: 10.2174/157340313805076359

Qu, Z., Garfinkel, A., Weiss, J. N., and Nivala, M. (2011). Multi-scale modeling in biology: how to bridge the gaps between scales? *Prog. Biophys. Mol. Biol.* 107, 21–31. doi: 10.1016/j.pbiomolbio.2011.06.004

Rocchetti, M., Malfatto, G., Lombardi, F., and Zaza, A. (2000). Role of the input/output relation of sinoatrial myocytes in cholinergic modulation of heart rate variability. *J. Cardiovasc. Electrophysiol.* 11, 522–530. doi: 10.1111/j.1540-8167.2000.tb00005.x

Rosen, M. R., Nargeot, J., and Salama, G. (2012). The case for the funny current and the calcium clock. *Heart Rhythm* 9, 616–618. doi: 10.1016/j.hrthm.2011.10.008

Sah, R., Mesirca, P., Van Den Boogert, M., Rosen, J., Mably, J., Mangoni, M. E., et al. (2013). Ion channel-kinase TRPM7 is required for maintaining cardiac automaticity. *Proc. Natl. Acad. Sci. U.S.A.* 110, E3037–E3046. doi: 10.1073/pnas.1311865110

Severi, S., Fantini, M., Charawi, L. A., and Difrancesco, D. (2012). An updated computational model of rabbit sinoatrial action potential to investigate the mechanisms of heart rate modulation. *J. Physiol.* 590, 4483–4499. doi: 10.1113/jphysiol.2012.229435

Stern, M. D., Maltseva, L. A., Juhaszova, M., Sollott, S. J., Lakatta, E. G., and Maltsev, V. A. (2014). Hierarchical clustering of ryanodine receptors enables emergence of a calcium clock in sinoatrial node cells. *J. Gen. Physiol.* 143, 577–604. doi: 10.1085/jgp.201311123

Stieber, J., Hofmann, F., and Ludwig, A. (2004). Pacemaker channels and sinus node arrhythmia. *Trends Cardiovasc. Med.* 14, 23–28. doi: 10.1016/j.tcm.2003.09.006

Vassalle, M. (1995). The pacemaker current (I(f)) does not play an important role in regulating SA node pacemaker activity. *Cardiovasc. Res.* 30, 309–310. doi: 10.1016/0008-6363(95)00028-3

Verheijck, E. E., Wilders, R., Joyner, R. W., Golod, D. A., Kumar, R., Jongsma, H. J., et al. (1998). Pacemaker synchronization of electrically coupled rabbit sinoatrial node cells. *J. Gen. Physiol.* 111, 95–112. doi: 10.1085/jgp.111.1.95

Vinogradova, T. M., Brochet, D. X., Sirenko, S., Li, Y., Spurgeon, H., and Lakatta, E. G. (2010). Sarcoplasmic reticulum Ca^{2+} pumping kinetics regulates timing of local Ca^{2+} releases and spontaneous beating rate of rabbit sinoatrial node pacemaker cells. *Circ. Res.* 107, 767–775. doi: 10.1161/CIRCRESAHA.110.220517

Vinogradova, T. M., Zhou, Y. Y., Bogdanov, K. Y., Yang, D., Kuschel, M., Cheng, H., et al. (2000). Sinoatrial node pacemaker activity requires $Ca^{(2+)}$/calmodulin-dependent protein kinase II activation. *Circ. Res.* 87, 760–767. doi: 10.1161/01.RES.87.9.760

Voigt, N., Heijman, J., Wang, Q., Chiang, D. Y., Li, N., Karck, M., et al. (2014). Cellular and molecular mechanisms of atrial arrhythmogenesis in patients with paroxysmal atrial fibrillation. *Circulation* 129, 145–156. doi: 10.1161/CIRCULATIONAHA.113.006641

Wilders, R. (2007). Computer modelling of the sinoatrial node. *Med. Biol. Eng. Comput.* 45, 189–207. doi: 10.1007/s11517-006-0127-0

Wydeven, N., Posokhova, E., Xia, Z., Martemyanov, K. A., and Wickman, K. (2014). RGS6, but not RGS4, is the dominant regulator of G protein signaling (RGS) modulator of the parasympathetic regulation of mouse heart rate. *J. Biol. Chem.* 289, 2440–2449. doi: 10.1074/jbc.M113.520742

Yang, J., Huang, J., Maity, B., Gao, Z., Lorca, R. A., Gudmundsson, H., et al. (2010). RGS6, a modulator of parasympathetic activation in heart. *Circ. Res.* 107, 1345–1349. doi: 10.1161/CIRCRESAHA.110.224220

Yaniv, Y., Ahmet, I., Liu, J., Lyashkov, A. E., Guiriba, T. R., Okamoto, Y., et al. (2014a). Synchronization of sinoatrial node pacemaker cell clocks and its autonomic modulation impart complexity to heart beating intervals. *Heart Rhythm* 11, 1210–1219. doi: 10.1016/j.hrthm.2014.03.049

Yaniv, Y., Lyashkov, A. E., Sirenko, S., Okamoto, Y., Guiriba, T. R., Ziman, B. D., et al. (2014b). Stochasticity intrinsic to coupled-clock mechanisms underlies beat-to-beat variability of spontaneous action potential firing in sinoatrial node pacemaker cells. *J. Mol. Cell. Cardiol.* 77, 1–10. doi: 10.1016/j.yjmcc.2014.09.008

Yaniv, Y., Maltsev, V. A., Escobar, A. L., Spurgeon, H. A., Ziman, B. D., Stern, M. D., et al. (2011). Beat-to-beat $Ca^{(2+)}$-dependent regulation of sinoatrial

nodal pacemaker cell rate and rhythm. *J. Mol. Cell. Cardiol.* 51, 902–905. doi: 10.1016/j.yjmcc.2011.08.029

Yaniv, Y., Sirenko, S., Ziman, B. D., Spurgeon, H. A., Maltsev, V. A., and Lakatta, E. G. (2013a). New evidence for coupled clock regulation of the normal automaticity of sinoatrial nodal pacemaker cells: bradycardic effects of ivabradine are linked to suppression of intracellular $Ca^{(2)(+)}$ cycling. *J. Mol. Cell. Cardiol.* 62, 80–89. doi: 10.1016/j.yjmcc.2013.04.026

Yaniv, Y., Spurgeon, H. A., Ziman, B. D., and Lakatta, E. G. (2013b). $Ca^{(2)+}$/calmodulin-dependent protein kinase II (CaMKII) activity and sinoatrial nodal pacemaker cell energetics. *PLoS ONE* 8:e57079. doi: 10.1371/journal.pone.0057079

Yaniv, Y., Stern, M. D., Lakatta, E. G., and Maltsev, V. A. (2013c). Mechanisms of beat-to-beat regulation of cardiac pacemaker cell function by $Ca^{(2)(+)}$ cycling dynamics. *Biophys. J.* 105, 1551–1561. doi: 10.1016/j.bpj.2013.08.024

Younes, A., Lyashkov, A. E., Graham, D., Sheydina, A., Volkova, M. V., Mitsak, M., et al. (2008). $Ca^{(2+)}$ -stimulated basal adenylyl cyclase activity localization in membrane lipid microdomains of cardiac sinoatrial nodal pacemaker cells. *J. Biol. Chem.* 283, 14461–14468. doi: 10.1074/jbc.M707540200

Zaza, A., and Lombardi, F. (2001). Autonomic indexes based on the analysis of heart rate variability: a view from the sinus node. *Cardiovasc. Res.* 50, 434–442. doi: 10.1016/S0008-6363(01)00240-1

Zaza, A., Robinson, R. B., and Difrancesco, D. (1996). Basal responses of the L-type Ca^{2+} and hyperpolarization-activated currents to autonomic agonists in the rabbit sino-atrial node. *J. Physiol.* 491(Pt 2), 347–355. doi: 10.1113/jphysiol.1996.sp021220

Zhang, H., Holden, A. V., Kodama, I., Honjo, H., Lei, M., Varghese, T., et al. (2000). Mathematical models of action potentials in the periphery and center of the rabbit sinoatrial node. *Am. J. Physiol. Heart Circ. Physiol.* 279, H397–H421.

Zhang, R., Khoo, M. S., Wu, Y., Yang, Y., Grueter, C. E., Ni, G., et al. (2005). Calmodulin kinase II inhibition protects against structural heart disease. *Nat. Med.* 11, 409–417. doi: 10.1038/nm1215

Conflict of Interest Statement: The authors declare that the research was conducted in the absence of any commercial or financial relationships that could be construed as a potential conflict of interest.

Received: 30 November 2014; paper pending published: 20 December 2014; accepted: 17 January 2015; published online: 13 February 2015.

*Citation: Yaniv Y, Lakatta EG and Maltsev VA (2015) From two competing oscillators to one coupled-clock pacemaker cell system. Front. Physiol. **6**:28. doi: 10.3389/fphys.2015.00028*

This article was submitted to Cardiac Electrophysiology, a section of the journal Frontiers in Physiology.

frontiers in
PHYSIOLOGY

MINI REVIEW ARTICLE
published: 09 February 2015
doi: 10.3389/fphys.2015.00034

Endosome-based protein trafficking and Ca^{2+} homeostasis in the heart

***Jerry Curran*[1,2]*, *Michael A. Makara*[1,2] *and Peter J. Mohler*[1,2,3]**

[1] *The Dorothy M. Davis Heart and Lung Research Institute, The Ohio State University Wexner Medical Center, Columbus, OH, USA*
[2] *Department of Physiology and Cell Biology, The Ohio State University Wexner Medical Center, Columbus, OH, USA*
[3] *Department of Internal Medicine, The Ohio State University Wexner Medical Center, Columbus, OH, USA*

Edited by:
Christopher Huang, University of Cambridge, UK

Reviewed by:
Ravi C. Balijepalli, University of Wisconsin, USA
Jin O-Uchi, Thomas Jefferson University, USA

***Correspondence:**
Jerry Curran, The Davis Heart and Lung Research Institute, The Ohio State University, 473 W. 12th Ave., Columbus, OH 43210, USA
e-mail: jerry.curran@osumc.edu

The ability to dynamically regulate, traffic, retain, and recycle proteins within the cell membrane is fundamental to life and central to the normal function of the heart. In the cardiomyocyte, these pathways are essential for the regulation of Ca^{2+}, both at the level of the plasma membrane, but also in local cellular domains. One intracellular pathway often overlooked in relation to cardiovascular Ca^{2+} regulation and signaling is the endosome-based trafficking pathway. Highlighting its importance, this system and its molecular components are evolutionarily conserved across all metazoans. However, remarkably little is known of how endosome-based protein trafficking and recycling functions within mammalian cells systems, especially in the heart. As the endosomal system acts to regulate the expression and localization of membrane proteins central for cardiac Ca^{2+} regulation, understanding the *in vivo* function of this system in the heart is critical. This review will focus on endosome-based protein trafficking in the heart in both health and disease with special emphasis for the role of endocytic regulatory proteins, C-terminal Eps15 homology domain-containing proteins (EHDs).

Keywords: endosome, protein trafficking, cardiac membrane excitability, Ca^{2+} homeostasis, heart failure

INTRODUCTION

The capacity of a cell to regulate protein expression and localization within the plasma membrane is central to life. Endosome-based systems mediate a wide range of cellular processes including anterograde trafficking of newly formed proteins out of the Golgi apparatus to their proper locales, internalization of membrane proteins targeted for recycling or degradation, and nutrient endocytosis. Studying these systems in the intact mammalian cellular environment has proven difficult, mostly due to the lack of available tools and model systems. Only within the last 15 years have we begun teasing out the role of endosome-based protein trafficking and targeting recycling *in vivo*. We now know that endosome-based systems are critical for such cellular processes as cell motility (Traynor and Kay, 2007), cell division (Boucrot and Kirchhausen, 2007), cell-cell junction regulation (Palacios et al., 2002), epithelial polarity (Shivas et al., 2010), and neuronal plasticity (Wang et al., 2008). A growing body of evidence has implicated endosomal trafficking in the development and regulation of membrane excitability in neurons (Sun et al., 2014), pancreatic cells (Manna et al., 2010), and cardiac muscle cells (McEwen et al., 2007; Kruse et al., 2009; Ishii et al., 2012; Curran et al., 2014).

In cardiomyocytes, membrane excitability depends on the proper expression and organization of multiple ion channels, pumps, exchangers, and transporters within the plasma membrane to regulate intracellular ion signaling pathways. As the endosomal system acts to regulate the expression and localization of membrane proteins, the potential exists that this system may be able to modulate excitability in the heart. This regulatory capacity, therefore, makes it an attractive candidate for new therapeutic intervention in the treatment of arrhythmia and sudden cardiac death.

ENDOSOMAL TRANSPORT AND CARDIAC EXCITABILITY

Only recently were efforts undertaken to determine the *in vivo* role of endosomal pathways in the cardiomyocyte. With the development of new tools, years of discovery in surrogate cell systems may now be translated into mammalian cardiovascular biology. Years of investigation have demonstrated that C-terminal Eps15 homology domain-containing (EHD) proteins have a functional role in each segment of endosome-mediated recycling, degradation, and trafficking. EHDs have therefore recently attracted significant attention as potential therapeutic targets to modulate endosomal function (Gudmundsson et al., 2010, 2012; Curran et al., 2014). As cardiac arrhythmia may arise from dysfunctional expression and organization of multiple membrane proteins leading to altered Na^{+} and Ca^{2+} homeostasis, therapeutically modulating EHD proteins may prove efficacious in the treatment of arrhythmia and sudden cardiac death.

EHDs are endocytic regulatory proteins. Discovered in the last decade, four EHD gene products (EHD1–4) are ubiquitously, albeit differentially-expressed across all tissue types (Pohl et al., 2000). These proteins are highly conserved throughout mammalian biology. Indeed, the human and mouse isoforms of EHD1 share 99.6% sequence similarity (Naslavsky and Caplan, 2005). EHD orthologs in non-mammalian species conserve this

similarity as well. These data strongly indicate that this family of proteins plays a similar and central role in metazoan cell biology.

The protein family acquires its name from the presence of an epidermal growth factor receptor substrate 15 (Eps15) homology (EH) domain within the C-terminus (**Figures 1A,B**) (Lee et al., 2005). By itself, the EH domain is well known to mediate protein/protein interactions (Salcini et al., 1997; Paoluzi et al., 1998; Doria et al., 1999; Confalonieri and Di Fiore, 2002; Naslavsky and Caplan, 2005). This domain typically interacts with proteins that contain an NPF (asparagine-proline-phenylalanine) motif (Morgan et al., 2003; Henry et al., 2010; Kieken et al., 2010). Over 50 proteins containing at least one EH domain have been identified in the eukaryotic proteome (Polo et al., 2003; Miliaras and Wendland, 2004). In the *C. elegans* proteome there are more than 800 proteins that contain at least one NPF motif, with more expected in eukaryotes (Pant et al., 2009). Therefore, the potential for protein/protein interactions in this system is substantial. With particular importance to this review, proteins containing an EH domain are often associated with vesicular trafficking, transport, and sorting (Santolini et al., 1999; Confalonieri and Di Fiore, 2002).

Amongst the identified proteins containing one or more EH domains, the overwhelming majority of them contain this domain within the N-terminus. Only a small handful have an EH domain in the C-terminus (Confalonieri and Di Fiore, 2002). Notably however, EHD1–4 all express the EH domain within the C-terminus. The EHD family share high homology with the *C. elegans* endocytic regulator protein, receptor-mediated endocytosis 1 (RME-1), which also has a C-terminal EH domain. RME-1 is known to mediate endosomal trafficking. Therefore, the distinctive location of the EH domain in mammalian paralogs suggested an *in vivo* functional role of these proteins. When RME-1 function is disrupted in *C. elegans*, endosome-based protein recycling is significantly impaired (Grant et al., 2001). Critically, Lin et al. found that expressing the human RME-1 ortholog, EHD1, in *C. elegans* could fully rescue this phenotype (Lin et al., 2001). This is unambiguous evidence that not only are C-terminal EHD proteins directly involved in endosomal trafficking, but their function is highly conserved across metazoans.

One or more EHDs have been demonstrated to play key roles within every endosome-based protein trafficking compartment.

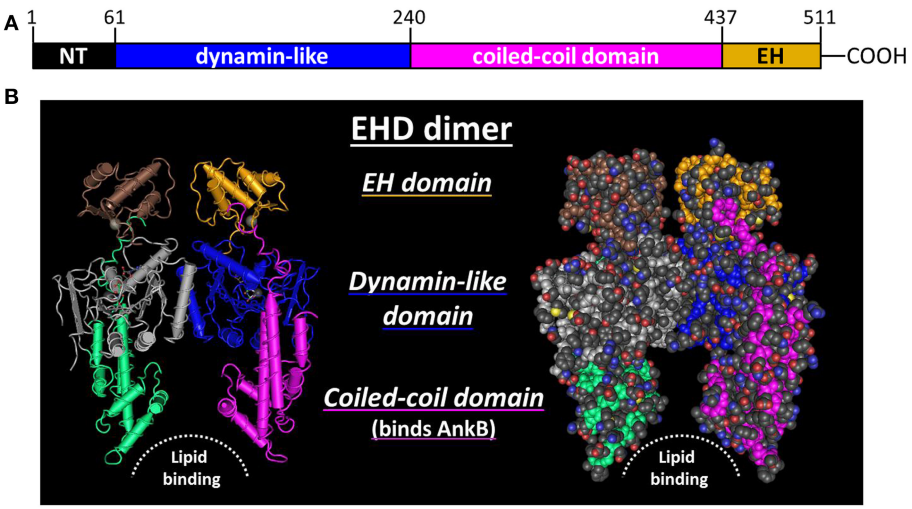

C

Sequence homology % (EH domain identity %)	EHD4	EHD3	EHD2
EHD1	74.1% (68.1%)	86.5% (81.5%)	70.3% (58.7%)
EHD2	67.9% (53.0%)	70.5% (57.3%)	
EHD3	74.3% (66.7%)		

FIGURE 1 | EHD protein structure and sequence homology. (A) Each EHD protein is contains an N-terminal region (NT), a dynamin-like domain, a coiled-coil domain, and a C-terminal EH domain. Typically, the EH domain mediates protein:protein interactions with EHDs. **(B)** Ribbon and space filling models of an EHD protein, based on the known crystal structure of EHD2 determined by Daumke et al. (2007). **(C)** The homology of total amino acid sequence and EH domain identity amongst the four EHD proteins expressed in mammals (Naslavsky and Caplan, 2011). Note that the overall sequence homology is greater than the homology shared amongst the EH domains.

EHDs promote anterograde trafficking from the TGN to the plasma membrane, along with internalization, recycling, and degradation pathways (see Naslavsky and Caplan for an expert review, Naslavsky and Caplan, 2011). While the specific molecular roles of EHD1–4 at the level of the vesicle remains poorly defined, they are hypothesized to serve two simultaneous functions. First, EHDs act as scaffolding proteins for key molecular players within the endosome. EHD1–4 have all been demonstrated to associate with Rab effector proteins (e.g., Rab11-Fip2, Rabenosyn-5, MICAL-L1) within membranous vesicular compartments *in vivo* (Naslavsky et al., 2004, 2006; George et al., 2007; Sharma et al., 2008, 2010). EHD proteins may recruit Rab effector proteins to the vesicle, although this function is not consistently observed (Naslavsky et al., 2004, 2006). Once present within the vesicle, the Rab effector can bind to individual Rab proteins that, in turn, recruit motor proteins such as myosin and dynein (Roland et al., 2007; Horgan and McCaffrey, 2011; Schafer et al., 2014). Indeed, recent reports have linked EHD1 with dynein motors (Rahajeng et al., 2010).

A second, more established role for EHDs is that of membrane scission. An elegant study by Daumke et al. demonstrated that when the G domain of an EHD is bound to ATP it will dimerize, forming either hetero- or homo-dimers (**Figure 1B**). This creates a membrane binding pocket within the protein complex (Daumke et al., 2007). These dimers then oligomerize to form ring-like structures around membranous. Upon ATP hydrolysis, the membrane binding pocket collapses, destabilizing the associated membrane, effectively pinching off the vesicle from the tubule to facilitate its transport. Indeed, based on this function, EHD4 is often termed "Pincher" in the literature (Shao et al., 2002; Smith et al., 2004). Combined with the scaffolding role and the association with Rab and Rab effectors, these findings nicely situate EHD proteins to be central players in endosome-based protein trafficking *in vivo*.

EHD PROTEINS IN HEART

Nearly all that is known regarding the EHD protein family has resulted from investigations using surrogate cell systems or model organisms. The study of endosomal systems *in vivo* has been hampered by the lack of appropriate tools. Only recently has a concerted effort been made to develop the molecular and biochemical tools and animal models necessary to study these systems *in vivo*. For this reason, remarkably little is known not just about how these systems function in the heart but even about the identity of the various molecular players involved.

In 2010, Gudmundsson et al. were the first to report that EHD1–4 were differentially expressed in the four chambers of the heart (Gudmundsson et al., 2010). EHD1–4 were each shown to localize within the perinuclear junction and also in discrete puncta spanning from the nucleus out to the plasma membrane, locales consistent with their role in endosomal trafficking (Sharma et al., 2009). Further, a direct protein/protein interaction was reported between EHD3 and the cytoskeletal membrane adapter protein, ankyrin-B (AnkB) (Gudmundsson et al., 2010). Interestingly, this protein/protein interaction was not mediated through the EH domain of EHD3 but rather through the coiled-coil domain. Early in the initial studies of EHD1–4, Naslavsky and Caplan astutely noted that the overall identity shared by EHD1–4 was higher than that shared between their individual EH domains (**Figure 1C**). They speculated that the conserved functions of EHD1–4 may not rely on the EH domain (Naslavsky and Caplan, 2005). The surprising finding that EHD3 interacts with AnkB through the coiled-coil domain supports this speculation and has potentially broader functional implications for EHD1–4.

Recall, the EH domain directly mediates protein/protein interactions. Moreover, in the case of EHD proteins, the EH domain has been demonstrated to mediate interactions with Rab effectors and Rab proteins. By interacting with cargo proteins, such as AnkB, through the coiled-coil region, this would free up the EH domain to still conduct its business with the motor protein complex (Rabs/Rab effectors). This places the EHD protein in a central position within the vesicular complex. It not only binds to, and recruits the motor complex, it may also simultaneously mediate cargo retention within the endosome. This observation may prove fundamental to our understanding of how EHD-dependent endosomal trafficking occurs *in vivo*.

In the heart, AnkB regulates cardiac calcium and contractility by controlling the proper targeting and retention of the Na/Ca exchanger (NCX), Na/K ATPase (NKA), inositol 1,4,5-trisphosphate receptor, and protein phosphatase 2A (Mohler et al., 2005; Degrande et al., 2013). Their appropriate subcellular localization is critical to maintaining proper cardiac function. The importance of the relationship between AnkB and these proteins is highlighted in patients harboring single point variants within *ANK2*, encoding for AnkB (Mohler et al., 2003, 2007). These variants result in a loss-of-function of AnkB and the mislocalization of the associated proteins. Consequently, cardiac function is severely compromised. These patients suffer from a complex arrhythmogenic phenotype ranging from ventricular and atrial fibrillation, sinus node disease, atrioventricular conduction block, and sudden cardiac death (Mohler et al., 2003).

Given the direct interaction between AnkB and EHD3, it was hypothesized that silencing EHD3 expressing in the cardiomyocyte would result a mislocalization of AnkB and its binding partners. Indeed, this was observed. Upon EHD3 silencing by siRNA, AnkB and NCX localization were disrupted. Both proteins were mislocalized within a perinuclear compartment. These data suggest that the cell is still synthesizing the protein, but it was not being trafficked to or retained at the proper subcellular location. In line with this, the NCX-mediated membrane current (I_{NCX}) was significantly downregulated (Gudmundsson et al., 2010). Interestingly, this same report also demonstrated that upon EHD3 overexpression in wild type myocytes, I_{NCX} increased. This suggests that endosomal pathways could potentially be targeted to fine tune membrane excitability. This was the first evidence that EHD3 (or any EHD) played a functional role in cardiomyocytes to regulate intracellular calcium.

EHD3 MEDIATES MEMBRANE EXCITABILITY AND Ca^{2+} HOMEOSTASIS *IN VIVO*

Using newly established mouse models of EHD deficiency, Curran et al. provided the first data on the role of EHDs in the intact heart. EHD3 was found to play critical roles in maintaining membrane excitability and proper Ca^{2+} homeostasis *in vivo*

(Curran et al., 2014). Hearts from EHD3$^{-/-}$ mice showed dysregulated AnkB and NCX trafficking and targeting. In isolated adult ventricular myocytes lacking EHD3, these proteins were mislocalized within a perinuclear compartment. Interestingly, in the EHD3$^{-/-}$ mouse, NCX protein expression was down by only 20%, while I_{NCX} was down by approximately 50%. A similar finding was reported for the L-type Ca channel (LTCC). The loss of EHD3 led to significant mislocalization of the protein. While overall LTCC protein expression was down less than 20%, the peak LTCC-mediated membrane current ($I_{Ca,L}$) was down by approximately 67%. Together, these data suggest that the myocyte is still synthesizing the NCX and LTCC protein, but the loss of EHD3 has limited its ability to properly traffic them to their correct subcellular localizations. Currently, there is no known interaction between the LTCC and AnkB, implying that the LTCC is being trafficked in an EHD3-dependent manner that does not require AnkB. This expands the purview of EHD3 function beyond that of just AnkB-mediated targeting to include direct or indirect interactions with other ion channels and transporters.

The LTCC and NCX are intimately involved in EC coupling and are central players in the maintenance of Ca^{2+} homeostasis in the heart (Bers, 2002). The $I_{Ca,L}$ triggers further Ca^{2+} release from the sarcoplasmic reticulum (SR) through the SR Ca^{2+} release channel, ryanodine receptor (RyR), a process called Ca^{2+}-induced Ca^{2+} release (Bers, 2001). This Ca^{2+} release induces muscle contraction. The amount of Ca^{2+} released ultimately dictates the strength of contraction. Ca^{2+} release is primarily dictated by two mechanisms: the size of the Ca^{2+} trigger and the size of the SR Ca^{2+} load. If one of these is downregulated and the other remains the same, the result will be diminished Ca^{2+} release and strength of contraction, or vice versa.

Therefore, one would expect that dysregulation of the LTCC and NCX observed in the EHD3-deficient mouse would have ramifications on EC coupling. Indeed, in ventricular myocytes isolated from EHD3$^{-/-}$ mice, the average SR Ca^{2+} load was increased approximately 40%. This is likely a compensatory response to the downregulation of the $I_{Ca,L}$ and I_{NCX}. The loss of these two membrane currents would favor Ca^{2+} retention in the cell, thereby increasing the SR Ca^{2+} concentration (Bers et al., 1996; McCall et al., 1998). This increase in SR Ca^{2+} concentration would have the effect of sensitizing the RyR to Ca^{2+}, thereby promoting increased Ca^{2+} release in the face of downregulated Ca^{2+} trigger (Bassani et al., 1995). In this fashion, contractility was maintained in the EHD3-deficient heart, similar to observations in mice deficient in NCX (Pott et al., 2005).

EHD3-dependent trafficking mechanisms will likely include other ion channels and transporters. The action potential duration (APD) of EHD3$^{-/-}$ myocytes was approximately 60% shorter compared to WT (Curran et al., 2014). While the NCX and the LTCC both play roles in mediating the APD, even if combined the amount of membrane current lost due to dysregulation of these proteins in the EHD3$^{-/-}$ heart cannot account for such a drastic shortening of the APD. This strongly suggests that EHD3 mediates the trafficking of other ion channels or regulatory proteins pertinent to developing the action potential. Future investigations should aim at uncovering the relationship between EHD3 and these other proteins, particularly the family of potassium channels.

HEART RHYTHM, AUTOMATICITY, AND CONDUCTION DEFECTS IN EHD3-DEFICIENT HEARTS

Beyond their roles in Ca^{2+} homeostasis and contraction in the heart, the NCX and LTCC also mediate automaticity and action potential conduction (Lyashkov et al., 2007; Monfredi et al., 2013a,b). In particular, they play vital roles within the "Ca^{2+} clock" machinery of the sinoatrial node (SAN) where they facilitate spontaneous membrane depolarization and the origin of the cardiac action potential (Maltsev and Lakatta, 2009; Lakatta et al., 2010). Further, LTCC function is required for the proper conduction of the action potential from the atria to the ventricle through the atrioventricular node (Zhang et al., 2011). Disruption of NCX and LTCC function would be expected to have considerable consequences on cardiac rhythm and action potential conduction.

EHD3 is expressed in the SAN (Curran et al., 2014). Given the functional role of EHD3 in trafficking and targeting the NCX and LTCC, dysregulation of cardiac automaticity in these mice would be predicted. Indeed, significant increases in heart rate variability and SAN pause were observed in the EHD3-deficient mouse. Furthermore, incidences of antrioventricular (AV) node conduction block were routinely detected. These observations strongly suggest that EHD3-dependent endosomal trafficking is required for proper cardiac automaticity and conduction. While no data yet exists investigating EHD3 function directly in SAN or AV node cells, it is intriguing to envision that NCX and LTCC trafficking and function are dysregulated in a similar manner as is observed in the ventricle. It is likely that the rhythm and conduction disturbances observed in EHD3-deficient mice are directly related to dysregulated NCX and LTCC function.

EHD PROTEINS AND HEART FAILURE

In nearly all forms of heart failure, a common observation is the increased expression and function of NCX within the membrane. While initially a compensatory mechanism, this increased NCX expression eventually becomes maladaptive and supplies an arrhythmogenic substrate (Pogwizd et al., 1992, 1999). This membrane remodeling is not limited to human, as increased NCX expression is commonly observed in animal models of heart failure (Baartscheer et al., 2003; Wei et al., 2007; Wang et al., 2009; Kohlhaas and Maack, 2010). This suggests that this response is evolutionarily conserved. Development of a specific pharmacological inhibitor of the NCX aimed at attenuating arrhythmogenesis is an area of active research. However, success in this endeavor has been elusive.

Recent data has indicated that EHD3 is also increased in human heart failure and in all animal models of heart failure yet examined (Gudmundsson et al., 2012). This observation coupled with what is now known about EHD3-dependent NCX trafficking in the heart provides a plausible molecular mechanism by which the heart mediates NCX expression in response to heart failure. These data imply that EHD3 may be involved in the electrical remodeling of the plasma membrane associated with heart failure. If this is the case, EHD-dependent endosomal trafficking may

provide a new approach to developing novel therapeutics against arrhythmia. A significant amount of work must be undertaken to more fully describe the function and molecular machinery of these endosomal trafficking pathways in the heart.

CONCLUSION AND FUTURE DIRECTIONS

A deeper understanding of endosomal trafficking may offer new avenues for therapies against arrhythmia and heart failure. The vast majority of arrhythmias are associated with ion channel or transporter dysfunction. For this reason, the field has pushed for ion channel-based therapeutic strategies. While the logic behind this approach is sound, it has unfortunately been met with limited success. In fact, as the CAST-II trial revealed, when anti-arrhythmic drugs were administered to patients, the rate of arrhythmogenesis in these patients increased (Greene et al., 1992). A secondary approach is therefore needed. Targeting the endosomal trafficking of specific ion channels and transporters may provide that approach.

ACKNOWLEDGMENT

This work was funded by NIH Grants F32 HL114252 (to Jerry Curran), HL084583, HL083422, HL114383 (to Peter J. Mohler), and the American Heart Association.

REFERENCES

Baartscheer, A., Schumacher, C. A., Belterman, C. N., Coronel, R., and Fiolet, J. W. (2003). $[Na^+]i$ and the driving force of the Na^+/Ca^{2+}-exchanger in heart failure. *Cardiovasc. Res.* 57, 986–995. doi: 10.1016/S0008-6363(02)00848-9

Bassani, J. W., Yuan, W., and Bers, D. M. (1995). Fractional SR Ca release is regulated by trigger Ca and SR Ca content in cardiac myocytes. *Am. J. Physiol.* 268, C1313–C1319.

Bers, D. M. (2001). *Excitation-Contraction Coupling and Cardiac Contractile Force.* (Dordrecht: Kluwer Academic Publishers). doi: 10.1007/978-94-010-0658-3

Bers, D. M. (2002). Cardiac excitation-contraction coupling. *Nature* 415, 198–205. doi: 10.1038/415198a

Bers, D. M., Bassani, J. W., and Bassani, R. A. (1996). Na-Ca exchange and Ca fluxes during contraction and relaxation in mammalian ventricular muscle. *Ann. N.Y. Acad. Sci.* 779, 430–442. doi: 10.1111/j.1749-6632.1996.tb44818.x

Boucrot, E., and Kirchhausen, T. (2007). Endosomal recycling controls plasma membrane area during mitosis. *Proc. Natl. Acad. Sci. U.S.A.* 104, 7939–7944. doi: 10.1073/pnas.0702511104

Confalonieri, S., and Di Fiore, P. P. (2002). The Eps15 homology (EH) domain. *FEBS Lett.* 513, 24–29. doi: 10.1016/S0014-5793(01)03241-0

Curran, J., Makara, M. A., Little, S. C., Musa, H., Liu, B., Wu, X., et al. (2014). EHD3-dependent endosome pathway regulates cardiac membrane excitability and physiology. *Circ. Res.* 115, 68–78. doi: 10.1161/CIRCRESAHA.115.304149

Daumke, O., Lundmark, R., Vallis, Y., Martens, S., Butler, P. J., and McMahon, H. T. (2007). Architectural and mechanistic insights into an EHD ATPase involved in membrane remodelling. *Nature* 449, 923–927. doi: 10.1038/nature06173

Degrande, S. T., Little, S. C., Nixon, D. J., Wright, P., Snyder, J., Dun, W., et al. (2013). Molecular mechanisms underlying cardiac protein phosphatase 2A regulation in heart. *J. Biol. Chem.* 288, 1032–1046. doi: 10.1074/jbc.M112.426957

Doria, M., Salcini, A. E., Colombo, E., Parslow, T. G., Pelicci, P. G., and Di Fiore, P. P. (1999). The eps15 homology (EH) domain-based interaction between eps15 and hrb connects the molecular machinery of endocytosis to that of nucleocytosolic transport. *J. Cell Biol.* 147, 1379–1384. doi: 10.1083/jcb.147.7.1379

George, M., Ying, G., Rainey, M. A., Solomon, A., Parikh, P. T., Gao, Q., et al. (2007). Shared as well as distinct roles of EHD proteins revealed by biochemical and functional comparisons in mammalian cells and *C. elegans. BMC Cell Biol.* 8:3. doi: 10.1186/1471-2121-8-3

Grant, B., Zhang, Y., Paupard, M. C., Lin, S. X., Hall, D. H., and Hirsh, D. (2001). Evidence that RME-1, a conserved *C. elegans* EH-domain protein, functions in endocytic recycling. *Nat. Cell. Biol.* 3, 573–579. doi: 10.1038/35078549

Greene, H. L., Roden, D. M., Katz, R. J., Woosley, R. L., Salerno, D. M., and Henthorn, R. W. (1992). The Cardiac Arrhythmia Suppression Trial: first CAST…then CAST-II. *J. Am. Coll. Cardiol.* 19, 894–898. doi: 10.1016/0735-1097(92)90267-Q

Gudmundsson, H., Curran, J., Kashef, F., Snyder, J. S., Smith, S. A., Vargas-Pinto, P., et al. (2012). Differential regulation of EHD3 in human and mammalian heart failure. *J. Mol. Cell. Cardiol.* 52, 1183–1190. doi: 10.1016/j.yjmcc.2012.02.008

Gudmundsson, H., Hund, T. J., Wright, P. J., Kline, C. F., Snyder, J. S., Qian, L., et al. (2010). EH domain proteins regulate cardiac membrane protein targeting. *Circ. Res.* 107, 84–95. doi: 10.1161/CIRCRESAHA.110.216713

Henry, G. D., Corrigan, D. J., Dineen, J. V., and Baleja, J. D. (2010). Charge effects in the selection of NPF motifs by the EH domain of EHD1. *Biochemistry* 49, 3381–3392. doi: 10.1021/bi100065r

Horgan, C. P., and McCaffrey, M. W. (2011). Rab GTPases and microtubule motors. *Biochem. Soc. Trans.* 39, 1202–1206. doi: 10.1042/BST0391202

Ishii, K., Norota, I., and Obara, Y. (2012). Endocytic regulation of voltage-dependent potassium channels in the heart. *J. Pharmacol. Sci.* 120, 264–269. doi: 10.1254/jphs.12R12CP

Kieken, F., Sharma, M., Jovic, M., Giridharan, S. S., Naslavsky, N., Caplan, S., et al. (2010). Mechanism for the selective interaction of C-terminal Eps15 homology domain proteins with specific Asn-Pro-Phe-containing partners. *J. Biol. Chem.* 285, 8687–8694. doi: 10.1074/jbc.M109.045666

Kohlhaas, M., and Maack, C. (2010). Adverse bioenergetic consequences of Na^+-Ca^{2+} exchanger-mediated Ca^{2+} influx in cardiac myocytes. *Circulation* 122, 2273–2280. doi: 10.1161/CIRCULATIONAHA.110.968057

Kruse, M., Schulze-Bahr, E., Corfield, V., Beckmann, A., Stallmeyer, B., Kurtbay, G., et al. (2009). Impaired endocytosis of the ion channel TRPM4 is associated with human progressive familial heart block type I. *J. Clin. Invest.* 119, 2737–2744. doi: 10.1172/JCI38292

Lakatta, E. G., Maltsev, V. A., and Vinogradova, T. M. (2010). A coupled SYSTEM of intracellular Ca^{2+} clocks and surface membrane voltage clocks controls the timekeeping mechanism of the heart's pacemaker. *Circ. Res.* 106, 659–673. doi: 10.1161/CIRCRESAHA.109.206078

Lee, D. W., Zhao, X., Scarselletta, S., Schweinsberg, P. J., Eisenberg, E., Grant, B. D., et al. (2005). ATP binding regulates oligomerization and endosome association of RME-1 family proteins. *J. Biol. Chem.* 280, 17213–17220. doi: 10.1074/jbc.M412751200

Lin, S. X., Grant, B., Hirsh, D., and Maxfield, F. R. (2001). Rme-1 regulates the distribution and function of the endocytic recycling compartment in mammalian cells. *Nat. Cell Biol.* 3, 567–572. doi: 10.1038/35078543

Lyashkov, A. E., Juhaszova, M., Dobrzynski, H., Vinogradova, T. M., Maltsev, V. A., Juhasz, O., et al. (2007). Calcium cycling protein density and functional importance to automaticity of isolated sinoatrial nodal cells are independent of cell size. *Circ. Res.* 100, 1723–1731. doi: 10.1161/CIRCRESAHA.107.153676

Maltsev, V. A., and Lakatta, E. G. (2009). Synergism of coupled subsarcolemmal Ca^{2+} clocks and sarcolemmal voltage clocks confers robust and flexible pacemaker function in a novel pacemaker cell model. *Am. J. Physiol. Heart Circ. Physiol.* 296, H594–H615. doi: 10.1152/ajpheart.01118.2008

Manna, P. T., Smith, A. J., Taneja, T. K., Howell, G. J., Lippiat, J. D., and Sivaprasadarao, A. (2010). Constitutive endocytic recycling and protein kinase C-mediated lysosomal degradation control K(ATP) channel surface density. *J. Biol. Chem.* 285, 5963–5973. doi: 10.1074/jbc.M109.066902

McCall, E., Ginsburg, K. S., Bassani, R. A., Shannon, T. R., Qi, M., Samarel, A. M., et al. (1998). Ca flux, contractility, and excitation-contraction coupling in hypertrophic rat ventricular myocytes. *Am. J. Physiol.* 274, H1348–H1360.

McEwen, D. P., Schumacher, S. M., Li, Q., Benson, M. D., Iniguez-Lluhi, J. A., Van Genderen, K. M., et al. (2007). Rab-GTPase-dependent endocytic recycling of Kv1.5 in atrial myocytes. *J. Biol. Chem.* 282, 29612–29620. doi: 10.1074/jbc.M704402200

Miliaras, N. B., and Wendland, B. (2004). EH proteins: multivalent regulators of endocytosis (and other pathways). *Cell Biochem. Biophys.* 41, 295–318. doi: 10.1385/CBB:41:2:295

Mohler, P. J., Davis, J. Q., and Bennett, V. (2005). Ankyrin-B coordinates the Na/K ATPase, Na/Ca exchanger, and InsP3 receptor in a cardiac T-tubule/SR microdomain. *PLoS Biol.* 3:e423. doi: 10.1371/journal.pbio.0030423

Mohler, P. J., Healy, J. A., Xue, H., Puca, A. A., Kline, C. F., Allingham, R. R., et al. (2007). Ankyrin-B syndrome: enhanced cardiac function balanced by risk of cardiac death and premature senescence. *PLoS ONE* 2:e1051. doi: 10.1371/journal.pone.0001051

Mohler, P. J., Schott, J. J., Gramolini, A. O., Dilly, K. W., Guatimosim, S., Dubell, W. H., et al. (2003). Ankyrin-B mutation causes type 4 long-QT cardiac

arrhythmia and sudden cardiac death. *Nature* 421, 634–639. doi: 10.1038/nature01335

Monfredi, O., Maltseva, L. A., Spurgeon, H. A., Boyett, M. R., Lakatta, E. G., and Maltsev, V. A. (2013b). Beat-to-beat variation in periodicity of local calcium releases contributes to intrinsic variations of spontaneous cycle length in isolated single sinoatrial node cells. *PLoS ONE* 8:e67247. doi: 10.1371/journal.pone.0067247

Monfredi, O., Maltsev, V. A., and Lakatta, E. G. (2013a). Modern concepts concerning the origin of the heartbeat. *Physiology (Bethesda)* 28, 74–92. doi: 10.1152/physiol.00054.2012

Morgan, J. R., Prasad, K., Jin, S., Augustine, G. J., and Lafer, E. M. (2003). Eps15 homology domain-NPF motif interactions regulate clathrin coat assembly during synaptic vesicle recycling. *J. Biol. Chem.* 278, 33583–33592. doi: 10.1074/jbc.M304346200

Naslavsky, N., Boehm, M., Backlund, P. S. Jr., and Caplan, S. (2004). Rabenosyn-5 and EHD1 interact and sequentially regulate protein recycling to the plasma membrane. *Mol. Biol. Cell* 15, 2410–2422. doi: 10.1091/mbc.E03-10-0733

Naslavsky, N., and Caplan, S. (2005). C-terminal EH-domain-containing proteins: consensus for a role in endocytic trafficking, EH? *J. Cell Sci.* 118, 4093–4101. doi: 10.1242/jcs.02595

Naslavsky, N., and Caplan, S. (2011). EHD proteins: key conductors of endocytic transport. *Trends Cell Biol.* 21, 122–131. doi: 10.1016/j.tcb.2010.10.003

Naslavsky, N., Rahajeng, J., Sharma, M., Jovic, M., and Caplan, S. (2006). Interactions between EHD proteins and Rab11-FIP2: a role for EHD3 in early endosomal transport. *Mol. Biol. Cell* 17, 163–177. doi: 10.1091/mbc.E05-05-0466

Palacios, F., Schweitzer, J. K., Boshans, R. L., and D'Souza-Schorey, C. (2002). ARF6-GTP recruits Nm23-H1 to facilitate dynamin-mediated endocytosis during adherens junctions disassembly. *Nat. Cell Biol.* 4, 929–936. doi: 10.1038/ncb881

Pant, S., Sharma, M., Patel, K., Caplan, S., Carr, C. M., and Grant, B. D. (2009). AMPH-1/Amphiphysin/Bin1 functions with RME-1/Ehd1 in endocytic recycling. *Nat. Cell Biol.* 11, 1399–1410. doi: 10.1038/ncb1986

Paoluzi, S., Castagnoli, L., Lauro, I., Salcini, A. E., Coda, L., Fre, S., et al. (1998). Recognition specificity of individual EH domains of mammals and yeast. *EMBO J.* 17, 6541–6550. doi: 10.1093/emboj/17.22.6541

Pogwizd, S. M., Hoyt, R. H., Saffitz, J. E., Corr, P. B., Cox, J. L., and Cain, M. E. (1992). Reentrant and focal mechanisms underlying ventricular tachycardia in the human heart. *Circulation* 86, 1872–1887. doi: 10.1161/01.CIR.86.6.1872

Pogwizd, S. M., Qi, M., Yuan, W., Samarel, A. M., and Bers, D. M. (1999). Upregulation of $Na^{(+)}/Ca^{(2+)}$ exchanger expression and function in an arrhythmogenic rabbit model of heart failure. *Circ. Res.* 85, 1009–1019. doi: 10.1161/01.RES.85.11.1009

Pohl, U., Smith, J. S., Tachibana, I., Ueki, K., Lee, H. K., Ramaswamy, S., et al. (2000). EHD2, EHD3, and EHD4 encode novel members of a highly conserved family of EH domain-containing proteins. *Genomics* 63, 255–262. doi: 10.1006/geno.1999.6087

Polo, S., Confalonieri, S., Salcini, A. E., and Di Fiore, P. P. (2003). EH and UIM: endocytosis and more. *Sci STKE* 2003:re17. doi: 10.1126/stke.2132003re17.

Pott, C., Philipson, K. D., and Goldhaber, J. I. (2005). Excitation-contraction coupling in Na^+-Ca^{2+} exchanger knockout mice: reduced transsarcolemmal Ca^{2+} flux. *Circ. Res.* 97, 1288–1295. doi: 10.1161/01.RES.0000196563.84231.21

Rahajeng, J., Giridharan, S. S., Naslavsky, N., and Caplan, S. (2010). Collapsin response mediator protein-2 (Crmp2) regulates trafficking by linking endocytic regulatory proteins to dynein motors. *J. Biol. Chem.* 285, 31918–31922. doi: 10.1074/jbc.C110.166066

Roland, J. T., Kenworthy, A. K., Peranen, J., Caplan, S., and Goldenring, J. R. (2007). Myosin Vb interacts with Rab8a on a tubular network containing EHD1 and EHD3. *Mol. Biol. Cell.* 18, 2828–2837. doi: 10.1091/mbc.E07-02-0169

Salcini, A. E., Confalonieri, S., Doria, M., Santolini, E., Tassi, E., Minenkova, O., et al. (1997). Binding specificity and *in vivo* targets of the EH domain, a novel protein-protein interaction module. *Genes Dev.* 11, 2239–2249. doi: 10.1101/gad.11.17.2239

Santolini, E., Salcini, A. E., Kay, B. K., Yamabhai, M., and Di Fiore, P. P. (1999). The EH network. *Exp. Cell Res.* 253, 186–209. doi: 10.1006/excr.1999.4694

Schafer, J. C., Baetz, N. W., Lapierre, L. A., McRae, R. E., Roland, J. T., and Goldenring, J. R. (2014). Rab11-FIP2 interaction with MYO5B regulates movement of Rab11a-containing recycling vesicles. *Traffic* 15, 292–308. doi: 10.1111/tra.12146

Shao, Y., Akmentin, W., Toledo-Aral, J. J., Rosenbaum, J., Valdez, G., Cabot, J. B., et al. (2002). Pincher, a pinocytic chaperone for nerve growth factor/TrkA signaling endosomes. *J. Cell Biol.* 157, 679–691. doi: 10.1083/jcb.200201063

Sharma, M., Giridharan, S. S., Rahajeng, J., Caplan, S., and Naslavsky, N. (2010). MICAL-L1: an unusual Rab effector that links EHD1 to tubular recycling endosomes. *Commun. Integr. Biol.* 3, 181–183. doi: 10.4161/cib.3.2.10845

Sharma, M., Giridharan, S. S., Rahajeng, J., Naslavsky, N., and Caplan, S. (2009). MICAL-L1 links EHD1 to tubular recycling endosomes and regulates receptor recycling. *Mol. Biol. Cell* 20, 5181–5194. doi: 10.1091/mbc.E09-06-0535

Sharma, M., Naslavsky, N., and Caplan, S. (2008). A role for EHD4 in the regulation of early endosomal transport. *Traffic* 9, 995–1018. doi: 10.1111/j.1600-0854.2008.00732.x

Shivas, J. M., Morrison, H. A., Bilder, D., and Skop, A. R. (2010). Polarity and endocytosis: reciprocal regulation. *Trends Cell Biol.* 20, 445–452. doi: 10.1016/j.tcb.2010.04.003

Smith, C. A., Dho, S. E., Donaldson, J., Tepass, U., and McGlade, C. J. (2004). The cell fate determinant numb interacts with EHD/Rme-1 family proteins and has a role in endocytic recycling. *Mol. Biol. Cell* 15, 3698–3708. doi: 10.1091/mbc.E04-01-0026

Sun, H., Lu, L., Zuo, Y., Wang, Y., Jiao, Y., Zeng, W. Z., et al. (2014). Kainate receptor activation induces glycine receptor endocytosis through PKC deSUMOylation. *Nat. Commun.* 5, 4980. doi: 10.1038/ncomms5980.

Traynor, D., and Kay, R. R. (2007). Possible roles of the endocytic cycle in cell motility. *J. Cell Sci.* 120, 2318–2327. doi: 10.1242/jcs.007732

Wang, S., Ziman, B., Bodi, I., Rubio, M., Zhou, Y. Y., D'Souza, K., et al. (2009). Dilated cardiomyopathy with increased SR Ca^{2+} loading preceded by a hypercontractile state and diastolic failure in the alpha(1C)TG mouse. *PLoS ONE* 4:e4133. doi: 10.1371/journal.pone.0004133

Wang, Z., Edwards, J. G., Riley, N., Provance, D. W. Jr., Karcher, R., Li, X. D., et al. (2008). Myosin Vb mobilizes recycling endosomes and AMPA receptors for postsynaptic plasticity. *Cell* 135, 535–548. doi: 10.1016/j.cell.2008.09.057

Wei, S. K., McCurley, J. M., Hanlon, S. U., and Haigney, M. C. (2007). Gender differences in Na/Ca exchanger current and beta-adrenergic responsiveness in heart failure in pig myocytes. *Ann. N.Y. Acad. Sci.* 1099, 183–189. doi: 10.1196/annals.1387.026

Zhang, Q., Timofeyev, V., Qiu, H., Lu, L., Li, N., Singapuri, A., et al. (2011). Expression and roles of Cav1.3 (alpha1D) L-type $Ca^{(2)+}$ channel in atrioventricular node automaticity. *J. Mol. Cell. Cardiol.* 50, 194–202. doi: 10.1016/j.yjmcc.2010.10.002

Conflict of Interest Statement: The authors declare that the research was conducted in the absence of any commercial or financial relationships that could be construed as a potential conflict of interest.

Received: 29 October 2014; accepted: 21 January 2015; published online: 09 February 2015.

*Citation: Curran J, Makara MA and Mohler PJ (2015) Endosome-based protein trafficking and Ca^{2+} homeostasis in the heart. Front. Physiol. **6**:34. doi: 10.3389/fphys.2015.00034*

This article was submitted to Cardiac Electrophysiology, a section of the journal Frontiers in Physiology.

frontiers in PHYSIOLOGY

REVIEW ARTICLE
published: 02 February 2015
doi: 10.3389/fphys.2015.00019

Functional role of voltage gated Ca^{2+} channels in heart automaticity

Pietro Mesirca[1,2,3]*, Angelo G. Torrente[1,2,3] and Matteo E. Mangoni[1,2,3]

[1] Laboratory of Excellence in Ion Channel Science and Therapeutics, Département de Physiologie, Institut de Génomique Fonctionnelle, Montpellier, France
[2] UMR-5203, Centre National de la Recherche Scientifique, Universités de Montpellier 1 and 2, Montpellier, France
[3] INSERM U 1191, Département de Physiologie, Universités de Montpellier 1 and 2, Montpellier, France

Edited by:
Ming Lei, University of Oxford, UK

Reviewed by:
Arie O. Verkerk, University of Amsterdam, Netherlands
Yue-kun Ju, University of Sydney, Australia

***Correspondence:**
Pietro Mesirca, Laboratory of Excellence in Ion Channel Science and Therapeutics, Département de Physiologie, Institut de Génomique Fonctionnelle; UMR-5203, Centre National de la Recherche Scientifique, Universités de Montpellier 1 and 2; INSERM U 1191, Département de Physiologie, Universités de Montpellier 1 and 2, 141 Rue de la Cardonille, 34094 Montpellier, France
e-mail: pietro.mesirca@igf.cnrs.fr

Pacemaker activity of automatic cardiac myocytes controls the heartbeat in everyday life. Cardiac automaticity is under the control of several neurotransmitters and hormones and is constantly regulated by the autonomic nervous system to match the physiological needs of the organism. Several classes of ion channels and proteins involved in intracellular Ca^{2+} dynamics contribute to pacemaker activity. The functional role of voltage-gated calcium channels (VGCCs) in heart automaticity and impulse conduction has been matter of debate for 30 years. However, growing evidence shows that VGCCs are important regulators of the pacemaker mechanisms and play also a major role in atrio-ventricular impulse conduction. Incidentally, studies performed in genetically modified mice lacking L-type $Ca_V1.3$ ($Ca_V1.3^{-/-}$) or T-type $Ca_V3.1$ ($Ca_V3.1^{-/-}$) channels show that genetic inactivation of these channels strongly impacts pacemaking. In cardiac pacemaker cells, VGCCs activate at negative voltages at the beginning of the diastolic depolarization and importantly contribute to this phase by supplying inward current. Loss-of-function of these channels also impairs atrio-ventricular conduction. Furthermore, inactivation of $Ca_V1.3$ channels promotes also atrial fibrillation and flutter in knockout mice suggesting that these channels can play a role in stabilizing atrial rhythm. Genomic analysis demonstrated that $Ca_V1.3$ and $Ca_V3.1$ channels are widely expressed in pacemaker tissue of mice, rabbits and humans. Importantly, human diseases of pacemaker activity such as congenital bradycardia and heart block have been attributed to loss-of-function of $Ca_V1.3$ and $Ca_V3.1$ channels. In this article, we will review the current knowledge on the role of VGCCs in the generation and regulation of heart rate and rhythm. We will discuss also how loss of Ca^{2+} entry through VGCCs could influence intracellular Ca^{2+} handling and promote atrial arrhythmias.

Keywords: heart automaticity, L-type Ca^{2+} channel, T-type Ca^{2+} channels, sinoatrial node, atrioventricular node

INTRODUCTION

Pacemaker activity in the heart is generated by specialized myocytes, able to generate periodical oscillations of their membrane potential. These cells are thus called "pacemaker" cells (Mangoni and Nargeot, 2008). Pacemaker cells are localized in the sino-atrial node (SAN), which is a thin tissue located in the right atrium (for anatomical description see Dobrzynski et al., 2005). Under physiological conditions the cardiac impulse has origin in the SAN. The pacemaker impulse spreads from the SAN to the cardiac conduction system (composed by the atrioventricular node and Purkinje fibers network), driving the contraction of the whole working myocardium. In comparison to the rest of the conduction system, the SAN generates the fastest intrinsic automaticity, thereby inhibiting pacemaking in the atrioventricular node (AVN) and the Purkinje fibers network. Nevertheless, in case of SAN failure, the AVN can take over as dominant pacemaker center. Under conditions of atrioventricular block, Purkinje fibers are able to generate viable rhythm, even if at relatively low rates (James, 2003; Dobrzynski et al., 2013).

The generation of the automaticity in cardiac pacemaker cells is due to the diastolic depolarization, a spontaneous slowly depolarizing phase of the action potential cycle. During this phase the membrane potential progressively becomes less negative until it reaches the threshold for triggering a new action potential. The SAN action potential cycle length determines the heart rate. At the level of the individual SAN cell, different classes of ion channels of the plasma membrane, the sarcoplasmic reticulum (SR) and mytochondria contribute to the generation and regulation of automaticity, but their respective functional roles and interactions are still not fully understood.

In the recent past, two distinct, but not mutually exclusively, hypotheses were proposed to explain the mechanism underling the cardiac automaticity: the so-called "membrane clock" model of pacemaking, which considers the "funny" current (I_f), an inward Na^+/K^+ current activated by membrane hyperpolarization at negative voltages (Brown et al., 1979) and regulated directly by cAMP (Difrancesco and Tortora, 1991) as the key initiator of the diastolic depolarization (Difrancesco, 1991). In the "calcium clock" model of pacemaking the key mechanism in the

diastolic depolarization is a spontaneous rhythmic phenomenon of Ca^{2+} release from the SR activating the Na^{+}/Ca^{2+} exchanger (NCX) in forward mode. This NCX mediated inward current is able to depolarize the membrane voltage to the threshold of the following action potential (Bogdanov et al., 2001; Vinogradova et al., 2002). Recently, the Ca^{2+} clock view of pacemaking has been updated into the "coupled-clock" model (Lakatta et al., 2010). In the coupled-clock model of pacemaking, the activity of membrane ion channels and spontaneous Ca^{2+} release mutually entrain to generate pacemaking (Lakatta et al., 2010; Monfredi et al., 2013). For a more extended description of the issues raised by the I_f - based and the Ca^{2+} or coupled-clock models of pacemaking, the reader is referred to recent review by the principal authors (Difrancesco, 2010; Lakatta et al., 2010; Monfredi et al., 2013).

However, either the I_f -based or the coupled clock models of pacemaking do not fully appreciate the role of VGCCs in pacemaking. Indeed, in the I_f -based model of pacemaking the L-type Ca^{2+} current ($I_{Ca,L}$) is considered only as a determinant of the action potential upstroke and duration (Difrancesco, 1993, 2010). In the coupled-clock model of pacemaking, $I_{Ca,L}$ is considered as a major mechanism to replenish SR Ca^{2+} content at each pacemaker cycle (Vinogradova et al., 2002). Finally, both the I_f -based and the coupled-clock models grant only a limited role to T-type VGCCs (Vinogradova et al., 2002).

However, during the last 10 years evidence accumulated showing that VGCCs contribute directly to pacemaking by carrying inward current during the diastolic depolarization phase (Zhang et al., 2002, 2011; Mangoni et al., 2003, 2006b; Marger et al., 2011a) or by stimulating the NCX activated by subsarcolemmal Ca^{2+} release during the diastolic depolarization (Lakatta et al., 2010). VGCCs also participate to the upstroke phase of the action potential (Hagiwara et al., 1988; Doerr et al., 1989; Marger et al., 2011a). Here we will focus on two distinct families of VGCCs, the L-type and the T-type Ca^{2+} channels. L-type VGCCs are expressed throughout the myocardium and are sensitive to antagonist and agonist dihydropyridines (DHPs) such as nifedipine and BAY K 8644 and are stimulated by PKA-dependent phosporylation (Striessnig, 1999; van der Heyden et al., 2005). In comparison with T-type channels, L-type VGCCs activate upon membrane depolarization at more positive potential, have Ca^{2+} and voltage dependent inactivation, as well as a higher single channel conductance (Perez-Reyes, 2003). T-type VGCCs are activated at more negative potentials than L-type VGCCs. The kinetic hallmark of native and heterogously expressed T-type mediated Ca^{2+} current is slow criss-crossing activation and fast voltage dependent inactivation (Carbone and Lux, 1987). **Table 1** summarizes the main characteristics of the L- and T-type VGCCs isoforms involved in cardiac automaticity. The elucidation of the functional role of the cardiac VGCCs can give important insights into the mechanisms underlying different SAN and conduction system pathologies. Indeed, failure of generating the cardiac impulse underlies SAN bradycardia and rhythmic disease. Diseases of the sinus node account for more than

Table 1 | Characteristics of the L- and T-type VGCCs isoforms involved in cardiac automaticity.

	L-type VGCC (Ca_v1)		T-type VGCC (Ca_v3)	
	$Ca_v1.2$	**$Ca_v1.3$**	**$Ca_v3.1$**	**$Ca_v3.2$**
Expression time	Embryonic stage	Embryonic stage	Start to increase in the perinatal period and becomes predominant in the adulthood	High in Embryonic heart tissue and then decrease and disappear in adult heart
Cardiac tissues expression	SAN, AVN, atria, PF networks, Ventricles	SAN, AVN, atria, PF networks, poorly or not expressed in ventricular	SAN, AVN, atria, PF networks, poorly or not expressed in ventricular tissue	SAN, AVN, atria, PF networks, poorly expressed in ventricular tissue
Voltage dependent activation	High threshold of activation (~ -40 mV) Fast activation	Lower threshold of activation than $Ca_v1.2$ (~ -55 mV) Fast activation	Lower threshold of activation (~ -70 mV) Slow activation	
Inactivation properties	Ca^{2+} and voltage dependent inactivation	Ca^{2+} and voltage dependent inactivation	Fast voltage dependent inactivation	
DHP sensitivity	High	Lower than $Ca_v1.2$	Low and very low	
Role in pacemaking	Control the Ca^{2+} dependent upstroke phase of action potential	Diastolic pacemaker current	Diastolic pacemaker current	
Knock-out mice phenotype	Lethal	Strong bradycardia, SAN arrhythmia, conduction system dysfunction	Mild bradycardia AV conduction disorders	No phenotype

1,000,000 electronic pacemaker implantations each year. SAN disease is characterized by various symptoms including severe sinus bradycardia, sinus pauses or arrest, chronotropic incompetence, sinus node exit block (Dobrzynski et al., 2007). Heart failure, cardiomyopathy, administration of antiarrhythmic drugs and other acquired cardiac conditions can induce SAN dysfunction. Nevertheless, in a significant number of patients, SAN dysfunction shows inherited features (Sarachek and Leonard, 1972; Lehmann and Klein, 1978; Mackintosh and Chamberlain, 1979; Dobrzynski et al., 2007; Sanders et al., 2014). Mutations in genes regulating L-type VDCCs involved in SAN automaticity such as L-type $Ca_v1.3$ (Mangoni et al., 2003; Baig et al., 2011) and T-type $Ca_v3.1$ (Marger et al., 2011a; Strandberg et al., 2013) are associated with various forms of previously unexplained tachy-brady syndromes and conduction defects (Mangoni and Nargeot, 2008; Pfeufer et al., 2010).

CARDIAC VOLTAGE GATED Ca^{2+} CHANNELS: MOLECULAR DETERMINANTS AND EXPRESSION

VGCCs are an important pathway for Ca^{2+} entry in pacemaker cells. In the mammalian heart, L- and T-type mediated Ca^{2+} currents are expressed in SAN, AVN, and Purkinje Fibers network and they have been consistently recorded in pacemaker SAN and AVN cells (Tseng and Boyden, 1989; Mangoni et al., 2003, 2006b; Marger et al., 2011a). Hagiwara et al. (1988) were the first to report the expression of $I_{Ca,L}$ in isolated SAN pacemaker cells and to describe its kinetic and pharmacologic properties. In particular, they defined $I_{Ca,L}$ as a "high"-threshold Ca^{2+} current activated from about -30 mV and distinguished from T-type mediated Ca^{2+} current ($I_{Ca,T}$), a "low" threshold Ca^{2+} current activated at −50 mV, suggesting that both currents participate the latter half of the slow diastolic depolarization (Hagiwara et al., 1988).

L-type VGCCs are hetero-oligomeric complexes constituted by a voltage sensitive pore, the so–called α1-subunits, together with different accessory subunits (α2δ, β, and γ) (Striessnig, 1999) and they are highly sensitive to DHP Ca^{2+} channels modulators. Four α1-subunits have been cloned and classified for the L- type Ca^{2+} channel, namely $Ca_v1.1$, $Ca_v1.2$ $Ca_v1.3$, and $Ca_v1.4$ (Catterall et al., 2003). $Ca_v1.1$ subunits are expressed in the skeletal muscle, where they couple membrane excitation to contraction (Tanabe et al., 1988; Tuluc et al., 2009), $Ca_v1.4$ expression is predominant in the retina, spinal cord and immune cells (McRory et al., 2004; Striessnig and Koschak, 2008). $Ca_v1.2$ and $Ca_v1.3$ are expressed in neurons, as well as in cells from the neuroendocrine and cardiovascular systems (Catterall, 2000). $Ca_v1.2$ is expressed in the whole heart but predominantly in atria and ventricles; $Ca_v1.3$ expression is predominant in the supraventricular regions with higher amounts of $Ca_v1.3$ in the rhythmogenic centers (Marionneau et al., 2005). Electrophysiological measurements showed clear differences between $Ca_v1.3$ and $Ca_v1.2$ mediated $I_{Ca,L}$. $Ca_v1.3$-mediated $I_{Ca,L}$ activates at more negative voltages and displays slower current inactivation during depolarization allowing these channels to mediate long lasting Ca^{2+} influx during weak depolarization (Platzer et al., 2000; Koschak et al., 2001). As showed by Hagiwara (Hagiwara et al., 1988), T-type VGCCs are activated at more negative potentials than L-type VGCCs. Moreover, $I_{Ca,T}$ have faster voltage-dependent inactivation and inactivation is complete at more negative membrane potentials than $I_{Ca,L}$ (Perez-Reyes, 2003) (**Table 1**).

Three genes encoding for T-type α-subunits have been cloned and named $Ca_v3.1$, $Ca_v3.2$, and $Ca_v3.3$. While the $Ca_v3.3$ isoform is not present in the heart, the expression of $Ca_v3.1$ and $Ca_v3.2$ isoforms in the myocardium varies according to the developmental status of the tissue. $Ca_v3.2$ constitutes the predominant T-type isoform in embryonic heart tissue (Ferron et al., 2002); $Ca_v3.1$ channels expression increases during perinatal period and reaches its maximal in adulthood (Marshall et al., 1993). In adult SAN $Ca_v3.1$ expression is higher than $Ca_v3.2$ (Bohn et al., 2000). Contrary to the Ca_v1 family, the Ca_v3 family is almost insensible to DHPs and at present, no selective inhibitor to discriminate the contribution of $Ca_v3.1$ and $Ca_v3.2$ channels to the total $I_{Ca,T}$ is available.

REGULATION OF L- AND T-TYPE Ca^{2+} CHANNELS IN CARDIAC TISSUES

Cardiac VGCCs are subject of multiple regulatory mechanisms involving both intramolecular regulatory sites and interactions with cellular second messengers and kinases.

Ca^{2+} influx through VGCCs can "auto-regulate" the channel activity in a negative (CDI, Ca^{2+}-dependent inactivation) or positive (CDF, Ca^{2+}-dependent facilitation) manner. L-type Ca^{2+} channels undergo calmoduline-mediated CDI or calmoduline kinase II (CaMKII)-mediated CDF (Christel and Lee, 2012). On the contrary only CaMKII-mediated CDF has been described for T-type Ca^{2+} channels (Christel and Lee, 2012).

It has been shown that SAN L-type Ca^{2+} channels undergo voltage-dependent inactivation (VDI) and facilitation (VDF) (Mangoni et al., 2000; Christel et al., 2012). Christel et al. (2012) showed that $Ca_v1.2$-mediated $I_{Ca,L}$ undergoes stronger VDI than $Ca_v1.3$-mediated $I_{Ca,L}$ and that $Ca_v1.3$-mediated $I_{Ca,L}$ exhibited stronger VDF than $Ca_v1.2$ -mediated $I_{Ca,L}$. Numerical modeling simulations predicted that VDF was responsible of 25% increase in $Ca_v1.3$-mediated $I_{Ca,L}$ which, as a consequence, induced a small positive chronotropic effect. These data further support the importance of $Ca_v1.3$ Ca^{2+} channels regulation in cardiac pacemaker activity.

L-type Ca^{2+} channels are also potently regulated by cAMP-dependent protein kinase A (De Jongh et al., 1996; Ramadan et al., 2009). Regulation of T-type Ca^{2+} channels by cAMP dependent protein kinase A is still controversial (Chemin et al., 2006), however, in a recent work Li et al. (2012) found that in cardiac myocytes the activity of $Ca_v3.1$ T-type VGCCs was significantly increased by isoproterenol, a β-adrenergic agonist, and that this regulation was strictly connected to the adenylate cyclase/cAMP/PKA machinery similar to L-Type Ca^{2+} channels. One of the most important differences in the pharmacologic modulation of T- and L-type Ca^{2+} channels rises from their different sensitivity to DHPs. DHPs are known to act on $I_{Ca,L}$ without affecting $I_{Ca,T}$ (Hagiwara et al., 1988). Nevertheless, this concept has been challenged by different studies showing an effect of certain types of DHPs also on different subunits of T-type VGCCs (Bladen et al., 2014a,b). L-type Ca^{2+} channel voltage-dependence and expression are potently regulated by β subunits

(see Buraei and Yang, 2010, for recent review). In the SAN, the predominant β subunit isoform expressed appears to be β2 (Marionneau et al., 2005). Co-expression of the β2 subunit with the $Ca_v1.2$ α1 subunit induces slowing of the voltage dependent inactivation of $I_{Ca,L}$ (Cens et al., 1996). It has been proposed that β subunits regulate α1 protein trafficking (Buraei and Yang, 2013). It will be interesting to investigate whether β2 subunits regulates L-type Ca^{2+} channel trafficking in the cardiac conduction system. It has been showed that L-type Ca^{2+} channels, even to a lesser extent than other VGCCs such as T-type Ca^{2+} channels, are regulated also by phospholipids (Suh and Hille, 2005).

FUNCTIONAL ROLE OF L-TYPE AND T-TYPE Ca^{2+} CHANNELS IN CARDIAC AUTOMATICITY

L-TYPE Ca^{2+} CHANNELS

Evidence for the importance of L-type Ca^{2+} current in SAN pacemaking have been reported by different studies (see Mangoni et al., 2006a, for review). Kodama et al. (1997) showed that blocking $I_{Ca,L}$ by 2 μM nifedipine abolished the action potential in the primary central pacemaker area in rabbit SAN but not in spontaneously beating tissue from the periphery of the SAN. In contrast, they showed that tetrodotoxin 20 μM had no effect on electrical activity in the primary central pacemaker area, but depolarized the takeoff potential, decreased the upstroke velocity and slowed the spontaneous activity in nodal tissue from SAN periphery. These results are in line with the view that the rabbit pacemaker action potential strongly depends from $I_{Ca,L}$ in the central area of SAN but not in the periphery, where it is more sensitive to Na^+ current (I_{Na}). The heterogeneity of sensitivity to $I_{Ca,L}$ in pacemaker cells highlights the problem of isolating the contribution of $I_{Ca,L}$ to the diastolic depolarization phase from its contribution to the upstroke phase of the cardiac action potential.

Doerr et al. (1989) tried to overcome this major problem using the action potential clamp technique to evaluate the contribution of $I_{Ca,L}$ in the pacemaker cycles in rabbit isolated SAN cells. They reported a net methoxyverapamil (L-type Ca^{2+} channels blocker)-sensitive current measurable during the early diastolic depolarization as well a long lasting component during the plateau phase. Verheijck et al. (1999) have recorded the net nifedipine-sensitive $I_{Ca,L}$ at different times during action potential cycle. Notably, they provided direct evidence that $I_{Ca,L}$ can be activated at potential as negative as −60 mV, typical of the early diastolic depolarization phase, and then increases up to the threshold potential supplying inward current during the entire diastolic depolarization. In comparison to the previous study by Hagiwara et al. (1988), Verheijck and co-workers recorded $I_{Ca,L}$ starting from negative holding potentials (−90 mV), preventing partial steady-state inactivation of $I_{Ca,L}$ at negative voltages. Second, Verheijck and co-workers employed a recording protocol combining current clamp, to let the cell to depolarize and repolarize spontaneously, with voltage clamping at discrete voltages spanning the diastolic depolarization to record $I_{Ca,L}$. This strategy allowed accurate measurement of the $I_{Ca,L}$ current density in this phase.

Moreover, they demonstrated the presence of a "low-voltage"-activated $I_{Ca,L}$ component, pharmacologically distinct from $I_{Ca,T}$, in the diastolic depolarization range, opening the way to the description of the functional role of $Ca_v1.3$ L-type channels in pacemaking.

The first *in vivo* evidence of the contribution of $I_{Ca,L}$ in cardiac pacemaker was provided by Lande et al. (2001); they recorded DHP-induced bradycardia in anesthetized mice. Subsequently, the unexpected result that electrocardiogram (ECG) recordings revealed SAN dysfunction (bradycardia and arrhythmia) in mice lacking L-type $Ca_v1.3$ channels was the first genetic evidence of their importance in heart automaticity (Platzer et al., 2000). Two independent studies showed that $Ca_v1.3$ channels have a key role in automaticity both *in vitro* (**Figure 1A**) and *in vivo* (**Figures 1B,C**) (Zhang et al., 2002; Mangoni et al., 2003) also unmasking important differences between $Ca_v1.3$-mediated and $Ca_v1.2$-mediated $I_{Ca,L}$ (**Figure 2A**). The heart chambers histology and thickness as well SAN and AVN structure did not show any differences between $Ca_v1.3^{-/-}$ and the wild type mice, suggesting that inactivation of $Ca_v1.3$ channels has no effect on heart structure (Matthes et al., 2004). Inactivation of $Ca_v1.3$-mediated $I_{Ca,L}$ impairs pacemaking and atrioventricular conduction, but has no effect on myocardial contractility (Matthes et al., 2004). Zhang et al. (2005) showed that intracardiac atrial stimulation induced atrial fibrillation and atrial flutter in $Ca_v1.3^{-/-}$ mice but not in wild-type littermates even in the absence of vagal stimulation with carbachol, a muscarinic agonist which is known to induce atrial fibrillation in control mice (Kovoor et al., 2001). In contrast, no ventricular arrhythmias were induced in either the wild-type or mutant mice (Zhang et al., 2005). These data further support the view of an important functional role of $Ca_v1.3$ in the atria.

Using a knock-in mouse strain in which the DHP sensitivity in $Ca_v1.2$ α1 subunits was eliminated ($Ca_v\ 1.2^{DHP-/-}$), without affecting channel function and expression, it has been possible to separate the DHP effects of $Ca_v1.2$ from those of $Ca_v1.3$ and other L-Type Ca^{2+} channels.

The heart rate reducing effect induced by DHP (isradipine) in $Ca_v1.2^{DHP-/-}$ mice demonstrated that $Ca_v1.3$ is the major L-Type Ca^{2+} channel controlling diastolic depolarization (Sinnegger-Brauns et al., 2004).

Recently, Christel et al. (2012) showed a differential degree of co-localization between the ryanodine receptors (RYRs) of the SR and $Ca_v1.3$ or $Ca_v1.2$ channels in primary SAN pacemaker cells. The strong co-localization of $Ca_v1.3$ with RYR2 may be relevant for the functional role of RYR-mediated Ca^{2+} release in pacemaking (Vinogradova et al., 2002). During the late phase of the diastolic depolarization, RYR-mediated Ca^{2+} release promotes NCX activation, which accelerates reaching the threshold of the SAN action potential upstroke (Vinogradova et al., 2002). Close apposition of $Ca_v1.3$ with RYRs may facilitate SR Ca^{2+} release since $I_{Ca,L}$ stimulates RYR open probability. In this respect, numerical simulations predicted that the slope of rise of diastolic RYR-dependent Ca^{2+} release increased as a function of $Ca_v1.3$-mediated $I_{Ca,L}$ half-activation voltage (Christel et al., 2012). The coupling of this SR Ca^{2+} release to the depolarizing influence of NCX should accelerate attainment of the threshold for action potential firing of SAN cells (Vinogradova et al., 2002). L-type Ca^{2+} channels, and in particular $Ca_v1.3$ channels, have been shown to physically associate with RYR2 in the nervous system

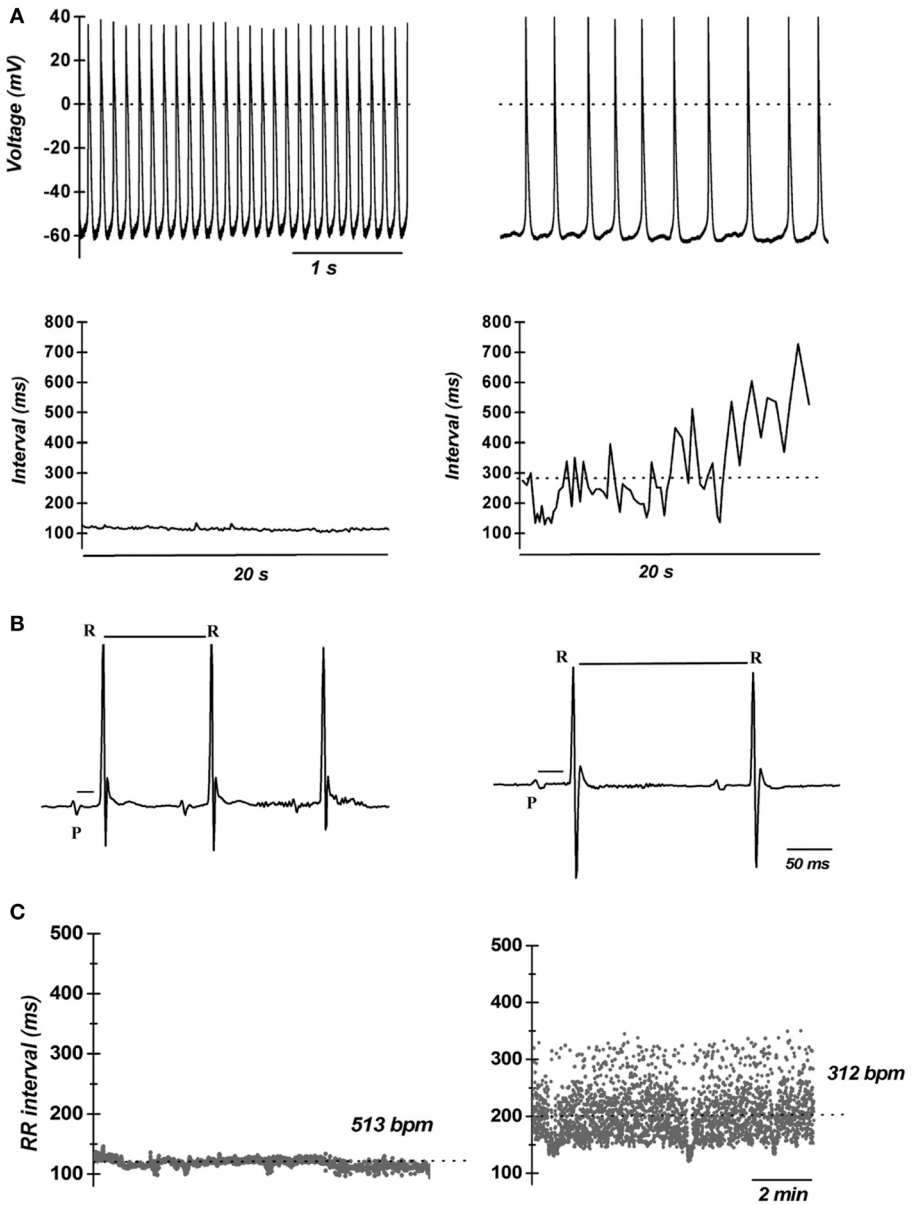

FIGURE 1 | Importance of L-type VGCCs in cardiac automaticity. (A) Representative recordings of consecutive action potentials recorded in pacemaker cells from wild-type (top left panel) and $Ca_v1.3^{-/-}$ mice (top right panel). Cellular arrhythmia is evident as irregular cycle length duration in $Ca_v1.3^{-/-}$ cells (bottom right panel) compared with wild-type cells (bottom left panel). Dotted lines indicate the zero voltage level (Data from Mangoni et al., 2003). **(B)** Telemetric ECGs showing prolongation of RR interval PQ interval in $Ca_v1.3^{-/-}$ mice (top right panel) with respect to wild type littermates (top left panel). **(C)** Dot plot of beat to beat variability in wild-type (left panel) and $Ca_v1.3^{-/-}$ mice (right panel) observed during 10 min recordings. Note the dispersion of the RR intervals in $Ca_v1.3$ knockout mice, revealing strong sinus arrhythmia. The dotted lines indicate the average heart rate as the number of beats per minutes (bpm) (reprinted from Mangoni et al., 2006a, with permission from Elsevier).

(Ouardouz et al., 2003; Kim et al., 2007). It will be interesting to investigate whether such a coupling also exists in SAN cells. As previously mentioned, $Ca_v1.3^{-/-}$ mice show slowing of atrioventricular conduction suggesting that these channels are important in AVN physiology (**Figure 2B**). It has been shown that $Ca_v1.3$ channels play a key role in pacemaking of AVN cells (Marger et al., 2011a; Zhang et al., 2011). In $Ca_v1.3^{-/-}$ AVN cells pacemaker activity is stopped and exhibited a depolarized membrane potential of -30 mV (Marger et al., 2011a) likely due the loss of crosstalk between $Ca_v1.3$ channels and SK2 K^+ channels. Indeed, functional coupling between $Ca_v1.3$ and SK channels has been reported in mouse atrial myocytes (Lu et al., 2007), where $Ca_v1.3$ loss-of-function prolongs the action potential duration via reduction in the activity of SK channels. Interestingly, Zhang et al. (2008) showed that mice lacking SK2 channels exhibited significant sinus bradycardia with prolongation of the

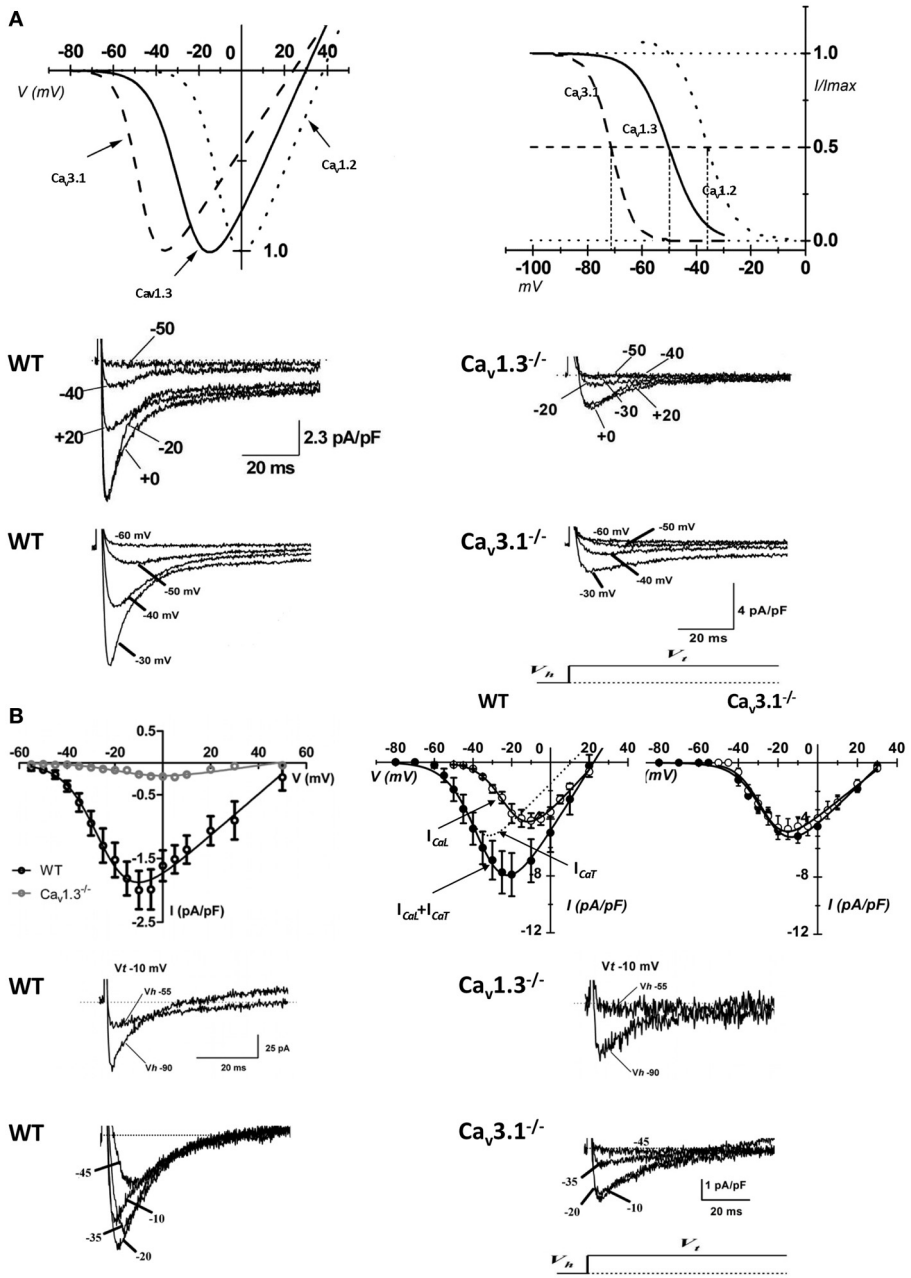

FIGURE 2 | Properties of VGCCs in cardiac pacemaker cells. (A) I–V curve (top left panel) and steady-state inactivation (top right panel) of native SAN $Ca_v3.1$ (dashed curve), $Ca_v1.3$ (solid curve), and $Ca_v1.2$ (dotted curve) channels (reprinted from Mangoni et al., 2006a, with permission from Elsevier). Examples of voltage dependent calcium currents recorded in pacemakers cells from WT (middle and bottom left panel), $Ca_v1.3^{-/-}$ (middle right panel) and $Ca_v3.1^{-/-}$ mice (bottom right panel). **(B)** Top left panel: I–V curve of L-type Ca^{2+} channels obtained from WT (black open circles) and $Ca_v1.3^{-/-}$ (gray open circles) isolated AVN cells. Top right panels: current to voltage relationship in isolated AVN cells from WT and $Ca_v3.1^{-/-}$ mice. Sample traces of $I_{Ca,L}$ (middle panels) and $I_{Ca,T}$ (bottom panels) recorded in isolated AVN cells from WT, $Ca_v1.3^{-/-}$ and $Ca_v3.1^{-/-}$ mice. For $I_{Ca,L}$ recordings the holding potential (V_h) was set at −55 mV, for $Ca_v3.1$ at −90 mV. Test potential (V_t) is reported near the trace (reprinted from Mangoni et al., 2006b with permission from Wolters Kluwer Health).

atrioventricular conduction intervals (PQ intervals), thus revealing a function role of these channels in AVN automaticity.

Saturating doses of the non-selective β-adrenergic agonist isoproterenol did not restore pacemaking in $Ca_v1.3^{-/-}$ AVN cells. Cellular automaticity could be initiated by injection of hyperpolarizing current to drive the membrane voltage to the maximum diastolic potential of −60 mV recorded in wild-type AVN cells. When this maximum diastolic potential voltage is maintained by constant hyperpolarizing current injection, AVN cells were able to fire spontaneous action potentials. However,

this firing was very slow and arrhythmic. Furthermore, the slope of the diastolic depolarization in current injected $Ca_v1.3^{-/-}$ cells was very low. Indeed, during the diastolic phase, only sub-threshold low amplitude oscillations of the membrane potential were recorded. These oscillations occasionally met the threshold to evoke an action potential (Marger et al., 2011a). These data indicated that $Ca_v1.3$ channels have a key role in the generation of the diastolic depolarization in AVN pacemaker cells (Marger et al., 2011a). β-adrenergic stimulation induced by isoproterenol was able to increase the firing rate in current-injected $Ca_v1.3^{-/-}$ AVN cells. However, the firing rate of isoproterenol treated $Ca_v1.3^{-/-}$ myocytes did not reach the value of control AVN cells (Marger et al., 2011a).

The lack of spontaneous automaticity in $Ca_v1.3^{-/-}$ AVN cells *in vitro* does not imply un-excitability *in vivo*. A potential explication is that $Ca_v1.3^{-/-}$ cells embedded in tissue are kept at hyperpolarized membrane voltages by the electrotonic influence of the atrium (Verheijck et al., 2002), allowing the discharge of the I_{Na} dependent action potential in the presence of SAN impulse (Marger et al., 2011a). Incidentally, Marger et al. (2011b) showed that I_{Na} has an important role in the AVN automaticity as 20 μM TTX completely stop firing in AVN cells. Finally, it is well known that AVN is composed by different cell types, automatic and non-automatic, interacting each other and eventually implicated in different conduction pathways. These aspects too can explain the reason why $Ca_v1.3^{-/-}$ mice do not show complete atrioventricular block.

T-TYPE CALCIUM CHANNELS

$I_{Ca,T}$ has been consistently found in all the three rhytmogenic centers of the heart: the SAN (Hagiwara et al., 1988; Fermini and Nathan, 1991), the AVN (Liu et al., 1993) and Purkinje fibers (Hirano et al., 1989; Tseng and Boyden, 1989) suggesting that T-type VGCCs may constitute a relevant mechanism in the generation of the diastolic depolarization.

Genetically modified mice with target inactivation of $Ca_v3.2$ and $Ca_v3.1$ subunit importantly helped to elucidate the role of T-type channel isoforms in cardiac pacemaking and impulse conduction (**Figure 2A**) (Chen et al., 2003; Mangoni et al., 2006b; Thuesen et al., 2014).

In comparison to wild-type littermates mice lacking $Ca_v3.2$ T-type channels do not show any significant differences in heart rate or the ECG waveform morphology; furthermore, no cardiac arrhythmias were observed in $Ca_v3.2$ deficient mice indicating that $Ca_v3.2$ mediated $I_{Ca,T}$ do not contribute significantly to the generation and the conduction of the cardiac impulse (Chen et al., 2003).Contrary to what reported for $Ca_v3.2$ deficient mice, genetic inactivation of the $Ca_v3.1$ T-type Ca^{2+} channels in mice results in a moderate bradycardia and significant slowing of AV conduction. Moreover, SAN and AVN cells of $Ca_v3.1^{-/-}$ hearts do not show residual $Ca_v3.2$ mediated $I_{Ca,T}$. Niwa et al. (2004) and Ferron et al. (2002) showed that the embryonic myocardium express $Ca_v3.2$ channels, while the adult heart shows a higher expression of $Ca_v3.1$ channels. These results suggest that $Ca_v3.2$ underlies the functional T-type Ca^{2+} channels in the embryonic murine heart, and there is a subtype switching of transcripts from $Ca_v3.2$ to $Ca_v3.1$ in the perinatal period. As stated previously, ablation of $Ca_v3.1$ subunits causes heart rate reduction (around 10%) and prolongation of the PQ interval due to first-degree atrioventricular block (Mangoni et al., 2006b). Similar results are obtained in sedated $Ca_v3.1^{-/-}$ mice after autonomic blockade by atropine and propranolol indicating a direct impact of $Ca_v3.1$ subunits deletion in the SAN automaticity (Mangoni et al., 2006b) (**Figure 3**).

In agreement with this observation *in vivo*, pacemaker activity in isolated SAN cells is slowed by about 30% (Mangoni et al., 2006b). The relatively lower impact of $I_{Ca,T}$ loss of function on pacemaking *in vivo* compared to isolated cells can be explained supposing a shift of the leading pacemaker site in $Ca_v3.1^{-/-}$ SAN. This phenomenon is known as "pacemaker shift," and can be observed when the SAN is challenged with neurotransmitters or pharmacologic agents that regulate pacemaker activity (Boyett et al., 2000; Lang et al., 2011; Inada et al., 2014). In the case of $Ca_v3.1^{-/-}$ hearts, it can be hypothesized that the leading pacemaker site of intact SAN is shifted to a location that is less sensitive to $I_{Ca,T}$ than the leading site in wild-type hearts. In this respect, pacemaker shift can be viewed as a compensatory mechanism to keep SAN rate as high as possible in the absence of $Ca_v3.1$ channels. This hypothesis would need direct testing by employing optical or electrical mapping of pacemaking in wild-type and $Ca_v3.1^{-/-}$ SANs Similar hypothesis concerning pacemaker leading site shift have already been proposed to explain beat-to-beat variability, sinus node dysrhythmia and sinus pauses in mice lacking HCN1 channel (Fenske et al., 2013) or to partially explain the phenotype of human patients affected by "ankyrin B syndrome," a disease characterized by sinus node dysfunction and increased susceptibility to spontaneous atrial fibrillation cause by Ankyrin-B dysfunction (Wolf et al., 2013). Another possible hypothesis to explain the difference in the pacing rate between isolated SAN cells and the heart rate *in vivo* in $Ca_v3.1^{-/-}$ mice would be the functional coupling between cardiac fibroblast and SAN myocytes. Indeed, it has been proposed that cardiac connective tissue facilitates impulse conduction *in vivo* (Camelliti et al., 2004; Kohl and Gourdie, 2014). Consequently, disruption of the electro-tonic coupling between fibroblast and $Ca_v3.1^{-/-}$ SAN cells during the cell isolation process could contribute reduce the pacing rate of isolated knockout myocytes. This hypothesis could also hold for other murine models lacking ion channels involved in pacemaker activity.

The prolongation of PQ interval in $Ca_v3.1^{-/-}$ mice suggested an important role of $I_{Ca,T}$ in AVN pacemaker cells. No residual $I_{Ca,T}$ was recorded in $Ca_v3.1^{-/-}$ AVN cells (**Figure 2B**) and the loss of $Ca_v3.1$ mediated $I_{Ca,T}$ had remarkable effects on AVN cells automaticity. Pacemaker activity in $Ca_v3.1^{-/-}$ AVN isolated cells was irregular and slower (40%) than that of control cells (Marger et al., 2011a) suggesting that the relative importance of these channels in AVN automaticity may be even higher than that of SAN.

The importance of T-type channels in automaticity has been also investigated also in the ventricular conduction system. Le Quang et al. (2013) performed a clever study on the role of $Ca_v3.1$ T- type Ca^{2+} channels subunits in escape rhythms and in bradycardia induced ventricular tachyarrhythmia after atrioventricular

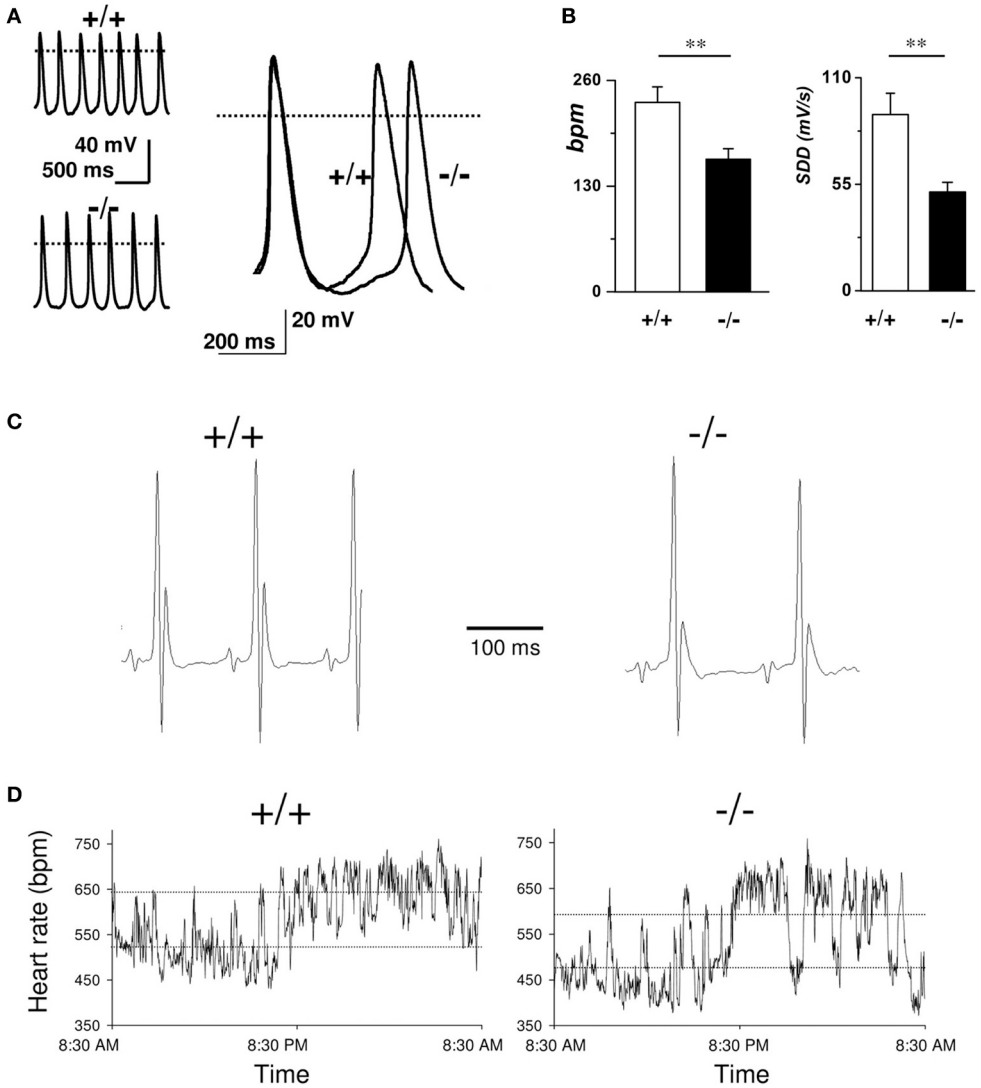

FIGURE 3 | Role of T-type VGCCs in cardiac automaticity. **(A)** Representative sweeps of spontaneous action potentials obtained from SAN cells from WT (upper left trace) and $Ca_v3.1^{-/-}$ mice (lower left trace). Right panel: Superimposition of typical action potentials from a WT and from $Ca_v3.1^{-/-}$ SAN cell. **(B)** Histograms of the average bpm value and the slope of the diastolic depolarization (SDD). **(C)** Representative telemetric ECG recordings obtained on WT (left panel) and $Ca_v3.1^{-/-}$ animals (right panel). **(D)** Variation of heart rate (in bpm) in WT (left panel) and $Ca_v3.1^{-/-}$ mice (right panel) over a 24-h period. Dashed lines indicate mean day and night heart rates (reprinted from Mangoni et al., 2006b with permission from Wolters Kluwer Health).

block. Adult male mice lacking $Ca_v3.1$ alpha subunits after induction of complete atrioventricular block showed slower escape rhythms, greater mortality and higher frequency of torsades de pointes than control mice. This study suggests that $Ca_v3.1$ channels play an important role in infra-nodal escape automaticity. Loss of $Ca_v3.1$ channels also worsens bradycardia-related mortality, increases bradycardia-associated adverse remodeling, and enhances the risk of malignant ventricular tachyarrhythmia following atrioventricular block.

Although data from different studies show clearly the involvement of $I_{Ca,T}$ in cardiac automaticity and impulse conduction, mechanistic description of how T channels contribute to the diastolic depolarization is still lacking. Protas et al. (2001) proposed, for rabbit SAN cells, the existence of T-type window current component in the diastolic depolarization, but such a window current was not recorded either in the original study by Hagiwara et al. (1988) or Mangoni et al. (2006b) leaving this aspect still controversial. A previous study by our group employing numerical modeling of pacemaker activity of SAN and AVN mouse cells suggested that about 25 pA/pF of $Ca_v3.1$-mediated $I_{Ca,T}$ flows during the diastolic depolarization (Hagiwara et al., 1988; Mangoni et al., 2006b; Marger et al., 2011a). Such a current density would be in theory sufficient to functionally contribute to the diastolic depolarization, since previous modeling work indicated that given the very high membrane resistance of SAN pacemaker cells at the maximum diastolic potential, a net inward current density

as low as 1 pA/pF could initiate the diastolic depolarization (Difrancesco, 1993; Verheijck et al., 1999). Another hypothesis on how T-type channels can contribute to the pacemaking has emerged from the study by Huser et al. (2000). The paper states that in cat SAN and latent atrial pacemaker cells, the activation of T-type calcium channels during the late phase of the depolarization triggers elementary Ca^{2+} release events (Ca^{2+} sparks) from the SR which in turns stimulate NCX current to depolarize the pacemaker potential to threshold. These data were confirmed using 40 μM nickel (blocker of low voltage activated $I_{Ca,T}$). Effectively, nickel reduced Ca^{2+} sparks and the slope of the diastolic depolarization, suggesting a functional coupling between T-type channels and SR (Lipsius et al., 2001), which could explain previous results showing that prevention of SR Ca^{2+} release with 10 μM ryanodine reduced T-type Ca^{2+} current (Li et al., 1997). However, Vinogradova et al. (2002) showed that nickel 50 μM slightly decreased the spontaneous cycle length of rabbit SAN cells and did not decrease the number of SR Ca^{2+} release suggesting a cell-type dependent role of $I_{Ca,T}$ in beating rate, SR Ca^{2+} release and diastolic depolarization. Therefore, the fact that $I_{Ca,T}$ appears to play a more important role in cat atrial latent pacemaker activity (Huser et al., 2000) than in primary pacemaker activity of rabbit SAN cells might be explained on the basis of a more negative maximum diastolic potential in atrial subsidiary vs. SAN cells (Vinogradova et al., 2002).

DISEASES OF HEART RHYTHM AND CARDIAC VGCCs

During the last years, mutations in ion channels contributing to cardiac automaticity in humans have been described (Dobrzynski et al., 2007; Sanders et al., 2014). These mutations underlie complex arrhythmic profiles in affected patients. Typical clinical profiles include bradycardia due to sinus node dysfunction (Baig et al., 2011), atrioventricular block (Brucato et al., 2000) and ventricular tachycardia (Ueda et al., 2004). In particular, the discovery of two congenital pathologies of heart automaticity and atrioventricular conduction that could be attributed to a down regulation or loss-of-function of $Ca_v1.3$ and/or $Ca_v3.1$ channels highlights the physiological relevance of VGCCs in the determination of heart rate and atrioventricular conduction in humans. In this context genetically modified mice lacking $Ca_v1.3$ or $Ca_v3.1$ channels are important tools to test mechanistic hypothesis linking ion channel loss-of-function to bradycardia in affected subjects and for testing potential therapeutic strategies.

Mice lacking $Ca_v1.3$-mediated $I_{Ca,L}$ are phenotypically characterized by bradycardia and deafness (Platzer et al., 2000; Mangoni et al., 2003). Similar dysfunctions were discovered in two consanguineous families from Pakistan (Baig et al., 2011). Deep hearing loss and SAN dysfunction in these individuals closely are reminiscent of the phenotype of $Ca_v1.3^{-/-}$ mice. Because of the association between deafness and bradycardia, this newly described disease was named Sino-atrial Node Dysfunction and Deafness syndrome (SANDD). Patients with SANDD present SAN bradycardia at rest and exhibit variable degree of atrioventricular block and dissociated rhythms. This last observation can be explained by a recent result showing that $Ca_v1.3$ is important for automaticity of mice AVN cells (Marger et al., 2011a) (**Figure 4A**). No short or long QT syndrome (LQTS) was reported in SANDD patients, indicating that $Ca_v1.3$ channels do not directly participate to ventricular repolarization in humans. On the other hand recent data indicate that mutations in genes affecting regulation of $Ca_v1.2$ channels can affect action potential duration. Particularly, mutations in calmodulin have been shown to be associated with cathecolaminergic polymorphic ventricular tachycardia (CPVT) and cardiac arrest (Nyegaard et al., 2012; Crotti et al., 2013). Limpitikul et al. (2014) showed that expression of mutated calmodulin suppressed Ca^{2+}/calmodulin mediated CDI in native $Ca_v1.2$ channels of ventricular myocytes. Suppression of CDI increased action potential durations and augmented the SR Ca^{2+} content. These works indicate that alteration in $Ca_v1.2$ channels can induce LQTS (Limpitikul et al., 2014).

Recently, Neco et al. (2012), using a mouse model of CPVT carrying a mutation in RYR2 ($RyR2^{R4496C}$), demonstrated a strong implication of SAN L-type channels in bradycardia associated with CPVT syndrome. $RyR2^{R4496C}$ mice manifested alteration in Ca^{2+} homeostasis together with SAN dysrhythmia (SAN pauses) and impaired positive chronotropic response to β-adrenergic stimulation. Isolated $RyR2^{R4496C}$ SAN cells showed Ca^{2+}-dependent decrease of $I_{Ca,L}$ density, together with depletion of SR Ca^{2+} load during the diastolic phase, two factors that impaired the generation of SAN action potential. Ca^{2+} dependent inactivation by excessive RYR dependent Ca^{2+} release provides a new mechanistic rationale of SAN dysfunction in CPVT disease. It has been shown that not only inherited, but also acquired cardiomyopathy can involve L-type $Ca_v1.3$. Rose et al. (2011) described a strong cardiac phenotype in a mouse model of chronic iron overload (CIO). SAN cells from CIO mice showed a strong decrease in $Ca_v1.3$-mediated $I_{Ca,L}$ density. This decrease in $I_{Ca,L}$ induced bradycardia, sinus pauses, prolonged PQ intervals and second degree heart block *in vivo*.

Congenital heart block (CHB) disease is another pathology in which cardiac VGCCs are strongly implicated. CHB disease affects fetuses and newborns. CHB is an acquired autoimmune disease that occurs during pregnancies of rheumatic mothers, but also in healthy mothers. CHB is usually diagnosed between weeks 18 and 24 of pregnancy by fetal echocardiography techniques. Although it may initially appear as a first- or second-degree atrioventricular block, most cases present with fetal bradycardia and complete third-degree atrioventricular block. Other arrhythmias, including sinus bradycardia, diverse atrial rhythms, and junctional ectopic and ventricular tachycardia, have also been reported in the context of CHB (Ambrosi et al., 2014). While the etiology of this disease has remained obscure for long time, there is now strong evidence that loss-of-function of $Ca_v1.3$ and $Ca_v3.1$ channels underlie this pathology (Strandberg et al., 2013). Hu et al. (2004) have reported inhibition of $I_{Ca,L}$ and $I_{Ca,T}$ by immunoglobulin G isolated from mothers having CHB-affected children. SAN bradycardia and CHB can be explained at least in part by down regulation of $Ca_v1.3$ and $Ca_v3.1$ channels by maternal antibodies (Hu et al., 2004) suggesting a strict correlation between loss of function of $Ca_v1.3$ and $Ca_v3.1$ VGCCs and CHB. Results published by our group (Marger et al., 2011a) further support this hypothesis. Indeed, we studied heart rate and atrioventricular conduction in mice with combined inactivation of $Ca_v1.3$ and $Ca_v3.1$ channels ($Ca_v1.3^{-/-}/Ca_v3.1^{-/-}$) showing that $Ca_v3.1$

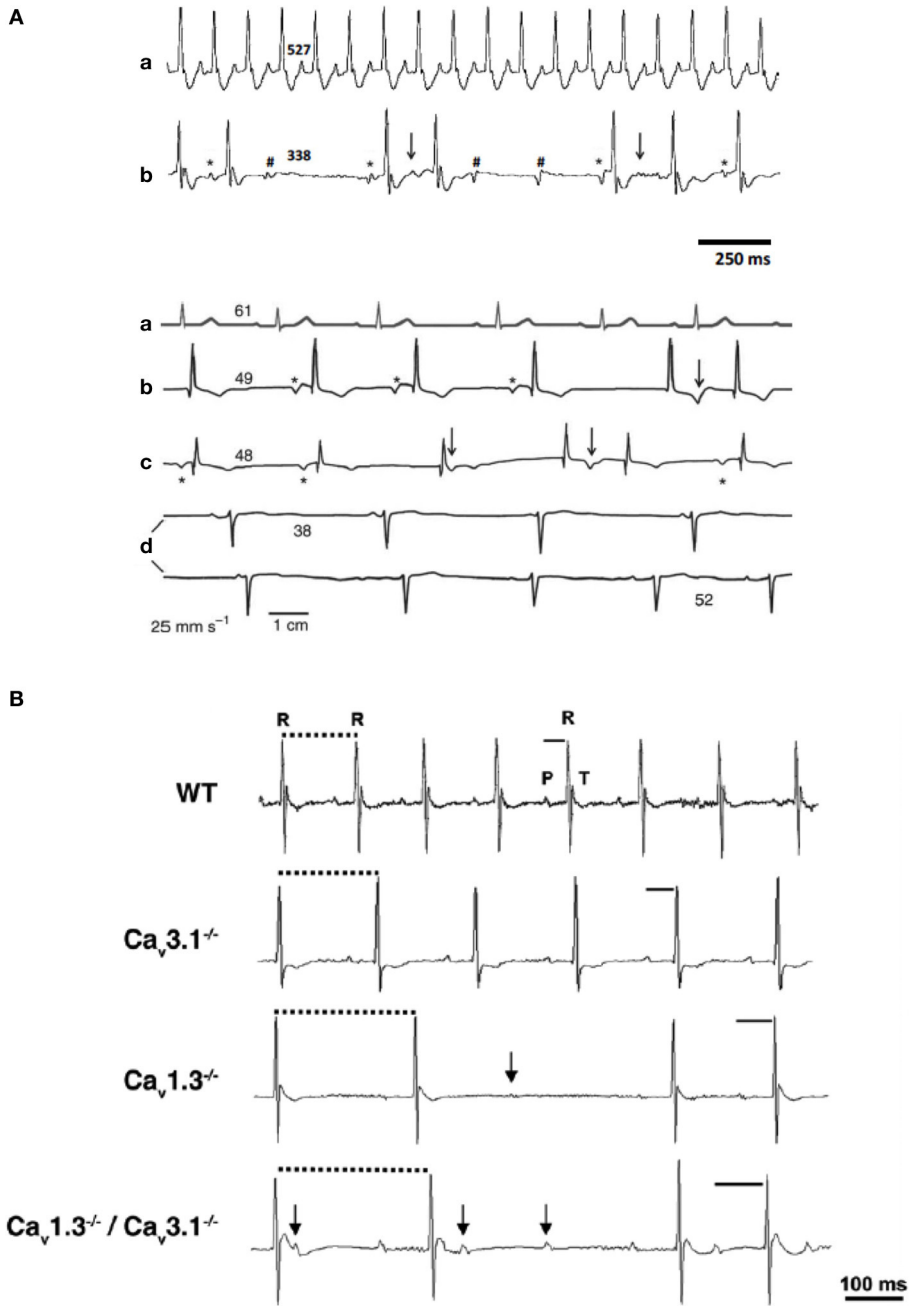

FIGURE 4 | Cardiac VGCCs in cardiac automaticity pathology. (A) ECG sample recordings from WT (a) and $Ca_v1.3^{-/-}$ mice (b). **(B)** ECG recordings from a healthy person (a) and three individuals with SANDD syndrome (b–d). Asterisks mark P waves that precede QRS complexes; arrows indicate waveforms that suggest P waves coinciding with T waves; hashes indicate not conducted P waves. Numbers indicate heart rate (bpm) calculated from the corresponding beat-to-beat R-R interval (adapted from Baig et al., 2011). **(B)** Telemetric surface ECGs of freely moving WT, $Ca_v3.1^{-/-}$, $Ca_v1.3^{-/-}$, and $Ca_v1.3^{-/-}/Ca_v3.1^{-/-}$ mice showed additive effect of Ca_v gene inactivation on atrioventricular conduction dysfunction. Solid bars indicate PQ interval, dotted bars indicate RR intervals and arrows indicate isolated P waves (reprinted from Marger et al., 2011a with permission from Taylor and Francis LLC http://www.tandfonline.com).

and $Ca_v1.3$ inactivation have an additive effect on atrioventricular conduction (**Figure 4B**). Indeed, while inactivation of $Ca_v3.1$ channels alone causes moderate dysfunction of atrioventricular conduction, association with $Ca_v1.3$ inactivation induces severe atrioventricular block. Some $Ca_v1.3^{-/-}/Ca_v3.1^{-/-}$ mice display complete block with dissociated atrial and ventricular. Disruption of both $Ca_v1.3$ and $Ca_v3.1$ subunits has also additive effects on AVN cells pacemaking. $Ca_v1.3^{-/-}/Ca_v3.1^{-/-}$ AVN cells display poor or absent automaticity, thus stressing the importance of voltage-dependent Ca^{2+} channels in pacemaker activity of these

cells. These results indicate that $Ca_v1.3^{-/-}/Ca_v3.1^{-/-}$ mice constitute a faithful animal model of CHB and could be used for testing of new therapies (Marger et al., 2011a).

In conclusion, work on mouse models of SANDD and CIO ($Ca_v1.3$ channels), CPVT ($I_{Ca,L}$), and CHB ($I_{Ca,L}$ and $I_{Ca,T}$) demonstrates that despite the differences between mouse and human cardiac rhythm the mouse is a valuable model for studying the role of ion channels in human pathologies of heart rhythm.

CONCLUDING REMARKS

The relevance of VGCCs in the generation and regulation of cardiac pacemaking, atrioventricular conduction and heart rate determination is now well established. Importantly, the functional role of VGCCs such as $Ca_v1.3$ and $Ca_v3.1$ channels seems to be conserved between rodents and humans. $I_{Ca,L}$ and $I_{Ca,T}$ play a major role in atrioventricular conduction as underscored by the presence of dissociated rhythms in $Ca_v1.3^{-/-}$ mice and SANDD patients (Baig et al., 2011) or in $Ca_v1.3^{-/-}/Ca_v3.1^{-/-}$ mice and CHB patients (Marger et al., 2011a). Future studies will further address the role of VGCCs in pacemaker activity and in particular their importance in respect to other ion channels involved in automaticity such as HCN4 and RYRs.

REFERENCES

Ambrosi, A., Sonesson, S. E., and Wahren-Herlenius, M. (2014). Molecular mechanisms of congenital heart block. *Exp. Cell Res.* 325, 2–9. doi: 10.1016/j.yexcr.2014.01.003

Baig, S. M., Koschak, A., Lieb, A., Gebhart, M., Dafinger, C., Nurnberg, G., et al. (2011). Loss of Ca(v)1.3 (CACNA1D) function in a human channelopathy with bradycardia and congenital deafness. *Nat. Neurosci.* 14, 77–84. doi: 10.1038/nn.2694

Bladen, C., Gadotti, V. M., Gunduz, M. G., Berger, N. D., Simsek, R., Safak, C., et al. (2014a). 1,4-Dihydropyridine derivatives with T-type calcium channel blocking activity attenuate inflammatory and neuropathic pain. *Pflugers Arch.* doi: 10.1007/s00424-014-1566-3. [Epub ahead of print].

Bladen, C., Gunduz, M. G., Simsek, R., Safak, C., and Zamponi, G. W. (2014b). Synthesis and evaluation of 1,4-dihydropyridine derivatives with calcium channel blocking activity. *Pflugers Arch.* 466, 1355–1363. doi: 10.1007/s00424-013-1376-z

Bogdanov, K. Y., Vinogradova, T. M., and Lakatta, E. G. (2001). Sinoatrial nodal cell ryanodine receptor and $Na^{(+)}$-$Ca^{(2+)}$ exchanger: molecular partners in pacemaker regulation. *Circ. Res.* 88, 1254–1258. doi: 10.1161/hh1201.092095

Bohn, G., Moosmang, S., Conrad, H., Ludwig, A., Hofmann, F., and Klugbauer, N. (2000). Expression of T- and L-type calcium channel mRNA in murine sinoatrial node. *FEBS Lett.* 481, 73–76. doi: 10.1016/S0014-5793(00)01979-7

Boyett, M. R., Honjo, H., and Kodama, I. (2000). The sinoatrial node, a heterogeneous pacemaker structure. *Cardiovasc. Res.* 47, 658–687. doi: 10.1016/S0008-6363(00)00135-8

Brown, H., Difrancesco, D., and Noble, S. (1979). Cardiac pacemaker oscillation and its modulation by autonomic transmitters. *J. Exp. Biol.* 81, 175–204.

Brucato, A., Cimaz, R., Catelli, L., and Meroni, P. (2000). Anti-Ro-associated sinus bradycardia in newborns. *Circulation* 102, E88–E89. doi: 10.1161/01.CIR.102.11.e88

Buraei, Z., and Yang, J. (2010). The ss subunit of voltage-gated Ca^{2+} channels. *Physiol. Rev.* 90, 1461–1506. doi: 10.1152/physrev.00057.2009

Buraei, Z., and Yang, J. (2013). Structure and function of the beta subunit of voltage-gated $Ca^{(2)(+)}$ channels. *Biochim. Biophys. Acta* 1828, 1530–1540. doi: 10.1016/j.bbamem.2012.08.028

Camelliti, P., Green, C. R., Legrice, I., and Kohl, P. (2004). Fibroblast network in rabbit sinoatrial node: structural and functional identification of homogeneous and heterogeneous cell coupling. *Circ. Res.* 94, 828–835. doi: 10.1161/01.RES.0000122382.19400.14

Carbone, E., and Lux, H. D. (1987). Kinetics and selectivity of a low-voltage-activated calcium current in chick and rat sensory neurons. *J. Physiol.* 386, 547–570. doi: 10.1113/jphysiol.1987.sp016551

Catterall, W. A. (2000). Structure and regulation of voltage-gated Ca^{2+} channels. *Annu. Rev. Cell Dev. Biol.* 16, 521–555. doi: 10.1146/annurev.cellbio.16.1.521

Catterall, W. A., Striessnig, J., Snutch, T. P., and Perez-Reyes, E. (2003). International union of pharmacology. XL. Compendium of voltage-gated ion channels: calcium channels. *Pharmacol. Rev.* 55, 579–581. doi: 10.1124/pr.55.4.8

Cens, T., Mangoni, M. E., Richard, S., Nargeot, J., and Charnet, P. (1996). Coexpression of the beta2 subunit does not induce voltage-dependent facilitation of the class C L-type Ca channel. *Pflugers Arch.* 431, 771–774.

Chemin, J., Traboulsie, A., and Lory, P. (2006). Molecular pathways underlying the modulation of T-type calcium channels by neurotransmitters and hormones. *Cell Calcium* 40, 121–134. doi: 10.1016/j.ceca.2006.04.015

Chen, C. C., Lamping, K. G., Nuno, D. W., Barresi, R., Prouty, S. J., Lavoie, J. L., et al. (2003). Abnormal coronary function in mice deficient in alpha1H T-type Ca^{2+} channels. *Science* 302, 1416–1418. doi: 10.1126/science.1089268

Christel, C., and Lee, A. (2012). Ca^{2+}-dependent modulation of voltage-gated Ca^{2+} channels. *Biochim. Biophys. Acta* 1820, 1243–1252. doi: 10.1016/j.bbagen.2011.12.012

Christel, C. J., Cardona, N., Mesirca, P., Herrmann, S., Hofmann, F., Striessnig, J., et al. (2012). Distinct localization and modulation of Cav1.2 and Cav1.3 L-type Ca^{2+} channels in mouse sinoatrial node. *J. Physiol.* 590, 6327–6342. doi: 10.1113/jphysiol.2012.239954

Crotti, L., Johnson, C. N., Graf, E., De Ferrari, G. M., Cuneo, B. F., Ovadia, M., et al. (2013). Calmodulin mutations associated with recurrent cardiac arrest in infants. *Circulation* 127, 1009–1017. doi: 10.1161/CIRCULATIONAHA.112.001216

De Jongh, K. S., Murphy, B. J., Colvin, A. A., Hell, J. W., Takahashi, M., and Catterall, W. A. (1996). Specific phosphorylation of a site in the full-length form of the alpha 1 subunit of the cardiac L-type calcium channel by adenosine 3',5'-cyclic monophosphate-dependent protein kinase. *Biochemistry* 35, 10392–10402. doi: 10.1021/bi953023c

Difrancesco, D. (1991). The contribution of the 'pacemaker' current (if) to generation of spontaneous activity in rabbit sino-atrial node myocytes. *J. Physiol.* 434, 23–40. doi: 10.1113/jphysiol.1991.sp018457

Difrancesco, D. (1993). Pacemaker mechanisms in cardiac tissue. *Annu. Rev. Physiol.* 55, 455–472. doi: 10.1146/annurev.ph.55.030193.002323

Difrancesco, D. (2010). The role of the funny current in pacemaker activity. *Circ. Res.* 106, 434–446. doi: 10.1161/CIRCRESAHA.109.208041

Difrancesco, D., and Tortora, P. (1991). Direct activation of cardiac pacemaker channels by intracellular cyclic AMP. *Nature* 351, 145–147. doi: 10.1038/351145a0

Dobrzynski, H., Anderson, R. H., Atkinson, A., Borbas, Z., D'Souza, A., Fraser, J. F., et al. (2013). Structure, function and clinical relevance of the cardiac conduction system, including the atrioventricular ring and outflow tract tissues. *Pharmacol. Ther.* 139, 260–288. doi: 10.1016/j.pharmthera.2013.04.010

Dobrzynski, H., Boyett, M. R., and Anderson, R. H. (2007). New insights into pacemaker activity: promoting understanding of sick sinus syndrome. *Circulation* 115, 1921–1932. doi: 10.1161/CIRCULATIONAHA.106.616011

Dobrzynski, H., Li, J., Tellez, J., Greener, I. D., Nikolski, V. P., Wright, S. E., et al. (2005). Computer three-dimensional reconstruction of the sinoatrial node. *Circulation* 111, 846–854. doi: 10.1161/01.CIR.0000152100.04087.DB

Doerr, T., Denger, R., and Trautwein, W. (1989). Calcium currents in single SA nodal cells of the rabbit heart studied with action potential clamp. *Pflugers Arch.* 413, 599–603. doi: 10.1007/BF00581808

Fenske, S., Krause, S. C., Hassan, S. I., Becirovic, E., Auer, F., Bernard, R., et al. (2013). Sick sinus syndrome in HCN1-deficient mice. *Circulation* 128, 2585–2594. doi: 10.1161/CIRCULATIONAHA.113.003712

Fermini, B., and Nathan, R. D. (1991). Removal of sialic acid alters both T- and L-type calcium currents in cardiac myocytes. *Am. J. Physiol.* 260, H735–H743.

Ferron, L., Capuano, V., Deroubaix, E., Coulombe, A., and Renaud, J. F. (2002). Functional and molecular characterization of a T-type $Ca^{(2+)}$ channel during fetal and postnatal rat heart development. *J. Mol. Cell. Cardiol.* 34, 533–546. doi: 10.1006/jmcc.2002.1535

Hagiwara, N., Irisawa, H., and Kameyama, M. (1988). Contribution of two types of calcium currents to the pacemaker potentials of rabbit sino-atrial node cells. *J. Physiol.* 395, 233–253. doi: 10.1113/jphysiol.1988.sp016916

Hirano, Y., Fozzard, H. A., and January, C. T. (1989). Characteristics of L- and T-type Ca^{2+} currents in canine cardiac Purkinje cells. *Am. J. Physiol.* 256, H1478–H1492.

Hu, K., Qu, Y., Yue, Y., and Boutjdir, M. (2004). Functional basis of sinus bradycardia in congenital heart block. *Circ. Res.* 94, e32–38. doi: 10.1161/01.RES.0000121566.01778.06

Huser, J., Blatter, L. A., and Lipsius, S. L. (2000). Intracellular Ca^{2+} release contributes to automaticity in cat atrial pacemaker cells. *J. Physiol.* 524(Pt 2), 415–422. doi: 10.1111/j.1469-7793.2000.00415.x

Inada, S., Zhang, H., Tellez, J. O., Shibata, N., Nakazawa, K., Kamiya, K., et al. (2014). Importance of gradients in membrane properties and electrical coupling in sinoatrial node pacing. *PLoS ONE* 9:e94565. doi: 10.1371/journal.pone.0094565

James, T. N. (2003). Structure and function of the sinus node, AV node and his bundle of the human heart: part II–function. *Prog. Cardiovasc. Dis.* 45, 327–360. doi: 10.1053/pcad.2003.1

Kim, S., Yun, H. M., Baik, J. H., Chung, K. C., Nah, S. Y., and Rhim, H. (2007). Functional interaction of neuronal Cav1.3 L-type calcium channel with ryanodine receptor type 2 in the rat hippocampus. *J. Biol. Chem.* 282, 32877–32889. doi: 10.1074/jbc.M701418200

Kodama, I., Nikmaram, M. R., Boyett, M. R., Suzuki, R., Honjo, H., and Owen, J. M. (1997). Regional differences in the role of the Ca^{2+} and Na^{+} currents in pacemaker activity in the sinoatrial node. *Am. J. Physiol.* 272, H2793–H2806.

Kohl, P., and Gourdie, R. G. (2014). Fibroblast-myocyte electrotonic coupling: does it occur in native cardiac tissue? *J. Mol. Cell. Cardiol.* 70, 37–46. doi: 10.1016/j.yjmcc.2013.12.024

Koschak, A., Reimer, D., Huber, I., Grabner, M., Glossmann, H., Engel, J., et al. (2001). alpha 1D (Cav1.3) subunits can form l-type Ca^{2+} channels activating at negative voltages. *J. Biol. Chem.* 276, 22100–22106. doi: 10.1074/jbc.M101469200

Kovoor, P., Wickman, K., Maguire, C. T., Pu, W., Gehrmann, J., Berul, C. I., et al. (2001). Evaluation of the role of I(KACh) in atrial fibrillation using a mouse knockout model. *J. Am. Coll. Cardiol.* 37, 2136–2143. doi: 10.1016/S0735-1097(01)01304-3

Lakatta, E. G., Maltsev, V. A., and Vinogradova, T. M. (2010). A coupled SYSTEM of intracellular Ca^{2+} clocks and surface membrane voltage clocks controls the timekeeping mechanism of the heart's pacemaker. *Circ. Res.* 106, 659–673. doi: 10.1161/CIRCRESAHA.109.206078

Lande, G., Demolombe, S., Bammert, A., Moorman, A., Charpentier, F., and Escande, D. (2001). Transgenic mice overexpressing human KvLQT1 dominant-negative isoform. Part II: pharmacological profile. *Cardiovasc. Res.* 50, 328–334. doi: 10.1016/S0008-6363(01)00232-2

Lang, D., Petrov, V., Lou, Q., Osipov, G., and Efimov, I. R. (2011). Spatiotemporal control of heart rate in a rabbit heart. *J. Electrocardiol.* 44, 626–634. doi: 10.1016/j.jelectrocard.2011.08.010

Lehmann, H., and Klein, U. E. (1978). Familial sinus node dysfunction with autosomal dominant inheritance. *Br. Heart J.* 40, 1314–1316. doi: 10.1136/hrt.40.11.1314

Le Quang, K., Benito, B., Naud, P., Qi, X. Y., Shi, Y. F., Tardif, J. C., et al. (2013). T-type calcium current contributes to escape automaticity and governs the occurrence of lethal arrhythmias after atrioventricular block in mice. *Circ. Arrhythm. Electrophysiol.* 6, 799–808. doi: 10.1161/CIRCEP.113.000407

Li, J., Qu, J., and Nathan, R. D. (1997). Ionic basis of ryanodine's negative chronotropic effect on pacemaker cells isolated from the sinoatrial node. *Am. J. Physiol.* 273, H2481–H2489.

Li, Y., Wang, F., Zhang, X., Qi, Z., Tang, M., Szeto, C., et al. (2012). beta-Adrenergic stimulation increases Cav3.1 activity in cardiac myocytes through protein kinase A. *PLoS ONE* 7:e39965. doi: 10.1371/journal.pone.0039965

Limpitikul, W. B., Dick, I. E., Joshi-Mukherjee, R., Overgaard, M. T., George, A. L. Jr., and Yue, D. T. (2014). Calmodulin mutations associated with long QT syndrome prevent inactivation of cardiac L-type $Ca^{(2+)}$ currents and promote proarrhythmic behavior in ventricular myocytes. *J. Mol. Cell. Cardiol.* 74, 115–124. doi: 10.1016/j.yjmcc.2014.04.022

Lipsius, S. L., Huser, J., and Blatter, L. A. (2001). Intracellular Ca^{2+} release sparks atrial pacemaker activity. *News Physiol. Sci.* 16, 101–106.

Liu, Y., Zeng, W., Delmar, M., and Jalife, J. (1993). Ionic mechanisms of electronic inhibition and concealed conduction in rabbit atrioventricular nodal myocytes. *Circulation* 88, 1634–1646. doi: 10.1161/01.CIR.88.4.1634

Lu, L., Zhang, Q., Timofeyev, V., Zhang, Z., Young, J. N., Shin, H. S., et al. (2007). Molecular coupling of a Ca^{2+}-activated K^{+} channel to L-type Ca^{2+} channels via alpha-actinin2. *Circ. Res.* 100, 112–120. doi: 10.1161/01.RES.0000253095.44186.72

Mackintosh, A. F., and Chamberlain, D. A. (1979). Sinus node disease affecting both parents and both children. *Eur. J. Cardiol.* 10, 117–122.

Mangoni, M. E., Couette, B., Bourinet, E., Platzer, J., Reimer, D., Striessnig, J., et al. (2003). Functional role of L-type Cav1.3 Ca^{2+} channels in cardiac pacemaker activity. *Proc. Natl. Acad. Sci. U.S.A.* 100, 5543–5548. doi: 10.1073/pnas.0935295100

Mangoni, M. E., Couette, B., Marger, L., Bourinet, E., Striessnig, J., and Nargeot, J. (2006a). Voltage-dependent calcium channels and cardiac pacemaker activity: from ionic currents to genes. *Prog. Biophys. Mol. Biol.* 90, 38–63. doi: 10.1016/j.pbiomolbio.2005.05.003

Mangoni, M. E., Fontanaud, P., Noble, P. J., Noble, D., Benkemoun, H., Nargeot, J., et al. (2000). Facilitation of the L-type calcium current in rabbit sino-atrial cells: effect on cardiac automaticity. *Cardiovasc. Res.* 48, 375–392. doi: 10.1016/S0008-6363(00)00182-6

Mangoni, M. E., and Nargeot, J. (2008). Genesis and regulation of the heart automaticity. *Physiol. Rev.* 88, 919–982. doi: 10.1152/physrev.00018.2007

Mangoni, M. E., Traboulsie, A., Leoni, A. L., Couette, B., Marger, L., Le Quang, K., et al. (2006b). Bradycardia and slowing of the atrioventricular conduction in mice lacking CaV3.1/alpha1G T-type calcium channels. *Circ. Res.* 98, 1422–1430. doi: 10.1161/01.RES.0000225862.14314.49

Marger, L., Mesirca, P., Alig, J., Torrente, A., Dubel, S., Engeland, B., et al. (2011a). Functional roles of Ca(v)1.3, Ca(v)3.1 and HCN channels in automaticity of mouse atrioventricular cells: insights into the atrioventricular pacemaker mechanism. *Channels (Austin)* 5, 251–261. doi: 10.4161/chan.5.3.15266

Marger, L., Mesirca, P., Alig, J., Torrente, A., Dubel, S., Engeland, B., et al. (2011b). Pacemaker activity and ionic currents in mouse atrioventricular node cells. *Channels (Austin)* 5, 241–250. doi: 10.4161/chan.5.3.15264

Marionneau, C., Couette, B., Liu, J., Li, H., Mangoni, M. E., Nargeot, J., et al. (2005). Specific pattern of ionic channel gene expression associated with pacemaker activity in the mouse heart. *J. Physiol.* 562, 223–234. doi: 10.1113/jphysiol.2004.074047

Marshall, P. W., Rouse, W., Briggs, I., Hargreaves, R. B., Mills, S. D., and McLoughlin, B. J. (1993). ICI D7288, a novel sinoatrial node modulator. *J. Cardiovasc. Pharmacol.* 21, 902–906. doi: 10.1097/00005344-199306000-00008

Matthes, J., Yildirim, L., Wietzorrek, G., Reimer, D., Striessnig, J., and Herzig, S. (2004). Disturbed atrio-ventricular conduction and normal contractile function in isolated hearts from Cav1.3-knockout mice. *Naunyn Schmiedebergs Arch. Pharmacol.* 369, 554–562. doi: 10.1007/s00210-004-0940-7

McRory, J. E., Hamid, J., Doering, C. J., Garcia, E., Parker, R., Hamming, K., et al. (2004). The CACNA1F gene encodes an L-type calcium channel with unique biophysical properties and tissue distribution. *J. Neurosci.* 24, 1707–1718. doi: 10.1523/JNEUROSCI.4846-03.2004

Monfredi, O., Maltseva, L. A., Spurgeon, H. A., Boyett, M. R., Lakatta, E. G., and Maltsev, V. A. (2013). Beat-to-beat variation in periodicity of local calcium releases contributes to intrinsic variations of spontaneous cycle length in isolated single sinoatrial node cells. *PLoS ONE* 8:e67247. doi: 10.1371/journal.pone.0067247

Neco, P., Torrente, A. G., Mesirca, P., Zorio, E., Liu, N., Priori, S. G., et al. (2012). Paradoxical effect of increased diastolic Ca^{2+} release and decreased sinoatrial node activity in a mouse model of catecholaminergic polymorphic ventricular tachycardia. *Circulation* 126, 392–401. doi: 10.1161/CIRCULATIONAHA.111.075382

Niwa, N., Yasui, K., Opthof, T., Takemura, H., Shimizu, A., Horiba, M., et al. (2004). Cav3.2 subunit underlies the functional T-type Ca^{2+} channel in murine hearts during the embryonic period. *Am. J. Physiol. Heart Circ. Physiol.* 286, H2257–H2263. doi: 10.1152/ajpheart.01043.2003

Nyegaard, M., Overgaard, M. T., Sondergaard, M. T., Vranas, M., Behr, E. R., Hildebrandt, L. L., et al. (2012). Mutations in calmodulin cause ventricular tachycardia and sudden cardiac death. *Am. J. Hum. Genet.* 91, 703–712. doi: 10.1016/j.ajhg.2012.08.015

Ouardouz, M., Nikolaeva, M. A., Coderre, E., Zamponi, G. W., McRory, J. E., Trapp, B. D., et al. (2003). Depolarization-induced Ca^{2+} release in ischemic spinal cord white matter involves L-type Ca^{2+} channel activation of ryanodine receptors. *Neuron* 40, 53–63. doi: 10.1016/j.neuron.2003.08.016

Perez-Reyes, E. (2003). Molecular physiology of low-voltage-activated t-type calcium channels. *Physiol. Rev.* 83, 117–161. doi: 10.1152/physrev.00018.2002

Pfeufer, A., van Noord, C., Marciante, K. D., Arking, D. E., Larson, M. G., Smith, A. V., et al. (2010). Genome-wide association study of PR interval. *Nat. Genet.* 42, 153–159. doi: 10.1038/ng.517

Platzer, J., Engel, J., Schrott-Fischer, A., Stephan, K., Bova, S., Chen, H., et al. (2000). Congenital deafness and sinoatrial node dysfunction in mice lacking class D L-type Ca^{2+} channels. *Cell* 102, 89–97. doi: 10.1016/S0092-8674(00)00013-1

Protas, L., Difrancesco, D., and Robinson, R. B. (2001). L-type but not T-type calcium current changes during postnatal development in rabbit sinoatrial node. *Am. J. Physiol. Heart Circ. Physiol.* 281, H1252–H1259.

Ramadan, O., Qu, Y., Wadgaonkar, R., Baroudi, G., Karnabi, E., Chahine, M., et al. (2009). Phosphorylation of the consensus sites of protein kinase A on alpha1D L-type calcium channel. *J. Biol. Chem.* 284, 5042–5049. doi: 10.1074/jbc.M809132200

Rose, R. A., Sellan, M., Simpson, J. A., Izaddoustdar, F., Cifelli, C., Panama, B. K., et al. (2011). Iron overload decreases CaV1.3-dependent L-type Ca^{2+} currents leading to bradycardia, altered electrical conduction, and atrial fibrillation. *Circ. Arrhythm. Electrophysiol.* 4, 733–742. doi: 10.1161/CIRCEP.110.960401

Sanders, P., Lau, D. H., and Kalman, J. K. (2014). "Sinus node abnormalities," in *Cardiac Electrophysiology: from Cell to Bedside, 6th Edn.*, eds D. P. Zipes and J. Jalife (Philadelphia, PA: Elsevier Saunders), 691–696.

Sarachek, N. S., and Leonard, J. L. (1972). Familial heart block and sinus bradycardia. Classification and natural history. *Am. J. Cardiol.* 29, 451–458. doi: 10.1016/0002-9149(72)90432-8

Sinnegger-Brauns, M. J., Hetzenauer, A., Huber, I. G., Renstrom, E., Wietzorrek, G., Berjukov, S., et al. (2004). Isoform-specific regulation of mood behavior and pancreatic beta cell and cardiovascular function by L-type Ca^{2+} channels. *J. Clin. Invest.* 113, 1430–1439. doi: 10.1172/JCI200420208

Strandberg, L. S., Cui, X., Rath, A., Liu, J., Silverman, E. D., Liu, X., et al. (2013). Congenital heart block maternal sera autoantibodies target an extracellular epitope on the alpha1G T-type calcium channel in human fetal hearts. *PLoS ONE* 8:e72668. doi: 10.1371/journal.pone.0072668

Striessnig, J. (1999). Pharmacology, structure and function of cardiac L-type Ca(2+) channels. *Cell. Physiol. Biochem.* 9, 242–269. doi: 10.1159/000016320

Striessnig, J., and Koschak, A. (2008). Exploring the function and pharmacotherapeutic potential of voltage-gated Ca^{2+} channels with gene knockout models. *Channels (Austin)* 2, 233–251. doi: 10.4161/chan.2.4.5847

Suh, B. C., and Hille, B. (2005). Regulation of ion channels by phosphatidylinositol 4,5-bisphosphate. *Curr. Opin. Neurobiol.* 15, 370–378. doi: 10.1016/j.conb.2005.05.005

Tanabe, T., Beam, K. G., Powell, J. A., and Numa, S. (1988). Restoration of excitation-contraction coupling and slow calcium current in dysgenic muscle by dihydropyridine receptor complementary DNA. *Nature* 336, 134–139. doi: 10.1038/336134a0

Thuesen, A. D., Andersen, H., Cardel, M., Toft, A., Walter, S., Marcussen, N., et al. (2014). Differential effect of T-type voltage-gated Ca^{2+} channel disruption on renal plasma flow and glomerular filtration rate *in vivo*. *Am. J. Physiol. Renal Physiol.* 307, F445–F452. doi: 10.1152/ajprenal.00016.2014

Tseng, G. N., and Boyden, P. A. (1989). Multiple types of Ca^{2+} currents in single canine Purkinje cells. *Circ. Res.* 65, 1735–1750. doi: 10.1161/01.RES.65.6.1735

Tuluc, P., Molenda, N., Schlick, B., Obermair, G. J., Flucher, B. E., and Jurkat-Rott, K. (2009). A CaV1.1 Ca^{2+} channel splice variant with high conductance and voltage-sensitivity alters EC coupling in developing skeletal muscle. *Biophys. J.* 96, 35–44. doi: 10.1016/j.bpj.2008.09.027

Ueda, K., Nakamura, K., Hayashi, T., Inagaki, N., Takahashi, M., Arimura, T., et al. (2004). Functional characterization of a trafficking-defective HCN4 mutation, D553N, associated with cardiac arrhythmia. *J. Biol. Chem.* 279, 27194–27198. doi: 10.1074/jbc.M311953200

van der Heyden, M. A., Wijnhoven, T. J., and Opthof, T. (2005). Molecular aspects of adrenergic modulation of cardiac L-type Ca^{2+} channels. *Cardiovasc. Res.* 65, 28–39. doi: 10.1016/j.cardiores.2004.09.028

Verheijck, E. E., van Ginneken, A. C., Wilders, R., and Bouman, L. N. (1999). Contribution of L-type Ca^{2+} current to electrical activity in sinoatrial nodal myocytes of rabbits. *Am. J. Physiol.* 276, H1064–H1077.

Verheijck, E. E., Wilders, R., and Bouman, L. N. (2002). Atrio-sinus interaction demonstrated by blockade of the rapid delayed rectifier current. *Circulation* 105, 880–885. doi: 10.1161/hc0702.104128

Vinogradova, T. M., Bogdanov, K. Y., and Lakatta, E. G. (2002). beta-Adrenergic stimulation modulates ryanodine receptor $Ca^{(2+)}$ release during diastolic depolarization to accelerate pacemaker activity in rabbit sinoatrial nodal cells. *Circ. Res.* 90, 73–79. doi: 10.1161/hh0102.102271

Wolf, R. M., Glynn, P., Hashemi, S., Zarei, K., Mitchell, C. C., Anderson, M. E., et al. (2013). Atrial fibrillation and sinus node dysfunction in human ankyrin-B syndrome: a computational analysis. *Am. J. Physiol. Heart Circ. Physiol.* 304, H1253–H1266. doi: 10.1152/ajpheart.00734.2012

Zhang, Q., Timofeyev, V., Lu, L., Li, N., Singapuri, A., Long, M. K., et al. (2008). Functional roles of a Ca^{2+}-activated K^+ channel in atrioventricular nodes. *Circ. Res.* 102, 465–471. doi: 10.1161/CIRCRESAHA.107.161778

Zhang, Q., Timofeyev, V., Qiu, H., Lu, L., Li, N., Singapuri, A., et al. (2011). Expression and roles of Cav1.3 (alpha1D) L-type $Ca^{(2)+}$ channel in atrioventricular node automaticity. *J. Mol. Cell. Cardiol.* 50, 194–202. doi: 10.1016/j.yjmcc.2010.10.002

Zhang, Z., He, Y., Tuteja, D., Xu, D., Timofeyev, V., Zhang, Q., et al. (2005). Functional roles of Cav1.3(alpha1D) calcium channels in atria: insights gained from gene-targeted null mutant mice. *Circulation* 112, 1936–1944. doi: 10.1161/CIRCULATIONAHA.105.540070

Zhang, Z., Xu, Y., Song, H., Rodriguez, J., Tuteja, D., Namkung, Y., et al. (2002). Functional Roles of Ca(v)1.3 (alpha(1D)) calcium channel in sinoatrial nodes: insight gained using gene-targeted null mutant mice. *Circ. Res.* 90, 981–987. doi: 10.1161/01.RES.0000018003.14304.E2

Conflict of Interest Statement: The authors declare that the research was conducted in the absence of any commercial or financial relationships that could be construed as a potential conflict of interest.

Received: 21 November 2014; accepted: 12 January 2015; published online: 02 February 2015.

Citation: Mesirca P, Torrente AG and Mangoni ME (2015) Functional role of voltage gated Ca^{2+} channels in heart automaticity. Front. Physiol. ***6****:19. doi: 10.3389/fphys.2015.00019*

This article was submitted to Cardiac Electrophysiology, a section of the journal Frontiers in Physiology.

frontiers in PHYSIOLOGY

ORIGINAL RESEARCH ARTICLE
published: 02 February 2015
doi: 10.3389/fphys.2015.00018

Ca^{2+} cycling properties are conserved despite bradycardic effects of heart failure in sinoatrial node cells

Arie O. Verkerk[1]*, Marcel M. G. J. van Borren[1,2], Antoni C. G. van Ginneken[1] and Ronald Wilders[1]

[1] *Department of Anatomy, Embryology and Physiology, Academic Medical Center, University of Amsterdam, Amsterdam, Netherlands*
[2] *Laboratory of Clinical Chemistry and Haematology, Rijnstate Hospital, Arnhem, Netherlands*

Edited by:
Ming Lei, University of Oxford, UK

Reviewed by:
Henggui Zhang, The University of Manchester, UK
Christopher Huang, University of Cambridge, UK

****Correspondence:***
Arie O. Verkerk, Department of Anatomy, Embryology and Physiology, Academic Medical Center, University of Amsterdam, Meibergdreef 15, 1105 AZ Amsterdam, Netherlands
e-mail: a.o.verkerk@amc.uva.nl

Background: In animal models of heart failure (HF), heart rate decreases due to an increase in intrinsic cycle length (CL) of the sinoatrial node (SAN). Pacemaker activity of SAN cells is complex and modulated by the membrane clock, i.e., the ensemble of voltage gated ion channels and electrogenic pumps and exchangers, and the Ca^{2+} clock, i.e., the ensemble of intracellular Ca^{2+} ($[Ca^{2+}]_i$) dependent processes. HF in SAN cells results in remodeling of the membrane clock, but few studies have examined its effects on $[Ca^{2+}]_i$ homeostasis.

Methods: SAN cells were isolated from control rabbits and rabbits with volume and pressure overload-induced HF. $[Ca^{2+}]_i$ concentrations, and action potentials (APs) and Na^+–Ca^{2+} exchange current (I_{NCX}) were measured using indo-1 and patch-clamp methodology, respectively.

Results: The frequency of spontaneous $[Ca^{2+}]_i$ transients was significantly lower in HF SAN cells (3.0 ± 0.1 ($n = 40$) vs. 3.4 ± 0.1 Hz ($n = 45$); mean ± SEM), indicating that intrinsic CL was prolonged. HF slowed the $[Ca^{2+}]_i$ transient decay, which could be explained by the slower frequency and reduced sarcoplasmic reticulum (SR) dependent rate of Ca^{2+} uptake. Other $[Ca^{2+}]_i$ transient parameters, SR Ca^{2+} content, I_{NCX} density, and I_{NCX}-$[Ca^{2+}]_i$ relationship were all unaffected by HF. Combined AP and $[Ca^{2+}]_i$ recordings demonstrated that the slower $[Ca^{2+}]_i$ transient decay in HF SAN cells may result in increased I_{NCX} during the diastolic depolarization, but that this effect is likely counteracted by the HF-induced increase in intracellular Na^+. β-adrenergic and muscarinic stimulation were not changed in HF SAN cells, except that late diastolic $[Ca^{2+}]_i$ rise, a prominent feature of the Ca^{2+} clock, is lower during β-adrenergic stimulation.

Conclusions: HF SAN cells have a slower $[Ca^{2+}]_i$ transient decay with limited effects on pacemaker activity. Reduced late diastolic $[Ca^{2+}]_i$ rise during β-adrenergic stimulation may contribute to an impaired increase in intrinsic frequency in HF SAN cells.

Keywords: heart failure, pacemaker activity, intracellular Ca^{2+}, Ca^{2+} clock, membrane clock, sinoatrial node, action potentials, sodium-calcium exchanger

INTRODUCTION

Pacemaker activity of the sinoatrial node (SAN) is controlled by a complex system of clocks composed of time- and voltage-dependent sarcolemmal currents, designated the voltage or membrane clock (Mangoni and Nargeot, 2008), and tightly coupled sarcoplasmic reticulum (SR) Ca^{2+} cycling molecules together with the Na^+–Ca^{2+} exchange current (I_{NCX}), named the Ca^{2+} clock (Lakatta et al., 2010). The primary mechanism of SAN pacemaking is heavily debated (DiFrancesco and Robinson, 2002; Kodama et al., 2002;Vinogradova et al., 2002b; Honjo et al., 2003; Lakatta et al., 2003; Lipsius and Bers, 2003; Bers, 2006a; Lakatta and DiFrancesco, 2009; DiFrancesco, 2010; Maltsev and Lakatta, 2010a, 2012; Verkerk and Wilders, 2010; Himeno et al., 2011a,b; Maltsev et al., 2011; DiFrancesco and Noble, 2012a,b; Lakatta and Maltsev, 2012), but it likely involves a tight collaboration of both clock systems, because intracellular Ca^{2+} ($[Ca^{2+}]_i$) affects various membrane currents directly, e.g., I_{NCX} (Blaustein and Lederer, 1999), hyperpolarization-activated current (I_f) (Rigg et al., 2003), slow component of delayed rectifier K^+ current (I_{Ks}) (Tohse, 1990), long lasting Ca^{2+} current ($I_{Ca,L}$) (Sipido et al., 1995), transient Ca^{2+} current ($I_{Ca,T}$) (Lacinová et al., 2006), Cl^- current (Arai et al., 1996; Verkerk et al., 2002), and/or indirectly via calmodulin-dependent protein kinase II (CaMKII) (Wu and Anderson, 2014), and changes in membrane current affect pacemaker rate with resultant changes in $[Ca^{2+}]_i$ (Lakatta et al., 2010; van Borren et al., 2010).

Heart failure (HF) reduces pacemaker activity of SAN cells through an increase in intrinsic cycle length (Opthof et al., 2000; Witte et al., 2000; Verkerk et al., 2003; Du et al., 2007). Previously, it has been shown that this was al least due to

remodeling of components of the membrane clock. HF impairs the membrane clock by downregulation of I_f in the SAN of rabbit (Verkerk et al., 2003) and downregulation of the corresponding hyperpolarization-activated (HCN) channel subunits, HCN4 and HCN2, in the SAN of dogs (Zicha et al., 2005). In addition, TTX-sensitive neuronal Na^+ channels, $Na_v1.1$ and $Na_v1.6$, are downregulated in SAN tissue of HF rats (Du et al., 2007). Finally, HF upregulates I_{Ks} in HF SAN cells of rabbit (Verkerk et al., 2003), but since I_{Ks} plays a limited role in pacemaker activity without adrenergic stimulation (Lei et al., 2000), this change in membrane clock is hardly involved in the increase in intrinsic cycle length during HF (Verkerk et al., 2003).

To date, the effect of HF on $[Ca^{2+}]_i$ homeostasis in atrial and ventricular myocytes has been studied in detail (for reviews, see Bers, 2006b; Bers et al., 2006; Kho et al., 2012; Eisner et al., 2013; Luo and Anderson, 2013; Neef and Maier, 2013), but the effect of HF on $[Ca^{2+}]_i$ in SAN cells is hardly known. Shinohara et al. (2010) found that HF, induced by rapid ventricular pacing, results in Ca^{2+} clock malfunction in SAN of dogs, characterized by a reduction of the slope of late diastolic Ca^{2+} elevation (LDCAE) as well as unresponsiveness to isoproterenol and caffeine in intact SAN. Especially the reduced slope of the LDCAE, with associated decrease in localized Ca^{2+} releases (LCRs) or Ca^{2+} sparks (Bogdanov et al., 2006; Maltsev et al., 2006; Joung et al., 2009, 2010; van Borren et al., 2010), may have implications for the Ca^{2+} clock (Stern et al., 2014).

In the present study, we evaluated the $[Ca^{2+}]_i$ homeostasis in isolated control (CTRL) and HF SAN cells using a well-established rabbit model of volume and pressure overload-induced HF. We found a slower spontaneous $[Ca^{2+}]_i$ transient frequency in HF SAN cells, indicating that the intrinsic cycle length was prolonged. HF slowed the $[Ca^{2+}]_i$ transient decay without changes in diastolic and systolic $[Ca^{2+}]_i$ concentrations, LDCAE, and SR Ca^{2+} content. The reduced $[Ca^{2+}]_i$ transient decay velocity was partially, but not completely, explained by the slower intrinsic frequency of HF SAN cells. Neither the I_{NCX} density nor the I_{NCX}-$[Ca^{2+}]_i$ relationship were affected by HF. Combined action potential and $[Ca^{2+}]_i$ measurements demonstrated that the decreased $[Ca^{2+}]_i$ transient decay velocity has limited effect on I_{NCX} during diastolic depolarization.

MATERIALS AND METHODS

CELL PREPARATION

The investigation was approved by the local ethics committee and conformed to the guiding principles of the *Declaration of Helsinki*. HF was induced in 5-month-old male New-Zealand White rabbits by combined volume- and pressure-overload in 2 sequential surgical procedures as described previously (Vermeulen et al., 1994; Verkerk et al., 2011). In short, volume overload was produced by rupture of the aortic valve until pulse pressure was increased by about 60–90%. Three weeks later, pressure overload was created by suprarenal abdominal aorta constriction of approximately 50%. Four months after the last operation, the rabbits were anaesthetized [ketamine (50 mg im; Eurovet, Bladel, The Netherlands) and xylazine (10 mg im; Eurovet, Bladel, The Netherlands)], heparinized (5000 IU, LEO Pharma, Breda, The Netherlands), and killed by intravenous injection of pentobarbital (240 mg; Ceva Sante Animale B.V., Maassluis, The Netherlands). Relative heart weight (i.e., heart weight to body weight ratio), relative lung weight (i.e., lung weight to body weight ratio), and presence of ascites were analyzed as described previously (Vermeulen et al., 1994). Sham-operated rabbits undergoing thoracotomy and age-matched non-operated rabbits do not differ in various heart failure parameters (Vermeulen et al., 1994) and important cellular parameters for hypertrophy and ionic remodeling (Verkerk et al., 2011). In the present study, therefore, non-operated age-matched healthy animals served as control (CTRL). A total of 12 HF and 13 CTRL rabbits were used.

Single SAN cells were enzymatically isolated from the entire SAN region as described previously (Verkerk et al., 2009). Small aliquots of cell suspension were put in a recording chamber on the stage of an inverted microscope. Cells were allowed to adhere for 5 min after which superfusion with Tyrode's solution was started. Tyrode's solution (36 ± 0.2°C) contained (in mM): NaCl 140, KCl 5.4, $CaCl_2$ 1.8, $MgCl_2$ 1.0, glucose 5.5, HEPES 5.0, pH 7.4 (NaOH). Spindle and elongated spindle-like cells displaying regular contractions were selected for measurements.

CALCIUM MEASUREMENTS

$[Ca^{2+}]_i$ was measured in spontaneously active indo-1 (Molecular Probes, Eugene, OR, USA) loaded myocytes as described previously in detail (van Borren et al., 2010). Such signals are a measure of global $[Ca^{2+}]_i$ transients, which are triggered by Ca^{2+} influx through sarcolemmal Ca^{2+} channels activated during spontaneous action potentials. As indicated in the Introduction section, these spontaneous action potentials in SAN cells likely involve a tight collaboration of both membrane and Ca^{2+} clock systems. Of note, in this study we used the term "spontaneous $[Ca^{2+}]_i$ transient" analog to "spontaneous action potentials," without assumptions regarding the primary cause of the spontaneous activity. As before, we discerned and analyzed five distinct phases in $[Ca^{2+}]_i$ transients of SAN cells (van Borren et al., 2010): (1) minimum diastolic $[Ca^{2+}]_i$ concentration, (2) maximum systolic $[Ca^{2+}]_i$ concentration, (3) maximum rate of the fast systolic $[Ca^{2+}]_i$ rise, (4) time constant of monoexponential $[Ca^{2+}]_i$ transient decay, and (5) mean rate of the slow diastolic $[Ca^{2+}]_i$ rise during the final third of diastolic depolarization until the fast systolic $[Ca^{2+}]_i$ transient. Ten consecutive spontaneous $[Ca^{2+}]_i$ transients were used to determine the average parameters. To date, SR Ca^{2+} content and the rate of Ca^{2+} uptake into the SR by sarco/endoplasmic reticulum Ca^{2+}-ATPase (SERCA) in cardiac working myocytes are frequently measured using caffeine-induced $[Ca^{2+}]_i$ transients combined with simultaneous I_{NCX} recordings with the patch clamp methodology (Varro et al., 1993), which also allows specific pre-pacing protocols. In SAN cells, however, we were unable to measure reliably the I_{NCX} during caffeine-induced Ca^{2+} transients, due to cell membrane rupture resulting in large "leak" currents in response to the strong and fast caffeine-induced contractions. Therefore, we assessed SR Ca^{2+} content as the fractional release of SR Ca^{2+} (Bers, 1987; Bassani et al., 1992) by comparing the amplitude of the spontaneous $[Ca^{2+}]_i$ transients (average of the preceding six successive spontaneous $[Ca^{2+}]_i$ transients) with that of 20 mM caffeine-evoked $[Ca^{2+}]_i$ transient in the presence of 5 mM $NiCl_2$, to block the

I_{NCX}. The rate of decay was obtained by fitting single exponential functions to the decay phase of the caffeine-evoked $[Ca^{2+}]_i$ transients.

ELECTROPHYSIOLOGY

Action potentials and I_{NCX} were recorded by the amphotericin-perforated patch-clamp technique using an Axopatch 200B amplifier (Molecular Devices, USA). Patch pipettes (borosilicate glass, 2–5 MΩ) were filled with solution containing (in mM): K-gluc 120, KCl 20, NaCl 5, amphotericin-B 0.22, NMDG-Cl (*N*-methyl-D-glucammonium chloride) 10, HEPES 10, pH 7.2 (KOH 5.5). Series resistance was compensated by ≥80%, and potentials were corrected for the calculated liquid junction potential. Action potentials were low-pass filtered (cut-off frequency: 1 kHz) and digitized at 1 kHz; I_{NCX} was filtered and digitized at 1 and 0.2 kHz, respectively. Voltage control and data acquisition were accomplished using pCLAMP 8 software (Molecular Devices, USA), while custom software was used for data analysis. Cell membrane capacitance was estimated by dividing the time constant of the decay of the capacitive transient in response to 5 mV hyperpolarizing voltage clamp steps from 0 mV by the series resistance, and amounted to 50.0 ± 6.9 pF in CTRL ($n = 5$) and 56.1 ± 8.1 pF in HF ($n = 5$) SAN cells (mean ± SEM, $P > 0.05$), in line with the values of 50 ± 4 ($n = 23$) and 52 ± 3 pF ($n = 24$) that we observed in a previous study (Verkerk et al., 2003). I_{NCX} density and the I_{NCX}-$[Ca^{2+}]_i$ relationship were measured as described previously (Weber et al., 2003). In short, a slow depolarizing voltage ramp from −85 to 120 mV results in an increase in $[Ca^{2+}]_i$ due to Ca^{2+} entry through NCX operating in reverse mode (net outward I_{NCX}). Upon fast repolarization, Ca^{2+} removal occurs resulting in a $[Ca^{2+}]_i$ decline due to Ca^{2+} efflux through NCX operating in forward mode (net inward I_{NCX}) (Weber et al., 2003). The relationship between $[Ca^{2+}]_i$ and I_{NCX} is membrane potential dependent, with a steeper relationship at more negative membrane potentials (Hove-Madsen and Tort, 2001). We used a repolarizing potential of −60 mV, which is close to the maximal diastolic potential of both CTRL and HF SAN cells (Verkerk et al., 2003). Thapsigargin (2.5 μM) was added to the Tyrode's solution to block SERCA. In addition, chromanol (5 μM) and E4031 (5 μM) were present to block the slow and rapid components of the delayed rectifier K^+ current, while CsCl (5 mM) was present to block I_f. All drugs were obtained from Sigma (Zwijndrecht, The Netherlands) except for E4031, which was a gift from Eisai (Tokyo, Japan), and noradrenaline (Centrafarm, Etten-Leur, The Netherlands). I_{NCX} densities were calculated by dividing current amplitudes by the cell membrane capacitance.

NUMERICAL RECONSTRUCTION OF SODIUM-CALCIUM EXCHANGE CURRENT

For the numerical reconstruction of I_{NCX} on the basis of the simultaneously recorded experimental data on the membrane potential (V_m) and $[Ca^{2+}]_i$ (combined voltage and calcium clamp, van Borren et al., 2007), we adopted the I_{NCX} formulation of the Lindblad et al. model for a rabbit atrial myocyte (Lindblad et al., 1996), with I_{NCX} scaled down to 78% of its control value, based on mRNA data from Allah et al. (2011). We thus followed the approach of our previous study in which we reconstructed rabbit SAN I_{NCX} in order to compare it with human SAN I_{NCX} (Verkerk et al., 2013).

The Lindblad et al. (1996) equations not only require values for V_m and $[Ca^{2+}]_i$, but also for $[Ca^{2+}]_e$, $[Na^+]_e$ and $[Na^+]_i$, which denote the extracellular Ca^{2+} concentration, the extracellular Na^+ concentration, and the intracellular Na^+ concentration, respectively. $[Ca^{2+}]_e$ and $[Na^+]_e$ were set to 1.8 and 140 mM, respectively, in accordance with the aforementioned Tyrode's solution, whereas $[Na^+]_i$ was set to 5 mM, based on the pipette solution. In some reconstructions, $[Na^+]_i$ was raised to 7.5 mM, as indicated.

STATISTICS

Data are mean ± SEM. Groups of HF SAN cells were compared with groups of CTRL SAN cells using Fisher's exact test, Two-Way Repeated Measures ANOVA followed by pairwise comparison using the Student-Newman-Keuls test, and unpaired *t*-test. Paired *t*-tests were used to compare drug effects within a group. An *F*-test was used to compare frequency dependency between groups. $P < 0.05$ is considered statistically significant.

RESULTS

HF MODEL CHARACTERISTICS

Table 1 summarizes the general characteristics of the HF model. Consistent with previous reports of the volume- and pressure-overload rabbit model of HF (Vermeulen et al., 1994; Baartscheer et al., 2003a,b; Verkerk et al., 2003, 2011; Wiegerinck et al., 2006) body weight was similar, but heart weight was significantly higher in HF compared to CTRL rabbits. Consequently relative heart weight was significantly higher in HF rabbits. In addition, HF rabbits had an increased lung weight and relative lung weight. Moreover, six out of the 12 HF rabbits used in the present study exhibited ascites as assessed during autopsy, while none of the 13 CTRL rabbits did. Finally, we measured the weight of the right atrium to determine whether HF affects also the right atrium including the SAN. We found that both the absolute weight of the right atrium and the relative right atrial weight were significantly higher in HF rabbits.

HF REDUCES THE FREQUENCY AND Ca^{2+} TRANSIENT DECAY OF SAN CELLS

Figure 1A shows typical recordings of $[Ca^{2+}]_i$ transients from SAN cells of a CTRL and a HF rabbit; **Figure 1B** summarizes the

Table 1 | Characteristics of the control (CTRL) and heart failure (HF) model.

	CTRL (*N* = 13)	HF (*N* = 12)
Body weight (kg)	3.90 ± 0.09	3.92 ± 0.13
Heart weight (g)	9.0 ± 0.4	19.2 ± 1.3*
Relative heart weight (g kg^{-1})	2.31 ± 0.08	4.90 ± 0.26*
Lung weight (g)	12.2 ± 0.4	18.8 ± 1.3*
Relative lung weight (g kg^{-1})	3.13 ± 0.08	4.84 ± 0.35*
Presence of ascites (%)	0	50*
Right atrium weight (g)	0.37 ± 0.04	0.86 ± 0.16*
Relative right atrium weight (g kg^{-1})	0.09 ± 0.01	0.22 ± 0.04*

$P < 0.05$ vs. CTRL. N, number of rabbits.

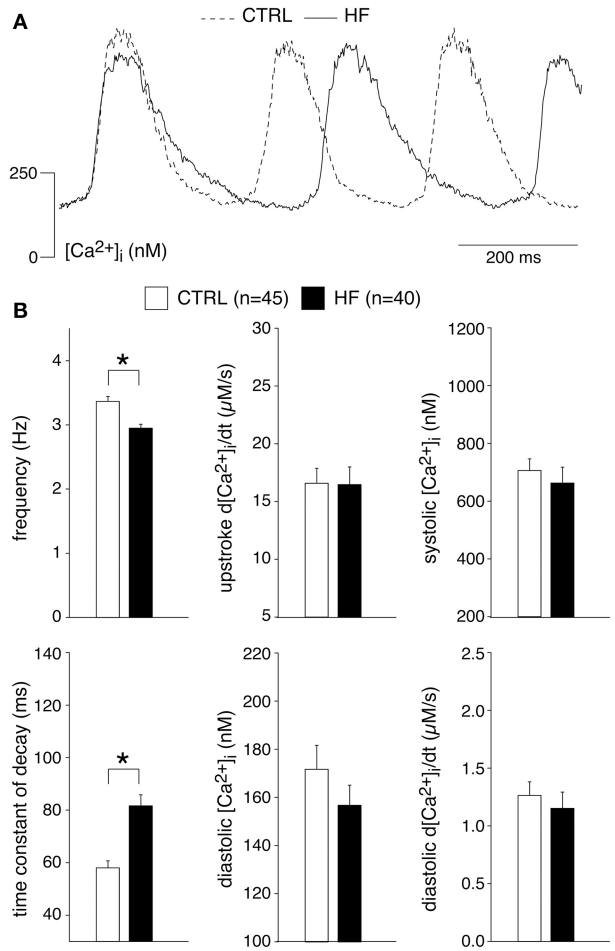

FIGURE 1 | Heart failure (HF) reduces the frequency and intracellular Ca^{2+} ($[Ca^{2+}]_i$) transient decay of sinoatrial (SAN) cells. (A) Representative $[Ca^{2+}]_i$ transients in a SAN cell isolated from a control (CTRL) and HF rabbit. **(B)** Average $[Ca^{2+}]_i$ transient characteristics. $^*P < 0.05$.

average $[Ca^{2+}]_i$ characteristics. In SAN cells, spontaneous action potentials are accompanied by $[Ca^{2+}]_i$ transients in a 1:1 fashion in CTRL (Li et al., 1997; Rigg et al., 2000; Lakatta et al., 2003; Joung et al., 2009, 2010; van Borren et al., 2010) as well as in HF SAN cells (see **Figure 7**, below). Thus, the rate of spontaneous SAN $[Ca^{2+}]_i$ transients is a measure of the intrinsic beating rate. We found a significantly lower frequency of spontaneous $[Ca^{2+}]_i$ transients in HF SAN cells [**Figure 1B**, top left; 2.95 ± 0.06 (HF) vs. 3.37 ± 0.08 (CTRL) Hz], indicating that intrinsic cycle length was prolonged in HF SAN cells. The upstroke velocity of the $[Ca^{2+}]_i$ transient and the systolic $[Ca^{2+}]_i$ transient concentration were not significantly different in HF SAN cells compared with CTRL SAN cells (**Figure 1B**, top right panels). The decay of the $[Ca^{2+}]_i$ transient was significantly slowed in HF SAN cells, as indicated by the significant increase in the time constant of decay (**Figure 1B**, bottom left). On average, $[Ca^{2+}]_i$ transient time constant of decay [81.6 ± 4.2 (HF) vs. 57.8 ± 2.6 (CTRL) ms] is ≈41% larger than in CTRL SAN cells. Neither the diastolic $[Ca^{2+}]_i$ concentration nor the late diastolic $[Ca^{2+}]_i$ rise (diastolic $d[Ca^{2+}]_i/dt$) were significantly different in HF SAN cells compared with CTRL SAN cells (**Figure 1B**, bottom right panels).

In ventricular myocytes, $[Ca^{2+}]_i$ transient parameters are action potential duration (Weber et al., 2003) and frequency-dependent (Hussain et al., 1997; Dibb et al., 2007), while in the SAN an increase in late diastolic $[Ca^{2+}]_i$ rise was observed at higher beating rates (Joung et al., 2009). The role of the action potential duration in the observed slower $[Ca^{2+}]_i$ transient decay is likely limited, because the action potential duration in CTRL and HF SAN cells is similar (Verkerk et al., 2003). However, the decay of the $[Ca^{2+}]_i$ transient has a strong frequency dependency with a slower decay at slower frequencies (Hussain et al., 1997; Dibb et al., 2007). Thus, the slower $[Ca^{2+}]_i$ transient decay that we observed in HF SAN cells may be related to its slower intrinsic frequency. To test this hypothesis, we determined the relationship between frequency and $[Ca^{2+}]_i$ properties by plotting each of the five $[Ca^{2+}]_i$ transient parameters of every cell against its own frequency. The data have been fitted with linear regression lines (**Figure 2**). The linear fits to the CTRL as well as HF SAN cell data have all slopes significantly different from zero (see **Table 2**). However, neither the slopes nor the intercepts are significantly different between CTRL and HF for each of the five parameters (**Table 2**). Thus, while there are clear relationships between all five $[Ca^{2+}]_i$ transient parameters and frequency, these relationships do not differ significantly between CTRL and HF SAN cells. The ≈41% difference in $[Ca^{2+}]_i$ transient time constant of decay between HF and CTRL cells (**Figure 1B**) is larger than expected from the linear regression of the $[Ca^{2+}]_i$ transient time constant of decay vs. frequency relationship. Using the slope and intercept of the regression line for all cells, which amount to 151 (intercept) and −26 (slope), respectively, the difference in frequency between HF and CTRL cells explains only a ≈17% difference.

From these data we conclude that HF reduces the frequency and slows the Ca^{2+} transient decay of SAN cells, the latter partially explained by the slower frequency in HF SAN cells.

HF DOES NOT AFFECT THE SR Ca^{2+} CONTENT OF SAN CELLS

Our experiments demonstrate a reduced $[Ca^{2+}]_i$ transient decay rate, partially explained by a slower intrinsic frequency. The decline of the $[Ca^{2+}]_i$ transient is mainly due to uptake into the SR through SERCA and extrusion of Ca^{2+} via the sarcolemmal Na^+–Ca^{2+} exchange (NCX), while mitochondrial Ca^{2+} uptake and sarcolemmal Ca-ATPase may contribute for a very small fraction (Bers, 2006b; Dibb et al., 2007). In ventricular myocytes, a slower decline of the $[Ca^{2+}]_i$ transient by downregulation of SERCA results in a reduced SR Ca^{2+} content (Bers, 2006b; Bers et al., 2006), while a slower decline of the $[Ca^{2+}]_i$ transient due to downregulation of the NCX may result in increased SR Ca^{2+} content (Bers, 2006b; Eisner et al., 2013). To gain insight into the relationship in SAN cells, we analyzed the amplitude of the normal spontaneous $[Ca^{2+}]_i$ transient as a fraction of the caffeine-evoked transient in the presence of 5 mM $NiCl_2$, termed fractional release, which is an estimate of the proportion of the SR Ca^{2+} content released during each spontaneous transient. **Figure 3A** shows typical recordings in SAN cells from a CTRL

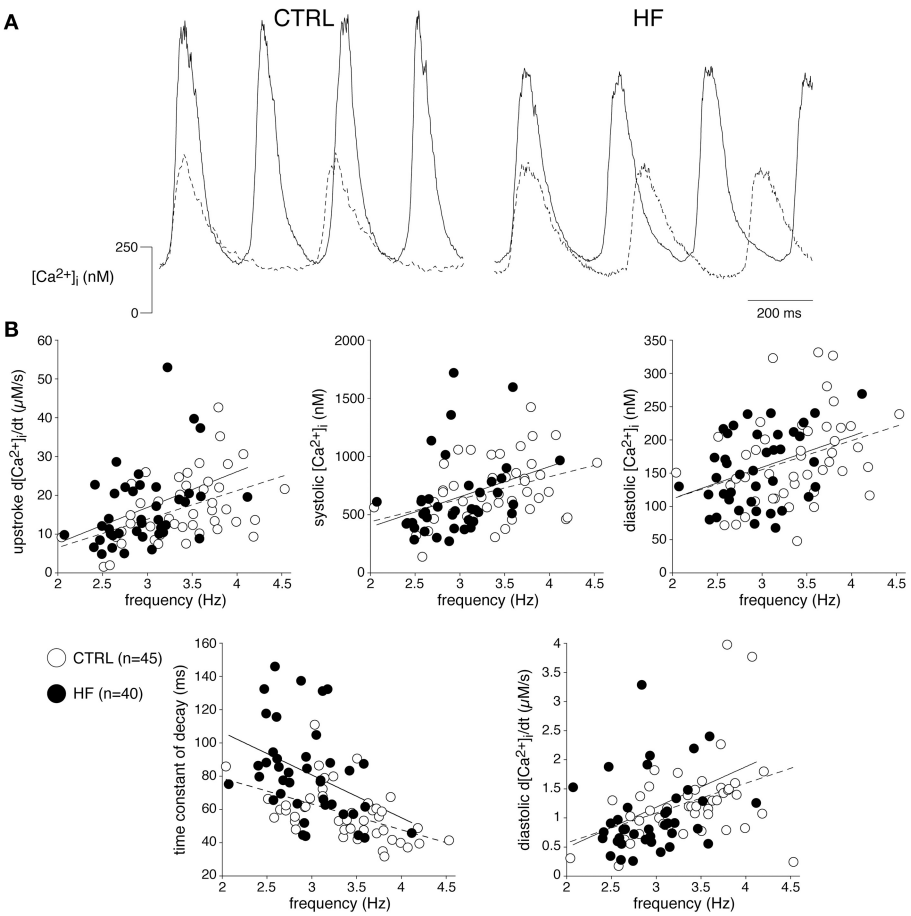

FIGURE 2 | The relationships between frequency and $[Ca^{2+}]_i$ transient parameters are not affected by HF. (A) Typical $[Ca^{2+}]_i$ transients of a fast (solid line) and slow (dashed line) beating CTRL and HF SAN cell. **(B)** Scatter plot of $[Ca^{2+}]_i$ transient parameters of all cells measured vs. frequency. Solid and dashed lines: linear fits to HF and CTRL data, respectively.

Table 2 | Frequency-dependency of $[Ca^{2+}]_i$ transient parameters in CTRL and HF SAN cells.

	CTRL ($n = 45$)		HF ($n = 40$)	
	Slope	**Intercept**	**Slope**	**Intercept**
Upstroke $d[Ca^{2+}]_i/dt$	7.3 ± 2.2	-8.1 ± 7.5	9.2 ± 3.6	-10.7 ± 10.6
Systolic $[Ca^{2+}]_i$	194 ± 73	55 ± 250	260 ± 121	-124 ± 359
Time constant of decay	-16 ± 4	110 ± 14	-26 ± 10	158 ± 29
Diastolic $[Ca^{2+}]_i$	44 ± 18	25 ± 62	47 ± 20	18 ± 59
Diastolic $d[Ca^{2+}]_i/dt$	0.51 ± 0.19	-0.45 ± 0.66	0.70 ± 0.34	-0.90 ± 1.0

*Regression lines as in **Figure 2**. Slope and intercept data are ± standard error. All slopes are significantly different from zero.*

and a HF rabbit. The averaged fractional release of CTRL and HF SAN cells did not differ significantly [0.23 ± 0.04 ($n = 23$) vs. 0.22 ± 0.03 ($n = 18$)] (**Figure 3B**). The caffeine-evoked transient in the presence of $NiCl_2$ can also be used to determine the aforementioned contribution of mitochondrial Ca^{2+} uptake and sarcolemmal Ca-ATPase, because SERCA and NCX function is effectively by-passed by caffeine and Ni^{2+}, respectively (Díaz et al., 2004). The time constant of decay of the caffeine-evoked $[Ca^{2+}]_i$ transient in the presence of 5 mM $NiCl_2$ was 3728 ± 474 (CTRL, $n = 23$) vs. 3654 ± 406 ms (HF, $n = 18$) (**Figure 3C**), indicating that mitochondrial Ca^{2+} uptake and sarcolemmal Ca-ATPase were not affected in HF SAN cells compared to CTRL SAN cells. The relative contribution of the mitochondrial Ca^{2+} uptake and sarcolemmal Ca-ATPase in Ca^{2+} removal was calculated by the use of the time constants of decay of the systolic $[Ca^{2+}]_i$ transient (**Figure 3C**, left) and those of caffeine-evoked $[Ca^{2+}]_i$ transient in the presence of Ni^{2+} (**Figure 3C**, middle) (Díaz et al., 2004). The percentage that mitochondrial Ca^{2+} uptake and sarcolemmal Ca-ATPase contribute to the $[Ca^{2+}]_i$ transient decay was 2.1 ± 0.3 and 2.6 ± 0.4 in CTRL and HF SAN cells, respectively (**Figure 3C**, right).

From these data we conclude that HF neither affects the SR Ca^{2+} content nor the mitochondrial Ca^{2+} uptake and sarcolemmal Ca-ATPase activity of SAN cells.

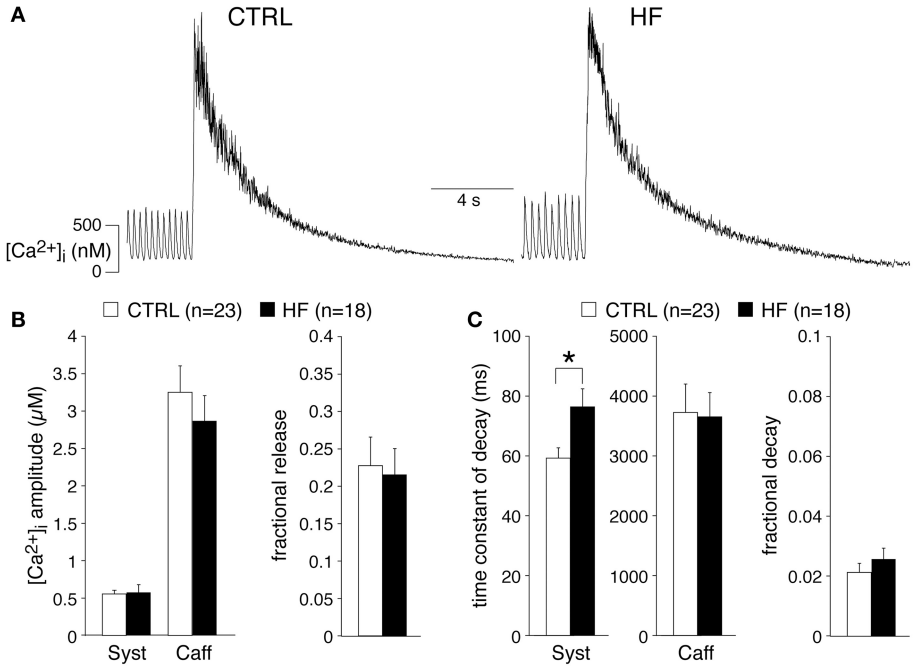

FIGURE 3 | HF does not affect the sarcoplasmic reticulum (SR) Ca^{2+} content of SAN cells. (A) Typical examples of $[Ca^{2+}]_i$ transients induced by application of 20 mM caffeine in the presence of 5 mM $NiCl_2$. **(B)** Average amplitudes of systolic (Syst) and caffeine-induced (Caff) $[Ca^{2+}]_i$ transients (left panel) and the average fractional release (right panel). **(C)** Average time constants of decay of the systolic and caffeine-induced $[Ca^{2+}]_i$ transients (left panels). Right: fractional contribution of mitochondrial Ca^{2+} uptake and sarcolemmal Ca-ATPase to the $[Ca^{2+}]_i$ transient decay. $*P < 0.05$.

HF AFFECTS NEITHER THE I_{NCX} NOR ITS $[Ca^{2+}]_i$ DEPENDENCY

Previously, the I_{NCX} density was found to be similar in CTRL and HF SAN cells of rabbit (Verkerk et al., 2003). These results were obtained by measurements of Ni^+-sensitive currents during a descending ramp, while the free $[Ca^{2+}]_i$ was buffered at 150 nM (Verkerk et al., 2003). HF may affect the relationship between $[Ca^{2+}]_i$ and I_{NCX} (Díaz et al., 2004). Therefore, we next determined the relationship between $[Ca^{2+}]_i$ and I_{NCX} as described previously by Weber et al. (2003). **Figures 4A,B**, show the protocol used and typical examples, respectively. A slowly depolarizing voltage ramp from −85 to 120 mV results in an increase in $[Ca^{2+}]_i$ due to Ca^{2+} entry through reverse mode NCX (**Figure 4B**). Upon repolarization to −60 mV, Ca^{2+} removal occurs (forward mode NCX) resulting in a $[Ca^{2+}]_i$ decline (**Figure 4B**, gray lines), which correlates well with the measured I_{NCX} (**Figure 4B**, black lines) (cf. Weber et al., 2003). **Figure 4C** shows the average I_{NCX}-$[Ca^{2+}]_i$ relationships obtained during the repolarization-induced $[Ca^{2+}]_i$ decline in CTRL and HF SAN cells. The I_{NCX}-$[Ca^{2+}]_i$ relationships are linear in the physiological range. Neither the I_{NCX} density nor the I_{NCX}-$[Ca^{2+}]_i$ relationships differ significantly between HF and CTRL SAN cells (**Figure 4C**). In addition, the time constants of both the $[Ca^{2+}]_i$ and I_{NCX} decline during the repolarizing step to −60 mV, another measure of NCX function (Weber et al., 2003), do not differ significantly between CTRL and HF SAN cells (**Figure 4D**).

From these data we conclude that HF does not affect the I_{NCX} density nor the I_{NCX}-$[Ca^{2+}]_i$ dependency. In addition, given the unaltered NCX and mitochondrial Ca^{2+} uptake and sarcolemmal Ca-ATPase activity of SAN cells, we conclude that the slower decay of the $[Ca^{2+}]_i$ transient is due to reduced SERCA activity.

HF HARDLY AFFECTS $[Ca^{2+}]_i$ MODULATION BY ACETHYLCHOLINE AND NORADRENALINE

$[Ca^{2+}]_i$ transients in SAN cells are importantly modulated by β-adrenergic (Rigg et al., 2000; Vinogradova et al., 2002a; Joung et al., 2009; van Borren et al., 2010) and muscarinic receptor (van Borren et al., 2010) stimulation. Most importantly, β-adrenergic stimulation increases the frequency and amplitude of $[Ca^{2+}]_i$ transients as well as local Ca^{2+} releases (LCRs) from the SR late during the diastolic depolarization (Vinogradova et al., 2002a; Joung et al., 2009; van Borren et al., 2010). Muscarinic receptor stimulation with acethylcholine decreases the frequency and amplitude of $[Ca^{2+}]_i$ transients and local Ca^{2+} releases from the SR (van Borren et al., 2010). Opthof et al. (2000) reported an increased sensitivity for acetylcholine in intact HF SAN preparations of rabbit, while Shinohara et al. (2010) found that intact SAN preparations of HF dogs were completely unresponsive to isoproterenol. Here, we tested the effects of β-adrenergic and muscarinic receptor stimulation on $[Ca^{2+}]_i$ transient parameters in CTRL and HF SAN cells. β-adrenergic stimulation with 500 nM noradrenaline significantly increased the frequency and the $[Ca^{2+}]_i$ transient parameters in both CTRL and HF SAN cells (**Figure 5**), except the time constant of decay, which was significantly decreased in the HF SAN cells. In presence of noradrenaline HF SAN cells still have a significantly lower frequency and slower decay phase compared to CTRL SAN cells (**Figure 5B**, left), while

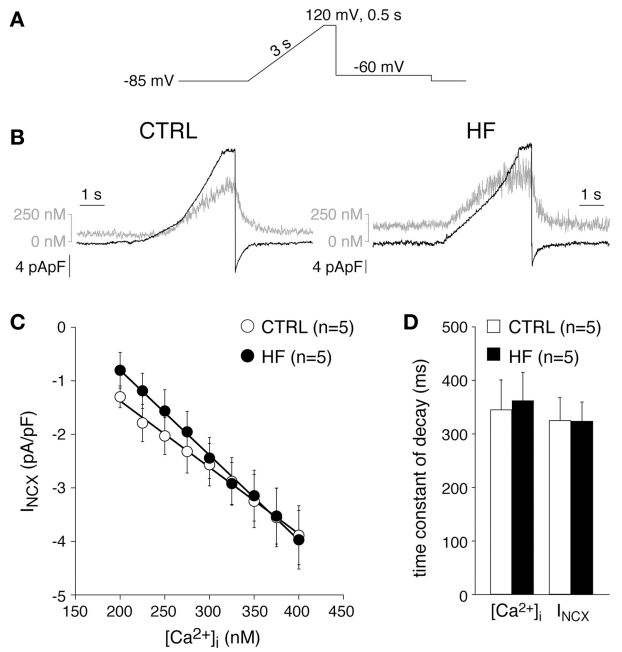

FIGURE 4 | HF affects neither the Na^+–Ca^{2+} exchange current (I_{NCX}) nor its $[Ca^{2+}]_i$ dependency. (A) Voltage clamp protocol used. **(B)** Typical changes in $[Ca^{2+}]_i$ and I_{NCX} (gray and black traces, respectively) in response to the voltage clamp protocol of **(A)**. **(C)** Average I_{NCX}-$[Ca^{2+}]_i$ relationships obtained during the repolarization-induced $[Ca^{2+}]_i$ decline. Solid lines: linear fits. **(D)** Average time constants of the $[Ca^{2+}]_i$ and I_{NCX} decline during the repolarizing step to −60 mV.

now also the late diastolic $[Ca^{2+}]_i$ rise is significantly lower in HF SAN cells (**Figure 5B**, bottom right).

Muscarinic receptor stimulation with 50 nM acetylcholine significantly decreased the frequency and $[Ca^{2+}]_i$ transients parameters in both CTRL and HF SAN cells, with exception of the time constant of decay which was significantly increased in both groups of cells (**Figure 6**). In presence of acetylcholine, only the frequency differs significantly between HF and CTRL SAN cells.

From these data we conclude that HF does not affect importantly the $[Ca^{2+}]_i$ modulation by acethylcholine and noradrenaline. However, in presence of noradrenaline, HF SAN cells have a reduced late diastolic $[Ca^{2+}]_i$ rise compared to CTRL SAN cells and this might have implications for pacemaker activity formation during β-adrenergic stimulation.

EFFECTS OF HF ON THE I_{NCX} DURING THE DIASTOLIC DEPOLARIZATION PHASE

The $[Ca^{2+}]_i$ transients are longer in HF SAN cells, likely due to reduced SERCA activity. In general, it is assumed that this will promote NCX mediated Ca^{2+} extrusion, and thus will increase the I_{NCX}-mediated net inward current during the diastolic depolarization (Ju and Allen, 1998; Sanders et al., 2006; Lau et al., 2011). Such an effect may, at least partially, counteract the previously observed decrease in I_f-mediated inward current in our used model of HF (Verkerk et al., 2003). However, NCX function during the cardiac cycle is not only determined by $[Ca^{2+}]_i$, but also by the intracellular Na^+ ($[Na^+]_i$) concentration, and the membrane potential (V_m) (Blaustein and Lederer, 1999).

Next, we recorded action potentials (APs) simultaneously with $[Ca^{2+}]_i$ in combined $[Ca^{2+}]_i$ and patch clamp experiments, and calculated I_{NCX} during SAN APs using the measured $[Ca^{2+}]_i$ and V_m. Combined $[Ca^{2+}]_i$ and patch clamp experiments were performed in 7 CTRL and 5 HF SAN cells. The average $[Ca^{2+}]_i$ transient and AP parameters recapitulate the CTRL and HF SAN cell phenotype of the present paper (**Figure 1**) and of our previous study (Verkerk et al., 2003; **Figure 1**), although the differences in frequency and diastolic depolarization rate between CTRL and HF SAN cells did not reach the level of statistical significance due to the small number of cells (data not shown). **Figures 7A,B**, show a selected AP and $[Ca^{2+}]_i$ transient of a CTRL and HF SAN cell, which closely represent the mean differences in $[Ca^{2+}]_i$ transient and AP properties. **Figure 7C** shows the reconstructed I_{NCX}, based on the simultaneously recorded Ca^{2+} transients and APs of **Figures 7A,B**. In the CTRL SAN cell, I_{NCX} is inward for the entire AP, with a small amplitude early in the AP and a maximal amplitude late during repolarization. The I_{NCX} declined during the diastolic depolarization phase, consistent with the decrease in $[Ca^{2+}]_i$. In HF, I_{NCX} during the AP is close to that of the CTRL SAN cells, except that the amplitude is slightly larger during the diastolic depolarization. This is likely due to the slightly higher $[Ca^{2+}]_i$ in the diastolic depolarization phase, since the APs were almost identical and an identical $[Na^+]_i$ concentration of 5 mM was used for CTRL and HF SAN cells in both the pipette solution and calculations. **Figure 7D** extends our analysis to an increased $[Na^+]_i$, as frequently observed in ventricular myocytes of our used HF model (Baartscheer et al., 2003b). Elevation of the $[Na^+]_i$ by 50% to 7.5 mM, in line with the observations of Baartscheer et al. (2003b), decreased the diastolic I_{NCX} in both CTRL and HF SAN cells. Interestingly, I_{NCX} may become even shortly outward early during the AP. **Figure 7E** shows the I_{NCX} of the CTRL SAN cell with 5 mM $[Na^+]_i$ and the I_{NCX} of the HF SAN cell with 7.5 mM $[Na^+]_i$. It is evident that under these conditions I_{NCX} in HF SAN cell is close to that of the CTRL SAN, except for the outward I_{NCX} in the HF SAN cell. Similar results are obtained with the NCX model equations of Faber and Rudy (2000) (data not shown).

From these data we conclude that the decreased $[Ca^{2+}]_i$ transient decay in HF may result in slightly increased I_{NCX} during the diastolic depolarization phase, but that this effect is counteracted by a HF-induced increase in $[Na^+]_i$.

DISCUSSION

In the present study, we characterized the $[Ca^{2+}]_i$ cycling of single SAN cells isolated from CTRL rabbits and rabbits with volume and pressure overload-induced HF. The mechanisms behind $[Ca^{2+}]_i$ cycling in ventricular myocytes are diverse and complex (for reviews, see Guatimosim et al., 2002; Eisner et al., 2005; Bers, 2006b; Neef and Maier, 2013). In short, the $[Ca^{2+}]_i$ transient is triggered by Ca^{2+} influx through sarcolemmal Ca^{2+} channels, which results in release of Ca^{2+} from the SR via ryanodine-2 (RyR2) channels. This so-called Ca^{2+}-induced Ca^{2+} release (CICR) is importantly modulated by T-tubuli organization, with co-localization of $I_{Ca,L}$ and RyR2 channels (Øyehaug et al., 2013),

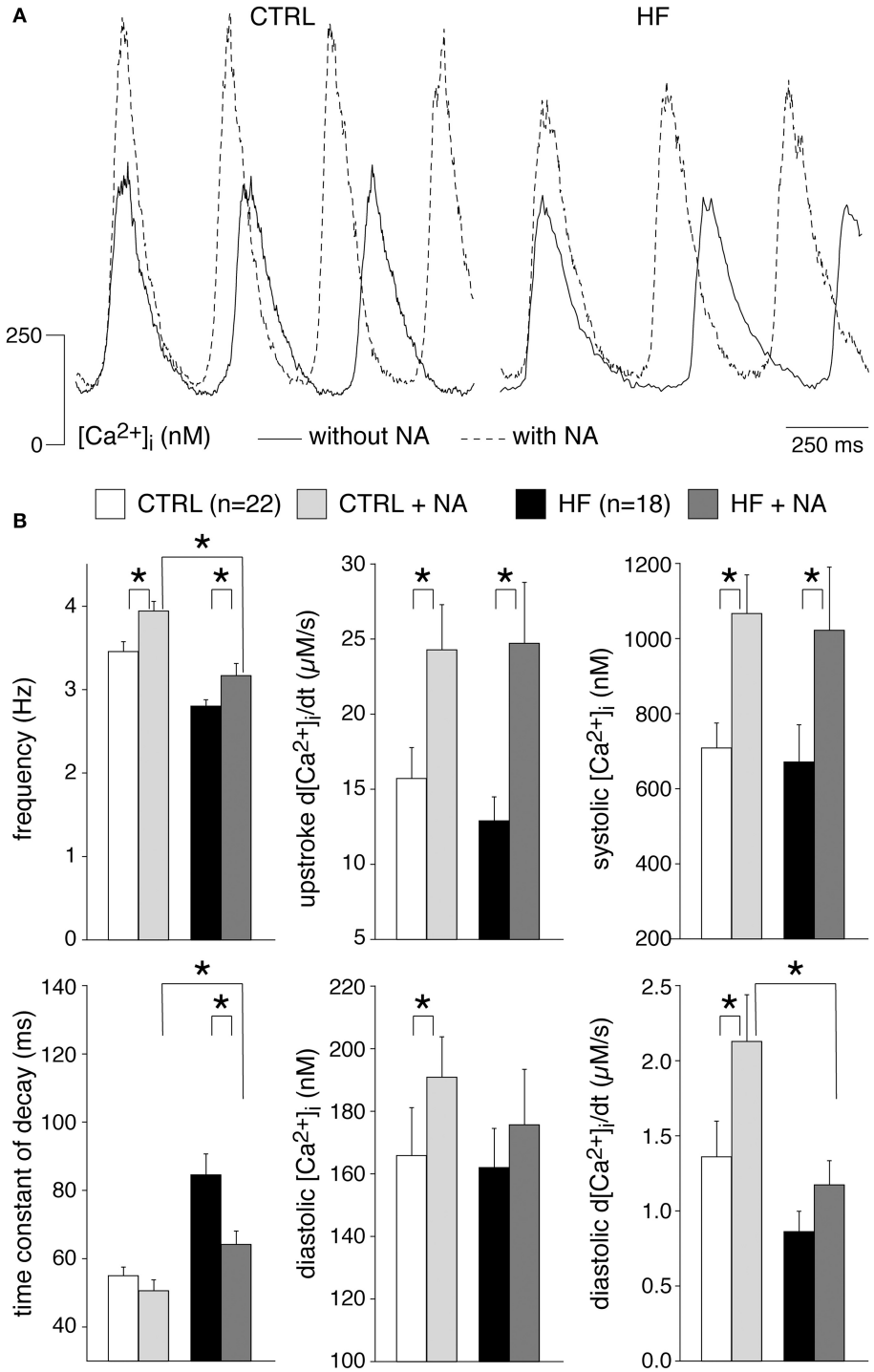

FIGURE 5 | Effects of 500 nM noradrenaline (NA) on the $[Ca^{2+}]_i$ transient parameters in CTRL and HF SAN cells. (A) Representative $[Ca^{2+}]_i$ transients in absence (solid lines) and presence (dashed lines) of NA. **(B)** Average $[Ca^{2+}]_i$ transient characteristics in absence and presence of NA. $^*P < 0.05$.

and the open probability of RyR2 channels (Guatimosim et al., 2002). The amplitude of the $[Ca^{2+}]_i$ transient depends importantly on the SR Ca^{2+} content (Bassani et al., 1992; Trafford et al., 2000, 2001; Díaz et al., 2004; Dibb et al., 2007; Briston et al., 2011). The decline of the $[Ca^{2+}]_i$ transient is mainly due to SR Ca^{2+} reuptake through SERCA and extrusion of Ca^{2+} via the NCX. Because NCX and SERCA activity compete during the decline of the $[Ca^{2+}]_i$ transient, any change in SERCA function indirectly affects NCX contribution and vice versa, resulting in changes in the Ca^{2+} content of the SR and consequently

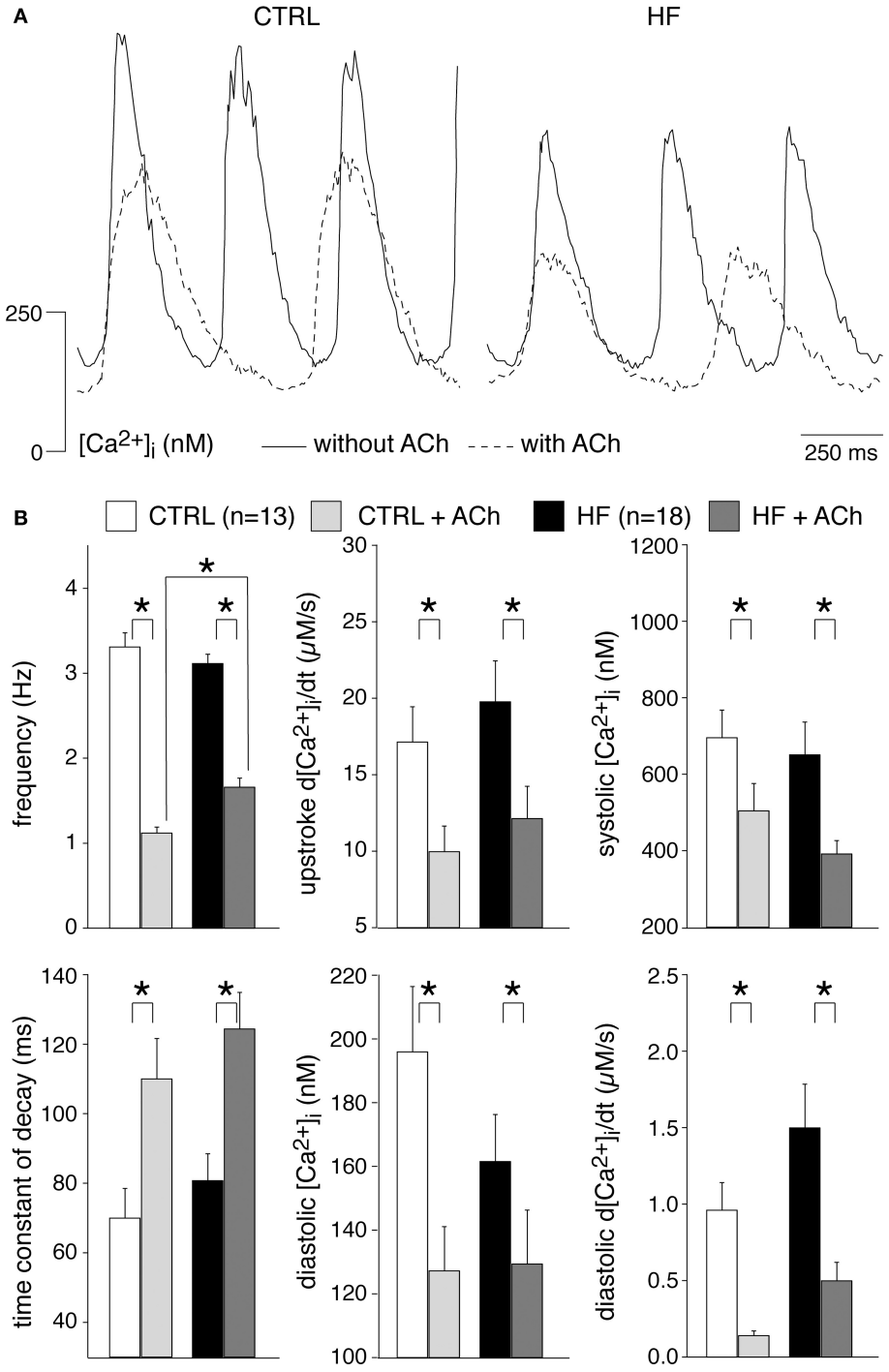

FIGURE 6 | Effects of 50 nM acetylcholine (ACh) on the $[Ca^{2+}]_i$ transient parameters in CTRL and HF SAN cells. (A) Representative $[Ca^{2+}]_i$ transients in absence (solid lines) and presence (dashed lines) of ACh. **(B)** Average $[Ca^{2+}]_i$ transient characteristics in absence and presence of ACh. $^*P < 0.05$.

$[Ca^{2+}]_i$ transient amplitudes (Eisner et al., 2005; Bers, 2006a; Neef and Maier, 2013). The diastolic Ca^{2+} concentration is regulated by the $[Ca^{2+}]_i$ transient decline, especially during rapid pacing (Laurita et al., 2003), and leak of RyR2 channels (Neef and Maier, 2013). Both a slower $[Ca^{2+}]_i$ transient decay and increased RyR2 channel leak results in elevation of the diastolic Ca^{2+} concentration. SAN cells exhibit also another $[Ca^{2+}]_i$ transient characteristic, i.e., rise of the diastolic $[Ca^{2+}]_i$, which is a key signature of pacemaking by the Ca^{2+} clock (for review, see Maltsev and Lakatta, 2008; Lakatta et al., 2010; Joung et al., 2011).

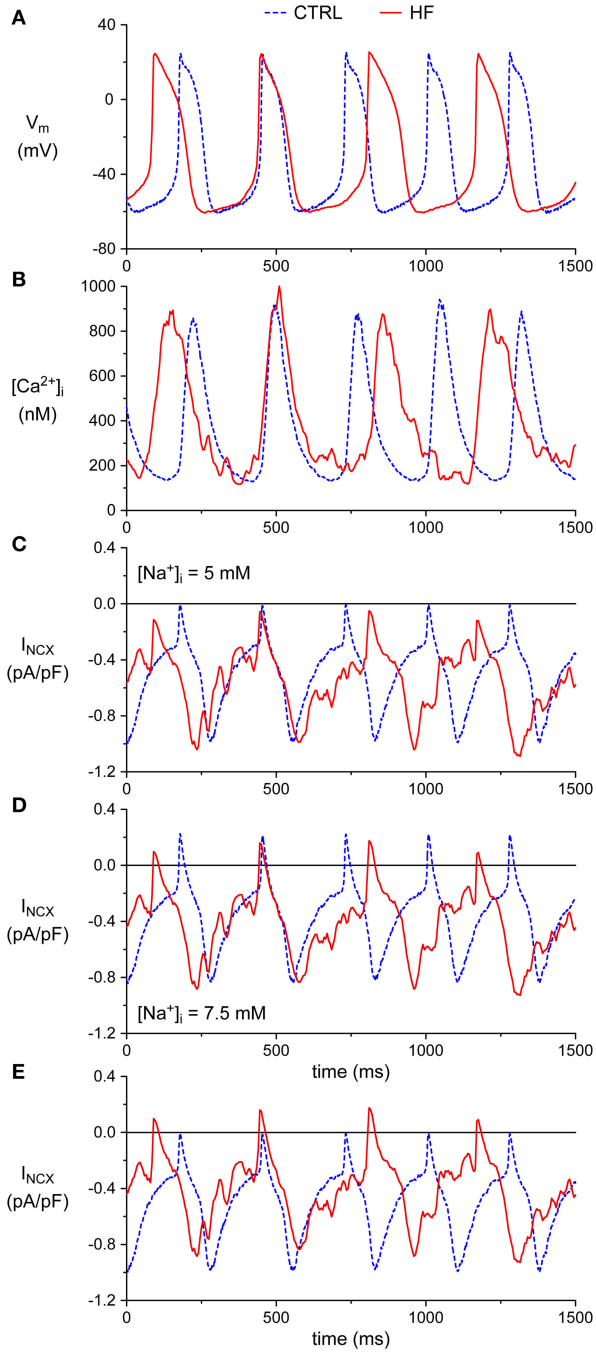

FIGURE 7 | Simultaneous action potential and $[Ca^{2+}]_i$ transient recordings from CTRL and HF SAN cells and associated numerical reconstruction of the I_{NCX}. **(A)** Recorded membrane potential (V_m). **(B)** Recorded intracellular $[Ca^{2+}]_i$ concentration. **(C)** Reconstructed I_{NCX}. **(D)** I_{NCX} upon elevation of the intracellular Na^+ concentration ($[Na^+]_i$) to 7.5 mM. **(E)** Selection of the I_{NCX} of the CTRL SAN cell of **(C)** ($[Na^+]_i$ of 5 mM) and HF SAN cell of **(D)** ($[Na^+]_i$ of 7.5 mM).

HF in ventricular myocytes may affect many $[Ca^{2+}]_i$ transient characteristics. It is reported that HF decreases the upstroke velocity of the $[Ca^{2+}]_i$ transient by T-tubuli disorganization (Øyehaug et al., 2013) and increased open probability of RyR2 channels (Guatimosim et al., 2002). An increase of RyR2 open probability, as may occur during HF in ventricular myocytes, also leads to an increased amount of Ca^{2+} sparks, resulting in an increased diastolic $[Ca^{2+}]_i$ concentration and reduced SR Ca^{2+} content since more Ca^{2+} is pumped out of the cell by the NCX (Neef and Maier, 2013). Furthermore, HF in ventricular mycoytes typically slows the $[Ca^{2+}]_i$ transient decay due to reduced SERCA function. Such reduced Ca^{2+} uptake by SERCA, in combination with a frequently observed upregulation of the NCX and consequently increased Ca^{2+} efflux, will reduce the SR Ca^{2+} content and systolic Ca^{2+} transient amplitude (for reviews, see Bers, 2006b; Eisner et al., 2013; Neef and Maier, 2013). Of note, the diastolic $[Ca^{2+}]_i$ concentration is frequently elevated by HF, due to the slower $[Ca^{2+}]_i$ transient decay and increased RyR2 channel leak.

We found that HF SAN cells have (1) a reduced frequency of spontaneous $[Ca^{2+}]_i$ transients, (2) a slower $[Ca^{2+}]_i$ transient decay, and (3) a reduced diastolic $[Ca^{2+}]_i$ rise during β-adrenergic stimulation, compared to CTRL SAN cells. Combined action potential and $[Ca^{2+}]_i$ measurements demonstrated that the decreased $[Ca^{2+}]_i$ transient decay in HF SAN cells may result in slightly increased I_{NCX} during the diastolic depolarization phase, but that this effect is counteracted by HF-induced increase in $[Na^+]_i$.

INTRINSIC CYCLE LENGTH IS PROLONGED IN HF SAN CELLS

We found a lower frequency of spontaneous $[Ca^{2+}]_i$ transients in HF SAN cells, indicating that intrinsic cycle length was prolonged in HF SAN cells (**Figure 1**). This finding agrees with previously findings in intact SAN (Opthof et al., 2000) and single SAN cells (Verkerk et al., 2003) of rabbit. The frequency of the intrinsic cycle length based on the $[Ca^{2+}]_i$ transients was 14% slower in HF SAN cells (**Figure 1**) and this percentage closely matches the increased intrinsic cycle length (15%) of our previous study with the same rabbit HF model and measured with perforated patch clamp methodology (Verkerk et al., 2003).

We found that the frequency of the spontaneous $[Ca^{2+}]_i$ transients in both CTRL and HF SAN cells influenced various $[Ca^{2+}]_i$ transient characteristics, including diastolic and systolic $[Ca^{2+}]_i$ concentrations, systolic $[Ca^{2+}]_i$ rise and decay, and late diastolic $[Ca^{2+}]_i$ rise (**Figure 2**, **Table 2**). All parameters, except the $[Ca^{2+}]_i$ transient time constant of decay, increased upon increased frequencies. The frequency dependency was not significantly different in HF compared to CTRL SAN cells (**Figure 2**, **Table 2**). Nevertheless, the frequency dependency relationships might have influenced some principal findings because spontaneous activity is lower in HF SAN cells. The relative small difference in intrinsic cycle length of CTRL and HF SAN cells, the rather large variation between cells, and the modest steepness of the frequency-dependencies (**Table 2**, **Figure 2**) may all have contributed to the absence of significant differences in frequency dependency between HF and CTRL SAN cells.

Recently, Herrmann et al. elegantly solved the problem of intrinsic rate differences in SAN cells by using electrical field stimulation (Herrmann et al., 2013). Using this approach, they investigated the contribution of the murine sodium-calcium exchanger

protein NCX1 to cardiac pacemaking in transgenic mice selectively lacking NCX1 in the cardiac pacemaking and conduction system. Among other things, they found that $[Ca^{2+}]_i$ transients measured during electrical field stimulation were of smaller magnitude and decelerated kinetics in NCX1 knockout cells.

$[Ca^{2+}]_i$ TRANSIENT CHARACTERISTICS IN HF SAN CELLS

$[Ca^{2+}]_i$ transient under basal conditions

We observed that HF results in a slower $[Ca^{2+}]_i$ transient decay (**Figure 1**). The $[Ca^{2+}]_i$ transient time constant of decay was increased by 41% in HF cells, which is larger than expected from the $[Ca^{2+}]_i$ transient time constant of decay vs. frequency relationship that explains only a ≈17% difference. HF affected neither the I_{NCX} density and I_{NCX}-$[Ca^{2+}]_i$ relationship (**Figure 4**) nor the mitochondrial Ca^{2+} uptake and sarcolemmal Ca-ATPase (**Figure 3**), indicating that downregulation of SERCA activity also contributes to the slower $[Ca^{2+}]_i$ transient decay. Any contribution of (changes in) T-tubular organization, sarcolemmal calcium currents, and action potential duration can be ruled out because T-tubuli are absent in rabbit SAN cells (Masson-Pévet et al., 1979), and $I_{Ca,T}$ and $I_{Ca,L}$ densities as well as action potential duration are unaffected in HF rabbit SAN cells (Verkerk et al., 2003).

HF in SAN cells did not affect the diastolic and systolic $[Ca^{2+}]_i$ concentrations, systolic $[Ca^{2+}]_i$ rise, late diastolic $[Ca^{2+}]_i$ rise (**Figure 1**), and SR Ca^{2+} content (**Figure 3**). The unaffected diastolic Ca^{2+} concentration, at first sight, might appear to be inconsistent with the decrease of the $[Ca^{2+}]_i$ transient decline. It should be noted, however, that HF SAN cells have a lower frequency due to their longer diastolic depolarization phase (Verkerk et al., 2003), which leaves more time for Ca^{2+} reuptake and/or removal. The unchanged slope of the LDCAE, associated with LCRs and Ca^{2+} sparks, suggests that RyR2 open probability is not affected in HF SAN cells. Our finding contrasts findings in a canine model of rapid pacing-induced heart failure, where it was found, using isolated right atrial preparations, that LDCAE was reduced (Shinohara et al., 2010). Differences in HF model, species and preparations might contribute to the contrasting findings.

The unaltered SR Ca^{2+} content agrees with the unaffected $[Ca^{2+}]_i$ transient amplitude in HF SAN cells, but is somewhat surprising given that reduced SERCA activity is supposed to result in a lower SR Ca^{2+} content. The latter is due because NCX and SERCA activity compete for Ca^{2+} during the $[Ca^{2+}]_i$ transient decline, and reduced SERCA function thus indirectly favors greater Ca^{2+} efflux via the NCX (for reviews, see Guatimosim et al., 2002; Eisner et al., 2005; Bers, 2006b; Neef and Maier, 2013). We observed a similar SR Ca^{2+} content in HF and CTRL SAN cells despite the slower $[Ca^{2+}]_i$ transient decline in HF SAN cells. This suggests a compensatory increase in Ca^{2+} influx. $I_{Ca,T}$ and $I_{Ca,L}$ densities were not affected in HF SA node cells (Verkerk et al., 2003), but we cannot exclude that the longer diastolic depolarization phase in HF SAN cells (Verkerk et al., 2003) may result in a larger background Ca^{2+} influx via L-type Ca^{2+} channels (Verheijck et al., 1999). Alternatively, increased $[Na^+]_i$ as occurs during HF may promote Ca^{2+} influx via reversed NCX activity (Despa et al., 2002). Indeed, by reconstruction of the I_{NCX}, based on action potentials and simultaneously measured $[Ca^{2+}]_i$ transients, we found that the I_{NCX} became outward, thus resulting in Ca^{2+} influx, early during the AP (**Figures 7D,E**) under conditions of elevated $[Na^+]_i$ as occur during HF.

$[Ca^{2+}]_i$ transient during β-adrenergic and muscarinic receptor stimulation

We found that the β-adrenergic and muscarinic receptor stimulation was hardly affected by HF. In both CTRL and HF SAN cells, acetylcholine significantly decreased the frequency and $[Ca^{2+}]_i$ transients parameters, with exception of the time constant of decay which was significantly increased in both groups of cells (**Figure 6**). The ACh induced effects were largely similar in CTRL and HF SAN cells. Noradrenaline, on the other hand, significantly increased the frequency and most $[Ca^{2+}]_i$ transient parameters in both CTRL and HF SAN cells (**Figure 5**), leading to preserved $[Ca^{2+}]_i$ transient differences between the CTRL and the HF SAN cells. However, in presence of noradrenaline the late diastolic $[Ca^{2+}]_i$ rise was significantly lower in HF SAN cells compared to HF SAN cells. The lower late diastolic $[Ca^{2+}]_i$ rise in HF SAN cells in presence of noradrenaline is in agreement with findings in canine right atrial preparations by Shinohara et al. (2010).

IMPLICATION OF HF-INDUCED $[Ca^{2+}]_i$ TRANSIENT CHANGES IN PACEMAKER ACTIVITY

Overall, the effects of HF on $[Ca^{2+}]_i$ transients in rabbit SAN cells were modest. The decrease in frequency of the spontaneous $[Ca^{2+}]_i$ transient in HF SAN cells is completely explained by the previously observed slower intrinsic cycle length (Verkerk et al., 2003). The slower $[Ca^{2+}]_i$ transient decay will promote Ca^{2+} transport across the sarcolemma by the NCX (Bers et al., 2006), an electrogenic process that delivers inward current at diastolic potentials. The observed slower $[Ca^{2+}]_i$ transient decay may thus result in increased I_{NCX} during the diastolic depolarization phase, thereby partially counteracting the previously observed decrease in I_f-mediated inward current in HF (Verkerk et al., 2003). Indeed, reconstructed I_{NCX}, based on the simultaneously recorded Ca^{2+} transients and APs, demonstrated a slightly larger amplitude during the diastolic depolarization phase (**Figure 7C**). However, when we incorporated an increased $[Na^+]_i$, as frequently observed in ventricular myocytes, including those from our rabbit HF model (Baartscheer et al., 2003b), the I_{NCX} in the diastolic depolarization phase is close to that of the CTRL SAN (**Figure 7E**). Thus, the slower $[Ca^{2+}]_i$ transient decay in HF has likely a limited role in the slower intrinsic cycle length in HF SAN cells. The slope of late diastolic $[Ca^{2+}]_i$ elevation, associated with localized Ca^{2+} releases (LCRs) or Ca^{2+} sparks (Bogdanov et al., 2006; Maltsev et al., 2006; Joung et al., 2009, 2010; van Borren et al., 2010), was unaffected under basal conditions, suggesting that the Ca^{2+} clock is not the primary cause of the slower intrinsic cycle length in HF SAN cells. Considering the importance of late diastolic $[Ca^{2+}]_i$ rise in setting pacemaker activity, however, the lower late diastolic $[Ca^{2+}]_i$ rise in HF SAN cells in presence of noradrenaline suggest that an impaired increase in intrinsic frequency under such conditions may be related to reduced Ca^{2+} clock function.

LIMITATIONS

We used indo-1 to measure $[Ca^{2+}]_i$, because this ratiometric indicator is less prone to cell contractions and loss of dye. However, indo-1 had an adverse effect on cell viability and rendered many smaller cells quiescent (Lancaster et al., 2004). We cannot rule out the possibility that indo-1 has affected the principal findings, but we assume that its effect is limited because the differences in spontaneous activity of CTRL and HF SAN cells in our present study are highly similar to the differences that we observed with perforated patch clamp measurements (Verkerk et al., 2003).

In our study, we used the complete SAN for cell isolation. However, the SAN is not homogeneous in its composition. This seems valid for membrane currents (Boyett et al., 2000), but also the expression of several calcium handling proteins varies across the node (Musa et al., 2002; Lancaster et al., 2004), all of which are expressed at a lower level in the center of the SAN compared with the periphery, although such findings are debated (Lyashkov et al., 2007). Cells from the center and periphery may differ in cell capacitance. We exclude cell location-dependency as an explanation for our principal findings because cell capacitance did not differ between control and HF.

We reconstructed I_{NCX} based on simultaneous measurements of $[Ca^{2+}]_i$ and spontaneous action potentials as well as the $[Na^+]_i$ of 5 and 7.5 mM used in our pipette solution and found in our model of HF previously (Baartscheer et al., 2003b). Data on $[Na^+]_i$ in SAN cells are extremely sparse and we were not succesful in $[Na^+]_i$ measurements with benzofuran isophthalate (SBFI) ourselves. However, the used 5 mM $[Na^+]_i$ is close to the concentrations of 4.5 and 4.0 mM in rabbit multicellular SAN preparations and single SAN cells, respectively, found by Choi et al. (1999). In our reconstructions, we used the Lindblad et al. (1996) equations for I_{NCX}. We could not make use of I_{NCX} equations from more recent models, in particular the rabbit SAN cell models by Maltsev and Lakatta (2010b) and Severi et al. (2012), because these require data on the concentration of Ca^{2+} in a sarcolemmal subspace rather than global $[Ca^{2+}]_i$.

CONCLUSIONS

In our rabbit model of HF, SAN cells have reduced SERCA activity and reduced intrinsic frequency, both resulting in a slower Ca^{2+} decay. The decreased $[Ca^{2+}]_i$ transient decay in HF SAN cells may result in slightly increased I_{NCX} during the diastolic depolarization phase, but this effect is likely counteracted by HF-induced increase in $[Na^+]_i$. Reduced late diastolic $[Ca^{2+}]_i$ rise during β-adrenergic stimulation may contribute to the impaired increase in frequency under this condition in HF SAN cells.

ACKNOWLEDGMENTS

The authors thank Charly Belterman, Jan Zegers, Berend de Jonge, and Jan Bourier for their excellent technical assistance.

REFERENCES

Allah, E. A., Tellez, J. O., Yanni, J., Nelson, T., Monfredi, O., Boyett, M. R., et al. (2011). Changes in the expression of ion channels, connexins and Ca^{2+}-handling proteins in the sino-atrial node during postnatal development. *Exp. Physiol.* 96, 426–438. doi: 10.1113/expphysiol.2010.055780

Arai, A., Kodama, I., and Toyama, J. (1996). Roles of Cl^- channels and Ca^{2+} mobilization in stretch-induced increase of SA node pacemaker activity. *Am. J. Physiol.* 270, H1726–H1735.

Baartscheer, A., Schumacher, C. A., Belterman, C. N. W., Coronel, R., and Fiolet, J. W. T. (2003a). SR calcium handling and calcium after-transients in a rabbit model of heart failure. *Cardiovasc. Res.* 58, 99–108. doi: 10.1016/S0008-6363(02)00854-4

Baartscheer, A., Schumacher, C. A., van Borren, M. M. G. J., Belterman, C. N. W., Coronel, R., and Fiolet, J. W. T. (2003b). Increased Na^+/H^+-exchange activity is the cause of increased $[Na^+]_i$ and underlies disturbed calcium handling in the rabbit pressure and volume overload heart failure model. *Cardiovasc. Res.* 57, 1015–1024. doi: 10.1016/S0008-6363(02)00809-X

Bassani, R. A., Bassani, J. W. M., and Bers, D. M. (1992). Mitochondrial and sarcolemmal Ca^{2+} transport reduce $[Ca^{2+}]_i$ during caffeine contractures in rabbit cardiac myocytes. *J. Physiol.* 453, 591–608. doi: 10.1113/jphysiol.1992.sp019246

Bers, D. M., Despa, S., and Bossuyt, J. (2006). Regulation of Ca^{2+} and Na^+ in normal and failing cardiac myocytes. *Ann. N.Y. Acad. Sci.* 1080, 165–177. doi: 10.1196/annals.1380.015

Bers, D. M. (1987). Ryanodine and the calcium content of cardiac SR assessed by caffeine and rapid cooling contractures. *Am. J. Physiol.* 253, C408–C415.

Bers, D. M. (2006a). The beat goes on: diastolic noise that just won't quit. *Circ. Res.* 99, 921–923. doi: 10.1161/01.RES.0000249859.10103.a9

Bers, D. M. (2006b). Altered cardiac myocyte Ca regulation in heart failure. *Physiology (Bethesda)* 21, 380–387. doi: 10.1152/physiol.00019.2006

Blaustein, M. P., and Lederer, W. J. (1999). Sodium/calcium exchange: its physiological implications. *Physiol. Rev.* 79, 763–854.

Bogdanov, K. Y., Maltsev, V. A., Vinogradova, T. M., Lyashkov, A. E., Spurgeon, H. A., Stern, M. D., et al. (2006). Membrane potential fluctuations resulting from submembrane Ca^{2+} releases in rabbit sinoatrial nodal cells impart an exponential phase to the late diastolic depolarization that controls their chronotropic state. *Circ. Res.* 99, 979–987. doi: 10.1161/01.RES.0000247933.66532.0b

Boyett, M. R., Honjo, M., and Kodama, I. (2000). The sinoatrial node, a heterogeneous pacemaker structure. *Cardiovasc. Res.* 47, 658–687. doi: 10.1016/S0008-6363(00)00135-8

Briston, S. J., Caldwell, J. L., Horn, M. A., Clarke, J. D., Richards, M. A., Greensmith, D. J., et al. (2011). Impaired β-adrenergic responsiveness accentuates dysfunctional excitation–contraction coupling in an ovine model of tachypacing-induced heart failure. *J. Physiol.* 589, 1367–1382. doi: 10.1113/jphysiol.2010.203984

Choi, S., Wang, D. Y., Noble, D., and Lee, C. O. (1999). Effect of isoprenaline, carbachol, and Cs^+ on Na^+ activity and pacemaker potential in rabbit SA node cells. *Am. J. Physiol.* 276, H205–H214.

Despa, S., Islam, M. A., Weber, C. R., Pogwizd, S. M., and Bers, D. M. (2002). Intracellular Na^+ concentration is elevated in heart failure but Na/K pump function is unchanged. *Circulation* 105, 2543–2548. doi: 10.1161/01.CIR.0000016701.85760.97

Díaz, M. E., Graham, H. K., and Trafford, A. W. (2004). Enhanced sarcolemmal Ca^{2+} efflux reduces sarcoplasmic reticulum Ca^{2+} content and systolic Ca^{2+} in cardiac hypertrophy. *Cardiovasc. Res.* 62, 538–547. doi: 10.1016/j.cardiores.2004.01.038

Dibb, K. M., Eisner, D. A., and Trafford, A. W. (2007). Regulation of systolic $[Ca^{2+}]_i$ and cellular Ca^{2+} flux balance in rat ventricular myocytes by SR Ca^{2+}, L-type Ca^{2+} current and diastolic $[Ca^{2+}]_i$. *J. Physiol.* 585, 579–592. doi: 10.1113/jphysiol.2007.141473

DiFrancesco, D. (2010). Considerations on the size of currents required for pacemaking. *J. Mol. Cell. Cardiol.* 48, 802–803. doi: 10.1016/j.yjmcc.2009.11.022

DiFrancesco, D., and Noble, D. (2012a). The funny current has a major pacemaking role in the sinus node. *Heart Rhythm* 9, 299–301. doi: 10.1016/j.hrthm.2011.09.021

DiFrancesco, D., and Noble, D. (2012b). Rebuttal: "The funny current in the context of the coupled clock pacemaker cell system." *Heart Rhythm* 9, 457–458. doi: 10.1016/j.hrthm.2011.09.023

DiFrancesco, D., and Robinson, R. B. (2002). β-Modulation of pacemaker rate: novel mechanism or novel mechanics of an old one? *Circ. Res.* 90:e69. doi: 10.1161/01.RES.0000014803.05780.E7

Du, Y., Huang, X., Wang, T., Han, K., Zhang, J., Xi, Y., et al. (2007). Downregulation of neuronal sodium channel subunits $Na_v1.1$ and $Na_v1.6$ in the sinoatrial node from volume-overloaded heart failure rat. *Pflügers Arch.* 454, 451–459. doi: 10.1007/s00424-007-0216-4

Eisner, D., Caldwell, J., and Trafford, A. (2013). Sarcoplasmic reticulum Ca-ATPase and heart failure 20 years later. *Circ. Res.* 113, 958–961. doi: 10.1161/CIRCRESAHA.113.302187

Eisner, D. A., Diaz, M. E., Li, Y., O'Neill, S. C., and Trafford, A. W. (2005). Stability and instability of regulation of intracellular calcium. *Exp. Physiol.* 90, 3–12. doi: 10.1113/expphysiol.2004.029231

Faber, G. M., and Rudy, Y. (2000). Action potential and contractility changes in $[Na^+]_i$ overloaded cardiac myocytes: a simulation study. *Biophys. J.* 78, 2392–2404. doi: 10.1016/S0006-3495(00)76783-X

Guatimosim, S., Dilly, K., Santana, L. F., Jafri, M. S., Sobie, E. A., and Lederer, W. J. (2002). Local Ca^{2+} signaling and EC coupling in heart: Ca^{2+} sparks and the regulation of the $[Ca^{2+}]_i$ transient. *J. Mol. Cell. Cardiol.* 34, 941–950. doi: 10.1006/jmcc.2002.2032

Herrmann, S., Lipp, P., Wiesen, K., Stieber, J., Nguyen, H., Kaiser, E., et al. (2013). The cardiac sodium-calcium exchanger NCX1 is a key player in the initiation and maintenance of a stable heart rhythm. *Cardiovasc. Res.* 99, 780–788. doi: 10.1093/cvr/cvt154

Himeno, Y., Toyoda, F., Matsuura, H., and Noma, A. (2011a). Reply to "Letter to the editor: 'Validating the requirement for beat-to-beat coupling of the Ca^{2+} clock and M clock in pacemaker cell normal automaticity.'" *Am. J. Physiol. Heart Circ. Physiol.* 300, H2325–H2326. doi: 10.1152/ajpheart.00317.2011

Himeno, Y., Toyoda, F., Satoh, H., Amano, A., Cha, C. Y., Matsuura, H., et al. (2011b). Minor contribution of cytosolic Ca^{2+} transients to the pacemaker rhythm in guinea pig sinoatrial node cells. *Am. J. Physiol. Heart Circ. Physiol.* 300, H251–H261. doi: 10.1152/ajpheart.00764.2010

Honjo, H., Inada, S., Lancaster, M. K., Yamamoto, M., Niwa, R., Jones, S. A., et al. (2003). Sarcoplasmic reticulum Ca^{2+} release is not a dominating factor in sinoatrial node pacemaker activity. *Circ. Res.* 92, e41–e44. doi: 10.1161/01.RES.0000055904.21974.BE

Hove-Madsen, L., and Tort, L. (2001). Characterization of the relationship between Na^+-Ca^{2+} exchange rate and cytosolic calcium in trout cardiac myocytes. *Pflügers Arch.* 441, 701–708. doi: 10.1007/s004240000470

Hussain, M., Drago, G. A., Colyer, J., and Orchard, C. H. (1997). Rate-dependent abbreviation of Ca^{2+} transient in rat heart is independent of phospholamban phosphorylation. *Am. J. Physiol.* 273, H695–H706.

Joung, B., Chen, P.-S., and Lin, S.-F. (2011). The role of the calcium and the voltage clocks in sinoatrial node dysfunction. *Yonsei Med. J.* 52, 211–219. doi: 10.3349/ymj.2011.52.2.211

Joung, B., Lin, S.-F., Chen, Z., Antoun, P. S., Maruyama, M., Han, S., et al. (2010). Mechanisms of sinoatrial node dysfunction in a canine model of pacing-induced atrial fibrillation. *Heart Rhythm* 7, 88–95. doi: 10.1016/j.hrthm.2009.09.018

Joung, B., Tang, L., Maruyama, M., Han, S., Chen, Z., Stucky, M., et al. (2009). Intracellular calcium dynamics and acceleration of sinus rhythm by β-adrenergic stimulation. *Circulation* 119, 788–796. doi: 10.1161/CIRCULATIONAHA.108.817379

Ju, Y.-K., and Allen, D. G. (1998). Intracellular calcium and Na^+-Ca^{2+} exchange current in isolated toad pacemaker cells. *J. Physiol.* 508, 153–166. doi: 10.1111/j.1469-7793.1998.153br.x

Kho, C., Lee, A., and Hajjar, R. J. (2012). Altered sarcoplasmic reticulum calcium cycling – targets for heart failure therapy. *Nat. Rev. Cardiol.* 9, 717–733. doi: 10.1038/nrcardio.2012.145

Kodama, I., Honjo, H., and Boyett, M. R. (2002). Are we lost in the labyrinth of the sinoatrial node pacemaker mechanism? *J. Cardiovasc. Electrophysiol.* 13, 1303–1305. doi: 10.1046/j.1540-8167.2002.01303.x

Lacinová, L., Kurejová, M., Klugbauer, N., and Hofmann, F. (2006). Gating of the expressed T-type $Ca_V3.1$ calcium channels is modulated by Ca^{2+}. *Acta. Physiol.* 186, 249–260. doi: 10.1111/j.1748-1716.2006.01539.x

Lakatta, E. G., and DiFrancesco, D. (2009). What keeps us ticking: a funny current, a calcium clock, or both? *J. Mol. Cell. Cardiol.* 47, 157–170. doi: 10.1016/j.yjmcc.2009.03.022

Lakatta, E. G., and Maltsev, V. A. (2012). Rebuttal: what I_f the shoe doesn't fit? "The funny current has a major pacemaking role in the sinus node." *Heart Rhythm* 9, 459–460. doi: 10.1016/j.hrthm.2011.09.024

Lakatta, E. G., Maltsev, V. A., Bogdanov, K. Y., Stern, M. D., and Vinogradova, T. (2003). Cyclic variation of intracellular calcium: a critical factor for cardiac pacemaker cell dominance. *Circ. Res.* 92, e45–e50. doi: 10.1161/01.RES.0000055920.64384.FB

Lakatta, E. G., Maltsev, V. A., and Vinogradov, T. M. (2010). A coupled SYSTEM of intracellular Ca^{2+} clocks and surface membrane voltage clocks controls the timekeeping mechanism of the heart's pacemaker. *Circ. Res.* 106, 659–673. doi: 10.1161/CIRCRESAHA.109.206078

Lancaster, M. K., Jones, S. A., Harrison, S. M., and Boyett, M. R. (2004). Intracellular Ca^{2+} and pacemaking within the rabbit sinoatrial node: heterogeneity of role and control. *J. Physiol.* 556, 481–494. doi: 10.1113/jphysiol.2003.057372

Lau, D. H., Roberts-Thomson, K. C., and Sanders, P. (2011). Sinus node revisited. *Curr. Opin. Cardiol.* 26, 55–59. doi: 10.1097/HCO.0b013e32834138f4

Laurita, K. R., Katra, R., Wible, B., Wan, X. P., and Koo, M. H. (2003). Transmural heterogeneity of calcium handling in canine. *Circ. Res.* 92, 668–675. doi: 10.1161/01.RES.0000062468.25308.27

Lei, M., Brown, H. F., and Terrar, D. A. (2000). Modulation of delayed rectifier potassium current, i_K, by isoprenaline in rabbit isolated pacemaker cells. *Exp. Physiol.* 85, 27–35. doi: 10.1111/j.1469-445X.2000.01915.x

Li, J., Qu, J., and Nathan, R., D (1997). Ionic basis of ryanodine's negative chronotropic effect on pacemaker cells isolated from the sinoatrial node. *Am. J. Physiol.* 273, H2481–H2489.

Lindblad, D. S., Murphey, C. R., Clark, J. W., and Giles, W. R. (1996). A model of the action potential and underlying membrane currents in a rabbit atrial cell. *Am. J. Physiol.* 271, H1666–H1696.

Lipsius, S. L., and Bers, D. M. (2003). Cardiac pacemaking: I_f vs. Ca^{2+}, is it really that simple? *J. Mol. Cell. Cardiol.* 35, 891–893. doi: 10.1016/S0022-2828(03)00184-6

Luo, M., and Anderson, M. E. (2013). Mechanisms of altered Ca^{2+} handling in heart failure. *Circ. Res.* 113, 690–708. doi: 10.1161/CIRCRESAHA.113.301651

Lyashkov, A. E., Juhaszova, M., Dobrzynski, H., Vinogradova, T. M., Maltsev, V. A., Juhasz, O., et al. (2007). Calcium cycling protein density and functional importance to automaticity of isolated sinoatrial nodal cells are independent of cell size. *Circ. Res.* 100, 1723–1731. doi: 10.1161/CIRCRESAHA.107.153676

Maltsev, V. A., and Lakatta, E. G. (2008). Dynamic interactions of an intracellular Ca^{2+} clock and membrane ion channel clock underlie robust initiation and regulation of cardiac pacemaker function. *Cardiovasc. Res.* 77, 274–284. doi: 10.1093/cvr/cvm058

Maltsev, V. A., and Lakatta, E. G. (2010a). Funny current provides a relatively modest contribution to spontaneous beating rate regulation of human and rabbit sinoatrial node cells. *J. Mol. Cell. Cardiol.* 48, 804–806. doi: 10.1016/j.yjmcc.2009.12.009

Maltsev, V. A., and Lakatta, E. G. (2010b). A novel quantitative explanation for the autonomic modulation of cardiac pacemaker cell automaticity via a dynamic system of sarcolemmal and intracellular proteins. *Am. J. Physiol. Heart Circ. Physiol.* 298, H2010–H2023. doi: 10.1152/ajpheart.00783.2009

Maltsev, V. A., and Lakatta, E. G. (2012). The funny current in the context of the coupled-clock pacemaker cell system. *Heart Rhythm* 9, 302–307. doi: 10.1016/j.hrthm.2011.09.022

Maltsev, V. A., Vinogradova, T. M., and Lakatta, E. G. (2006). The emergence of a general theory of the initiation and strength of the heartbeat. *J. Pharmacol. Sci.* 100, 338–369. doi: 10.1254/jphs.CR0060018

Maltsev, V. A., Vinogradova, T. M., Stern, M. D., and Lakatta, E. G. (2011). Validating the requirement for beat-to-beat coupling of the Ca^{2+} clock and M clock in pacemaker cell normal automaticity. *Am. J. Physiol. Heart Circ. Physiol.* 300, H2323–H2324. doi: 10.1152/ajpheart.00110.2011

Mangoni, M. E., and Nargeot, J. (2008). Genesis and regulation of the heart automaticity. *Physiol. Rev.* 88, 919–982. doi: 10.1152/physrev.00018.2007

Masson-Pévet, M., Bleeker, W. K., and Gros, D. (1979). The plasma membrane of leading pacemaker cells in the rabbit sinus node. A qualitative and quantitative ultrastructural analysis. *Circ. Res.* 45, 621–629. doi: 10.1161/01.RES.45.5.621

Musa, H., Lei, M., Honjo, H., Jones, S. A., Dobrzynski, H., Lancaster, M. K., et al. (2002). Heterogeneous expression of Ca^{2+} handling proteins in rabbit sinoatrial node. *J. Histochem. Cytochem.* 50, 311–324. doi: 10.1177/002215540205000303

Neef, S., and Maier, L. S. (2013). Novel aspects of excitation-contraction coupling in heart failure. *Basic Res. Cardiol.* 108:360. doi: 10.1007/s00395-013-0360-2

Opthof, T., Coronel, R., Rademaker, H. M., Vermeulen, J. T., Wilms-Schopman, F. J., and Janse, M. J. (2000). Changes in sinus node function in a rabbit model of heart failure with ventricular arrhythmias and sudden death. *Circulation* 101, 2975–2980. doi: 10.1161/01.CIR.101.25.2975

Øyehaug, L., Loose, K. Ø., Jølle, G. F., Røe, Å. T., Sjaastad, I., Christensen, G., et al. (2013). Synchrony of cardiomyocyte Ca^{2+} release is controlled by T-tubule organization, SR Ca^{2+} content, and ryanodine receptor Ca^{2+} sensitivity. *Biophys. J.* 104, 1685–1697. doi: 10.1016/j.bpj.2013.03.022

Rigg, L., Heath, B. M., Cui, Y., and Terrar, D. A. (2000). Localisation and functional significance of ryanodine receptors during β-adrenoceptor stimulation in the

guinea-pig sino-atrial node. *Cardiovasc. Res.* 48, 254–264. doi: 10.1016/S0008-6363(00)00153-X

Rigg, L., Mattick, P. A. D., Heath, B. M., and Terrar, D. A. (2003). Modulation of the hyperpolarization-activated current (I_f) by calcium and calmodulin in the guinea-pig sino-atrial node. *Cardiovasc. Res.* 57, 497–504. doi: 10.1016/S0008-6363(02)00668-5

Sanders, L., Rakovic, S., Lowe, M., Mattick, P. A., and Terrar, D. A. (2006). Fundamental importance of Na^+-Ca^{2+} exchange for the pacemaking mechanism in guinea-pig sino-atrial node. *J. Physiol.* 571, 639–649. doi: 10.1113/jphysiol.2005.100305

Severi, S., Fantini, M., Charawi, L. A., and DiFrancesco, D. (2012). An updated computational model of rabbit sinoatrial action potential to investigate the mechanisms of heart rate modulation. *J. Physiol.* 590, 4483–4499. doi: 10.1113/jphysiol.2012.229435

Shinohara, T., Park, H.-W., Han, S., Shen, M. J., Maruyama, M., Kim, D., et al. (2010). Ca^{2+} clock malfunction in a canine model of pacing-induced heart failure. *Am. J. Physiol. Heart. Circ. Physiol.* 299, H1805–H1811. doi: 10.1152/ajpheart.00723.2010

Sipido, K. R., Callewaert, G., and Carmeliet, E. (1995). Inhibition and rapid recovery of Ca^{2+} current during Ca^{2+} release from sarcoplasmic reticulum in guinea pig ventricular myocytes. *Circ. Res.* 76, 102–109. doi: 10.1161/01.RES.76.1.102

Stern, M. D., Maltseva, L. A., Juhaszova, M., Sollott, S. J., Lakatta, E. G., and Maltsev, V. A. (2014). Hierarchical clustering of ryanodine receptors enables emergence of a calcium clock in sinoatrial node cells. *J. Gen. Physiol.* 143, 577–604. doi: 10.1085/jgp.201311123

Tohse, N. (1990). Calcium-sensitive delayed rectifier potassium current in guinea pig ventricular cells. *Am. J. Physiol.* 258, H1200–H1207.

Trafford, A. W., Díaz, M. E., and Eisner, D. A. (2001). Coordinated control of cell Ca^{2+} loading and triggered release from the sarcoplasmic reticulum underlies the rapid inotropic response to increased L-type Ca^{2+} current. *Circ. Res.* 88, 195–201. doi: 10.1161/01.RES.88.2.195

Trafford, A. W., Díaz, M. E., Sibbring, G. C., and Eisner, D. A. (2000). Modulation of CICR has no maintained effect on systolic Ca^{2+}: simultaneous measurements of sarcoplasmic reticulum and sarcolemmal Ca^{2+} fluxes in rat ventricular myocytes. *J. Physiol.* 522, 259–270. doi: 10.1111/j.1469-7793.2000.t01-2-00259.x

van Borren, M. M. G. J., Verkerk, A. O., Wilders, R., Hajji, N., Zegers, J. G., Bourier, J., et al. (2010). Effects of muscarinic receptor stimulation on Ca^{2+} transient, cAMP production and pacemaker frequency of rabbit sinoatrial node cells. *Basic. Res. Cardiol.* 105, 73–87. doi: 10.1007/s00395-009-0048-9

van Borren, M. M. G. J., Zegers, J. G., Verkerk, A. O., and Wilders, R. (2007). Computational model of rabbit SA node pacemaker activity probed with action potential and calcium transient clamp. *Conf. Proc. IEEE Eng. Med. Biol. Soc.* 2007, 156–159. doi: 10.1109/IEMBS.2007.4352246

Varro, A., Negretti, N., Hester, S. B., and Eisner, D. A. (1993). An estimate of the calcium content of the sarcoplasmic reticulum in rat ventricular myocytes. *Pflügers Arch.* 423, 158–160. doi: 10.1007/BF00374975

Verheijck, E. E., van Ginneken, A. C. G., Wilders, R., and Bouman, L. N. (1999). Contribution of L-type Ca^{2+} current to electrical activity in sinoatrial nodal myocytes of rabbits. *Am. J. Physiol.* 276, H1064–H1077.

Verkerk, A. O., Baartscheer, A., de Groot, J. R., Wilders, R., and Coronel, R. (2011). Etiology-dependency of ionic remodeling in cardiomyopathic rabbits. *Int. J. Cardiol.* 148, 154–160. doi: 10.1016/j.ijcard.2009.10.047

Verkerk, A. O., den Ruijter, H. M., Bourier, J., Boukens, B. J., Brouwer, I. A., Wilders, R., et al. (2009). Dietary fish oil reduces pacemaker current and heart rate in rabbit. *Heart Rhythm* 6, 1485–1492. doi: 10.1016/j.hrthm.2009.07.024

Verkerk, A. O., van Borren, M. M. G. J., and Wilders, R. (2013). Calcium transient and sodium-calcium exchange current in human versus rabbit sinoatrial node pacemaker cells. *ScientificWorldJournal* 2013:507872. doi: 10.1155/2013/507872

Verkerk, A. O., and Wilders, R. (2010). Relative importance of funny current in human versus rabbit sinoatrial node. *J. Mol. Cell. Cardiol.* 48, 799–801. doi: 10.1016/j.yjmcc.2009.09.020

Verkerk, A. O., Wilders, R., Coronel, R., Ravesloot, J. H., and Verheijck, E. E. (2003). Ionic remodeling of sinoatrial node cells by heart failure. *Circulation* 108, 760–766. doi: 10.1161/01.CIR.0000083719.51661.B9

Verkerk, A. O., Wilders, R., Zegers, J. G., van Borren, M. M. G. J., Ravesloot, J. H., and Verheijck, E. E. (2002). Ca^{2+}-activated Cl^- current in rabbit sinoatrial node cells. *J. Physiol.* 540, 105–117. doi: 10.1113/jphysiol.2001.013184

Vermeulen, J. T., McGuire, M. A., Opthof, T., Coronel, R., de Bakker, J. M. T., Klöpping, C., et al. (1994). Triggered activity and automaticity in ventricular trabeculae of failing human and rabbit hearts. *Cardiovasc. Res.* 28, 1547–1554. doi: 10.1113/jphysiol.2001.013184

Vinogradova, T. M., Bogdanov, K. Y., and Lakatta, E. G. (2002a). β-adrenergic stimulation modulates ryanodine receptor Ca^{2+} release during diastolic depolarization to accelerate pacemaker activity in rabbit sinoatrial nodal cells. *Circ. Res.* 90, 73–79. doi: 10.1161/hh0102.102271

Vinogradova, T. M., Bogdanov, K. Y., and Lakatta, E. G. (2002b). Novel perspectives on the beating rate of the heart. *Circ. Res.* 91:e3. doi: 10.1161/01.RES.0000031164.28289.55

Weber, C. R., Piacentino, V. III, Houser, S. R., and Bers, D. M. (2003). Dynamic regulation of sodium/calcium exchange function in human heart failure. *Circulation* 108, 2224–2249. doi: 10.1161/01.CIR.0000095274.72486.94

Wiegerinck, R. F., Verkerk, A. O., Belterman, C. N., van Veen, T. A. B., Baartscheer, A., Opthof, T., et al. (2006). Larger cell size in rabbits with heart failure increases myocardial conduction velocity and QRS duration. *Circulation* 113, 806–813. doi: 10.1161/CIRCULATIONAHA.105.565804

Witte, K., Hu, K., Swiatek, J., Müssig, C., Ertl, G., and Lemmer, B. (2000). Experimental heart failure in rats: effects on cardiovascular circadian rhythms and on myocardial β-adrenergic signaling. *Cardiovasc. Res.* 47, 350–358. doi: 10.1016/S0008-6363(00)00099-7

Wu, Y., and Anderson, M. E. (2014). CaMKII in sinoatrial node physiology and dysfunction. *Front. Pharmacol.* 5:48. doi: 10.3389/fphar.2014.00048

Zicha, S., Fernandez-Velasco, M., Lonardo, G., L'Heureux, N., and Nattel, S. (2005). Sinus node dysfunction and hyperpolarization-activated (HCN) channel subunit remodeling in a canine heart failure model. *Cardiovasc. Res.* 66, 472–481. doi: 10.1016/j.cardiores.2005.02.011

Conflict of Interest Statement: The authors declare that the research was conducted in the absence of any commercial or financial relationships that could be construed as a potential conflict of interest.

Received: 09 November 2014; accepted: 12 January 2015; published online: 02 February 2015.

Citation: Verkerk AO, van Borren MMGJ, van Ginneken ACG and Wilders R (2015) Ca^{2+} cycling properties are conserved despite bradycardic effects of heart failure in sinoatrial node cells. Front. Physiol. ***6****:18. doi: 10.3389/fphys.2015.00018*

This article was submitted to Cardiac Electrophysiology, a section of the journal Frontiers in Physiology.

frontiers in
PHYSIOLOGY

REVIEW ARTICLE
published: 29 January 2015
doi: 10.3389/fphys.2015.00013

Regulation of Ca^{2+} transient by PP2A in normal and failing heart

Ming Lei[1], Xin Wang[2], Yunbo Ke[3]* and R. John Solaro[3]

[1] *Department of Pharmacology, University of Oxford, Oxford, UK*
[2] *Faculty of Life Science, University of Manchester, Manchester, UK*
[3] *Department of Physiology and Biophysics, Center for Cardiovascular Research, University of Illinois at Chicago, Chicago, IL, USA*

Edited by:
Antonius Baartscheer, Academic Medical Center, Netherlands

Reviewed by:
Ravi C. Balijepalli, University of Wisconsin, USA
Thomas Hund, Ohio State University, USA

****Correspondence:***
Yunbo Ke, Department of Physiology and Biophysics, Center for Cardiovascular Research, University of Illinois at Chicago, 835 S. Wolcott Ave., Chicago, IL 60612, USA
e-mail: yke@uic.edu

Calcium transient in cardiomyocytes is regulated by multiple protein kinases and phosphatases. PP2A is a major protein phosphatase in the heart modulating Ca^{2+} handling through an array of ion channels, antiporters and pumps, etc. The assembly, localization/translocation, and substrate specificity of PP2A are controlled by different post-translational mechanisms, which in turn are linked to the activities of upstream signaling molecules. Abnormal PP2A expression and activities are associated with defective response to β-adrenergic stimulation and are indication and causal factors in arrhythmia and heart failure.

Keywords: calcium handling, ion channels, phosphatase, FTY720, arrhythmia, heart failure

INTRODUCTION

Cyclic and effective cardiac contraction and relaxation depend on the appropriately timed generation and spread of cardiac electrical activity. At the cellular level, excitation-contraction (E-C) coupling is initiated by action potential depolarization resulting, via a cascade of events, in an increase in intracellular calcium concentration, which ultimately leads to activation of myofilament and muscle contraction; subsequent removal of intracellular calcium via a number of mechanisms results in detachment of myosin cross-bridges and relaxation. Excitation and contraction involve multiple trans-membrane (e.g., ion channels) and intracellular proteins (e.g., Ca^{2+} handling and sarcomeric proteins) and are highly regulated by multiple extra- and intra-cellular signaling pathways that frequently converge at protein phosphorylation.

Studies of reversible protein phosphorylation in the heart date back to early seventies of last century when it was reported that cardiac troponin I (cTnI) was phosphorylated and dephosphorylated in the same manner as the protein substrates involved in glycogen metabolism (England et al., 1972; Stull et al., 1972). cTnI is the inhibitory component of heterotrimeric troponin complex and a major phosphoprotein in ventricular myocytes. cAMP dependent protein kinase (PKA), a downstream effector of β-adrenergic stimulations, phosphorylates cTnI at serine 23 and 24 (Cole and Perry, 1975; Solaro et al., 1976). Phosphorylation of cTnI promotes Ca^{2+} release from the myofilament and promotes cardiac relaxation (Robertson et al., 1982; Kentish et al., 2001). PP2A came into spotlight of heart research following another line of observation in late 1980s and early 1990s. It was found that an extract from black sea sponge, okadaic acid, has positive inotropic effect on electro-mechanic properties of ventricular muscle and enhances pacemaker activities in rabbit SA node preparation (Kodama et al., 1986; Kondo et al., 1990). Okadaic acid inhibits protein phosphatase PP2A at very low concentration leading to increased phosphorylation in numerous proteins of mammalian cells, including a number of ion channels and myofilament regulatory proteins. Thus, PP2A coordinates cardiac excitation and contraction.

The catalytic subunit of PP2A is highly conserved from yeast to humans and is homologous to the counterpart of PP1 complex, another major protein phosphatase in mammalian cells, which consists of catalytic and regulatory/targeting subunit with more than more than 200 isoforms (Depaoli-Roach et al., 1994; Peti et al., 2013). PP1 and PP2A are responsible for greater than 90% of protein dephosphorylation in the heart and they often share the same protein substrates and serine/threonine sites of dephosphorylation (Luss et al., 2000). However, their relative contributions to specific protein substrates o are often different, which is reflected in dephosphoryation of L-type Ca^{2+} channels (PP2A preferred) and phospholamban (PP1 preferred). For a long time, mammalian protein phosphatases had been considered constitutively active with the regulatory function fulfilled solely by protein kinases. This notion has become obsolete with discovery of multiple regulatory mechanisms for protein phosphatases, especially those that link phosphatase activities to extracellular cues (Cohen, 1988). The importance of regulation of phosphatases in heart pathophysiology becomes more obvious when altered PP2A expression and activities are closely associated with heart diseases (Ai and Pogwizd, 2005; Ke et al., 2008; Wijnker et al., 2011).

PP2A AND ITS REGULATION BY UPSTREAM SIGNALS IN THE HEART

PP2A actually refer to a large family of distinct heterotrimeric protein phosphatases that share a common core enzyme

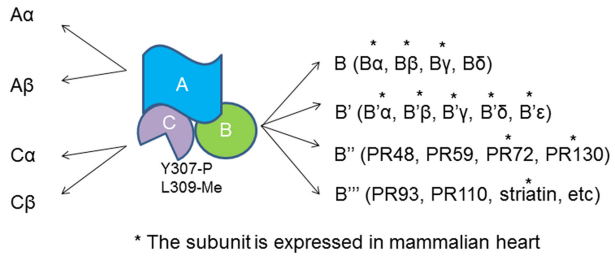

FIGURE 1 | PP2A heterotrimer and the subunits. Both A and C subunit have two isoforms, α and β. The catalytic C subunit can be tyrosine phosphorylated at tyrosine 307 and methylated at Leucine 309. *The B subunit is expressed and identified in cardiomyocytes.

consisting of a scaffolding (A) and a catalytic (C) subunits that associate with a B subunit (**Figure 1**). A subunit contains multiple HEAT repeats and forms a horse shoe structure that bind to both B and C subunits (Groves et al., 1999). HEAT repeat exists in proteins with different functions that form helical structures and provide structural flexibility to PP2A-A subunit (Grinthal et al., 2010). Formation of the PP2A heterotrimer follows a sequential pattern in that the core enzyme AC arises first and then binds to the B subunit. The Tyrosine 307 and Leucine 309 show reversible phosphorylation and methylation that determine the phosphatase localization and substrate specificity (Chen et al., 1992; Chung et al., 1999). Methylation of Leucine 309 diverts the C-terminal carboxyl group from a repulsive negative charge interaction and facilitates assembly of ABC holoenzyme (Cho and Xu, 2007).

The regulatory subunits of PP2A have many members with large sequence diversity and are coded by at least 17 distinct genes. At least 11 of them are expressed in cardiomyocytes with Bα and γ the most studied cardiac isoforms (**Figure 1**). Bα is abundant in cytoplasm in cardiomyocyte that associates with ankyrin-B, an adapter protein required for normal subcellular localization of the Na/Ca exchanger, Na/K ATPase (Bhasin et al., 2007). Overexpression of Bα leads to reduced phosphorylation cTnI, myosin-binding protein C and phospholamban, and repressed response of L-type Ca^{2+} channel current to stimulation of isoproterenol (Kirchhefer et al., 2014a). Bγ is expressed in the nuclear. In mouse model deficient in Bγ, an incomplete ventricular septum occurs during development. PR72 binds to Ca^{2+} resulting in conformational changes in the scaffolding subunit. Another Ca^{2+} responsive B subunit expressed in cariomyocytes is striatin that directly interacts with calmodulin (Chen et al., 2014; Hwang and Pallas, 2014). It remains unclear if PP2As containing these B subunits control cyclic dephophorylation on any protein substrates. A genome wide association studies has identified a deletion mutation that links abnormal striatin mRNA accumulation to arrhythmogenic right ventricular cardiomyopathy in canine model (Meurs et al., 2010).

Both PP1 and PP2A have native inhibitors in mammalian cells. Inhibitor I of PP1 is a phosphoprotein regulated by β-adrenergic stimulation and is important for modulation of Ca^{2+} re-uptake through phospholamban. I1 and I2 PP2A are specific PP2A inhibitors (Li et al., 1995). Their expression and functional role in cardiomyocytes is underexplored. PP2A is also up-regulated by small molecular weight chemicals, both native and artificial. C_2 and C_6 ceramides activates PP2A in different types of mammalian cells (Dobrowsky et al., 1993). FTY720 (fingolimod) is a synthetic analog of C_2 and C_6 ceramide and an immunosuppressor used for treatment of multiple schlerosis (Kappos et al., 2006). Like C_2 and C_6 ceramide, FTY720 activates PP2A without knowing exactly what the molecular mechanism of activation. P^{21} activated kinase-1 (Pak1), an upstream activator for PP2A, is activated by FTY720 and C2/C6 ceramides *on vitro* and *in vivo* (Ke and Solaro, 2008; Egom et al., 2010; Liu et al., 2011b).

Accumulating evidence has indicated that PP2A activities are up-regulated by stimulation of the inhibitory G proteins, Gi through different intermediate signaling processes (Ke et al., 2008). Treatment of ventricle cardiomyocytes with agonists that turn on receptors coupled to inhibitory G proteins (Gi/Go) leads to reduced phosphorylation on PKA substrates without any change in intracellular cAMP, suggesting phosphatases are responsible for reduction in protein phosphorylation (Gupta et al., 1993, 1994). In cardiomyocytes, methylation of PP2Ac is reduced when the cells are treated with pertussis toxin and the same result is generated by inhibition of p38 MAP kinase (Liu and Hofmann, 2002, 2003). Cdc42 and Rac1 have been shown to be the downstream effectors for Gi in cardiomycytes and other mammalian cells. The constitutively active Pak1, the downstream effectors for Cdc42 and Rac1 induces activation of PP2A and dephosphorylation of myofilament regulatory proteins (Ke et al., 2004). PI3K is another possible link between Gi and PP2A activities that enhances carboxylmethylation at leu309 (Longman et al., 2014) (**Figure 2**).

REGULATION OF Ca^{2+} HANDLING PROTEINS BY PP2A

The calcium transient starts through depolarization-activated Ca^{2+} channels. The inward calcium current triggers Ca^{2+} release from the sarcoplasmic reticulum mediated primarily by ryanodine receptors. The Ca^{2+} binds to troponin C of troponin/tropomyosin complex and activates myofilaments. During relaxation, cytosolic Ca^{2+} is pumped back into sarcoplasmic reticulum by SR Ca ATPase (SERCA) and is removed from the cells by Na^+/Ca^{2+} exchanger. Protein kinases and PP2A associate with all of these key regulatory machinery and shape the dynamics of Ca^{2+} flow (**Table 1**, **Figure 2**).

PP2A IS A MAJOR PHOSPHATASE FOR L-TYPE CA^{2+} CHANNELS (LTCC)

The voltage gated influx of Ca^{2+} through LTCC is highly responsive to β-adrenergic stimulation. PKA phosphorylates LTCC at the cytoplasmic, carboxyl end of alpha subunit of LTCC at Ser1928, Ser1866 (Chen et al., 2002; Hall et al., 2006), phosphorylation of S1512 and S1570 by Cam Kinase II may also play an auxiliary role modulating the channel activities (Blaich et al., 2010). The β-adrenergic effect on LTCC is reversed by PP2A, which associates with the channels at the PKA sites (Davare et al., 2000). In pacemaker cells, activation of PP2A by its upstream signal, Pak1, represses isoproterenol stimulated enhancement of the channel activities (Ke et al., 2007).

THE ROLES OF PP2A ON RYANODINE RECEPTOR (RyR) REGULATION

Ca^{2+} induced Ca^{2+} release through LTCC and ryanodine receptors is enhanced by β-adrenergic signaling cascades. Ser2808 and

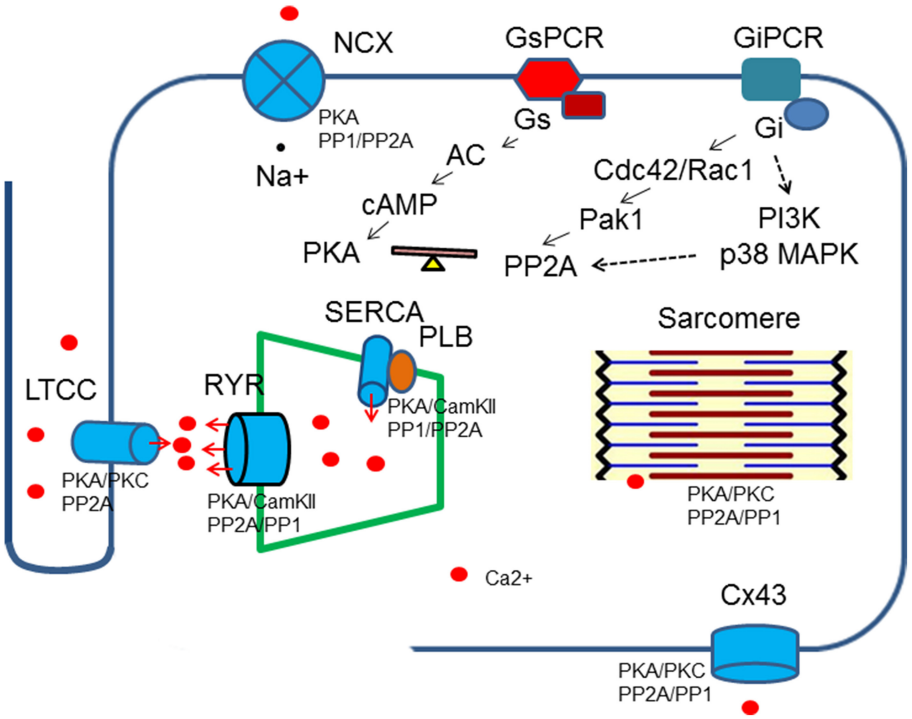

FIGURE 2 | Regulation of Ca^{2+} transient by protein kinases and phosphatases. Protein kinases and phospahtases are associated with key Ca^{2+} transient regulatory proteins, which in turn are linked to upstream signaling cascades. A balance of protein kinase and phosphatase activities is required to maintain normal cardiac functions. Breakdown of the balance occurs at different levels: genetic mutations, gene expressions, post-translational modifications and excessive or deficient neuro-hormonal cues.

Table 1 | Major targets regulating Ca^{2+} transient and regulated by PP2A.

Targets	Reported phosphorylation sites	Protein kinases	Protein phosphatases	Effects of PP2A on channel activities	References
L type Ca^{2+} channels	Ser1928 Ser1866	PKA	PP2A	↓	Chen et al., 2002; Hall et al., 2006 Davare et al., 2000; Shi et al., 2012
Ryanodine receptors	Ser2808	PKA, CamKII	PP2A	↓↑	Marx et al., 2000; Xiao et al., 2005, 2006; Meng et al., 2007; Liu et al., 2011a; Zhang et al., 2012
	Ser2030		PP1		Liu et al., 2014
Phospho-lamban	Ser16 and Thr17	PKA CamKII	PP1 PP2A	Release of inhibition on SERCA	MacDougall et al., 1991; Luo et al., 1994; Jackson and Colyer, 1996; Chu and Kranias, 2002
Connexin 43	Ser368 Ser262	PKC PKA	PP2A PP1	↓	Doble et al., 2000; Ai and Pogwizd, 2005; Srisakuldee et al., 2009
NCX	?	PKA PKC	PP2A PP1	↓?	Wei et al., 2003, 2007 Schulze et al., 2003; Zhang and Hancox, 2009

Ser2030 are considered as the PKA sites. Early studies suggest that hyperphosphorylation of RyR at Ser 2808 is responsible for increased leak for Ca^{2+} and associated with heart failure. Surprisinglya recent study has shown that in genetically modified mice with Ser2808 rendered unphosphorylatable, Ca^{2+} leak increases, instead of decrease with exacerbation of Ca^{2+}-dependent cardiomyopathy (Liu et al., 2014). On the other hand, Yang et al. recently indicate that a reduced degradation of β2-AR due to Rnd3 deficiency results in enhanced PKA activities and increased Ca^{2+} leak from RyR (Yang et al., 2015). PP1

and PP2A form complexes on ryanodine receptors. In saponin permeabilized myocytes, exposure of PP1 and PP2A dramatically increased Ca sparks with a significant decrease of SR Ca store (Terentyev et al., 2003). On the other hand, targeting of PP2A regulatory subunit B56α by microRNA miR-1 leads to hyperphosphorylation of RyR at the CamKII sites and increases Ca^{2+} release and promote cardiac arrhythmogenesis (Terentyev et al., 2009; Belevych et al., 2011). PP2A is also responsible for dephosphorylation of RyR from the CamKII sites which have now been considered to play an even more important roles enhancing Ca^{2+} leak from the channel.

PP2A IS NOT A MAJOR PROTEIN PHOSPHATASE FOR PHOSPHOLAMBAN

SERCA, a calcium transport ATPase for Ca^{2+} reuptake from cytosol to SR partners with phospholamban that is phosphorylated at Ser16 and threonine17 by PKA and CamKII, respectively. Phospholamban inhibits SERCA activities and the inhibition is released by PKA phosphorylation and Ser16. PP1 is the major phosphatase that removes phosphate from both locations. PP2A plays a minor role (30%) of dephosphorylation (MacDougall et al., 1991). In mice with overexpression of the regulatory subunit of PP2A, the isoproterenol stimulated phosphorylation of phosholamban and cTnI is partially reduced with increased basal contractility of the heart, likely due to elevated diastolic Ca^{2+} level and increased myofilament activities (Kirchhefer et al., 2014a).

THE ACTIVITIES OF CONNEXIN 43 ARE INHIBITED BY PP2A

The gap junction channel protein connexin 43 conducts ions and other small molecules between two adjacent myocytes. The conductivity of connexin 43 is enhanced by PKA and reduced by PP2A as demonstrated by intercellular dye coupling (Ai and Pogwizd, 2005; Ai et al., 2011).

PP2A AND Na/Ca EXCHANGER

The cardiac Na/Ca^{2+} exchanger (NCX) is involved in the extrusion of cytosolic Ca^{2+} with a major role in the decay phase of the intracellular Ca^{2+} transient. PP1 and PP2A form complex with Na/Ca exchanger (Schulze et al., 2003). Stimulation of PKA activities by dibutyryl cyclic AMP and inhibition of PP2A by okadaic acid inhibits NCX activities (Lin et al., 1994). However, studies from other groups reported mixed results regarding the role of β-adrenergic stimulation on NCX activities (Zhang and Hancox, 2009). Wei et al. indicated that hyperphosphorylation of NCX is associated with an increased NCX current. In failing heart, low phosphatase activity and hyperphosphorylation is responsible for impaired sensitivity to β-adrenergic stimulation (Wei et al., 2007).

ABERRANT EXPRESSION, LOCALIZATION, AND ACTIVITIES OF PP2A IN ARRHYTHMIA AND HEART FAILURE

The importance of PP2A in the heart resides in its capacity to antagonize the effects of β-adrenergic stimulation with reduction of the amplitude of Ca transient and meanwhile increasing the Ca^{2+} sensitivity of myofilament in force development. Therefore, abnormality in PP2A expression, localization and activities are frequently associated with heart failure. However, the role of PP2A as a causal or beneficial factor in heart failure remains unclear.

EXPRESSION AND ACTIVITIES OF PP2A IN HEART FAILURE

In a rat model with chronic isoproterenol infusion that lead to cardiac hypertrophy and heart failure, PP2A activities increased significantly at day 2 (Boknik et al., 2000). In HF induced by tachypacing in sheep, increased PP1 and PP2A activities are associated with diminished response to β-adrenergic stimulation in amplitude of Ca^{2+} transient compared to normal heart (Briston et al., 2011). Overexpression of the catalytic subunit of PP2A (PP2A-C) by transgenic approach in mouse heart leads to left ventricular hypertrophy and reduced contractility along with an increase of PP2A activities in myocardium (Gergs et al., 2004). A more detailed analysis of expression and localization of different PP2A B subunits in cardiomyocytes from normal and failing hearts indicate that proper targeting and localization of PP2A holoenzyme are important for normal cardiac functions (DeGrande et al., 2013). On the other hand, in human heart with ischemic cardiomyopathy (ICM) and dilated cardiomyopathy (DCM), expression of both PP2A-C and PP2A-B α are reduced by half or more compared to the non-failing heart. Studies in transgenic mice over-expressing the regulatory subunit Bα indicate that this subunit directs PP2A core enzyme to Ca^{2+} release channels and myofilament regulatory proteins (Kirchhefer et al., 2014a). Although there is no change in PP2A activities in the ICM and DCM samples, the total protein phosphatase activities and PP1 activities increases with reduced phosphorylation on cTnI (Wijnker et al., 2011). Hyperphosphorylation of ryanodine by enhanced β-adrenergic stimulation and reduced phosphatase activities results in "Ca^{2+} leak" from sarcoplasmic reticulum in failing heart (Marx et al., 2000; Reiken et al., 2001).

REDUCED PP2A ACTIVITIES ARE ASSOCIATED WITH ARRHYTHMIA AND ATRIAL FIBRILLATION (AF)

As reduced density of L-type Ca^{2+} current is characteristic of AF, increased PP2A activities were considered as an cause for the cardiac condition (Christ et al., 2004). Further analysis indicates that reduction of L-type calcium current density is due to a transcriptional downregulation of the pore forming alpha (1c)-subunit of LTCC, while single channel peak average current is 1.7-fold higher in AF than the control due to a 3.1-fold higher open probability of LCC. Inhibition of PP2A by okadaic acid only increases Ica in control but not in AF, suggesting phosphorylation of LCC in AF is high (Klein et al., 2003). Down regulation of PP2A-Bα by microRNA miR-1 is associated with elevated phosphorylation of RyR at CamKII site, but not the PKA sites with enhanced frequency of spontaneous Ca^{2+} sparks and arrhythmogenic oscillations of intracellular Ca^{2+} (Terentyev et al., 2009).

POST-TRANSLATIONAL MODIFICATIONS AND MUTATION OF PP2A ASSOCIATED WITH HEART FAILURE

Kirchhefer et al. reported that Bα of PP2A is phosphorylated at Ser41 by PKC α and phosphorylation at this site lead to reduction of the phosphatase activities. In failing human heart, phosphorylation of Bα is 7-fold higher (Kirchhefer et al., 2014b). The

A subunit is also phosphorylated and phosphorylation attenuates assembly of PP2A heterotrimer and reduces PP2A activities characterized by increased phosphorylation occurred to a large number of proteins in cells expressing the peudophosphorylated constructs. Unlike phosphorylated Bα, in a rat model of heart failure phosphorylation at this subunit is reduced leading to higher PP2A activities. In transgenic mice expressing a truncated A subunit that is a dominant negative mutant disrupting normal PP2a assembly, dilated cardiomyopathy developed with increased end-diastolic and end-systolic dimensions and decreased fractional shortening (Brewis et al., 2000).

THE ROLES OF PP2A IN SENSITIZING β-ADRENERGIC STIMULATION

Loss of response to β-adrenergic stimulation is a hall mark of end stage heart failure. Previously, it is believed that increased phosphatase activity is a major cause for desensitizing β-adrenergic stimulation as the β-adrenergic stimulation are effectively and rapidly damped by enhanced phosphatase activities. Accumulating evidence suggest that this may not be true because in failing heart, phosphorylation on L-type Ca^{2+} channels, ryanodine receptors and NCX are usually high. Phosphatases, especially PP2A can make them more responsive to β-adrenergic signals by bringing down phosphorylation levels. Recent studies by Zheng et al suggest that pyruvate restores β-adrenergic sensitivity of L-type Ca^{2+} channels in failing rat heart through PP2A (Zheng et al., 2013).

PERSPECTIVE

Structural diversity and complex regulation of PP2A constitute a significant challenge in understanding its function in the heart. Emerging evidence begins to point out connections between specific PP2A heterotrimers and their protein substrates in cardiomyocytes, but definitive results are still scarce. Application of general PP2A inhibitors for heart diseases may not be applicable as these inhibitors usually are tumorigenic. However, cardiac conditions including heart failure may become ameliorated by elevating PP2A activities. FTY720 (fingolimod), a FDA recently approved drug activates PP2A and target novel anti-adrenergic signaling pathways mediated by Pak1 (Egom et al., 2010). FTY720 protect heart against ischemia-reperfusion induced arrhythmia and has demonstrated anti-hypertrophic effect in mouse TAC model (Liu et al., 2011b, 2013). Its roles in modulation of Ca^{2+} transient in failing heart in animal models and in humans deserve further investigation.

ACKNOWLEDGMENT

This work is supported by NIH Grant HL 064035 (R. John Solaro), PO1 HL 062426 (R. John Solaro) and the Medical Research Council (G10002647: Ming Lei, Xin Wang, Elizabeth J. Cartwright, R. John Solaro, Yunbo Ke).

REFERENCES

Ai, X., Jiang, A., Ke, Y., Solaro, R. J., and Pogwizd, S. M. (2011). Enhanced activation of p21-activated kinase 1 in heart failure contributes to dephosphorylation of connexin 43. *Cardiovasc. Res.* 92, 106–114. doi: 10.1093/cvr/cvr163

Ai, X., and Pogwizd, S. M. (2005). Connexin 43 downregulation and dephosphorylation in nonischemic heart failure is associated with enhanced colocalized protein phosphatase type 2A. *Circ. Res.* 96, 54–63. doi: 10.1161/01.RES.0000152325.07495.5a

Belevych, A. E., Sansom, S. E., Terentyeva, R., Ho, H. T., Nishijima, Y., Martin, M. M., et al. (2011). MicroRNA-1 and -133 increase arrhythmogenesis in heart failure by dissociating phosphatase activity from RyR2 complex. *PLoS ONE* 6:e28324. doi: 10.1371/journal.pone.0028324

Bhasin, N., Cunha, S. R., Mudannayake, M., Gigena, M. S., Rogers, T. B., and Mohler, P. J. (2007). Molecular basis for PP2A regulatory subunit B56alpha targeting in cardiomyocytes. *Am. J. Physiol. Heart Circ. Physiol.* 293, H109–H119. doi: 10.1152/ajpheart.00059.2007

Blaich, A., Welling, A., Fischer, S., Wegener, J. W., Kostner, K., Hofmann, F., et al. (2010). Facilitation of murine cardiac L-type Ca(v)1.2 channel is modulated by calmodulin kinase II-dependent phosphorylation of S1512 and S1570. *Proc. Natl. Acad. Sci. U.S.A.* 107, 10285–10289. doi: 10.1073/pnas.0914287107

Boknik, P., Fockenbrock, M., Herzig, S., Knapp, J., Linck, B., Luss, H., et al. (2000). Protein phosphatase activity is increased in a rat model of long-term beta-adrenergic stimulation. *Naunyn Schmiedebergs. Arch. Pharmacol.* 362, 222–231. doi: 10.1007/s002100000283

Brewis, N., Ohst, K., Fields, K., Rapacciuolo, A., Chou, D., Bloor, C., et al. (2000). Dilated cardiomyopathy in transgenic mice expressing a mutant A subunit of protein phosphatase 2A. *Am. J. Physiol. Heart Circ. Physiol.* 279, H1307–H1318.

Briston, S. J., Caldwell, J. L., Horn, M. A., Clarke, J. D., Richards, M. A., Greensmith, D. J., et al. (2011). Impaired beta-adrenergic responsiveness accentuates dysfunctional excitation-contraction coupling in an ovine model of tachypacing-induced heart failure. *J. Physiol. (Lond).* 589, 1367–1382. doi: 10.1113/jphysiol.2010.203984

Chen, C., Shi, Z., Zhang, W., Chen, M., He, F., Zhang, Z., et al. (2014). Striatins contain a noncanonical coiled coil that binds protein phosphatase 2A A subunit to form a 2:2 heterotetrameric core of striatin-interacting phosphatase and kinase (STRIPAK) complex. *J. Biol. Chem.* 289, 9651–9661. doi: 10.1074/jbc.M113.529297

Chen, J., Martin, B. L., and Brautigan, D. L. (1992). Regulation of protein serine-threonine phosphatase type-2A by tyrosine phosphorylation. *Science* 257, 1261–1264. doi: 10.1126/science.1325671

Chen, X., Piacentino, V. III, Furukawa, S., Goldman, B., Margulies, K. B., and Houser, S. R. (2002). L-type Ca^{2+} channel density and regulation are altered in failing human ventricular myocytes and recover after support with mechanical assist devices. *Circ. Res.* 91, 517–524. doi: 10.1161/01.RES.0000033988.13062.7C

Cho, U. S., and Xu, W. (2007). Crystal structure of a protein phosphatase 2A heterotrimeric holoenzyme. *Nature* 445, 53–57. doi: 10.1038/nature05351

Christ, T., Boknik, P., Wohrl, S., Wettwer, E., Graf, E. M., Bosch, R. F., et al. (2004). L-type Ca^{2+} current downregulation in chronic human atrial fibrillation is associated with increased activity of protein phosphatases. *Circulation* 110, 2651–2657. doi: 10.1161/01.CIR.0000145659.80212.6A

Chu, G., and Kranias, E. G. (2002). Functional interplay between dual site phospholambam phosphorylation: insights from genetically altered mouse models. *Basic Res. Cardiol.* 97(Suppl. 1), I43–I48. doi: 10.1007/s003950200028

Chung, H., Nairn, A. C., Murata, K., and Brautigan, D. L. (1999). Mutation of Tyr307 and Leu309 in the protein phosphatase 2A catalytic subunit favors association with the alpha 4 subunit which promotes dephosphorylation of elongation factor-2. *Biochemistry* 38, 10371–10376. doi: 10.1021/bi990902g

Cohen, P. (1988). Protein phosphorylation and hormone action. *Proc. R. Soc. Lond. B Biol. Sci.* 234, 115–144. doi: 10.1098/rspb.1988.0040

Cole, H. A., and Perry, S. V. (1975). The phosphorylation of troponin I from cardiac muscle. *Biochem. J.* 149, 525–533.

Davare, M. A., Horne, M. C., and Hell, J. W. (2000). Protein phosphatase 2A is associated with class C L-type calcium channels (Cav1.2) and antagonizes channel phosphorylation by cAMP-dependent protein kinase. *J. Biol. Chem.* 275, 39710–39717. doi: 10.1074/jbc.M005462200

DeGrande, S. T., Little, S. C., Nixon, D. J., Wright, P., Snyder, J., Dun, W., et al. (2013). Molecular mechanisms underlying cardiac protein phosphatase 2A regulation in heart. *J. Biol. Chem.* 288, 1032–1046. doi: 10.1074/jbc.M112.426957

Depaoli-Roach, A. A., Park, I. K., Cerovsky, V., Csortos, C., Durbin, S. D., Kuntz, M. J., et al. (1994). Serine/threonine protein phosphatases in the control of cell function. *Adv. Enzyme Regul.* 34, 199–224. doi: 10.1016/0065-2571(94)90017-5

Doble, B. W., Ping, P., and Kardami, E. (2000). The epsilon subtype of protein kinase C is required for cardiomyocyte connexin-43 phosphorylation. *Circ. Res.* 86, 293–301. doi: 10.1161/01.RES.86.3.293

Dobrowsky, R. T., Kamibayashi, C., Mumby, M. C., and Hannun, Y. A. (1993). Ceramide activates heterotrimeric protein phosphatase 2A. *J. Biol. Chem.* 268, 15523–15530.

Egom, E. E., Ke, Y., Musa, H., Mohamed, T. M., Wang, T., Cartwright, E., et al. (2010). FTY720 prevents ischemia/reperfusion injury-associated arrhythmias in an *ex vivo* rat heart model via activation of Pak1/Akt signaling. *J. Mol. Cell. Cardiol.* 48, 406–414. doi: 10.1016/j.yjmcc.2009.10.009

England, P. J., Stull, J. T., and Krebs, E. G. (1972). Dephosphorylation of the inhibitor component of troponin by phosphorylase phosphatase. *J. Biol. Chem.* 247, 5275–5277.

Gergs, U., Boknik, P., Buchwalow, I., Fabritz, L., Matus, M., Justus, I., et al. (2004). Overexpression of the catalytic subunit of protein phosphatase 2A impairs cardiac function. *J. Biol. Chem.* 279, 40827–40834. doi: 10.1074/jbc.M405770200

Grinthal, A., Adamovic, I., Weiner, B., Karplus, M., and Kleckner, N. (2010). PR65, the HEAT-repeat scaffold of phosphatase PP2A, is an elastic connector that links force and catalysis. *Proc. Natl. Acad. Sci. U.S.A.* 107, 2467–2472. doi: 10.1073/pnas.0914073107

Groves, M. R., Hanlon, N., Turowski, P., Hemmings, B. A., and Barford, D. (1999). The structure of the protein phosphatase 2A PR65/A subunit reveals the conformation of its 15 tandemly repeated HEAT motifs. *Cell* 96, 99–110. doi: 10.1016/S0092-8674(00)80963-0

Gupta, R. C., Neumann, J., Boknik, P., and Watanabe, A. M. (1994). M2-specific muscarinic cholinergic receptor-mediated inhibition of cardiac regulatory protein phosphorylation. *Am. J. Physiol.* 266, H1138–H1144.

Gupta, R. C., Neumann, J., Durant, P., and Watanabe, A. M. (1993). A1-adenosine receptor-mediated inhibition of isoproterenol-stimulated protein phosphorylation in ventricular myocytes. Evidence against a cAMP-dependent effect. *Circ. Res.* 72, 65–74. doi: 10.1161/01.RES.72.1.65

Hall, D. D., Feekes, J. A., Arachchige Don, A. S., Shi, M., Hamid, J., Chen, L., et al. (2006). Binding of protein phosphatase 2A to the L-type calcium channel Cav1.2 next to Ser1928, its main PKA site, is critical for Ser1928 dephosphorylation. *Biochemistry* 45, 3448–3459. doi: 10.1021/bi051593z

Hwang, J., and Pallas, D. C. (2014). STRIPAK complexes: structure, biological function, and involvement in human diseases. *Int. J. Biochem. Cell Biol.* 47, 118–148. doi: 10.1016/j.biocel.2013.11.021

Jackson, W. A., and Colyer, J. (1996). Translation of Ser16 and Thr17 phosphorylation of phospholamban into Ca^{2+}-pump stimulation. *Biochem. J.* 316(Pt 1), 201–207.

Kappos, L., Antel, J., Comi, G., Montalban, X., O'Connor, P., Polman, C. H., et al. (2006). Oral fingolimod (FTY720) for relapsing multiple sclerosis. *N. Engl. J. Med.* 355, 1124–1140. doi: 10.1056/NEJMoa052643

Ke, Y., Lei, M., Collins, T. P., Rakovic, S., Mattick, P. A., Yamasaki, M., et al. (2007). Regulation of L-type calcium channel and delayed rectifier potassium channel activity by p21-activated kinase-1 in guinea pig sinoatrial node pacemaker cells. *Circ. Res.* 100, 1317–1327. doi: 10.1161/01.RES.0000266742.51389.a4

Ke, Y., Lei, M., and Solaro, R. J. (2008). Regulation of cardiac excitation and contraction by p21 activated kinase-1. *Prog. Biophys. Mol. Biol.* 98, 238–250. doi: 10.1016/j.pbiomolbio.2009.01.007

Ke, Y., and Solaro, R. J. (2008). Use of a decoy peptide to purify p21 activated kinase-1 in cardiac muscle and identification of ceramide-related activation. *Biologics* 2, 903–909.

Ke, Y., Wang, L., Pyle, W. G., de Tombe, P. P., and Solaro, R. J. (2004). Intracellular localization and functional effects of P21-activated kinase-1 (Pak1) in cardiac myocytes. *Circ. Res.* 94, 194–200. doi: 10.1161/01.RES.0000111522.02730.56

Kentish, J. C., McCloskey, D. T., Layland, J., Palmer, S., Leiden, J. M., Martin, A. F., et al. (2001). Phosphorylation of troponin I by protein kinase A accelerates relaxation and crossbridge cycle kinetics in mouse ventricular muscle. *Circ. Res.* 88, 1059–1065. doi: 10.1161/hh1001.091640

Kirchhefer, U., Brekle, C., Eskandar, J., Isensee, G., Kucerova, D., Mueller, F. U., et al. (2014a). Cardiac function is regulated by B56α-mediated targeting of PP2A to contractile relevant substrates. *J. Biol. Chem.* 289, 33862–33873. doi: 10.1074/jbc.M114.598938

Kirchhefer, U., Heinick, A., Konig, S., Kristensen, T., Muller, F. U., Seidl, M. D., et al. (2014b). Protein phosphatase 2A is regulated by protein kinase Calpha (PKCalpha)-dependent phosphorylation of its targeting subunit B56alpha at Ser41. *J. Biol. Chem.* 289, 163–176. doi: 10.1074/jbc.M113.507996

Klein, G., Schroder, F., Vogler, D., Schaefer, A., Haverich, A., Schieffer, B., et al. (2003). Increased open probability of single cardiac L-type calcium channels in patients with chronic atrial fibrillation. role of phosphatase 2A. *Cardiovasc. Res.* 59, 37–45. doi: 10.1016/S0008-6363(03)00357-2

Kodama, I., Kondo, N., and Shibata, S. (1986). Electromechanical effects of okadaic acid isolated from black sponge in guinea-pig ventricular muscles. *J. Physiol. (Lond).* 378, 359–373. doi: 10.1113/jphysiol.1986.sp016224

Kondo, N., Kodama, I., Kotake, H., and Shibata, S. (1990). Electrical effects of okadaic acid extracted from black sponge on rabbit sinus node. *Br. J. Pharmacol.* 101, 241–246. doi: 10.1111/j.1476-5381.1990.tb12694.x

Li, M., Guo, H., and Damuni, Z. (1995). Purification and characterization of two potent heat-stable protein inhibitors of protein phosphatase 2A from bovine kidney. *Biochemistry* 34, 1988–1996. doi: 10.1021/bi00006a020

Lin, L. F., Kao, L. S., and Westhead, E. W. (1994). Agents that promote protein phosphorylation inhibit the activity of the Na^+/Ca^{2+} exchanger and prolong Ca^{2+} transients in bovine chromaffin cells. *J. Neurochem.* 63, 1941–1947. doi: 10.1046/j.1471-4159.1994.63051941.x

Liu, B., Ho, H. T., Velez-Cortes, F., Lou, Q., Valdivia, C. R., Knollmann, B. C., et al. (2014). Genetic ablation of ryanodine receptor 2 phosphorylation at Ser-2808 aggravates $Ca^{(2+)}$-dependent cardiomyopathy by exacerbating diastolic Ca^{2+} release. *J. Physiol. (Lond).* 592, 1957–1973. doi: 10.1113/jphysiol.2013.264689

Liu, J., Sirenko, S., Juhaszova, M., Ziman, B., Shetty, V., Rain, S., et al. (2011a). A full range of mouse sinoatrial node AP firing rates requires protein kinase A-dependent calcium signaling. *J. Mol. Cell. Cardiol.* 51, 730–739. doi: 10.1016/j.yjmcc.2011.07.028

Liu, Q., and Hofmann, P. A. (2002). Antiadrenergic effects of adenosine A(1) receptor-mediated protein phosphatase 2a activation in the heart. *Am. J. Physiol. Heart Circ. Physiol.* 283, H1314–H1321.

Liu, Q., and Hofmann, P. A. (2003). Modulation of protein phosphatase 2a by adenosine A1 receptors in cardiomyocytes: role for p38 MAPK. *Am. J. Physiol. Heart Circ. Physiol.* 285, H97–H103.

Liu, W., Zi, M., Naumann, R., Ulm, S., Jin, J., Taglieri, D. M., et al. (2011b). Pak1 as a novel therapeutic target for antihypertrophic treatment in the heart. *Circulation* 124, 2702–2715. doi: 10.1161/CIRCULATIONAHA.111.048785

Liu, W., Zi, M., Tsui, H., Chowdhury, S. K., Zeef, L., Meng, Q. J., et al. (2013). A novel immunomodulator, FTY-720 reverses existing cardiac hypertrophy and fibrosis from pressure overload by targeting NFAT (Nuclear Factor of Activated T-cells) signaling and periostin. *Circ. Heart Fail.* 6, 833–844. doi: 10.1161/CIRCHEARTFAILURE.112.000123

Longman, M. R., Ranieri, A., Avkiran, M., and Snabaitis, A. K. (2014). Regulation of PP2AC carboxylmethylation and cellular localisation by inhibitory class G-protein coupled receptors in cardiomyocytes. *PLoS ONE* 9:e86234. doi: 10.1371/journal.pone.0086234

Luo, W., Grupp, I. L., Harrer, J., Ponniah, S., Grupp, G., Duffy, J. J., et al. (1994). Targeted ablation of the phospholamban gene is associated with markedly enhanced myocardial contractility and loss of beta-agonist stimulation. *Circ. Res.* 75, 401–409. doi: 10.1161/01.RES.75.3.401

Luss, H., Klein-Wiele, O., Boknik, P., Herzig, S., Knapp, J., Linck, B., et al. (2000). Regional expression of protein phosphatase type 1 and 2A catalytic subunit isoforms in the human heart. *J. Mol. Cell. Cardiol.* 32, 2349–2359. doi: 10.1006/jmcc.2000.1265

MacDougall, L. K., Jones, L. R., and Cohen, P. (1991). Identification of the major protein phosphatases in mammalian cardiac muscle which dephosphorylate phospholamban. *Eur. J. Biochem.* 196, 725–734. doi: 10.1111/j.1432-1033.1991.tb15871.x

Marx, S. O., Reiken, S., Hisamatsu, Y., Jayaraman, T., Burkhoff, D., Rosemblit, N., et al. (2000). PKA phosphorylation dissociates FKBP12.6 from the calcium release channel (ryanodine receptor): defective regulation in failing hearts. *Cell* 101, 365–376. doi: 10.1016/S0092-8674(00)80847-8

Meng, X., Xiao, B., Cai, S., Huang, X., Li, F., Bolstad, J., et al. (2007). Three-dimensional localization of serine 2808, a phosphorylation site in cardiac ryanodine receptor. *J. Biol. Chem.* 282, 25929–25939. doi: 10.1074/jbc.M704474200

Meurs, K. M., Mauceli, E., Lahmers, S., Acland, G. M., White, S. N., and Lindblad-Toh, K. (2010). Genome-wide association identifies a deletion in the 3' untranslated region of striatin in a canine model of arrhythmogenic right ventricular cardiomyopathy. *Hum. Genet.* 128, 315–324. doi: 10.1007/s00439-010-0855-y

Peti, W., Nairn, A. C., and Page, R. (2013). Structural basis for protein phosphatase 1 regulation and specificity. *FEBS J.* 280, 596–611. doi: 10.1111/j.1742-4658.2012.08509.x

Reiken, S., Gaburjakova, M., Gaburjakova, J., He Kl, K. L., Prieto, A., Becker, E., et al. (2001). beta-adrenergic receptor blockers restore cardiac calcium release channel (ryanodine receptor) structure and function in heart failure. *Circulation* 104, 2843–2848. doi: 10.1161/hc4701.099578

Robertson, S. P., Johnson, J. D., Holroyde, M. J., Kranias, E. G., Potter, J. D., and Solaro, R. J. (1982). The effect of troponin I phosphorylation on the Ca^{2+}-binding properties of the Ca^{2+}-regulatory site of bovine cardiac troponin. *J. Biol. Chem.* 257, 260–263.

Schulze, D. H., Muqhal, M., Lederer, W. J., and Ruknudin, A. M. (2003). Sodium/calcium exchanger (NCX1) macromolecular complex. *J. Biol. Chem.* 278, 28849–28855. doi: 10.1074/jbc.M300754200

Shi, J., Gu, P., Zhu, Z., Liu, J., Chen, Z., Sun, X., et al. (2012). Protein phosphatase 2A effectively modulates basal L-type $Ca^{(2+)}$ current by dephosphorylating Ca(v)1.2 at serine 1866 in mouse cardiac myocytes. *Biochem. Biophys. Res. Commun.* 418, 792–798. doi: 10.1016/j.bbrc.2012.01.105

Solaro, R. J., Moir, A. J., and Perry, S. V. (1976). Phosphorylation of troponin I and the inotropic effect of adrenaline in the perfused rabbit heart. *Nature* 262, 615–617. doi: 10.1038/262615a0

Srisakuldee, W., Jeyaraman, M. M., Nickel, B. E., Tanguy, S., Jiang, Z. S., and Kardami, E. (2009). Phosphorylation of connexin-43 at serine 262 promotes a cardiac injury-resistant state. *Cardiovasc. Res.* 83, 672–681. doi: 10.1093/cvr/cvp142

Stull, J. T., Brostrom, C. O., and Krebs, E. G. (1972). Phosphorylation of the inhibitor component of troponin by phosphorylase kinase. *J. Biol. Chem.* 247, 5272–5274.

Terentyev, D., Belevych, A. E., Terentyeva, R., Martin, M. M., Malana, G. E., Kuhn, D. E., et al. (2009). miR-1 overexpression enhances $Ca^{(2+)}$ release and promotes cardiac arrhythmogenesis by targeting PP2A regulatory subunit B56alpha and causing CaMKII-dependent hyperphosphorylation of RyR2. *Circ. Res.* 104, 514–521. doi: 10.1161/CIRCRESAHA.108.181651

Terentyev, D., Viatchenko-Karpinski, S., Gyorke, I., Terentyeva, R., and Gyorke, S. (2003). Protein phosphatases decrease sarcoplasmic reticulum calcium content by stimulating calcium release in cardiac myocytes. *J. Physiol. (Lond).* 552, 109–118. doi: 10.1113/jphysiol.2003.046367

Wei, S. K., Ruknudin, A., Hanlon, S. U., McCurley, J. M., Schulze, D. H., and Haigney, M. C. (2003). Protein kinase A hyperphosphorylation increases basal current but decreases beta-adrenergic responsiveness of the sarcolemmal Na^{+}-Ca^{2+} exchanger in failing pig myocytes. *Circ. Res.* 92, 897–903. doi: 10.1161/01.RES.0000069701.19660.14

Wei, S. K., Ruknudin, A. M., Shou, M., McCurley, J. M., Hanlon, S. U., Elgin, E., et al. (2007). Muscarinic modulation of the sodium-calcium exchanger in heart failure. *Circulation* 115, 1225–1233.

Wijnker, P. J., Boknik, P., Gergs, U., Muller, F. U., Neumann, J., dos Remedios, C., et al. (2011). Protein phosphatase 2A affects myofilament contractility in non-failing but not in failing human myocardium. *J. Muscle Res. Cell Motil.* 32, 221–233. doi: 10.1007/s10974-011-9261-x

Xiao, B., Jiang, M. T., Zhao, M., Yang, D., Sutherland, C., Lai, F. A., et al. (2005). Characterization of a novel PKA phosphorylation site, serine-2030, reveals no PKA hyperphosphorylation of the cardiac ryanodine receptor in canine heart failure. *Circ. Res.* 96, 847–855. doi: 10.1161/01.RES.0000163276.26083.e8

Xiao, B., Zhong, G., Obayashi, M., Yang, D., Chen, K., Walsh, M. P., et al. (2006). Ser-2030, but not Ser-2808, is the major phosphorylation site in cardiac ryanodine receptors responding to protein kinase A activation upon beta-adrenergic stimulation in normal and failing hearts. *Biochem. J.* 396, 7–16. doi: 10.1042/BJ20060116

Yang, X., Wang, T., Lin, X., Yue, X., Wang, Q., Wang, G., et al. (2015). Genetic deletion of Rnd3/RhoE results in mouse heart calcium leakage through upregulation of protein kinase a signaling. *Circ. Res.* 116, e1–e10. doi: 10.1161/CIRCRESAHA.116.304940

Zhang, H., Makarewich, C. A., Kubo, H., Wang, W., Duran, J. M., Li, Y., et al. (2012). Hyperphosphorylation of the cardiac ryanodine receptor at serine 2808 is not involved in cardiac dysfunction after myocardial infarction. *Circ. Res.* 110, 831–840. doi: 10.1161/CIRCRESAHA.111.255158

Zhang, Y. H., and Hancox, J. C. (2009). Regulation of cardiac Na^{+}-Ca^{2+} exchanger activity by protein kinase phosphorylation—still a paradox? *Cell Calcium* 45, 1–10. doi: 10.1016/j.ceca.2008.05.005

Zheng, M. Q., Li, X., Tang, K., Sharma, N. M., Wyatt, T. A., Patel, K. P., et al. (2013). Pyruvate restores beta-adrenergic sensitivity of L-type $Ca^{(2+)}$ channels in failing rat heart: role of protein phosphatase. *Am. J. Physiol. Heart Circ. Physiol.* 304, H1352–H1360. doi: 10.1152/ajpheart.00873.2012

Conflict of Interest Statement: The authors declare that the research was conducted in the absence of any commercial or financial relationships that could be construed as a potential conflict of interest.

Received: 24 November 2014; accepted: 09 January 2015; published online: 29 January 2015.

Citation: Lei M, Wang X, Ke Y and Solaro RJ (2015) Regulation of Ca^{2+} transient by PP2A in normal and failing heart. Front. Physiol. ***6****:13. doi: 10.3389/fphys.2015.00013 This article was submitted to Cardiac Electrophysiology, a section of the journal Frontiers in Physiology.*

Advantages of publishing in Frontiers

OPEN ACCESS
Articles are free to read, for greatest visibility

COLLABORATIVE PEER-REVIEW
Designed to be rigorous – yet also collaborative, fair and constructive

FAST PUBLICATION
Average 85 days from submission to publication (across all journals)

COPYRIGHT TO AUTHORS
No limit to article distribution and re-use

TRANSPARENT
Editors and reviewers acknowledged by name on published articles

SUPPORT
By our Swiss-based editorial team

IMPACT METRICS
Advanced metrics track your article's impact

GLOBAL SPREAD
5'100'000+ monthly article views and downloads

LOOP RESEARCH NETWORK
Our network increases readership for your article

Frontiers
EPFL Innovation Park, Building I • 1015 Lausanne • Switzerland
Tel +41 21 510 17 00 • Fax +41 21 510 17 01 • info@frontiersin.org
www.frontiersin.org

Find us on